

**Tectonic evolution of the Svecofennian crust in southern Finland -
a basis for characterizing bedrock technical properties**



**Tectonic evolution of the Svecofennian
crust in southern Finland –
a basis for characterizing
bedrock technical properties**

Edited by
Matti Pajunen

Contributors:

Meri-Liisa Airo, Tuija Elminen, Alaric Hopgood,
Hannu Huhma, Tapio Koistinen, Irmeli Mänttari,
Satu Mertanen, Reijo Niemelä, Matti Pajunen,
Juha Salmelainen, Markus Vaarma, Pekka Wasenius
and Marit Wennerström

ISBN 978-952-217-044-6 (paperback)
ISBN 978-952-217-045-3 (PDF)
ISSN 0782-8535

Otavan Kirjapaino 2008

Pajunen, M. (ed.) 2008. Tectonic evolution of the Svecofennian crust in southern Finland – a basis for characterizing bedrock technical properties. *Geological Survey of Finland, Special Paper 47*, 326 pages, 185 figures, 17 tables and 10 appendices.

The increasing need for raw materials and usable bedrock resources, especially in densely populated urban areas, has set new demands for geological information on bedrock properties. For example, underground construction for varied purposes has recently greatly increased. In the Precambrian shield areas, such as in the Fennoscandian Shield, the main concerns in underground construction predominantly arise from the brittle structures in bedrock, such as the zones of weakness and jointing. In the main, this can also be generalized to many other bedrock applications, e.g. underground planning, prospecting for groundwater and construction material or studying the migration of harmful constituents in bedrock.

In this volume of the *Geological Survey of Finland, Special Paper 47*, the main goals were to study the structural evolution of the southern Svecofennian domain, and to develop geological and geophysical methods for this information to be exploited for applicational purposes. The project was carried out in southern Finland, in the Helsinki capital area, with some correlations with the Pori area in southwestern Finland. The volume includes related papers describing successive studies, from ductile evolution during the Svecofennian orogeny at 1.9–1.8 Ga to the brittle phases of post-Svecofennian deformations, such as faulting and jointing. Structural analyses are based on extensive field data and careful analyses of key outcrops. A new tectonic model of the Svecofennian orogeny, a description of fault structures and kinematics, and regional jointing systematics in the study area are presented. Interpretations of ductile and brittle structural evolution benefitted the analysis of aerogeophysical data and geophysical modelling. TIMS and SIMS datings and palaeomagnetic studies carried out to establish the timing of magmatic, metamorphic and structural events.

The tectonic structures were used as a basis for the geotechnical classification of bedrock properties. The old Svecofennian ductile structural framework of the crust effectively determined the locations and characters of the post-Svecofennian brittle structures, faulting and jointing, and was used as a main factor in dividing the study area into tectonically coherent sub-areas. The kinematically and structurally classified faults were combined with geomechanical classifications by comparing them to the same, geomechanically classified, zones in tunnels. Jointing properties were used to classify the consistency/brokenness of the tectonically or lithologically coherent sub-areas. The new geotechnical classification is presented as a construction suitability of the bedrock in the Espoo, Helsinki and Vantaa areas.

The way to formulate and use geological and geophysical information varies depending on the target application. Therefore, more work and co-operation between geoscientists and other users should be carried out to explore the possibilities for using the geological information in various applications in an optimal way.

Key words (GeoRef Thesaurus, AGI): crust, tectonics, structural geology, bedrock, structural analysis, engineering properties, Proterozoic, Paleoproterozoic, Svecofennian, Espoo, Helsinki, Vantaa, Finland

Matti Pajunen
Geological Survey of Finland,
P.O. Box 69, FI-02151 Espoo, Finland

E-mail: matti.pajunen@gtk.fi

CONTENTS

Introduction.....	7
<i>Matti Pajunen</i>	
Tectonic evolution of the Svecofennian crust in southern Finland.....	15
<i>Matti Pajunen, Meri-Liisa Airo, Tuija Elminen, Irmeli Mänttari, Reijo Niemelä, Markus Vaarma, Pekka Wasenius and Marit Wennerström</i>	
Integrated structural succession and age constraints on a Svecofennian key outcrop in Västerviken, southern Finland	161
<i>Matti Pajunen, Alaric Hopgood, Hannu Huhma and Tapio Koistinen</i>	
Fault structures in the Helsinki Area, southern Finland.....	185
<i>Tuija Elminen, Meri-Liisa Airo, Reijo Niemelä, Matti Pajunen, Markus Vaarma, Pekka Wasenius and Marit Wennerström</i>	
Paleomagnetic evidence for Mesoproterozoic – Paleozoic reactivation of the Paleoproterozoic crust in southern Finland.....	215
<i>Satu Mertanen, Meri-Liisa Airo, Tuija Elminen, Reijo Niemelä, Matti Pajunen, Pekka Wasenius and Marit Wennerström</i>	
Orientation and properties of jointing in Helsinki area, southern Finland	253
<i>Marit Wennerström, Meri-Liisa Airo, Tuija Elminen, Reijo Niemelä, Matti Pajunen, Markus Vaarma and Pekka Wasenius</i>	
Aerogeophysical approach to ductile and brittle structures in the densely populated urban Helsinki area, southern Finland	283
<i>Meri-Liisa Airo, Tuija Elminen, Satu Mertanen, Reijo Niemelä, Matti Pajunen, Pekka Wasenius and Marit Wennerström</i>	
Construction suitability of bedrock in the Helsinki area based on the tectonic structure of the Svecofennian crust of southern Finland	309
<i>Matti Pajunen, Meri-Liisa Airo, Tuija Elminen, Reijo Niemelä, Juha Salmelainen, Markus Vaarma, Pekka Wasenius and Marit Wennerström</i>	

INTRODUCTION

M. Pajunen

Recently, the requirements for geological information on bedrock properties have extended to cover the various needs of infrastructural developments. In Finland, underground construction has significantly increased in the densely built urban areas, and more underground structures, including traffic tunnels, walkways, car parking, service tunnels, waste management and sport centres, are to be hidden below the surface (e.g. Roinisto 1986 and Rönkä & Ritola 1997). In the near future, underground planning and the identification of usable bedrock resources for further construction will become more significant (e.g. Tarkkala 2004). Prospecting for groundwater (e.g. Mälkki 1999) or studying of the migration of harmful constituents in bedrock (e.g. Asikainen & Kahlos 1979) would benefit from more precise data on fracturing patterns. Concern over the state of the environment also necessitates the location of surficial actions of society, such as the waste disposal sites, to be more carefully determined from the geological point of view. The increasing need for raw materials, building rocks (e.g. Selonen & Suominen 2003) or rock aggregates (e.g. Kuula-Väisänen & Uusinoka 2001 and Nurmi et al. 2001), and also for landscaping open pits or road cuts, requires data on brittle structures. Recent technical solutions have improved ground storing heat pumping systems in which water in bedrock fractures acts as transporting medium. In addition to the fabric of society, the geological structure of the bedrock must also be taken into account during the early stages of planning processes. Therefore, it has become necessary to also concentrate on the basic geological factors that are important in meeting of these growing needs. This presents the challenge of determining what kind of basic information is needed for different applications and how these data should be formulated to more usable and reliable form.

The purpose of this volume is to examine and identify the important factors in analysing geological data for applications based on the tectonic evolution of the Svecofennian domain in southern Finland. The main goal in these studies has been to formulate the geological data primarily for underground construction or communal planning processes. These studies would not have been possible

without the extensive geological and geophysical mapping (e.g. Airo 2005) and research carried out in Finland since the end of the 19th century.

The Precambrian bedrock in central and southern Finland consists of two major domains: the Archaean craton in the northeast and the Paleoproterozoic Svecofennian domain in the southwest (Korsman et al. 1997). The Svecofennian domain, which collided against the Archaean continent at c. 1.9–1.88 Ga ago (e.g. Wegmann 1928 and Koistinen 1981), shows a complex accretion of terrains with wide lithological, tectonic and metamorphic variation. Hietanen (1975) published the first plate tectonic construction of the domain. Subsequently, several authors (e.g. Gaál 1982, Gaál & Gorbatshev 1987 and Park et al. 1984) have developed new tectonic constructions. The studies of Korsman et al. (1984) advanced the tectono-thermal crustal models by evidencing tectono-metamorphic discordances between different terranes in the southern Svecofennian domain. The c. 100 km broad, E-W-trending granite migmatite belt in the south exhibits tectonic and magmatic activity that occurred about 50 Ma later. Korsman et al. (op. cit) also found that the so-called Savo schist belt bordering the Archaean craton in the west was intruded by c. 1.93 Ga old tonalites, i.e. c. 40 Ma older than granitoids characterizing the other parts of the Svecofennian domain. Kontinen (1987) described the early Proterozoic ophiolite from the Kainuu schist belt. Lahtinen (1994) noticed the primitive nature of the early island arc, the Savo schist belt, and published his multi-stage accretion model on the Svecofennian orogeny. The model was based on extensive data from tectono-metamorphic analyses (e.g. Hopgood et al. 1983, Kilpeläinen 1988, Hölttä 1988, Pajunen 1988, Nironen 1989, Tuisku & Laajoki 1990 and Kilpeläinen & Rastas 1990 and Ehlers et al. 1993), isotopic studies (e.g. Vaasjoki & Sakko 1988, Huhma 1986 and Suominen 1991), seismic data (Luosto et al. 1990, BABEL Working Group 1993 and Korja et al. 1993), and electromagnetic analyses of the crust and lithosphere (Korja 1990, 1993 and Korja & Hjelt 1993). The model was adapted to cover the Fennoscandian Shield by Nironen (1997). The crustal model produced in the GGT/SVEKA Transect

program (Korsman et al. 1999) combined the tectonic-metamorphic and magmatic history of the crust with the deeper crustal structure based on seismic and electromagnetic data, and benefited the new tectono-metamorphic interpretations (e.g. Kilpeläinen 1998, Väisänen & Hölttä 1999 and Pajunen & Poutiainen 1999). Increasing amount of age data, primarily in the southernmost Finland (e.g. Mouri et al. 1999, Lahtinen et al. 2002, Väisänen et al. 2002, Väisänen et al. 2004 and Kurhila et al. 2005), have led to several new interpretations of the Svecofennian collision and collapse history (e.g. Väisänen 2002, Pajunen et al. 2004, Rutland et al. 2004, Lahtinen et al. 2005 and Korja & Heikkinen 2005). The latest tectonic models are related to the FIRE reflection seismic lines (compiled in Kukkonen & Lahtinen 2006).

The post-Svecofennian tectonic events in the cooled crust are still a less-known part of the evolutionary history in Finland. Nearly all the bedrock applications that supply the needs of society are dependent on the fracturing properties for bedrock. Thus, the requirements of information on post-Svecofennian semi-brittle to brittle faulting and jointing patterns will increase in the near future in Finland.

During this long geological time, after the emplacement of the “post-orogenic” granites at 1.8–1.77 Ga (e.g. Vaasjoki 1995 and Eklund & Shebanov 2005), several important geotectonic events occurred: post-Svecofennian crustal uplift, the extensional rapakivi stage at 1.65–1.54 Ga (Vaasjoki 1977a and Haapala et al. 2005), formation of the c. 1.3–1.2 Ga sediment basins and related mafic magmatism (e.g. Kohonen et al. 1993), the Caledonian orogeny at 450 Ma ago (e.g. Vaasjoki 1977b and Mertanen et al. 2004) and post-glacial uplift that began at c. 10 000–8000 years ago and is still continuing and exhibited as recent seismic activity (e.g. Kuivamäki et al. 1998). All these events (and possibly others) left their signatures as semi-brittle to brittle structures or as reactivation of the pre-existing structures (e.g. Mertanen et al. 2001 and Pajunen et al. 2001a), but only a few studies have sought to understand their evolution in depth. The majority of interpretations of regional faulting patterns have been based on topographic and geophysical lineament analyses (e.g. Talvitie 1971, Parkkinen 1975 and Kuivamäki 2000), and some arguments on the age relations or kinematics of the fractural crustal features have been presented (e.g. Talvitie 1971). A few more local studies of fault zones have described the relative age relations and characters of the fault rocks (e.g. Halden 1982, Pajunen 1986, Ploegsma 1989, Pietikäinen 1994, Lindroos et al. 1996, Heermans & Wijbrans 1999 and Pajunen et al. 2001a), some of which have shown Svecofennian precursors

for the faults. Korja & Heikkinen (1995) described the major listric fault structures that were related to extensional processes during the rapakivi stage.

Several studies have been carried out on joint characters for local-scale modelling of the properties of rock masses (Barton & Stephansson 1990) and analyses of fluid flow in fractural systems (National Research Council 1996). The jointing properties and patterns have received little attention during the mapping programs in Finland. Studies have generally concentrated on local construction tasks; in Finland, several of these have been related to the final disposal of spent nuclear fuel in bedrock (e.g. Anttila et al. 1992, Anttila et al. 1999, Posiva Oy 2005, Paulamäki et al. 2006 and Mattila et al. 2008). Analyses of jointing patterns have rarely been based on field measurements covering larger areas or correlated with lithological variations or with other tectonic structures. Regional-scale interpretations described by Pajunen et al. (2001a) have provided evidence of connections between the ductile structure of the crust and the jointing pattern. The close relationships between jointing patterns and folding and faulting were also detected in the Helsinki area during the preliminary stages of the studies of this Special Paper (Pajunen et al. 2002a). Accordingly, the regional jointing patterns and joint kinematics in the Svecofennian bedrock are still largely unknown.

This volume presents geological data, based on the tectonic evolution of the crust, in a useful form especially targeted at underground construction and planning. This research was initiated in a research project of the Geological Survey of Finland carried out in the Pori area, southwestern Finland, from 1998–2000 (Pajunen et al. 2001a). The study concentrated on structural succession in the area, including preliminary analysis of brittle faulting and jointing properties; the studies were continued from 2006–2007 in co-operation with the cities of Pori and Rauma, Posiva Ltd and the Satakuntaliitto. The developments of these studies were extended to the surroundings of the Helsinki capital area in 1999–2002 in a collaborative project with the cities of Espoo, Helsinki and Vantaa, the planning companies Rockplan Ltd and Viatek Ltd and the Technological Agency of Finland (Tekes). The early results of the project were presented by Pajunen et al. (2001a), in Wennerström et al. (2006) and in unpublished reports (Pajunen et al. 2002a, b, c and d).

Our purpose is to successively describe the tectonic history of the Svecofennian bedrock, from the early ductile Svecofennian structures to the late formation of brittle faulting and jointing. The papers are the results of intensive co-operation within the study group, and with non-geologists users, and are thematically tied to each other resulting in this

volume of the *Geological Survey of Finland, Special Paper 47*, including the following papers:

Paper I:

Pajunen, M., Airo, M.-L., Elminen, T., Mänttari, I., Niemelä, R., Vaarma, M., Wasenius, P. & Wennerström, M. 2008. Tectonic evolution of the Svecofennian crust in southern Finland. Geological Survey of Finland, Special Paper 47, 15–160.

The paper summarizes the tectono-metamorphic, magmatic and kinematic evolution of the Svecofennian orogeny in southern Finland based on study carried out in the Helsinki and Pori regions. The analysis is based on observations of structural succession at key outcrops (cf. Paper II), new structurally-fixed TIMS and SIMS age data, pre-existing geological research and mapping, and on modelling of aerogeophysical data (cf. Paper VI). A new tectonic evolution model is presented for the Svecofennian orogeny. The significance of the Svecofennian structures in reorienting the post-Svecofennian deformation is briefly discussed (cf. Papers III and V). The Svecofennian tectonic evolution forms the framework for analyzing brittle structures for the technical application exemplified in Paper VII.

Paper II:

Pajunen, M., Hopgood, A., Huhma, H. & Koistinen, T. 2008. Integrated structural succession and age constraints on a Svecofennian key outcrop in Västerviken, southern Finland. Geological Survey of Finland, Special Paper 47, 161–184.

This paper describes detailed structures on the complexly deformed and metamorphosed Västerviken key outcrop in Karjalohja. The outcrop provides an excellent example of the local structural succession of key structures, migmatization phases and tectono-thermal discordances. Detailed structural studies of this kind are important in understanding and compiling the successions of the major crustal events on a regional scale (cf. Paper I).

Paper III:

Elminen, T., Airo, M.-L., Niemelä, R., Pajunen, M., Vaarma, M., Wasenius, P. & Wennerström, M. 2008. Fault structures in the Helsinki Area, southern Finland. Geological Survey of Finland, Special Paper 47, 185–213.

This paper describes the shear and fault zones in the Helsinki area, the locations of which were estab-

lished in the field or by using topographic and geophysical interpretations. The relationships between the structurally and kinematically classified fault generations were correlated with the Svecofennian structural framework (cf. Paper I) and the post-Svecofennian structural history. The faults classified due to their fault rock characteristics, ages (cf. Paper IV) and kinematics are used in the geotechnical classification of the zones of weakness (cf. Paper VII). These faults, in addition to the Svecofennian structural framework, determine the sub-areas for the jointing characterization (cf. Papers V and VII).

Paper IV:

Mertanen, S., Airo, M.-L., Elminen, T., Niemelä, R., Pajunen, M., Wasenius, P. & Wennerström, M. 2008. Paleomagnetic evidence for Mesoproterozoic – Paleozoic reactivation of the Paleoproterozoic crust in southern Finland. Geological Survey of Finland, Special Paper 47, 215–252.

This paper presents paleomagnetic results from shear and fault zones in the Helsinki area, where sampling was related to structural observations (cf. Papers I and III). The main result of the study was that the zones have been reactivated in several geological processes, seen as different remanent magnetization components. Due to partial reheating and fluid flow movements in the pre-existing shear and fault zones (cf. Paper I), new magnetic minerals were able to precipitate. The occurrence of different magnetic minerals coupled with paleomagnetic dating provides information on the heating periods and fluid activity along the zones and can be used in explaining the tectonic and crustal processes following the Svecofennian orogeny (cf. Paper III). Along with kinematic analyses, the study aids in the overall characterization of the geotechnical features of the bedrock (cf. Paper VII).

Paper V:

Wennerström, M., Airo, M.-L., Elminen, T., Niemelä, R., Pajunen, M., Vaarma, M. & Wasenius, P. 2008. Orientation and properties of jointing in Helsinki area, southern Finland. Geological Survey of Finland, Special Paper 47, 253–282.

Recently, the significance of research into the fracturing and jointing of bedrock has increased due to the increased need for the data in various applications and construction projects (cf. Paper VII). This paper, based on studies carried out in the Helsinki area, is the first approach to regionally characterizing jointing patterns in Finland. Extensive regional

field data on jointing properties were collected using a field mapping scheme developed during the project. The variation in jointing patterns and properties in the tectonic sub-areas is described in the context to the structural framework (cf. Papers I and III).

Paper VI:

Airo, M.-L., Elminen, T., Mertanen, S., Niemelä, R., Pajunen, M., Wasenius, P. & Wennerström, M. 2008. Aerogeophysical approach to ductile and brittle structures in the densely populated urban Helsinki area, southern Finland. Geological Survey of Finland, Special Paper 47, 283–308.

In Finland wide areas are overlain by glaciogenic sediments and show poor outcropping. Due to limited possibilities to obtain geological information in such areas, geophysical methods play an important role. Existing airborne geophysical data cover the Helsinki study area, including magnetic, electromagnetic and gamma-ray spectrometric data (standard: nominal terrain clearance 35 m, flight line spacing of 200 m). More detailed and specialized airborne measurements were conducted at denser flight line spacing of 100 m when testing the possibilities to more precisely analyze the bedrock properties in densely constructed urban areas. Interpretation of the airborne geophysical data aimed at 1) outlining the regional structural framework and its possible control on the present structural pattern of the bedrock, and 2) expanding standard interpretation methods to identify shallow, near-surface geological features. This succeeded through the use of directional analysis of magnetic horizontal derivatives. This paper describes how the airborne geophysical data were processed and interpreted for use

as background data in analyses carried out in related studies (Papers I, II, V and VII) and discusses restrictions in the interpretation of data from densely populated urban areas when seeking to avoid artificial noise problems.

Paper VII:

Pajunen, M., Airo, M.-L., Elminen, T., Niemelä, R., Salmelainen, J., Vaarma, M., Wasenius, P. & Wennerström, M. 2008. Construction suitability of bedrock in the Helsinki area based on the tectonic structure of the Svecofennian crust of southern Finland. Geological Survey of Finland, Special Paper 47, 309–326.

All the previously-presented studies (cf. Papers I-VI) supported the production of a construction suitability model described in this paper. When introducing geological-geophysical data for different applications, new approaches are needed to make the analyses usable. The purpose of this paper is to test the possibilities to formulate geological data for geotechnical use; here, data for community planning and underground building were set as the principal targets. The results were presented in the map of the “The Construction Suitability of Bedrock 1:50 000 – Espoo, Helsinki & Vantaa”. The geologically classified field data (Papers III and V) were combined with the pre-existing geomechanical classifications based on jointing properties and weakness zones. The lithologically and structurally coherent sub-areas, bordered by ductile to brittle shear/fault zones, were classified using jointing properties (Paper III) as a basis for qualification. The weakness zones were classified by correlating them with the corresponding technically classified zones in tunnels.

ACKNOWLEDGEMENTS

It is evident that penetrative interpretation of crustal evolution of this kind implies considerable co-operation and discussion both with the geological and geophysical counterparts, and also with various potential users of the information. The first steps to open routes for such co-operation between geoscientists and other users, finally leading to these studies, were initiated by Kalevi Korsman from the Geological Survey of Finland (retired) and by Jarmo Roinisto from the Rockplan Ltd back in 1997. Their input and help have been important throughout the projects represented here. Tapio Koistinen has helped us greatly in the structural analyses and cor-

relations with different parts of the Svecofennian domain.

The field observations of Göran Sandholm, Nicklas Nordbäck, Rod Holcombe and several students working as field assistants were of great help. The aerogeophysicist group of the Geological Survey of Finland took part in the aerogeophysical field measurements and data processing, and the personnel of the mineralogical and isotope geology laboratories at the Geological Survey of Finland have provided an important input to the project. Christer Ahlsved and Nils Gustavsson helped us by constructing IT applications. Anneli Lindh and Mirjam

Ajlani completed several drawings and maps of the papers for publication.

The three-year project in Espoo, Helsinki and Vantaa area was funded by the Technological Agency of Finland (Tekes), the cities of Helsinki, Espoo and Vantaa, and by the planning companies Rockplan Ltd. and Viatek Ltd. The studies in the Pori area were carried out in co-operation with the cities of Pori and Rauma, Posiva Ltd and Satakuntaliitto.

Several people from the geotechnical divisions of the participant cities kindly organized the material for correlation purposes.

The English of the preface was corrected by Roy Siddall.

The editor and contributors wish to express their warmest thanks to all above-mentioned and to those not named but who have contributed to the projects in different ways.

REFERENCES

- Airo, M.-L. (ed.) 2005.** Aerogeophysics in Finland 1972–2004. Methods, System characteristics and applications. Geological Survey of Finland, Special Paper 39. 197 p.
- Anttila, P., Paulamäki, S., Lindberg, A., Paananen, M., Koistinen, T., Front, K. & Pitkänen, P. 1992.** The geology of the Olkiluoto area, summary report. Tiivistelmä: Olkiluodon alueen geologiset olosuhteet: yhteenvetoraportti. Helsinki: Voimayhtiöiden ydinjätetoimikunta, Report YJT-92-28. 37 p. (in Finnish)
- Anttila, P., Ahokas, H., Front, K., Hinkkanen, H., Johansson, E., Paulamäki, S., Riekkola, R., Saari, J., Saksa, P., Snellman, M., Wikström, L. & Öhberg, A. 1999.** Final disposal of spent nuclear fuel in Finnish bedrock – Olkiluoto site report. Tiivistelmä: Käytetyn polttoaineen loppusijoitus Suomen kallio-perään – Olkiluodon paikkaraportti. Helsinki: Posiva Oy, Posiva-raportti 99-10. 206 p.
- Asikainen, M. & Kahlos, H. 1979.** Anomalously high concentrations of uranium, radium and radon in water from drilled wells in the Helsinki region. *Geochimica et Cosmochimica Acta* 43, 1681–1686.
- BABEL Working Group 1993.** Integrated seismic studies of the Baltic Shield using data in the Gulf of Bothnia region. *Geophysical Journal International* 112 (3), 305–324.
- Barton, N. & Stephansson, O. 1990.** Rock Joints. Rotterdam: A. A. Balkema. 814 p.
- Ehlers, C., Lindroos, A. & Selonen, O. 1993.** The late Svecofennian granite-migmatite zone of southern Finland – a belt of transpressive deformation and granite emplacement. *Precambrian Research* 64, 295–309.
- Eklund, O. & Shebanov, A. 2005.** Prolonged postcollisional shoshonitic magmatism in the southern Svecofennian domain – a case study of the Åva granite-lamprophyre ring complex. In: Rämö, O. T. (ed.) *Granitic systems – Ilmari Haapala Volume*. *Lithos* 80 (1–4), 229–247.
- Gaál, G. 1982.** Proterozoic tectonic evolution and late Svecofennian plate deformation of the Central Baltic Shield. *Geologische Rundschau* 71 (1), 158–170.
- Gaál, G. & Gorbatshev, R. 1987.** An outline of the Precambrian evolution of the Baltic Shield. *Precambrian Research* 35, 15–52.
- Haapala, I., Rämö, O. T. & Frindt, S. 2005.** Comparison of Proterozoic and Phanerozoic rift-related basaltic-granitic magmatism. *Lithos* 80, 1–32.
- Halden, N. M. 1982.** Structural, metamorphic and igneous history of migmatites in the deep levels of a wrench fault regime, Savonranta, eastern Finland. *Transactions of the Royal Society of Edinburgh, Earth Sciences* 73 (1), 17–30.
- Heeremans, M. & Wijbrans, J. 1999.** Late Proterozoic tectonic events in southern Finland, constrained by Ar-40/Ar-39 incremental heating and single spot fusion experiments on K-feldspars. *Terra Nova* 11 (5), 216–222.
- Hietanen, A. 1975.** Generation of potassium-poor magmas in the northern Sierra Nevada and the Svecofennian of Finland. *J. Res. U.S. Geol. Surv.* 3, 631–645.
- Hölttä, P. 1988.** Metamorphic zones and the evolution of granulite grade metamorphism in the early Proterozoic Pielavesi area, central Finland. Geological Survey of Finland, Bulletin 344. 50 p.
- Hopgood, A., Bowes, D., Kouvo, O. & Halliday, A. 1983.** U-Pb and Rb-Sr isotopic study of polyphase deformed migmatites in the Svecokareliides, southern Finland. In: Atherton, M. & Gribble, C. (eds.) *Migmatites, melting and metamorphism*. Nantwich: Shiva, 80–92.
- Huhma, H. 1986.** Sm-Nd, U-Pb and Pb-Pb isotopic evidence for the origin of the Early Proterozoic Svecofennian crust in Finland. Geological Survey of Finland, Bulletin 337. 48 p.
- Kilpeläinen, T. 1988.** Evolution of deformation and metamorphism as a function of time in the Rantasalmi-Sulkava area, southeastern Finland. In: Korsman, K. (ed.) *Tectono-metamorphic evolution of the Raaheladoga zone*. Geological Survey of Finland, Bulletin 343, 77–87.
- Kilpeläinen, T. 1998.** Evolution and 3D modelling of structural and metamorphic patterns of the Palaeoproterozoic crust in the Tampere-Vammala area, southern Finland. Geological Survey of Finland, Bulletin 397. 124 p.
- Kilpeläinen, T. & Rastas, J. 1990.** Etelä-Suomen lehtiitijakson tektonis-metamorfisesta kehityksestä. University of Turku, Institute of Geology and Mineralogy, Publication No 21. 37 p. (in Finnish).

- Kohonen, J., Pihlaja, P., Kujala, H. & Marmo, J. 1993.** Sedimentation of the Jotnian Satakunta sandstone, western Finland. Geological Survey of Finland, Bulletin 369. 24 p.
- Koistinen, T. J. 1981.** Structural evolution of an early Proterozoic stratabound Cu-Co-Zn deposit, Outokumpu, Finland. Transactions of the Royal Society of Edinburgh, Earth Sciences 72, 115–158.
- Kontinen, A. 1987.** An early Proterozoic ophiolite – the Jormua mafic-ultramafic complex, north-eastern Finland. Precambrian Research 35, 313–341.
- Korja, A. 1995.** Structure of the Svecofennian crust – growth and destruction of the Svecofennian orogen. Institute of Seismology, University of Finland, Report S–31.
- Korja, A., Korja, T., Luosto, U. & Heikkinen, P. 1993.** Seismic and geoelectric evidence for collisional and extensional events in the Fennoscandian Shield – implications for Precambrian crustal evolution. Tectonophysics 219, 129–152.
- Korja, A. & Heikkinen, P. 1995.** Proterozoic extensional tectonics of central Fennoscandian Shield: a result from the Baltic and Bothnian echoes from the Lithosphere experiment. Tectonics 14, 504–517.
- Korja, A. & Heikkinen, P. 2005.** The accretionary Svecofennian orogen – insight from the BABEL profiles. Precambrian Research 136 (3–4), 241–268.
- Korja, T. 1990.** Electrical conductivity of lithosphere. Magnetotelluric studies in the Fennoscandian Shield, Finland. Acta Univ. Oulu, v. A215. 55p.
- Korja, T. 1993.** Electrical conductivity distribution of the lithosphere in the central Fennoscandian Shield. In: Gorbatshev, R. (ed.) The Baltic Shield. Precambrian Research 64 (1–4), 85–108.
- Korja, T. & Hjelt, S.-E. 1993** Electromagnetic studies in the Fennoscandian Shield – electrical conductivity of the Precambrian crust. Phys. Earth Planet. Inter., v. 81, 107–138.
- Korsman, K., Hölttä, P., Hautala, T. & Wasenius, P. 1984.** Metamorphism as an indicator of evolution and structure of the crust in Eastern Finland. Geological Survey of Finland, Bulletin 328. 40 p.
- Korsman, K., Koistinen, T., Kohonen, J., Wennerström, M., Ekdahl, E., Honkamo, M., Idman, H. & Pekkala, Y. (eds.) 1997.** Bedrock map of Finland 1:1 000 000. Geological Survey of Finland.
- Korsman, K., Korja, T., Pajunen, M. & Virransalo, P. 1999.** The GGT/SVEKA transect: structure and evolution of the continental crust in the Paleoproterozoic Svecofennian orogen in Finland. International Geology Review 41, 287–333.
- Kuivamäki, A. 2000.** Lineament database of the Finnish potential repository sites for calculation of bedrock movements induced by earthquakes (without appendices 14). Helsinki, Finland: Posiva Oy, Working Report 2000–12. 56 p.
- Kuivamäki, A., Vuorela, P. & Paananen, M. 1998.** Indications of postglacial and recent bedrock movements in Finland and Russian Karelia. Nuclear Waste Disposal Research. Geological Survey of Finland, Report YST–99. 92 p.
- Kukkonen, I. & Lahtinen, R. (eds.) 2006.** Finnish Reflection Experiment FIRE 2001–2005. Geological Survey of Finland, Special Paper 43. 247 p.
- Kurhila, M., Vaasjoki, M., Mänttari, I., Rämö, T. & Nironen, M. 2005.** U-Pb ages and Nd isotope characteristics of the lateorogenic, migmatizing microcline granites in southwestern Finland. Bulletin of the Geological Society of Finland 77 (2), 105–128.
- Kuula-Väisänen, P. & Uusinoka, R. (eds.) 2001.** Aggregate 2001 – environment and economy. Aggregate 2001, Helsinki, Finland 6–10 August 2001, vol. 1 and 2. 509 p.
- Lahtinen, R. 1994.** Crustal evolution of the Svecofennian and Karelian domains during 2.1–1.79 Ga, with special emphasis on the geochemistry and origin of 1.93–1.91 Ga gneissic tonalites and associated supra-crustal rocks in the Rautalampi area, central Finland. Geological Survey of Finland, Bulletin 378. 128 p.
- Lahtinen, R., Huhma, H. & Kousa, J. 2002.** Contrasting source components of the Paleoproterozoic Svecofennian metasediments : detrital zircon U-Pb, Sm-Nd and geochemical data. Precambrian Research 116 (1–2), 81–109.
- Lahtinen, R., Korja, A. & Nironen, M. 2005.** Paleoproterozoic tectonic evolution. In: Lehtinen, M., Nurmi, P. A. & Rämö, O. T. (eds.) Precambrian Geology of Finland. Key to the Evolution of the Fennoscandian Shield. Amsterdam: Elsevier Science B.V., 481–531.
- Lindroos, A., Romer, R. L., Ehlers, C. & Alviola, R. 1996.** Late-orogenic Svecofennian deformation in SW Finland constrained by pegmatite emplacement ages. Terra Nova 8 (6), 567–574.
- Luosto, U., Tiira, T., Korhonen, H., Azbel, I., Burmin, V., Buyanov, A., Kosminskaya, I., Ionkis, V. & Sharov, N. 1990.** Crust and upper mantle structure along the DSS Baltic profile in SE Finland. Geophysical Journal International 101, 89–110.
- Mälkki, E. 1999.** Pohjavesi ja pohjaveden ympäristö. Tampere: Tammer-paino Oy. 304 p. (in Finnish)
- Mattila, J., Aaltonen, I., Kempainen, K., Wikström, L., Paananen, M., Paulamäki, S., Front, K., Gehör, S., Kärki, A. & Ahokas, T. 2008.** Geological model of the Olkiluoto site, Version 1.0. Posiva Oy, Working Report 2007–92. 509 p.
- Mertanen, S., Pajunen, M. & Elminen, T. 2001.** Applying palaeomagnetic method for dating young geological events. In: Autio, S. (ed.) Geological Survey of Finland, Current Research 1999–2000. Geological Survey of Finland, Special Paper 31, 123–129.
- Mertanen, S., Pajunen, M. & Elminen, T. 2004.** Multiple remagnetization events of shear zones in southern Finland. In: Mertanen, S. (ed.) Supercontinents, remagnetizations and geomagnetic modelling. 5th Nordic Paleomagnetic Workshop, Suitia-Helsinki, Finland, September 25–30, 2004, 39–44.
- Mouri, H., Korsman, K. & Huhma, H. 1999.** Tectono-metamorphic evolution and timing of the melting processes in the Svecofennian tonalite-trondhjemite migmatite belt: An example from Luopioinen, Tampere area, southern Finland. Bulletin of the Geological Society of Finland 71, 31–56.

- National Research Council 1996.** Rock fractures and fluid flow. Washington, D.C: National Academy Press. 551 p.
- Nironen, M. 1989.** Emplacement and structural setting of granitoids in the early Proterozoic Tampere and Savo Schist Belts, Finland – implications for contrasting crustal evolution. Geological Survey of Finland, Bulletin 346. 83 p.
- Nironen, M. 1997.** The Svecofennian Orogen: a tectonic model. *Precambrian Research* 86 (1–2), 21–44.
- Nurmi, H., Sipilä, P. & Vuokko, J. 2001.** Occurrence and quality variations of rock aggregates in Finland. Aggregate 2001, Helsinki, Finland 6–10 August 2001, vol. 1, 55–57.
- Pajunen, M. 1986.** Deformation analysis of cataclastic structures and faults in the Tervo area, central Finland. Geological Survey of Finland, Bulletin 339, 16–31.
- Pajunen, M. 1988.** Tectono-metamorphic evolution of the Hallaperä pyrrhotite-pyrite ore deposit, Central Finland. Geological Survey of Finland, Bulletin 343, 51–76.
- Pajunen, M. & Poutiainen, M. 1999.** Palaeoproterozoic prograde metasomatic-metamorphic overprint zones in Archaean tonalitic gneisses, eastern Finland. *Bulletin of the Geological Society of Finland* 71, 73–132.
- Pajunen, M., Airo, M.-L., Wennerström, M., Niemelä, R. & Wasenius, P. 2001a.** Preliminary report: The “Shear zone research and rock engineering” project, Pori area, south-western Finland. Geological Survey of Finland, Special Paper 31, 7–16.
- Pajunen, M., Elminen, T., Airo, M.-L. & Wennerström, M. 2001b.** Structural evolution of bedrock as a key to rock mechanical properties. In *Rock Mechanics. A Challenge for Society. Proceeding of Regional Symposium EUROCK 2001*. Rotterdam: A. A. Balkema. 143–148.
- Pajunen, M., Airo, M.-L., Elminen, T., Niemelä, R. J., Vaarma, M., Wasenius, P. & Wennerström, M. 2002a.** Kallioperän rakennettavuusmalli taajamiin. Menetelmänkehitys ja ohjeistus. Raportti I. Geological Survey of Finland, unpublished report K.21.42/2002/5. 95 p. (in Finnish)
- Pajunen, M., Airo, M.-L., Elminen, T., Niemelä, R., Salmelainen, J., Vaarma, M., Wasenius, P. & Wennerström, M. 2002b.** Rakennettavuuskartan selitys. ”Kallioperän rakennettavuusmalli taajamiin” -projekti. Raportti II. Geological Survey of Finland, unpublished report K.21.42/2002/4. 42 p. (in Finnish)
- Pajunen, M., Airo, M.-L., Elminen, T., Niemelä, R., Salmelainen, J., Vaarma, M., Wasenius, P. & Wennerström, M. 2002c.** Projekti pähkinänkuoressa. ”Kallioperän rakennettavuusmalli taajamiin” -projekti. Raportti III. Geological Survey of Finland, unpublished report K.21.42/2002/4. 28 p. (in Finnish)
- Pajunen, M., Airo, M.-L., Elminen, T., Niemelä, R., Salmelainen, J., Vaarma, M., Wasenius, P. & Wennerström, M. 2002d.** Kallioperän rakennettavuuskartta 1:50 000 – Espoo, Helsinki, Vantaa. ”Kallioperän rakennettavuusmalli taajamiin” – projekti. Geological Survey of Finland, unpublished report K.21.42/2002/7. (in Finnish)
- Pajunen, M., Elminen, T., Airo, M.-L. & Wennerström, M. 2004.** Structural evolution of Svecofennian crust in southern Finland. The 26th Nordic Geological Winter Meeting, January 6th–9th 2004, Uppsala Sweden. *GFF* 126, (1), 32–33.
- Park, A. F., Bowes, D. R., Halden, N. M. & Koistinen, T. J. 1984.** Tectonic evolution at an early Proterozoic continental margin: the Svecofennian of eastern Finland. *Journal of Geodynamics* 1 (3–5), 359–386.
- Parkkinen, J. 1975.** Deformation analysis of a Precambrian mafic intrusive, Haukivesi area, Finland. Geological Survey of Finland, Bulletin 278. 61 p.
- Paulamäki, S., Paananen, M., Gehör, S., Kärki, A., Front, K., Aaltonen, I., Ahokas, T., Kemppainen, K., Mattila, J. & Wikström, L. 2006.** Geological model of the Olkiluoto Site, Version O. Posiva Oy, Working Report 2007–37. 355 p.
- Pietikäinen, K. 1994.** The geology of the Paleoproterozoic Pori shear zone, southwestern Finland, with special reference to the evolution of veined gneisses from tonalitic protoliths. PhD thesis, Michigan Technological University. 130 p.
- Ploegsma, M. 1989.** Shear zones in the West Uusimaa area, SW Finland. Amsterdam: Vrije Universiteit. 134 p.
- Posiva Oy 2005.** Olkiluoto site description. Report May 2005. Posiva Oy, POSIVA 2005–03. 444 p.
- Roinisto, J. (ed.) 1986.** Kalliorakentaminen Suomessa. Rakentajain kustannus, Maanalaisten tilojen rakentamisyhdistys r.y. Jyväskylä: Gummerus Oy. 190 p.
- Rönkä, K. & Ritola, J. (eds.) 1997.** Kalliorakentamisen neljäs aalto: ympäristövastuullinen maanalainen rakentaminen, suunnittelu ja toteutus. MTR (Maanalaisten tilojen rakentamisyhdistys r.y.), VTT (Valtion teknillinen tutkimuskeskus, yhdyskuntateknikka). Porvoo: WSOY. 137 p.
- Rutland, R. W. R., Williams, I. S. & Korsman, K. 2004.** Pre-1.91 Ga deformation and metamorphism in the Paleoproterozoic Vammala Migmatite Belt, southern Finland, and implications for Svecofennian tectonics. *Bulletin of the Geological Society of Finland* 76, 93–140.
- Selonen, O. & Suominen, V. (eds.) 2003.** Nordic stone. Paris: UNESCO, IAEG. 64 p.
- Suominen, V. 1991.** The chronostratigraphy of southwestern Finland with special reference to Postjotnian and Subjotnian diabases. Geological Survey of Finland, Bulletin 356. 100 p.
- Talvitie, J. 1971.** Seismotectonics of the Kuopio region, Finland. *Bulletin de la Commission Géologique de Finlande* 248. 41 p.
- Tarkkala, J. 2004.** Helsingin maanalaisten toimintojen osayleiskaava, suunnitteluohjelma. Helsingin kaupunkisuunnitteluviraston yleissuunnitteluosaston selvityksiä 2004:8. Helsingin kaupunki. (in Finnish)
- Tuisku, P. & Laajoki, K. 1990.** Metamorphic and structural evolution of the Early Proterozoic Puolankajärvi formation, Finland – II. The pressure-temperature-deformation-composition path. *J. Metamorphic Geol.* 8, 375–391.

- Vaasjoki, M. 1977a.** Rapakivi granites and other post-orogenic rocks in Finland: their age and the lead isotopic composition of certain associated galena mineralizations. Geological Survey of Finland, Bulletin 294. 64 p.
- Vaasjoki, M. 1977b.** Phanerozoic resetting of U- Pb ages in some South-Finnish uraninites. In: ECOG V. Fifth European Colloquium of Geochronology, Cosmochronology and Isotope Geology, Pisa, September 5.10, 1977. 2 p.
- Vaasjoki, M. 1995.** Rengon Rouvinmäen kvartsimont-sodioriitti: uusi posttektoninen granitoidi. Summary: The Rouvinmäki quartzmonzodiorite at Renko: a new posttectonic granitoid. *Geologi* 47 (6), 79–81.
- Vaasjoki, M. & Sakko, M. 1988.** The evolution of the Raahe-Ladoga zone in Finland: isotopic constraints. Geological Survey of Finland, Bulletin 343, 7–32.
- Väisänen, M. 2002.** Tectonic evolution of the palaeoproterozoic Svecofennian orogen in Southwestern Finland. *Annales Universitatis Turkuensis, A II*, 154. 143 p.
- Väisänen, M. & Hölttä, P. 1999.** Structural and metamorphic evolution of the Turku migmatite complex, southwestern Finland. *Bulletin of the Geological Society of Finland* 71, 177–218.
- Väisänen, M., Mänttari, I. & Hölttä, P. 2002.** Svecofennian magmatic and metamorphic evolution in southern Finland as revealed by U-Pb zircon SIMS geochronology. *Precambrian Research* 116, 111–127.
- Väisänen, M., Andersson, U. B., Huhma, H. & Mouri, H. 2004.** Age of late Svecofennian regional metamorphism in southern Finland and south-central Sweden. The 26th Nordic Geological Winter Meeting, January 6th–9th 2004, Uppsala, Sweden. Abstract volume. GFF 126, 40.
- Wegmann, C. E. 1928.** Über die Tektonik der jüngeren Faltung in Ostfinnland. *Fennia* 50, 1–22.
- Wennerström, M., Airo, M.-L., Elminen, T., Pajunen, M. & Salmelainen, J. 2006.** Structural evolution of the crust as a means of determining the technical properties of bedrock in the Helsinki capital region. In: Proceedings of the IAEG2006 Congress of 'Engineering geology for tomorrow's cities'. Nottingham, United kingdom, 6–10 September 2006. Paper number 86. 9 p.

TECTONIC EVOLUTION OF THE SVECOFENNIAN CRUST IN SOUTHERN FINLAND

by

*Matti Pajunen**, *Meri-Liisa Airo*, *Tuija Elminen*, *Irmeli Mänttari*, *Reijo Niemelä*, *Markus Vaarma*, *Pekka Wasenius* and *Marit Wennerström*

Pajunen, M., Airo, M.-L., Elminen, T., Mänttari, I., Niemelä, R., Vaarma, M., Wasenius, P. & Wennerström, M. 2008. Tectonic evolution of the Svecofennian crust in southern Finland. *Geological Survey of Finland, Special Paper 47*, 15–160, 53 figures, 1 table and 9 appendices.

The present-day constitution of the c. 1.9–1.8 Ga old Svecofennian crust in southern Finland shows the result of a complex collision of arc terranes against the Archaean continent. The purpose of this study is to describe structural, metamorphic and magmatic succession in the southernmost part of the Svecofennian domain in Finland, in the Helsinki area. Correlations are also carried out with the Pori reference area in southwestern Finland. A new tectonic model on the evolution of the southern Svecofennian domain is presented. The interpretation is based on field analyses of structural successions and magmatic and metamorphic events, and on interpretation of the kinematics of the structures. The structural successions are linked to new TIMS and SIMS analyses performed on eight samples and to published age data.

The Svecofennian structural succession in the study area is divided into deformation phases D_A - D_1 ; the post-Svecofennian events are combined as a D_p phase. Kinematics in the progressively-deforming transtensional or transpressional belts complicates analysis of the overprinting relations due to their simultaneous contractional and extensional structures. In this work the Svecofennian structural succession in the study area is related to major geotectonic Events 1–5, E_1 - E_5 , on the basis of their characteristic kinematics and tectono-metamorphic and magmatic features.

Geotectonic event E_1 includes the D_A deformation (corresponding to the D_1 in the northern Svecofennian units) that deformed the oldest supracrustal sequences, including volcanic Series I. The horizontal D_A structures formed during c. N-S shortening. Event 1 is suggested as an early major thrusting deformation at c. 1.9–1.88 Ga ago. The crust thickened and crustal slices from different depths, and geotectonic and depositional environments, were juxtaposed.

Geotectonic event E_2 includes the D_B deformation (D_2 in the north). It is related to a crustal extension that caused a strong vertical shortening and prograde low-pressure (andalusite-sillimanite type) metamorphism. Extension is related to an island arc collapse; this collapse did not occur in the Archaean domain. The younger volcanic Series II evolved during the collapse and is proposed to represent intra-arc volcanism. Large amounts of syn-/late D_B intermediate igneous rocks were also emplaced. E_2 shows diachronic evolution, getting younger towards south; the age of E_2 in the south is c. 1.88–1.87 Ga.

The E_2 extension was rapidly followed by a N-S shortening event, E_3 , that formed the contractional D_C structures (D_3 in the north) in the south at c. 1.87 Ga; E_3 was also a diachronic event. According to the structure and age correlations, the northern Svecofennian units already underwent E_3 contraction during the southern E_2 extensional stage. This supposes that the crust as a whole was under a compressional regime and that E_2 was a southwards-migrating localized event. In the Archaean continent and close to its border zone, the escape of crustal blocks towards the NNW-NNE occurred; movements occurred along the old Archaean or pre-collisional Proterozoic N-S-trending shear zones. After E_3 the Svecofennian and Archaean domains formed a coherent continent and, therefore, the later geotectonic events occurred in this new continental crust.

Geotectonic event E_4 deformed the new continental crust and is in the south predominantly connected to the evolution of the Southern Finland Granitoid Zone (SFGZ). The E_3 N-S stress field rotated into a SW-NE orientation. The pre-SFGZ crust in the south is characterized by the D_{C+D} dome-and-basin interferences formed at c. 1.87 Ga due to the SW-NE transpressional deformation D_D (D_4 in the north). At that time, in the northern units, the wide-scale oblique contractional folding, eastwards transport and clockwise rotation of crustal blocks occurred. The deformation pattern of crustal blocks, like the Pomarkku and Vaasa blocks during D_4 (D_D in the south) and the Central Finland block during D_F at c. 1.86–1.85 Ga, as well as related shear zone patterns, are interpreted as a product of escape tectonics related to the SW-NE transpression. Simultaneously with the termination of the D_4 deformation in the north at 1868 ± 3 Ma, evolution of the Southern Finland Granitoid Zone (SFGZ) was initiated by the early D_E tonalites in the south. The SFGZ shows a very complex pattern of D_E , D_F , D_G and D_H structures that formed in kinematics representing different local stress fields. Intense intermediate to felsic D_E magmatism occurred in the oblique SE-extensional zones between the active N-trending deformation zones, the Baltic Sea-Bothnian Bay Zone (BBZ), Riga Bay Karelia Zone (RKZ) and the Transscandinavian Igneous Belt (TIB). In the erosion level, progressive extensional evolution led to the development of the pull-part basins with supracrustal sequences exemplified by the Jokela supracrustal association. The peak of D_E extensional evolution is represented by gabbro intrusions at c. 1.84 Ga; this mafic and intense intermediate magmatism may be related to the volcanism in the pull-apart basins. The Porkkala-Mäntsälä shear/fault zone and the wide-scale F_G folding are results of a short-lasting N-S shortening D_G at c. 1.85 Ga. In southern Finland the late E_4 evolution, from c. 1.84 to 1.80 Ga, is characterized by SE-NW transpression during D_H . Sinistral movements in the N-trending shear zones, like the Vuosaari-Korso shear/fault zone, oblique dextral movements in the E-W-trending Hyvinkää and Southern Finland shear/fault zones, oblique contractional D_H folds and the oblique extensional or spot-like granites and diabase dykes resulted. The localized D_E SE-NW extension in the SFGZ turned to SE-NW transpression due to rotation of the zone under an overall SW-NE transpression between the major N-trending deformation zones, the Baltic Sea-Bothnian Bay Zone (BBZ), Riga Bay-Karelia Zone (RKZ) and Transscandinavian Igneous Belt (TIB).

The evolution of the major N-trending D_1 deformation zones, the BBZ, RKZ and TIB, already started during the D_D deformation, but their latest phase, related here to the E_5 , deformed the Southern Finland Granitoid Zone (SFGZ) and the E-W-trending shear zones. The D_{G+H+I} dome-and-basin interferences determining the present exposition of the geotectonic and metamorphic units were formed. The youngest dated Svecofennian rock in the study area is a <1.8 Ga old amphibolite facies diabase dyke, which confines the fade of the Svecofennian orogeny in southernmost Finland.

The post-Svecofennian deformations and magmatic events, included here as a combined D_p , are strongly controlled by the older Svecofennian structures. In the study area the c. 1.65 Ga Bodom and Obbnäs rapakivi granite magmas were channelled by the intersections of the major Svecofennian crustal shear structures, like the southern Finland, Porkkala-Mäntsälä and the D_1 shear zones/faults, and the low-angle structures like the $S_{E/H}$ foliation planes controlled their emplacement. On a wider scale, rapakivis are located in close association with the major Svecofennian D_1 deformation zones such as the Baltic Sea-Bothnian Bay Zone (BBZ) and Riga Bay-Karelia Zone (RKZ).

Tectonic and kinematic analysis combined with the tectonically-fixed age data on magmatic events establishes that the Svecofennian orogeny was a continuous diachronic event getting younger towards the south/southwest. The Svecofennian island arc system collided obliquely against the Archaean continent simultaneously with the growth of an island arc. The Svecofennian arc components were accreted to the Archaean continent to form a new continental crust. The continent was deformed during the continued transpressional orogen into major crustal blocks that transported and rotated with simultaneously formed extensional zones – e.g. the pull-apart basins and granitoid zones – and strike slip terranes. The tectonic pattern is characteristic for terranes formed by escape tectonics.

In summary, the tectonic evolution of the Svecofennian orogeny is related to one oblique collision of the active, growing Svecofennian island arc system against the Archaean continent, and to subsequent transpressional continental deformation characterized by escape tectonics.

Key words (GeoRef Thesaurus, AGI): crust, tectonics, structural geology, structural analysis, deformation, folds, shear zones, Svecofennian Domain, Proterozoic, Paleoproterozoic, Uusimaa, Southern Finland

* *Geological Survey of Finland, P.O. Box 96, FI-02151 Espoo, Finland*

* *E-mail: matti.pajunen@gtk.fi*

INTRODUCTION

At the very beginning of last century, J. J. Sederholm (1907, 1923, 1926, compiled works in 1967), the architect of modern geological research and mapping in Finland (e.g. Scheinin & Korsman 2007), described with amazing accuracy the 1.9–1.8 Ga Svecofennian supracrustal sequences and migmatites (interpreted as Archaean at his time) in the southernmost part of the country. His main emphasis was on structures and the genesis of migmatites, melting and granitization in the deeper crustal levels. Sederholm (1926) carefully analysed the relationships between different magmatic and migmatization events. For example, mafic dykes intruded into the brittle fractures of Hanko-Inkoo granite, and both the granite and dyke were migmatized by a later granitic event, thus confirming the polyphase tectono-thermal evolution of the crust. The observation definitely evidences that there was a cooling stage between the two granitic events; this discordance was later re-established, for instance, by Pajunen et al. (2008). In the southern Svecofennian domain, Korsman et al. (1984) described a tectono-metamorphic discordance (geosuture in Korsman et al. 1988) between the northern Tonalite Migmatite Belt (TMB) and the southern Granite Migmatite Belt (GMB) (Figure 1). These kinds of discordances, combined with kinematic and thermal data, have a great importance in constructing crustal evolution models. Several models of the history of Svecofennian evolution have been developed since the first plate tectonic model of Hietanen (1975). These accretion and collision-extension models (e.g. Koistinen 1981, Edelman & Jaanus-Järkkälä 1983, Gaál & Gorbachev 1987, Ekdahl 1993, Korja et al. 1993, Lahtinen 1994, Ruotoistenmäki 1996, Nironen 1997, Kilpeläinen 1998, Korsman et al. 1999, Väisänen 2002, Pajunen et al. 2002, 2004 and Lahtinen et al. 2005), accompanied with considerable age data (e.g. Patchett et al. 1981, Huhma 1986, Vaasjoki & Sakko 1988 and Suominen 1991), are a good basis for further research on Svecofennian evolution. Unfortunately, the interesting results of the Finnish Reflection Experiment FIRE 2001–2005 (Kukkonen & Lahtinen 2006) were published too late to be discussed in details here.

In the northern Tonalite Migmatite Belt (TMB) the crust was largely stabilized at 1.88 Ga ago, whereas in the southern Granite Migmatite Belt (GMB) the thermal peak was achieved c. 50 Ma later (Korsman et al. 1984 and 1999). The differences in timing of thermal and deformation events, and the depth of concurrent deformations between the units (e.g. Kilpeläinen 1998), have a crucial bearing on characters of concomitant tectonic struc-

tures in these regions. While ductile deformation occurred in the south, the northern units behaved in a more rigid and brittle way (Pajunen et al. 2001b). Recently, more reasonable information on the semi-brittle to brittle structures has been needed, because society has increased the requirements for geological information. Especially the analysis of semi-ductile to brittle structural data has prime importance for several applications. The late Svecofennian ductile to semi-ductile tectonic events are important for the present-day arrangement of tectonic units and distribution of lithologies, but are only seldom described (Ehlers et al. 1993, Pietikäinen 1994 and Pajunen et al. 2001a). How the Svecofennian structures influenced the post-Svecofennian geotectonic structures, like the extension-related rapakivi magmatism at c. 1.65–1.57 Ga ago (Vaasjoki 1977a, Rämö 1991, Korja & Heikkinen 1995, Kosunen 2004 and Haapala et al. 2005), the subsequent formation of the sandstone basin (Kohonen et al. 1993) and related mafic magmatism at 1.25 Ga in the Pori area, or the Caledonian or even post-glacial events, is still an open question.

The aim of this paper is to explain how tectonic, magmatic and thermal evolution yielded the present configuration of rock types and structures in the study area in the surroundings of Helsinki (Figure 1). The results presented in a preceding unpublished report by Pajunen et al. (2002) showed that tectono-metamorphic and magmatic evolution in southernmost Finland is more complicated than can be summarized from the earlier studies. There are several reasons for this complexity, for example: 1) the tectono-thermal events and their products cover the whole time-scale of Svecofennian history, from 1.9 to 1.8 Ga; the crust was strongly modified during the anorogenic rapakivi-stage c. 1.65–1.54 Ga ago (Vaasjoki 1977a, Korsman et al. 1997 and Haapala et al. 2005) and later Mesoproterozoic extension and magmatism 1.25 Ga ago (Kohonen et al. 1993); some reactivation occurred during the Caledonian orogeny c. 450 Ma ago (Vaasjoki 1977b and Mertanen et al. 2008) and even the post-glacial time (Kuivamäki et al. 1998), 2) the bedrock is characterized by a complex polyphase tectonic history (e.g. Laitala 1973a, Hopgood 1984 and Pajunen et al. 2008) that caused strong fragmentation and reorganization of the various tectonic units, 3) the thermal state and rigidity of different units varied during the concomitant deformation, causing differing kinematic behaviour and deformation patterns that are difficult to correlate between the separate units, 4) several metamorphic mineral growth stages (e.g. Korsman et al. 1984, 1999 and Kilpeläinen 1998),

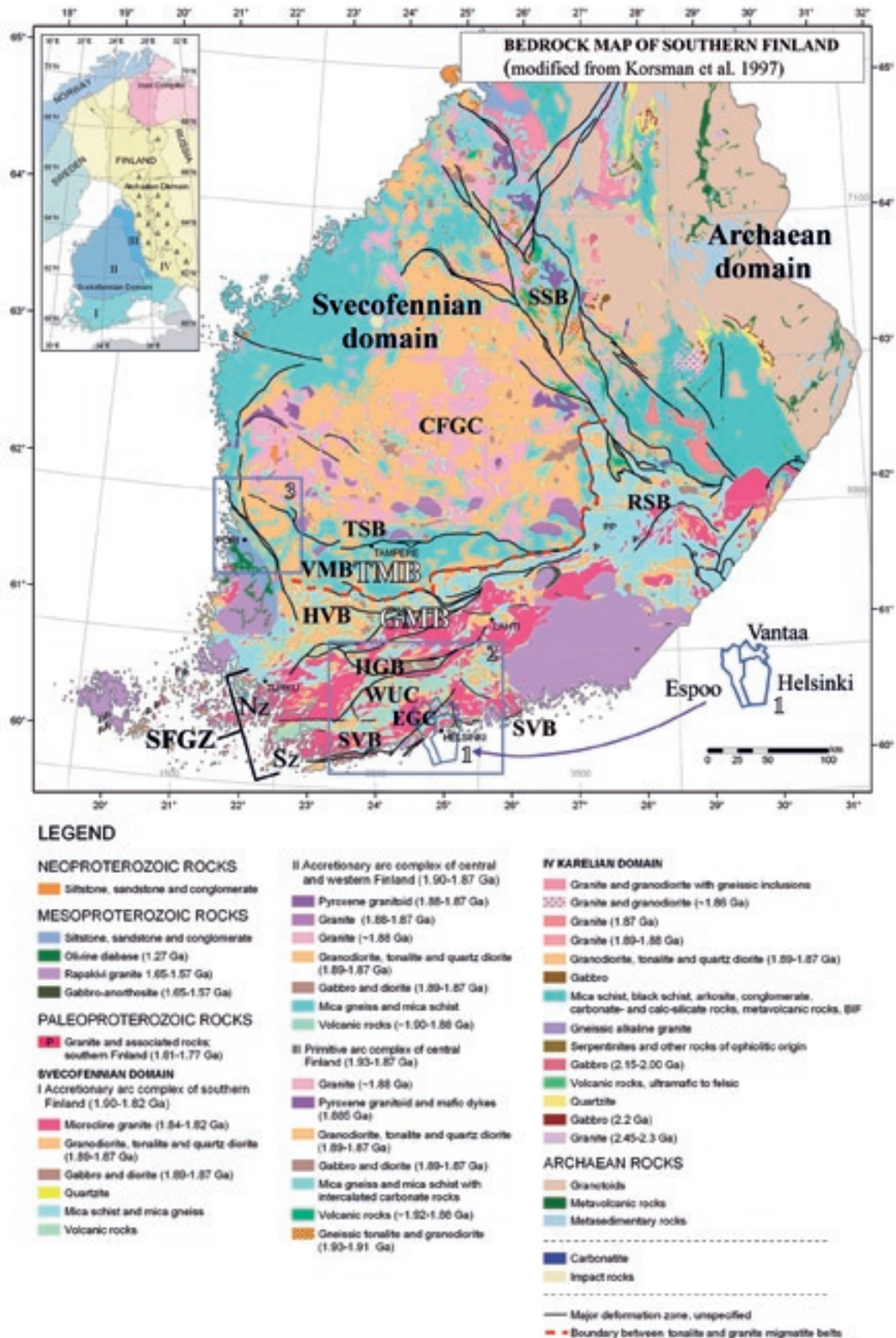


Figure 1. The study areas on the geological map of Finland (Korsman et al. 1997): 1. Detailed study area in Espoo, Helsinki and Vantaa; 2. Study area for the observations on key outcrops and interpretation of the pre-existing data; and 3. Pori reference area (Pajunen et al. 2001a). Abbreviations: GMB = Granite Migmatite Belt (I in inset), TMB = Tonalite Migmatite belt (II in inset), SSB = Savo Schist Belt (III in inset), Karelian unit (IV in inset), RSB = Rantasalmi-Sulkava area, VMB = Vammala Migmatite Belt, TSB = Tampere Schist Belt, HVB = Häme Volcanic Belt, HGB = Hyvinkää Gabbroic-volcanic Belt, WUC = West Uusimaa Complex, SVB = Southern Volcanic-sedimentary Belt, CFGC = Central Finland Granitoid Complex, SFGZ = Southern Finland Granitoid Zone, northern zone of the SFGZ = Nz, southern zone of the SFGZ = Sz and EGC = Espoo Granitoid Complex. Base map © National Land Survey of Finland, permit No. 13/MML/08.

strong melting and granitization (e.g. Härme 1965), have often destroyed the earlier structures and effectively obscure the preceding metamorphic signatures, 5) primary supracrustal features are largely destroyed and the stratigraphic interpretations generally justify only tectonic stratigraphy of variable crustal slices, and 6) isotopic information on early events is sometimes difficult to obtain due to later higher-grade overprint, inheritance or rejuvenation.

Analysis of tectonic evolution of the southern Svecofennian domain is based on detailed field observations on structures in the study area; much weight will be put on descriptions of structures in the field. The descriptions and interpretations focus predominantly on the Granite Migmatite Belt (GMB) in Espoo, Helsinki and Vantaa (Figure 1, area 1). In understanding regional Svecofennian evolution in the southernmost part of Finland, it was also necessary to carry out some studies and correlations outside the detailed area (Figure 1, area 2). Some revision of the early observations of Pajunen et al. (2001a) was also made in the Tonalite Migmatite Belt (TMB) in the Pori area (Figure 1, area 3). Some characteristic structures in the study area are impossible to analyze without considering a wider, Fennoscandian context. Supporting interpretations outside the detailed study area are separately described in Appendices 1–7. The structural model is fixed with some new TIMS and SIMS age data on the key rocks (Appendix 8). Figures in the Appendices are referred to in the main text in the form Appendix-Fig. 1-1a (Figure 1a in Appendix 1); the

main text Figures are referred to in the Appendices correspondingly to the main text. Tables in appendices are named as App-Table 1–4. Postulations on how the southern Svecofennian structures controlled post-Svecofennian deformation, especially during the Palaeoproterozoic-Mesoproterozoic rapakivi event, are briefly discussed.

The results represented here are based on projects organized by the Geological Survey of Finland (GTK): 1) “Construction potential modelling of bedrock in urban areas” during 1999–2002 near Helsinki in southernmost Finland (Pajunen et al. 2001b and preliminary report, Pajunen et al. 2002), with field revision during the field seasons 2003 and 2004; 2) “Shear/fault zone research and rock engineering”, which was carried out in 1998–1999 in the Pori area in western Finland (Pajunen et al. 2001a), where some revision was made in 2006–2007 by the “Bedrock stress field in Satakunta/GeoSatakunta” project.

M. Pajunen takes the full responsibility for the geological interpretations presented in this paper. M.-L. Airo modified and interpreted the geophysical data and constructed the cross-sections (cf. Airo et al. 2008). T. Elminen and M. Wennerström interpreted the semi-brittle to brittle structures that are discussed in more detail in Elminen et al. (2008) and Wennerström et al. (2008). M. Pajunen, T. Elminen, M. Wennerström, Vaarma, R. Niemelä and P. Wasenius took part in the regional and thematic mapping necessary for this analysis. I. Mänttari performed the U-Pb age determinations.

GEOLOGICAL OUTLINE

Svecofennian evolution

The Palaeoproterozoic 1.9–1.8 Ga Svecofennian domain is situated in the central part of the Fennoscandian Shield area (Koistinen et al. 2001). According to refraction seismic studies (e.g. Luosto et al. 1990, Grad & Luosto 1992 and Korsman et al. 1999), the crust in southernmost Finland is c. 48–50 km thick. In the central and eastern parts of the Svecofennian domain, in the Proterozoic-Archaeon border zone, it is considerably thicker, up to 65 km. The reflection seismic data of FIRE (Kukkonen & Lahtinen 2006) and BABEL (Korja & Heikkinen 1995 and 2005) indicate a layered crust with wide-scale, low-angle tectonic structures characterizing large areas in central and southern Finland.

The complex collision of the Svecofennian units against the Archaean domain occurred along a suture zone at 1.90–1.88 Ga (e.g. Wegmann 1928,

Koistinen 1981, Lahtinen 1994 and Korsman et al. 1999). The suture is verified by remnants of a c. 1.95 Ga oceanic crust (Kontinen 1987) and turbiditic sediments (area IV in inset in Figure 1) that was overthrust towards the NNE over the Archaean continent (Koistinen 1981). The effects of Svecofennian tectonic activity extended far northeast of the suture zone (e.g. Kontinen et al. 1992 and Pajunen & Poutiainen 1999). Pajunen and Poutiainen (1999) identified two Svecofennian tectono-thermal overprinting events in the Archaean domain. The first event was related to barrowian-type (kyanite-staurolite) heating after collision at c. 1.90 Ga and the later one to c. 1.85 Ga dilatational fluid activity (Mg-metasomatism in sillimanite stability field) and magmatism. The later event was caused by magmatic underplating, resulting in the thick crust of the area (cf. Luosto et al. 1990, Korja et al. 1993 and Korsman et al. 1999). The U-Pb zircon ages in mafic

granulite xenoliths from the lower crust in kimberlites in eastern Finland evidence high temperatures in the lower crust still occurring c. 1.80–1.73 Ga ago (Hölttä et al. 2000 and Peltonen et al. 2006).

The Svecofennian domain consists of juvenile (Huhma 1986) crust showing increasing maturity of island arcs towards south and west. The NW-SE trending Savo Schist Belt (SSB, the Pyhäsalmi primitive island arc, c. 1.93–1.91 Ga) borders the Archaean unit. In the southern and western part of the Svecofennian domain, more mature island arc belts, like the Tampere Schist Belt (TSB, c. 1.9–1.89 Ga) and the Häme Volcanic Belt (HVB) (Kähkönen 1989, Lahtinen 1994 and Hakkarainen 1994), are located. The volcanic sequences (c. 1.90–1.87 Ga) in the Orijärvi area of the Southern Volcanic-sedimentary Belt (SVB) show back-arc basin geochemical characteristics (Väisänen & Mänttari 2002). Laitala (1973a) described the structures in the volcanic series (c. 1.89 Ga) in the eastern part of the belt in Pellinki. The Hyvinkää Gabbroic-volcanic Belt (HGB) shows several large, c. 1.88 Ga gabbro intrusions (Patchett et al. 1981) in a volcanic environment (Härme 1978). Wide areas between the volcanic units are characterized by predominantly migmatized pelitic to psammitic rocks. In the southernmost Svecofennian domain, near the coast and in the archipelago, the volcanic rocks are felsic to mafic, sometimes with well-preserved pillow lava structures. Layers of carbonate rocks and silicate-facies iron formations indicate a shallow-marine depositional environment of the sediments (e.g. Ehlers & Lindroos 1990). Carbonate rocks and pillow lavas diminish northwards and volcanism changes to intermediate, pyroclastic and epiclastic (Kähkönen 1987). Sedimentary rocks deposited in deep water with intermediate to mafic volcanic rocks dominate further north in the Tonalite Migmatite Belt (TMB) (Korsman et al. 1984 and Kähkönen 1987). The majority of these supracrustal rocks were deposited at c. 1.9 Ga during the earliest stage of Svecofennian evolution (Huhma et al. 1991), but some, like the Tiirismaa quartzite near Lahti (Lehijärvi 1964), have younger zircons indicating deposition after 1.87–1.86 Ga (Lahtinen et al. 2002).

Several pulses of magmatic rocks representing different tectono-magmatic settings intrude the supracrustal sequences. Sederholm (1932a) divided the intrusive rocks in Finland into four groups that essentially still represent a helpful basis for classification: I – synorogenic mafic to felsic intrusive rocks (c. 1.89–1.87 Ga); II – late-orogenic felsic intrusive rocks (c. 1.84–1.81 Ga); III – post-orogenic granites and mafic dykes (c. 1.80–1.77 Ga); IV – anorogenic rapakivi granites and related intrusive rocks (c. 1.65–1.57 Ga) (cf. Vaasjoki 1977a, Nurmi

& Haapala 1986 and Suominen 1991). The Central Finland Granitoid Complex (CFGC) is a coherent area of predominantly felsic granitoids with narrow zones of supracrustal rocks (Korsman et al. 1997). The CFGC shows a two-stage magmatic history: the older syntectonic plutonic pulse is c. 1.89–1.88 Ga in age and the later late/post-orogenic granitoids are c. 1.88–1.87 Ga old (Nironen 2003). A crustal component older than 1.92 Ga in the CFGC (e.g. Lahtinen & Huhma 1997) is postulated by Lahtinen et al. (2005) as the signature of an unexposed early microcontinent. A large amount of late-orogenic granites are exposed in a c. 100 km wide ENE-WSW-trending zone along the coast of the Gulf of Finland, in the southernmost Svecofennian area (Sederholm 1932a and Korsman et al. 1997), which is named Southern Finland Granitoid Zone (SFGZ). Related granitic rocks also cut the Archaean crust in eastern Finland; Sm-Nd data demonstrate Archaean contamination in these granitoids (Huhma 1986). Corresponding granitic units also exist in Sweden and northern Estonia (Koistinen et al. 1996 and 2001). Rämö et al. (2004) found variations in the Sm-Nd isotopic compositions in the late-orogenic granites between the northern (Nz in Figure 1) and southern zones (Sz in Figure 1) of the SFGZ. The c. 1.80–1.79 Ga old (Suominen 1991 and Vaasjoki 1995) post-tectonic granite intrusions locally caused metamorphic contact aureoles into the Granite Migmatite Zone (GMB) country rocks (Rastas 1990).

The tectono-metamorphic discordance between the Tonalite Migmatite Belt (TMB) and the Granite Migmatite Belt (GMB) (Korsman et al. 1984) forms a rather sharp boundary zone (Koistinen et al. 1996 and Korsman et al. 1999); Korsman et al. (1988) proposed that it represents a geosuture between the belts. The Rantasalmi-Sulkava area (RSB) was overthrust towards north upon the Savo Schist Belt (SSB). In spite of the differences in crustal structure, the pressure estimates representing the Svecofennian peak metamorphic conditions are consistently around 5 kbar in the whole Svecofennian area (Korsman et al. 1999), and even in the Archaean domain (Tuisku & Laajoki 1990 and Pajunen & Poutiainen 1999).

The high-T/low-p (andalusite-sillimanite-type) metamorphism in the Savo Schist Belt (SSB) was connected to the c. 1.89–1.88 Ga magmatic activity. The crust stabilized soon after emplacement of 1884 ± 5 Ma pyroxene-bearing granitoids. The contact metamorphism generated by these rocks overprints the regional metamorphism (e.g. Korsman et al. 1984, Hölttä 1988, Hölttä et al. 1988 and Hölttä & Pajunen 1988). In western Finland, corresponding post-tectonic pyroxene-bearing granitoids are younger, c. 1.87 Ga (Mäkitie & Lahti 2001). In the tectono-metamorphic model of Korsman et al. (1999), based on the

refraction seismic structure of the crust (Luosto et al. 1984), magmatic underplating was proposed as the main source of crustal heat flow and the reason for the invariable pressure estimates. Pajunen and Poutiainen (1999) also supported the idea of lower-crustal disturbance as a heat source for the 1.85 Ga tectono-thermal process in the Archaean domain.

In the Rantasalmi-Sulkava area (RSB) of the Granite Migmatite Belt (GMB), penetrative tectonic, metamorphic and magmatic processes peaked c. 1.82–1.81 Ga ago (Korsman et al. 1984, 1988 and 1999). However, in the southern Savo Schist Belt (SSB) c. 1.84 Ga lamprophyre dykes intruded into an already cooled crust (Neuvonen et al. 1981). In the RSB the high-T/low-p metamorphism shows prograde zoning from andalusite stability in the north to granulite facies migmatitic garnet-cordierite gneisses in the south (Korsman 1977 and Korsman et al. 1984). However, the intrusion age of a pyroxene-bearing granitoid in the Granite Migmatite Belt (GMB) in the Turku area is 1878 ± 19 Ma (Väisänen et al. 2002), and the results of Hopgood et al. (1983) indicate that there was an earlier, c. 1.88–1.87 Ga, tectono-metamorphic event in the GMB.

Several models for the metamorphic evolution in the GMB have been proposed. An early interpretation of Korsman (1977) explained the progressive metamorphic zoning in the Rantasalmi-Sulkava area (RSB) as due to crustal thickening. Schreurs and Westra (1986) connected the granulite facies metamorphism in the West Uusimaa granulite Complex (WUC, cf. Parras 1958) to CO₂ influx. Väisänen (2002), on the other hand, proposed that the high heat flow in the granulite area in Turku (Väisänen & Hölttä 1999) was caused by crustal collapse (cf. model of Platt & England 1993). Ehlers et al. (1993) interpreted the late-orogenic granite magmatism in the Southern Finland Granitoid Zone (SFGZ) as syntectonic with SE-NW transpression at c. 1.84–1.81 Ga. According to Puura et al. (2004), further south in Estonia the ages of 1778 ± 2 Ma for mona-

zite and 1728 ± 24 Ma for garnet in high-grade gneisses refer to still later events or cooling than in southern Finland.

Post-Svecofennian events

The late Palaeo- to Mesoproterozoic rapakivi stage (group IV of Sederholm 1932a) is the latest major tectono-magmatic event producing great amounts of mafic and granitic rocks (e.g. Sederholm 1932a, Rämö 1991, Heeremans 1997, Kosunen 2004 and Haapala et al. 2005). The rocks of the rapakivi suite are younger in western Finland (1.59–1.54 Ga) and in Russian Karelia (1.5–1.3 Ga) than in the detailed study area near Helsinki (1.67–1.62 Ga) (Vaasjoki 1977a and Haapala et al. 2005). The formation of the rapakivi suite, including related anorthosites and diabase dyke swarms, represented an extensional event that affected the whole crust, as suggested by listric faults identified below the Åland rapakivi batholith (Korja & Heikkinen 1995). In the Pori area, Mesoproterozoic c. 1.25 Ga mafic sills and laccoliths occur within the sandstone basin (Korsman et al. 1997 and Kohonen et al. 1993). These events reactivated older faults (Mertanen 2001, Mertanen et al. 2001, 2004, 2008 and Elminen et al. 2008), and later during the Caledonian orogeny some heating and reactivation (Vaasjoki 1977b and Mertanen et al. 2008) of the predominantly brittle faults occurred. The more systematic joint patterns were also formed during these latest stages of crustal evolution (Pajunen et al. 2001a and Wennerström et al. 2008). The present-day seismic activity and several post-glacial faults demonstrate that the recent c. WNW-ESE-oriented stress field (Stephansson et al. 1986), and even the local stress variations due to present gravity contrasts caused by differences in densities of rock types (Elo et al. 2007), still causes reactivation in the old fracture zones (e.g. Kuivamäki et al. 1998).

METHODS AND DATA

Field data

Tectonic interpretation is based on the field analyses of rock types and structures. The majority of observations are from the detailed study area (Figure 1, area 1). Approximately 1550 outcrops (Figures 2a, Pajunen et al. 2002) were studied; c. 200 exposures were investigated more carefully for their structural, metamorphic and magmatic characteristics, but detailed metamorphic analysis was beyond the scope of

this study. Nearly 400 thin sections, including those collected during the regional mapping (see below), were investigated for structural and metamorphic characterization. Some correlations and sampling outside the detailed area (Figure 1, area 2) was concentrated on key outcrops hosting important geological information. The tectonic interpretation made in the Pori area (Figure 1, area 3) by Pajunen et al. (2001a) was based on c. 650 outcrops (Figure 2b), some of which are revisited during this study.

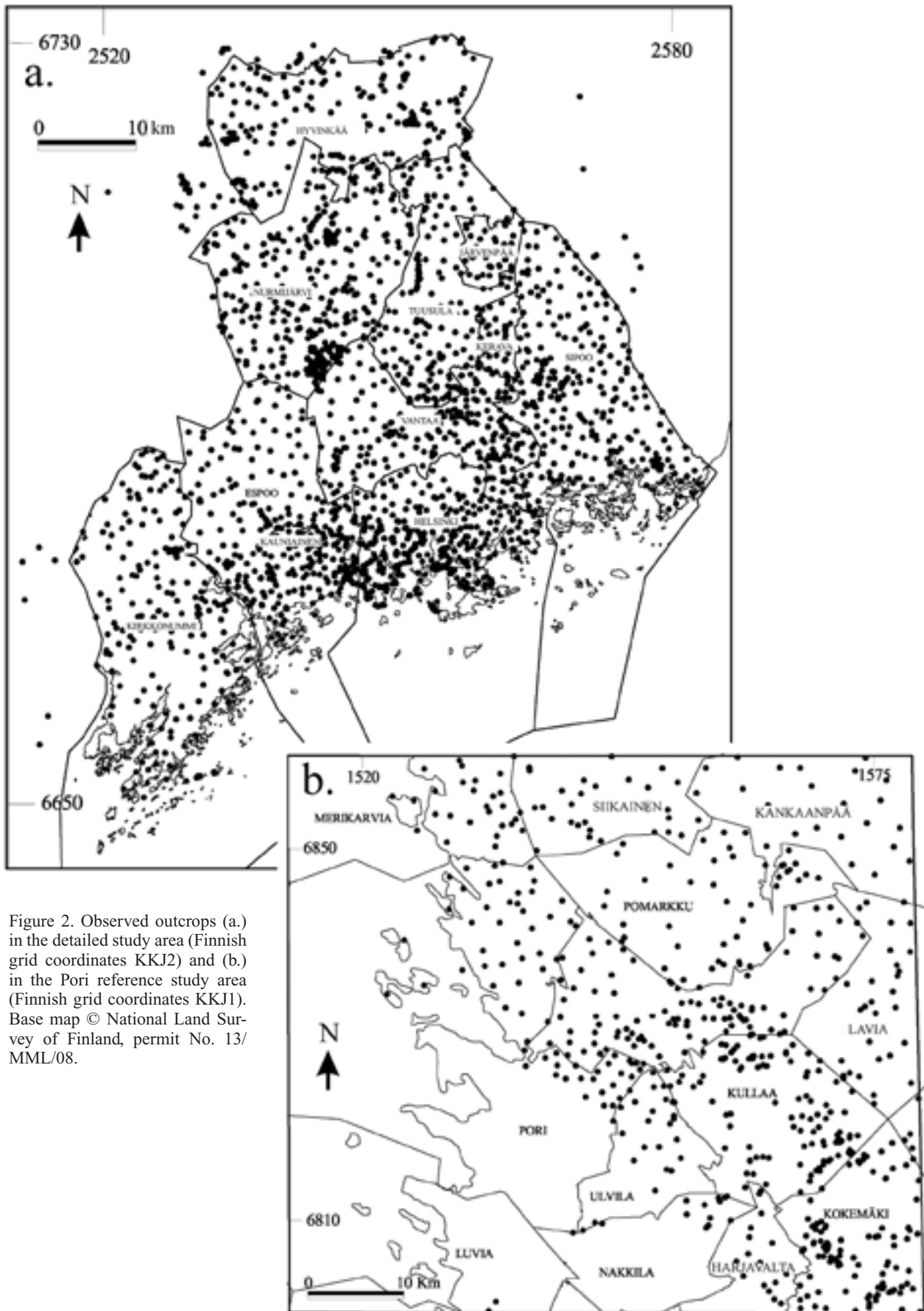


Figure 2. Observed outcrops (a.) in the detailed study area (Finnish grid coordinates KKJ2) and (b.) in the Pori reference study area (Finnish grid coordinates KKJ1). Base map © National Land Survey of Finland, permit No. 13/MML/08.

Structural analysis

Analysis of structural sequences is based on overprinting relationships of tectonic, magmatic and metamorphic events. The sequences of different structural features were established by analyzing the relationships of the structures and interference patterns on outcrops using the method described by Hopgood (1980, 1984 and 1999). To be able to make a regional correlation of structural sequences in and between the polydeformed and metamorphosed areas, the thermal history, mineral growth and magmatic events have to be considered, as well as the relative ages of events. Regional variation in strain during deformation has an important effect on the resulting tectonic configuration (e.g. Ramsay & Huber 1983); strain and stress terminology follows Marrett and Peacock (1999). In this work, the kinematic reconstructions are based on the analysis of tectonic transport directions in the high strain shear zones, folding, foliation, boudinage structures, stretching/intersection lineations and shear band structures in the field. Rough estimations of strain are based on folding patterns, foliation intensities and the behaviour of competent objects in ductile groundmass.

When dealing with the Svecofennian history (e.g. Korsman et al. 1999, Pajunen et al. 2004 and Lahtinen et al. 2005) of the study area, it is not easy to correlate structures of one area to another. Where did the earliest events occur with respect to their present-day neighbouring units or tectonic slices? When were different crustal units/slices accreted to each other? Even though the crustal units share their primary lithology, earliest deformation events and even ages with each other whether it is not always self-evident, if they were together during the tectonic process. This problem is represented schematically in Figure 3. Especially in the strongly metamorphosed and tectonically segmented areas, like in southern Finland, correlation of the earliest tectonic structures from one area to another is difficult. Missing structures, not developed in sheltered blocks, may also confuse the structural succession.

In polydeformed and metamorphosed areas the analysis of structural succession is not straightforward; the metamorphic mineral growth history and age dating of processes are needed. The deformation products differ in the deeper parts of the crust from those simultaneously forming shallower crustal levels. Some rocks may have been affected by deformation under low-grade brittle conditions, or were even still depositing, whereas the lower crust already suffered a high-grade metamorphism and ductile metamorphism. Infra-supracrustal structures of this kind were exemplified by Kilpeläinen (1998),

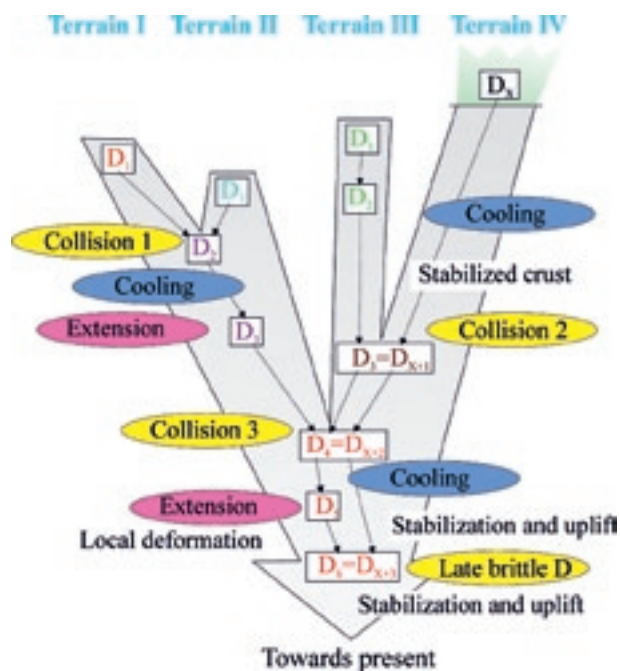


Figure 3. Schematic model describing the successive series of deformation events in different units; the oldest D_1 deformation event is overprinted by the subsequent deformations $D_{1,2,3,\dots}$. Depending on the timing of the collisional, extensional and stabilization stages of the crust, the deformation history is the same or different in different units. Generally, the latest deformation events show a coherent history over wide areas, such as in the Fennoscandian Shield.

who noted that the well-preserved lower-grade rocks in the Tampere Schist Belt (TSB) were not affected by the earliest deformation seen in the corresponding high-grade gneisses south of it in the Vammala Migmatite Belt (VMB) (Figure 1). On the other hand, Rutland et al. (2004) proposed an age difference and discordance between them. As discussed above, Sederholm already presented similar ideas of the “tectono-thermal discordances” from southern Finland in 1926.

Heterogeneous strain partitioning during deformation complicates the correlation of tectonic structures. Strain localization into narrow shear zones may show some bending or folding restricted to these zones, whereas wide areas may be left unaffected. Thus, an important structure for reconstructing the regional tectonic history may be absent or very weak. This kind of partitioning is common under low-grade upper crustal conditions during the earliest and latest episodes of crustal history. Under higher-grade conditions, deformation is more penetrative and partitioning affects the rock on a smaller scale, e.g. along the fold limbs. When dealing with multistage tectono-magmatic history, deformation partitioning due to temperature and ductility contrasts is a phenomenon that strongly controls the tectonic construction. Local irregularities in the distribution of heat input or syntectonic magmatism may disturb the otherwise regular fold interference

patterns. These kinds of regional variations in strain and heat flow characterize, for example, the regions deformed in transpressional/-tensional belts (Holdsworth et al. 1998), or orogen-parallel extension zones in compressional orogens, like in the Himalayas (Zhang et al. 2000 and Murphy 2002). Tectonic structures indicating simultaneous shortening and dilatation in different parts of the region were developed.

The small-scale structures identified on outcrops do not necessarily reflect the major structures of the crust, like those seen in the reflection seismic data. For example, steeply- and tightly-folded units often represent on a wider scale a quite horizontal, only internally steep and tightly-folded slice. Internal structures are often unaffected by horizontal deformations such as overthrusting or extensional shearing/flattening (Figure 4). Such situations are typical in the southern Svecofennian domain. On a wider scale, thermal-driven differences in the competences of rocks or units may cause drastic modifications, even to the major crustal structure; Koistinen (1981) and Koistinen et al. (1996) described such effects in the boundary zone of the Archaean domain.

A range of magmatic intrusions and dykes are useful for structural correlation (cf. Sederholm 1926). They are often widespread and intruded into different tectonic domains, thus fixing the structural history of the domains. Intrusive rocks show tectonic structures such as foliation, shear bands or

metamorphic mineral assemblages that are often easier to interpret than those distinguished, for instance, in the complexly deformed pelitic rocks. However, magmatic rocks representing the same event may have different styles of intrusion depending on the local tectonic-metamorphic conditions or emplacement depth.

On the other hand, intrusive rocks and alteration caused by magmatic fluids may obscure and destroy pre-existing structures. Fortunately, early structures may sometimes still be identifiable, although their manifestation has changed. Figures 5a and b show an example of remnant foliation after granitization (cf. Härme 1965) on an outcrop scale. Sometimes only small remnants of original gneisses are preserved in schlieren migmatites (Figure 5c). On a regional scale, the remnants of gneiss belts may remain as narrow remnant chains between or within the intrusive or strongly migmatitic areas. Belts of this kind are often still interpretable from the geophysical data.

Crustal-scale long-wavelength folds, bends and warps (cf. Pajunen et al. 2008) are mostly difficult to observe on an outcrop scale, especially on the flat ice-polished outcrops. Nevertheless, they are significant in analyzing the major characteristics of tectonic units, e.g. the distribution of litho-stratigraphic units, exposures from various crustal depths evident from variations in the metamorphic grade and characters in magmatism, variation of crustal

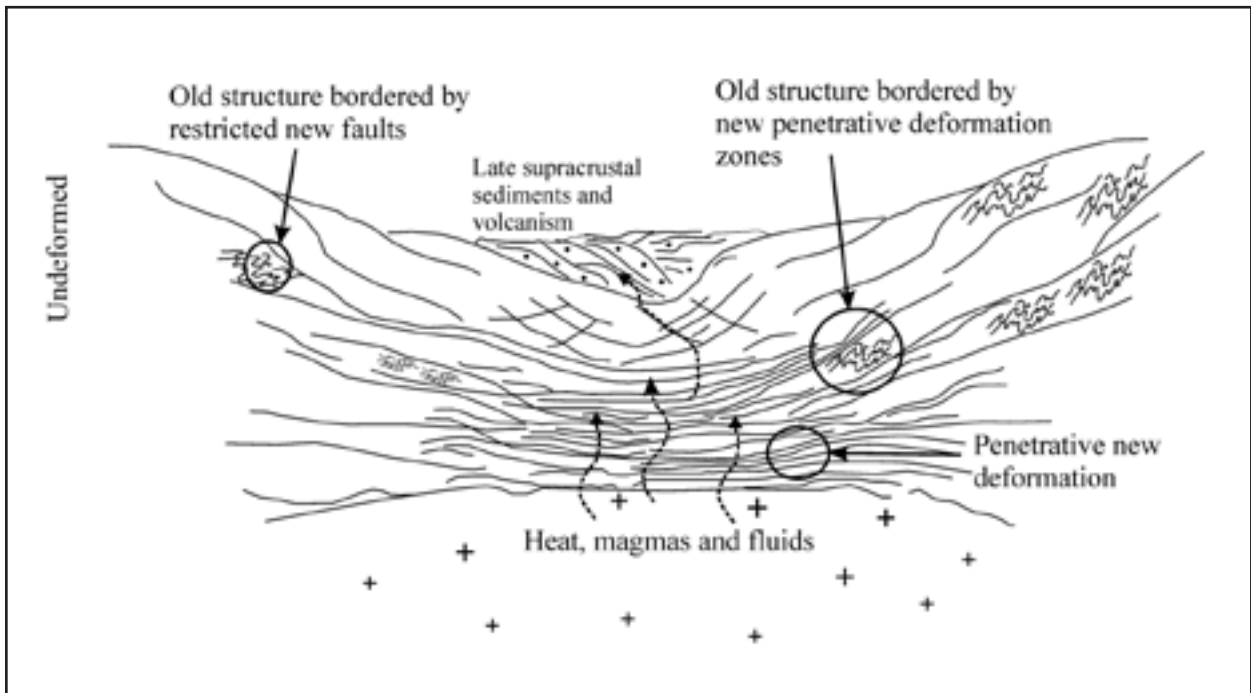


Figure 4. The type of deformation, penetrative or zoned, varies with crustal depth and thermal conditions. For example, the deformation pattern in the extensional event may produce penetratively deformed parts in the crust, where the pre-existing structures are totally destroyed. The less deformed parts of the crust locally show the older deformation structures preserved; depending on the strength of deformation, the directions of the old structures may also be preserved. Near the surface the deformation may, however, show only weak and narrow deformation zones and fault structures that are often overlain by soft sediments.

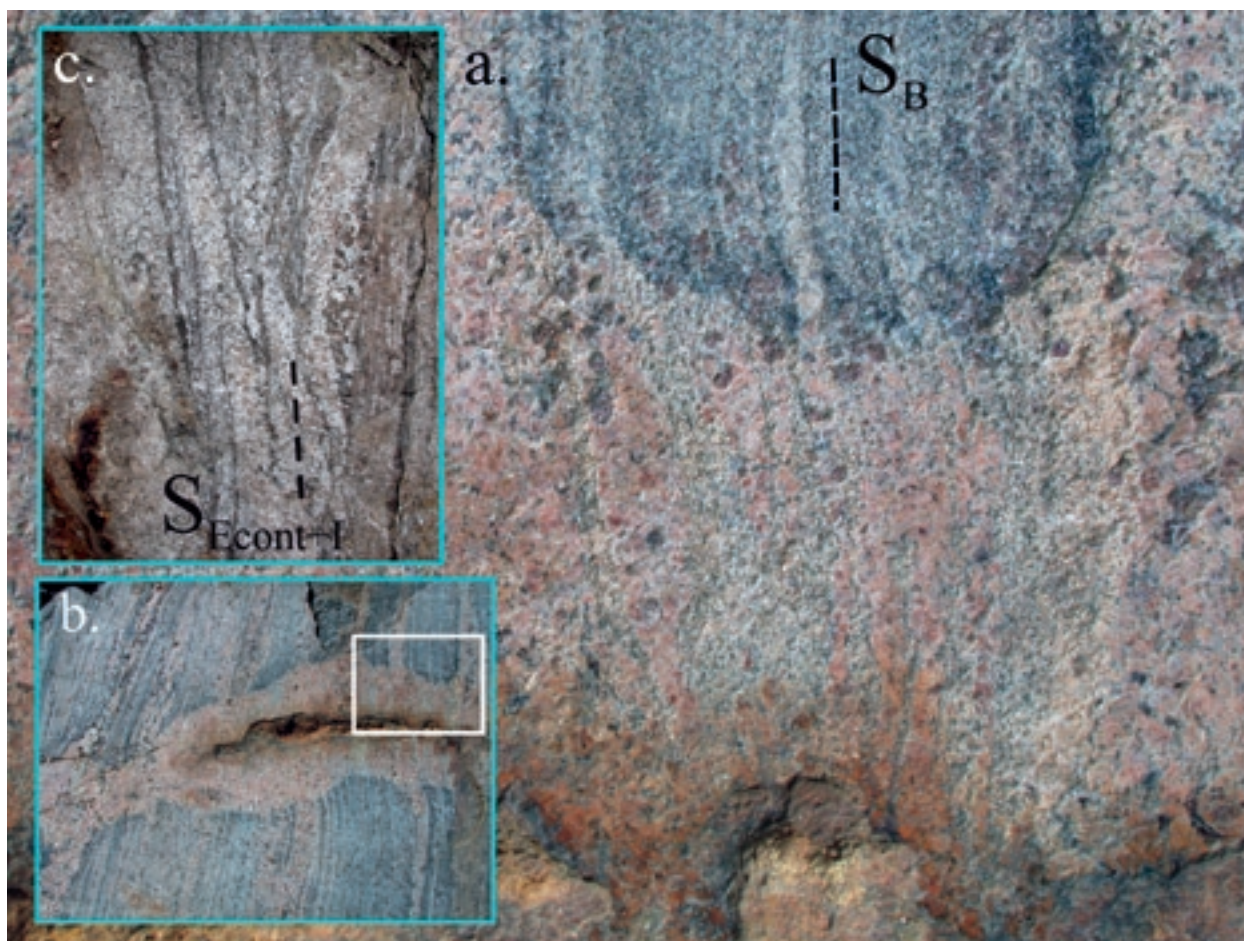


Figure 5. Granitized garnet-bearing mica gneiss in Sipoo (Finnish grid coordinates KKJ2 2568.78E 6695.45N). Figure (a.) shows a detail of the granitization surroundings of the fracture in figure (b.). The pre-existing structure is still visible in the altered gneiss. Width of the area of the figure is c. 1.5 m. (c.) Granitization and melting is almost penetrative in schlieren mica gneiss in Nurmi-järvi, Klaukkala (Finnish grid coordinates KKJ2 2542.76E 6696.12N). The pre-existing structure is hardly visible, but the major trends of the gneisses are often preserved and identifiable on geophysical maps. Width of the area of the figure is c. 1 m. Photos by M. Pajunen.

deformation style, and so on. According to several metamorphic studies (e.g. Korsman et al. 1984 and 1999), strong magmatic activity under a high thermal gradient caused a rapid temperature increase downwards during the peak metamorphism in the southern Svecofennian domain. Therefore, the late/post-metamorphic open fold structures and faults have an important effect on the metamorphic configuration on the present-day erosion level, e.g. in antiformal or synformal tectonic settings. The results of these open fold deformations vary depending on the pre-existing structural setting; areas with steep and horizontal structures produce very different patterns, as schematized in Figure 6.

The open structures form a framework into which the earlier structures should be fixed. The small-scale structures are the results of major tectonic processes, but they are often affected by local heterogeneities. Our approach is first to deal with the structures from a regional point of view to reconstruct the tectonic framework in which the detailed study area is located. Our purpose is not to try to explain all the structures caused by local heterogeneities,

but to provide a generalized structural framework by describing several examples for further, more detailed analyses (e.g. Hopgood et al. 1983, Hopgood 1984 and Pajunen et al. 2008) that are helpful in resolving local structural problems.

The general structural framework of the Fennoscandian Shield was compiled by using the published geological (e.g. Korsman et al. 1997 and Koistinen et al. 2001), magnetic (Korhonen et al. 2002a), gravity (Korhonen et al. 2002b) and Moho depth (Korsman et al. 1999) maps, and the low- and high-altitude aeromagnetic magnetic data of the Geological Survey of Finland (GTK). By correlating structural information on lithological and magnetic or gravity maps, it is evident that the “post- and late orogenic” magmatic and migmatization events locally effectively reduced or destroyed the early structures of supracrustal belts. Remnants of supracrustal belts are commonly more poorly exposed than granitoids characterizing the geological maps. Even though the pre-migmatization rock was supracrustal in origin, the large granitic component (>50%) determines the rock as granitoid on

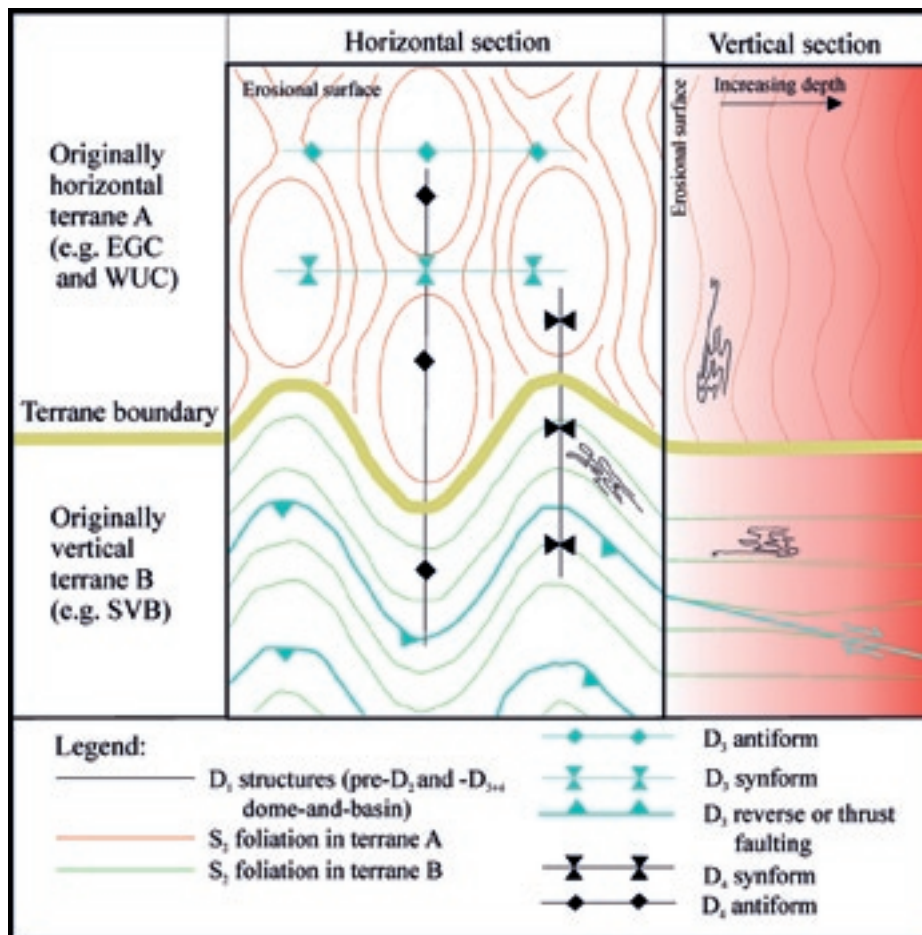


Figure 6. Two generations of open folding in originally steeply and horizontally deformed areas in horizontal and vertical sections. The characters of the deformation structures and the regional pattern vary between tectonic units. The structural analysis thus demands careful correlation of structures with metamorphic and magmatic events. $D_{1,2,3,\dots}$ refer to successive deformation events and the abbreviations (EGC = Espoo Granitoid Complex, WUC = West Uusimaa granulite Complex and SVB = Southern Finland Volcanic-sedimentary Belt) exemplify the units in the study area (see Figure 1).

the lithological maps of GTK. Thus, we suggest that the relic geophysical signatures, indicating the pre-magmatic/migmatization structural trends of the belts, are often still identifiable. The structural interpretations represented here are based on these assumptions.

As discussed previously, the problems in analysing the succession of tectonic structures are multiple. The structural events of this study are not directly consistent with the previously published descriptions, because some structures identified in the study area are missing as such in the other domains, or the way structures are interpreted differs. To avoid confusion while keeping doors open for later modification, we label the structures as follows. The structures formed by the first identified regional deformation phase D_A are F_A = folding, S_A = foliation or axial plane, L_A = lineation and M_A = metamorphism; the second, respectively, D_B , F_B , S_B , L_B , M_A ; the third D_C , F_C , S_C , L_C , M_A ... The bedding is termed S_0 . When discussing or referring to the earlier published results, we follow the labels applied by the

previous authors. The naming of structures follows a regional scheme: the earliest structure in a late rock series is named according to the regional structural succession. For example, the foliation S_E in older sequences may represent the first foliation in a sequence formed later; we also label it as S_E . We prefer this solution because the structures in both the old and the young series are related to the same tectonic event. Such naming requires the identification of key features such as regional folding, characteristic foliation or dated magmatic rocks (volcanic/intrusive) that enable correlation. Difficulties arise in naming structures formed during continued transcurrent events comprising simultaneous shortening/contraction (labelled e.g. $D_{E,cont}$), dilatation/extension (labelled e.g. $D_{E,ext}$), which overprint during progressive deformation. In the descriptions we primarily follow the overprinting relations on outcrops.

The field structures are then assigned to regional major geotectonic events labelled Event 1 – E_1 , Event 2 – E_2 , Event 3 – E_3 ...

Pre-existing geological data

Structural domains and tectonic formlines were constructed using structural field data, tectonic elements from geological maps and the digitalized geological data sets of the Geological Survey of Finland (GTK). The following geological bedrock maps of scale 1:100 000 were used: 2013 (Jussarö, Laitala 1973b), 2014 (Tammisaari, Koistinen 1992), 2023 (Suomusjärvi, Salli 1955), 2024 (Somero, Simonen 1955 and 1956), 2032 (Siuntio, Laitala 1960), 2034 (Helsinki, Laitala 1967 and 1991), 2041 (Lohja, Laitala 1994), 2042 (Karkkila, Härme 1953), 2043 (Kerava, Härme 1969), 2044 (Riihimäki, Kaitaro 1956), 2113 (Forssa, Neuvonen 1954), 2131 (Hämeenlinna, Simonen 1949), 2133 (Kärkölä, Lehijärvi 1961), 3012 (Pellinki, Laitala 1965), 3021 (Porvoo, Laitala 1964), 3022 (Lapinjärvi, Laitakari & Simonen 1962 and 1963), 3023+3014 (Kotka, Simonen & Laitala 1970), 3024 (Karhula, Simonen 1965), 3111 (Lahti, Lehijärvi 1964), and 3113 (Kouvola, Simonen & Lehijärvi 1963).

The majority of the maps are old; at the time of their production, modern tectonic study methods were just being developed. Generally, the main foliations on outcrops are shown on the maps. The foliation trends in Figure 7 were constructed by combining several foliation measurements with average dip values. Each trend line represents the foliation trend inside a certain lithological unit. Without familiarity with the tectonic and magmatic history of the rock it is not possible in most cases to identify the deformation event that produced the depicted foliation. According to our observations, especially the horizontal structures, which seem to characterize wide areas of southern Finland, are underestimated on the maps. For example, the dome-and-basin structures that characterize the magnetic maps are difficult to construct from these tectonic elements. Similar problems arose when dealing with fold axes (which fold phase?) and lineations (stretching or intersection lineation, or slicken line striation?). According to our experience, most granitic areas show measurable foliations on outcrops, but these are not shown on the maps.

Magmatic processes are important when interpreting the tectonic evolution of the crust. In southern Finland, different types of granitoids are not sufficiently classified and outlined on the maps. Their composition and amount of strain vary from foliated tonalites to weakly-deformed granites and, finally, to non-deformed pegmatitic granites and even migmatitic mica gneisses. Therefore, the regional distribution of various granitoids can only be discussed in a very general sense.

Aerogeophysical data

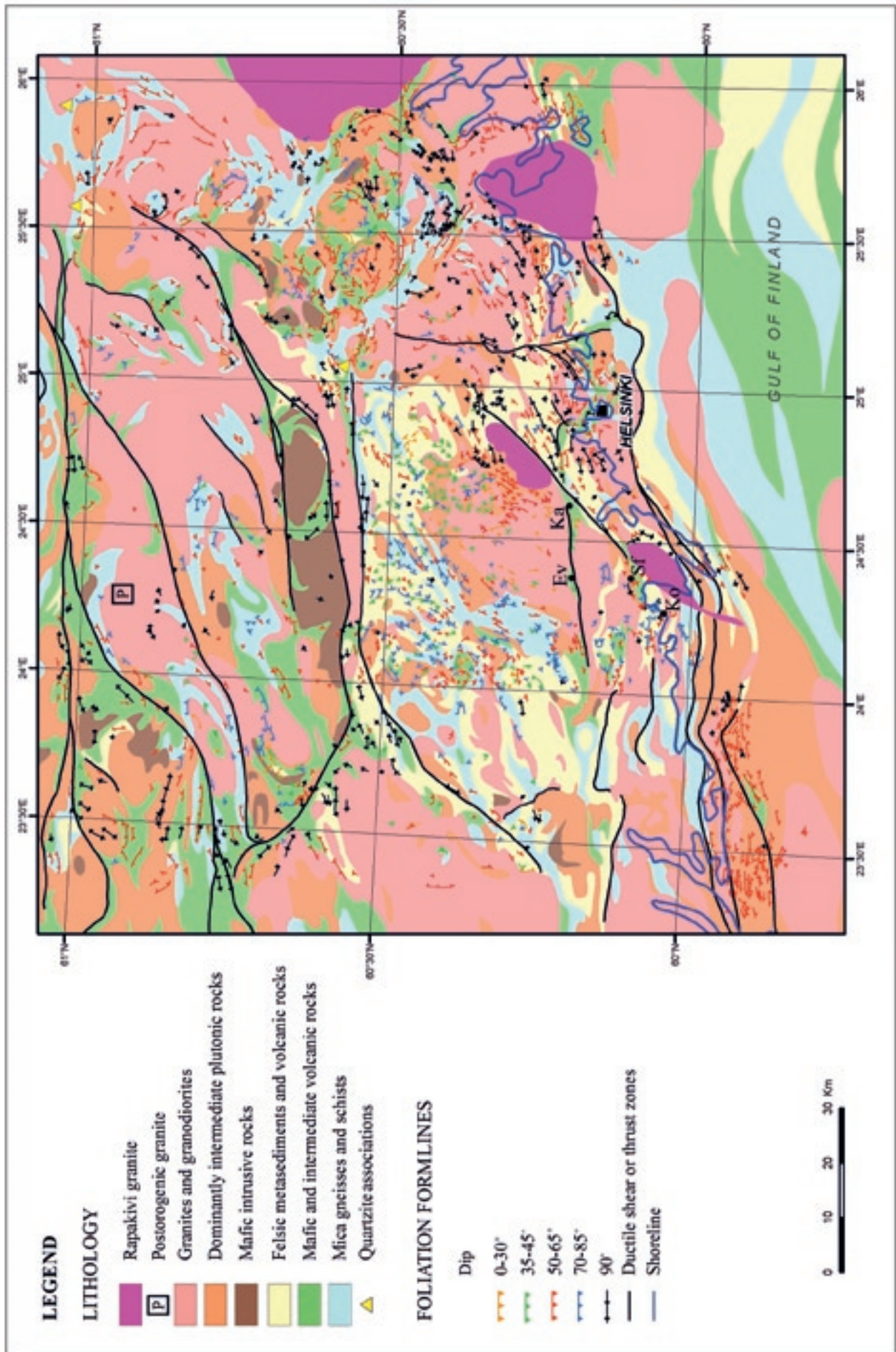
The field observations on outcrops mostly show the structures on a “miniature” scale. The magnetic data were useful for the regional tectonic analyses. Wide areas only show small variations in the intensity of the magnetic field. In such areas, different methods of processing the aeromagnetic data were used for detailed analyses; the methods are described in detail in Airo (1999) and Airo et al. (2008). Topographic maps were often useful in constructing the regional structures. They were informative in granitoid dominant areas, which were homogeneous in the geophysical data, but clearly show structural trends in the topographic patterns. Geophysical interpretations were confirmed by detailed field observations on the key outcrops.

Aeroradiometric data were used in estimating the distribution of some late magmatic events (Th/U ratio). The use of radiation data is limited, because it often reflects the soil properties or radiation may be buffered in lakes and swamps. The non-geological noise diminishes the usefulness of aeroelectromagnetic data. Regional gravity data with a 5 km and a denser grid of 250 m collected by the Geodetic institute and by the Geological Survey of Finland (GTK) were of benefit in analyzing wide-scale structures, unit boundaries and crustal fracture zones.

Geochronology

The major tectonic events are dated using the U-Pb TIMS and SIMS methods. Samples were fixed to the successive structural and magmatic events observed in the field. The dating methods and results are provided in Appendix 8. The ages for the rocks that are structurally fixed into tectonic evolution are presented in App-Table 3.

Figure 7. Lithology and foliation trends in the study area. Foliation trends are compiled using the bedrock maps on the scale 1 : 100 000 of GTK. Ev = Evitskog, Ka = Kauklahti, Ko = Kopparnäs and Sf = Sarfvik. Base map © National Land Survey of Finland, permit No. 13/MML/08.



TECTONIC FRAMEWORK OF THE STUDY AREAS IN THE SOUTHERN FENNOSCANDIAN SHIELD IN FINLAND

The lithology and timing of major tectonic events of the Fennoscandian Shield are represented on the geological map of Koistinen et al. (2001). Recently, Lahtinen et al. (2005) compiled a tectonic model for the shield. Relating the local structures in the study areas to structural evolution on the crustal scale first requires the determination of their setting in the structural framework of the southern Fennoscandian Shield in Finland.

The Archaean and Svecofennian domains can be divided into different tectonic units using major tectonic boundaries, shear/fault zones of varying origin. The southern Svecofennian domain of the

Fennoscandian Shield is divided into c. N-trending tectonic units along the eastern margin of the Transscandinavian Igneous Belt (TIB, see Högdahl et al. 2004) in Sweden, the deformation zones from the southern Baltic Sea to the eastern coast of the Bothnian Bay (Baltic Sea-Bothnian Bay Zone, BBZ) and from Riga Bay, Lithuania, to the Vyborg rapakivi and to Karelia in southeastern Finland (Riga Bay-Karelia Zone, RKZ). These deformation zones are shown on the magnetic map of Korhonen et al. (2002a) (Figure 8).

The Transscandinavian Igneous Belt (TIB) is dominated by magmatism that overprints the earlier

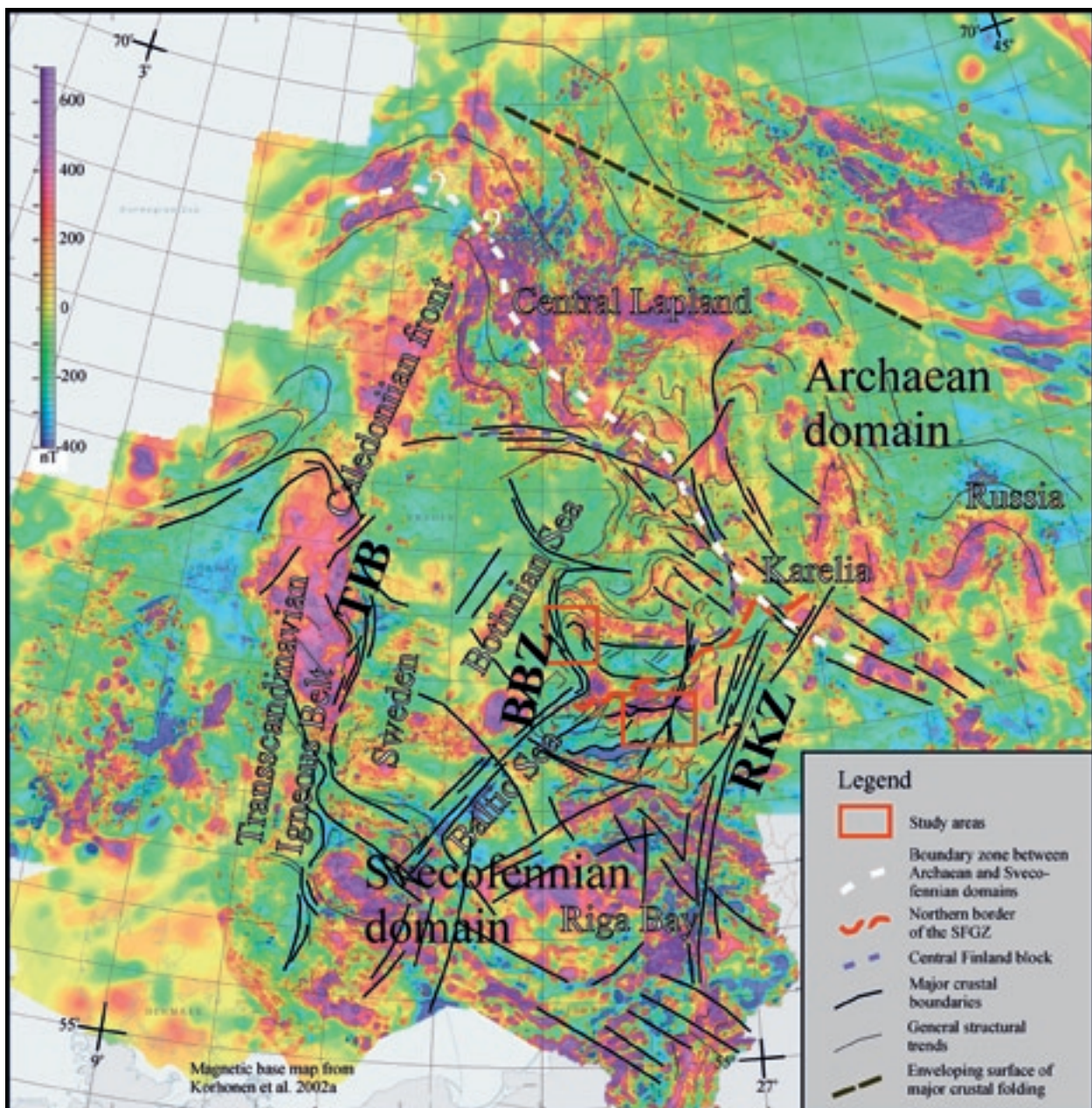


Figure 8. The major crustal structures and domains of the southern Fennoscandian Shield on the magnetic map of Korhonen et al. (2002a). BBZ = Baltic Sea-Bothnian Bay Zone, RKZ = Riga Bay-Karelia Zone and TIB = Transscandinavian Igneous Belt.

Svecofennian structural trends. The age of the TIB magmatism ranges from 1.85 to 1.65 Ga (Högdahl et al. 2004). The oldest granitoids are situated in the eastern margin of the belt (Koistinen et al. 2001). A c. N-trending deformation zone characterizes the TIB. To the east of the zone the structural trend is bent from c. WNW to NW due to a crustal-scale dextral drag of the earlier structures. The magnetic anomalies are weaker below the Caledonian front to the west of the TIB, where the large-scale crustal bend shows a NNE-trending axial trace (Figure 8). According to Bergman et al. (2006), the so-called Storsjön-Edsby Deformation Zone is a dextral transpressional zone that was active in the time interval of c. 1.7–1.3 Ga.

The Baltic Sea-Bothnian Zone (BBZ) is exposed in its northernmost part in the Pori area. The structural characteristics established from the magnetic pattern supports the more ductile deformation in the northern part (ductile bended shear zones) of the BBZ than in its southern parts (more sharply cutting faults). The Pori area is characterized by NNW-trending crustal blocks, e.g. the Pomarkku block (Po in Figure 9) (Pietikäinen 1994 and Pajunen et al. 2001a), that are bordered by the major sinistral NNW-SSE-/N-S-trending Kynsikangas shear/fault zone in the west and the dextral shear zones like the Kankaanpää shear zone in the east (Figure 10). A similar block structure is exposed towards the north

up to the Vittinki zone, and is also characteristic in the east, in the Central Finland Granitoid Complex (CFGC) (Figures 9 and 10). The northern end of the BBZ is located in the Vaasa area (Va in Figure 9) along the Vittinki shear/fault zone (Figure 10). According to Rutland et al. (2004), the Vaasa area was pushed into its present setting from the WNW.

In its southern parts, in the Paleozoic area of the Baltic countries, the Riga Bay-Karelia Zone (RKZ) appears as sharp faults. It disappears in the Vyborg rapakivi massive area and forms a complex, ductile structural pattern to the north and northeast of the rapakivi intrusion. The crustal segment between the BBZ and RKZ in southern Finland is characterized by large-scale warping with a c. N-trending axial plane. Closer to the BBZ and RKZ zones the folds become tighter and the major shear and fault zones parallel to the axial planes of the folds (see also Lindroos et al. 1996). The detail study area is situated in the western branch of the RKZ. The area is characterized by wide-scale open to tight folding with a c. N-trending axial plane paralleling the Vuosaari-Korso shear/fault zone (Figure 10).

An ENE-trending belt of late Svecofennian granitoids, the Southern Finland Granitoid Zone (SFGZ), characterizes the southern study area. The major crustal N-trending deformation zones, the Riga Bay-Karelia Zone (RKZ) and Baltic Sea-Bothnian Zone (BBZ), deform the SFGZ.

STRUCTURAL UNITS IN THE SOUTHERN SVECOFENNIAN DOMAIN

The southern Svecofennian domain is composed of several tectonic units showing varying depositional, tectono-metamorphic and magmatic characteristics (Figure 9). The shapes of the units are determined by wide-scale folding and faulting patterns, and by the competences of rock and tectonic units during deformation. The major crustal high-strain and fault/shear zones and stacked zones/units are indicated in Figure 10. Naturally, this kind of division is somewhat artificial; the units often show features in common or they may simply represent corresponding rocks from different crustal depths. In fact, the division should be carried out in three dimensions constrained in time; an ambitious challenge only shortly assessed here.

The study areas are situated in the major tectonic units of the Granite Migmatite Belt (GMB) and Tonalite Migmatite Belt (TMB). Our observations are from key outcrops in the Southern Volcanic-sedimentary Belt (SVB), West Uusimaa granulite Complex (WUC), Hyvinkää Gabbroic-volcanic Belt (HGB), Jokela supracrustal association (Jo in Figure

9) and the Espoo Granitoid Complex (EGC). We place the main emphasis on the EGC, because it excellently shows the wide variation in magma phases, and on the SVB, which was preserved from the intense magmatism of the EGC. Supracrustal rocks within the EGC show characteristics similar to those in the SVB and WUC. The HGB represents a tectonic slice lying upon the EGC and WUC. The Jokela supracrustal association is a late sedimentary-volcanic sequence. These units include the majority of the lithological and structural characteristics important in constructing the tectono-metamorphic and magmatic scheme for the southernmost Svecofennian domain.

The Hämeenlinna shear/fault and the stacked zone north of it border the Granite Migmatite Belt (GMB) against the Tonalite Migmatite Belt (TMB). The stacked slices of the GMB are NW-trending in the west and N- and NE-trending in the east (Figure 10). The western end of the TMB-GMB discordance was mapped later by Korsman et al. (1997). The general structural trend of the TMB is E-W, but it is

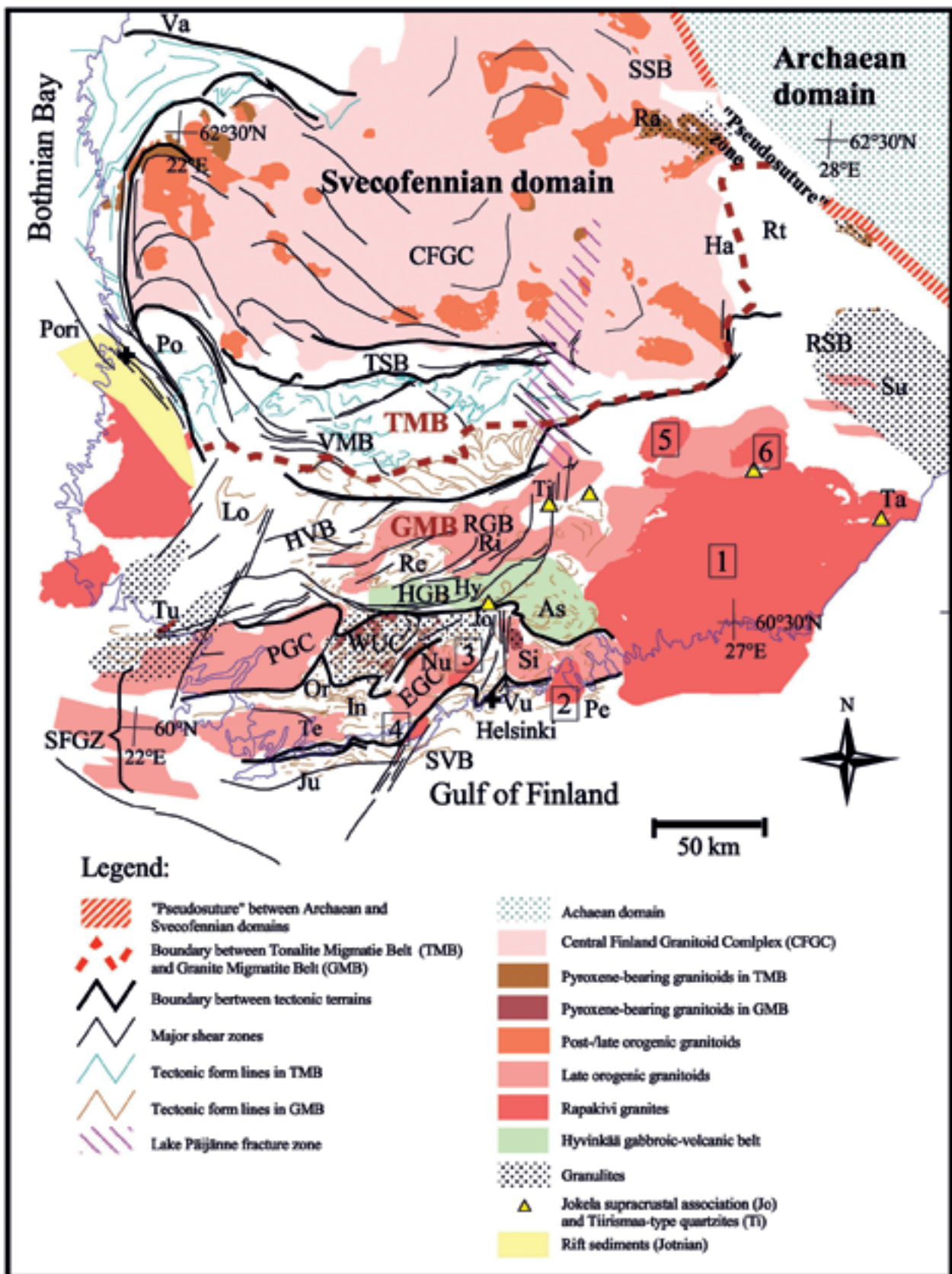


Figure 9. Geotectonic units in southern Finland. Abbreviations: SFGZ = Southern Finland Granitoid Zone, CFGC = Central Finland Granitoid Complex, TMB = Tonalite Migmatite Belt, GMB = Granite Migmatite Belt, SSB = Savo Schist Belt, RSB = Rantasalmi-Sulkava area/Belt, TSB = Tampere Schist Belt, VMB = Vammala Migmatite Belt, HVB = Häme Volcanic Belt, HGB = Hyvinkää Gabbroic-volcanic Belt, WUC = West Uusimaa granulite Complex, SVB = Southern Volcanic-sedimentary Belt, EGC = Espoo Granitoid Complex, RGC = Riihimäki Granitoid Complex, PGC = Perniö Granitoid Complex; Po = Pomarkku block, Nu = Nuukio area, Va = Vaasa area, Lo = Loimaa area, Tu = Turku area, Re = Renko area, Pe = Pellinki area, In = Inkoo area Or = Orijärvi area, Ju = Jussarö area, Vu = Vuosaari area, Hy = Hyvinkää area, As = Askola area; Jo = Jokela supracrustal association, Ti = Tiirismaa quartzite, Rt = Rantasalmi area, Su = Sulkava area, Ra = Rautalampi area, Ha = Haukivuori area, Ta = Taalikkala "roof pendant"; rapakivi granites: 1 = Vyborg, 2 = Onäs, 3 = Bodom, 4 = Obbnäs, 5 = Ahvenisto and 6 = Suomenniemi. Base map © National Land Survey of Finland, permit No. 13/MML/08.

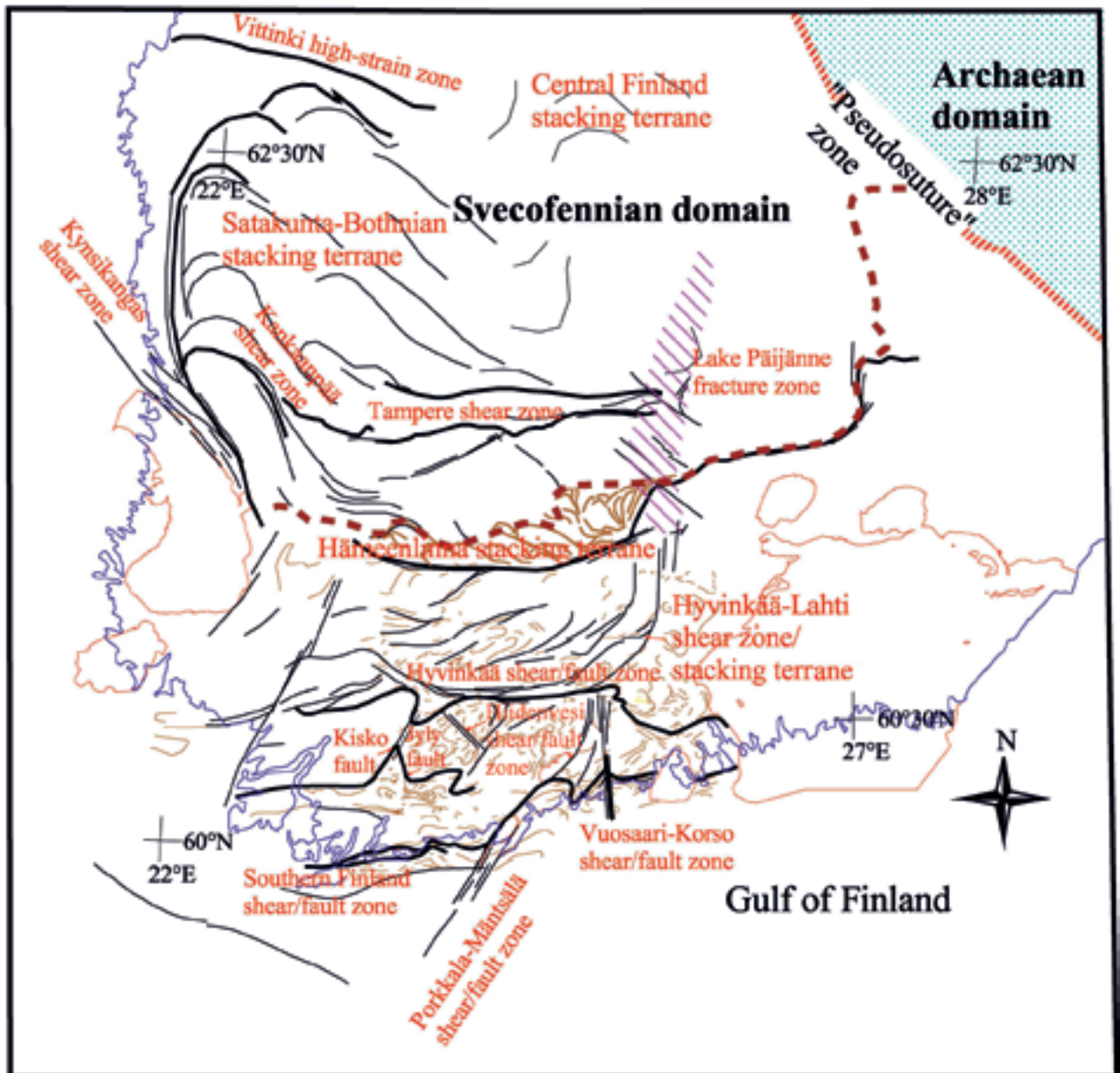


Figure 10. Major unit boundaries, shear and fault zones, in Southern Finland. Base map © National Land Survey of Finland, permit No. 13/MML/08.

bent towards the NW in the Pori area (e.g. Pomarkku block, Po in Figure 9) and reoriented into the N-NW trend near the Archaean-Proterozoic border zone in the east (e.g. Koistinen et al. 1996 and Korsman et al. 1997). The lower-grade Tampere Schist Belt (TSB) is bordered by the TMB in the south and by the Central Finland Granitoid Complex (CFG) in the north. The CFG is characterized by crustal-scale NW-stacked structures (Figures 8 and 10). The structural characteristics of the northern units, the Central Finland Granitoid Complex (CFG), Vammala Migmatite Belt (VMB), Hämeenlinna Volcanic Belt (HVB), Tampere Schist Belt (TSB), Rantasalmi-Sulkava area (RSB) and Savo Schist Belt (SSB) are briefly discussed.

The volcanic and sedimentary sequences of the Southern Volcanic-sedimentary Belt (SVB) in southernmost Finland form continuous E-trending

belts ranging from the southwestern archipelago (e.g. Ehlers & Lindroos 1990) to the Inkoo (e.g. Eskola 1914, Sederholm 1926, Hopgood 1984, Bleeker & Westra 1987 and Kilpeläinen & Rastas 1990) and Pellinki areas (e.g. Sederholm 1923 and Laitala 1973a and 1984) (Figure 9). The SVB is cut and bent by the Porkkala-Mäntsälä and Vuosaari-Korso shear/fault structures (Figure 10) (Elminen et al. 2008). Psammitic-pelitic metasediments with carbonaceous interlayers, various felsic gneisses and mafic to intermediate volcanic rocks characterize the SVB supracrustal lithology. Generally, the rocks are migmatitic and intruded by the later granitoids. The pelitic layers are intensely affected by melting. Felsic gneisses are felsic volcanic rocks, psammitic metasediments or, locally, even deformed granitoids; mostly the related rock associations give reference to their origin. Non-migmatitic, amphibolite

facies areas such as in the Pellinki (Pe in Figure 9) (Laitala 1973a and 1984), Orijärvi (Or in Figure 9) (e.g. Eskola 1914, 1915 and Tuominen 1957) and Vuosaari areas (Vu in Figure 9) clearly show the primary features like bedding, pillow lava, amygdale and porphyric structures. The Orijärvi area is characterized by Zn-Cu-Pb ores, associated with altered rocks such as coarse-grained cordierite-anthophyllite rocks (Eskola 1914 and 1915), and skarn-iron ores, iron formations (e.g. Eskola 1914, Latvalahti 1979 and Saltikoff et al. 2002) and carbonate rock horizons (Bleeker & Westra 1987 and Reinikainen 2001), indicating a shallow-water depositional environment. Väisänen and Mänttari (2002) proposed a back-arc basin origin for the volcanogenic rocks and divided them into two sequences at c. 1.90–1.89 Ga and c. 1.88–1.87 Ga; in the following they are referred to as volcanic Series I and II, respectively. The Orijärvi granodiorite was interpreted as syngenetic with the earlier volcanic sequences (Väisänen & Mänttari 2002). Hopgood et al. (1976 and 1983) and Hopgood (1984) described gabbroic-tonalitic associations from the Jussarö-Skåldö area (Ju in Figure 9): mafic magmatic series have the same age as the early volcanism (Hopgood et al. 1983).

The granulite-facies West Uusimaa granulite Complex (WUC) (Eskola 1914, 1915 and Parras 1958) is exposed between amphibolite-facies gneisses and granitoid complexes. It is sharply bordered by the Hyvinkää high strain zone in the north (Figures 9 and 10) against the Hyvinkää Gabbroic-volcanic Belt (HGB). Lithologically, the WUC represents the granulite-facies counterpart of the Southern Volcanic-sedimentary Belt (SVB) and the Espoo Granitoid Complex (EGC) rocks (e.g. Eskola 1914, 1915, Parras 1958, Schreurs & Westra 1986 and Kilpeläinen & Rastas 1990); the occurrence of orthopyroxene- and two-pyroxene-bearing assemblages is characteristic. Small granulite remnants overprinted by retrograde parageneses occur in the central Sipoo area (Si in Figure 9).

The Hyvinkää Gabbroic-volcanic Belt (HGB) has a complex internal structure and is squeezed between the Hyvinkää shear/fault zone and the sheared structures bordering the Renko area (Re in Figure 9). The Hyvinkää-Lahti shear zone, in the continuation of the combined Porkkala-Mäntsälä and Vuosaari-Korso shear/fault zones, continues further north to the Päijänne fracture pattern, already described by Sederholm (1932b) (Figures 9 and 10). The Hyvinkää-Lahti shear/fault zone separates the Hyvinkää unit of the HGB (Hy in Figure 9) from the eastern Askola unit (As in Figure 9). Large layered gabbro massifs and supracrustal sequences characterize the western part. Volcanic rocks and mica gneisses locally show primary features such as bed-

ding, agglomerate and pillow lava structures. Roundish dome-and-basin structures with gabbroic-volcanic rock associations squeezed between the domes typify the eastern part. The dome interiors are composed of granodioritic-tonalitic intrusive rocks and migmatitic mica gneisses.

The supracrustal Jokela association (Jo in Figure 9), including quartzites similar to those in Tiirismaa (Ti in Figure 9) (Lehijärvi 1964), is exposed near Hyvinkää. The association shows a depositional succession composed of sedimentary and volcanic sequences. It is important in establishing the regional structures and metamorphism because of its young depositional age dated by Lahtinen et al. (2002) using detrital zircons.

The ENE-trending Southern Finland Granitoid Zone (SFGZ) cuts the structural trend of the Granite Migmatite Belt (GMB) and is thus tectonically differentiated from the GMB. It also penetrates the Archaean domain. The southern belt, from Tenhola (Te in Figure 9) to Nuksio (Nu) and Sipoo (Si), is here referred to as the Espoo Granite Complex (EGC) (Figure 9). It is cut by the Vyborg rapakivi (1 in Figure 9) massive in the east. The northern zone, the Riihimäki Granite Complex (RGC), extends ENE to the Rantasalmi-Sulkava area (RSB) and the Archaean domain, up to the Riga Bay-Karelia Zone (RKZ). In the west, the Perniö Granite Complex (PGC) continues from the Kisko fault (Figure 10) to Turku. According to our limited observations, the lithology and structural settings of the Perniö (PGC) and Riihimäki Granite Complexes (RGC) are quite similar to that of the Espoo Granitoid Complex (EGC) (cf. Ehlers et al. 1993 and Lindroos et al. 1996). Rämö et al. (2004) described some geochemical differences between the northern (Nz in Figure 1) and southern granitic units (Sz in Figure 1).

The Espoo Granitoid Complex (EGC) covers a significant part of the detailed study area. Its contacts with the supracrustal associations of the Southern Volcanic-sedimentary Belt (SVB) are generally tectonic, e.g. along the Southern Finland shear/fault zone (cf. Koistinen et al. 1996). The EGC is bordered in the north along low-angle shear zones with the granulitic West Uusimaa granulite Complex (WUC), which, according to tectonic observations, underlies the EGC. The observation is supported by the continuation and weakening of the magnetic anomalies of the WUC below the EGC. Felsic and intermediate intrusive rocks characterize the EGC. Gneissic tonalites were intruded and migmatized by later granites; thus, many rocks shown as granitic-granodioritic on the geological maps were originally more tonalitic in composition. Gabbroic rocks occur as restricted intrusions or fragments within granitoids. Intermediate and to a lesser extent mafic

dykes form important reference features in analyzing the deformation scheme. We have not studied the lamprophyre dykes described by Eskola (1954) and Suominen (1997); the first one is situated in the courtyard of a prison and the other in a wastewater tunnel in Helsinki.

The Palaeo- to Mesoproterozoic rapakivi granites and related diabase dykes cut the rocks of the Espoo Granitoid Complex (EGC) and the Southern Volcanic-sedimentary Belt (SVB) in a semi-ductile to brittle manner. The names of the rapakivis in the study are given in Figure 9. Diabase dykes form at least two sets of dykes that are c. WNW- and NW-trending; some dykes showing a W trend may be related to a younger dyke group (Mertanen et al. 2008). Near the Vuosaari-Korso shear/fault zone occur penetratively-altered diabase dykes showing

ghost-like blasto-ophitic structure. Some diabase dykes intruded close to the erosion level and rapidly cooled, as evidenced by their shock-like and chilled microstructures.

The over 600 m thickness of the Mesoproterozoic sandstone and related mafic laccoliths (Kohonen et al. 1993) in the fault-bounded basin in the Pori area (Figure 11) also indicates that late brittle movements distinctly modified the crustal structure (Pajunen et al. 2001a). The movements must have been even larger than is estimated from the thickness of the very low-grade sandstone sequence, because the recent cross-section represents a locally ductile drag-folded section. Late NW-trending normal fault structures exist in the study area (Elminen et al. 2008); their effect on the metamorphic pattern is still an open question.

OVERVIEW OF STRUCTURES IN THE STUDY AREA

A two-stage thermal evolution of the southern Svecofennian domain has been established in several studies since the interpretations of Sederholm (1926) and Korsman et al. (1984). However, the data of Pajunen et al. (2002) demonstrated that the tectonic evolution is more complex. In order to follow the structural succession, we provide a short overview prior to the descriptions. The early structures, D_A - D_D , deformed the early supracrustal sequences and magmatic rocks. The high- to medium-grade horizontal structure, predominantly D_B , was folded into tight, ellipsoidal dome-and-basin patterns, D_{C+D} (Figure 11) with an originally c. E-trending longitudinal axis. A complex series of dilatational to contractional structures followed the D_A - D_D . We label the earliest dilatational and flat-lying structures as

D_E , and related intrusive rocks are divided into early, mid- and late D_E phases according to their relationships to the successive magmatic sequence. The D_E structures were followed by structures formed by N-S-shortening D_G and later NW-SE shortening D_H , which was accompanied by strong granitic magmatism. D_F deformation appears as E-W-contracting structures that caused major block movements in the northern Svecofennian domain in eastern Finland; it was simultaneous with the D_E in the south, where only local shear zones are related to this deformation. The large-scale warping with N- to NNE-trending steep axial planes has deformed all the earlier structures and is labelled as D_I . The post-Svecofennian structures, e.g. those related to the rapakivi event, are generalized as D_P structures.

WIDE-SCALE FOLD STRUCTURES – FRAMEWORK FOR DETAILED STRUCTURAL ANALYSIS

The thermal gradient was high during Svecofennian evolution (Korsman 1977 and Korsman et al. 1984 and 1999). It caused rapid changes in metamorphic conditions with depth. This had an important effect on regional variation in metamorphic grade, magma production and the characters of tectonic structures. In the southern Svecofennian domain the late, wide-scale folding and warping structures (D_G , D_H and D_I) substantially modified the tectonic geometry. These structures also deformed the magmatic rocks of the Southern Finland Granitoid Zone (SFGZ), although to varying extents. The regional-scale open

fold or warp structures with unpretentious axial plane properties are generally difficult to identify on outcrops. However, the interference structures formed a wide synform-antiform pattern that is clearly visible on lithological, tectonic (Figures 7 and 11) and magnetic maps. This interference pattern is accompanied by major shear and fault zones (Figure 10) and determines the recent regional distribution of lithological, structural and metamorphic units in the southern Svecofennian domain (Figure 11). The folds are therefore described prior to the older structures.

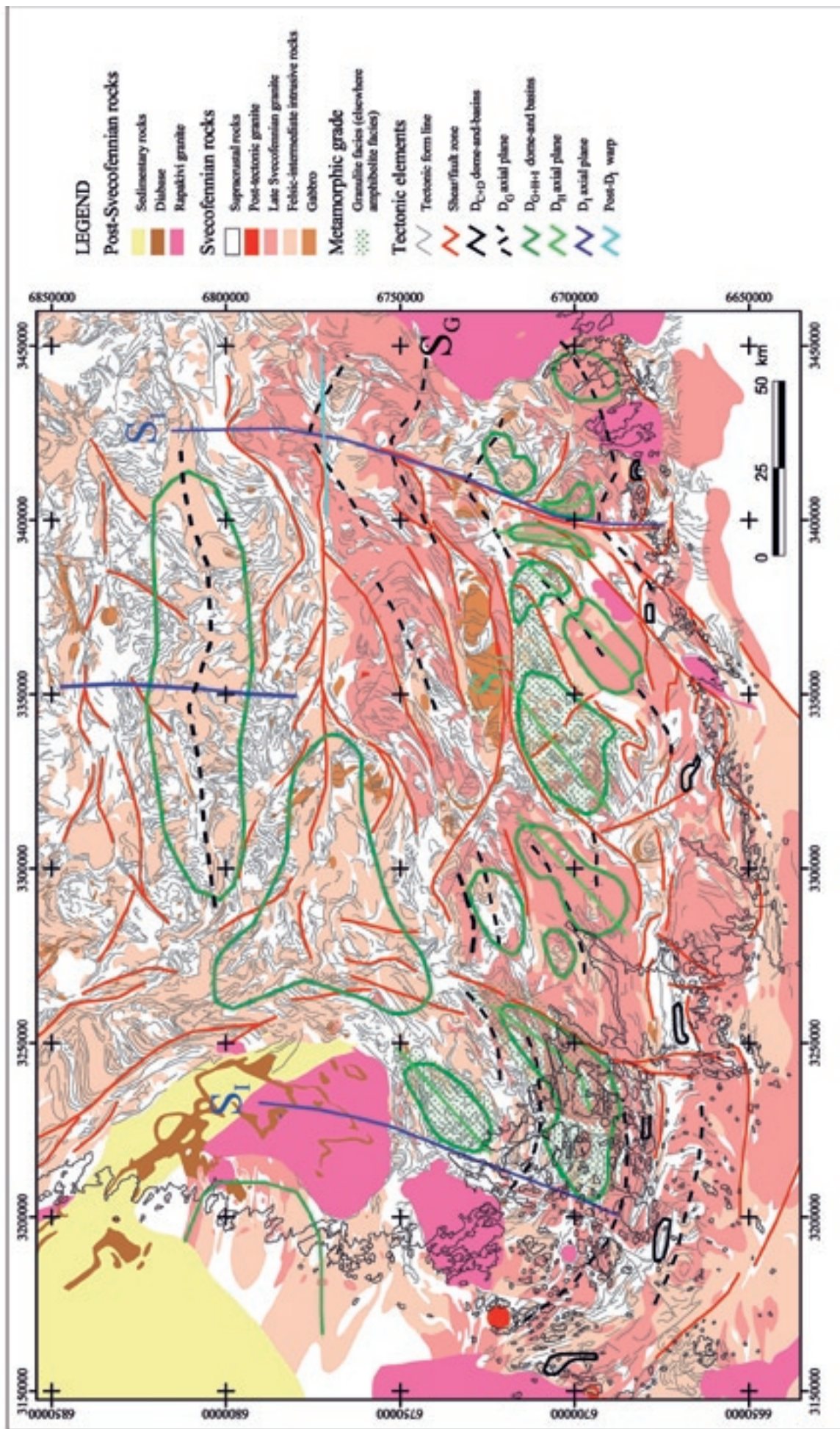


Figure 11. Large-scale fold structures and tectonic formlines in southern Finland. The formlines are constructed predominantly by using magnetic and structural element data of the Geological Survey of Finland (Finnish grid coordinates KJ3). Base map © National Land Survey of Finland, permit No. 13/MML/08.

Open folds with E-trending axial planes (F_G)

Originally open folds and warps (F_G), with an approximately vertical E-trending axial planes, indicate N-S shortening of the crust. On the present-day erosion level these folds determine the distribution of the E-W-trending granitoid-dominant complex, such as the Espoo Granitoid Complex (EGC) and Riihimäki Granitoid Complex (RGC), and the earlier supracrustal-magmatic units (Figure 11). This fold structure, together with the regional folds with NE-trending axial planes (F_H), determines the large-scale NE-trending dome-and-basin pattern characterizing the study area; the exposure of the West Uusimaa granulite Complex (WUC) and granitoid areas southeast of it, provides a good example. These folds are seldom identified on an outcrop scale.

Open folds with NE-trending axial planes (F_H)

Large-scale folds with NE-trending axial planes (F_H) (Figure 11) are constructed in Figures 12a and b from magnetic and gravity data. Up to 3 km for the amplitude and c. 8 km for the wavelength of the folding can be estimated. The axial plane estimated from field observations and the magnetic anomaly pattern is NE-trending, indicating NW-SE shortening. The folds are open and overturned northwestwards on the western limb of the major fold with a N-trending axial plane (F_I) (Figure 12c). The structure on the upwards-continued aeromagnetic map in Figure 12a indicates that shortening (D_{H+I}) extended into deeper levels of the crust. This ductile folding is identifiable in the southern part of the Svecofennian domain, especially in the Southern Finland Granitoid Zone (SFGZ). In the north, e.g. in the Tonalite Migmatite Belt (TMB), the crust deformed in a more localized manner, e.g. along the ENE-NE- and WNW-NW-trending crustal shear/fault zones that deform the major folds with E-trending axial planes (Figure 11). This indicates that the folding (F_H) represents a high-T event in the south, whereas stabilization/cooling at that time occurred far in the north. The foliation trends in the border zones of the tectonic units often reveal south-eastwards dipping high-strain zones (Figure 12b), e.g. the West Uusimaa granulite Complex-Espoo Granitoid Complex (WUC-EGC) boundary zone (Figure 9).

Open warps with N-trending axial planes (F_I)

In southern Finland the early tight (D_{C+D}) and also the less strained dome-and-basins (D_{G+H}) trend

approximately E-ENE (Figure 11). These structures are openly warped/folded (D_I) with wavelength up to 300 km and a steep axial plane trending c. N (010°).

The most intense bends exist in the detailed study area and in western Finland, from the SW archipelago to the Pori area. These coincide with the Baltic Sea-Bothnian Bay Zone (BBZ) and Riga Bay-Karelia Zone (RKZ), exemplified by the Vuosaari-Korso shear/fault zone in the detailed study area (Figures 8 and 10). In the northern parts of the detailed study area, ductile folding with a N-NNE-directional axial plane developed, indicating E-W shortening. The early dome-and-basin structures (D_{G+H}) tightened and were refolded/drag-folded into a N direction, especially near the Vuosaari-Korso zone. The open folds with a NW-trending axial plane to the west of Obbnäs rapakivi granite (4 in Figure 9) are related to this deformation (D_I) (Figure 11); its axial plane (S_I) is bent into a N-NNE-trend further north. The axial structure shows varying ductility characters; it is more ductile in the granite-dominant areas and deforms the NE-trending axial plane (S_H). Corresponding folds also exist in the southern Sipoo area, where they form complex dome-and-basin interferences (D_{G+H+I}).

The shapes and setting of the granulite-facies areas, the West Uusimaa granulite Complex (WUC) and central Sipoo area (Si in Figure 9), are a consequence of the large-scale dome-and-basin geometry (D_{G+H+I}) (Figure 11). The high-grade rocks are exposed in the antiformal settings of the structures. The corresponding interference pattern (predominantly D_{G+H}) also defines the large, open tectonic dome-and-basins such as the Nuuksio synform (Nu in Figure 9), which was reoriented in the N-trending Vuosaari-Korso axial zone (S_I). The supracrustal Southern Volcanic-sedimentary Belt (SVB) is predominantly characterized by the earlier isoclinal dome-and-basin geometry (D_{C+D}), which in the study area is complexly deformed by the crustal-scale the Vuosaari-Korso (D_I) and Porkkala-Mänt-sälä shear/fault zones (D_G) (Figures 10 and 11).

Small amounts of granite veins locally intruded into the N-trending axial planes (S_I), indicating high temperatures during deformation, but the latest semi-brittle axial plane structures provide evidence of decreasing temperatures during its later stages. Semi-brittle to sharp brittle faults with a N-NNE orientation, and dense jointing cutting the open fold pattern described from the Vuosaari-Korso shear/fault zone, indicate late reactivation of the zone (Elminen et al. 2008 and Wennerström et al. 2008). The character of the structure (D_I) changes from ductile in the area of the Southern Finland Granitoid Zone (SFGZ) to brittle in the Lake Päijänne fracture

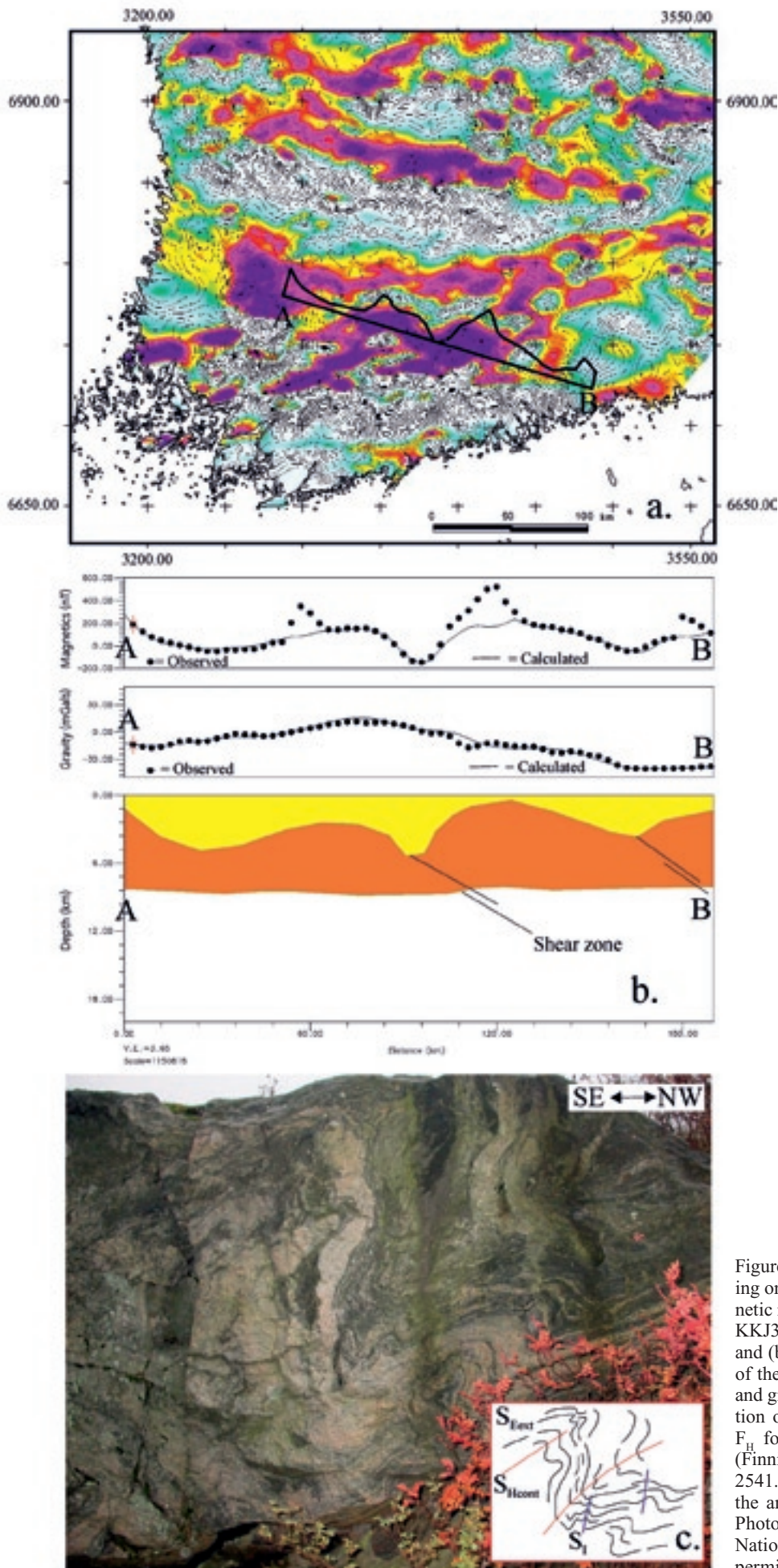


Figure 12. (a.) Large-scale D_H folding on the upwards-continued magnetic map (Finnish grid coordinates KKJ3) with the interpreted profile and (b.) geophysical interpretations of the structure from aeromagnetic and gravity data. (c.) A vertical section of northwestwards overturned F_H fold in Nurmijärvi, Klaukkala (Finnish grid coordinates KKJ2 2541.83E 6696.47N); width of the area of the figure is c. 1.5 m. Photo by M. Pajunen. Base map © National Land Survey of Finland, permit No. 13/MML/08.

zone (Figure 10 and Sederholm 1932b), in the Tonalite Migmatite Belt (TMB) and the Central Finland Granitoid Complex (CFG). This suggests different thermal evolutions in the areas; the northern units were cooled at the time of ductile deformation and magmatism in the south.

Open warps with E-trending axial planes (post- D_1)

The ductile N-S axial plane (S_1) is openly warped in c. N-NNE-shortening: the post- D_1 warp in Figure 11. The semi-brittle structures in the Vuosaari-

Korso shear/fault zone also show such open bending and the early tight domes-and-basins (D_{C+D}) are deformed in a complex manner south of the Vuosaari area (Vu in Figure 9). We have not established whether these late structures are related to the latest Svecofennian events that occurred essentially later in Estonia (Puura et al. 2004) than observed so far in Finland. The latest movements in the N-trending axial zones (D_1) are related to post-Svecofennian events (D_p) prior to or during the rapakivi stage, and even to later stages of crustal evolution (cf. Mertanen et al. 2001, 2008 and Bergman et al. 2006).

DETAILED DESCRIPTION OF STRUCTURAL SUCCESSION

Structural evolution preceding the Southern Finland Granitoid Zone

Primary associations and D_A deformation

The earliest identified tectonic structures in the study area are the intrafolial isoclinal F_A folds preserved in the compositionally-layered volcanic or metasedimentary rocks. A migmatitic mica gneiss outcrop in the Espoo Granitoid Complex (EGC) at the Hakkila site, Vantaa, excellently shows the relations between the early structural events and the primary sedimentary-volcanic structure (Figure 13a). In a schollen fragment of the mica gneiss, a layered felsic rock, a psammitic portion of the mica gneiss, is cut by a zoned mafic dyke (Figure 13b). The felsic rock has a weak, nearly bedding/ S_0 -parallel S_A foliation (Figure 13c). It was lithified and D_A -deformed before the intrusion of the mafic dyke into a brittle fracture at a high angle to S_0 and S_A . The dyke has narrow, altered, chilled margins, seen as a grain-size decrease towards the contact, indicating intrusion into a cool environment. On the same outcrop the primary bedding, S_0 , of psammitic metasediment shows remnant isoclinal F_A folds (Figure 13d) with weak penetrative S_A foliation, which was later strengthened and migmatized by D_B . The S_A foliation and a weak F_A folding remnant beside the mafic dyke (Figure 13c; white arrow) constrains the structure in the schollen fragment to those (Figure 13d) in the gneiss nearby. The mafic dyke was M_B -metamorphosed and D_B -deformed. The D_B structures in the surrounding mica gneiss are strongly overprinted by later deformations. The mafic fragmentary (possible agglomerate, Figure 13e) and layered volcanic rocks (Figure 13f) show M_B metamorphic parageneses, but their relations to D_A are not known.

Garnet-bearing migmatitic felsic gneiss (Figures 14a-d) from the Southern Sedimentary-volcanic Belt (SVB) at the Kalkkiranta site, on the Sipoo coast, includes intra-folial F_A folds (Figure 14c) in a D_B -foliated rock. It also has D_B -boudinaged and rotated amphibolite fragments (Figure 14d). F_A folds also occur in the associated, shallow-water, impure limestones/marbles in the Kalkkiranta mine. Due to later higher-grade processes, carbonates were often remobilized into dilatational fractures, like in the West Uusimaa granulite Complex (WUC, Appendix 2). A garnet-bearing, intermediate dyke with chilled margins cut the F_A -folded gneiss (Figures 14a and b) and was deformed and metamorphosed in D_B . This post- D_A to pre-/early D_B dyke shows a corresponding setting to the volcanic dykes in Hakkila. Boudinaged mafic fragments have a strong lineation (Figure 14e) similar to the F_A -folded felsic host gneiss; it is an intersection lineation, $L_{A+B/C}$ (structural relations summarized in the inset in Figure 14).

Thus, two tectonically-differentiated volcanic sequences occur: the earlier volcanic Series I (pre- D_A) including the F_A folds, and the later volcanic Series II (post- D_A to pre-/early D_B) cutting the D_A structures. Both are deformed and metamorphosed during the D_B . The described tectonic relationships also support the view that at least part of the psammitic to pelitic sediments were lithified and deformed, before the mafic dykes and the closely-associated volcanic rocks were formed.

The F_A folds are flame- or sharp-hinged with thickened hinges and thinned limbs (Figure 15a). The flame-shaped F_A hinges are interpreted as being a result of low-temperature deformation, which caused a brittle to semi-brittle, spaced, fracture foliation in the S_A axial plane. The spaced segments were transposed along the foliation planes under continuous D_A flattening. Later higher-grade ductile

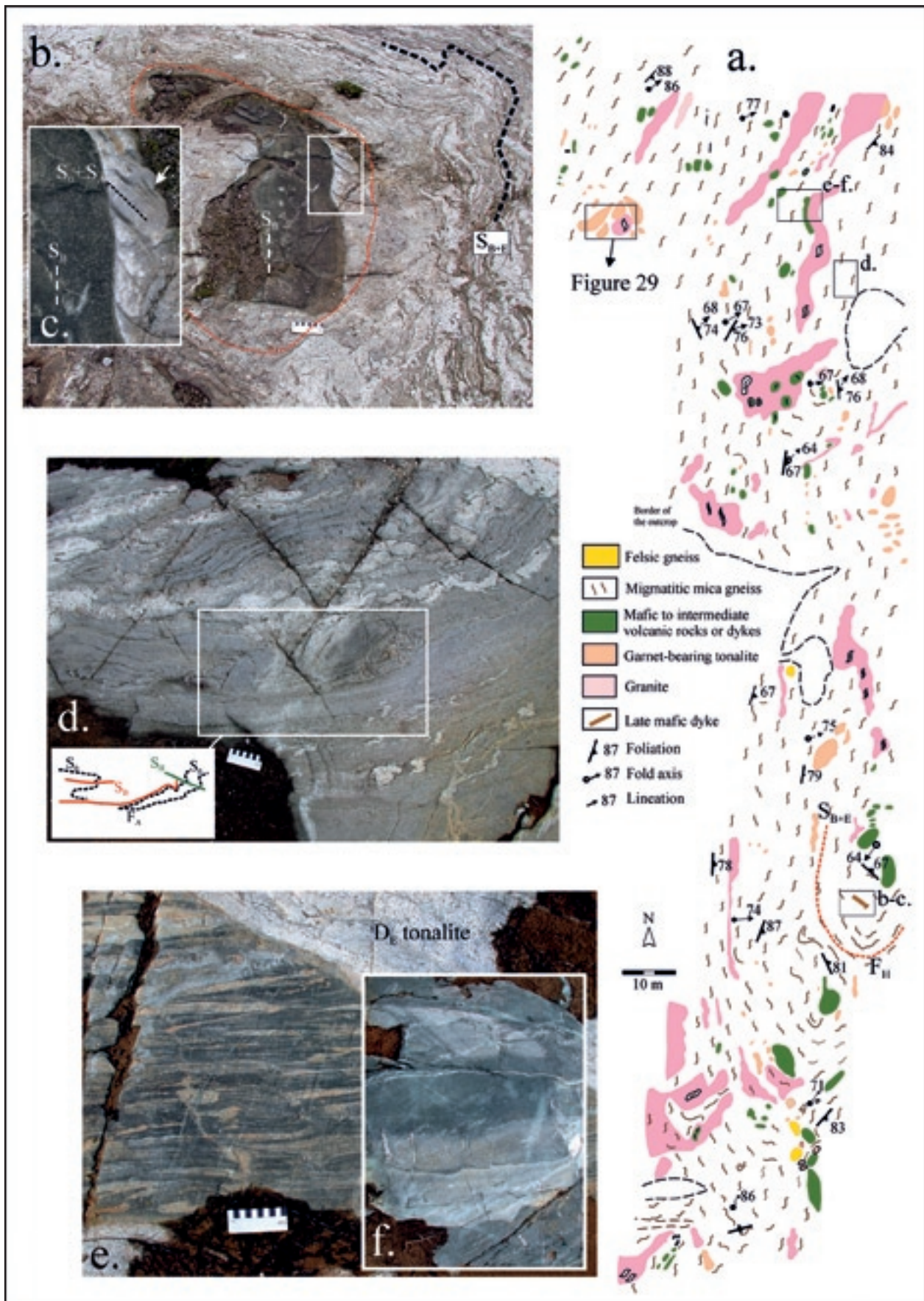


Figure 13. (a.) Detailed map of a migmatitic mica gneiss outcrop in Hakkila, Vantaa (Finnish grid coordinates KKJ2 2560.64E 6687.59N). The locations of Figures 29 and 13b-f are shown with boxes. (b.) Fragment of an amphibolitic dyke (red dot line) in migmatitic mica gneiss. Scale bar is 10 cm in length. (c.) A detail in (b.) (white box) showing the dyke edge against the psammitic portion of the mica gneiss; the dyke was intruded into D_A -deformed rock; (d.) F_A and F_B folding in psammitic layers of migmatitic mica gneiss. Scale bar is 10 cm in length. (e.) Fragment of fragmentary mafic volcanic rock cut by D_E tonalite. Scale bar is 10 cm in length. (f.) Layered volcanic rock in migmatitic mica gneiss. Width of the area of the figure is c. 2 m. Photos by M. Pajunen.

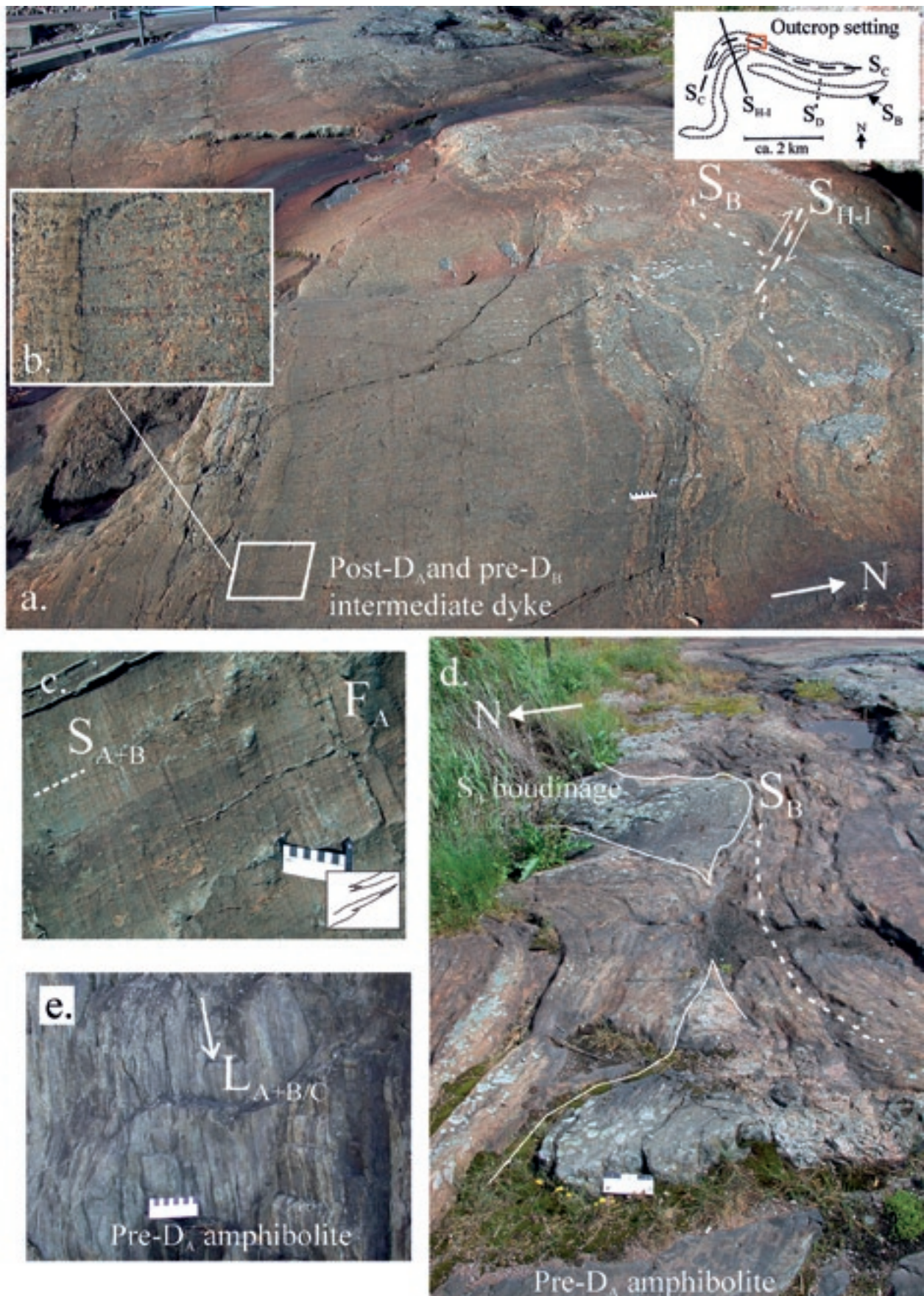


Figure 14. (a) A metamorphosed intermediate dyke cutting migmatitic garnet-bearing felsic gneiss with a chilled margin in an intermediate dyke shown in Figure (b). Scale bar is 10 cm in length. (c.) F_A folds in felsic gneiss. Scale bar is 10 cm in length. (d.) D_B boudinage structure of amphibolitic layers in migmatitic felsic gneiss. Scale bar is 15 cm in length. (e.) $L_{A+B/C}$ lineation in a D_B -boudinaged amphibolite. Scale bar is 10 cm in length. Kalkkiranta, Sipoo (Finnish grid coordinates KKJ2 2577.26E 6683.23N). Photos by M. Pajunen.

deformation and metamorphism transformed the folds into a flame shape. These types of “low-temperature” fold hinges also characterize the earliest fold phases elsewhere (cf. Koistinen 1981, Hopgood 1984 and Pajunen et al. 2008). However, the later more ductile folds, refolding the earlier schistosity or foliation, show more or less rounded and unbroken hinges. S_A is weak foliation. At present it is composed of biotite and is sometimes crenulated by S_B . It parallels the F_A limbs and bedding S_0 . Generally, D_A phases were consumed by the later mineral growth, particularly D_B ; pelitic layers were effectively melted during the later high-grade events. No mineral, veining or melting phase can be connected to D_A . Hitherto, there are no direct indications of metamorphic conditions during D_A . The brittle character of the contact relations between the felsic gneiss and the post- D_A volcanic dyke, and the “low-temperature” flame-hinged F_A folds, indicate low-grade conditions during D_A . Kilpeläinen and Rastas (1990) described early, low-T quartz segregations from the andalusite schists of the Orijärvi area; we relate the quartz veins in the Vetio andalusite-cordierite schist to a later prograde metamorphism following the cooling stage after the early tectonothermal events D_{A-D} ; the veins are related to D_H (Appendix-Fig. 4-1).

The isoclinal F_A folds are identified from the steep supracrustal units, in sections perpendicular to S_0 ; in horizontal sections, F_A folds are seldom recognisable (cf. Figure 6). Indications on depositional top directions are rare and not helpful for lithostratigraphic analysis. The primary associations show strong shortening, but the original D_A strain cannot be estimated, because the following D_B shows the main compressional axis roughly paralleling that of D_A . In the E-W-trending, upright parts of the Southern Volcanic-sedimentary Belt (SVB), not strongly affected by the later high-grade crustal bends, the sub-horizontal F_A axes trend c. E-W (cf. Pajunen et al. 2008), roughly referring to N-S-directional tectonic transport. However, the axes can be followed only a few meters on the outcrops and, when taking into account the effects of the later deformations, like rotation due to D_B shearing (Figures 14d and 15b), this estimation should be regarded as suggestive. The rarity of the F_A folds may indicate that they were originally very large.

Age of D_A deformation and correlations

According to recent observations the age of D_A deformation in the Espoo Granitoid Complex (EGC) and Southern Sedimentary-volcanic Belt (SVB) is between the ages of the early volcanic rocks (Series I) and later volcanic rocks (Series II), i.e. 1.90–1.88

Ga and 1.88–1.87 Ga, respectively (Väisänen & Mänttari 2002). The age of Series II is approximately the same as that of intrusive D_B magmatism: these relations are discussed in more detail later. The 1.90–1.89 Ga age of volcanism in the Tampere Schist Belt (TSB) (Kähkönen 1989), corresponds to that of the early volcanic Series I.

The oldest dated granitoid in the study area is the 1898 ± 2 Ma Orijärvi granodiorite, which is interpreted as co-magmatic with the bimodal volcanism in the Orijärvi area (Väisänen & Mänttari 2002). According to Suominen (1991), the syntectonic Algersö granodiorite in Föglö, in the southwestern archipelago SW of Turku, is 1899 ± 8 Ma in age (Southern Volcanic-sedimentary Belt, SVB). There have so far been no descriptions of the relations between D_A structures and these oldest granitoids.

The earliest structurally-fixed magmatic rocks in the study area are mafic rocks dated by Hopgood et al. (1983) in the Jussarö-Skåldö area (Ju in Figure 9) (ages are discussed under D_B). Hopgood et al. (1983) proposed a primary volcanic-volcanogenic origin for the rock assemblage. Hopgood (1984) described two intrafolial fold sets from the Skåldö-Jussarö area, F_{aa} and F_{ab} ; S_{aa} is folded around F_{ab} fold hinges. The tightly refolded, round-hinged folds (Figure 13d) are rare in our data and we relate them to the D_B flattening. This does not contradict the possibility of local isoclinal folds (F_{ab}) between F_A and F_B of this study – we have limited data from the well-exposed, clean coastal outcrops studied by Hopgood (1984). Hopgood et al. (1983) and Hopgood (1984) did not describe F_A folds from the mafic agmatitic rocks, but they related the gabbro foliation to the earliest deformation phase in the area. Nevertheless, the foliation-forming mineral assemblage of the rocks indicates metamorphism under amphibolite facies conditions, which according to our observations points to conditions not achieved until D_B . We relate the post- D_A /pre- D_B mafic and intermediate dykes (Figures 13b and 14a and b) of the study area to the later volcanic rocks, Series II.

Summarizing, we have not identified D_A structures from the later volcanic Series II (post- D_A to pre/early- D_B) or from the gabbroic-tonalitic association (pre-/early D_B) in the Southern Sedimentary-volcanic Belt (SVB, see D_B description). The Hyvinkää Gabbroic-volcanic Belt (HGB, Appendix 3) and the high-grade gneisses of an upper tectonic unit of the southern Svecofennian domain, referred to here as the Upper Tectonic Unit (UTU) (Appendix 6), do not show F_A folds either. The evolution of the Jokela sedimentary-volcanic association is dated to considerably later, post-dating D_C (Appendix 5). No F_A folds are defined from the Vetio andalusite-cordierite schist in the Orijärvi area (Appendix 4), either.

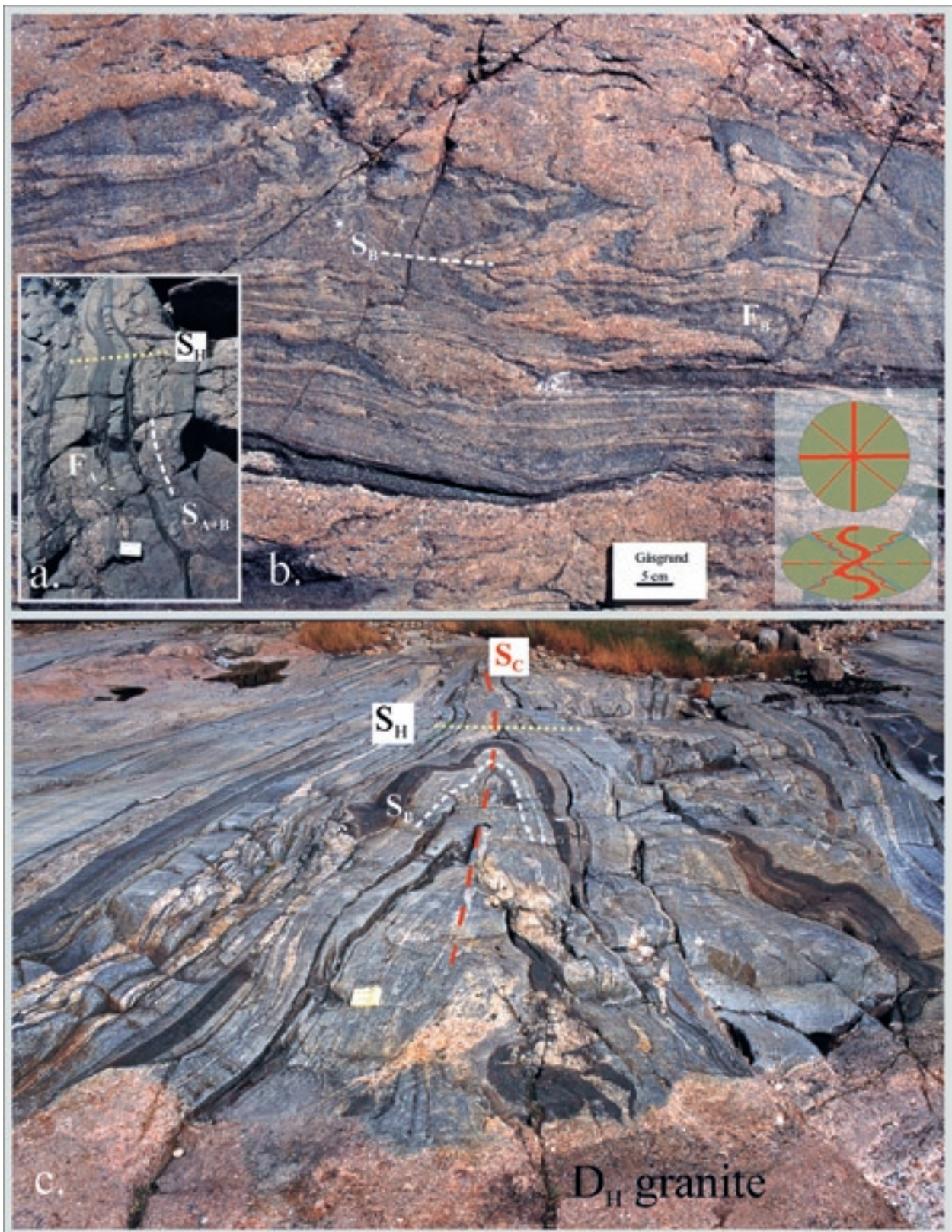


Figure 15. (a.) Flame-hinged F_A folding in felsic gneiss with mafic layers. The F_A axis is close to horizontal. S_{A+B} is c. ENE-WSW-trending; scale bar is 7 cm in length. (b.) D_B folding and migmatization in mica gneiss. Anti-clockwise D_B rotation of competent fragments and shearing parallel to S_B foliation planes indicate that the D_B strain was not pure shear strain in the study area (the pure shear strain flow model with related folding and boudinage patterns is shown in the inset). S_B is c. ENE-WSW-trending. (c.) An F_C fold in layered felsic gneiss cut by a D_H granite dyke. S_C is c. ENE-WSW-trending; scale bar is 7 cm in length. Gåsgrundet, Espoo (Finnish grid coordinates KJ2 2541.86E 6664.80N). Photos by M. Pajunen.

D_B deformation – extensional event with intense crustal flattening

The D_A structures and the early supracrustal sequences, including both the volcanogenic Series I and II, were deformed in a strong, penetrative D_B deformation that occurred under progressive metamorphic conditions. D_B structures also characterize the gabbroic associations described by Hopgood (1984). Intense vertical shortening deformation, melting and intense intrusive magmatism typify the D_B.

F_B folds are isoclinal to tight with thickened, roundish hinges and thinned or boudinaged limbs (Figures 13d and 15b). Penetrative, or locally zoned, S_B mineral foliation developed sub-parallel/parallel to S₀ and S_A. The F_B folds are only occasionally observed to refold the primary bedding S₀ or S_A (Figure 13d), because the early structures were originally close to horizontal position. Generally, D_B only strengthened the F_A folds. However, isoclinal to tight F_B folds in the syn-D_B migmatizing neosome veins are typical (Figures 15b). Deformation was often localized in D_B shear zones along the F_B fold limbs and, in places, competent boudinage fragments were rotated due to D_B shearing (Figure 14d). A melt fraction developed into the pressure minimums of the boudinaged necks. L_B lineation is weak, but an intersection lineation is evident, for example, in amphibolites; L_{A+B/C} in the early volcanic amphibolites (Series I, Figure 14e) and L_{B/C} in the later ones (Series II, Appendix-Fig. 3-2c).

The D_B neosome veins are quartzo-feldspathic or trondhjemitic in composition during the early stages; later more granitic melts were formed (Figure 13b and 15b). According to Mouri et al. (1999), the composition of neosomes depends on the activity (aH₂O) of participating fluid components and the primary rock composition. D_B migmatization was polyphase due to successive melting and intrusive magma events under continuous flattening and heating. In the Southern Finland Granitoid Zone (SFGZ) it is sometimes impossible to fix the neosome phase to just the D_B because of strong later melting events. On an outcrop scale, the D_B structures often are quite similar to D_{E+H} structures, especially where a weak D_B is overprinted by a strong D_{E+H}. The S_B represents the main foliation in the supracrustal areas of weak D_{E+H}. The similarity of the D_B and D_{E+H} structures has been one of the major “stumbling blocks” in analyzing the structural successions in the southern Svecofennian domain: they may both represent the second deformation event in a particular area, but there is an important time gap between them. The problem becomes particularly evident in areas where only a few structurally-fixed date deter-

minations are in use. The identification is straightforward if a cooling stage can be established between the events (e.g. Sederholm 1926 and Pajunen et al. 2008).

Koistinen et al. (1996, Figures 26 and 27, page 50) provide an example of weakly lineated, chocolate tablet D₂ boudinage from Uusikaupunki, c. 80 km SSW of Pori, indicating weakly ellipsoidal flattening strain. We have not found good three-dimensional sections to analyze the kinematics of D_B boudinage structures. The subhorizontal to horizontal position of the S_B can be constructed by analyzing the position of the enveloping surface of F_{C+D} domes, but only on an outcrop-scale. On a map-scale, the ductile D_B shearing and later structures between the domes complicate such analysis. The observations suggest that the main strain was sub-/horizontal flattening; the strain was not just pure shear, as modelled in the inset Figure 15b, but the rotated D_B boudinages (Figure 14d) and shearing along the F_B limbs (Figure 15b) refer to some shear component during the deformation.

Structures in magmatic rocks related to D_B deformation

The early Svecofennian magmatic rocks are foliated, complexly deformed and intruded by several later magma and migmatization events. They have amphibolite to granulite facies mineral parageneses. Analysis of the tectonic setting of these intrusive rocks necessitates the description of their field relations with respect to the early structures in their hosts as well as to the later structures existing in them. Hence, the following examples also describe the post-D_B structures that will be discussed in more detail later.

Structures in pre-/early D_B gabbroic associations

The earliest magmatic rocks related to deformation are banded or layered mafic rocks showing variation in composition from assimilated ultramafic remnants to gabbros and diorites in the Jussarö-Skåldö area (Ju in Figure 9). Hopgood et al. (1983) and Hopgood (1984) proposed a primary volcanic-volcanogenic origin for the rock assemblage. The gabbros were intruded and injected by tonalitic magmas and by amphibolitic dykes. In Simijärvi (Si in Figure 16), to the south and east of the Orijärvi area (Or in Figure 9), occur corresponding, locally sheared, gabbroic rocks (Figures 17a and b). The Salittu ultramafic rock (Sa in Figure 16) is situated to the N of Simijärvi. The association is exposed along a rather coherent zone in the southern coast and archipelago in the Southern Volcanic-sedimentary Belt

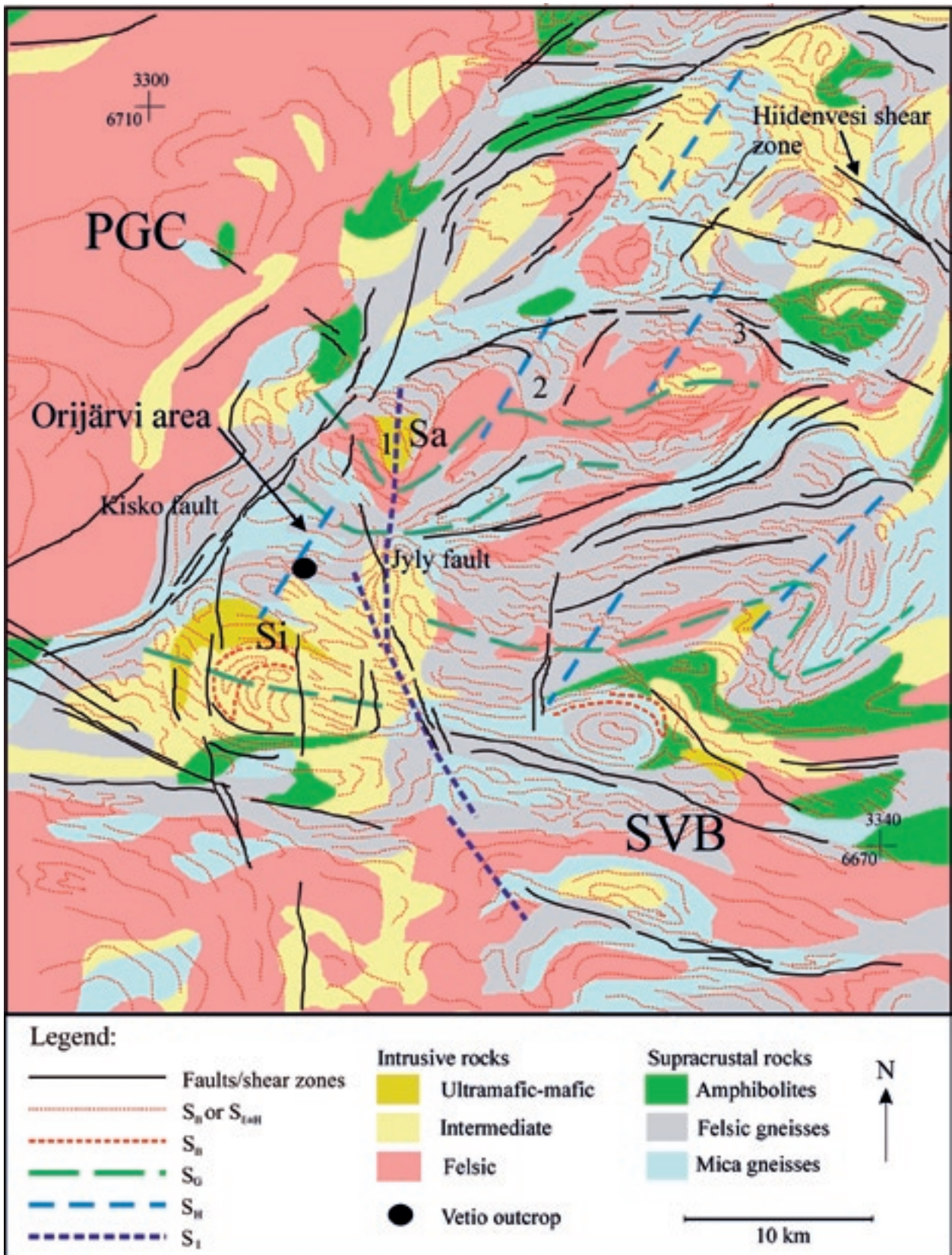


Figure 16. Tectonic structure of the Orijärvi area. Si = Simijärvi, Sa = Salittu, 1–3 mafic to ultramafic rock in tectonically similar settings (see text) (Finnish grid coordinates KKI3).

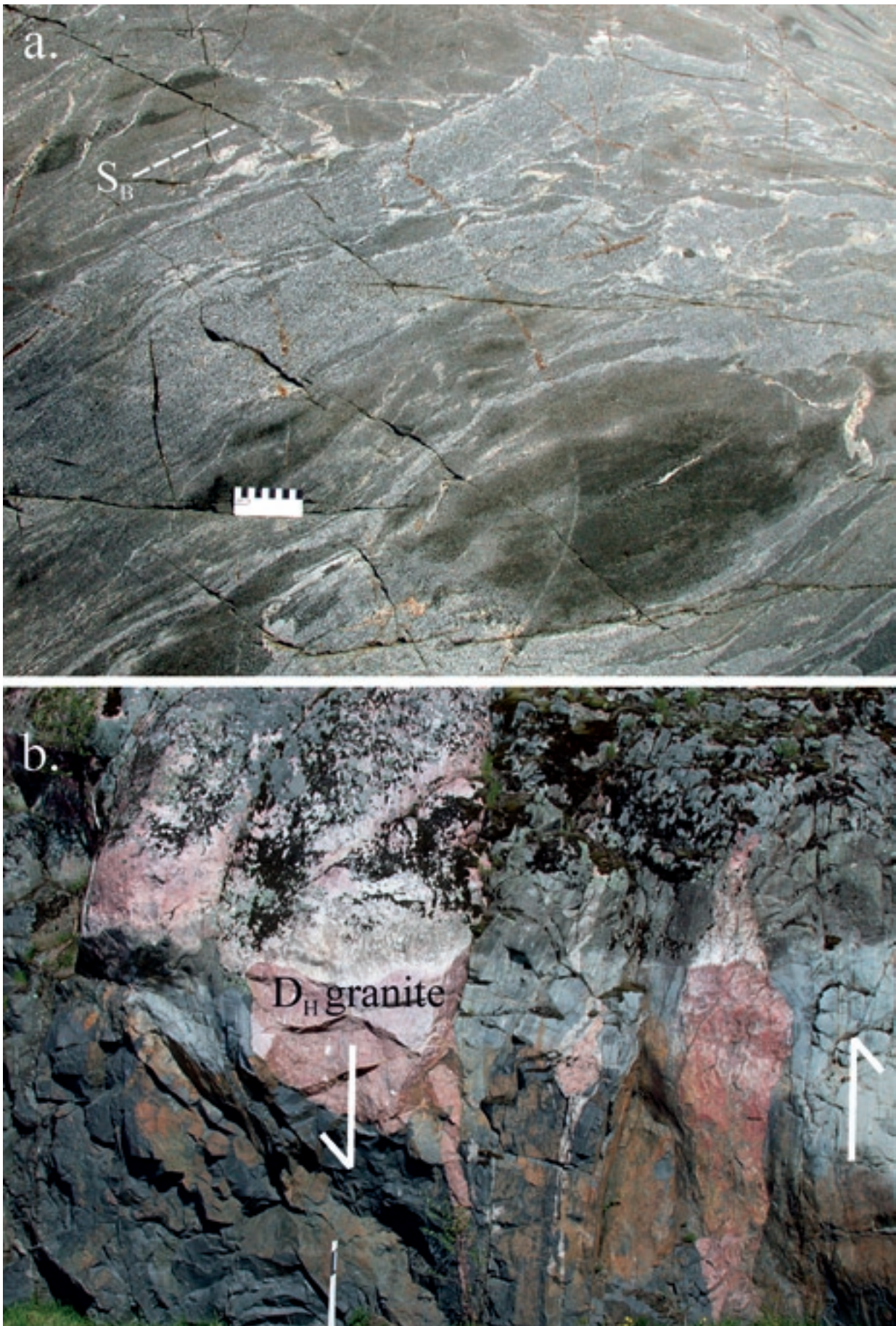


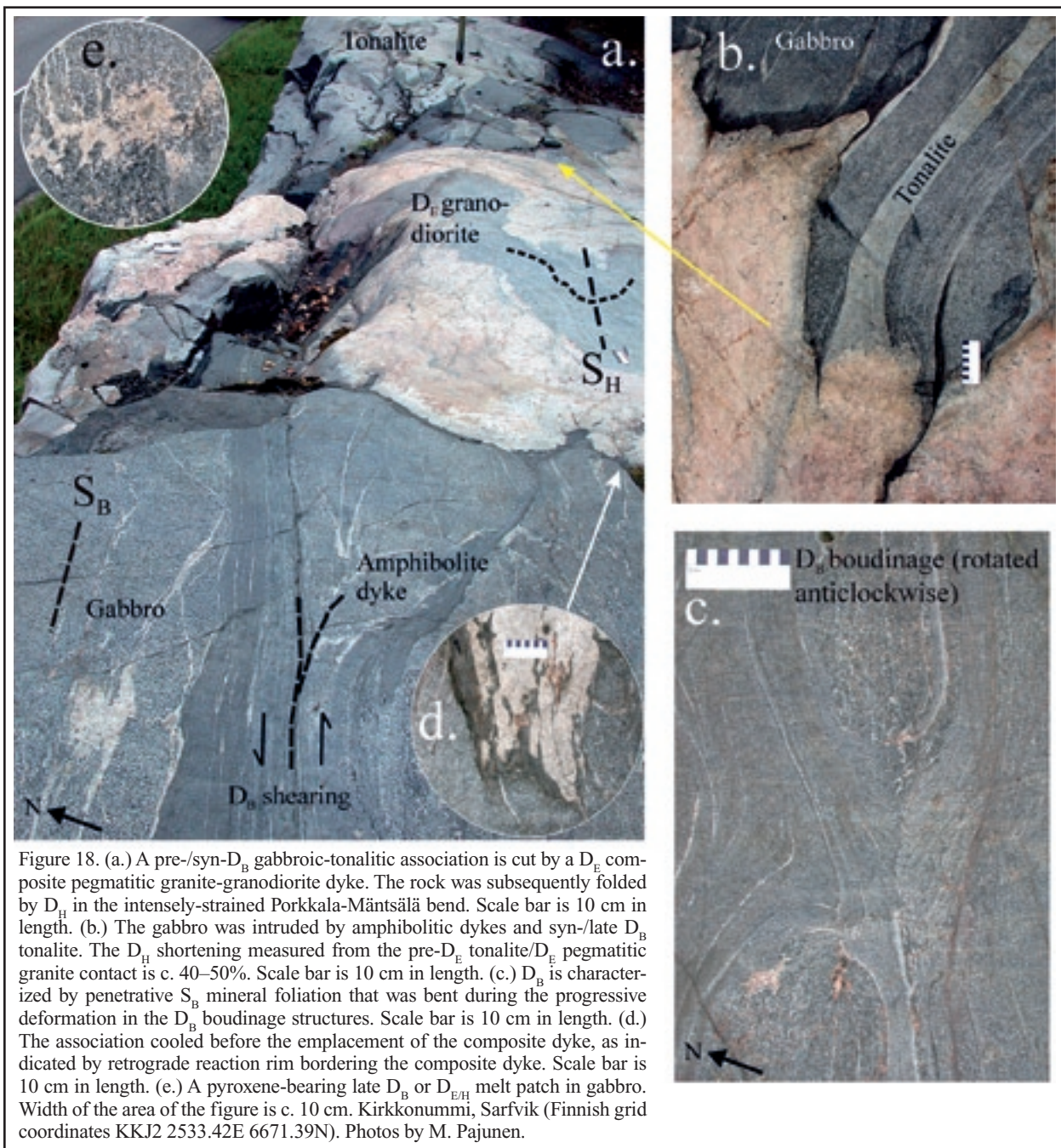
Figure 17. (a.) A pre-/early D_B gabbroic-tonalitic association with tonalitic magma cutting and assimilating the gabbro and ultramafic fragments. Scale bar is 10 cm in length. (b.) Strongly-sheared gabbroic rock on the same outcrop representing deformation in the Southern Finland shear zone. Width of the area of the figure is c. 3 m. Bollstad N, Inkoo (Finnish grid coordinates KKJ2 2494.50E 6661.50N). Photos by M. Pajunen.

(SVB), e.g. Kopparnäs in Siuntio, Sarfvik and Evitskog in Kirkkonummi, and Kauklahti in Espoo (locations are shown in Figure 7). The sinistral Porkkala-Mäntsälä shear zone in the east cuts the zone.

The Sarfvik site is an example of the structural relationships of the gabbroic association and the Porkkala-Mäntsälä crustal bend. The medium-grained gabbro (Figure 18a) was intruded by a gneissic tonalite (Figure 18b). The gabbro has an amphibolite-facies, penetrative mineral foliation, S_B , which locally appears as shear foliation. The gabbro shows weakly rotated D_B boudinage structures (Figure 18c). We have not identified D_A structures in the rocks. Hopgood et al. (1983) also did not describe folds that can be correlated to F_A of this study from the Jussarö-Skåldö area. They related

the foliation to the first deformational phase. We suggest that it corresponds to S_B : the metamorphic assemblages related to the penetrative foliation and weakly rotated boudinages are characteristic for D_B . Thus, we link the rocks to a pre-/early D_B gabbroic association. The D_B structures were later cut by granitoids (Figures 18a and b) showing a retrograde reaction rim against the gabbro (Figure 18d) and overprinted by later metamorphic events, such as high-grade melt patches related to the late stage of D_B or $D_{E/H}$ (Figure 18e). The D_E granitoid in Sarfvik does not show such high-grade mineral assemblages.

The post- D_B deformations in the gabbroic rocks have been studied at the Kauklahti site (Figure 21a), in the amphibolitic wedge shown on the geological map (Laitala 1960 and 1961, Ka in Figure 7) to the



southwest of the Bodom rapakivi intrusion (3 in Figure 9) and to the west of the Porkkala-Mäntsälä shear/fault zone (Figure 10). A low-angle, E-W-trending gabbroic wedge dips gently towards the north, below the granitoids of Nuuksio (Nu in Figure 9). The gabbro was foliated, boudinaged and sheared and resembles a layered volcanic rock (Figure 19b); we interpret the layered structure as tectonic caused by the shearing of an originally heterogeneous ultramafic-mafic to tonalitic rock. The structures indicate intense flattening with contemporaneous shearing in amphibolite facies conditions. The S-C intersection and slicken line lineations in the shear planes indicate reverse top-to-SE faulting with a dilatation zone in the NW, i.e., in the direction of the West Uusimaa granulite Complex (WUC). We relate the shear planes to the $D_{E,ext}$ dilatation; further NW from the Porkkala-Mäntsälä shear/fault zone the $S_{E,ext}$ foliation is only gently to openly folded by later deformations, which is typical for the $D_{E'}$, but not the case with the tightly D_{C+D} -folded D_B structures. Instead, the S_B , corresponding to that in Sarfviik, is preserved as penetrative min-

eral foliation in the gabbroic boudinage fragments. Recumbent F_E folds are very small and deform the felsic veins or, due to progressive deformation, more seldomly the sheared layering S_E itself. The kinematic setting (D_E) is exactly the same as at the Klaukkala site, described later. The described $D_{E,ext}$ structures are re-boudinaged during $D_{H,ext}$ with pegmatitic granitic melt emplaced in the boudinage neck (Figure 19c). The $S_{E,ext}$ -layered structure was overturned towards the south, supposedly as F_G folds, and refolded by the $F_{H,cont}$ folds overturned northwestwards (Figure 19d). The latest granites of the Espoo Granitoid Complex (EGC) cut the gabbroic association and the shear foliation (S_E). In the western extension of the Kauklahti gabbroic association, in Evitskog, Kirkkonummi (Ev in Figure 7), the strongly deformed and assimilated remnants of mafic rock, corresponding to that in Kauklahti, are preserved as inclusions in a D_H granite. This supports the view that the main deformation in the Kauklahti site occurred before the D_H deformation.

According to the structural interpretation, based on field observations, regional geophysical data and

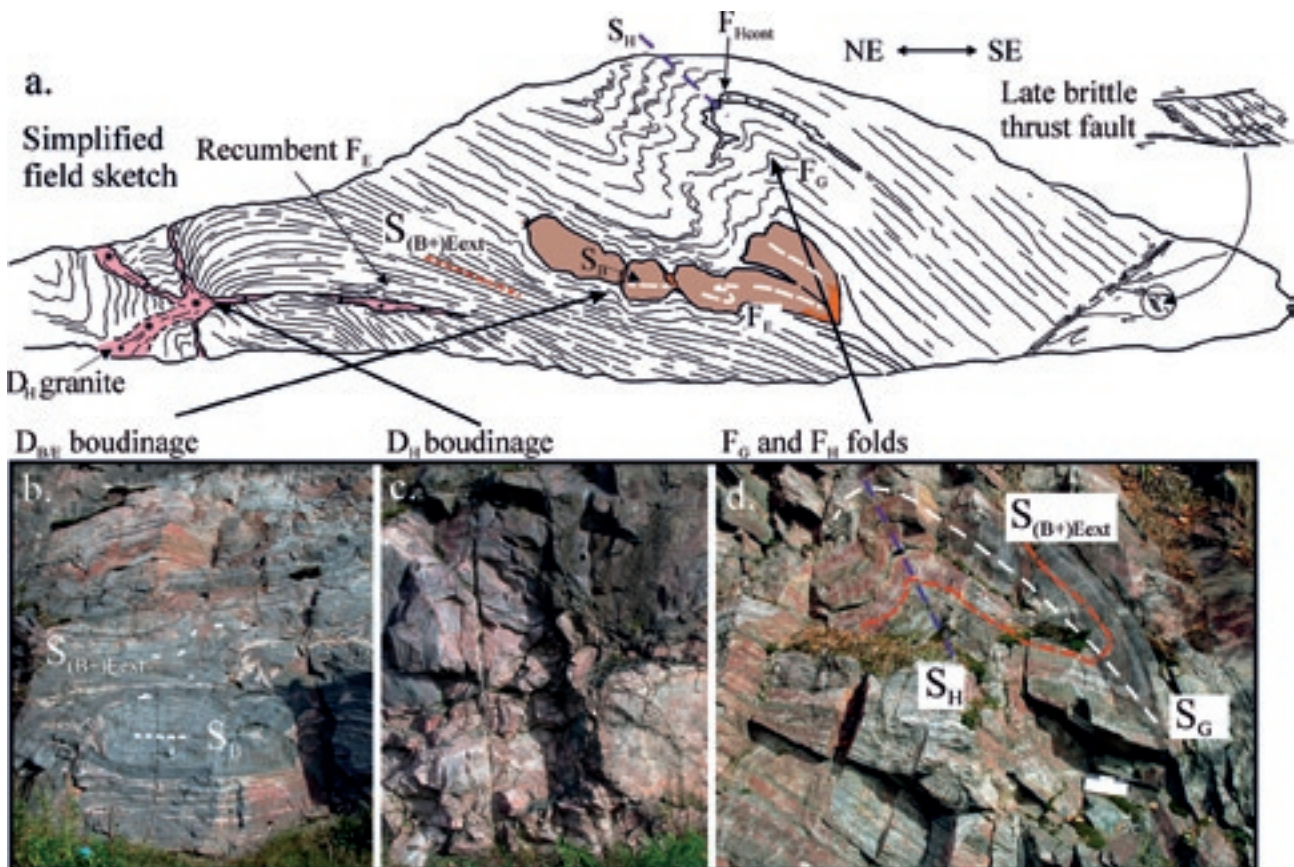


Figure 19. (a.) A simplified field sketch of a road cut showing layered amphibolitic gneiss interpreted as strongly D_E -deformed pre-/early D_B gabbroic rock. (b.) S_B is preserved in the gabbroic boudinage fragments; the main foliation is linked to $S_{E,ext}$, indicating top-to-SE movement. The initiation of D_E boudinaged gabbroic fragments possibly has its roots in D_B (cf. Figure 18c). Width of the area of the figure is c. 2 m. (c.) The D_E structures are re-boudinaged by the D_H with pegmatitic granite intruded into the boudinage neck. Width of the area of the figure is c. 1.5 m. (d.) The D_E structures are refolded by the c. south-eastwards overturned F_G and c. north-westwards overturned $F_{H,cont}$ folds. The post-Svecofennian brittle thrust fault deforms all the structures. Scale bar is 15 cm in length. Kauklahti, Espoo (Finnish grid coordinates KJK2 2532.08E 6675.58N). Photos by M. Pajunen.

the geological map of Koistinen (1992), the locally-sheared gabbroic association (Figures 17a and b) at Simijärvi (Si in Figure 16) forms a refolded synformal structure that can be correlated to the D_{C+D} domes-and-basins in the surrounding Southern Volcanic-sedimentary Belt (SVB). This D_{C+D} structure was refolded by F_G folding with an E-trending axial plane and by F_I folding with a NNW-trending axial plane. The S_I axial plane bends to a north trend further north and refolds the E-W-trending S_G at Salittu (Sa in Figure 16). The Salittu ultramafic rock (cf. Mikkola 1955) is situated in a northwards-opening fold structure (F_{G+I}), near the northern border of the granitic zone. The tectonic setting of the granitic zone is controlled by the F_G folding. Mafic rocks (amphibolites) in corresponding settings exist to the ENE of Salittu (2 and 3 in Figure 16). On a structural basis the Salittu (1) and mafic rocks ENE of it (2 and 3) are related to the mafic association in Simijärvi due to the large-scale, open F_G folding. Thus, the tectonic setting of the Simijärvi and Salittu ultramafic-mafic associations suggests their close relations (Figure 16). Their genetic relation to the lower-grade rocks in Orijärvi has not yet been based on structure.

Due to their high competence the ultramafic-gabbroic rocks were resistant to small-scale folding, but a regional folding pattern (Figure 16) can be constructed from the mapping and geophysical data. These medium-grained rocks are S_B -foliated with amphibolite facies assemblages, but locally strong later events overprint the D_B structures, like D_{E-H} in Kauklahti. The magmatic structures in the medium-grained rocks, such as assimilation and mobile magma contacts without chilled effects (Figure 17a), point to processes that occurred quite deep in the crust. The compositional variation from ultramafic and gabbroic to dioritic and tonalitic may represent a differentiated magma evolution. For these reasons, we suppose that these rocks are not tightly associated with the lower-grade, volcanic rocks in Orijärvi nearby, but the contacts are tectonic as often suggested by the discordant geophysical features and by the sheared structures (Figure 17b and 18a). This does not preclude a genetic connection to the volcanic associations as postulated by Hopgood et al. (1983) and Väisänen and Mänttari (2002). We have not identified D_A structures from these rocks to support the possibility that D_A transported these rocks close to the lower-grade gneisses. It is also possible that these kinds of rocks evolved at different times with respect to D_A , just as is the case with the volcanic sequences, Series I and II. Our observations so far fix these S_B -foliated rocks, without identified D_A structures, to formation during the early stage of D_B .

Structures in syn-/late D_B tonalitic rocks

In the southern Svecofennian units, gneissic intrusive rocks are widespread. They cut the supracrustal associations, except for the Jokela supracrustal association (Appendix 5). These intrusive rocks are homogeneous and vary in composition from tonalites to granodiorites. Tonalites locally have pyroxene (cf. the West Uusimaa granulite Complex, WUC), which generally retrogressed to pale clin amphibole, like in Sipoo (Si in Figure 9). Several pulses of later magmatic rocks cut these granitoids (e.g. Figure 18a and b). The following key examples from Pornainen and Sipoo summarize the characteristics of these gneissic tonalites.

The contact relationships between the gneissic tonalite and migmatitic mica gneiss are exposed at the Hirvensuo site, Pornainen, within a wide, open synform with a N-trending axial plane. On the outcrop, migmatitic mica gneiss forms a tight synform few meters wide in tonalite (Figure 20a). A strong S_B foliation and isoclinally F_B folded neosome veins of the gneiss indicate intense D_B deformation. The D_B structures were deformed by the synform F_C , with a moderately plunging F_C axis. The D_C structures are refolded by F_I folding; the synform thus represents a D_{C+I} structure. The tonalite intruded along the S_B plane and was folded by F_C . S_C is the first dominant mineral foliation identified in the tonalite. Close to the contacts, tonalite is only weakly S_B -oriented (Figure 20a), but farther from the contact, in the homogeneous parts, a steep S_C dominates; thus, it is syn-/late tectonic to D_B . A narrow, folded intermediate dyke cuts the mica gneiss, tonalite and the D_C synform (Figure 20b). Dykes cut S_C foliation in tonalite with bulging contacts (Figure 20c). We relate these post- D_C dykes to the D_E event; the syn-/late D_B tonalite and the dykes underwent a new prograde metamorphism during the proceeding D_E . In the following we refer to the intermediate D_E dykes in the corresponding tectonic setting as microtonalites, even though they show small variations in their composition and in their relations to D_E structures. Weak spaced foliation S_{Econt} formed in tonalites; it is penetrative in microtonalites. New granitic melt and segregation patches locally destroyed the S_C and S_{Econt} foliations. The prograde metamorphism also produced garnet-bearing granitic dykes and granite dykes (D_E or D_H) with a pegmatitic margin and medium-grained centre (Figure 20d) showing a pinch-and-swell-structure. The continuing magmatism (D_E - D_H) indicates that rather high temperatures prevailed during late deformation events.

Often the contacts between tonalite and supracrustal rocks are strongly deformed, or gradational due to later migmatization or magma pulses. Figure

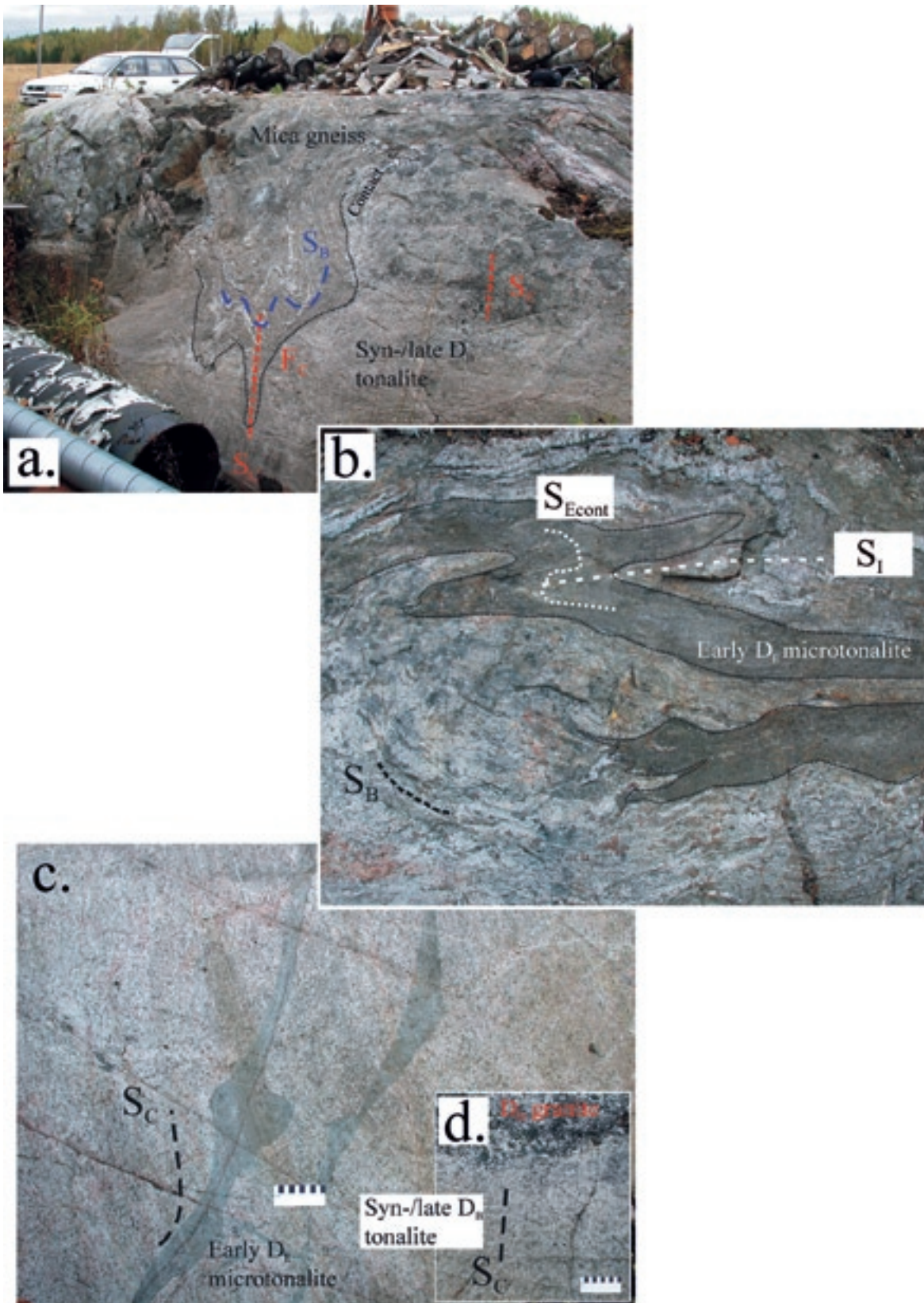


Figure 20. (a.) D_B deformed and migmatized mica gneiss forming a synformal structure in syn-/late D_B tonalite. Tonalite was intruded into the S_B plane, but its first penetrative foliation is S_C ; S_B formed only close to contact. N is to the right; width of the area of the figure is c. 5 m. (b.) The gneiss and synformal structure are cut by intermediate early D_E microtonalite dyke. Folding with a c. N-trending axial plane is interpreted as F_D ; the synform is thus a D_{C-1} structure. The dyke acquired foliation S_{Econt} before the folded structure, indicating an increase in temperature following the dyke intrusion. (Note: the earliest stages of D_E and the latest D_D were produced by the same regional stress field close to each other during progressive deformation – The F_D folding can not be excluded in this case). N is to the right; width of the area of the figure is c. 1 m. (c.) The microtonalite dykes in the tonalite are bulbous and cut the S_C indicating emplacement into a ductile environment under elevated temperatures; the M_E temperature increase is also indicated by the melt segregation patches in tonalite. Scale bar is 10 cm in length. (d.) A D_H pegmatitic granite dyke cuts the tonalite and S_C . Scale bar is 10 cm in length. Hirvensuo, Pornainen (Finnish grid coordinates KkJ2 2572.79E 6704.48N). Photo by M. Pajunen.

21a illustrates a sheared and folded contact against the migmatitic mica gneiss, locally including amphibolitic remnants, at the Vilonoja site, Pornainen. It is a primary magmatic contact, which was extensively deformed to an isoclinally-folded structure (sketch in Figure 21b). The D_B neosome veins of mica gneiss in the isoclinal folds, squeezed into tonalite, are strongly deformed; a less deformed mica gneiss structure is shown in Figures 22a and b. The tonalite is S_C -foliated and cut by later magmatic and migmatitic pulses. It is interpreted as syn-/late tectonic to D_B . It was intruded by felsic granitoid with a dark retrograde alteration zone along the contact (Figure 21c); the rock was deformed and migmatized by later granite melt that often concentrated into shear bands. We relate the felsic granitoid dyke to the early/mid- D_E tonalites and the granite to the later D_E or D_H phase. Correspondingly, the mica gneiss was also intruded by D_E melts (see Figure 22a) and in places shows a strong, steep, spaced S_{E-cont} foliation that developed during proceeding de-

formation to form extensional shear bands (Figure 22c, the pre- S_{E-cont} structure is shown in Figure 22a and b). The horizontal S_E foliation is interpreted as extensional S_{E-ext} and the steep S_E as contractional S_{E-cont} occurring rather simultaneously. The later D_H , characterized by intense granite production cannot be ruled out, because c. E-W-trending shearing also occurred during it. However, the axial planes of contradictional F_{H-cont} folds are NE-trending (see later). In places, penetrative D_E structures completely destroy the early D_{A-D} structures.

The Hindsby tonalite is c. 5*3 km wide, homogeneous, medium-grained and intrusive, and is exposed in a c. SSE-plunging open antiformal setting at the Staffas site in Sipoo (Hindsby tonalite location in Appendix-Fig. 6-2d). It clearly shows the internal structural evolution of this intrusive phase. Its contacts are mostly covered; the observed ones are against the later pegmatitic granite displacing the foliated tonalite (Figure 23a), or tectonic along the Vuosaari-Korso structure (Figure 23b). The

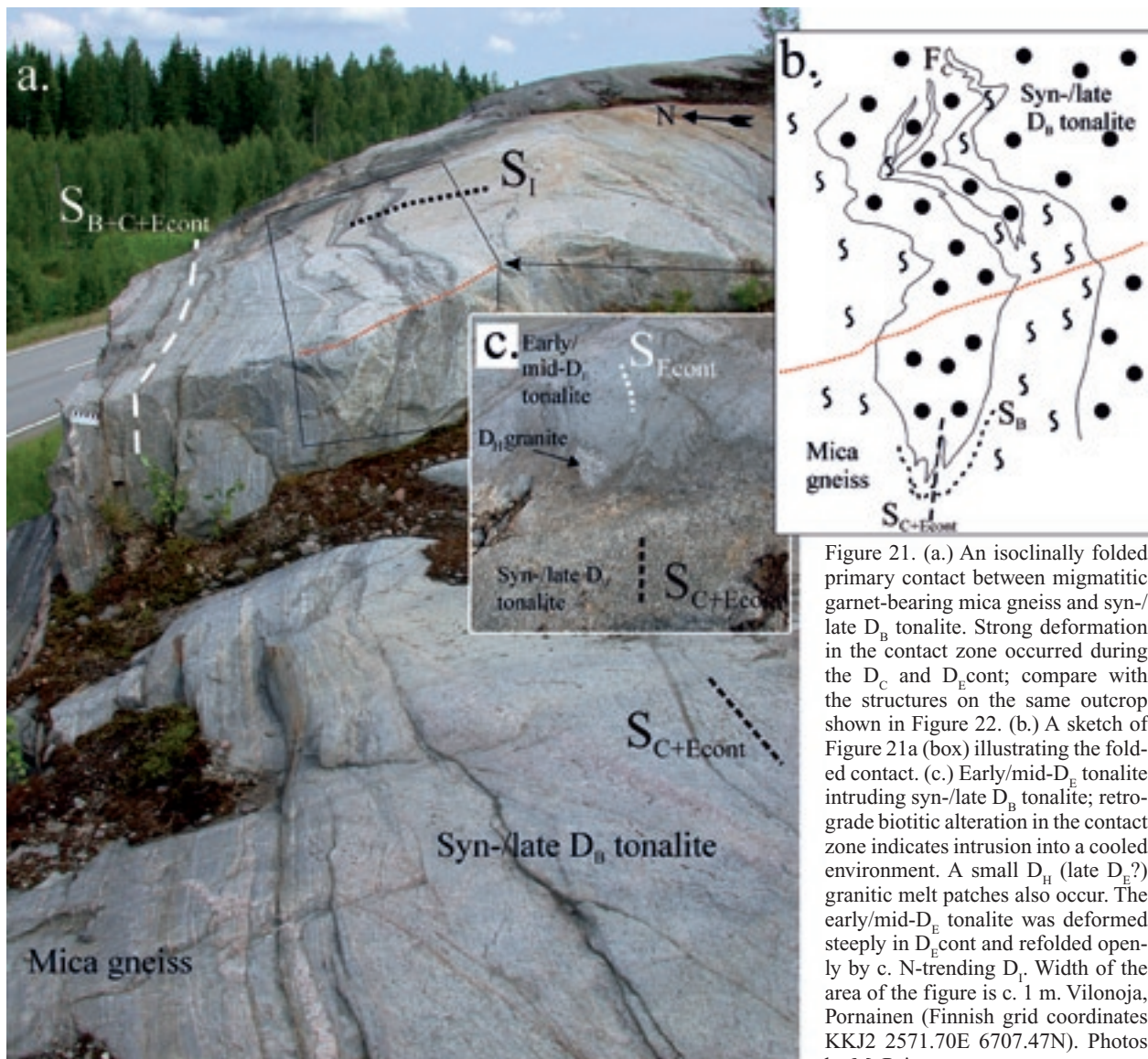


Figure 21. (a.) An isoclinally folded primary contact between migmatitic garnet-bearing mica gneiss and syn-/late D_B tonalite. Strong deformation in the contact zone occurred during the D_C and D_{E-cont} ; compare with the structures on the same outcrop shown in Figure 22. (b.) A sketch of Figure 21a (box) illustrating the folded contact. (c.) Early/mid- D_E tonalite intruding syn-/late D_B tonalite; retrograde biotitic alteration in the contact zone indicates intrusion into a cooled environment. A small D_H (late $D_{E?}$) granitic melt patches also occur. The early/mid- D_E tonalite was deformed steeply in D_{E-cont} and refolded openly by c. N-trending D_I . Width of the area of the figure is c. 1 m. Vilonoja, Pornainen (Finnish grid coordinates KJ2 2571.70E 6707.47N). Photos by M. Pajunen.

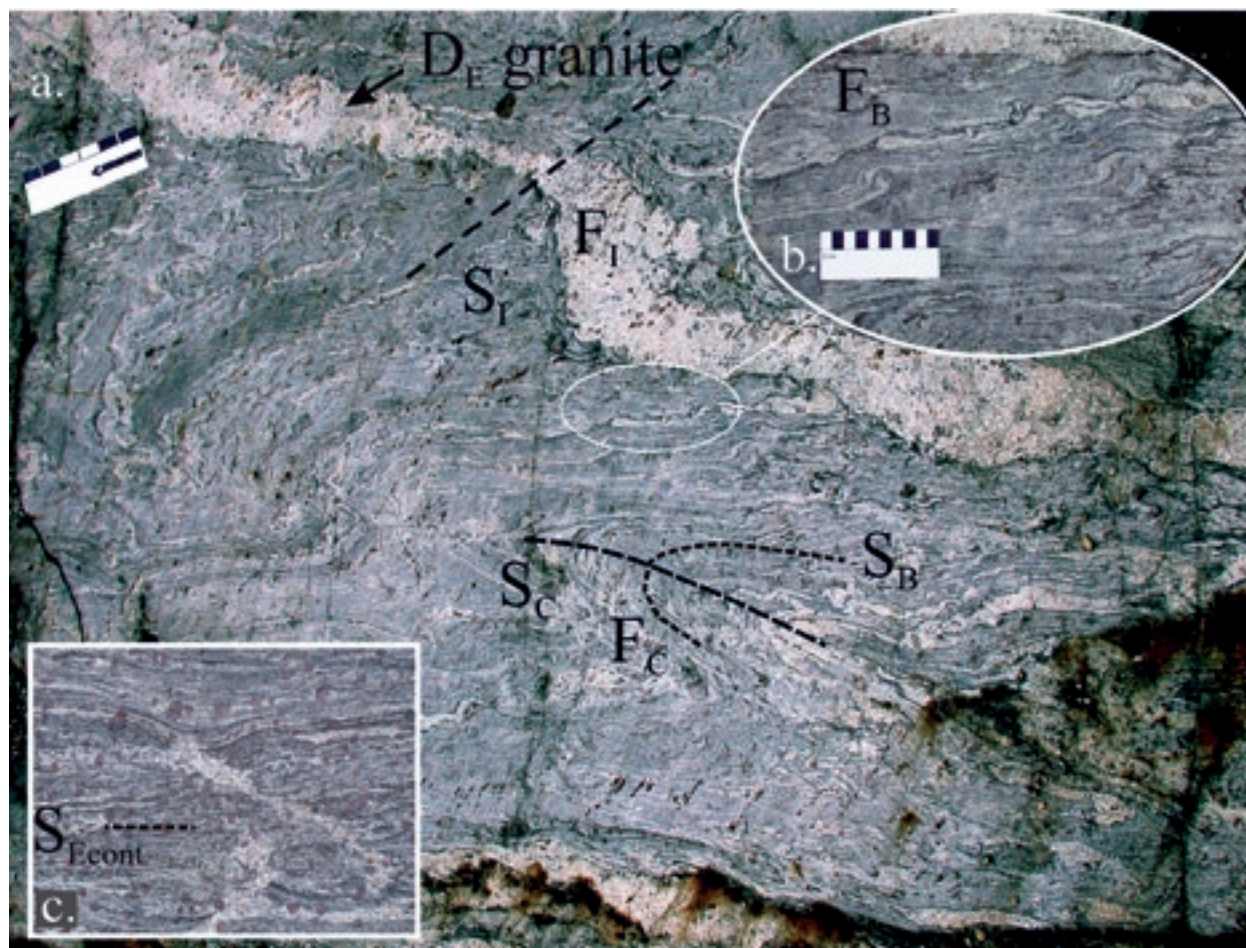


Figure 22. (a.) Migmatitic garnet-bearing mica gneiss showing the relationships between the D_B , D_C , D_E and D_I structures and related migmatization events. Scale bar is 15 cm in length. (b.) F_B folds in trondhjemitic neosome in mica gneiss. Scale bar is 10 cm in length. (c.) Extensional granitic D_E melt fraction in mica gneiss. Width of the area of the figure is c. 1 m. Vilonoja, Pornainen (Finnish grid coordinates KKKJ2 2571.70E 6707.47N). Photos by M. Pajunen.

deformation succession of the tonalite (Figure 24a) is determined by the following structures: 1) intrusion (likely as described above); 2) the formation of early foliation S_C – preserved in a dextrally-rotated fragment in the microtonalite dyke, elsewhere strengthened by later events (see point 4); 3) the generation of early quartz veins indicating low-grade fracturing deformation; 4) the intrusion of an intermediate microtonalite dyke with chilled margins (Figure 24b), which along with the fragments in the dyke (Figure 24c) demonstrates intrusion into cool tonalite; 5) the formation of new steep spaced foliation, S_{Econt} (Figures 24a, b and c), which also developed as penetrative in the dyke; 6) an increase in temperature causing partial decomposition of biotite to form garnet and granitic melt, and forming an amphibolite-facies assemblage in the dyke; patchy destruction of the previous structures (Figure 25a); 7) the formation of D_E shear bands with medium-grained coarsening or granitic melt/segregation in the highest-strained zones (Figure 25b); 8) foliated, slightly pinching-and-swelling D_H pegmatitic granite dykes (Figure 24a, upper left corner); 9) the formation of shear bands with granite or quartz in the

highest-strained zones – they are less common and locally lower-grade shearing is related to them (Figure 25c), and we interpret that they represent D_I (correlate to point 10); 10) semi-ductile shearing (Figure 23b) along the border zone – the eastern contact is bordered by the steep Vuosaari-Korso shearing structures showing east-side-up movement of $D_{I+(P?)}$ (cf. Elminen et al. 2008).

The structures in the syn-/late D_B tonalites give evidence for a cooling stage before the intrusion of the intermediate microtonalite dykes (e.g. early quartz veins, straight contacts of dykes with chilled margins). The evolution was followed by an increase in temperature that caused the continuing processes, the generation of a foliation, the formation of extensional shear bands and the decomposition of biotite forming garnet and granitic melt patches; these are related to the complex extensional D_E - D_H events. We relate the retrogression of pyroxene in the D_B tonalites to this new D_E melting and fluidization, and prograde metamorphism. Open warping of the main foliation and later lower-grade shear bands, representing the later shortening events, also give evidence for cooling towards the end of the succession.

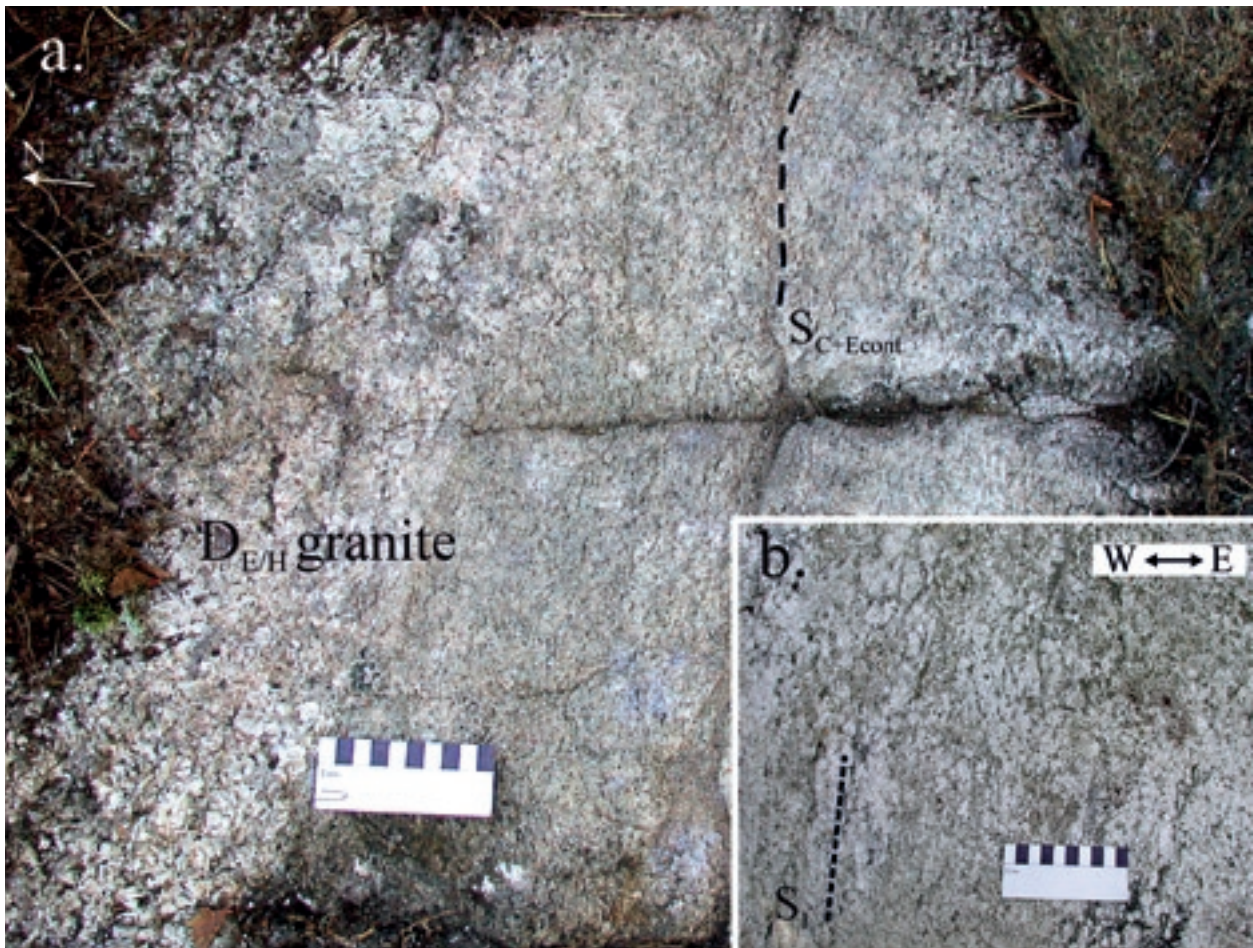


Figure 23. (a.) The E-trending northern contact between the Hindsby syn-/late D_B tonalite and D_E pegmatitic granite. Scale bar is 10 cm in length. Högbacka, Sipoo (Finnish grid coordinates KKKJ2 2565.71E 6694.91N). (b.) Vertical section of sheared contact of the Hindsby tonalite against the Vuosaari-Korso shear/fault zone. Scale bar is 10 cm in length. Stormossen, Sipoo (Finnish grid coordinates KKKJ2 2565.36E 6691.71N). Photos by M. Pajunen.

Age of D_B deformation and correlations

The earliest structurally-fixed magmatic rocks in the Southern Volcanic-sedimentary Belt (SVB) are the rocks of the gabbroic association showing a penetrative S_B . Hopgood et al. (1983) dated magmatic gabbros at 1885 ± 7 Ma, and banded dioritic gneiss, a neosome for agmatite, at 1895 ± 13 Ma from the Jussarö-Skåldö area. Structurally comparable mafic rocks in the Hyvinkää Gabbroic-volcanic Belt (HGB) show similar D_B evolution of the gabbros and the closely-related supracrustal associations without D_A structures (Appendix 3). The published age of the Hyvinkää gabbro (Patchett & Kouvo 1986 and Patchett et al. 1981) is 1880 ± 5 Ma, which is same as the age of 1880 ± 3 Ma for the plagioclase porphyrite in Hyvinkää (Suominen 1988). Within the error limits, this is the same age as for the younger, post- D_A to early- D_B volcanic Series II, dated from Orijärvi (Väisänen & Mänttari 2002). The post- D_A /pre- D_B mafic and intermediate dykes (Figures 13b and 14a and b) of the study area belong to the younger volcanic Series II. The ages from Jussarö-Skåldö (Hopgood et al. 1983) have such a large

error that both alternatives, the pre- D_A volcanic Series I and early D_B Series II, hold true. Thus, further work is needed to establish the setting of these mafic associations and to test whether the gabbroic associations represent two different sequences. The ages from the Hyvinkää gabbros prove their intrusion close to the regional D_B , because the age is close to that obtained from the syn-/late D_B tonalites. The structures formed in D_A were weak and could have been destroyed by the stronger D_B . This leaves the possibility that the southern gabbroic association belongs to the older, pre- D_A phase.

The maximum age of D_B in the Southern Volcanic-sedimentary Belt (SVB) and in the Espoo Granitoid Complex (EGC) can be established by the age of the post- D_A and pre- D_B volcanic sequence at c. 1.88–1.87 Ga. The syn-/late D_B tonalites intruded into the S_B plane of coexisting supracrustal rocks with strong D_B flattening and migmatization. The first penetrative foliation in these tonalite is S_C . These observations bind D_B deformation and migmatization between the ages of the later volcanic sequence and the tonalite intrusion. A magmatic age of 1873 ± 7 Ma (SIMS U/Pb zircons) was obtained



Figure 24. (a.) A metamorphosed early D_E intermediate microtonalite dyke cutting the syn-/late D_B tonalite (Hindsby intrusion) and pegmatitic D_H granite dykes (black arrow, upper-left corner). Hammer is 47 cm in length; N is to the left. (b.) The dyke shows a chilled margin that indicates intrusion into cooled rock. Width of the area of the figure is c. 0.4 m. (c.) The tonalite is S_C foliated and overprinted by the steep spaced $S_{E,cont}$, which also deforms the dyke as penetrative foliation. The $S_{E,cont}$ shows a small shear component deforming the dyke margins. In the central part of the dyke $S_{E,cont}$ foliation is c. dyke-parallel. The fragment of tonalite in the dyke (c.) is S_C foliated, slightly rotated, and $S_{E,cont}$ is bent to surround it; the observation provides evidence of emplacement of the dyke post- D_C and prior to the strongest $D_{E,cont}$ deformation. The medium-grade metamorphic parageneses in the dyke indicates the new metamorphic event after intrusion into cooled rock. Width of the area of the figure is c. 0.7 m. Staffas, Sipoo (Finnish grid coordinates KKKJ2 2568.93E 6694.67N). Photos by M. Pajunen.

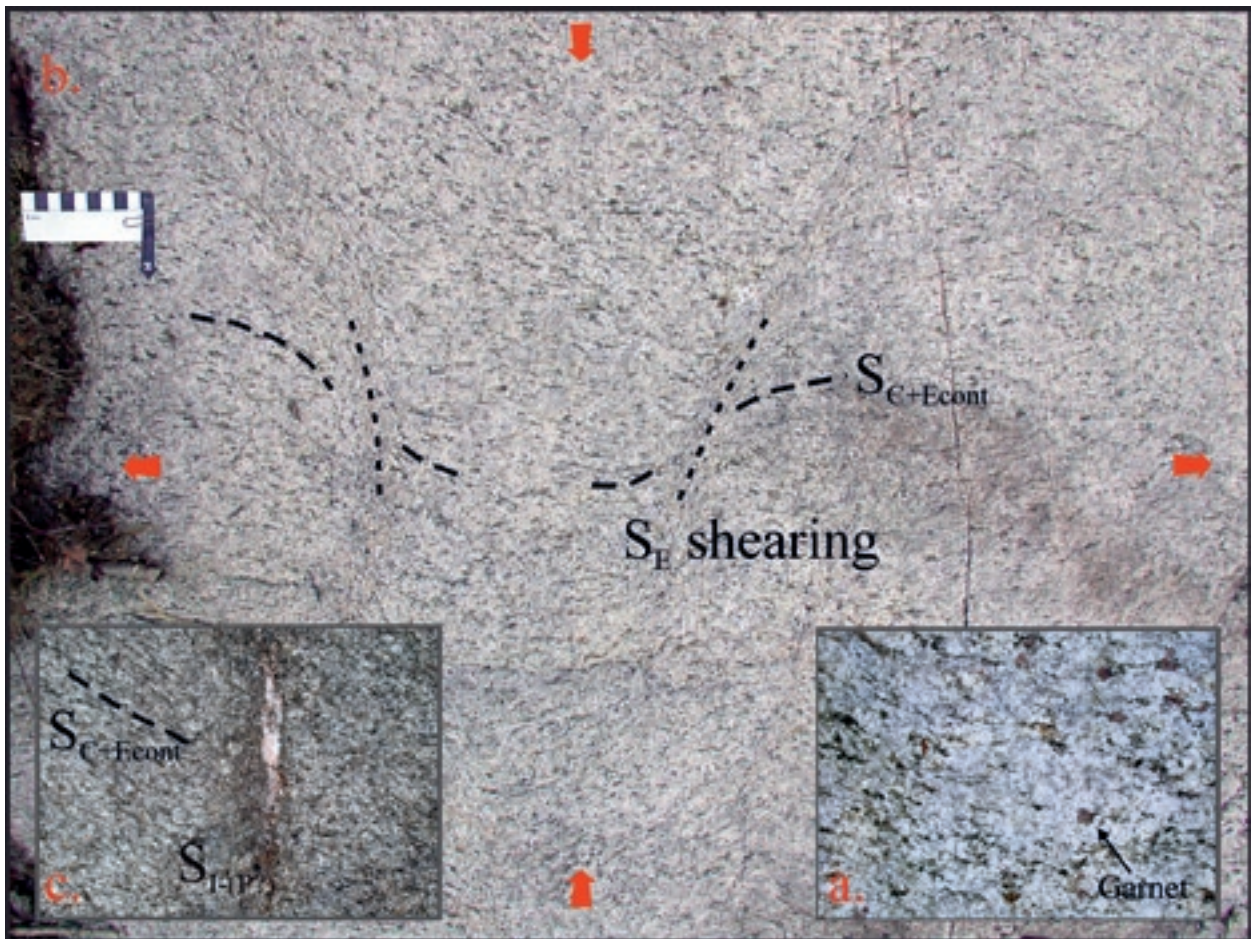


Figure 25. (a.) D_E granitic remelting patches in the syn-/late D_B tonalite. Biotite has decomposed to garnet and granitic melt. Width of the area of the figure is c. 20 cm. (b.) D_E shear band structures in syn-/late D_B tonalite; shear bands are characteristic for this magma phase. The shear bands are formed in N-S contraction. Scale bar is 10 cm in length. (c.) Later lower-grade shear bands in syn-/late D_B tonalite include quartz veining, instead of granite, in the shear plane. Drag folds related to shearing indicate c. E-W contraction that is characterizing the D_I . Width of the area of the figure is c. 30 cm. Stormossen, Sipoo (Finnish grid coordinates KJ2 2565.36E 6692.07N). Photos by M. Pajunen.

from the Bollstad syn-/late D_B tonalite in Inkoo (mixed age of 1855 ± 6 Ma for zircons was obtained by TIMS method) (Appendix 8). A concordant age of 1829 ± 3 Ma (TIMS U/Pb monazite) for metamorphic monazite in this tonalite was obtained (Appendix 8). The Hindsby syn-/late D_B tonalite (sample A1738 Staffas), Sipoo, gives ages of 1876 ± 8 Ma (SIMS U/Pb zircons, Appendix 8) for the older zircon population, and of 1841 ± 4 Ma and 1801 ± 7 Ma for younger zircons. On the structural basis the age group of 1876 ± 8 Ma could represent the age of the intrusion, whereas the age of 1841 ± 4 Ma could be related to later metamorphism and lead loss; the tonalite shows typically small melt patches related to D_E (Figure 25a). The youngest ages are related to M_H metamorphism and older zircons are inherited.

The ages of 1.88–1.87 Ga are typical for the “syntectonic granitoids” and neosomes in southern Finland (Hopgood et al. 1983, Huhma 1986, Vaasjoki & Sakko 1988, Nironen 1999, Mouri et al. 1999, Väisänen et al. 2002 and Skyttä et al. 2006).

The ages are on average 10 Ma younger than corresponding rocks in the northern units in the Tonalite Migmatite Belt (TMB) (e.g. Huhma 1986, Vaasjoki & Sakko 1988 and Nironen 1989). The tectono-metamorphic characteristics of the northern units (Pietikäinen 1994, Koistinen et al. 1996, Kilpeläinen 1998, Korsman et al. 1999, Nironen 1999, Pajunen et al. 2001a and Rutland et al. 2004), like the strong nearly-horizontal S_2 and flat-lying recumbent F_2 folds, prove strong vertical shortening deformation D_2 at c. 1.89–1.88 Ga; “syntectonic” intrusive rocks of this age also characterize the major parts of the Central Finland Granitoid Complex (CFGC) (Nironen 2003). The intense magmatism and migmatization, oblate horizontal flattening strain (cf. Koistinen et al. 1996) and widespread high-T/low-p metamorphism support an extensional D_2 event. D_2 is very similar to the c. 10 Ga younger D_B in the southern Granite Migmatite Belt (GMB). This suggests a different evolution of northern D_2 from the southern D_B , or that evolution was diachronic, becoming younger towards the south. In such a model

the Tonalite Migmatite Belt (TMB) was situated in the border zone of the intense D_B extensional belt. During the stage of local D_B extension in the south the TMB was already under contraction (D_3 , see later). To the north of the GMB-TMB border, in the TMB, there are also granitoids of 1.88–1.87 Ga in age (cf. Kilpeläinen 1998), like the syn-/late D_B tonalite ages in the south. This suggests that the TMB and GMB were close to each other during their intrusion. Thus, the original accretion of the GMB and TMB already occurred during the southern D_A .

In the low-grade gneisses in Orijärvi area (Vetio outcrop, Appendix 4), the first foliation and the early andalusite-cordierite growth are related to the D_B , corresponding the higher-grade extensional D_B deformation in the lower crustal sections. Heating occurred under subsidence of the upper crustal sections. The metamorphic evolution is very similar in the andalusite schists in the Tampere schist belt (TSB, Kilpeläinen 1998) and in the Rantasalmi area (Ra in Figure 9, Korsman 1977 and Korsman & Kilpeläinen 1986). Large andalusite porphyroblasts are c. S_0 -parallel and are overprinted by prograde metamorphism. Correspondingly, the TSB began to sub-

side during the northern D_2 extension. The TSB is situated upon an E-W-trending electric conductive zone dipping north (Korja 1990) between the Vammala Migmatite Belt (VMB) and the Central Finland Granitoid Complex (CFGC). The zone has been regarded as a suture zone along which the conductive schists of an accretionary prism of the VMB were pushed below the CFGC (e.g. Lahtinen 1994, Kilpeläinen 1998 and Korsman et al. 1999).

Deformation D_C – N-S shortening

The predominantly horizontal D_B flattening was followed by a high-T, ductile shortening event, D_C , which deformed the early supracrustal and magmatic series to isoclinal or tight, originally E-W-trending folds with steep axial planes. In the study area, the D_C structures are best preserved in the Southern Volcanic-sedimentary Belt (SVB) in areas that were not effectively overprinted by the later D_E - D_H events. Examples of D_C structures are given in Figures 11, 15c, 20 a, 22a, 26b, 27a and b and 28 a and c. Figures 27a and b give an example of a garnet-amphibole rock, a silicate-facies iron formation of the

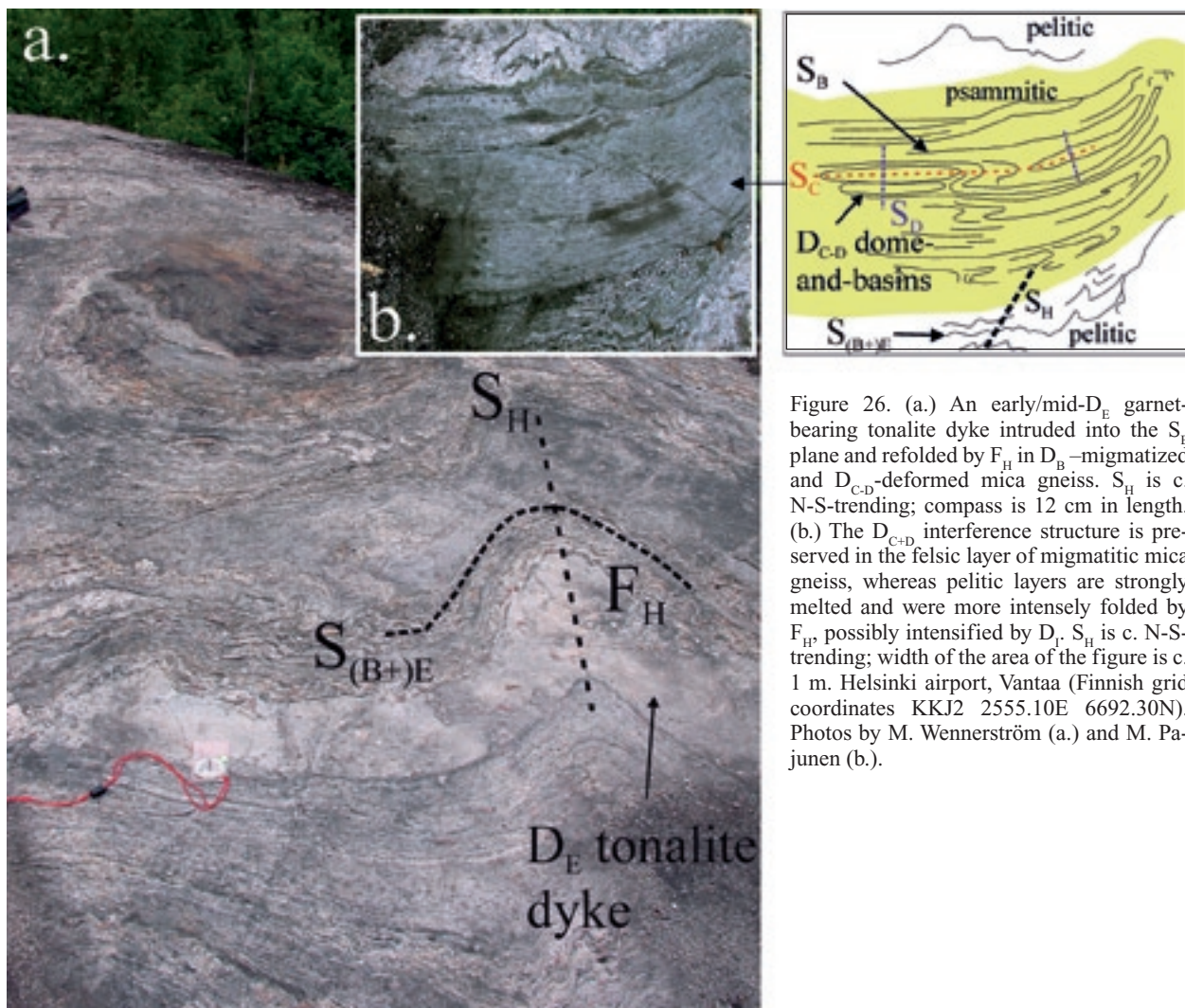


Figure 26. (a.) An early/mid- D_E garnet-bearing tonalite dyke intruded into the S_E plane and refolded by F_H in D_B -migmatized and D_{C-D} -deformed mica gneiss. S_H is c. N-S-trending; compass is 12 cm in length. (b.) The D_{C-D} interference structure is preserved in the felsic layer of migmatitic mica gneiss, whereas pelitic layers are strongly melted and were more intensely folded by F_H , possibly intensified by D_I . S_H is c. N-S-trending; width of the area of the figure is c. 1 m. Helsinki airport, Vantaa (Finnish grid coordinates KJ2 2555.10E 6692.30N). Photos by M. Wennerström (a.) and M. Pajunen (b.).

Southern Volcanic-sedimentary Belt (SVB), from Nöykkiö, Espoo. The outcrop is situated close to the Porkkala-Mäntsälä high-strain zone. The competent garnet-amphibole rock, however, shows only moderately strained D_{C+D} structures refolding S_B . The

D_{C+D} structures are overprinted by steep shear zones (Figure 27c) and weak folding that are related to the Porkkala-Mäntsälä shear/fault zone. The rock also shows patchy melting structures due to D_E .

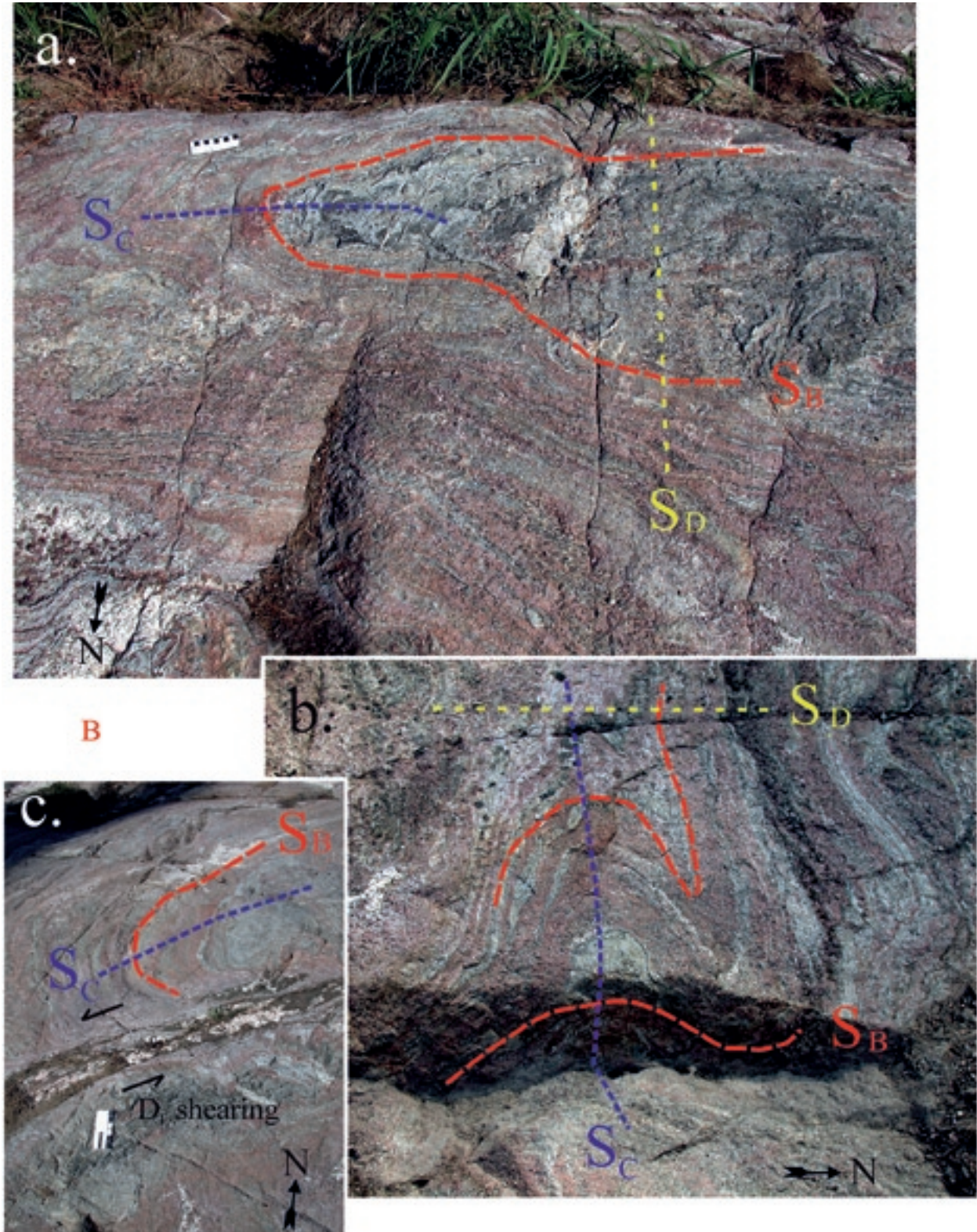


Figure 27. (a) D_{C+D} interference pattern in a competent garnet-amphibole rock (silicate facies iron formation); the F_C axis is dipping towards W. Scale bar is 10 cm in length. (b.) Vertical section of the same interference structure; the F_C axis is dipping towards W. Width of the area of the figure is c. 1 m. (c.) A D_F shear zone, related to deformation in the Porkkala-Mäntsälä zone under N-S contraction, cuts the D_{C+D} dome-and-basin structure; the F_C axis is dipping towards E. Scale bar is 15 cm in length. Nöykkiö, Espoo (Finnish grid coordinates KKKJ2 2536.88E 6672.79N). Photos by M. Pajunen.

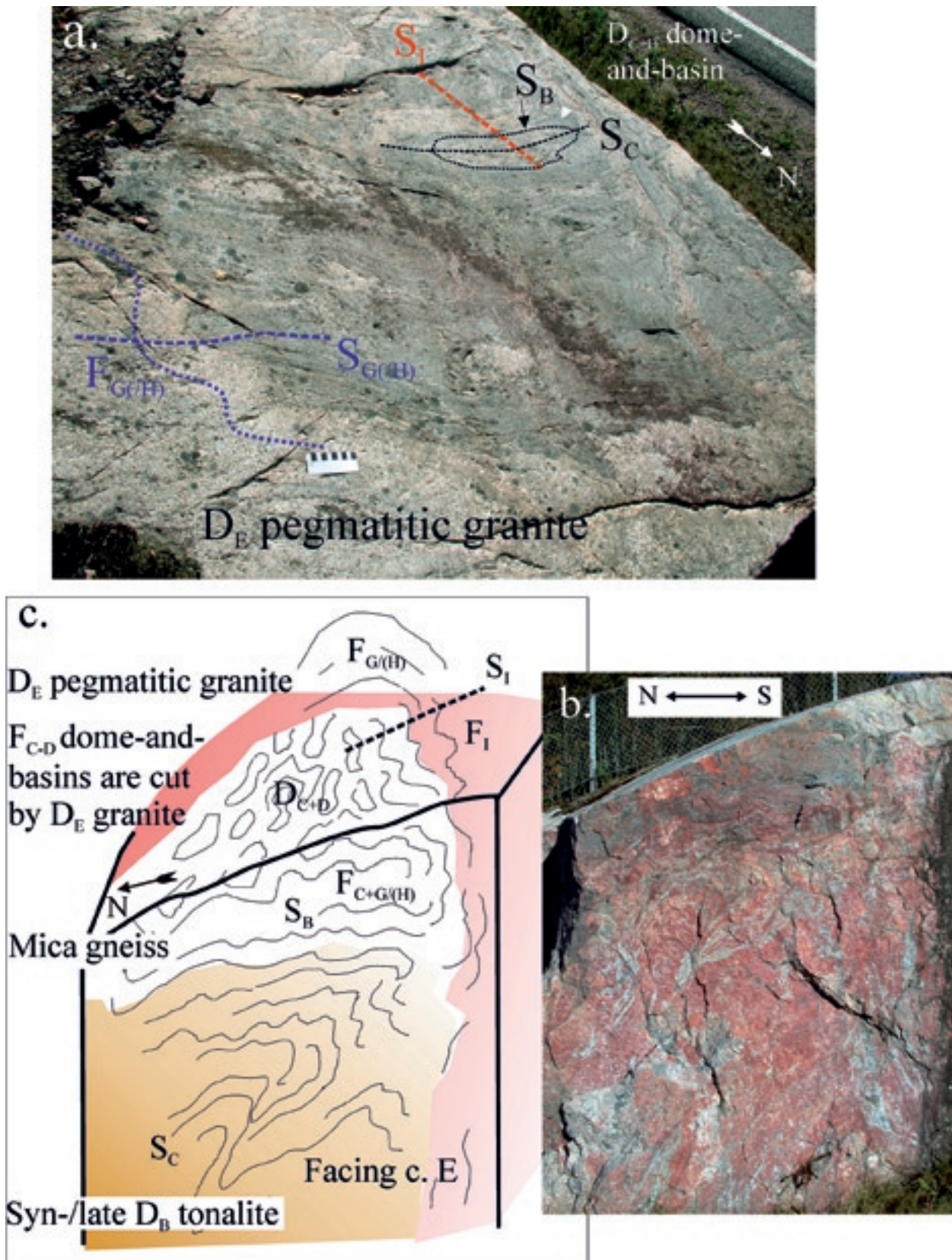


Figure 28. Migmatitic felsic gneiss with a deformed S_{C+D} dome-and-basin interference structure on the horizontal surface (a.); scale bar is 10 cm in length. Vertical surface is shown in (b.); width of the area of the figure is c.2 m. Indistinct relations between the gneiss and tonalitic rock are due to strong granitic melting and intruded dykes. (c.) Interpretation of structure: The S_B foliation plane in felsic gneiss is folded to form D_{C+D} dome-and-basin structures. The D_{C+D} dome-and-basin interference structure is cut by $F_{G(H)}$ -folded D_E pegmatitic granite. $F_{G(H)}$ intensified the F_C folds, because the axial planes S_C and $S_{G(H)}$ are approximately parallel. The first foliation in the strongly granitized syn-/late D_B tonalite including remnants of the mica gneiss is S_C (cf. the mica gneiss-tonalite contact in Figure 21). Thus, in the mica gneiss $F_{G(H)}$ refolds the foliation $S_{B+later}$, whereas in the tonalite it refolds $S_{C+later}$. The vertical section shows a southwards-overturned structure, interpreted as $F_{G(H)}$, which was refolded by F_1 with a c. NW-trending axial plane. This complicated structure is preserved in between the strongly migmatitic rocks characterizing the southern Sipoo area. Söderkulla, Sipoo (Finnish grid coordinates KKKJ2 2571.49E 6689.11N). Photos by M. Pajunen.

In the Espoo Granitoid Complex (EGC) the D_C structures have been hidden or destroyed by later deformations, metamorphism and magmatism. The vast majority of the felsic magmatism in the EGC post-dates D_C . For example, in the southern Sipoo area, to the east of the Vuosaari-Korso shear/fault zone, granitic rocks are often nebulitic or schlieren migmatitic. The complexity of structures is exemplified by migmatitic granite at the Söderkulla site, Sipoo (Figures 28a-c). A mica gneiss-tonalite remnant within the granitic unit shows D_{C+D} dome-and-basins deforming the early D_B migmatization and S_B foliation of the mica gneiss, and the S_C foliation of tonalite. No D_A features were preserved/identified. These structures were cut by D_E pegmatitic granite, which, along with the early structures, was overturned southwards by $F_{G(H)}$ folds with c. E-trending axial planes. There are some kinematic observations indicating to D_G tectonic transport southwards (Figure 19). However, the F_H folds are mostly overturned towards NW, such as to the west of the Vuosaari-Korso zone (Figure 12c). The latest ductile deformation identified at e Söderkulla site is open D_I folding with c. NW-trending axial planes. The deformations $D_{G(H)+I}$ form an open dome-and-basin structure upon the D_{C+D} ones.

The tight to isoclinal F_C folds are round-hinged, without significant thickening of hinges or thinning on limbs. In the pre- D_C rocks, with strong S_B foliation and migmatization, no significant mineral growth occurred in the S_C axial plane. S_C is indistinct, or weak crenulation and only locally some melt remobilization sometimes occurred in the axial planes. S_C is the first penetrative foliation in the syn-/late D_B tonalites. Minor new D_C mineral growth suggests a decrease in temperature after the peak metamorphic conditions during the D_B . However, close timing of D_B and D_C is suggested by the large amounts of syn-/late D_B tonalites showing S_C as their first foliation. The biotitic-hornblende tonalite foliation indicates amphibolite facies conditions.

D_D deformation – E-W shortening and D_{C+D} dome-and-basin structures

Refolding of F_C folds by the ductile F_D folds with c. N-trending, steep axial planes formed the dome-and-basin interferences, D_{C+D} , seen on both the map scale (Figure 11) and outcrop scale (Figures 26b, 27a and b, 28a and c). The F_D folds are open to tight, more open than the F_C folds. No significant mineral growth in the S_D axial plane has been identified. The D_{C+D} dome-and-basin structures are deformed by the later tectonic events, e.g. by the less-strained, map-scale $D_{G(H)+I}$ interference structures (Figure 11).

On outcrops they only openly to weakly re-fold the D_{C+D} structures (Figures 22, 26a and b).

Regional analysis of the F_G and F_D folding patterns requires investigation of their foliation-fold axis-lineation relationships, which is not possible by using our limited-area field observations alone. On the outcrop scale the structures are mostly small, only partly exposed or reoriented by the later deformations, so that the analysis does not give regionally correlative results. A generalized idea of D_{C+D} dome-and-basin forms and related kinematics can be obtained by studying the D_{C+D} structures using the geological maps of the GTK on the scale 1 : 100 000. The following preliminary analysis is carried out using tectonic measurements on the maps, in the areas not intensely intruded by magmas of the Southern Finland Granitoid Zone (SFGZ) or not located in zones of intense D_{H+I} deformation.

The Pellinki area (Pe in Figure 9) shows a D_{C+D} structural pattern with S_C dipping steeply south (the main foliation S_B is mostly dipping 90–70° towards south). The orientations of F_C fold axes and $L_{A+B/C}$ lineations (generations established by correlation to the study area) give steeply a northwards overturned, isoclinal-tight fold pattern for the F_C , and a westwards overturned moderate pattern for the F_D (the interpreted F_C fold axes are generally steeper on the western end of the D_{C+D} domes than on the eastern end, and opposite for the synformal structures). This indicates N-S shortening during D_C and E-W shortening during D_D . Analysis from the southwestern archipelago to the SW of Turku gives similar kinematics for the D_C , but F_D folds show an eastwards overturned pattern. Analysis of the borders of the major N-trending tectonic block, between the Baltic Sea-Bothnian Bay Zone (BBZ) and the Riga Bay–Karelia Zone (RKZ), suggests opposite overthrusting patterns in the western and eastern parts of the block during the D_D (Figure 8). This may indicate that the bordering structure of the block dips towards the west in the BBZ and towards east in the RKZ. A rough estimate of D_C shortening based on the forms of the F_C folds in the Southern Volcanic-sedimentary Belt (SVB) gives a value of about 40–50%; that of D_D is somewhat less, with shortening of c. 20–30%. These analyses are preliminary and further research is needed to specify the regional variations in D_C and D_D kinematics more comprehensively.

Ages of D_C and D_D deformations and correlations to the northern tectonic units

Structural and mineral growth relations indicate that the compressional D_C evolution rapidly followed the formation of the later volcanic Series II and the

syn-/late D_B tonalites at c. 1.88–1.87 Ga. The D_3 deformation in the Tonalite Migmatite Belt (TMB) can be dated at c. 1.89–1.88 Ga by following the deformation succession of Kilpeläinen (1998), and the ages of syntectonic Hämeenkyrö and Värmälä intrusions (Nironen 1989) (Appendix 1). The E-W-trending D_3 in the northern units is slightly older than D_C in the south; it is about the age range of the southern D_B . Compression in the north was, accordingly, simultaneous with D_B in the south. Because of the rapid evolution from D_B to D_C in the study area, and the contemporaneous extensional D_B in the south and contractional D_3 in the north, we suggest that the crust was in its entirety under a compressional stress field, i.e., under continuous collision towards the north. The northern D_2 and southern D_B are similar strong deformations, accompanied by prograde, high-T/low-p metamorphism (e.g. Korsman et al. 1999). We suggest they represent an extensional crustal evolution between the compressional D_A (or D_1 in the north) and D_C (or D_3 in the north). The evolution from the northern D_2 at c. 1.88–1.89 Ga to the southern D_B at 1.88–1.87 Ga was a diachronic process that progressed southwards. Similarly, the D_3 (north) and D_C (south) represent evolution that was diachronic, getting younger southwards. The end of D_C is determined by the rotation of the N-S stress field to SW-NE during D_D . In the study area the setting of the oldest dated early D_E Hakkila tonalite cutting the D_D structures is 1868 ± 3 Ma old (see later discussion and Appendix 8).

The D_{C-D} folding pattern in the Southern Finland Volcanic-sedimentary Belt (SVB) is systematic, but is more complex further north. In the Pori area Pajunen et al. (2001a) described F_4 folding with a N-trending axial plane deforming the D_{2-3} structures, and Nironen (1999) described a D_4 structure refolding earlier structures into the Pomarkku block structure in the Loimaa area (see Figures 9 and 11). The tectonic formline pattern shown in Figure 11 suggests that corresponding dome-and-basin deformation (D_{3-4}) also occurred in the Vammala migmatite belt (VMB), but it was deformed by a complex sliced structural pattern with c. NW- and NE-trending deformation zones. These zones characterize the Hämeenlinna stacked terrane (Figure 10) in the border zone between the Granite Migmatite Belt (GMB) and the Vammala Migmatite Belt (VMB) in the Tonalite Migmatite Belt (TMB). The Pomarkku block structure represents the western end of this structure; we relate the block formation to c. SW-NE transpression D_4/D_D (Appendix 7 and Appendix-Fig. 7-1c).

In the Central Finland Granitoid Complex (CFG), D_3 produced the northwestwards stacked structure (Figures 8, 9 and 10) that was later sliced

by NW-trending D_4 (D_b shear zones of Pajunen 1986) and later N-trending (D_d shear zones of Pajunen 1986) shear zones. The 1.89–1.88 Ga (Vaasjoki & Sakko 1988) granitoids in the CFGC are generally deformed and locally show low-angle foliation dipping SE (S_3). Kilpeläinen (2007) also described a low-angle shear zone from the Savo Schist Belt (SSB) and CFGC border. Primarily, we suggest this to correspond to the D_3 stacking shear structures. The generation of this magmatic complex followed the accretion of the CFGC against the 1.93–1.91 Ga old primitive island arc of the Savo Schist Belt (SSB) and the Archaean continent. The CFGC was fixed to the SSB along a complex structure; originally it was deformed by the D_3 stacking northwestwards and slicing, which during later evolution was folded and fragmented by the zonal D_4 NW-trending shearing. The shear zones are characterized by a strong granite magmatism and granitization (Pajunen 1986 and Pääjärvi 1991) and by a linear gravity low (Korhonen et al. 2002b). Thus, D_3 resulted in a continued northwards collision, forming stacked units that became folded and fragmented during D_4 .

No age determination has been carried out to date for the D_D folding structures in the Granite Migmatite Belt (GMB), but correlation with the northern units is supportive. The D_4 block deformation can be dated with post-/late tectonic granitoids emplaced into the arched structures characterizing the block structure of the areas of Pomarkku block (Appendix 7 and Appendix-Fig. 7-1c) and Central Finland Granitoid Complex (CFGC) (Figure 9). The transpressional N-NW slicing, D_4 , together with the earlier NW-stacked D_3 structure, formed the arched structures into which these late/post-tectonic granitoids were intruded. According to our interpretation, these granitoids are syn- D_4 intrusions emplaced in oblique dilatational settings during the NE-SW transpression. These granitoids effectively destroyed the older collisional D_3 thrust structures in the CFGC. In the west, to the north of the Pomarkku block, a weakly deformed quartz monzonite, dated at 1872 ± 2 Ma (Mäkitie & Lahti 2001), is a typical syn- D_4 intrusion. In the CFGC corresponding intrusions vary in age, being younger towards the west: 1886 ± 6 to 1885 ± 5 Ma (E part), 1882 ± 2 to 1880 ± 3 Ma (central part), 1880 ± 5 to 1874 ± 4 Ma (SE part), 1875 ± 2 Ma (S part) and 1872 ± 2 to 1870 ± 4 (W part) (ages from Mäkitie & Lahti 2001 and Nironen 2003; dating with large errors is excluded). The age of the ductile D_D folding in the south can be bracketed between the syn-/late D_B tonalite ages (1.88–1.87 Ga) and the early D_E tonalite dykes (the oldest dated Hakkila dyke is 1868 ± 3 Ma). Because the stress field remained in a NE-SW direction

during the early D_E deformation, a transitional transformation from D_D to D_E is suggested.

In eastern Finland, in the Proterozoic allochthonous sequences lying upon the Archaean basement, the earliest deformations, D_{1-2} , are related to thrusting and crustal thickening at c. 1.9 Ga ago (Koistinen 1981). This collision juxtaposed a 1.93–1.91 Ga old primitive island arc (Lahtinen 1994, Kousa et al. 1994 and Korsman et al. 1999) – the Savo Schist Belt (SSB) – and the Archaean domain, causing the obduction of 1.95 Ga ophiolites, described by Kontinen (1987), together with the early rift and passive margin sediments (Koistinen 1981). Prior to the 1.95 Ga rifting the Archaean continent was covered by platform sediments that are now preserved near the craton border zone and between the wide tectonic slices of the Archaean unit. These tectonic slices of the Archaean domain have a surprisingly similar geometry to the D_4 slices in the northern Svecofennian unit, e.g. the Pomarkku block. These structures formed earlier in the east than in the west. The Proterozoic-Archaean boundary zone was already strongly deformed before the intrusion of the 1884 ± 5 Ma orthopyroxene-bearing monzonites (Hölttä 1988). Their contact aureoles cut the regional fold structures in the Savo Schist Belt (SSB), but some ductile shearing in the contact aureole (Hölttä et al. 1988) proves that deformation was already localized at the time of monzonite intrusion. These intrusions terminate the main stage of deformation and metamorphism near the craton boundary. We propose a corresponding generation for the major geometry in the Archaean domain and in its boundary zone to that further west: D_3 N-S compression and $D_{4/D}$ SW-NE transpression. The craton boundary area did not undergo an extensional event characterizing its evolution, such as $D_{2/B}$ in the southern Svecofennian domain. The thick crust is preserved in the craton boundary area, and it thins towards the southwest (Luosto et al. 1990). The continued $D_{3/C}$ north-south compression followed by $D_{4/D}$ SW-NE transpression prevented the major extensional thinning of the crust. Korsman et al. (1999) already suggested this kind of continuous compression model to explain the preservation of the thick crust.

We suggest that the syn- D_4 granitoids determine the age of the D_4 arching and fragmentation in the north. The younger Härkmeri quartz monzonite, dated at 1868 ± 3 Ma (Lehtonen et al. 2005), caused a metamorphic contact aureole on regional metamorphic assemblages and cut the D_4 block structure in the north (Appendix 7). The age of the intrusion establishes the end of D_4 in the western Tonalite Migmatite Belt (TMB) and the Central Finland Granitoid Complex (CFGC). To the north of the Vitinki zone the strongly migmatitic Vaasa area (Va in

Figure 9), which continues to the Swedish coast, has, according to Rutland et al. (2004), been pushed from the west to its present setting. We agree with the eastward movement of the unit and suppose the deformation to be related to syn- D_4 . Movements have occurred still later during the D_F deformation (see later). Thus, the termination of the D_4 in Central Finland occurred primarily between 1884 ± 5 Ma in the east and 1868 ± 3 Ma in the west. D_4 development thus shows a similar diachronic evolution, becoming younger towards southwest that became evident from the earlier tectonic events $D_{2/B}$ and $D_{3/C}$. In the south the ductile F_D folding occurred simultaneously with the northern D_4 fragmentation, but it continued longer due to the continuing NE-SW stress field under increasing high heat flow.

Structures related to the evolution of the Southern Finland Granitoid Zone

In the Southern Finland Granitoid Zone (SFGZ), structures in intrusive rocks play a key role in analyzing the geotectonic evolution of the zone; therefore, the structural relationships of intrusive rocks on representative outcrops will be discussed in detail.

From D_D to D_E deformation – begin of the Southern Finland Granitoid Zone evolution

In the study area the Hakkila early D_E garnet-bearing tonalite dyke (Figure 29) has an age of 1868 ± 3 Ma (SIMS U/Pb zircons, Appendix 8). This granitoid phase intruded into dilatational structures in a hot and ductile environment, into migmatitic mica gneiss, that was already deformed into D_{C-D} dome-and-basin structures. Thus, D_D is at least partly older than these tonalitic intrusives. These early D_E tonalitic intrusions determine the beginning of D_E deformation in the study area; they also establish the beginning of evolution of the Southern Finland Granitoid Zone (SFGZ). The tonalite age is exactly the same as that of the Härkmeri quartz monzonite (Lehtonen et al. 2005) cutting the D_4 structure to the north of the Pomarkku block (Appendix 7). The monzonite determines the termination of the major deformations in the north.

The age data demonstrate that tectonic evolution changed rapidly from the extensional D_B to the contractional D_C and transpressional D_D , and finally to the dilatational events labelled here as D_E . These changes occurred in the study area between the intrusion of the syn-/late D_B tonalites at c. 1876 ± 8 Ma and the garnet-bearing early D_E tonalites at c. 1868 ± 3 Ma. This also means that the discordances

described as characterizing the southern Svecofenian domain are transitional and the evolution was more continuous. Deformation did not affect the whole crust, accreted during its early tectonic evolution, to the same extent, but began to deform it in more zoned and patchy pattern.

The SFGZ, formed predominantly during the D_E and D_H , shows large variations in magmatic, metamorphic and structural characteristics in different parts of the zone and during different stages of the evolution of the zone. The composition of magmatism changed with time; it was tonalite-dominant in the early stages (D_E) and changed to granitic during its late evolution (D_H); small amounts of mafic intrusive rocks also evolved. The major N-trending Baltic Sea-Bothnian Bay Zone (BBZ) and Riga Bay Karelia Zone (RKZ) are related to the D_I deformation; the evolution of these structures was partly concurrent with the SFGZ evolution, but the late stages of the D_I structures deformed the SFGZ (Figure 11).

D_E deformation – oblique extension under NE-SW transpression

D_E structures and syn-tectonic intrusions overprint the D_{C+D} dome-and-basin structures. On outcrops, D_E structures are sometimes very similar to those of the D_B and need identification based on their relationships to the D_{C+D} or D_G and D_H structures. The depositional evolution of the Jokela supracrustal association is predominantly related to the D_E and is described in detail in Appendix 5.

Structures in early to mid- D_E tonalite-granodiorite dykes and intrusions

Metamorphosed, folded and fragmented garnet-bearing tonalitic dykes and larger intrusive bodies cut migmatitic gneisses in the Espoo Granitoid Complex (EGC), like at the Hakkila site in Vantaa (Figure 29, sketch of outcrop in Figure 13a) and the Hyrylä site in Tuusula (Figure 30a). The Hakkila rock cuts typical veined garnet-mica gneiss with preserved volcanic remnants, intense D_B migmatization and D_C deformation described above. Closeby, to the north of Helsinki-Vantaa airport, a corresponding garnet-bearing tonalite-granodiorite dyke intruded into the S_E plane (Figure 26a) and cuts the D_{C+D} (Figure 26b). The Hyrylä tonalite (Figure 30a) cuts a strongly foliated and migmatitic garnet-cordierite gneiss. The primary features of the gneiss almost disappeared and the dyke is less fragmented than that in Hakkila; this indicates more proceeded deformation in Hyrylä than in Hakkila. The contact zone of these dykes is granitic-pegmatitic, suggest-

ing that the early magma/migmatite phase intruded in slightly cooler conditions than the later medium-grained central tonalite pulse. The dykes have an early S_E cont mineral foliation parallel to the dykes. The folds have granitic neosome in axial planes and show mobile fragmentation. The folds are related to F_{H+I} and the composite pegmatitic granite-tonalite dykes are related to early D_E . These garnet-bearing tonalitic rocks represent the earliest D_E magma phases generated during the evolution of the Southern Finland Granitoid Zone (SFGZ) and cutting the D_{C+D} structures.

In Hyrylä, a larger garnet-bearing tonalite body, closely associated with and tectonically corresponding to the tonalite dyke, shows a nice layered pattern (Figure 30b). The steeply NW-dipping layers are systematic in showing narrow biotite-rich planes bordered against a coarser-grained granitic portion that in part grades into finer-grained tonalite. These layers are repeated and in places the new set cuts the earlier one with a low angle. We interpret the layers as magmatic; they formed during repeated magma injections and continuous dilatation. Some crystallization occurred between pulses, but the ductile character of the layer relations and garnet microstructure suggest crystallization from magma and indicate a high-temperature environment during the layer generation. The pegmatite-granite contacts locally show in-situ melting characteristics with the country rock migmatites. However, the central dykes sometimes sharply cut the pegmatite, indicating their longer transport distance. Dilatation occurred perpendicular to the NW-directional magmatic layering (Figure 30b) and is consistent with the SE extension; the dextral shear zone in Hyrylä (Figure 30c) was generated concurrently with the SE extension.

A similar pegmatitic granite-granodiorite dyke cuts the pre- D_B gabbro-tonalite association in Kirkkonummi, at the Sarfvik site. Discordance between the gabbro and the D_E dyke is shown in Figure 18a. The gabbro was cooled before the intrusion of the dyke, as shown by the retrograde alteration zone surrounding the dyke (Figure 18d). Medium-grained granodiorite in the dyke centre represents hotter magma with a longer transport distance – the same granodiorite cuts close by the country rock with intrusive contacts. The dyke intruded into a dilatational fracture, but the contact character indicates intrusion into a cooler environment than in Hakkila and Hyrylä, which are closer to the granulitic unit of the West Uusimaa granulite Complex (WUC). It also differs from the previous dykes by its more granitic composition and absent garnet. The intrusion into a cooler environment indicates either a later intrusion event or intrusion in the margin area of the major D_E

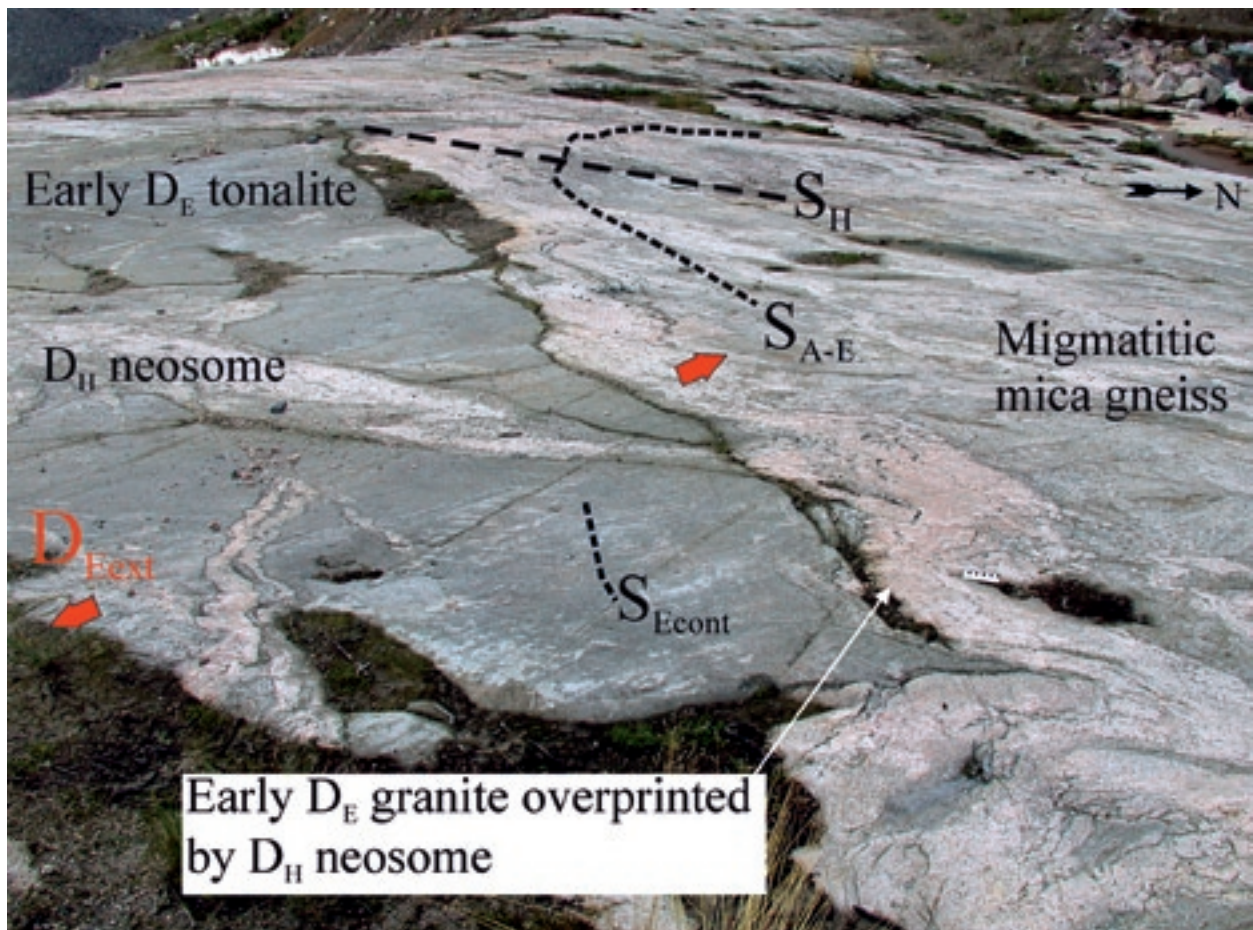


Figure 29. Garnet-bearing early D_E tonalite cutting migmatitic mica gneiss (see location in Figure 13). The dyke cuts the D_{A-D} structures (cf. Figure 26). The early intrusive phase of the dyke is represented by pegmatitic granite in the dyke margins. Tonalite intruded during progressive dilatation into the pegmatitic dyke phase. The composite dyke was deformed by progressive D_E (S_{Econt}) and fragmented by later by $D_{H(-)}$. A new granitic melt was also generated and it intruded into the $S_{H(-)}$ axial planes. Scale bar is 10 cm in length. Hakkila, Vantaa (Finnish grid coordinates KKKJ2 2560.64E 6687.59N). Photo by M. Pajunen.

event; there is no age data, but a situation close to the margin of the D_E granitoid area holds true. In Sarfvik, the later granite plays a minor role; only narrow pegmatitic veins cut the dyke there, but they blend into a pegmatitic border zone. This is why we suppose this granodiorite-pegmatitic granite phase to also be younger than the tonalitic phases and relate it to late D_E . The Sarfvik composite dyke was folded by c. ENE-trending D_H (Figure 18a) that caused shortening of c. 40–50% (Figure 18b).

Structural relationships of the widespread tonalitic intrusive rocks are often difficult to establish accurately. At the Jamppa site, Järvenpää, a garnet-bearing tonalite-granodiorite intruded into nearly horizontal and strongly sheared S_{Eext} foliation planes of a mica gneiss (Figure 31 a and b). Its intrusion occurred during the main phase of the D_E extensional shearing phase. Similar homogeneous, penetratively foliated tonalitic intrusions are common in the Southern Finland Granitoid Zone (SFGZ).

In all studied cases the early to mid- D_E garnet-bearing tonalitic-granodioritic compositions are intruded, migmatized or cut by later granitic pulses. The tonalites were dated using zircon U-Pb SIMS. The age of 1868 ± 3 Ma was interpreted to represent the magmatic age of the Hakkila dyke. An exceptionally old age of 3.30 Ga for one inherited zircon grain was observed in Hakkila (Appendix 8). The Hyrylä dyke was dated at 1860 ± 3 Ma; inherited zircon gave an age of c. 1.95 Ga (Appendix 8). The Maikkala pyroxene tonalite from Vihti (charnockite) represents a granulitic magmatic rock from the West Uusimaa granulite Complex (WUC); it gives TIMS ages of 1860 ± 5 Ma on zircon and of 1837 ± 3 Ma on monazite (Appendix 8); the U-Pb SIMS analysis of zircons give an age of 1862 ± 4 Ma for the rock and c. 1.83 Ga was obtained for a metamorphic zircon phase (Appendix 8). The ages of c. 1.86 Ga are regarded as magmatic ages of the early D_E tonalitic rocks, and the monazite and younger zircon ages of c. 1.84–1.83 Ga reflect metamorphism related to late D_E or D_H .

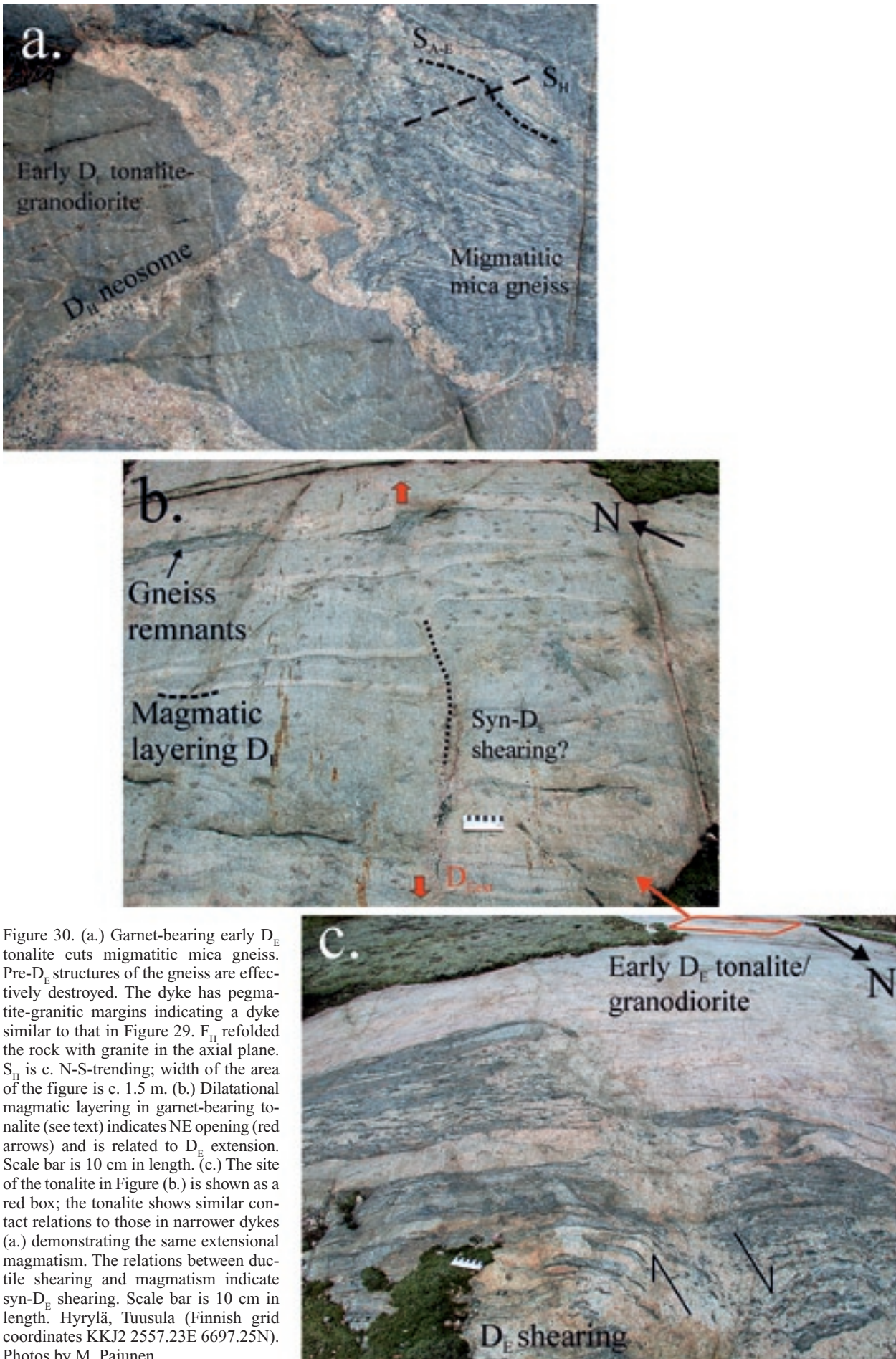


Figure 30. (a.) Garnet-bearing early D_E tonalite cuts migmatitic mica gneiss. Pre- D_E structures of the gneiss are effectively destroyed. The dyke has pegmatite-granitic margins indicating a dyke similar to that in Figure 29. F_H refolded the rock with granite in the axial plane. S_H is c. N-S-trending; width of the area of the figure is c. 1.5 m. (b.) Dilatational magmatic layering in garnet-bearing tonalite (see text) indicates NE opening (red arrows) and is related to D_E extension. Scale bar is 10 cm in length. (c.) The site of the tonalite in Figure (b.) is shown as a red box; the tonalite shows similar contact relations to those in narrower dykes (a.) demonstrating the same extensional magmatism. The relations between ductile shearing and magmatism indicate syn- D_E shearing. Scale bar is 10 cm in length. Hyrylä, Tuusula (Finnish grid coordinates KJK2 2557.23E 6697.25N). Photos by M. Pajunen.

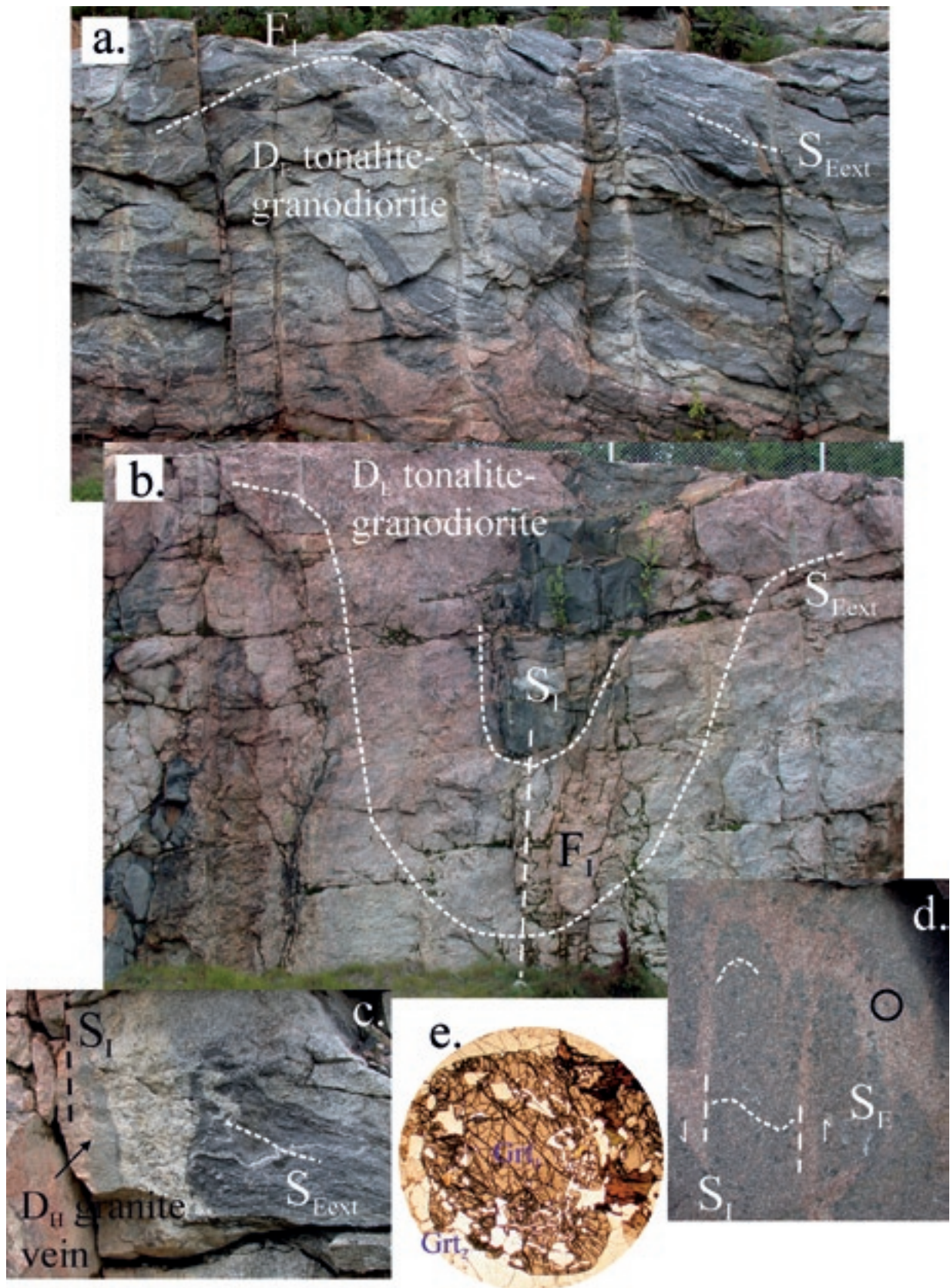


Figure 31. Nearly horizontal $S_{E\text{ext}}$ foliation intensely destroyed the pre-existing D_{A-D} structures and the early migmatization events in garnet-bearing mica gneiss. Garnet-bearing tonalite was intruded into the $S_{E\text{ext}}$ plane and refolded by open N-trending F_1 . Width of the area of the figure is c. 5 m; E is to the right. (b.) Large, tight to isoclinal F_1 folds (or F_H folds re-oriented by D_1) with steep axial planes S_1 ; the F_1 folds in this figure are exceptionally tight. The site is located close the major D_1 axial zone near the Vuosaari-Korso shear zone in the northern Espoo Granitoid Complex (EGC). Width of the area of the figure is c. 5 m; E is to the right. (c.) Medium-grained D_1 granite intruded into the F_1 axial plane. Width of the area of the figure is c. 1 m; E is to the right. (d.) D_1 structure with granite in the ductile D_1 shear planes. Width of the area of the figure is c. 0.5 m; E is to the right. (e.) The high temperature during D_1 in the northern EGC is indicated by the new garnet₂ generation surrounding the earlier garnet₁ core; the microstructure in both garnet generations indicates crystallization from melt. Diameter of the figure c. 1 cm. Jamma, Järvenpää (Finnish grid coordinates KKKJ2 2558.23E 6710.45N). Photo by M. Pajunen.

Structures in early to mid- D_E intermediate dykes – microtonalites

Intermediate intrusive dykes, microtonalites in the following, vary slightly in their composition. Such dykes are found in the southern archipelago (Sederholm 1926), in the western study area (Pajunen et al. 2008), widely in the Espoo Granitoid Complex (EGC) and in the Askola area of the Hyvinkää Gabbroic-volcanic Belt (HGB) (As in Figure 9 and Appendix 3). Generally, they are found/preserved in those areas where the latest granitic pulses of the Southern Finland Granitoid Zone (SFGZ) were not extensive or penetrative. These dykes exhibit quite well their relationships to their country rocks and are good reference rocks for structural analysis.

The contact structures of the dyke at the Staffas site, Sipoo (Figure 24), demonstrate microtonalite emplacement into the cooled syn-/late D_B tonalite. The microtonalite (Figures 20b and 24c) cuts the S_C foliation and was metamorphosed and partially melted by the later D_E events. In the granite-dominant areas the later D_H granites normally assimilate the dykes. Nevertheless, they still often show their sharp cutting relationships against their syn-/late D_B tonalitic and locally against the D_{A-D} -deformed migmatitic mica gneiss hosts. An example from the Hirvensuo site in Sipoo, in the eastern Espoo Granitoid Complex (EGC), describes the relationships of a microtonalite dyke to the migmatitic mica gneiss of a so-called Upper Tectonic Unit (UTU, Appendix 6) and to the syn-/late D_B tonalite (Appendix-Figs. 6-2a–d). The mica schist – dyke relations indicate that the mica gneiss was situated in the upper crust under low-grade conditions at the time of dyke emplacement, and the dyke contacts suggest already-cooled syn-/late D_B tonalite.

The studied microtonalite dykes have metamorphic mineral parageneses and predate the major granite events of D_H . At the Palojoki site, in Nurmijärvi, a weakly S_H -foliated microtonalite dyke cuts a high-grade migmatitic garnet-cordierite gneiss and pegmatitic granite (Figure 32a). The contacts to the granite are ductile and refer to intrusion into a hot rock shortly after the pegmatitic granite dykes related to D_E (Figure 32b). There is weak later shearing along the contacts of the dyke and assimilated granitic fragments in the dyke, but in general the effects of later alteration in the dyke are minor. The host rock shows ESE-WNW-trending, dextral D_E cont shear bands (Figure 32c) predating the D_E pegmatitic dykes. The structural setting of the dyke differs from those emplaced in tonalites (e.g. Figure 24a). The outcrop is located in the transitional area between the Espoo Granitoid Complex (EGC) and the West Uusimaa granulite Complex (WUC). The

dyke intruded into a deeper depth, which is supported by the tectonic D_{G+H} antiformal setting of the outcrop. In these deeper levels temperature also began to increase earlier and remained high for longer (the thermal gradient was high) than in the upper crustal levels. Our interpretation is that the dyke represents the corresponding intermediate magma to those microtonalites intruded in brittle conditions, but was intruded into an environment that had already achieved a higher temperature before dyke emplacement. The weak S_H as a only foliation in the rock also establishes it younger than the D_E tonalites and microtonalites described above.

The dykes are often steeply cutting their hosts, like the dyke in Nuuksio (Figure 33) that indicates dilatation in a c. SE-direction, but nearly horizontal dykes also occur, e.g. in the Sipoo area. The field observations provide evidence on the one hand of intrusion into a cool, brittle crust (Figure 24) that later underwent higher-grade metamorphism and, on the other hand, emplacement in a more ductile and heated environment (Figure 32b). Structurally, these dykes are in corresponding setting to the D_E tonalites described above. Thus, the microtonalites also show some variation in time of their emplacement.

No age has been determined from these sharply-cutting dykes from the study area. Microtonalites are widely distributed in eastern Finland, where they intrude the Proterozoic cover overthrust on the Archaean continent, in a N-trending zone of Svecofennian reactivation, close the craton boundary zone. Koistinen (1981) described fold structures in eastern Finland with N-trending axial planes, belonging to his structure D_4 (cf. Koistinen et al. 1996). It comprises zoned ductile folding that left large areas untouched. The deformation has been dated with the help of the syntectonic Maarianvaara granite to c. 1.86–1.85 Ga (Huhma 1981).

Structures in late D_E gabbros

Post- D_D mafic intrusive rocks are not common. We have found only few gabbros from in the northern Espoo Granitoid Complex (EGC). Often it is difficult to distinguish between these and the early/syn- D_B gabbros of the Hyvinkää Gabbroic-volcanic Belt (HGB) (Appendix 3) or the gabbroic-tonalite association in the south without linking them to the structural succession. An example from the Jyskelä site in Mäntsälä (Figure 34a) shows a medium-grained, foliated gabbro with local coarser-grained later ophitic portions – gabbro pegmatite (Figure 34b). In places the gabbro is homogeneous, medium-grained and only weakly deformed. The gabbro with a mingling-like structure with tonalite shows

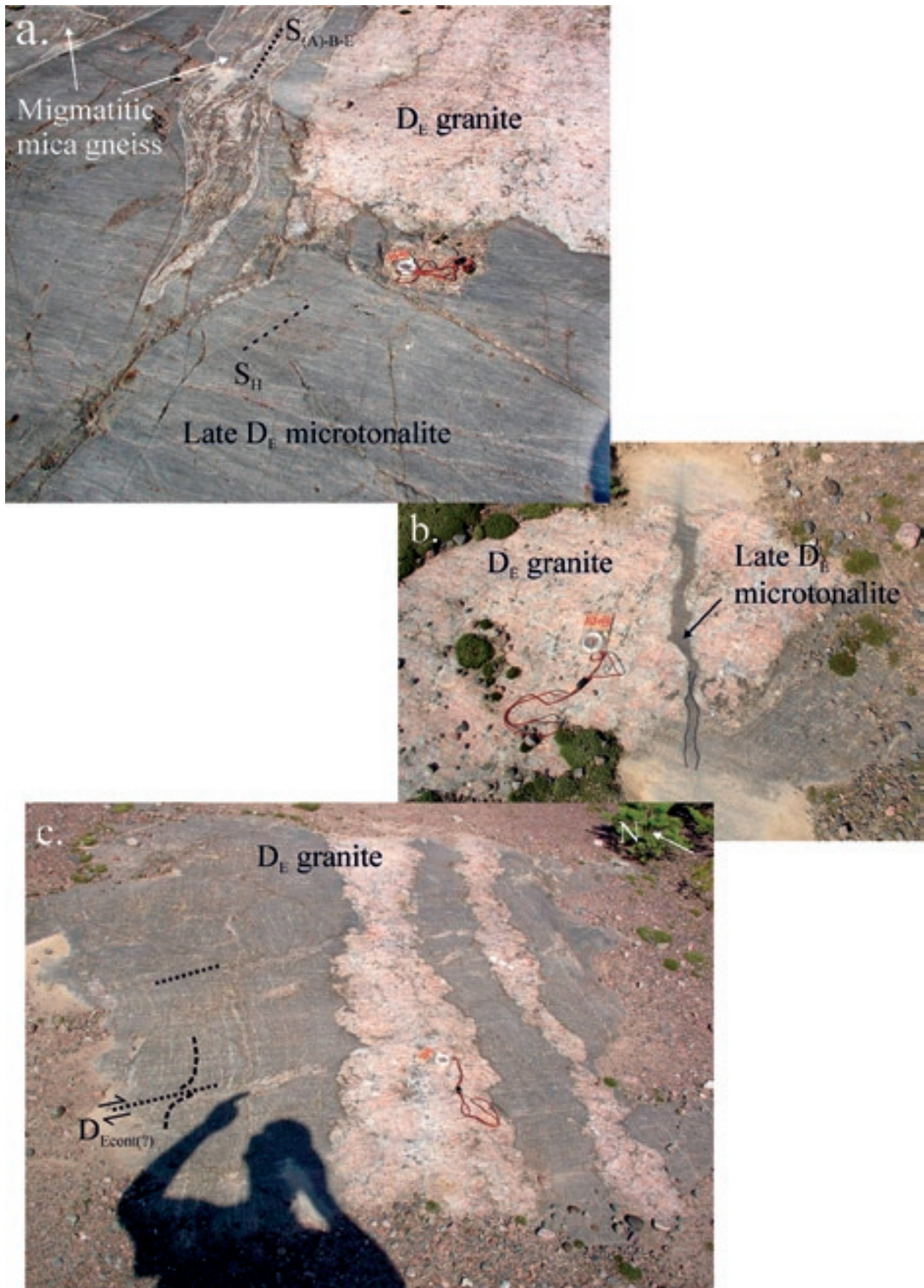


Figure 32. (a.) An intermediate weakly S_H -foliated microtonalite dyke cuts the high-grade, $D_{(A)-B-E}$ -deformed migmatitic mica gneiss represented by narrow zones in the upper-left part of the figure. Contacts against the D_E pegmatitic granite are sharp, but in figure (b.) the microtonalite is cutting the pegmatitic granite with bulbous margins suggesting ductile high-grade conditions during the microtonalite emplacement. (c.) The host migmatitic mica gneiss shows c. ESE-WNW-trending dextral $D_{Econt(?)}$ shear bands that predate the pegmatitic D_E granite dykes. Compass is 12 cm in length. Palojoki, Nurmijävi (Finnish grid coordinates KKJ2 2548.41E 6703.32N). Photos by M. Vaarma.

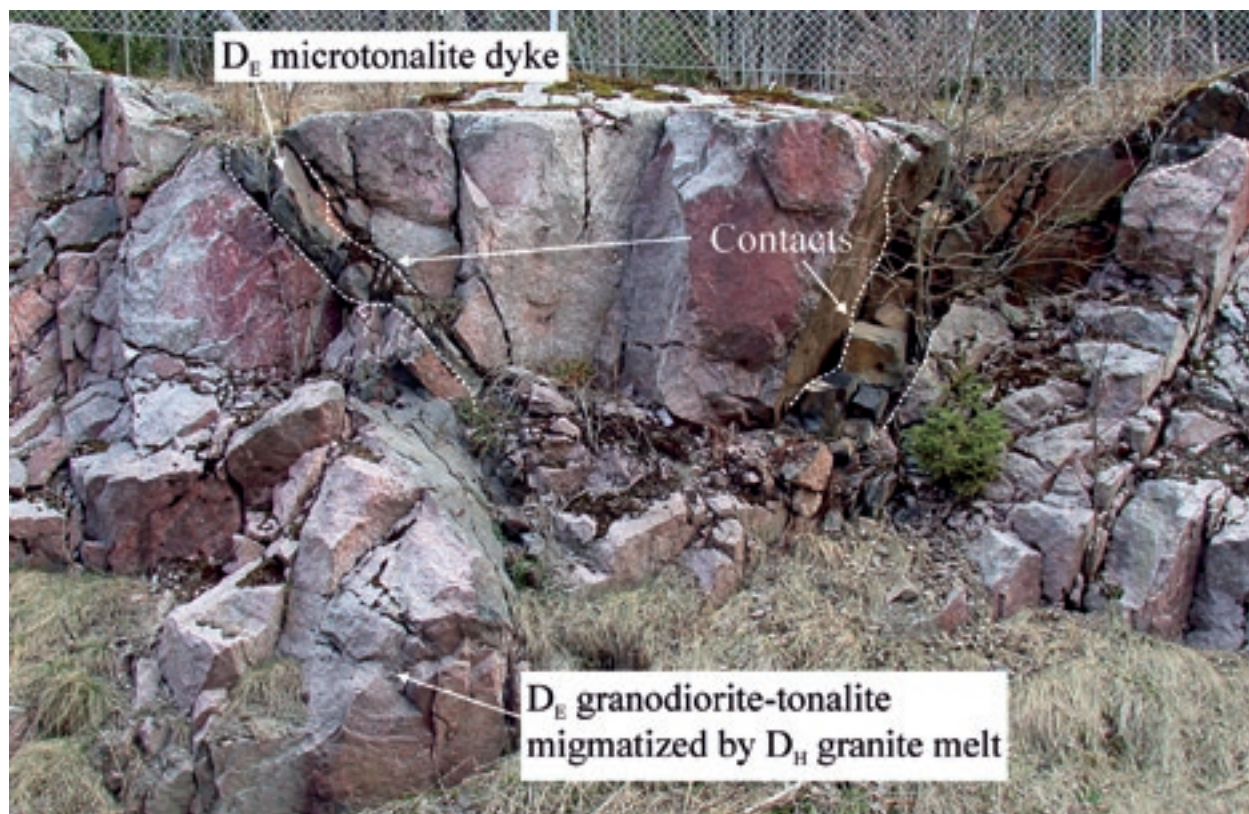


Figure 33. An intermediate dyke cutting the mid- D_E granodiorite/tonalite. The dyke and tonalite are both strongly altered by D_H granite-migmatization. Mustakallio, Nuuksio, Espoo (Finnish grid coordinates KKKJ2 2533.28E 6684.02N). Width of the area of the figure is c. 5 m; S is to the right. Photo by M. Pajunen.

weak foliation that formed in ductile and high-temperature conditions rapidly after the gabbro emplacement. We relate it to the extensional low-angle $S_{E,ext}$ foliation (Figures 34b and c). Granitic dykes intruding the gabbro show recumbent folding, and a retrograde alteration zone in the gabbro (Figure 34d); the reaction rim indicates a cooling period between the gabbro and granite intrusion. We relate the granite to the D_H that is associated with the recumbent folding to $F_{H,ext}$ with low-angle $S_{H,ext}$ foliation. The low-angle $S_{H,ext}$ overprints the earlier $S_{E,ext}$ and both are openly F_{G-H-I} -folded (Figure 34a and b). N-trending shear zones cutting the gabbro can be related to the late phase of the regional D_I or even to D_p . Thus, according to the structural observations, this gabbro is syn- D_E and nearly contemporaneous with tonalitic magmatism, as supported by the mingling-like structure. In the northern EGC in Karhunkorpi, Nurmijärvi, a gabbro has a similar tectonic setting. It is openly folded and it intruded into a horizontal S_E plane. The kinematic observations made from the horizontal $S_{E,ext}$ structures indicate extensional top-to-SE movement, so the extension is directed outwards from the granulite facies WUC area (see later).

The gabbro magmatism indicates a deep-seated heat source and the generation of magmas at this stage. The increase in temperature also caused the high-grade metamorphism that characterizes the northern parts of the Espoo Granitoid Complex (EGC) and the West Uusimaa granulite Complex (WUC). The homogeneous portion of the gabbro contains some zircon that was dated by the TIMS method to 1841 ± 7 Ma; the U-Pb SIMS analyses on zircons give, within error limits, the same age of 1838 ± 4 Ma (Appendix 8 and App-Table 3). The structural setting of intruding granite corresponds to the D_H pegmatitic granite in Bollstad (described later and Appendix 8), but the temperature has increased higher in Jyskelä, as indicated by more ductile deformation and the mingling-like structures. The gabbro is slightly older than the pegmatitic dykes in Bollstad (cf. Appendix 8); we relate it to late D_E , because it precedes the major D_H granite pulses. This also indicates that the horizontal $S_{E,ext}$ foliation was generated at 1.84 Ga; the observation made in the West Uusimaa Complex (WUC) established its generation after the intrusion of the Maikkala pyroxene-bearing tonalite (charnockite) (Appendix 8).

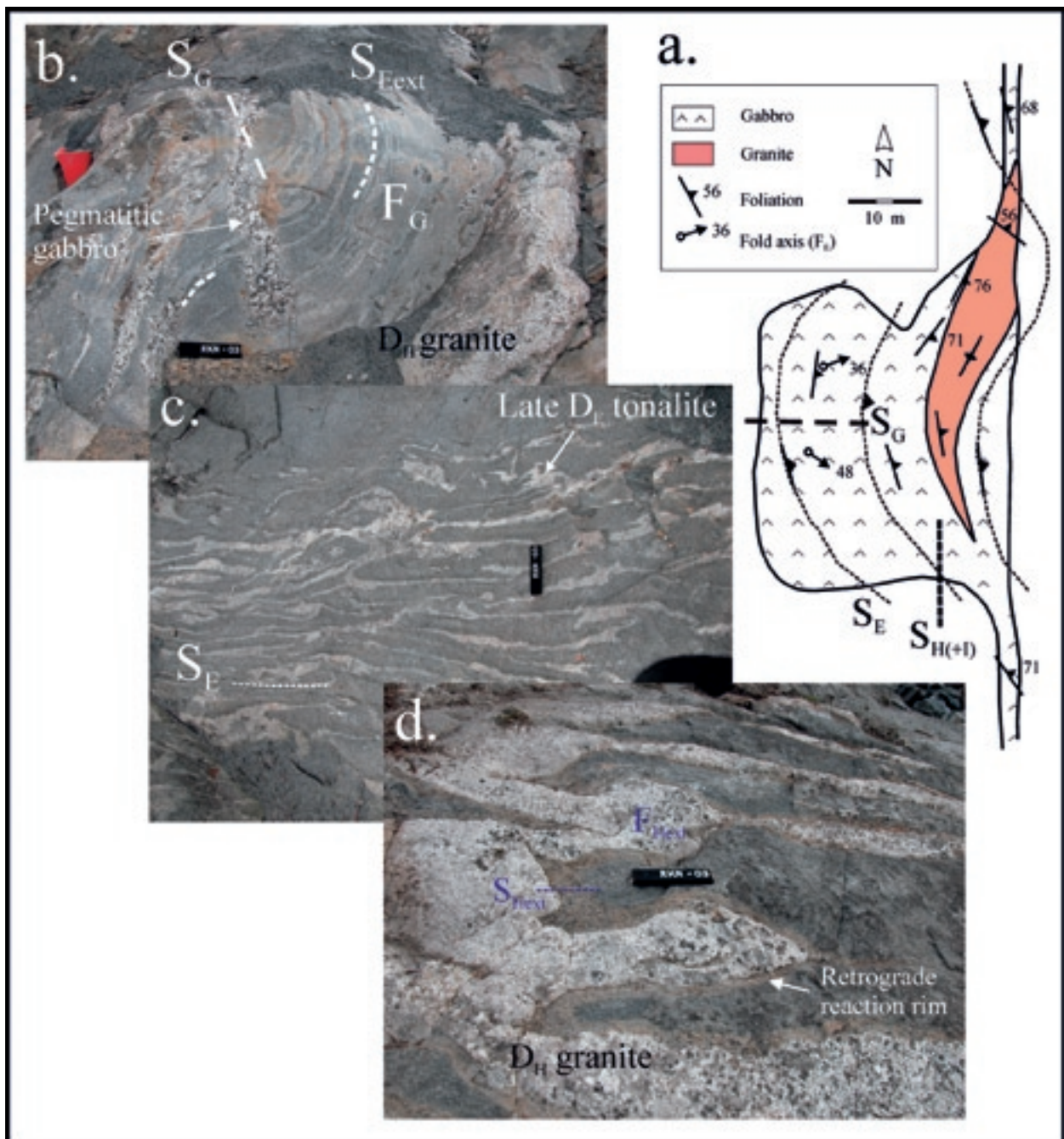


Figure 34. (a.) A sketch of the structural setting of the late D_E gabbro outcrop in Jyskelä, Mäntsälä (Finnish grid coordinates KKJ2 2562.56E 6711.55N). (b.) Late D_E gabbro is cut by a late D_H granite dyke and coarse-grained gabbro-pegmatite veins cutting the $S_{E\text{ext}}$ foliation refolded by F_G . Scale bar is 10 cm in length. (c.) A mingling structure between the gabbro and contemporaneous tonalite. $S_{E\text{ext}}$ foliation was rapidly generated after intrusion in high temperature conditions. The structure was later deformed by D_H (see d.). Scale bar is 10 cm in length. (d.) Intense D_H vertical shortening of gabbro is indicated by the isoclinal recumbent F_H folding of D_H granite dykes; a new foliation $S_{H\text{ext}}$ formed. Scale bar is 10 cm in length. Photos by R. Niemelä.

D_E structures and kinematics

The intensity and character of the D_E structures vary regionally due to deformational depth (schematized in Figure 4) and the time of their formation. The oldest dated D_E intrusion, the garnet-bearing early D_E tonalite in Hakkila, intruded into an approximately E-trending dilatational zone (Figure 29). Dilatation during the emplacement of the slightly younger gar-

net-bearing Hyrylä tonalite was c. SE-directional (Figure 30a); a similar direction of dilatation is also interpreted from the layered Hyrylä tonalite (Figure 30b) and from the shear zones related to its contacts (Figure 30c). However, the homogeneous Jamma tonalite was emplaced into horizontal S_E shear planes (Figures 31a and b) in the migmatitic mica gneiss.

The most intense D_E structure in the D_A - D_D deformed rocks is S_E foliation that developed as a

spaced crenulation cleavage. A map from the Klaukaka site in Nurmijärvi (Figure 35) shows the characteristic D_E - D_H relationships (Figure 12c). S_E is a regional, nearly horizontal shear foliation in the migmatitic gneiss. The horizontal S_E foliation plane intersects the pre-existing foliation (S_B of the mica gneiss), forming a SW-trending intersection lineation L_E (Figure 35d). Drag bends of the previous foliation by the S_E shearing indicate extensional top-to-SE movement – the dilatation zone is towards the NW, towards the high-grade West Uusimaa granulite Complex (WUC). Similar kinematic patterns of S_E were identified further south, e.g. at the Kauklahti site, Espoo (Figure 19). In the WUC and the northern Espoo Granitoid Complex (EGC), S_E is often developed as a spaced foliation that transposed and intensely fragmented the early D_B migmatite structures (Figures 12c and 36). Sometimes, the earlier D_A - D_D structures are completely destroyed, as in the felsic pyroxene gneiss in the WUC (Appendix-Fig. 2-1). The age of S_E in the WUC is younger than 1.86 Ga (Appendix 2). Contractional $S_{E,cont}$ is a spaced foliation in the syn-/late D_B tonalites (Figure 24). Shear bands with granitic melt are characteristic (Figures 22c and 25b). In the early D_E intrusive rocks, oblique contractional $S_{E,cont}$ is penetrative mineral foliation paralleling the dykes.

The age of Hakkila tonalite is precisely the same as the age of the granitoid that blocked the SW-transpressional $D_{4/D}$ evolution in the northern units (Appendix 7). Kinematically, the early D_E dilatational structures in the Espoo Granitoid Complex (EGC) fit well with this NE-SW transpressional stress field that acted during the $D_{4/D}$ between the major N-trending Baltic Sea-Bothnian Bay (BBZ) and the Riga Bay-Karelia Zones (RKZ) (Figure 8). D_E extension occurred in the oblique NE-E-trending dilatation zones in between the active dextral N-trending shear zones, the BBZ and RKZ. The continued NE-SW transpression caused local rotations of the dykes to produce closely related metamorphic steep penetrative $S_{E,cont}$ foliation paralleling the dykes. In addition to the early D_E tonalite dykes, these structures are also typical in the microtonalitic dykes. Under continuing extension and increasing temperature, oblique dilatation developed to horizontal extensional shearing with top-to-SE movement. Increased tonalitic to granodioritic magma emplaced into these $S_{E,ext}$ shear foliation planes. Thermal gradient was high during the late D_E and gabbroic intrusions emplaced into corresponding $S_{E,ext}$ shear planes. The increasing temperature produced polymetamorphic characters in the older syn-/late D_B tonalites that are intensely shear-banded and re-melted, which is not the case with the intermediate D_E granitoids.

The evolution of the Jokela supracrustal association (Jo on Figure 9) began during the early D_E deformation. In the upper crustal levels the oblique extension between the major N-trending BBZ and RKZ opened dilatational regions into a c. NE-E trend, into which the supracrustal sedimentary association began to accumulate. The continuing extension and clockwise rotation caused rapid deformation of the sequences, and increased heat flow due to the thinning crust caused volcanic activity in the subsiding sedimentary basin. We interpret the Jokela supracrustal association as a pull-apart basin formed in between the major N-trending deformation zones – the evolution of the association is discussed in detail in Appendix 5.

In summary, the D_E evolution in the Southern Finland Granitoid Zone (SFGZ) was a result of SW-NE transpression causing oblique SE-dilatation, extensional top-to-SE shearing and clockwise rotation between the active dextral N-trending transcurrent shear zones – the Baltic Sea-Bothnian Bay Zone (BBZ) and Riga Bay Karelia Zone (RKZ).

D_F deformation – E-W movement of the Central Finland block

The sinistral NW-trending Hiidenvesi shear zone (Figures 10 and 16) in the West Uusimaa granulite Complex (WUC) predates the major D_H granitic events; the NE-trending border zone of the Nuuksio granite area, characterized by a strong D_H granite magmatism, cuts it at the southeastern end. According to interpretation made from magnetic maps the shear zone continues below the Espoo Granitoid Complex (EGC), where it still acted as a zone of weakness during the rapakivi-related diabase magmatism. The generation of the shear zone indicates E-W contraction. However, in the study area the fold structures with c. N-trending axial planes are related to D_D deformation or, in the vicinity of the major N-trending, like the Vuosaari-Korso shear/fault zone, to D_I deformation. Folds related to this E-W contraction have not so far been found in the study area.

The observations of Koistinen (1981) in eastern Finland indicate contractional folding with N-trending axial planes at c. 1.86–1.85 Ga ago (see also Huhma 1981). The major sinistral ENE-E-trending deformation zone at the northern end of the Bothnian Bay (cf. Korja & Heikkinen 2005) and dextral movements in the Hyvinkää and southern Finland shear zones indicate the push of a large-scale crustal Central Finland block towards the east (Figure 8). This kind of deformation would explain the zones of folds with N-trending axial planes, the 1.85 Ga fluid activity in NW-trending shear zones and the

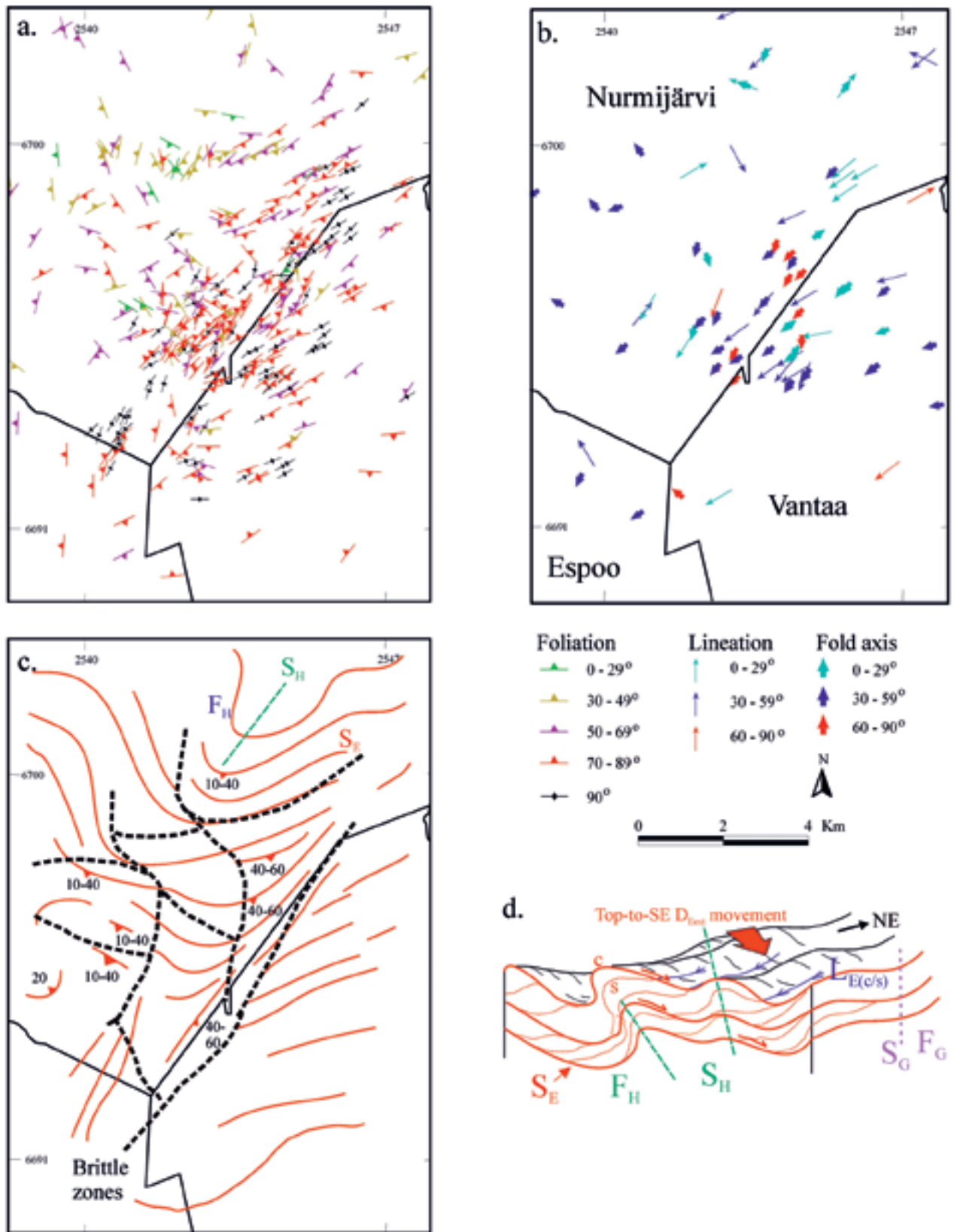


Figure 35. Tectonic element maps, Klaukkala, Nurmijärvi area (Finnish grid coordinates KJ2): (a.) foliations, (b.) lineations and (c.) S_E foliation plane formlines deformed by D_H , and major ductile to brittle shear/fault zones. (d.) A schematic tectonic model showing the relationships between structures and tectonic transport: lineation dipping towards the SW is predominantly an intersection lineation on the S_E ext shear planes (intersection between the S-C planes) that point to low-angle top-to-SE movement during D_E extension. The S_E planes are moderately to openly refolded by the D_H with a NE-trending axial plane (see Figure 12c.). Base map © National Land Survey of Finland, permit No. 13/MML/08.

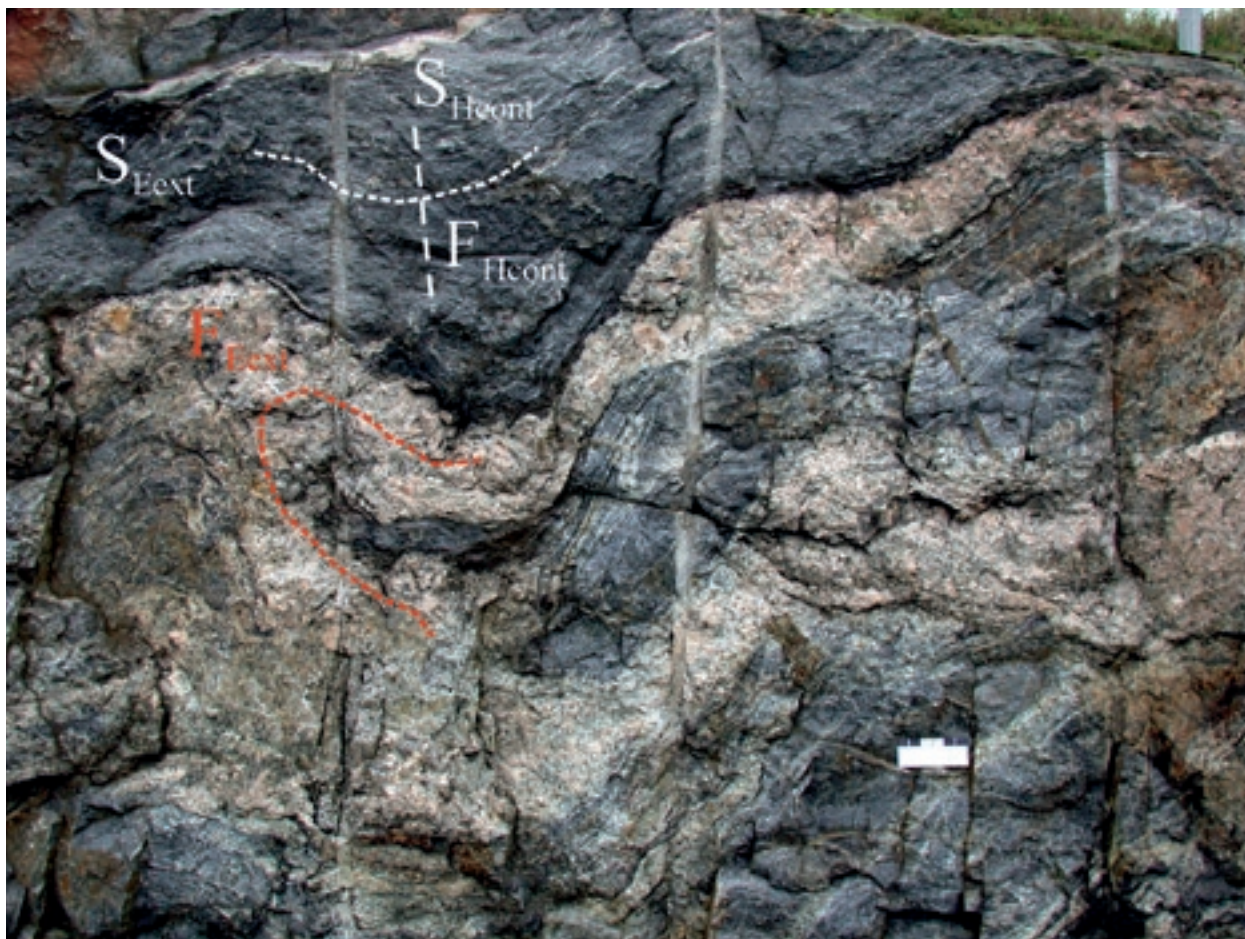


Figure 36. A migmatitic garnet-bearing mica gneiss, cut by D_{E-H} pegmatitic granite, shows strong extensional $S_{E,ext}$ foliation, presumably overprinted by the later $S_{H,ext}$, and is refolded by $F_{H,cont}$. The D_{A-D} structures are completely destroyed; relics of the early D_B neosome appear as remnants elongated in the direction of the S_E foliation planes. Scale bar is 15 cm in length; E is to the right. Bockbärgen NE, Vantaa (Finnish grid coordinates KJK2 2550.98E 6687.43N). Photo by M. Pajunen.

emplacement of felsic granitoids of that age in eastern Finland (Pajunen & Poutiainen 1999). Near the craton boundary, there are several NW-trending faults, sometimes showing sinistral movement (e.g. D_C in Pajunen 1986), and NE-trending dextral faults, such as the Auho fault (e.g. Kärki 1995) cutting the Kainuu schist belt. The fold structures and the shear zones were formed during E-W contraction labelled here as D_F deformation.

The SW-NE transpression during the D_E turned into E-W-directional contraction during the D_F at c. 1.86–1.85 Ga. The E-W-push of the Central Finland block did not have major effects on the structures in the southernmost part of Finland, because stress predominantly released along the major E-W-trending shear zones. The main reason for the D_F block movements is considered to exist further west; a large-scale ductile folding with N-NNE-trending axial planes in the western Fennoscandian Shield (Figure 8) may be causing pushing of the coherent Central Finland block towards the east. The E-W contraction may also represent a local rotation of the NE-SW transpressional stress, especially because in

the south the SW-NE transpression D_E occurred at the same time.

D_G deformation – N-S shortening

D_G deformation comprises N-S-oriented shortening that produced large-scale open folding with c. E-W-trending axial planes (Figure 11). The F_G folds developed in the intensely D_E -migmatized zones to gentle and sometimes even tight folds. S_G foliation is weak or missing. The D_G effects are difficult to distinguish in the areas where the earlier D_{C-D} dome-and-basins are in the same direction – only tightening or shearing of these early structures occurred. On outcrops the characters of D_G structures can be identified in those areas where the horizontal S_E and D_E granitoids predominate; they were not affected by the D_{A-D} events. The scarce observations on tectonic transport during the D_G indicate overturning towards south in Kauklahti (Figure 19d) and in southern Sipoo (Figure 28c). Although poorly detectable on the outcrop scale, the D_G has an important effect on the regional tectonic $D_{G+H±I}$ dome-and-

basin pattern, which strongly determined the present exposing of different tectonic units, such as the West Uusimaa granulite Complex (WUC) and Espoo Granitoid Complex (EGC) (Figure 11). Wide-scale folding with E-W-trending axial planes can be identified in the area of the whole Granite Migmatite Belt (GMB) (Figure 11). It could also partly explain the metamorphic pattern in the Tonalite Migmatite Belt (TMB), where the granitoid-dominant E-trending central zone is surrounded by lower-grade bordering areas (Figure 11).

Sinistral shearing of the Porkkala-Mäntsälä shear zone, bending the pre- D_G structures to sinistral drag folds, can be explained by the N-S shortening related to D_G deformation. Torvela et al. (2008) describe the dextral NW-trending South Finland shear zone from SW Finland in the southwestern archipelago. They dated its beginning at 1.85 Ga and related it to the Southern Finland shear zone of this study. However, according to our interpretation from aeromagnetic maps, the shear zone continues more or less straight towards the ESE. We relate it contemporaneously to the Porkkala-Mäntsälä shear zone produced due to c. N-S compression during the D_G . We suggest the age of c. 1.85 Ga for the D_G deformation.

D_H deformation – a major granitic event in the Southern Finland Granitoid Zone

In the Southern Finland Granitoid Zone (SFGZ), weakly oriented, medium to coarse-grained, reddish or greyish, often K-feldspar-porphyritic or “layered” granitic rocks (Figure 37a) are widely distributed. They are accompanied by several rather contemporaneous and heterogeneous magmatic, often pegmatite granitic, and migmatitic events. They intrude or migmatize the described D_E granitoids, including the pegmatite granitic border zones of the early/mid- D_E dykes (Figures 29 and 30a). In the Espoo Granitoid Complex (EGC), the Nuuksio area (Nu in Figure 9) forms a large open synformal D_{G+H} structure (Figure 11). It is one of the key areas illustrating how the late granitic intrusive and melting events “eat and hide” the structures formed during the earlier D_{A-E} evolution, and how the D_H magmatism and migmatization are related to the D_H structures. The Riihimäki Granitoid Complex (RGC), the Perniö Granitoid Complex (PGC) and the southern Sipoo area of the Espoo Granitoid Complex (EGC) are corresponding granitic units. However, early D_H evolution can be best examined outside the major D_H granite units; there, the relationships to the early structural evolution are better preserved. Some mafic dykes, cutting the Southern Volcanic-sedimentary Belt (SVB), are closely related to the D_H granite

magmatism and represent the latest magmatic events identified in the study area.

Description of D_H granites

The D_H granites cut the older structures in different ways; the melting structures and intrusives change from place to place due to characteristics of the syn-tectonic D_H deformation processes. Heterogeneous patchy melting of the older granitoids is a general phenomenon (Figure 37b); biotite decomposes to garnet and/or cordierite and granitic melt. Melt formed non-oriented in-situ patches sometimes accompanied by intruded granite dykes. In places, D_H granite occurs in shear bands (Figure 32c) that cut the foliated granitoids or gneisses. In the areas of horizontal deformation and strong granitic melting, the D_H granite was emplaced into the foliation or shear planes (Figure 37c) forming heterogeneously “layered” granites; they are characteristic, for example, in the Nuuksio synform. Non-foliated coarse-grained, garnet-bearing granite and older, foliated granitoid alternate within them (Figure 37a). When the amount of granite increases the older granitoids or gneisses are decomposed to biotite-rich schlierens in the younger granite (Figure 5c). If the contacts with pre-existing rocks are not visible on the outcrops, it is seldom possible to determine whether the pre-existing host rock was a metapelitic-psammitic metasedimentary rock, which is typical in the northern part of the Nuuksio and southern Sipoo areas, or a granitoid. In the Nuuksio area the weakly-oriented porphyritic granites show open folds with steep axial planes trending NE (S_H) or N ($S_{H±}$).

The areas dominated by the widespread D_H granites show a low U/Th radiation ratio, differing from the surrounding granitoid areas (Figure 38). The disturbing effects of water cover and overburden by glacial sediments place restrictions on analysis of the ratio (see Airo et al. 2008). When taking these restrictions and the featureless magnetic anomalies characterizing these areas into account, some estimation of the distribution of corresponding magmatic rocks can be carried out. Our conclusion is that the D_H granitic pulse does not appear as penetrative feature in the Southern Finland Granitoid Zone (SFGZ), but is concentrated in areas determined by local late heat flow and dilatation. The decreased U/Th ratios in granitic rocks indicate that repeated melting processes produced them. Some of these granites have very small amounts of zircon (M. Vaasjoki, pers. comm. 2004). We suppose that the low U/Th ratio was predominantly a result of remelting of earlier syn-/late D_B and early/mid- D_E intermediate granitoids. The early U-bearing phases were decomposed and soluted under increasing

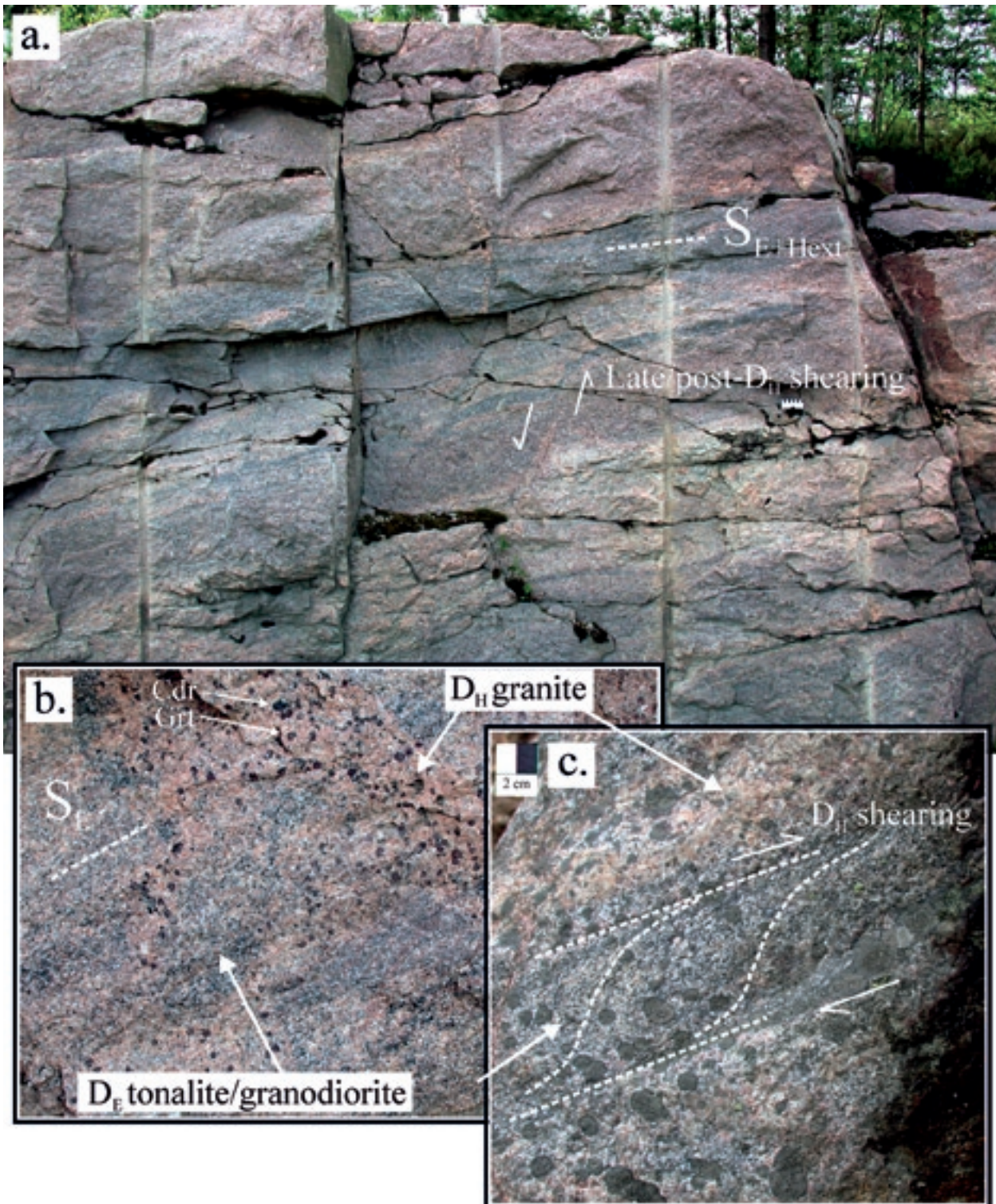


Figure 37. (a.) D_H remelting of early/mid- D_E tonalite/granodiorite producing a layered appearance characterizing the granitoids in the Nuuksio synform area. Scale bar is 10 cm in length; N is to the right. Ämmänsuo, Espoo (Finnish grid coordinates KKJ2 2531.22E 6681.43N). (b.) Patchy D_H remelting of early/mid- D_E granodiorite/tonalite in the Nuuksio synform. Biotite has decomposed to garnet, cordierite and granitic melt. Width of the area of the figure is c. 1 m. Solvalla, Espoo (Finnish grid coordinates KKJ2 2531.02E 6687.27N). (c.) Extensional D_H shearing deforming the pre-/syn- D_E tonalite. The shear plane was deformed by progressive F_{H+cont} folding into a secondary thrust zone position. The D_H granite intruded into the extensional S_{H+ext} shear plane. NE is to the right. Haramossen, Nuuksio, Espoo (Finnish grid coordinates KKJ2 2534.15E 6685.25N). Photos by M. Pajunen.

temperature and magmatic fluid production. Uranium was fixed into the increased metamorphic melt/fluids and escaped to the upper horizons in the crust. Indeed, this is supported by the uranium showings (Saltikoff et al. 2002) that are concentrated in semi-ductile/-brittle structures of the overlying tectonic sequences.

To the west of the Espoo Granitoid Complex (EGC), in the Bollstad site at Inkoo, the syn-/late D_B tonalite (cf. E_b tonalite of Pajunen et al. 2008) is cut

by D_H pegmatitic dykes and granitic veins that show isoclinal recumbent folding with horizontal axial planes (Figures 39a and c) indicating vertical shortening. The pegmatitic dyke was originally intruded into an upright position into a brittle crust that is suggested by the semi-ductile shearing structures related to the early development of the horizontal S_H foliation in the tonalite (Figure 39b). No retrograde mineral phases were formed during shearing, but a continuing vertical shortening under increased

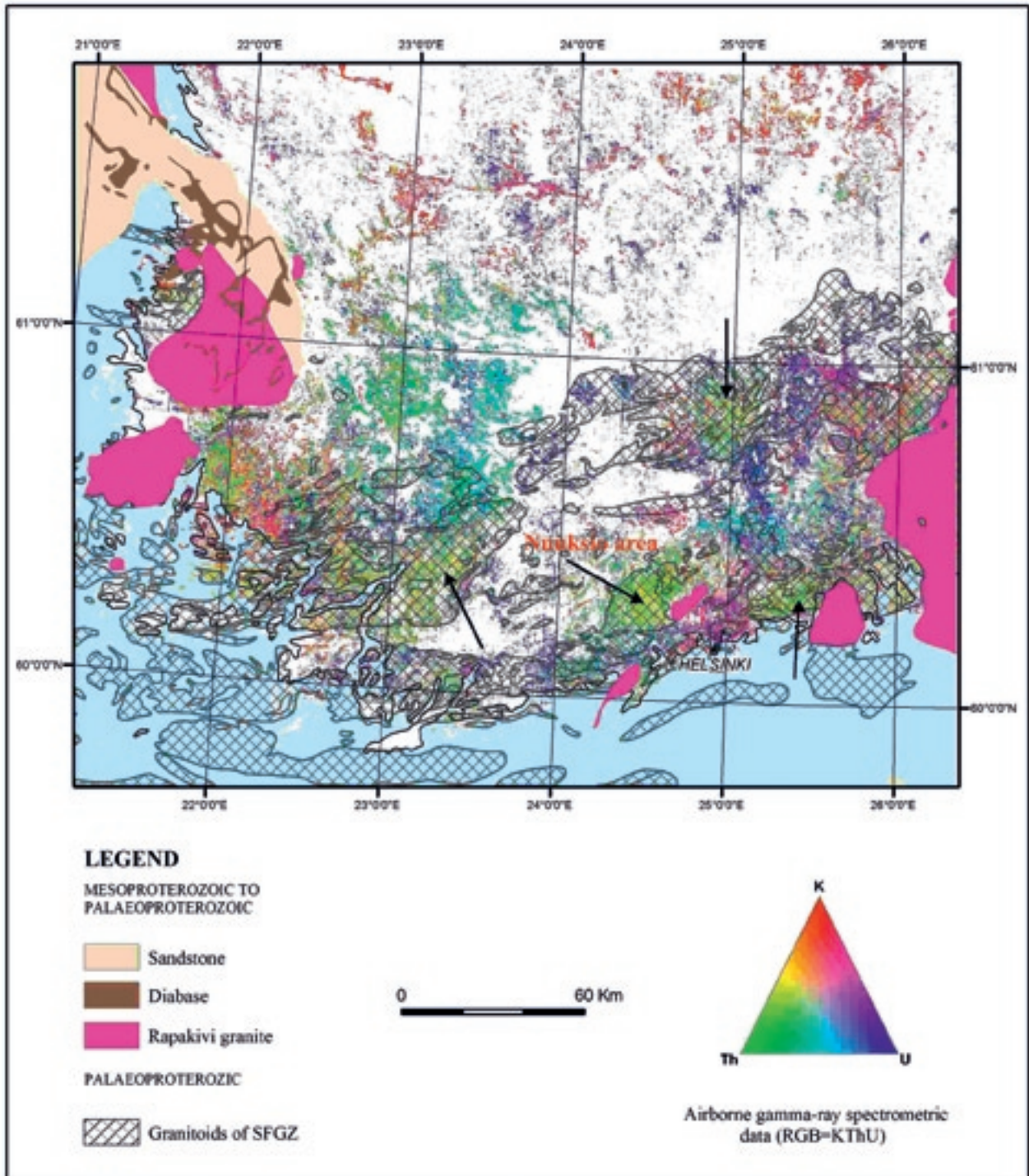


Figure 38. An aeroradiometric map showing the belt characterized by the D_E and D_H granitoids (Southern Finland Granitoid Zone, SFGZ – hatched). The area of intense D_H remelting of the early tonalitic/granodioritic rocks (Figure 37) in the Nuuksio area shows a lower U/Th ratio than in its surroundings. A similar ratio in the radiometric data is also found in the other granitoid complexes, as indicated by the arrows. Base map © National Land Survey of Finland, permit No. 13/MML/08.

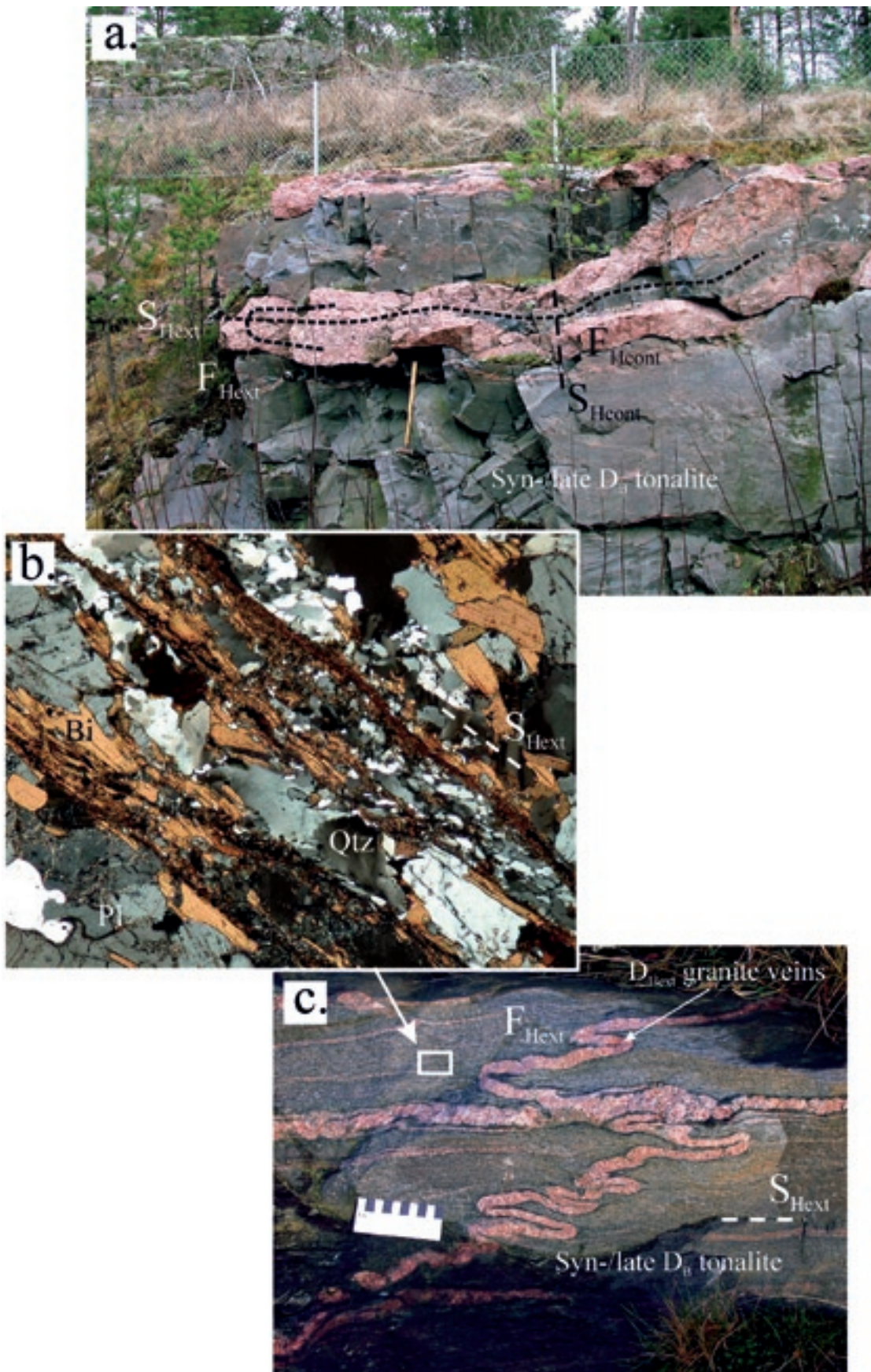


Figure 39. (a.) Isoclinal recumbent F_{Hext} folding in a D_H pegmatitic granite dyke strongly cutting deformed gneissic syn-/late D_B tonalite. The intrusion of the dyke indicates emplacement into steep position in the beginning of the D_H granitic phase in the area; the outcrop is located in the marginal area of the most intense D_H granitic area of Nuuksio (cf. Figure 38). Hammer is c. 65 cm in length; SE is to the right. (b.) Photo of microstructures in the tonalite. The development of S_H began as semi-ductile shearing, and under the increasing temperature spaced biotite foliation was produced; Bi = biotite, Pl = plagioclase and Qtz = quartz. Width of the figure area is c. 6 mm. (c.) Vertical D_H shortening in narrow granite veins in the gneissic tonalite that shows a strong S_{Hext} foliation. Scale bar is 10 cm in length. Bollstad, Inkoo (Finnish grid coordinates KKJ2 2497.78E 6662.16N). Photos by M. Pajunen.

temperature caused a horizontal penetrative S_H biotite foliation that characterizes wide areas in the environments. The pegmatitic dyke folded isoclinally and new syn- D_H granite veining developed (Figure 39c). Similar structures elsewhere deform the D_{C+D} dome-and-basins and also the earlier D_E structures and intrusions, like the late D_E gabbros (Figure 34d). The emplacement of the pegmatitic dyke represents the beginning of the D_H granitic event in Bollstad, outside the major D_H granite unit EGC. Open folds with c. NE-trending steep axial planes refold the recumbent F_H folds and form interference dome-and-basins with the F_G and F_I . The open large-scale folds were developed during the progressive D_H deformation into oblique contractional settings; the tectonic relationships of the recumbent fold interpreted as extensional $F_{H,ext}$ and the steep $F_{H,cont}$ folds are discussed below.

Description of D_H diabase dykes

In the southernmost Southern Finland Volcanic-sedimentary Belt (SVB), near the coast and on the islands of the Gulf of Finland, fine-grained diabase dykes occur showing fresh amphibolite facies hornblende-plagioclase paragenesis. They are found in places that were not intensely intruded by the D_H granites. The dykes cut the gneisses in a c. N-NNE or E-W direction and were, in all the studied cases, emplaced into central parts of the pegmatitic granite dykes.

Figure 40a shows an example in Espoo, the Rövaren site. The E-W-trending dyke cuts felsic gneiss that was intruded by pre-/early D_B amphibolite dyke boudinaged by D_B and folded by F_C . There are magmatic hybrid-/mingling-like structures between the diabase and granite margin (Figure 40b). At the Kopparnäs site, Inkoo, structurally and compositionally corresponding diabase dyke (Figure 40d) cuts the old structure of the gabbro-tonalite association in a N-S direction. The Rövaren dyke was weakly F_H folded with ENE-trending axial planes (Figure 40c) and the diabase dyke in Kopparnäs shows ductile, sinistral N-S-trending D_{H-1} shearing (Figure 40d) close to the contacts. The metamorphic paragenesis in the dykes and contact structures between the dykes and the pegmatitic granite supposes intrusion into a high temperature environment.

Age of D_H magmatism and metamorphism

The U-Pb TIMS age for the monazite of the Bollstad pegmatitic granite is 1828 ± 3 Ma (Appendix 8). This age provides a reference for the beginning of the D_H deformation in the area and suggests a discordance of c. 40 Ma after the intrusion of the

syn-/late D_B tonalite at 1873 ± 7 Ma in Bollstad (Appendix 8). Several studies since Sederholm (1927) have provided evidence that the crust of the Granite Migmatite Belt (GMB) stabilized and cooled between tectono-thermal events (e.g. Korsman et al. 1984, 1999 and Pajunen et al. 2008). Such cooling stages are described between the syn-/late D_B tonalites and the early/mid- D_E microtonalite dykes (Figures 24a and b), and retrograde reaction rims surrounding the mid- D_E granodiorites (Figures 18a and d) also indicate the preceding cooling stage of the country rock.

However, continuous thermal and magmatic evolution is supported by structural relationships between magma phases and by the ages of structurally-fixed magmatic rocks. For example, in the northern Espoo Granitoid Complex (EGC) compositionally varying magmatic and metamorphic activity continued in a ductile state practically without a break throughout the described 40 Ma period. High-T metamorphic conditions during this cap are supported by several observations of metamorphic zircons and monazites (Appendix 8). The Bollstad granite dykes indicate the beginning of the D_H pulse outside the major D_H granite units, but in the granitoid-dominant areas like the EGC (Figures 9 and 38) huge amounts of granodioritic to granitic magmas were produced. Kurhila et al. (2005) dated the granitic magmatism from the detailed study area in Nuukio at c. 1.85–1.82 Ga. On the basis of structures and remelting characteristics in the area (Figures 37a-c), we suppose that the youngest ages represent the D_H magmatism and remelting event of the earlier intrusive or supracrustal rocks. This is supported by the ages of the D_H leucosomes of granulitic metapelites ranging between 1.82–1.81 Ga (Korsman et al. 1984, 1988, 1999 and Väisänen et al. 2004). Intense crustal melting also produced wide, locally porphyritic granite intrusions. The cooled parts of the crust, beside the areas of intense D_H granitic magmatism, medium-grained to pegmatitic granite dykes with sharp contact were intruded, as exemplified in Figure 15c from the Southern Volcanic-sedimentary Belt (SVB).

The D_H diabase dyke from Kopparnäs yielded a small amount of zircon. For the most part, it has a SIMS U-Pb age of c. 1.83 Ga and only a few zircon grains with deviating appearance poorly determined an age of c. 1.78 Ga. It is considered, that the 1.83 Ga zircon undoubtedly is inherited and the 1.78 Ga is a maximum age for the diabase as mafic fine-grained rocks very seldom contain co-magmatic zircon. Three discordant U-Pb data points analyzed using TIMS reflect an average of c. 1.84 Ga for the very tiny inherited zircon in Kopparnäs diabase. The dyke shows an amphibolite facies mineral

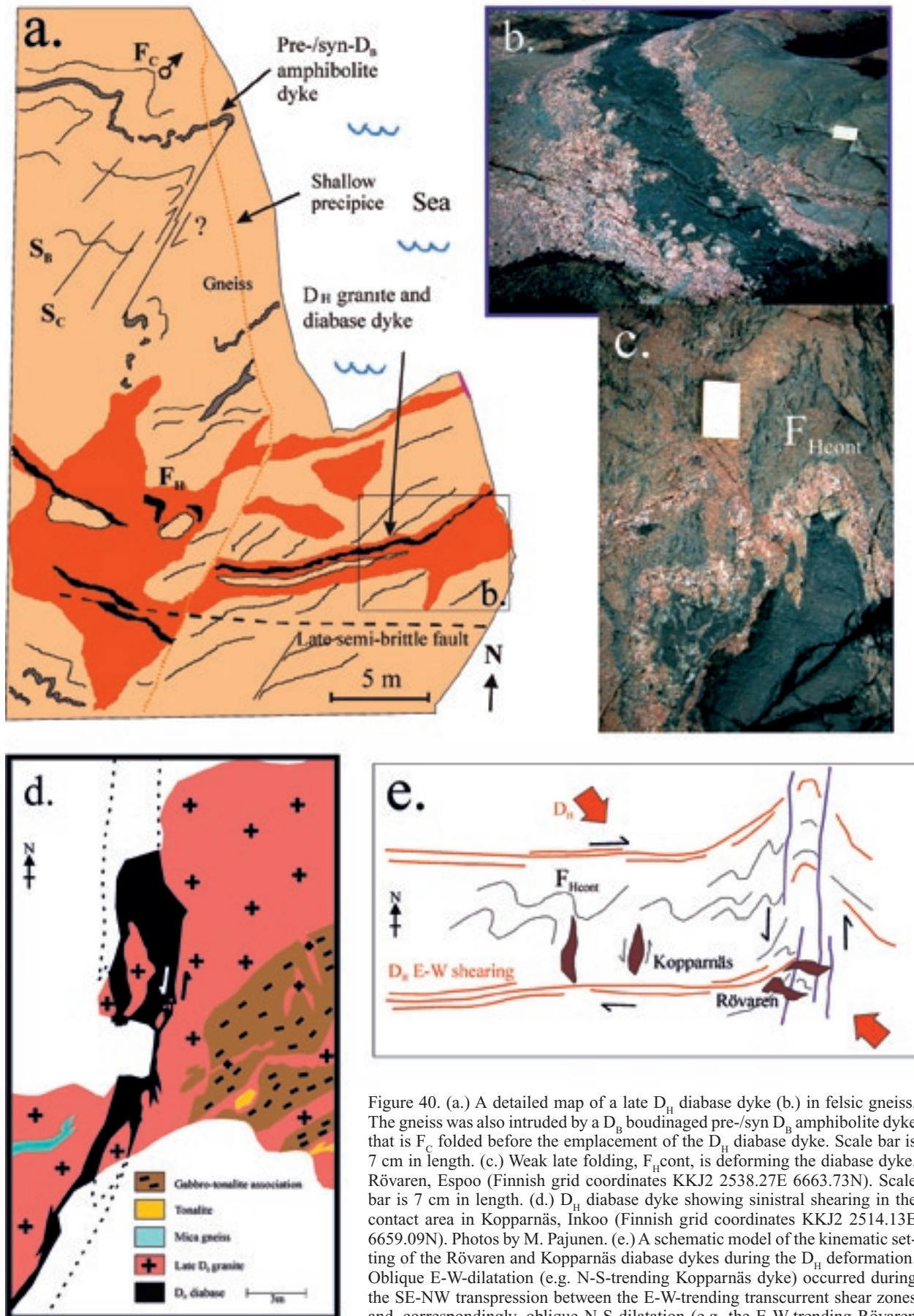


Figure 40. (a.) A detailed map of a late D_H diabase dyke (b.) in felsic gneiss. The gneiss was also intruded by a D_B boudinaged pre-/syn D_B amphibolite dyke that is F_C folded before the emplacement of the D_H diabase dyke. Scale bar is 7 cm in length. (c.) Weak late folding, F_{Hcont} , is deforming the diabase dyke. Rövaren, Espoo (Finnish grid coordinates KJ2 2538.27E 6663.73N). Scale bar is 7 cm in length. (d.) D_H diabase dyke showing sinistral shearing in the contact area in Kopparnäs, Inkoo (Finnish grid coordinates KJ2 2514.13E 6659.09N). Photos by M. Pajunen. (e.) A schematic model of the kinematic setting of the Rövaren and Kopparnäs diabase dykes during the D_H deformation. Oblique E-W-dilatation (e.g. N-S-trending Kopparnäs dyke) occurred during the SE-NW transpression between the E-W-trending transcurrent shear zones and, correspondingly, oblique N-S-dilatation (e.g. the E-W-trending Rövaren dyke) formed between the N-S-trending sinistral transcurrent zones.

assemblage; therefore the younger zircon age may represent a late metamorphism. However, no metamorphic rims on the young zircon grains have so far been detected. This age is within the error limits approximately the same as that of the post- F_1 pegmatitic granite (cf. Pajunen et al. 2008). In Estonia, even later ages for metamorphic minerals (1778 ± 2 Ma for monazite and 1728 ± 24 Ma for garnet) have been published (Puura et al. 2004).

D_H structures and kinematics

The most pronounced D_H structures are the recumbent F_H folds with horizontal S_H axial planes exemplified by the folded Bollstad (Figures 39a and c) or Jyskelä (Figure 34d) granite dykes. Vertical shortening estimated from the folded pegmatitic granite dykes is c. 70–75%. Some shearing along the S_H planes and a weak c. E-trending L_H lineation, indicating with weak E-W dilatation in Bollstad and Väster-viken (Pajunen et al. 2008), suggest somewhat smaller vertical shortening. The N-S or E-W trend of the D_H diabase dykes in the Southern Volcanic-sedimentary Belt (SVB) supposes E-W or N-S dilatation during their emplacement. In the NE margin of the Nuukio granite area (Nu in Figure 9), spaced shear structures indicate c. horizontal top-to-NW movement along the S_H planes (Figure 37c; note that later F_H folding, discussed later, turned the shear foliation S_H to a thrust fault position). Extensive magmatism and migmatization, vertical shortening and a contemporaneous increase in heat flow resulting in high-T/low-p metamorphism indicate that D_H deformation was related to crustal extension. Although on an outcrop scale the extensional D_H touched the rock often quite homogeneously, regionally there is much variation in its extent. In general, extensional D_H structures and related magmatism were more penetrative in the central parts of the granitoid areas (e.g. EGC), whereas in the bordering areas shearing or faulting left wide areas untouched (schematized in Figure 4). Our limited observations (extensional D_E and D_H structures are very similar on outcrops) on the directions of the extensional movements during the D_H refer to extension outwards from the granitic centres, for example from the Nuukio area (Nu in Figure 9). This is supported by the patchy distribution of the D_H granites interpreted from the radiometric map (Figure 38).

Folds with NE-trending steep axial planes deform granitoids of different ages to different extents: they deform openly to tightly the earlier S_E foliated rocks (Figure 12c and 36), form gentle folds in the D_H granites (Figure 39a) and refold only weakly and zoned the D_H diabases (Figure 40c). The decreasing contractional strain during this steep F_H folding,

from the earlier structures and magmas to the later ones, suggests this folding was concurrent with the evolution of the extensional deformation D_H . Thus, there are two types of F_H folding related to the late Southern Finland Granitoid Zone evolution: the extensional recumbent $F_{H,ext}$ folds and the contractional $F_{H,cont}$ folds with steep NE-trending axial planes. Due to progressive deformation the contractional and extensional F_H folds may occur on the same outcrops overprinting each other – slightly later contractional F_H folds overprint the extensional F_H folds (Figures 36 and 39a) – or they may form simultaneously in different areas.

The $F_{H,cont}$ refolded the earlier large-scale F_G folds with E-W-trending axial planes to D_{G+H} dome-and-basins (Figure 11). Locally, the steep $F_{H,cont}$ folds are overturned towards the NW (Figure 12c and 19a and d). It is possible that overthrusting along the pre-existing extensional SE-dipping S_E planes also occurred, but we have not observed this so far. The $F_{H,cont}$ folds only seldom have distinct axial plane foliation. In the tightly deformed high-T D_H zones, as in Klaukkala, Nurmijärvi (Figure 35), a weak gneissic $S_{H,cont}$ foliation exists in the D_H granites. The NE trend of the S_H planes is bent E-W in the northern border zone of the West Uusimaa Complex (WUC). This bending can be explained by the stopping effect during the collision of the hot WUC against the cooled Hyvinkää Gabbroic-volcanic Belt (HGB) along the dextral Hyvinkää shear zone.

The close relations of SE contractional $F_{H,cont}$ folds and the E-W dilatational structures is explained by D_H SE-NW transpression between the active E-W-trending transcurrent faults such as the southern Finland shear/fault zone and the Hyvinkää shear/fault zone. The evolution of these shear/fault zones shows a polyphase history that began during the D_E . Hitherto, we have had no observations of high-T, sinistral steep shearing that could be related to $D_{E,cont}$ in these zones; thus, rotation of the $D_{E,ext}$ into a steep position is suggested. Dextral shearing in these steep zones may have already started during the Central Finland block movements during the D_F , and continued dextral during the D_H transpression. The Hyvinkää gabbros were rotated clockwise during the dextral shear deformations (Appendix 3). The oblique overthrusting of the Hyvinkää Gabbroic-volcanic Belt (HGB) on the West Uusimaa granulite Complex (WUC) occurred due to the D_H SE-NW transpression. The transpression caused oblique E-W dilatation and simultaneous the patchy melting and intrusion of D_H granites that, in the lower-T areas, intruded into N-S-directional oblique dilatation fractures sharply cutting the earlier structures (Figure 15c).

The D_H SE-NW transpression also caused sinistral shearing in the N-S-trending shear zones. The N-S- and E-W-trending D_H diabase dykes indicate dilatation c. perpendicular to each other. The oblique E-W dilatation, the N-S-directed dykes, can be related to SE-NW transpression in between the active E-W-trending shear/fault zones (e.g. Hyvinkää and Southern Finland shear/fault zones). Similarly, the E-W-directed dykes were formed as oblique extension zones in between the N-S-directed shear/fault zones (e.g. in the Vuosaari-Korso shear/fault zone). Indeed, there are several minor shear/fault zones paralleling these major structures in the study area (cf. Elminen et al. 2008), suggesting several possibilities for such oblique dilatational settings. The kinematic setting of the D_H diabase dykes under SE-NW transpression is schematized in Figure 40e. As indicated by the diabase age, the D_H transpression still acted at c. 1.8 Ga ago, suggesting that the transformation to the D_1 deformation is more or less transitional.

D_1 deformation

The evolution of major N-trending crustal-scale high-strain D_1 zones, the Baltic Sea-Bothnian Bay Zone (BBZ), the Riga Bay-Karelia Zone (RKZ) and the Transscandinavian Igneous Belt (TIB) (Figure 8), began at least during D_D (Appendix 7). The Southern Finland Granitoid Zone (SFGZ) predominantly formed during the D_{E-H} . The late phase of the major N-trending high-strain zones, such as the Vuosaari-Korso shear/fault zone, deforms all the structures from the D_A to D_H and hence we prefer to differentiate the deformation event as a new phase D_1 . D_1 bent the SFGZ, and also the southern Finland and Hyvinkää shear/fault zones (Figure 11) sinistrally into a N-NNW direction.

The Vuosaari-Korso Shear/fault zone (Figure 10) represents a western branch of the Riga Bay-Karelia Zone (RKZ). In the strongest part of the Vuosaari-Korso D_1 zone the F_G and F_H folds were refolded or bent to a N-S direction in a ductile manner; the structural relationships are represented by the structures at the Jamma site, in Järvenpää, in the northern Espoo Granitoid Complex (EGC). The area is intensely D_E deformed with a strong nearly horizontal $S_{E,ext}$ that destroyed almost completely the earlier $D_{(A-)B-D}$ migmatite structures (Figure 31a). The $S_{E,ext}$ is a spaced or penetrative mineral foliation; D_E biotite is coarser-grained than D_B biotite. Garnet-bearing tonalite-granodiorite intruded into the S_E planes and was refolded by F_1 folding with N-trending axial planes (Figure 31b), which may represent a rotated F_H intensified by D_1 . The F_{H+1} folds developed to nearly isoclinal indicating c. E-W shortening. New

generation of pegmatitic to medium-grained granite intruded into the N-trending S_1 axial plane, which shows shearing with east-side-up movement (Figure 31c). This late granite also cuts or replaces the tonalitic-granodioritic D_E rock. Two garnet generations have been detected in the granite; a new garnet rim overgrows the earlier core. Both generations have a microstructure indicating crystallization from melt (Figure 31d and e). This leads to the conclusion that the thermal conditions were still high during this late phase of structural evolution, especially close to the D_1 axial zone in the Espoo Granitoid Complex (EGC) and West Uusimaa Complex (WUC).

The drag folds bending the earlier major structures in the D_1 zones indicate sinistral movement on the horizontal surface; the observations of vertical sections (Figure 31d) prove east-side-up movement. These structures and contractional F_1 folding showing varying intensity can be explained by c. ESE-WNW transpression during the D_1 deformation. In the southern part of the Vuosaari-Korso D_1 axial zone, in the Vuosaari triangle (Vu in Figure 9) and to the south of it in the Gulf of Finland, a complex pattern of magnetic anomalies was generated; the D_1 deforms the early D_{C+D} dome-and-basin structures. Sederholm (1932b) described brittle structures seen in bathymetric configuration in lake Päijänne, Central Finland: the Lake Päijänne fracture zone in Figure 10. Structurally, Päijänne is on the continuation of the axial trace D_1 . As described above, the bedrock to the north of Southern Finland Granitoid Zone (SFGZ) was already stabilized after D_D at c. 1.87–1.86 Ga ago. Thus, the D_1 was brittle in the Päijänne area at the time of ductile deformation in the southern part of the zone. The fracture pattern described by Sederholm (1932b) is consistent with c. E shortening characterizing the D_1 .

The tight-isoclinal ductile F_{H+1} folds (Figure 31b) demonstrate that the temperature was not reduced under ductile-brittle transition in the Espoo Granitoid Complex (EGC) and West Uusimaa granulite Complex (WUC). The age of 1804 ± 2 Ma for pegmatitic granite, fragmenting a host rock with pre-existing ductile folds with N-trending axial plane (F_g of Pajunen et al. 2008), corresponding to F_1 of this paper, proves that ductile folding with N-trending axial planes predates that age. However, ductile shear structures in the pegmatitic dyke contacts indicate that movements still continued afterwards.

So-called post-tectonic granitic intrusions of a c. 1.8 Ga age group consist of small stocks (indicated by the letter P in Figures 1 and 7) or late pegmatitic granite dykes (cf. Alviola et al. 2001). In Sulkava (Su in Figure 9), post-tectonic granite caused a low-pressure metamorphic contact aureole in a migmatitic garnet-cordierite gneiss (Rastas 1990). These

granites often occur in close association with the N-trending crustal D_1 zones, like the Sulkava stock in the Riga Bay-Karelia Zone (RKZ) and the Åva ring intrusion (Lindberg & Eklund 1988) in the Baltic Sea-Bothnian Bay Zone (BBZ). We prefer to relate these intrusions as syn-tectonic to the latest phase of the D_1 deformation. Presumably, they formed into patchy dilatational settings during the c. ESE-WNW transpressional D_1 regime; however, further structural research is needed for more precise determination of the tectonic setting of these granites.

The late evolution of the D_1 zones turned to lower grade processes, which can be seen as a change to more semi-ductile and partitioned deformation in the D_1 axial zones. Deformation concentrated into rather narrow fault zones with formation of mica-rich slickenside surfaces and protomylonitic to mylonitic structures. According to Elminen et al. (2008), late movements show steep sinistral east-side-up movement in the Vuosaari-Korso zone. This kind of movement is also evident in the Hyvinkää-Lahti shear/fault zone. These late microstructures, described in detail by Elminen et al. (2008), are at least partly related to post-Svecofennian events, D_p , such as to the rapakivi stage (e.g. Mertanen et al. 2008).

Evolution of the major shear/fault zones of Southern Finland

The Hyvinkää and Mäntsälä-Lahti shear/fault zones characterize the structural pattern in the northern study area, and the Southern Finland, Porkkala-Mäntsälä and Vuosaari-Korso shear/fault zones are important features in analyzing the tectonic evolution in the detail study area (Figures 10 and 41). The high strain zones with the same strike, i.e. the E-trending Hyvinkää and Southern Finland shear/fault zones and the N-NNE-trending Mäntsälä-Lahti and Vuosaari-Korso shear/fault zones, have much in common.

The Hyvinkää shear/fault zone

The Hyvinkää shear/fault zone is a c. 8 km wide complex high-strain zone between the Hyvinkää Gabbroic-volcanic Belt (HGB) and West Uusimaa granulite Complex (WUC). The zone is generally covered by thick overlays of sediments and outcropping is poor. It is composed of strongly sheared rocks (Figure 42a) and slices of heterogeneous granite and supracrustal rocks with intensely folded

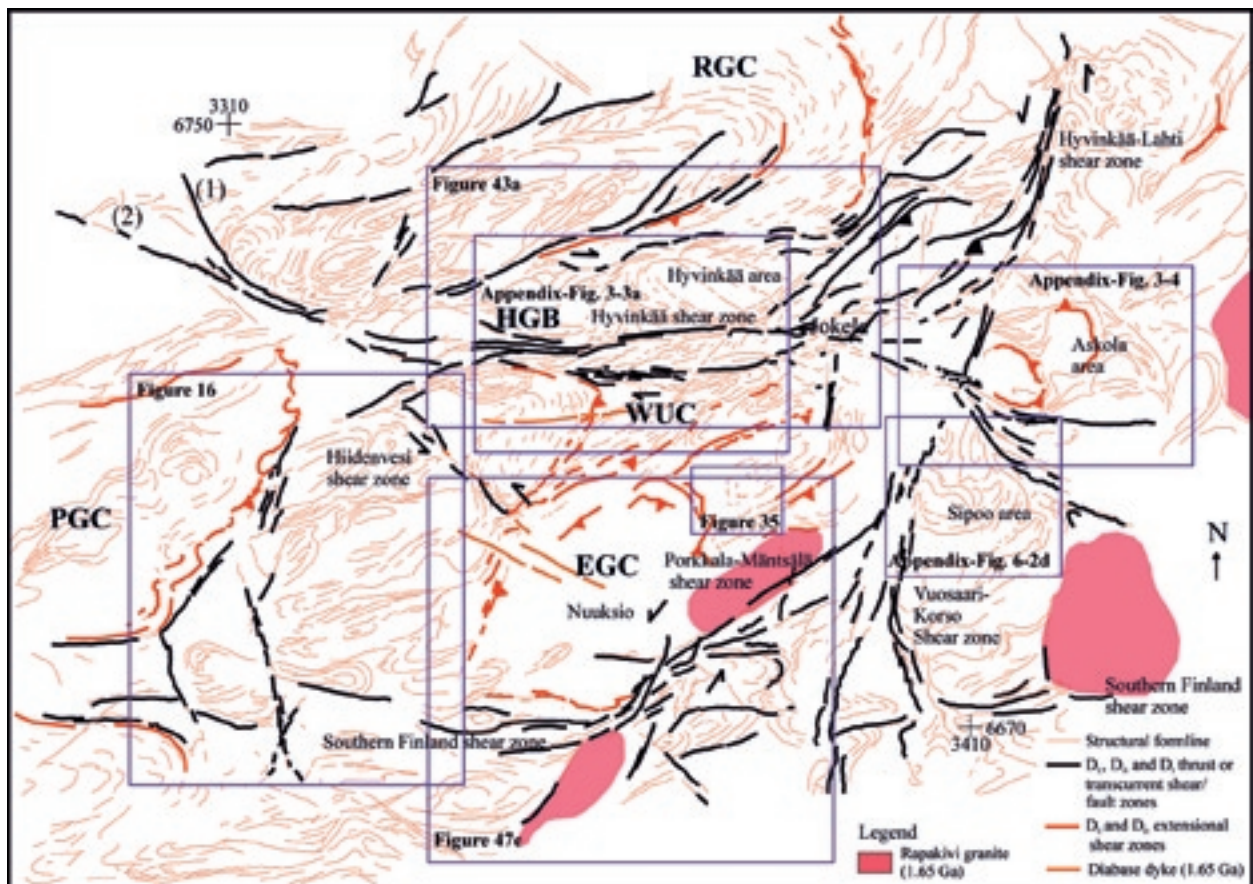


Figure 41. Structural relationships in the Espoo Granitoid granulite Complex (EGC), West Uusimaa granulite Complex (WUC) and Hyvinkää Gabbroic-volcanic Belt (HGB). The areas represented by detailed maps or sketches are shown by boxes. (1) and (2) = NW- and WNW-trending branches of the Hyvinkää shear/fault zone (see text).

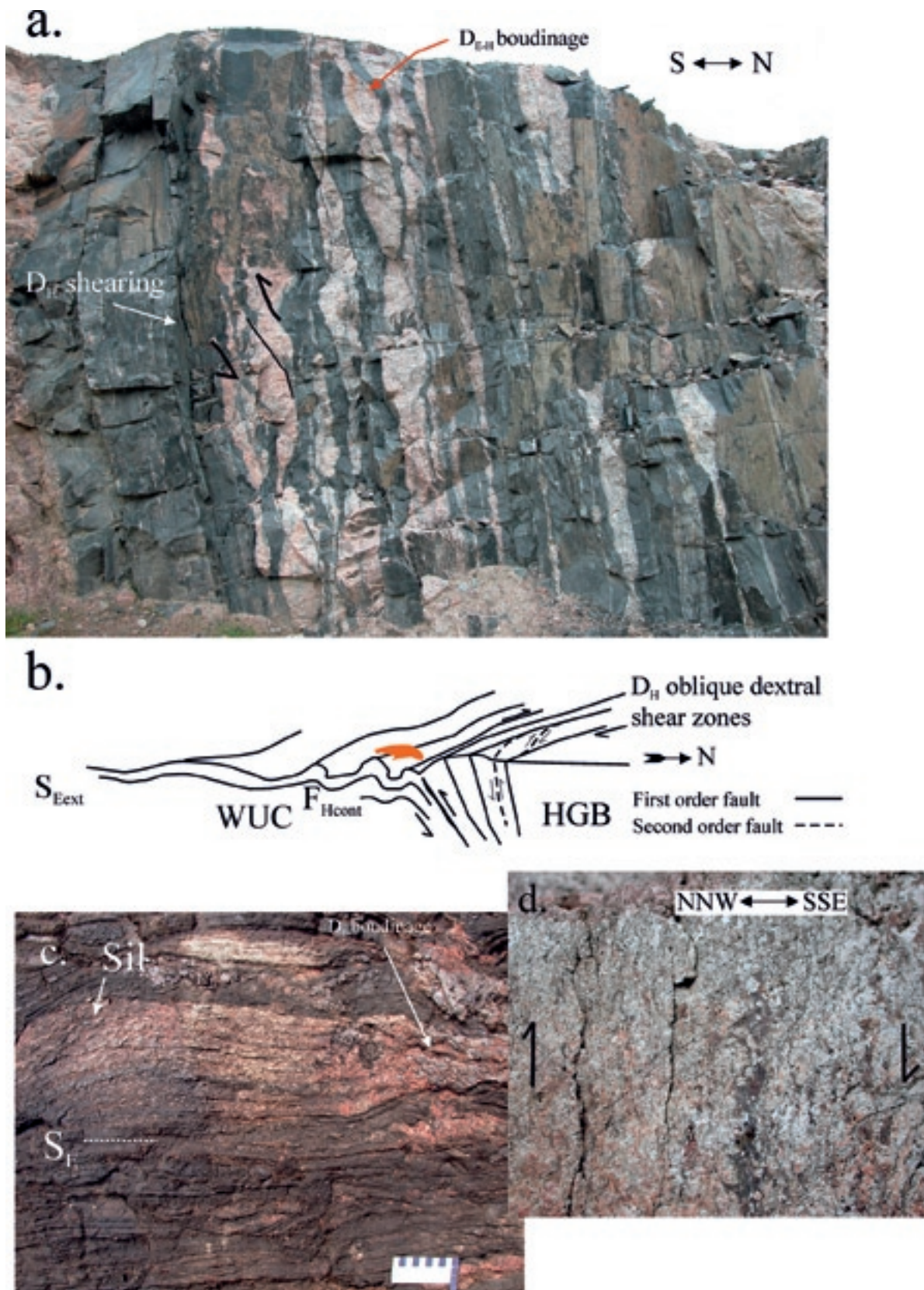


Figure 42. Structures in the polydeformed Hyvinkää shear/fault zone. (a.) A Hyvinkää high strain zone with a strong S_E plane in a steep position. The D_E granite dykes are boudinaged (D_E). Later oblique dextral D_H shearing with N-side-up movement deforms the structure. Width of the area of the figure is c. 6 m. Ylimmäinen, Karkkila (Finnish grid coordinates KKJ2 2534.70E 6715.07N). (b.) A sketch illustrating the F_{Hcont} folding of the S_{Eext} planes close to the Hyvinkää shear/fault zone. (c.) S_E foliation with sillimanite in the E-trending mica gneiss related to the Jokela supracrustal association. The outcrop is located in the Hyvinkää shear zone close to the West Uusimaa granulite Complex (WUC), where the gneisses and locally also the granites (see text) show progressive sillimanite growth related to the high-temperature during the deformation. Scale bar is 10 cm in length. Hyvinkää, Kettukallio (Finnish grid coordinates KKJ2 2552.98E 6721.53N). (d.) Protomylonitic granite in the second-order Hyvinkää shear zone; a vertical section showing NW-side-up movement in the dextral oblique shear zone. Width of the area of the figure is c. 1 m. Karkkila, Vaskijärvi (Finnish grid coordinates KKJ2 2518.18E 6717.12N). Photos by M. Pajunen.

internal structures representing the pre-high-strain zone history (Appendix-Fig. 3-2b). The well-preserved Jokela association (Appendix 5) is located in the eastern part of the zone. On the northern edge of the WUC the D_{G+H} interference structures were bent more or less into an E-W-direction against the HGB (Figure 41). Folding with a steep E-trending axial plane (Figure 42b) deformed the $S_{E\text{ext}}$ planes (cf. Appendix-Fig. 2-1) close to the zone into a vertical position; further from the zone the $S_{E\text{ext}}$ foliation is nearly horizontal and semi-openly refolded by the D_{G+H} .

The first-order structures of Hyvinkää high-strain zone are E-W-trending and refolded/bent by the open D_1 structure, like the Hyvinkää-Lahti shear zone. In the west, the Hyvinkää shear/fault zone continues towards the NW; it is divided into branches continuing to Somero and Koski areas ((1) in Figure 41) and, on the other hand, along the lake Painio shear/fault zone, southeast of Somero ((2) in Figure 41). Ductile and sharply-cutting brittle characteristics in the Painio shear/fault zone prove its reactivated evolution. According to geophysical data, the Hyvinkää high-strain zone also has an E-trending extension in the northern side of the Askola dome area (As in Figures 9 and 41), where it is sharply defined, also representing later reactivation of the Hyvinkää zone. Brittle slicken line striations dipping c. 30° to the east on the sheared foliation planes indicate late strike slip movements.

Close to the West Uusimaa granulite Complex (WUC), shearing structures are higher-grade and almost penetratively recrystallized when compared to those to the north of it. In the highest-grade zone in granites (observations only from boulders) and in mica gneisses, sillimanite was formed (Figure 42c) into the sheared foliation plane. Locally, sillimanite-bearing foliation and the folding with E-trending axial planes (Figure 42b) in the WUC are still overprinted by melt patches. These observations indicate that during the deformation, thermal heat flow was high in the vicinity of the hot WUC. We relate the sheared foliation to S_E that corresponds to S_E in the Jokela association (Appendix 5), where the foliation was refolded by later deformation events (Appendix-Fig. 5-3a). The observations suggest that the earliest phase of the evolution of the Hyvinkää shear zone was initiated during the extensional D_E phase (Figure 42a); however, most of the fault rock structures suggest shortening (Figure 42b).

On outcrops, the first-order, E-W-trending shear zones dip steeply (90–80°) to the north, and the second-order zones north of WUC are upright and trend ENE (Figure 42b). Kinematic interpretation of the E-trending first-order zones is based on pro-

tomylonitic foliation structures, S-C structures, rotational fragments and drag folds. These steep shear zones show N-side-up dextral oblique reverse movements. There are few observations on the ENE-trending steep second-order shear zones with NNW-side-up dextral oblique reverse movements (Figure 42d). The Hyvinkää gabbro massifs and their surroundings also show a map-scale dextral rotation (Appendix-Fig. 3-3). The E-axial folded structure in Figure 42b concurrent with the shear movements in the high-strain zones suggests a NW-SE transpressional stress field – this type of kinematics characterizes the D_H deformation.

The geophysical model in Figure 43 supports the tectonic interpretation based on field observations. The Hyvinkää high-strain zone forms a belt of tectonic slices narrowing downwards. The structure accompanied with dextral oblique kinematics of the shear zones postulates oblique N-side-up movement of the tectonic slices upon the thrust plane. The interpreted thrust plane, between the WUC and the overlying HGB, dips northwards below the HGB with a dipping angle of c. 20–30°.

Structures in $L_{B/C}$ lineated amphibolitic rock in the Hyvinkää Gabbroic-volcanic Belt (HGB), NE of the Hyvinkää gabbro massif, are schematized in Figure 44a. The amphibolite is cut by pegmatitic granite. Similar pegmatitic granites also cut the Hyvinkää gabbro massifs, supracrustal sequences of the HGB and the Jokela supracrustal association (Appendix-Fig. 5-2). In the internal parts of the HGB, they intruded as sharply-cutting dykes fragmenting a cooled and stabilized crust. We relate these pegmatite granites the D_H granites in the West Uusimaa granulite Complex (WUC) and Espoo Granitoid Complex (EGC). The amphibolite with strong lineation is cut by semi-brittle faults with spacing of several centimetres. The fault planes show slicken line striations that indicate thrusting towards the SSE. Under the microscope (Figure 44b) the rock has a complex pattern of narrow semi-brittle faults cutting the rock. The faults are openly folded by c. E-W contraction. We correlate the faults to oblique thrusting related to the transpressional collision, D_H , in the Hyvinkää high-strain zone and the open folding to the D_1 deformation. In general, the transpressional structures (D_H) in the cooled parts of the HGB are semi-brittle to brittle in character (Appendix-Fig. 3-1a).

Summarizing, the formation and kinematics of the high-strain zone between the West Uusimaa granulite Complex (WUC) and Hyvinkää Gabbroic-volcanic Belt (HGB) is related to continuing deformation events. The earliest structures were already formed during the extensional D_E . The strongest shearing structures formed during the crustal

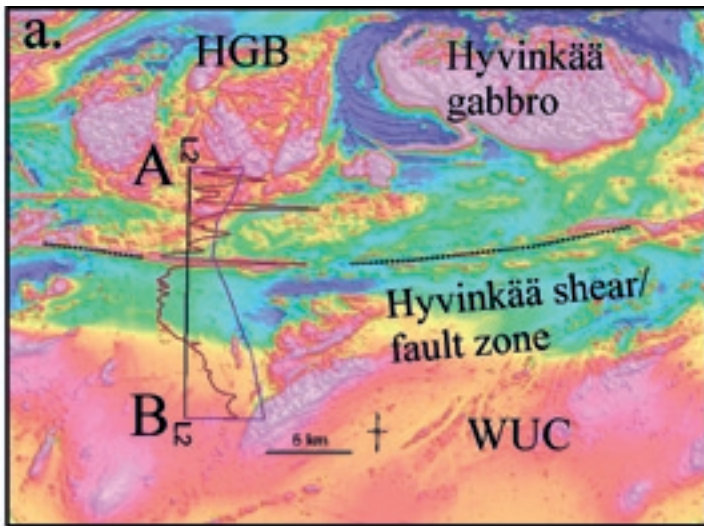
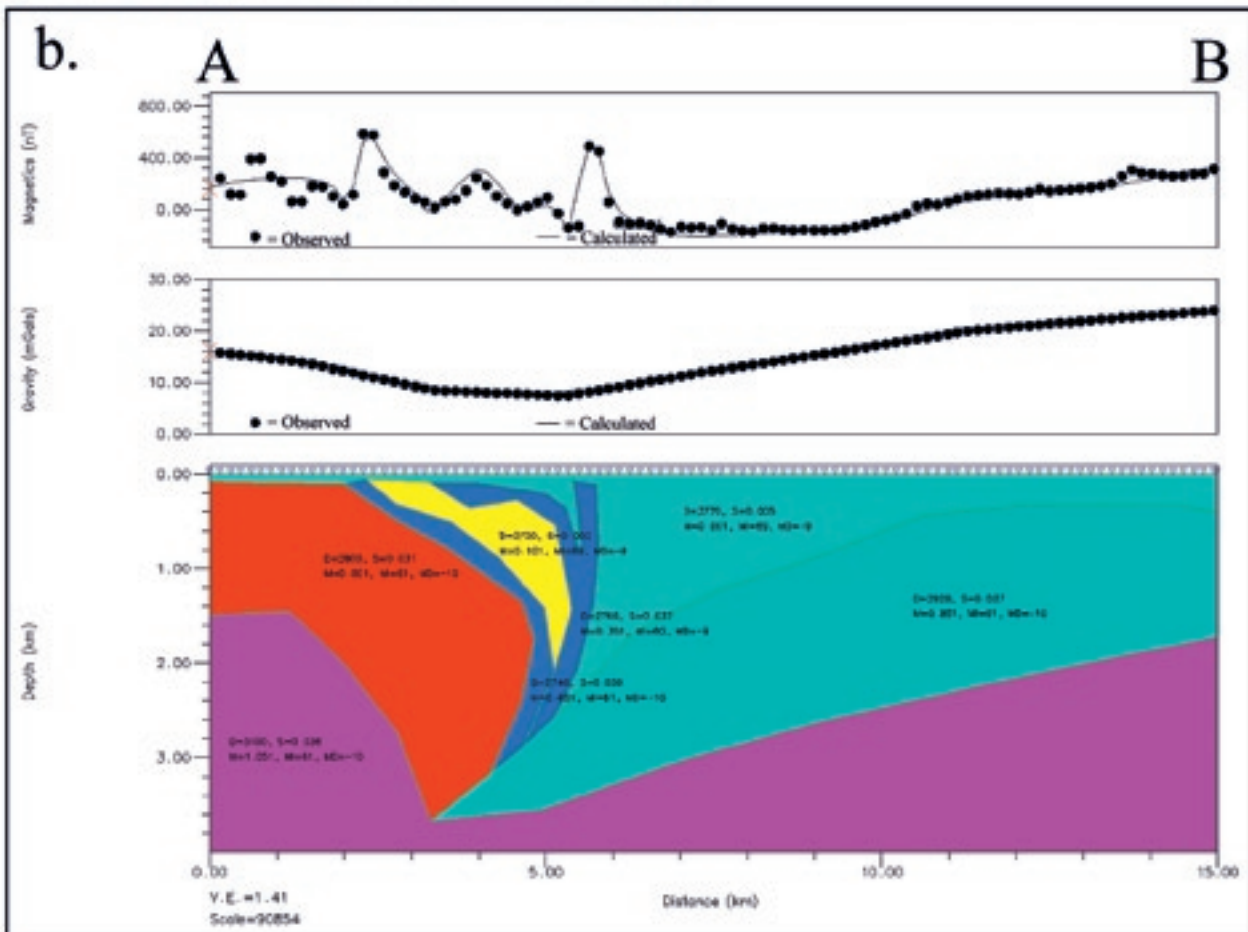


Figure 43. A geophysical model of the Hyvinkää shear/fault zone. (a.) Site of the cross section on a magnetic map and (b.) a geophysical model cross-cutting the Hyvinkää shear/fault zone. See the text for further discussion.



shortening in transpressional deformation D_{HT} . The bends and folds in the boundary zone are a consequence of heterogeneous strain in the border zone during continuing oblique overthrusting of the HGB onto the WUC. The late regional D_1 refolded the Hyvinkää zone extensively (Figure 41). During the final stage, movements occurred along E-trending semi-brittle faults due to blocking of the ductile structure under cooling.

The Hyvinkää-Lahti shear/fault zone

The SSW-NNE/SW-NE-trending Hyvinkää-Lahti shear/fault zone is located in the axial zone of D_1 (Figures 10 and 41). According to geophysical and tectonic interpretation, using map-scale bends of the earlier structures and the existence of higher-grade rocks in the Askola area, sinistral oblique E-side-up movement occurred in the zone; it is similar

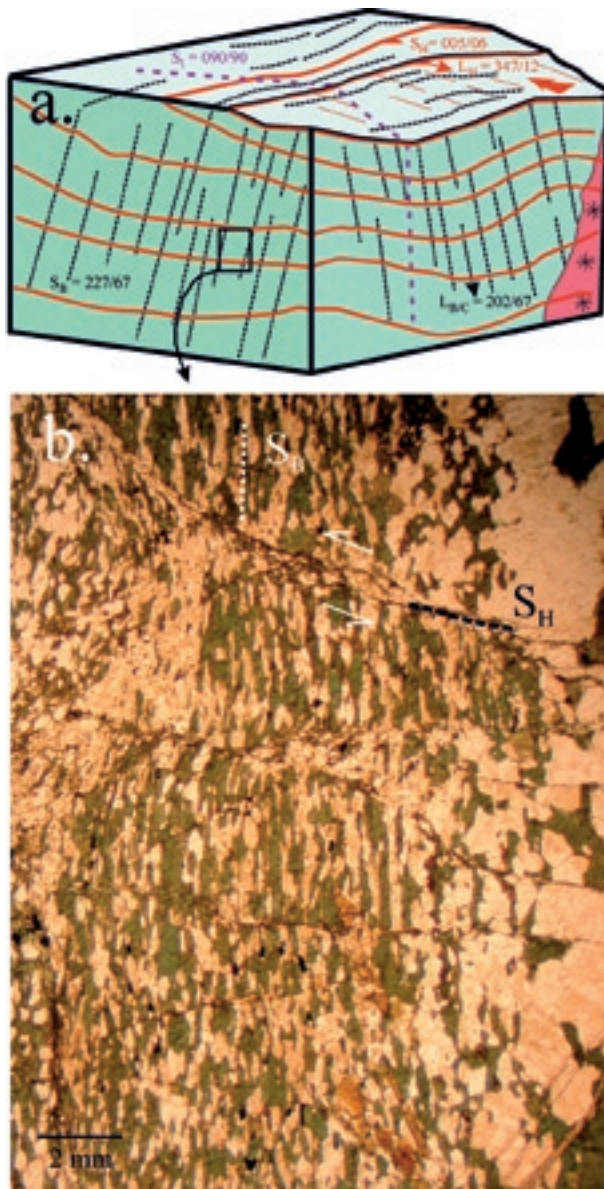


Figure 44. (a.) $L_{B/C}$ -lineated amphibolite showing D_1 folding of semi-brittle spaced thrust foliation planes, S_H , that were interpreted as a product of oblique c. SSE-thrusting on the northern side of the Hyvinkää gabbro; L_H is slickenline lineation on the S_H planes. The Hyvinkää Gabbroic-volcanic Belt (HGB) was a cooled and competent area during the late D_H event occurring in the granite-dominant units. Thus, the D_H and later structures are brittle and granites sharply cut the HGB (cf. Appendix-Fig. 3-1a). (b.) A microscopic photo of the amphibolite showing semi-brittle fractures. Hirvijärvi, Riihimäki (Finnish grid coordinates KJKJ2 2535.92 6729.82N). Photo by M. Pajunen.

to that Vuosaari-Korso zone (cf. Elminen et al. 2008). However, the D_1 bends the Hyvinkää shear structures into a NE-NNE direction and this causes complexity in this major crustal zone. On the NW-side of the zone, the magnetic signature of the sliced structure shows a SE-dipping pattern of anomalies. Our tectonic measurements from the area are limited, but in general, the tectonic measurements on the geological map (Kaitaro 1956) show a pattern that predominantly follows the earlier structures,

particularly the D_{G+H} pattern. The structures close to the most intense D_1 deformation zones are often dipping steeply to the SE, which, together with the magnetic pattern, indicates stacking towards the NW during D_1 .

The Hyvinkää-Lahti shear/fault zone, which is parallel to the axial plane of the open semi-ductile crustal bend F_1 , continues further north to the Lake Päijänne fracture zone (cf. Sederholm 1932). The differences in characteristics of this D_1 zone from the high-T ductile south to low-T brittle north are due to early stabilization of the northern Svecofennian crust.

Southern Finland shear/fault zone

The polyphase E-trending Southern Finland shear/fault zone represents a complex high strain zone (Figure 45a and b), which is faulted/sheared by the late phases of the Porkkala-Mäntsälä zone and extensively folded and faulted by the Vuosaari-Korso D_1 deformation zone. The Southern Finland shear/fault zone is composed of several parallel high-strain zones bordering the tectonic units, like those dominated by supracrustal (SVB) and granitic rocks (EGC). The most intense zone in the study area borders the non-migmatitic Pellinki area (Pe in Figure 9) and Vuosaari triangle (Vu in Figure 9) from the granitic units in the north. Elminen et al. (2008) describe in detail the late, ductile to brittle structures and kinematics of the Southern Finland shear/fault zone. Structures in the high-strain gneisses and mylonite gneisses exhibit a steep shear zone with dextral S-side-up oblique reverse movement (Elminen et al. op. cit.). In the stronger zones, intense spaced biotite shear foliation has been generated (Figures 45a and b). However, the metamorphic evidence, well-preserved non-migmatitic volcanic rocks in the Vuosaari triangle versus highly migmatitic rocks just north of the major shear zone, indicates opposite movement in this area. Stretching lineation in the sheared gneisses shows a moderate dip to east, indicating oblique movement.

The Southern Finland shear zone was already initiated during the extensional D_E deformation forming the early border zone between the granitoid and supracrustal belts. The D_G deformation (N-S shortening) intensified close to the zone to form steep southwards-overtaken folds (e.g. Figure 28) and reoriented the early phase (D_E) of the E-W-trending zone to a NE-SW trend (Porkkala-Mäntsälä zone). The main structures characterizing the Southern Finland shear zone were generated during the D_H SE-NW transpression. This produced the dextral oblique reverse movements in the steep Southern Finland shear/fault zone. Late reactivation was

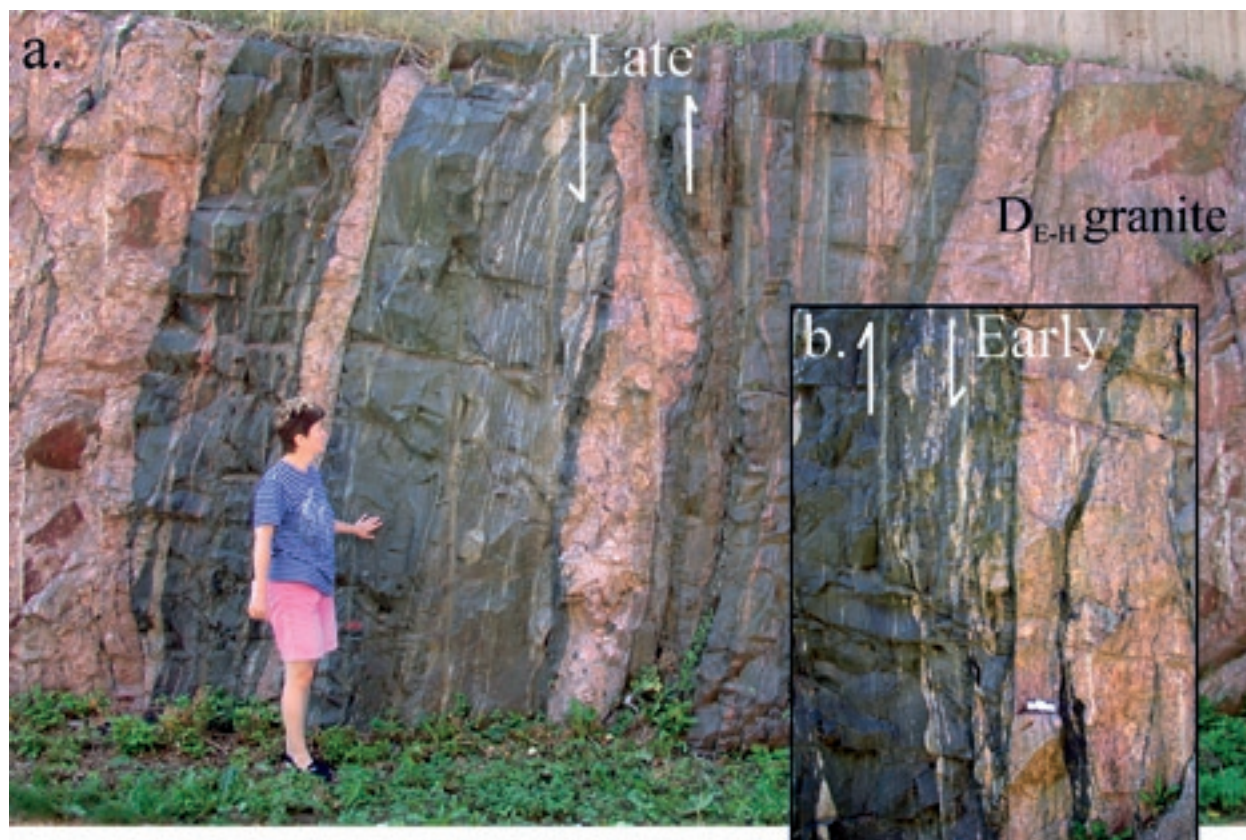


Figure 45. Structures in the Southern Finland shear/fault zone. The outcrop is situated in the strongly deformed and folded area between the Porkkala-Mäntsälä and Vuosaari-Korso zones. The outcrop shows opposite directions of movement on vertical surface: (a.) late movement north-side-up and (b.) early movement south-side-up movements. Scale bar is 15 cm in length. Otaniemi, Espoo (Finnish grid coordinates KKKJ2 2545.68E 6674.71N). Photos by M. Pajunen.

common in the Southern Finland shear/fault zone; nearly horizontal slicken line striations on the late E-trending steep fault planes indicate both sinistral and dextral strike-slip movement.

The structures observed in the Southern Finland shear/fault zone are very similar to those in the Hyvinkää shear/fault zone (compare Figures 42a and 45a). Dextral transpressional evolution in the Southern Finland Granitoid Zone (SFGZ) was postulated by Ehlers et al. (1993), but our observations indicate longer history for the zone; the SE-NW transpression only characterizes the latest SFGZ and major shear zone evolution.

Porkkala-Mäntsälä and Vuosaari-Korso shear/fault zones

The polyphase character of the Porkkala-Mäntsälä/ (Lahti) shear/fault zone was discussed in early papers, e.g. Härme (1969), and there have been several papers dealing with corresponding NE-trending shear/fault structures further west (compiled by Lindroos et al. 1996). We recommend the name Porkkala-Mäntsälä shear/fault zone because it is connected to the Vuosaari-Korso zone to the south

of the E-trending Hyvinkää zone (the name Vuosaari- or Helsinki-Päijänne would better describe the setting of the Vuosaari-Korso zone of this paper; Figures 9 and 10).

The Porkkala-Mäntsälä shear/fault zone steeply cuts the E-W-trending Southern Volcanic-sedimentary Belt (SVB) and Espoo Granitoid Complex (EGC), and also the Southern Finland shear zone. It bends the Southern Finland shear zone into a NE-direction. In the study area the early structures of the Porkkala-Mäntsälä zone are ductile sinistral bending of the earlier structures (Figure 46a) against the Nuuksio granitoid unit. In Figure 46b there is an example of migmatitic tonalitic gneiss in the NE-trending Porkkala-Mäntsälä zone at the Bemböle site in Espoo. Locally, as at the Bemböle site, the steep structures of the originally E-W-trending Southern Finland shear zone were bent into a NE direction, and these old structures oriented the shear movements in the Porkkala-Mäntsälä zone. A NE-trending crenulation cleavage (Figure 46c) and related steep-axial folds with NE-trending axial planes were formed in sinistral strike-slip movement under D_G N-S contraction. On the NW side of the Porkkala-Mäntsälä zone the $S_{E,ext}$ and D_G structures were

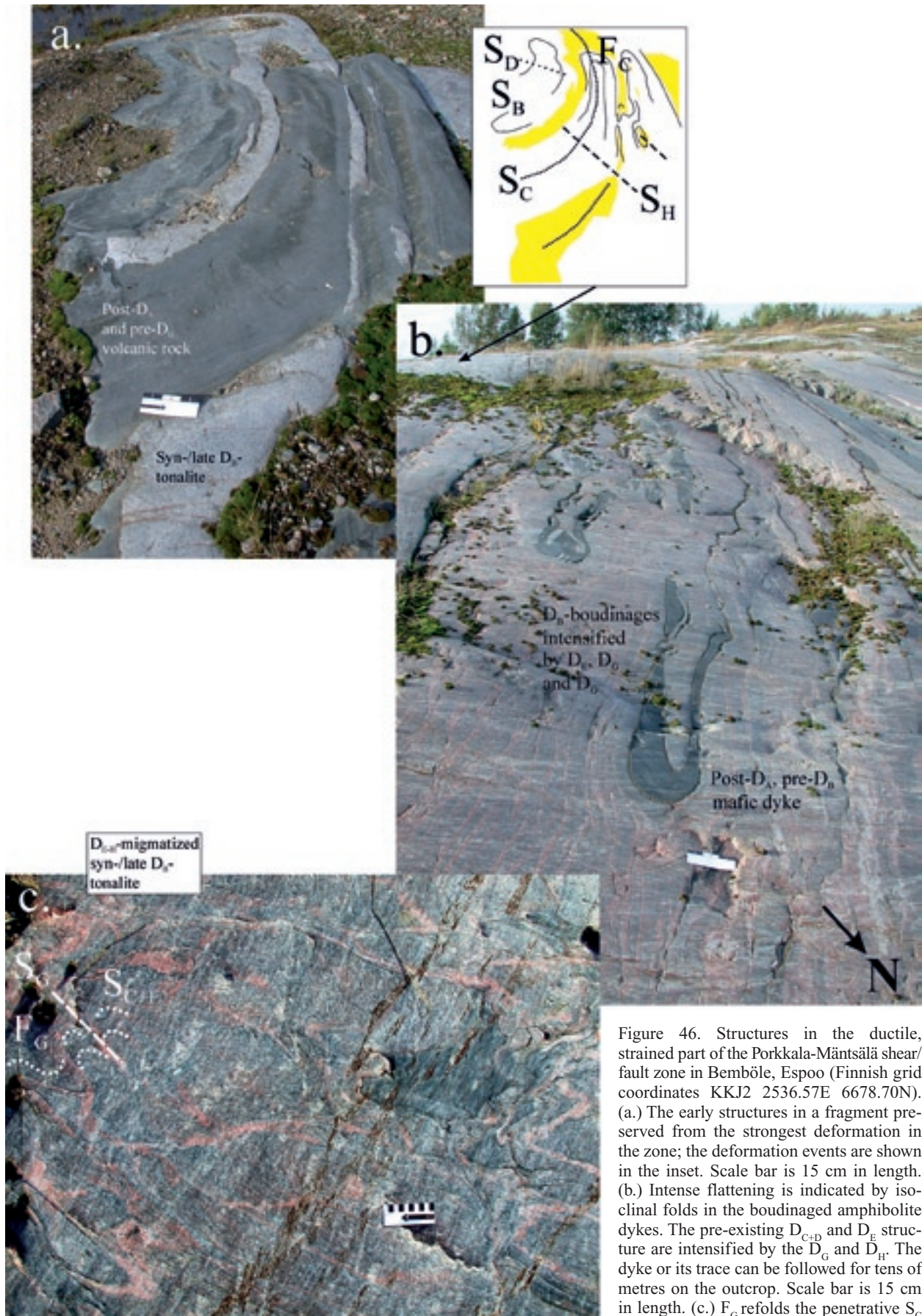


Figure 46. Structures in the ductile, strained part of the Porkkala-Mäntsälä shear/fault zone in Bemböle, Espoo (Finnish grid coordinates KKJ2 2536.57E 6678.70N). (a.) The early structures in a fragment preserved from the strongest deformation in the zone; the deformation events are shown in the inset. Scale bar is 15 cm in length. (b.) Intense flattening is indicated by isoclinal folds in the boudinaged amphibolite dykes. The pre-existing D_{C+D} and D_E structure are intensified by the D_G and D_H . The dyke or its trace can be followed for tens of metres on the outcrop. Scale bar is 15 cm in length. (c.) F_G refolds the penetrative S_C foliation and the spaced S_E of migmatized syn-/late D_B gneissic tonalite. Scale bar is 10 cm in length. Photos by M. Pajunen.

F_H -folded and overturned NW, e.g. in Kauklahti (Figures 19a and d). The F_H with NE-trending axial planes is a consequence of rotation of the stress field into SE-NW-directional transpression during the D_H .

In the high-grade parts of the Espoo Granitoid Complex (EGC) and West Uusimaa granulite Complex, continuing deformation caused intensifying and bending of the earlier D_H structures into a N direction by the D_P , still under high-grade ductile conditions. Sinistral E-side-up shearing (e.g. Figure 31d) occurred along the steep N-directional D_I shear/fault zones, as in the Vuosaari-Korso shear/fault zone. These kinds of sinistral shear zones are also found elsewhere in the study area (Figure 47a). The early stage N-S-trending sinistral shear zones are related to the SE-NW transpression during the D_H ; the D_H diabase dykes were intruded into oblique dilatational ($D_{H,ext}$) settings (Figure 40e). During the latest Svecofennian evolution the maximum principal stress rotated from SE-NW into a more easterly direction causing some ductile folding, F_{H+I} (Figure 31b), after which cooling and fading of the Svecofennian deformation caused transformation to more brittle events. Sinistral movements in the Vuosaari-Korso shear zone became brittle and localized in character. In the Porkkala-Mäntsälä fault zone, late movements were dextral (Figure 47b) and they are related to the post-Svecofennian events D_P . Elminen et al. (2008) relate dextral movements to the rapakivi stage.

The tectonic pattern produced by the shear/fault structures, especially D_H and D_P , and the low-angle D_E structures strongly oriented the post-Svecofennian tectonic reactivation and emplacement of the rapakivi intrusions (Figure 47c) in the area.

Structural setting of rapakivi granites – D_P

The rapakivis are divided to different age classes by Haapala et al. (2005). The rapakivi intrusions in the study area belong to the c. 1.67–1.62 Ga age group that forms a c. N-NNE-trending zone from Lithuania to Southern Finland. The intrusions located in a close association with the BBZ are dominated by rapakivis of 1.59–1.54 Ga in age. There are two small 1.65 Ga rapakivi intrusions in the detailed study area, Bodom and Obbnäs, and the Onas and Vyborg rapakivi intrusions are just east of it (Figure 9) (e.g. Vaasjoki 1977a).

The Bodom rapakivi is a NE-trending intrusion on the NW side of the Porkkala-Mäntsälä shear/fault zone. The intrusion is thinner at its northern end; the Svecofennian magnetic anomalies are distinguishable through the rapakivi mass. Its south-

western part forms a round stock without such a magnetic anomaly pattern. According to Kosunen (2004), it represents a younger intrusive phase. The internal structure of the batholith is well seen in the topographic pattern in the rapakivi area. The rapakivi is sharply bordered against the Porkkala-Mäntsälä fault, which drags the SE-border of intrusion under dextral movement D_P . This movement can also be seen in mylonitic shear zones overprinting the early sinistral D_G phase of the zone (Figure 47b). The topography in the Bodom rapakivi area exhibits an arched pattern; in the NE-part of the intrusion the Svecofennian remnants show similar arched forms (Laitala 1967). The magnetic patterns and the arched forms support narrow, sheet-like horizontal intrusions intruded in a laccolith-like manner. Sederholm (1923) argued that the western rapakivis might be sheet-like bodies. Magnetic patterns of the Bodom and Vyborg rapakivi massifs support such a structure. The nearly horizontal $S_{E/H}$ plane characterizing large areas in Nuuksio synform forms an appropriate structure for emplacement of these horizontal rapakivis (Figure 47c). The thickest part of the Bodom intrusion is in the SW. It is interpreted as the site of the intrusion channel, which is located in the intersection point of the Porkkala-Mäntsälä fault, Southern Finland shear zone and the N-trending D_I structure (Figure 47c). The rapakivi-related diabase dykes, especially in the western study area and in the West Uusimaa granulite Complex (WUC), also intruded at least partly into the pre-existing Svecofennian structures. An example is the Hiidenvesi D_F shear zone (Figures 10 and 41), which was hidden below the Espoo Granitoid Complex (EGC), but controls the orientation of the rapakivi-related diabbases. Fracturing and jointing (Wennerström et al. 2008) in the dyke direction was also generated in the above-lying Nuuksio granitoid area. Some diabbases are very fine-grained, indicating emplacement close to the present erosion level.

The Obbnäs intrusion does not show such a magnetic anomaly pattern as the Bodom intrusion. This is why we suppose it to be thicker and to represent a root section of the rapakivi intrusion corresponding to the SW stock of the Bodom batholith. In principle, its tectonic setting is similar in the intersection of the southern Finland shear zone, Porkkala-Mäntsälä shear/fault zone and D_I deformation zone as was described from Bodom. Airo et al. (2008) noticed gravity lows corresponding to those caused by the described rapakivi intrusions in the intersections of the Vuosaari-Korso and the Porkkala-Mäntsälä zone and further south at the intersection of the southern Finland and the Vuosaari-Korso zones. These anomalies may represent rapakivis that are not exposed on the present erosion level.

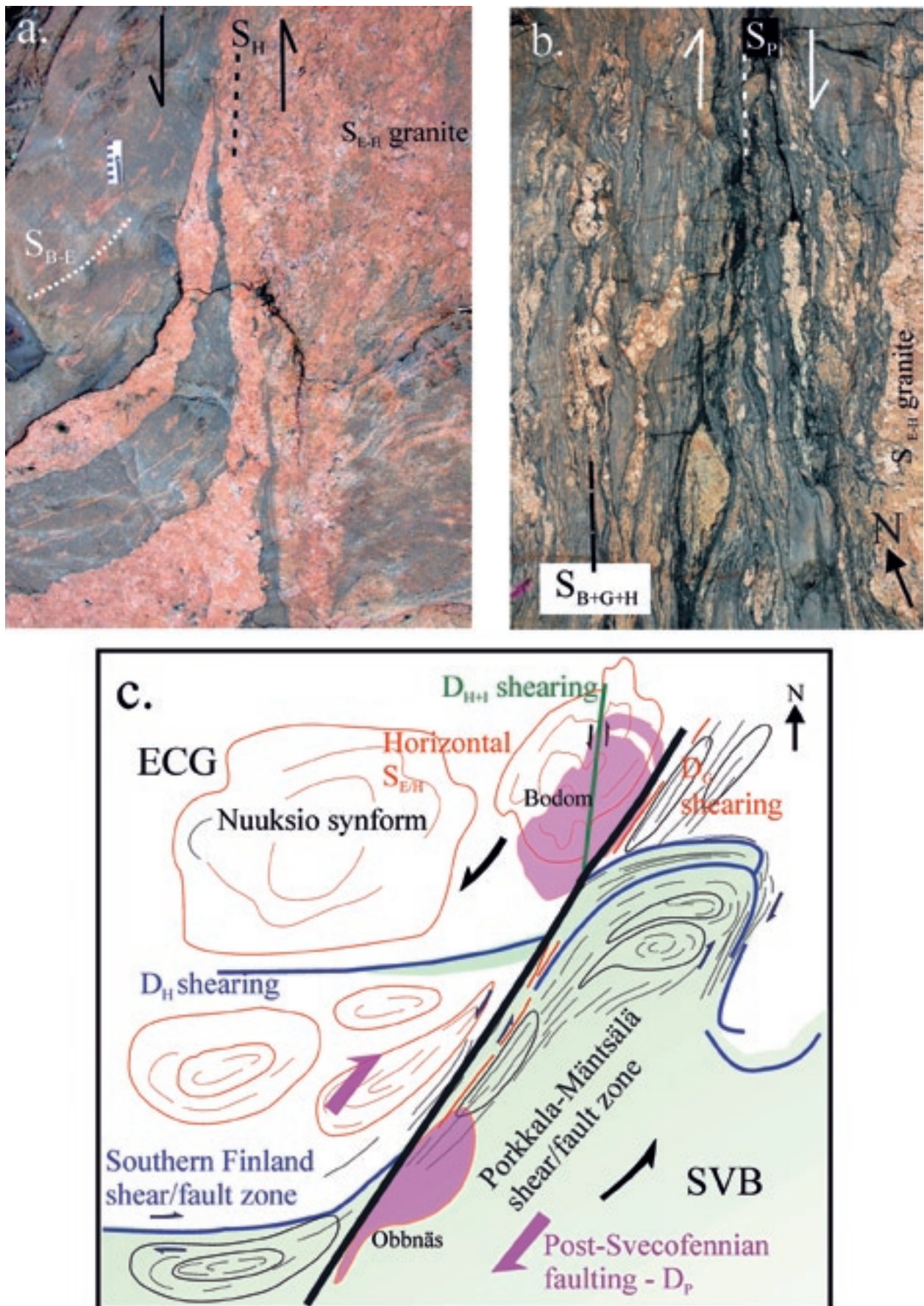


Figure 47. (a.) Sinistral N-trending $D_{H(c)}$ shearing. Scale bar is 10 cm in length. Kopparnäs, Inkoo (Finnish grid coordinates KKJ2 2514.13E 6659.09N). (b.) Post-Svecofennian dextral D_p faulting on the horizontal surface in the Porkkala-Mäntsälä shear/fault zone. The pre-existing strong D_E is rotated by the D_c into a SW-NE-trend. Width of the area of the figure is c. 70 cm. Porkkala, Kirkkonummi (Finnish grid coordinates KKJ2 2252.10E 6651.87N). (c.) The tectonic structure of the Porkkala-Mäntsälä zone in Espoo and structural setting of the Bodom and Obbnäs rapakivi intrusions. Photos by M. Pajunen.

The Vyborg rapakivi batholith is, according to the magnetic and gravity anomaly pattern, thickest in the western part of the batholith, and the Ahvenisto rapakivi intrusion (5 in Figure 9) is located in the northern extension on this pattern. Both are controlled by the N-trending structure D_1 shown in Figure 8. The magnetic pattern in the Vyborg rapakivi batholith also shows intrusive phases intruded linearly in the ENE direction. It is also evident that the western part of the Vyborg rapakivi represents such an intersection of major crustal fault zones as the Bodom and Obbnäs stocks; according to the magnetic anomaly pattern it thins towards the east from the D_1 zone.

Korja and Heikkinen (1995) described listric fault structures related to the extensional evolution of the rapakivi in Åland. This study shows that the late Svecofennian structures were of great importance for the post-Svecofennian tectonic and magmatic events in controlling where the crust was weakest. The ENE-trending phases in the Vyborg batholith emplaced into the N-trending D_1 zone fit

well the dextral kinematic pattern of movements observed in the Porkkala-Mäntsälä zone and in the N-trending major crustal deformation zones, the Baltic Sea-Bothnian Bay Zone (BBZ) and Riga Bay-Karelia Zone (RKZ) (Figure 8). The fault kinematics related to the rapakivi stage indicate c. N-S-directional extension (Elminen et al. 2008) in the study area. Bergman et al. (2006) described dextral transpression in the Storsjö-Edsby Deformation Zone in Sweden. In summary, the emplacement of the rapakivis may be related to dilatational settings during major c. N-trending dextral shearing in transpressional deformation (cf. Bergman et al. 2006), and magma channelling and emplacement were strongly controlled by the late Svecofennian structures, especially the intersections of the major shear/fault zones.

The relations of the latest brittle faults, like the thrust faults shown in Figure 19a, to the Svecofennian structures have not been studied so far; observations of such faults are limited on outcrops due to the weak character of the structures.

TECTONIC EVOLUTION OF THE SVECOFENNIAN DOMAIN IN FINLAND

Hietanen (1975) was the first to compile an evolutionary model based on the modern plate tectonic scheme in Finland. Koistinen (1981) described the structures related to the Svecofennian collision and overthrusting tectonics in the Archaean craton boundary. Korsman et al. (1984) described the tectono-metamorphic discordance between the southern (GMB) and northern (TMB) Svecofennian terranes, and proposed a suture zone between them (Korsman et al. 1988). Based on comprehensive pre-existing data, Lahtinen (1994) presented a model of the accretion history of the Svecofennian orogen suggesting that the Svecofennian domain was produced by complex accretion of several arcs against the Archaean continent. Kilpeläinen (1998) studied the relationships between the tectonic structures and metamorphic evolution in the Vammala Migmatite Belt (VMB) and Tampere Schist Belt (TMB) by analyzing folding patterns of metamorphic isograds related to different stages of tectonic evolution. He was able to establish the complex pattern of deformation and metamorphism in the deeper crust with concomitant deposition of sediments on the surface in the active collisional orogen. Since then, collision-accretion models have been expanded to include the deep crustal structure (Korsman et al. 1999) and widened to comprehend the whole Fennoscandian Shield (Nironen 1999). Lahtinen et al. (2005) divided Svecofennian evolu-

tion into several orogens. The latest models of the crustal structure developed using the reflection seismic data of the Finnish Reflection Experiment, FIRE 2001–2005, are compiled in Kukkonen and Lahtinen (2006).

The Svecofennian structural succession in southernmost Finland has received less attention. Laitala (1973a) analyzed the structures in the Pellinki area. Ehlers et al. (1993) divided the deformation in the southern Svecofennian domain into two major crust-forming stages: an early island arc orogen and collision and a later transpressional event responsible for the generation of the Southern Finland Granitoid Zone. Väisänen (2002) compiled the tectono-metamorphic evolution in southwestern Finland concentrating on the granulites in the Turku area; he placed special emphasis on the evolution of the Southern Finland Granitoid Zone and concluded it to be a result of crustal collapse. Pajunen et al. (2002) described the structural evolution in the Helsinki region; this paper is partly a revision of these early results. Skyttä et al. (2006) studied the structural succession and kinematics in Kisko, in the Orijärvi area. They describe the structures in the low-strained steep gneisses in the so-called Kisko Triangle (e.g. Väisänen & Mänttari 2002; cf. Vetio outcrop, Appendix 4) and in the highly-strained horizontal gneisses outside of the Triangle (cf. Pajunen et al. 2008).

Summary of Svecofennian structural succession and division into geotectonic events

The polyphase structural succession in the southern Svecofennian domain is complicated due to significant rotations of the stress field during the tectonic evolution. The relations of the observed structures appeared to be more complicated because of the contemporaneous formation of structures in contractional and extensional zones during progressive deformation. In the southern study area (1 and 2 in Figure 1) the Svecofennian structures are divided into D_A - D_I phases that can be identified using the overprinting relations of structures, metamorphic events and magmatism on outcrops. The Svecofennian structural succession in the study area (note that due to diachronic evolution the early deformations, D_A - D_D , occurred c. 10 Ma earlier in the north) can be divided into major geotectonic events (E) as follows:

Event 1: D_A deformed the early sedimentary rocks and the volcanogenic rocks of Series I c. 1.9–1.89 Ga ago. Kinematic observations suggest c. N-S compression during D_A causing approximately E-W-trending fold axes of isoclinal, originally recumbent F_A folds. The D_A represents the first major geotectonic Event 1 (E_1), which caused thickening of the early crust under low-temperature conditions.

Event 2: D_B is a crustal flattening phase that deformed the D_A structures under progressive metamorphism, intense magmatism and migmatization. The volcanogenic rocks of Series II were evolved. D_B occurred in the south at c. 1.88–1.87 Ga and is related to crustal extension under rather constant pressure conditions. D_B is regarded as the second major geotectonic Event 2 (E_2), which caused thinning of the E_1 crust.

Event 3: D_C deformed the previous structures during N-S compression to tight F_C folds in amphibolite facies conditions at c. 1.87 Ga ago. The D_C N-S shortening thickened the crust rapidly after E_2 and is separated here as the third major geotectonic Event 3 (E_3). As a result of the Events 1–3, a new Archaean-Svecofennian continental crust was formed.

Event 4: Event 4 (E_4) is linked to the complex structural, magmatic and metamorphic evolution in the new E_{1-3} continental crust. In the south, E_4 is predominantly connected to the evolution of the Southern Finland Granitoid Zone (SFGZ) during the D_{E-H} deformations. The D_D produced D_{C+D} interferences concurrently with the D_4 block movements in the north. Early E_4 evolution, predominantly D_E that

started at 1868 ± 3 Ma, occurred under SW-NE transpression associated with oblique extensional zones of intense intermediate to felsic magmatism. On the erosion surface the oblique extensional pull-apart basins were generated. Transition from SW-NE transpression to SE-NW transpression, during D_H , occurred at c. 1.85–1.84 Ga ago through short steps of varying stress fields – D_G and D_F . The E-W and N-S-trending major high-strain and shear/fault zones played a considerable role during the E_4 transpressional deformations.

Event 5: The latest major Svecofennian geotectonic Event 5 (E_5) is related to the deformation that concentrated in the major N-trending deformation zones, the Riga Bay-Karelia Zone (RKZ) and Transscandinavian Igneous Belt (TIB), and to a lesser extent the Baltic Sea-Bothnian Bay Zone (BBZ). The Southern Finland Granitoid Zone (SFGZ) was deformed in decreasing temperatures under c. ESE-WNW shortening, D_I , to wide-scale folds. At c. 1.8 Ga the crust started to cool, leading to fading of E_5 and the Svecofennian orogeny in Finland.

Table 1 summarizes the observed structures identified in different tectonic units in the southern study area. The structural observations suggest different structural histories in different units and crustal depths. Their occurrence on the recent erosion level is controlled, in addition to the major fault and shear zones, by the wide-scale folding patterns (Figure 11). The following differently deformed and metamorphosed tectonic units can be distinguished:

1. Early high-grade events (E_1 and/or E_{2-3}) overprinted by a later high-grade event (E_4) characterizing large areas of the southern Svecofennian domain – exemplified e.g. by Pajunen et al. (2008) by the Västerviken site in Karjalohja.
2. An early weakly-deformed, low-grade event (E_1 and/or E_{2-3}) that is later overprinted by a non-migmatitic low-grade (generally amphibolite facies) event (E_4) – exemplified by the Vetio site in Kisko (Appendix-Fig. 4-1).
3. Early low-grade event (E_1 and/or E_{2-3}) or late deposition (early E_4) overprinted by later a high-grade event (later E_4) – exemplified by the gneisses of the Upper Tectonic Unit (UTU) (Appendix-Figs. 6-2a–d).
4. Late deposition (early E_4) and a low-grade non-migmatitic (amphibolite facies) late event (later E_4) – exemplified by the rocks of the Jokela supracrustal association (Appendix 5).

The present data are insufficient to map the distribution of these tectono-thermally different units,

Table 1. Observed structures in the geotectonic terranes and tectonic units in the study area.

	SVB	EGC	HGB		UTU	Jokela supracrustal association	WUC (modified from Pajunen et al. 2008)	Orijärvi area
	<i>Supra- crustal rocks</i>	<i>Grani- toid area</i>	<i>Gabbros and supra- crustal rocks</i>	<i>Askola dome interiors, supra- crustal rocks</i>	<i>Migmatitic garnet- cordierite gneisses rocks</i>	<i>Pull-apart basin sedi- ments and volcanic rocks</i>	<i>Västerviken outcrop (modi- fied from Pajunen et al. 2008)</i>	<i>Vetio outcrop, andalusite- cordierite schist</i>
Volcanic Series I	X						X	
D _A	X			X			X	
Volcanic Series II	X		X					(?)
Pre-D _B intrusions	X		X				X	
D _B	X		X	X			X	(?)
Syn-/late D _B tonalites	X		X	X			(?)	
D _C	X		X	X			X	
D _D	X		X	?			?	
Cooling	X		X	X			X	X
D _E	X	X	X	X	X	X	X	X
Early/mid-D _E granitoids and dykes		X		X	X		X	
Late D _E gabbros		X					X	
D _F		X					X	
D _G	X	X	X		X	X	X	
D _H	X	X	X		X	X	X	X
D _H granitoids	X	X	X	X	(?)	X	X	
D _I	X	X	X		X	X	X	

but more careful structural mapping and correlation of structural, magmatic and metamorphic events is needed.

The first geotectonic Event 1 (E₁) – early collisions and crustal thickening

The structures of the earliest-observed Svecofennian deformations are not correlative between the major geotectonic terranes like, for example, in the Karelian terrane lying upon the Archaean continent, in the early Svecofennian Pyhäsalmi primitive island arc (Savo Schist Belt, SSB) or in the Southern Volcanic-sedimentary Belt (SVB). Koistinen (1981) interpreted that D₁ in the Karelian terrane, in the Outokumpu area, was related to the regional overthrusting of the Karelian supracrustal sequences and ophiolites upon the Archaean domain; the collision

began before 1.90 Ga. Weak pre-D₁ folds were also described, but their tectonic significance was not established (Koistinen 1981).

In the different units of the Svecofennian domain the early structures are quite similar intrafolial folds that in some measurable cases suppose approximately N-S transport (cf. Pajunen et al. 2008) causing crustal thickening. In the southern study area the earliest thickening event (E₁) occurred after the deposition of early volcanic Series I at c. 1.90–1.89 and before Series II 1.88–1.87 Ga ago. We suggest that E₁ was a low-grade, low-angle thrusting event, which had an important effect on the slicing of the earliest primary sequences and the thrusting of rocks from different crustal depths and geotectonic environments close to each other, close to their present-day positions in the D_{C-D} structures. We also suggest that the accretion of the southern units, the Tonalite Migmatite Belt (TMB) and the Granite Migmatite

Belt (GMB), occurred during the southern D_A . The maximum age of D_1 in the Vammala Migmatite Belt (VMB) is determined as c. 1.91 Ga, which indicates an earlier D_1 evolution when compared to the D_A to the south of it. Kinematic and age determination of the corresponding early structures and references to their ages in the Central Finland Granitoid Complex (CFGC) and Savo Schist Belt (SSB) are lacking.

The earliest structures from the Karelian terrane and southern Finland (SVB) suggest that the early overthrusting or collisions occurred in c. N-NNE compression. The pattern of fragmentation of the Archaean continent indicates that the collision was oblique. The E-W trend of the early structures in the Svecofennian domain suggests that the N-S collision occurred against the Archaean continent with its originally more or less NW-trending shore line (Figure 48). This can also be reconstructed from the

enveloping surface of major fold structures, caused by the major block structures further southeast, deforming the Archaean continent (Figure 8). Mantled gneiss domes (Eskola 1949), like the Pitkäranta dome in eastern Russian Karelia and the Kuopio mantled gneiss dome (Brun et al. 1981), were formed close to the collision zone, near the original Archaean-Svecofennian suture. They show ductile folding patterns that formed in the active collision zone, whereas domes further north from the original collision zone, like the Sotkuma dome close to the Karelian terrane-Archaean domain border, are more sliced in character. The distribution of different domes (ductile domes are located in the southern parts and less ductile sliced domes in the northern parts of the N-trending tectonic blocks that were separated from each other by dextral N-trending shear zones) support the early N-S collision. The

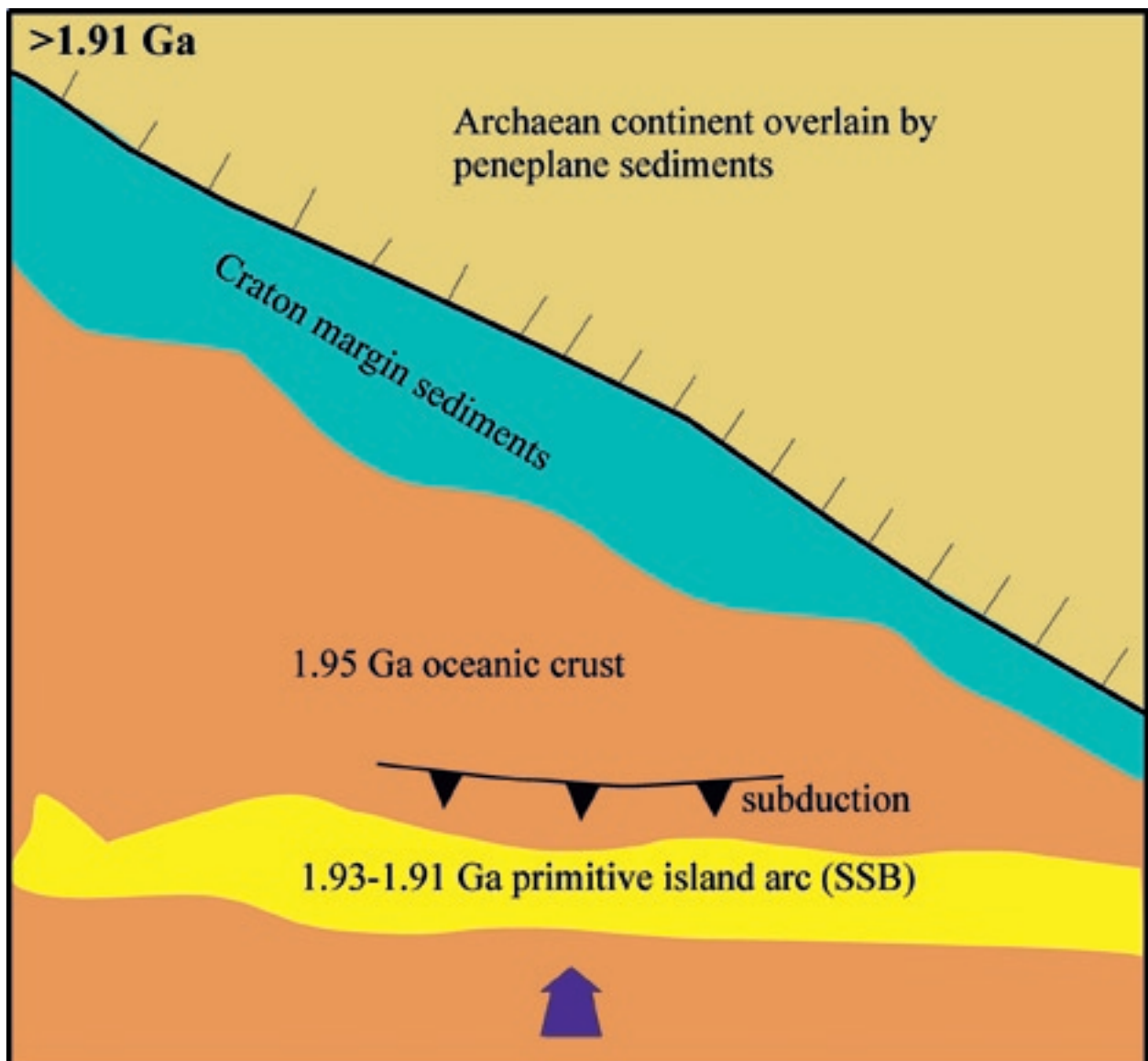


Figure 48. The pre-collisional stage and the generation of the Pyhäsalmi primitive island arc (Savo Schist Belt, SSB) by c. southwards subduction of 1.95 Ga oceanic crust.

early thickening event E_1 of the crust in the southern Svecofennian domain and contemporaneous events in the north are schematized in Figure 49. In the Karelian terrane, the second deformation event D_2 was related to continued collision (Koistinen 1981) and therefore differs markedly in character from the $D_{B/2}$ structures in the southern Svecofennian domain. When E_1 thickening occurred in the south

(Granite Migmatite Belt, GMB) the northern terranes (Tonalite Migmatite Belt, TMB) already underwent an extensional event thinning the crust. This supports the idea of diachronic evolution progressing towards the south, and suggests that the N-S collisional event continued during the contemporaneous local extensive events further north.

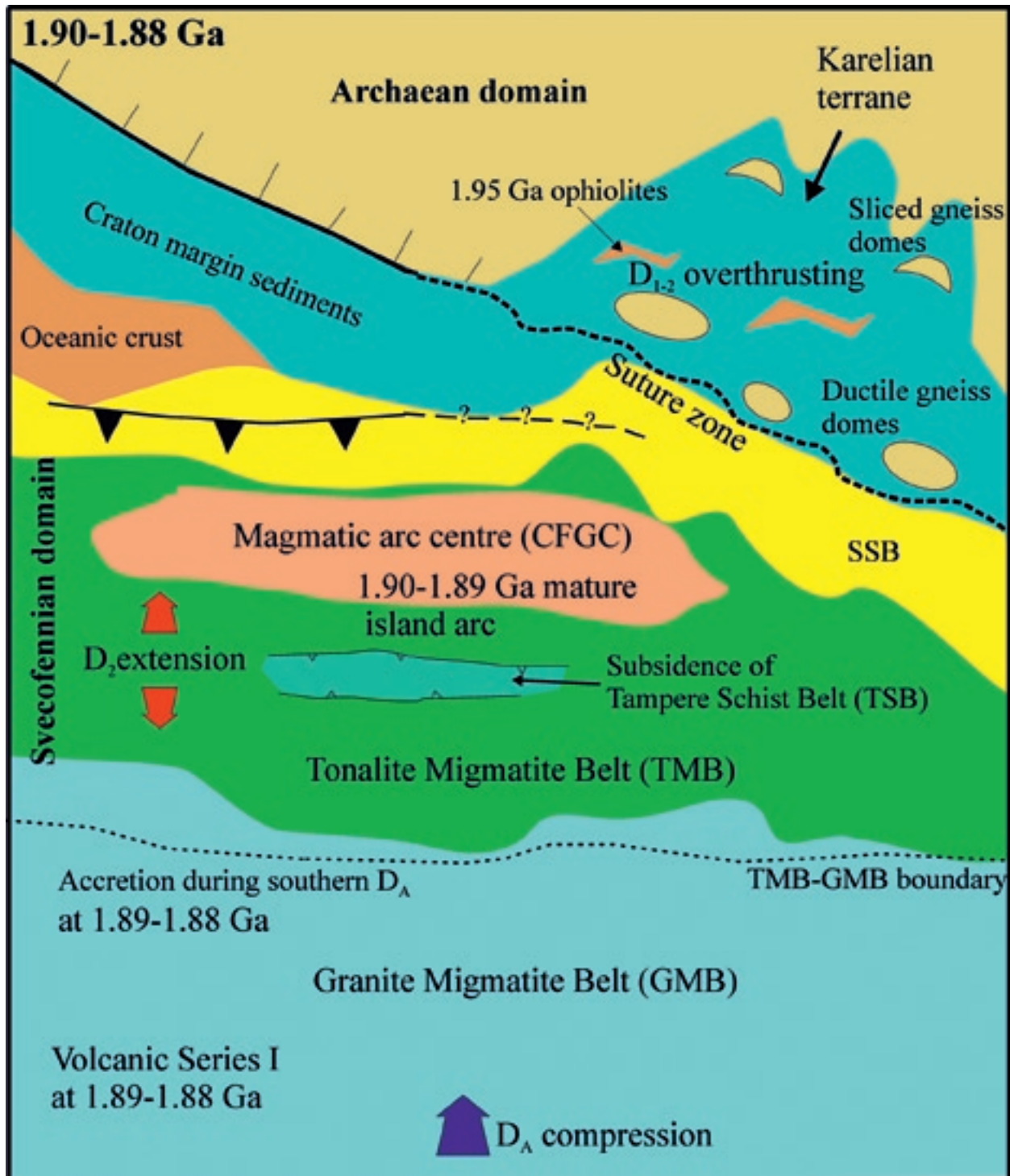


Figure 49. The first geotectonic Event 1 comprises crustal thickening by overthrusting in the southern Svecofennian domain and contemporaneous tectonic events in the north. CFGC = Central Finland Granitoid Complex and SSB = Savo Schist Belt.

The second geotectonic Event 2 (E_2) – collapse of the island arc causing crustal extension

Event 2 appears in the study area as intense vertical shortening of the early D_A structures, early/syn- D_B intrusive rocks and the volcanic Series I. The later volcanic Series II also underwent M_B metamorphism and D_B deformation. Deformation occurred under prograde metamorphic conditions, at low pressures (c. 4–5 kbar, Korsman et al. 1999), and the strain was strong flattening including a rotational shear strain component as indicated by rotated D_B boudinages. The maximum age of E_2 in the study area is fixed by the age of the volcanic sequence of Series II at c. 1.88–1.87 Ga (cf. Väisänen & Mänttari 2002). The syn-/late D_B tonalites, intruded into the S_B plane of strong D_B flattening and migmatization, are dated at 1.88–1.87 Ga (Appendix 8). Similar ages of “syntectonic granitoids” and neosomes are common in southernmost Finland (Hopgood et al. 1983, Huhma 1986, Vaasjoki & Sakko 1988, Nironen 1999, Mouri et al. 1999, Väisänen et al. 2002 and Skyttä et al. 2006).

We propose that D_B occurred in the arc environment (back arc basin environment of Väisänen & Mänttari 2002) that was already thickened by collision during the E_1 event. The later volcanic Series II represents an intra-arc extensional volcanism into the upper crust. The increased heat flow caused increased production of tonalitic magmas during the latest phases of the extensional E_2 . The S_C is dominantly the first strong penetrative foliation in the wider intrusions (e.g. Hindsby), but intrusion into S_B planes (Figure 20a) indicates their close association with the D_B . In the earlier or deeper-level D_B granitoids (cf. Skyttä et al. 2006 and Pajunen et al. 2008), and in the pre- D_B gabbroic-tonalitic rocks, amphibolite facies S_B foliation generally developed. A possible explanation for the extensional E_2 with the characteristic low-pressure prograde metamorphism, intensive migmatization and contemporaneous upper crustal volcanism, is the increased heat flow generated by upwelling of the lithosphere and sinking of the oceanic slab into the mantle, as modelled by Platt and England (1993). This extension caused subsidence in the upper crust and the low-grade, non-migmatitic rocks (Vuosaari triangle and Vetio, Appendix 4; cf. Kisko Triangle in Skyttä et al. 2006) underwent their first metamorphism.

The E_2 affected the whole area of the Granite Migmatite Belt (GMB), Hyvinkää Gabbroic-volcanic Belt (HGB) and Hämeenlinna Volcanic Belt (HVB). In the northern terranes, such as in the Vammala Migmatite Belt (VMB), D_2 is a similar strong, prograde flattening deformation to that in the GMB

(Koistinen et al. 1996, Pietikäinen 1994, Kilpeläinen 1998 and Pajunen et al. 2001a), but dated by magmatic rocks to c. 1.89–1.88 Ga (compiled in Korsman et al. 1999). “Syntectonic” magmas of this age also characterize major parts of the Central Finland Granitoid Complex (CFGC) (Nironen 2003). The ages are on average c. 10 Ma older in the northern terranes, like the Tonalite Migmatite Belt (TMB) (e.g. Huhma 1986, Vaasjoki & Sakko 1988 and Nironen 1989), than in the GMB, again proving the diachronic character of the Svecofennian orogeny. This suggests that the collapse structure caused by mantle upwelling began in the north and was migrating towards the south c. 10 Ma later. The structural observations indicate the co-existence of the geotectonic units already after D_A . The Tampere Schist Belt (TSB) began to subside during the northern D_2 extension correspondingly to the southern non-migmatitic units such as the Vuosaari triangle and Vetio (Appendix 4, cf. the Kisko Triangle, Skyttä et al. 2006).

Event 2 and corresponding structural characteristics in the southern Svecofennian domain are illustrated in Figure 50. The extensional evolution, D_B , in the south was coeval with the contractional structures D_3 in the north. This supports the conclusion of overall N-S compression and localized extension. This is why the extensional E_2 rapidly turned to the compressional event E_3 .

The third geotectonic Event 3 (E_3) – collision due to N-S compression

In the study area the E_2 extension was soon followed, or concomitantly affected, by the N-S shortening E_3 , which deformed the supracrustal series and the early magmatic rocks into tight, often northwards overturned folds with originally c. E-W-trending steep axial planes related to the D_C . In the study area the D_C structures are best preserved in the Southern Volcanic-sedimentary Belt (SVB). In the Espoo Granitoid Complex (EGC) the D_C structures are often difficult to identify because of the strong later deformations, metamorphism and magmatism. The observations on mineral growth in relation to the structural succession suggest that the temperature peak was already achieved during the extensional E_2 , but was still high, as can be concluded from the amphibolite facies S_C as the first foliation in the syn-/late D_B tonalites. The ductile folding character also establishes the evolution as closely following E_2 . The age determinations indicate that the compressional E_3 evolution rapidly followed the formations of the later volcanic Series II and syn-/late D_B tonalites. The E_3 ended in the study area certainly

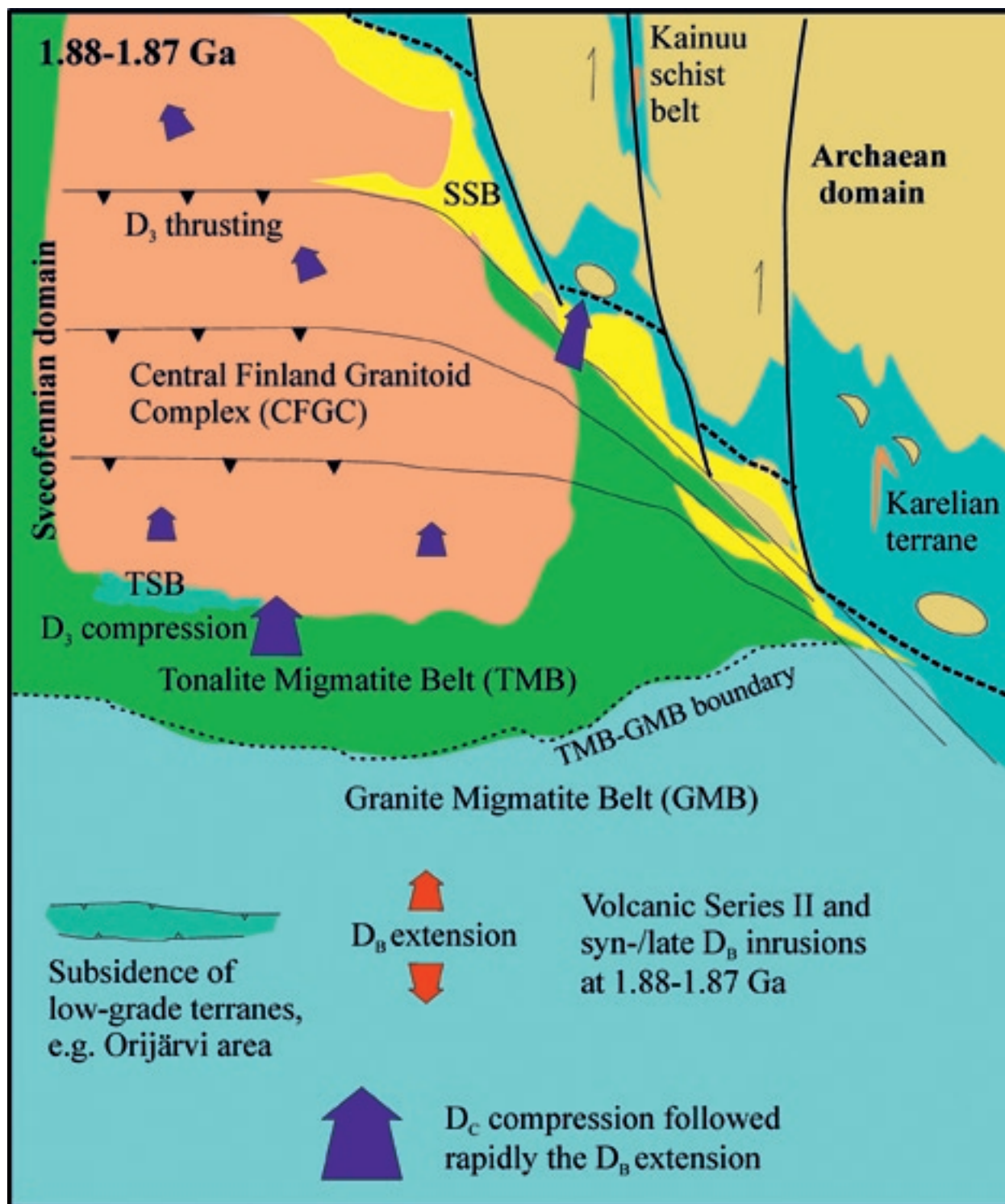


Figure 50. The second geotectonic Event 2 caused crustal thinning in the southern Svecofennian domain and contemporaneous overthrusting and thickening of the crust in the north. TSB = Tampere Schist Belt.

before the first D_E intrusion at 1868 ± 3 Ma (Hakkila, Appendix 8): it also cuts the D_D structures. The northern D_4 , simultaneously with the D_D in the south, fixes the age of the major geotectonic E_3 at 1.88–1.87 Ga, i.e. closely to the age of E_2 .

We interpret that E_3 was continued northward collision against the northern terranes. The struc-

tural relations in the southern Svecofennian domain are illustrated in Figures 50 and 51. In central Finland, D_3 is an overthrusting deformation with low-angle thrust planes dipping towards the southeast (cf. Sorjonen-Ward 2006). The Tampere Schist Belt (TSB) is located in the E-W-trending electric conductive zone between the Vammala Migmatite Belt

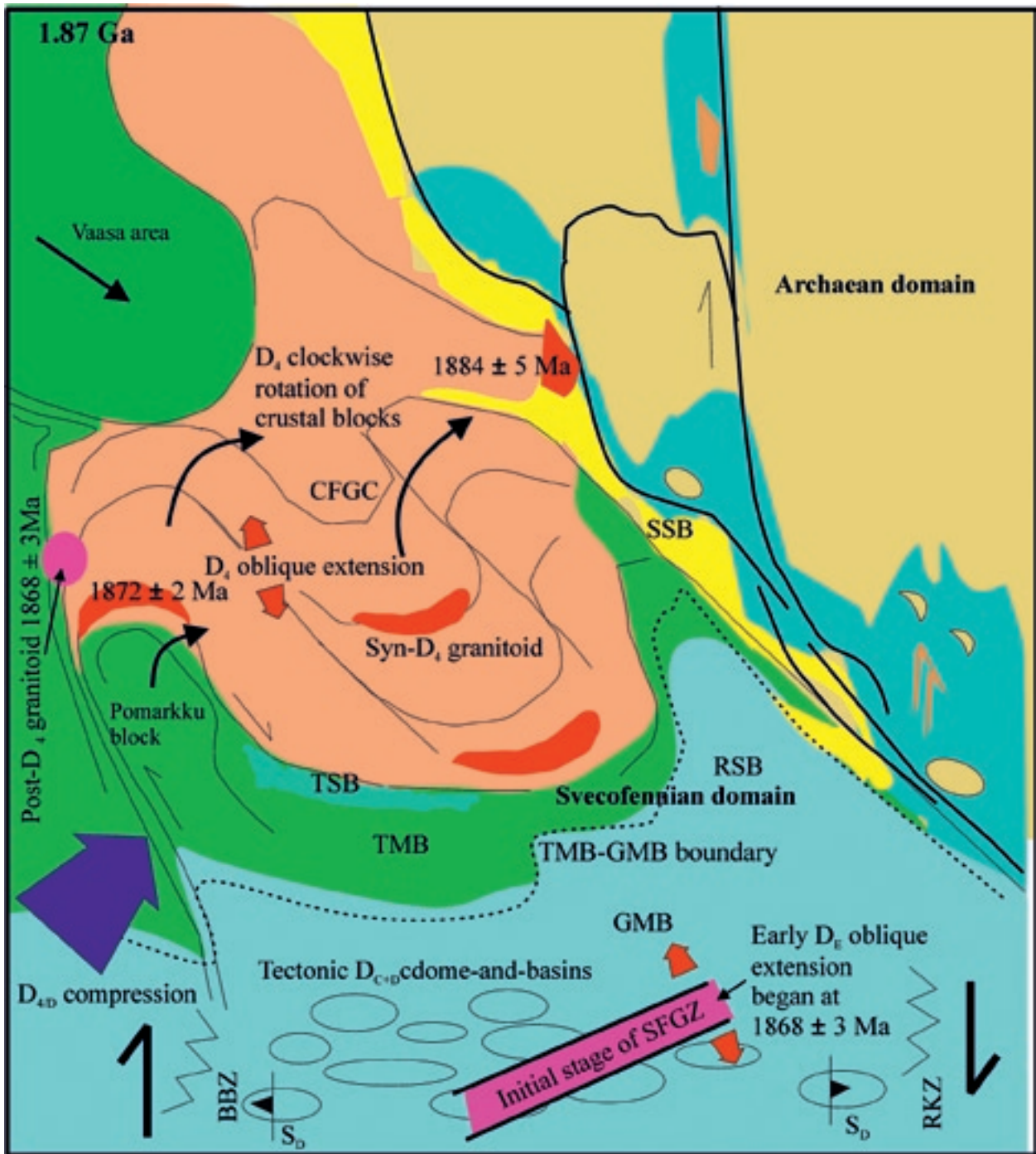


Figure 51. Relations between the northern D_4 and the southern D_5 deformations and the beginning of the fourth major geotectonic Event 4 – the beginning of evolution of the Southern Finland Granitoid Zone. Abbreviations: SSB = Savo Schist Belt, RSB = Rantasalmi-Sulkava area, TMB = Tonalite Migmatite Belt, GMB Granite Migmatite Belt, TSB = Tampere Schist Belt, SFGZ = Southern Finland Granitoid Zone, CFGC = Central Finland Granitoid Complex, BBZ = Baltic Sea-Bothnian Bay Zone and RKZ = Riga Bay-Karelia Zone.

(VMB) and the Central Finland Granitoid Complex (CFGC) (Korja 1990); the zone dips beneath the CFGC and is regarded as a suture zone along which the conductive schists of accretionary prism of the VMB were pushed below the CFGC (e.g. Lahtinen 1994, Kilpeläinen 1998 and Korsman et al. 1999). In the model presented here the zone is in a corre-

sponding setting to the D_3 zones in the northern margin of the Pomarkku block (Appendix 7 and Appendix-Fig. 7-1c). It can be interpreted as a crustal-scale thrust zone related to E_3 , presumably reactivating the E_2 extensional zones.

The strong crustal slicing and northwestwards stacked structure in the Central Finland Granitoid

Complex (CFG) may be due to the competent character of the CFGC when compared to the sediment-dominant units. We relate the major 1.89–1.88 Ga (Vaasjoki & Sakko 1988) granitoid pulse in the CFGC to the generation of a magmatic complex in the central arc that developed beside/upon or collided against the 1.93–1.91 Ga old primitive island arc (Savo Schist Belt, SSB). Anyhow, at present the contact between the CFGC and SSB is a tectonic zone that is characterized by strong granite magmatism, granitization and shearing (Pajunen 1986 and Pääjärvi 1991) and by a gravity low (Korhonen et al. 2002b), predominantly syn- D_3 . The CFGC does not show such a D_2 flattening as the supracrustal units of the Tonalite Migmatite Belt (TMB), again supporting its more competent character – extensional deformation mainly concentrated in zones. The D_3 in the north is slightly older than D_C in south; the D_3 is about the age range of the southern D_B . Hence, E_3 also becomes diachronic younger towards the south; at the time of thrusting in the north the southern crust underwent the extensional collapse E_2 .

Due to large differences in competencies between the Archaean continent and the active Svecofennian crust, deformation developed to dextral shearing along the NW- and N-trending shear zones along Archaean border zone (Figure 50). The Archaean continent fragmented to c. N-S-trending slices that slid dextrally towards north along with some rotation of the blocks. Movements partly occurred along pre-existing c. N-S-trending zones of weakness, for example, the structures related to the early break-up of the Archaean continent, the Early Proterozoic c. N-S-trending diabase dykes or the Siilinjärvi carbonatite occurrence (Korsman et al. 1997). Korsman et al. (1999) explained the preservation of thick crust in eastern Finland as a consequence of continued compression preventing thinning that in the southern and western Svecofennian domain is predominantly related to the extensional E_2 . Indeed, the Archaean region did not undergo the extensional E_2 , but the crust was thickening by oblique collision at that time. The extensional collapse was caused by the subsidence of the oceanic slab and upwelling of mantle. This did not occur in the Archaean area, which supports subduction away from the Archaean terrane. The late extensional structures, the D_E - D_H , did not notably affect the Archaean continent, with the exception of the easternmost Southern Finland Granitoid Zone or Central Lapland granitoid area, where the crust is thinner. These are the main reasons for the thick crust in eastern Finland.

After the major geotectonic Events 1–3 the Svecofennian arcs were accreted to the Archaean continent forming a new continental environment.

The fourth geotectonic Event 4 (E_4) – evolution of the Southern Finland Granitoid Zone

The fourth geotectonic event, E_4 (D_D - D_H), occurred in the new continental crust (Archaean and accreted Svecofennian) and is predominantly linked to the evolution of the Southern Finland Granitoid Zone (SFGZ) (D_E - D_H). E_4 shows a complicated history; the tectonic evolution of the SFGZ exhibits significant rotations of the stress field accompanied by enormous magma production.

Ductile F_D folds in the south refolded the earlier structures under decreased temperatures after E_{2-3} and produced the map- to outcrop-scale D_{C+D} dome-and-basin interferences, preserved well in the Southern Finland Volcanic-sedimentary Belt (SVB). The c. 1.88–1.87 Ga age of D_D is linked to the northern syn- D_4 granitoids (Appendix 7) emplaced into the D_4 oblique extensional zones under NE-SW transpression in between the major N-trending deformation zones, e.g. the Baltic Sea-Bothnian zone (BBZ) and the Riga Bay-Karelia zone (RKZ) (Figure 8). The F_D folds in the south are results of this transpressional deformation.

The transpressional D_{D4} evolution shows similar diachronic progression towards the southwest and south as occurred during the earlier geotectonic E_2 and E_3 . D_4 terminated in the Savo Schist Belt (SSB) at 1884 ± 5 Ma (Hölttä 1988) and in the western Tonalite Migmatite Belt (TMB) at 1868 ± 3 Ma (Lehtonen et al. 2005). In the north, the D_3 thrust planes (Figure 50) were deformed in the D_4 to arched structures and blocks that were bordered by c. NW-SE-trending shear zones/faults and were rotated clockwise; Figure 51 summarizes the results of the rotational deformation of the blocks. The Pomarkku block (Appendix 7) is a typical result of this transpression. The migmatitic Vaasa area (Va in Figure 9), which in the south is bordered by the Vittinki shear/fault zone (Figure 10), continues to the Swedish coast. According to Rutland et al. (2004), it was transported from the west on its present setting. We agree with the eastward movement of the unit and relate it to the deformation D_4 in the north; movements occurred still later during the short-lasting D_F E-W contraction. Similar block structures characterize the western parts of the Archaean craton. Further east, in Russia, the structure changes to open folding, as can be interpreted from the magnetic data (Figure 8). The N- and NW-trending, mainly dextral shear zones (e.g. Talvitie 1971) of the Ladoga-Bothnian Bay zone mark the present border zone between the Archaean and Svecofennian domains; the original Archaean-Svecofennian suture zone nowadays occurs as deformed pieces in

the southern borders of N-trending tectonic slices (Figure 50).

The termination of D_4 deformation and stabilization of the crust at 1868 ± 3 Ma (Lehtonen et al. 2005) in the north caused a jump of the major deformation towards the south into the area of the Southern Finland Granitoid Zone (SFGZ). The early evolution of the SFGZ is linked to the emplacement of the first dated early D_E tonalite at 1868 ± 3 Ma (Appendix 8). The southern Svecofennian domain cooled and became more competent after D_D . It was susceptible to oblique SE extension along the E-ENE-trending zones under the overall SW-NE transpression between the active major N-trending deformation zones, the Baltic Sea-Bothnian zone (BBZ), the Riga Bay-Karelia zone (RKZ) and Transscandinavian Igneous Belt (TIB). Thus, the earliest deformation in the SFGZ, the D_E , is characterized by similar SW-NE transpression to that which occurred during the $D_{D/4}$.

The earliest structures in the Southern Finland Granitoid Zone (SFGZ) are related to oblique extension in the ENE-trending zone. At greater crustal depths, nearly horizontal the extensional $S_{E,ext}$ shear foliation developed. Oblique contractional structures like the $S_{E,cont}$, produced by the progressive SW-NE transpression, appear more intensely in the early D_E magmatic rocks than in the later ones. The early D_E magmatism is represented by the garnet-bearing early D_E tonalites, microtonalite dykes and wider tonalitic to granodioritic intrusions at 1.87–1.86 Ga. Most microtonalites intruded into upper parts of the cooled crust, but some dykes and most of the tonalitic-granodioritic rocks were intruded into the high-grade ductile environment at greater depth. In eastern Finland, corresponding microtonalites are 1.86–1.85 Ga old (Huhma 1981). Continued extensional evolution in the SFGZ led to the enlargement of intermediate magma production and an increase in the metamorphic grade. The second major migmatization phase after E_2 evolved and the granulitic rocks of West Uusimaa Complex (WUC) were generated into the middle and, due to the high thermal gradient (cf. Korsman et al. 1999), even into the upper crust. The pyroxene tonalite from the WUC at 1860 ± 5 Ma (Appendix 8) predates the penetrative horizontal $S_{E,ext}$ characterizing the high-T areas of the SFGZ. The later metamorphic 1841 ± 4 Ma zircon phase and 1837 ± 3 Ma monazites in tonalites (Appendix 8) suggest continuing high heat flow. Channels also opened for deeper-derived mafic magmas that culminate the oblique extensional evolution in the SFGZ; the late D_E gabbro is dated at 1841 ± 7 Ma (Appendix 8).

In the upper crust the SE extension was more zoned and was characterized by faulting and shear-

ing. The Jokela supracrustal association, and corresponding rocks in the southern Svecofennian domain (yellow triangles in Figure 9), started their deposition with high-energy clastic sediments, quartzites and conglomerates (Appendix 5); corresponding associations also exist in Sweden. Sedimentation basins developed in between the active N-trending transcurrent shear zones, the Baltic Sea-Bothnian Bay zone (BBZ) and the Riga Bay-Karelia zone (RKZ), as oblique extensional pull-apart basins under the overall SW-NE transpression. Similar quartzites in Sweden suggest oblique extensional pull-apart-basins between the BBZ and the Transscandinavian Igneous Belt (TIB) (or unknown zones even further west, nowadays destroyed, for example, due to opening of the Iapetus Sea or the Caledonian orogeny). The subsidence of the Jokela supracrustal association proceeded with rapid steps as evidenced by the sharp change from high-energy clastic sandstone to mica gneiss, referring to more peaceful deeper-water sedimentation. The volcanic rocks within the Jokela association can be related to the increased deep-derived mafic or the intermediate magma production in the lower crustal levels during the D_E . This assumption of the genetic relations between the Jokela volcanogenic rocks and the deeper crustal intrusives is based on correlation of their structural successions, and requires further establishment, e.g. by geochemical methods.

In the study area, there are only scarce signatures of the E-W contradictory D_F that appears as a zoned fold deformation with N-trending axial planes in eastern Finland at c. 1.86–1.85 Ga ago (cf. Koistinen 1981). The deformation was concomitant with the early D_E in the south. The sinistral Hiidenvesi shear zone is linked to that stage. The related fold deformation has not been identified in the SFGZ. The D_F in eastern Finland is related to the transport of a large central Finland block shown in Figure 8 towards the east. The northern border of the block is the sinistral E-W-trending shear zone at the level of the northern end of the Bothnian Bay. In the south the bordering shearing occurred along the dextral E-W-trending Hyvinkää, Hämeenlinna and Tampere shear zones. The stress was released into these zones and no significant folding corresponding to the F_F (F_4 Koistinen et al. 1996) occurred to the south of the zones. The 1.85 Ga dilatational fluid activity causing strong metasomatic alterations in shear zones in the Archaean domain (Pajunen & Poutiainen 1999) and felsic granitoids of that age (compiled in Pajunen & Poutiainen op. cit.) in eastern Finland can be related to this deformation. Near the craton boundary, some NW-SE-trending shear zones show a sinistral sense of movement (e.g. D_c in Pajunen 1986) and NE-SW-trending shear zones are

dextral, like the Auho fault cutting the Kainuu schist belt (Kärki 1995); their formation or reactivation can be related to the E-W contraction. The D_F was localized in the northern part of the Svecofennian domain and the E-W stress field thus reflects these local conditions.

In the study area the large-scale F_G folds and the sinistral shearing along the Porkkala-Mäntsälä shear zone indicate a short transitional period of N-S contraction, before the stress field rotated into a SE-NW trend. Corresponding major shear zones in the c. SE-NW and also SW-NE directions characterize the crustal structure in the southwestern archipelago, where the beginning of the SE-NW shear zone is dated at c. 1.85 Ga (Torvela et al. 2008), and further south in the Baltic region (Figure 8). Such a wide-scale F_G folding related to the D_G also deforms the northern terranes, e.g. the Tonalite Migmatite Belt (TMB).

Rotation of the stress field from SW-NE affecting through S-N during the early E_4 to SE-NW during the late E_4 occurred rapidly at c. 1.84 Ga ago. The rotation indicates the start of the D_H deformation, the latest major evolutionary phase of the Southern Finland Granitoid Zone (SFGZ). The 1.83 Ga pegmatitic granitic dykes cutting the syn-/late D_B tonalite (Appendix 8) indicate the beginning of the D_H granitic pulse in the marginal area of the Espoo Granitoid Complex (EGC). The dyke-intrusive relations provide evidence that the crust stabilized and cooled for c. 40 Ma. Corresponding cooling stages are identified between early/mid- D_E microtonalites and syn-/late D_B tonalites, and Sederholm (1927) described a tectono-thermal gap between magma pulses in the Hanko-Inkoo area. However, in places, such as in the northern EGC or West Uusimaa granulite Complex (WUC), compositionally varying magmatic activity continued in a ductile state practically throughout the E_4 evolution. Hence, the contemporaneous igneous rocks show different characteristics depending on the thermal state of their emplacement environment.

The SE-NW transpression occurred in between the active E-W-trending Southern Finland and Hyvinkää shear zones. Ehlers et al. (1993) related the evolution of the Southern Finland Granite Zone (SFGZ) to SE-NW transpression, but the observations of this study demonstrate that the SFGZ evolution was a more complex and longer-lasting process. Transpression caused oblique contractional folding $F_{H,cont}$, forming the regional-scale D_{G+H} dome-and-basin interferences. The simultaneous oblique extension $D_{H,ext}$ caused strong vertical shortening, felsic magmatism and increased heat flow, causing a new pulse of migmatization. Huge amounts of granodioritic to granitic magmas were produced between 1.85–1.82 Ga, dated by Kurhila et al. (2005)

from the Espoo Granitoid Complex (EGC). The age of migmatization ranges between 1.82–1.81 Ga (Korsman et al. 1984, 1988, 1999 and Väisänen et al. 2004). This migmatization also occurred in the D_E granitoids. Differences in competencies, due to variations in thermal state and magmatic activity, caused variations in local deformation patterns. In the cooled areas no significant deformation occurred, whereas strong magmatism and deformation occurred in the areas nearby; e.g. Espoo Granitoid Complex (EGC) or the West Uusimaa Complex (WUC) as compared to the Southern Volcanic-sedimentary Belt (SVB). In the cooled parts of the crust outside the most active D_H extensional zones, medium-grained to pegmatitic granite dykes emplaced.

NW-SE transpression suggests c. E-directional dilatation or NW-N oblique extension between the E-W-trending dextral major shear zones. The granitic igneous activity during the late E_4 was scattered and concentrated in spots (Figure 38); spot-like dilatation centred during the late E_4 is supported by kinematic observations on the varying directions of dilatation in the surroundings of the Nuukio granitoid area. The contractional $F_{H,cont}$ folds openly deform even the latest identified granite pulses in the study area, presuming that NW-SE transpression acted very late in the SFGZ evolution. The latest Svecofennian rocks in the study area are <1.8 Ga diabase dykes intruded into c. E- or N-trending dilatation zones in the Southern Volcanic-sedimentary Belt (SVB). The amphibolite facies diabase dykes locally show contractional $F_{H,cont}$ and high temperature assimilation structures, indicating their hot emplacement environment. They are related kinematically to the D_H SE-NW-transpression, very close to the transition to E_5 ; their age is within the error limits the same as that of the latest dated F_1 granite dykes (E_5) in the area (c.f. Pajunen et al. 2008).

The evolution of southern Finland and the Hyvinkää shear/fault zones shows a polyphase history that began during the early SE-NW extensional E_4 . It continued during the oblique dextral movements causing clockwise rotation of the competent blocks, like the Hyvinkää gabbros, during the latest E_4 SE-NW transpression. The transpression also caused the oblique overthrusting of the Hyvinkää Gabbroic-volcanic Belt (HGB) upon the high-grade West Uusimaa Complex (WUC). The tectonic-metamorphic observations from the Jokela supracrustal association, the pull-apart basin that started its evolution during the early E_4 NE-SW transpression, reveal that a series of contractional structures formed under varying stress fields during the E_{4-5} evolution (D_F - D_1). During the latest E_4 , pegmatitic granite dykes intruded it.

Close to the border zone of the Archaean continent, dextral movements of crustal N-trending blocks characterize the oblique collisional structures formed during the E_3 event. During the continuing oblique collision under SW-NE transpression the E_3 the shear zones remained active and dextral movements continued. During the early E_4 evolution the northern Svecofennian crust in central Finland was deformed to form NW-trending crustal slices and blocks that rotated clockwise and transported eastwards. Correspondingly, the crustal blocks already formed during the E_3 were transported dextrally towards north; these blocks also show some rotation. The eastwards transport of the central Finland block during D_F E-W contraction exhibits a local event. During the late E_4 evolution, oblique extension zones represented by the Southern Finland Granitoid Zone were formed between the crustal-scale N-trending the Baltic Sea-Bothnian Bay Zone (BBZ), Riga Bay-Karelia Zone (RKZ) and Transscandinavian Igneous Belt (TIB). The evolution of the BBZ was predominantly related to the early E_4 SW-NE transpression. The TIB show a strong dextral component of movement, which is not the case with the RKZ; therefore, the E_4 granitic areas are much larger in the west than close the RKZ.

Magmatic rocks or thermal events at c. 1.87–1.84 Ga characterize the N-trending zones (e.g. Huhma 1981, Neuvonen et al. 1981, Pajunen & Poutiainen 1999, Koistinen et al. 2001 and Högdahl et al. 2004). Some observations of late movements and cordierite alteration in shear zones in central Finland, e.g. in Hallaperä sulphide ore in Kiuruvesi (Pajunen 1988) or close to the N-trending high-strain zone in the Haukivuori area (Ha in Figure 9), are very similar to the 1.85 Ga metasomatic zones in the Archaean continent (Pajunen & Poutiainen 1999), and also indicate crustal reactivation in the Savo Schist Belt (SSB) during the E_4 . In eastern Finland, granitoids related to E_4 are concentrated in a zone from the Maarianvaara granite in eastern Finland to the Kainuu schist belt and to the north, central Lapland. The central Lapland granite complex shows similar characteristics to the Southern Finland Granitoid Zone (SFGZ), but it was developed into Archaean crust similarly to the easternmost parts of the SFGZ in southeastern Finland (cf. Huhma 1981). We suggest that the evolution of these c. 1.86–1.80 Ga granitoid terranes is of similar origin during the E_4 . The 1.80 Ga granites in the Kajaani area (Korsman et al. 1997) can also be related to the E_4 evolution.

The E_{3-4} evolutions produced a complex structural pattern of rotated and moved crustal blocks. A continuous oblique collision model that was produced predominantly under SW-NE transpression can explain the structures. Local variations in the

stress field are due to continuing deformation that rotated originally extensional areas to contractional; e.g. the early E_4 oblique SE extension (D_E) in the Southern Finland Granitoid Zone rotated to SE-NW transpression (D_H) that caused shortening of the originally extensional zones. All this may occur by clockwise rotation of the zone itself under overall SW-NE transpression. Similarly, the complex rotational block patterns in central and eastern Finland can be explained by a continuous SW-NE transpression that caused the escape of crustal blocks towards the east and north.

Tectonic evolution and kinematics during the E_4 - E_5 evolution in the area of the Southern Finland Granitoid Zone are summarized in Figure 52.

The geotectonic Event 5 (E_5) – evolution following the Southern Finland Granitoid Zone

The major N-trending D_1 deformation zones the Transscandinavian Igneous Belt (TIB), Baltic Sea-Bothnian Bay Zone (BBZ) and the Riga Bay Karelia Zone (RKZ) provide evidence of a long-lasting history. Their latest structures deform the Southern Finland Granitoid Zone (SFGZ) and the E-W-trending Hyvinkää and Southern Finland shear/fault zones and are linked to a new geotectonic Event 5 (E_5). The stress field was c. ESE-E trending during the E_5 . In the detailed study area the effects of the E_5 are seen in the structural evolution of the Vuosaari-Korso shear/fault zone.

The distribution of the remnants of the Jokela association and related rocks (Figure 9), and the older non-migmatitic areas like the Vuosaari triangle (Vu in Figure 9) and the Orijärvi area (Kisko Triangle of Skyttä et al. 2006 and the Vetio outcrop in Appendix 4) are strongly controlled by the intersections of the major E-W-trending and the N-trending D_1 shear zones. The isoclinal F_1 folds (Figure 31b) in the axial area in the northern Espoo Granitoid Complex (EGC) demonstrate that the temperature was not reduced under the ductile-brittle boundary. The monazite age of 1804 ± 2 Ma is suggested to represent the age of pegmatitic granite (Pajunen et al. 2008) that cuts the ductile F_1 folding (F_g in Pajunen et al. op. cit.). Ductile shearing structures close to dyke contacts indicate ductile movements that are still continuing (Pajunen et al. op. cit.). The bedrock north of the Southern Finland Granitoid Zone (SFGZ) was stabilized at c. 1.87 Ga ago and the D_1 structures there are brittle, as in the Päijänne fracture zone. The fracture pattern described by Sederholm (1932b) is in good agreement with the E-W shortening during the D_1 .

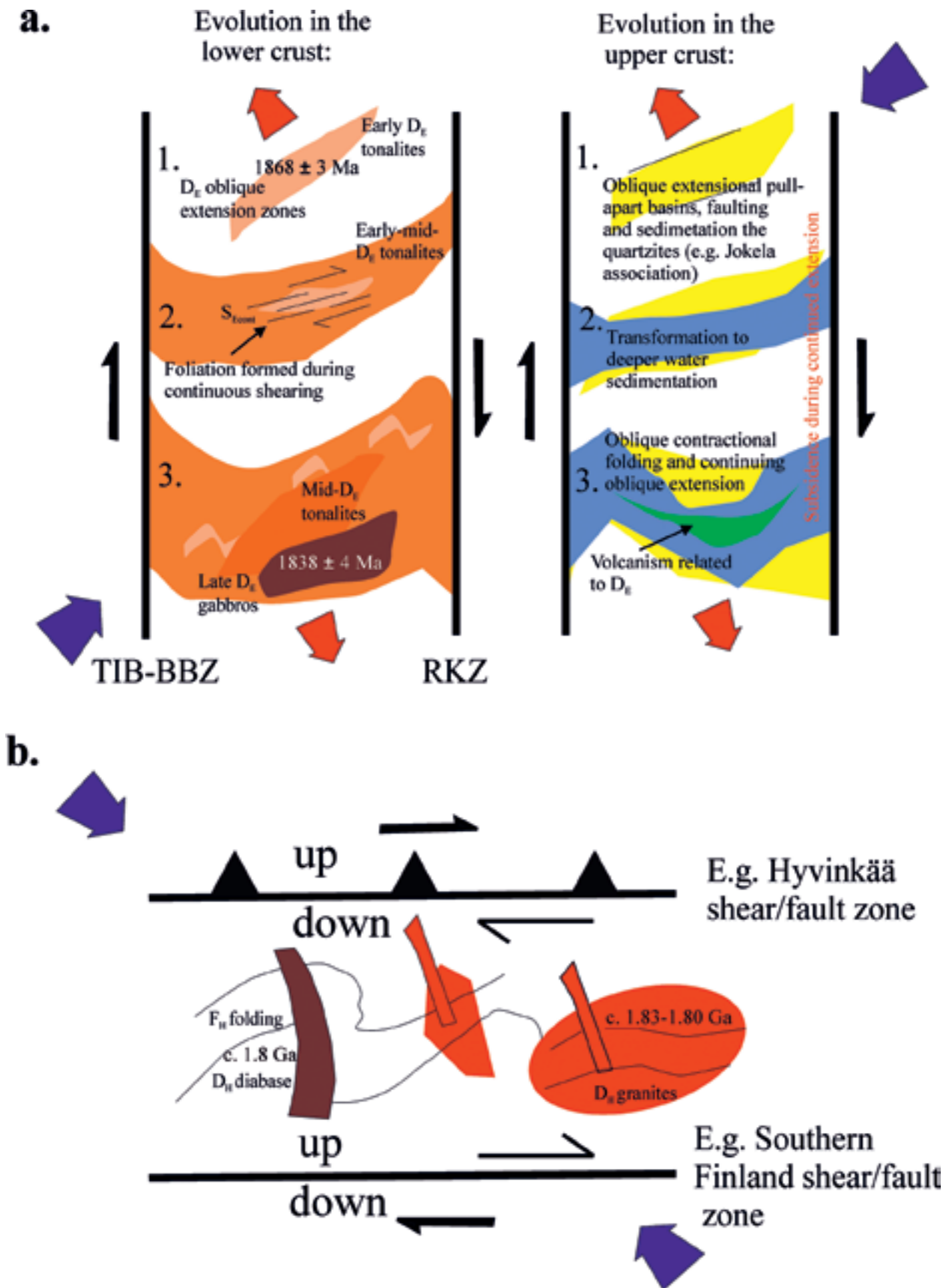


Figure 52. Schematic model of the evolution of Event 4 in (a.) during the oblique extension (D_e) under SW-NE transpression – in the lower crust on the left and in the erosion level on the right and (b.) during the (D_H) SE-NW transpression. E_4 includes the generations of the Southern Finland Granitoid Zone and the E_4 pull-apart basins.

So-called post-orogenic 1.8 Ga group granitic intrusions, locally showing low-pressure contact metamorphic aureoles (Rastas 1990), are small stocks or ring intrusions (Lindberg & Eklund 1988) that are often located in close association with the D_1 zones. The latest Svecofennian rocks in the study area are diabase dykes dated at c. 1.8 Ga in the Southern Volcanic-sedimentary Belt (SVB). They are connected according to their kinematics to the E_4 event (D_H). The diabase age is within the error limits the same as the F_1 granite (cf. Pajunen et al. 2008). The structural relations suggest that the jump from E_4 to E_5 involved only small rotation of the stress field. This and the structural relationships of the late magmatic rocks suggest that E_4 and E_5 are not strongly differentiated in their kinematics or in time.

The late stages of the E_5 deformation turned to lower-grade processes, which can be seen in a change of the shear structures to semi-ductile. In the latest stage, deformation concentrated into rather narrow zones with sinistral east-side-up movement and the formation of mica-rich slicken side surfaces and protomylonitic to mylonitic structures (Elminen et al. 2008). These late microstructures are predominantly related to post-Svecofennian events such as to the rapakivi stage (e.g. Mertanen et al. 2008). Kinematics of this kind are also evident in the Hyvinkää-Lahti shear/fault zone. The Svecofennian shear/fault zones controlled the movements in post-Svecofennian times and the intersections of the Svecofennian shear/fault zones effectively channelled the rapakivi granite magmatism. Figure 53a shows the occurrences of the rapakivi granites in the Fennoscandian Shield. The structures that have been active during the E_5 , like the Baltic Sea-Bothnian Bay Zone (BBZ) and Riga Bay-Karelia Zone (RKZ), strongly control the present setting of the rapakivi intrusions in Finland and Sweden. However, only preliminary results are currently available on the relations between the later structures such as brittle thrust faults (e.g. Pajunen et al. 2001a, Elminen et al. 2008 and Wennerström et al. 2008) and the Svecofennian structural framework.

In Estonia, late ages of metamorphic minerals, monazite and garnet (Puura et al. 2004), may indicate a diachronic jump of tectono-thermal processes towards the south, and that the Svecofennian orogeny continued with a new evolutionary step. Open warps with E-trending axial planes post-dating the D_1 structures (Figure 11) and sinistral movements along sharp faults deforming the Southern Finland Granitoid Zone suggest c. N-S contraction. The age and regional context of this deformation is not known.

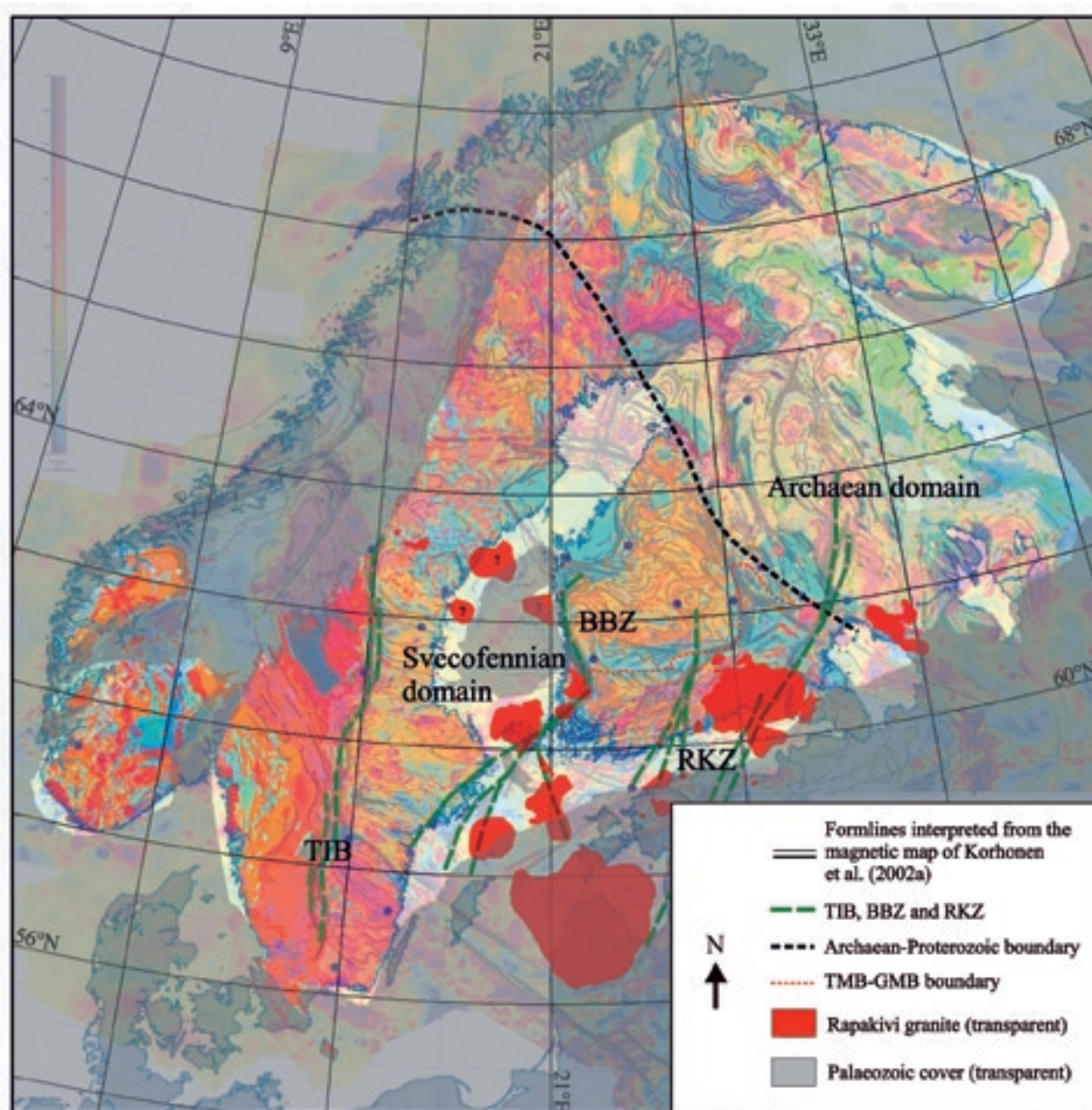
The Svecofennian orogeny – the result of oblique collision characterized by escape tectonics

There are several determinations of zircons and sphenes preceding the Svecofennian orogeny in metasedimentary rocks (e.g. Huhma et al. 1991, Lahtinen et al. 2002 and Rutland et al. 2004). The existence of these ages and Sm-Nd data from the Central Finland Granitoid Complex granitoids (Lahtinen & Huhma 1997) are proposed as evidence of pre-existing continental crust, such as microcontinents (e.g. Lahtinen et al. 2005) or pre-Svecofennian metamorphism and deformation (e.g. Rutland et al. 2004). Such old inherited zircons also occur in the igneous rocks in the study area, for example the inherited 3.3 Ga Archaean zircons in the Hakkila early D_E tonalite (Appendix 8). There are several possible source provenances for these old minerals or crustal geochemical components preceding the Svecofennian orogeny in the Svecofennian domain: 1) the Archaean continent; 2) an unknown removed continent formed by the break-up of the earlier Archaean (the removed continent may include crustal components of ages not identified in the Fennoscandian Shield, except the detrital zircons); 3) sedimentary sequences overlying the Archaean + Early Proterozoic (?) supercontinent before the break-up; 4) magmatism related to break-up of the supercontinent; 5) continental craton margin sedimentary sequences and 6) the 1.93–1.91 Ga Svecofennian primitive island arc sediments and volcanism. The old zircons are met widely, even in the most mature parts of the island arc, which is not expected in mature arcs initiated in the oceanic environment. In the tectonic model presented in this paper, the early sediments were formed from very variable sources and they were already mixed with volcanic sequences during the earliest collisional stages of the Svecofennian orogen. The continuing evolution that turned to transpressional collision that caused strong magmatism and remelting of the early associations, including the very heterogeneous set of the old minerals like zircons. This suggests that the evolution of the mature Svecofennian island arc and following collapse (E_2) occurred close to the Archaean continent, and no hidden microcontinents are needed to explain the pre-Svecofennian detrital zircons or crustal components.

After the early stages of the Svecofennian collision, E_{1-3} , the formation of tectonic block structures characterizes the orogeny. The main deformation migrated towards the south and southwest during diachronic transpression, which caused the movement of crustal blocks towards the north and east with accompanying rotation of the blocks. This deformation predominantly occurred in the newly-

formed continental crust. The deformation pattern is very similar to that in the continental crust formed by the extrusion/escape tectonics in the Himalayas (Tapponier et al. 1982). The escape tectonics model explains the regional patterns of extensional, contractional and strike-slip terranes formed in the continent-continent collision of the Indian plate against the Asian continent. According to Jacobs and Thomas (2004), a lateral escape tectonics model explains the tectonic movements of crustal blocks in the southern Neo-Proterozoic-early-Proterozoic Antarctic orogen. In the Svecofennian collision such an indenter described from the Himalayas, the Indian plate, is not known, and the main indenter for the long-lasting transpression remains open. A possible

interpretation is that the main indenter causing the Svecofennian transpressional structures has been somewhere in the south-southeast, but at present is hidden (removed?) due to the SE-NW-trending Tornquist zone (cf. Shomali et al. 2006) bordering the Fennoscandian Shield in the southwest. This type of escape tectonics model explains the present co-existence of different crustal blocks close to each other in the present-day tectonic constitution. Thus, the model of several orogens between microcontinents (e.g. Lahtinen et al. 2005) can be explained by one continued oblique Svecofennian orogen. A simplified escape tectonics model for the oblique collisional Svecofennian orogeny in Finland is presented in Figure 53b.



CONCLUDING REMARKS

A new model of Svecofennian tectonic evolution in southern Finland is presented, and some suggestions for the wider context of this model are also given. The model is based on observations of structural successions in the field and on regional correlations of structures described in previous studies. The successions were dated using structurally-fixed samples by SIMS and TIMS methods and by correlations with published age data. The data were collected in several projects of the Geological Survey of Finland in the Helsinki region and in the Pori area. The main conclusions and suggestions for the forthcoming studies and applied research are summarized as follows:

Results of the study:

1. Svecofennian structural evolution at 1.9–1.8 Ga in southern Finland was complex, showing successive major structures of the D_A – D_1 deformations, and the evolution was divided into major geotectonic Events 1–5 (E_{1-5}).
2. E_1 was the early Svecofennian c. N-S collisional event in the island arc and against the Archaean continent. E_2 is related to the collapse of the island arc. E_3 represents continuing N-S collision; during E_{1-3} a new continental crust was formed.

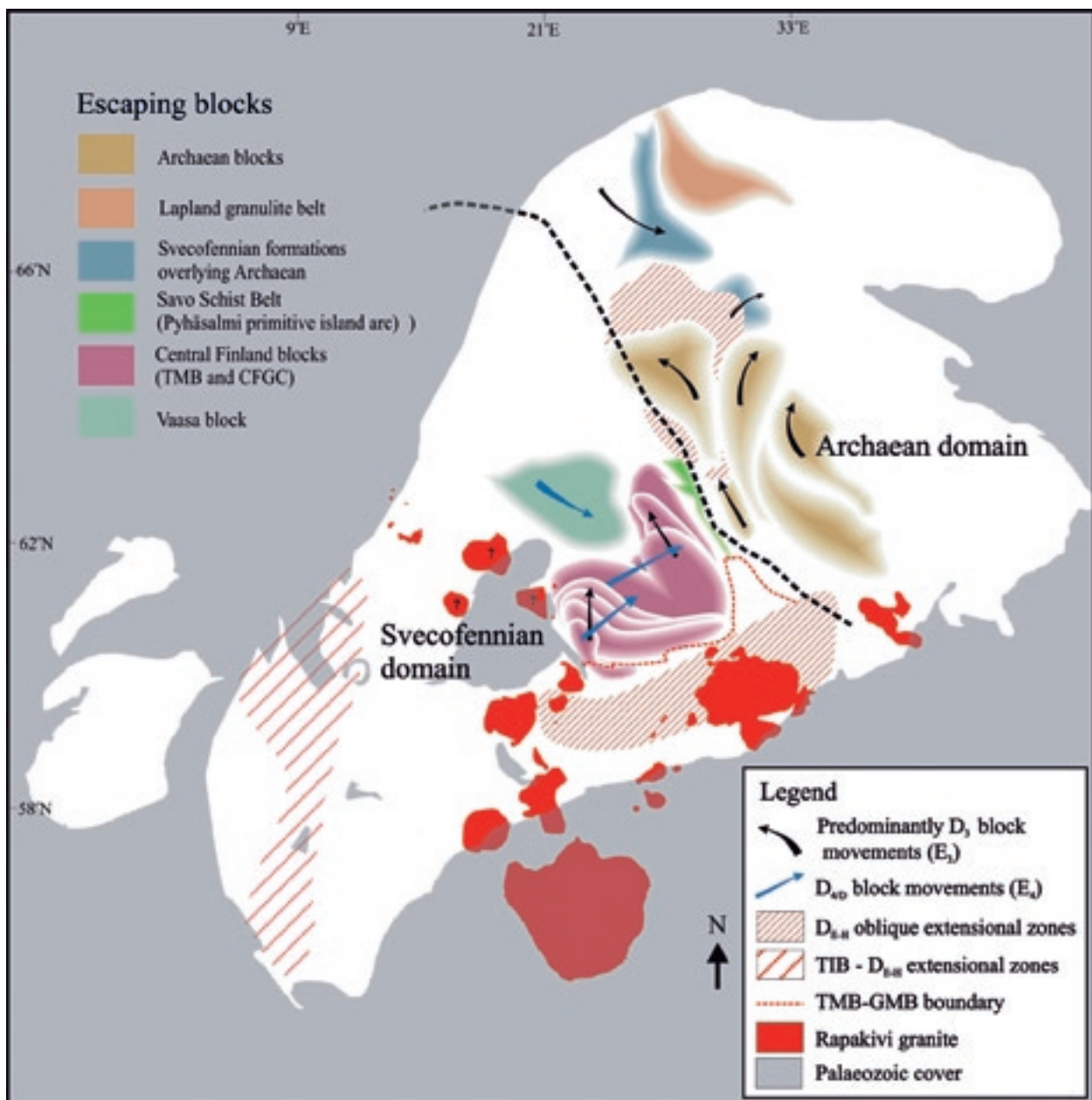


Figure 53. (b.) The escape tectonics model of the Svecofennian orogeny. The major extensional, contractional terranes and movements and rotations of the blocks are indicated. Base map © National Land Survey of Finland, permit No. 13/MML/08.

- E_4 includes a complex SW-NE transpressional evolution, showing local variations of the stress directions, in the E_{1-3} -generated continental crust, resulting in strong fragmentation and rotation of crustal blocks. The transpressional Southern Finland Granitoid Zone and pull-apart basins were developed. E_5 post-dates the main Southern Finland Granitoid Zone evolution and led to fading of the Svecofennian evolution in Southern Finland.
3. The tectonic evolution was diachronic, becoming younger towards the south and southwest; structural succession in the north occurred c. 10 Ma earlier than in the south.
 4. The Svecofennian orogeny represents one oblique collision of the growing and active Svecofennian island arc complex against the Archaean continent. The new continental crust, formed during the early evolution E_{1-3} , was followed by a complex transpressional E_4 characterized by escape tectonics. A complex pattern of contractional, transcurrent fault and extensional terranes developed. The transpressional evolution of the Svecofennian orogeny took c. 70 Ma and, in the present tectonic constitution, the kinematically different terranes form a complex structure of rotated and migrated crustal blocks.
 5. The thick crust in eastern Finland is a result of continuous collision that partly prevented thinning. The area did not undergo the E_2 collapse, such as thinning the crust in the Svecofennian domain. Instead, it was at that time under contractional and transpressional thickening. This tectonic pattern supports the idea of southwards subduction in which the Svecofennian island arc complex formed.
 6. The mature portions of the Svecofennian island arc formed close to the Archaean continent, and mixing of early sediments and volcanic sequences of Series I occurred during the earliest collisional stage E_1 . Remelting and mixing of the early components was extensive during the later evolution E_{2-4} . The later volcanism of Series II is related to the collapse stage E_2 of the arc.
 7. The pre-existing structures in the Archaean crust, such as the inclined shoreline with respect to the colliding arc or early zones of weakness in the Archaean crust, controlled the tectonic pattern formed by the escape tectonics, especially close to the Archaean border zone. The primary suture zone is fragmented into pieces and exhibits at present, if preserved at all, on the southern edges of the N-S-trending Archaean blocks. In the present constitution the Archaean-Svecofennian border is predominantly tectonic in character.
 8. The Southern Finland Granitoid Zone had a long evolution during E_4 . The evolution of the Central Lapland granitoid complex was corresponding but occurred in Archaean crust. The granitoid terranes represent the major extensional zones determined by the E_4 SW-NE transpressional escape tectonics model. The Baltic Sea-Bothnian Bay Zone, Transscandinavian Igneous Belt and Riga Bay-Karelia Zone represent the contractional transcurrent zones, and the areas between the extensional and transcurrent terranes are characterized by strike-slip tectonics and block structures, like large areas in Central Finland. According to our interpretation, the Baltic Sea-Bothnian Bay Zone stabilized earlier than the Transscandinavian Igneous Belt. The E_4 movements were less significant in the Riga Bay-Karelia Zone. Recent constitution of these terranes suggests that the major transcurrent zone was migrating toward west during E_4 . This is the reason for the wider occurrence of E_4 magmatism in the west than in the east.
 9. The high-T/low-p metamorphism in the Svecofennian domain is predominantly related to extensional stages of the orogeny, especially during the E_2 collapse and E_4 oblique extensional events.
 10. Even though the Svecofennian orogeny shows a continuing character with magmatic and metamorphic events covering the whole time frame, there are several tectono-thermal discordances of a more local character. This is why some tectonic units show earlier stabilization than their neighbouring ones. The Southern Finland Granitoid Zone and the northern terranes, e.g. the Tonalitic Migmatite Belt, provide examples. There are also more local discordances, as described from the study area. These differently-stabilized units show different later histories, which is important when comparing the evolution of the later semi-brittle to brittle structures in them. In the areas showing late Svecofennian high-T evolution the brittle evolution started in places c. 70 Ma later than in the earlier stabilized units.

11. Post-Svecofennian structures are effectively controlled by the Svecofennian orogeny. For example, the channelling and emplacement of the rapakivi intrusions in the study area show significant relations to the mid-late Svecofennian structures. Reactivation of the Svecofennian shear zones during the late Svecofennian or post-Svecofennian brittle regime was important. The present setting of the rapakivi occurrence is strongly controlled by the major N-S-trending transpressional transcurrent zones.

Further suggestions and remarks:

12. The presented tectonic model set a new basic for tectonic characterization of the Svecofennian domain.
13. The complex model of collision and escape tectonics has to be taken in to account when examining the plate tectonic constructions. Rotation and transport of the crustal blocks should be considered when interpreting, for example, the paleomagnetic orientations for continental constructions.
14. The evolution model presented here gives new possibilities to consider the genesis of ores and especially their later remobilization. There are examples of the remobilization and formation of new ore constituents during the mid-late Svecofennian evolution. Semi-brittle to brittle evolutionary stages also vary in time and kinematics in different geotectonic units. This variation should be taken in to account when prospecting and studying the mineralizations related to tectonic processes.
15. This study is part of a larger programme of research organized by the Geological Survey of Finland that is attempting to acquire basic geological information for helping and advising societies in their various activities, for example, such as construction, planning, ground water prospecting and nature protecting. This work concentrates on the ductile stages of crustal evolution and attempts to set the framework for identifying tectonic terranes showing different histories. The most important structures for various applications developed during the semi-

brittle to brittle stages of crustal evolution. As noted above, the occurrence brittle stages varies in time and place due to the complexity of the Svecofennian orogeny and due to the different timing of discordances during the orogeny. Therefore, the brittle structures, such as faulting and jointing patterns, should be analyzed with these variations in minds.

16. Several problems remained unsolved or need further research. For example:

- a. The earliest stages of the Svecofennian collision E_1 vary from place to place. For example, note the differences between D_{1-2} in the Archaean domain and D_A in southernmost part of the Svecofennian domain. The oblique collision suggests a complex process with transpressional structures even during the earliest stages, but no information is currently available. Whether early local contractional zones, e.g. early subduction zones, or extensional zones were related to E_1 remains open with the pre-existing data. Such early oblique tectonics could explain the complex variations in the characters of the earliest supracrustal sequences.
- b. The direction of the southwards-migrating E_2 collapse zone is not known with certainty. The occurrence of mafic magmatism related to it, like that of Hyvinkää, supposes a c. ESE-trending zone. Further study is also needed to establish the ages of this mafic magmatism in the southernmost part of the Svecofennian domain.
- c. There are no ages for the microtonalite phase related to the early E_4 in the southern Svecofennian domain, and the relationship between late migmatization and magmatism during the late E_4 needs further establishment. Kinematic observations on the spot-like oblique extension during the D_H are based on rather limited data so far. The tectonic setting of so-called post-orogenic granites has not entirely been studied.
- d. The connections between volcanism in the E_4 pull-apart basins and the contemporaneous magmatism needs further establishment.

17. Studies on relationships between the brittle structures, faults and joints, with respect to the structures controlled by the Svecofennian orogeny are presently taking their first steps in Finland and require a considerable input in the near future.

ACKNOWLEDGEMENTS

This study is compilation of several projects of the Geological Survey of Finland; the results were mainly produced in the project “Construction potential modelling of bedrock in urban areas” carried out in 1999–2002 in the Helsinki area. We thank the Technological Agencies of Finland (TEKES), Helsinki, Espoo and Vantaa cities and the private companies Viatek Ltd and Rockplan Ltd for their financial support in this project.

Kalevi Korsman and Tapio Koistinen have been very keen on the developments of this research, and have helped us during the work in many different ways. They both read the early version of the manuscript and suggested several important aspects to touch on more carefully. We are grateful to them for their kind and supporting help. Our great thanks to Nicklas Nordbäck, who helped us in detailed and regional mapping. Matti Karhunen, Leena Järvinen and Marita Niemelä are thanked for rock crushing, mineral separation and laboratory assistance, and Andrej Wennström and Jouko Pääkkönen for preparing the thin sections.

We want to thank the official reviewers of the early version of the paper, Carl Ehlers and Karin Högdahl, for their suggestions for major revisions to improve the paper. Kerstin Saalman reviewed this late version of the manuscript, which includes a lot of new data, and suggested several corrections; we thank her for her great help. This paper is a Nordsims publication # 206. The ion microprobe facility in Stockholm (Nordsims) is operated under an agreement between the joint Nordic research councils (NOS-N), the Geological Survey of Finland and the Swedish Museum of Natural History. The personnel of the NORDSIM laboratory, Martin Whitehouse, Lev Ilyinsky and Bodil Kajrup, are thanked.

Our greatest thanks to Roy Siddall for checking the English of the manuscript.

We are also grateful to many persons not named for their help during this process and hope that this co-operation will continue in the future during the more demanding stages of the forthcoming research work.

REFERENCES

- Airo, M.-L. 1999.** Aeromagnetic and petrophysical investigations applied to tectonic analysis in the northern Fennoscandian Shield. Geological Survey of Finland, Report of Investigation 145. 51 p.
- Airo, M.-L., Elminen, T., Mertanen, S., Niemelä, R., Pajunen, M., Wasenius, P. & Wennerström, M. 2008.** Aero-geophysical approach to ductile and brittle structures in the densely populated urban Helsinki area, southern Finland. In: Pajunen, M. (ed.) Tectonic evolution of the Svecofennian crust in southern Finland – a basis for characterizing bedrock technical properties. Geological Survey of Finland, Special Paper 47, 283–308.
- Alviola, R., Mänttari, I., Mäkitie, H. & Vaasjoki, M. 2001.** Svecofennian rare-element granitic pegmatites of the Ostrobothnia region, western Finland: their metamorphic environment and time of intrusion. In: Mäkitie, H. (ed.) Svecofennian granitic pegmatites (1.86–1.79 Ga) and quartz monzonite (1.87 Ga), and their metamorphic environment in the Seinäjoki region, western Finland. Geological Survey of Finland, Special Paper 30, 9–29.
- Bergman, S., Sjöström, H. & Högdahl, K. 2006.** Transpressive shear related to arc magmatism: The Paleoproterozoic Storsjön-Edsbyn Deformation Zone central Sweden. *Tectonics* 25, 1–16.
- Bleeker, W. & Westra, L. 1987.** The evolution of Mustio gneiss dome, Svecofennides of SW Finland. *Precambrian Research* 36, 227–240.
- Brun, J. P., Gapais, D. & Le Theoff, B. 1981.** The mantled gneiss domes of Kuopio (Finland): interfering diabirs. *Tectonophysics* 74, 283–304.
- Edelman, N. & Jaanus-Järkkälä, M. 1983.** A plate tectonic interpretation of the Precambrian of the Archipelago of southwestern Finland. Geological Survey of Finland, Bulletin 325. 33 p.
- Ehlers, C. & Lindroos, A. 1990.** Early Proterozoic Svecofennian volcanism and associated plutonism in Enklinge, SW Finland. *Precambrian Research* 47, 307–318.
- Ehlers, C., Lindroos, A. & Selonen, O. 1993.** The late Svecofennian granite-migmatite zone of southern Finland – a belt of transpressive deformation and granite emplacement. *Precambrian Research* 64, 295–309.
- Ekdahl, E. 1993.** Early Proterozoic Karelian and Svecofennian formations and the evolution of the Raahe-Ladoga ore zone, based on the Pielavesi area, Central Finland. Geological Survey of Finland, Bulletin 373. 137 p.
- Elminen, T., Airo, M.-L., Niemelä, R., Pajunen, M., Vaarma, M., Wasenius, P. & Wennerström, M. 2008.** Fault structures in the Helsinki Area, southern Finland. In: Pajunen, M. (ed.) Tectonic evolution of the Svecofennian crust in southern Finland – a basis for characterizing bedrock technical properties. Geological Survey of Finland, Special Paper 47, 185–213.

- Elo, S., Pirttijärvi, M. & Eskelinen, J. 2007.** “Maan-kuoren anomaalisten massojen vaikutus kallioperän yläosan jännitystilaan Suomessa”. In: Kaila, K. & Korja, T. (eds.) XXIII Geofysiikan Päivät, Oulu, 23.–24.05.2007. Oulu: Geofysiikan Seura, 35–39. (in Finnish)
- Eskola, P. 1914.** On the petrology of the Orijärvi region in southwestern Finland. *Bulletin de la Commission Géologique de Finlande* 40. 277 p.
- Eskola, P. 1915.** Om sambandet mellan kemisk och mineralogisk sammansättning hos Orijärvi traktens metamorfa bergarter. Summary of the contents: On the Relations between the Chemical and Mineralogical Composition in the Metamorphic Rocks of the Orijärvi Region. *Bulletin de la Commission Géologique de Finlande* 44, 1–107. Summary, 109–145.
- Eskola, P. 1949.** The problem of mantled gneiss domes. *J. Geol. London* 104, 461–476.
- Eskola, P. 1954.** Ein Lamprophyrgang in Helsinki und die Lamprophyrprobleme. *Tschermak's Mineralogische und Petrographische Mitteilungen* 3, 4, 1–4, 329–337.
- Gaál, G. & Gorbatschew, R. 1987.** An outline of the Precambrian evolution of the Baltic Shield. *Precambrian Research* 35, 15–52.
- Grad, M. & Luosto, U. 1992.** Fracturing of the crystalline uppermost crust beneath the SVEKA profile in Central Finland. *Geophysica* 28, 53–66.
- Haapala, I., Rämö, T. & Frindt, S. 2005.** Comparison of Proterozoic and Phanerozoic rift-related basaltic-granitic magmatism. *Lithos* 80, 1–32.
- Hakkarainen, G. 1994.** Geology and geochemistry of the Hämeenlinna-Somero Volcanic Belt, southwestern Finland: a Paleoproterozoic island arc. In: Nironen, M. & Kähkönen, Y. (eds.) *Geochemistry of Proterozoic supracrustal rocks in Finland*. IGCP Project 179 Stratigraphic methods as applied to the Proterozoic record and IGCP Project 217 Proterozoic geochemistry. Geological Survey of Finland, Special Paper 19, 85–100.
- Härme, M. 1953.** Karkkila. Geological Map of Finland 1:100 000, Pre-Quaternary Rocks, Sheet 2042. Geological Survey of Finland.
- Härme, M. 1965.** On the potassium migmatites of South Finland. *Bulletin de la Commission Géologique de Finlande* 219. 43 p.
- Härme, M. 1969.** Kerava. Geological Map of Finland 1:100 000, Pre-Quaternary Rocks, Sheet 2043. Geological Survey of Finland.
- Härme, M. 1978.** Pre-Quaternary Rocks of the Kerava and Riihimäki Map-Sheet area. Geological Map of Finland 1:100 000, Explanation to the Maps of Pre-Quaternary Rocks, Sheets 2043 and 2044. *Geologinen tutkimuslaitos*. 51 p. (in Finnish with English summary).
- Heeremans, M. 1997.** Silicic magmatism and continental lithosphere thinning; Inferences from field studies and numerical modelling of the Oslo Graben and the anorogenic crustal evolution of southern Finland. Publication no. 970122. Netherlands Research School of Sedimentary Geology. 197 p.
- Hietanen, A. 1975.** Generation of potassium-poor magmas in the northern Sierra Nevada and the Svecofennian of Finland. *J. Res. U.S. Geol. Surv.* 3, 631–645.
- Högdahl, K., Andersson, U. & Eklund, O. (eds.) 2004.** The Transscandinavian Igneous Belt (TIB) in Sweden: a review of its character and evolution. Geological Survey of Finland, Special Paper 37. 125 p.
- Holdsworth, R. E., Strachan, R. A. & Dewey, J. F. (eds.) 1998.** Continental transpressional and transtensional tectonics. London: Geological Society, Special Publications 135. 360 p.
- Hölttä, P. 1988.** Metamorphic zones and the evolution of granulite grade metamorphism in the early Proterozoic Pielavesi area, central Finland. Geological Survey of Finland, Bulletin 344. 50 p.
- Hölttä, P. & Pajunen, M. 1988.** The Pielavesi-Kiuruvesi area. In: Pajunen, M. (ed.) Project No. 235 “Metamorphism and geodynamics” excursion in Finland 15.6.–19.6.1988. Geological Survey of Finland, Guide 21, 13–18.
- Hölttä, P., Lahti, S. & Pajunen, M. 1988.** The Vaaraslahti pyroxene granitoid intrusion. In: Pajunen, M. (ed.) Project No. 235 “Metamorphism and geodynamics” excursion in Finland 15.6.–19.6.1988. Geological Survey of Finland, Guide 21, 19–22.
- Hölttä, P., Huhma, H., Mänttari, I. & Paavola, J. 2000.** P-T-t development of Archaean granulites in Varpaisjärvi, central Finland. II. Dating of high-grade metamorphism with the U-Pb and Sm-Nd methods. *Lithos* 50 (1–3), 121–136.
- Hopgood, A. M. 1980.** Polyphase fold analysis of gneisses and migmatites. *Transactions of the Royal Society of Edinburgh: Earth Sciences* 71, 55–68.
- Hopgood, A. M. 1984.** Structural evolution of Svecokarelian migmatites, southern Finland: a study of Proterozoic crustal development. *Transactions of the Royal Society of Edinburgh: Earth Sciences* 74, 229–264.
- Hopgood, A. M. 1999.** Determination of structural successions in migmatites and gneisses. Dordrecht: Kluwer Academic. 346 p.
- Hopgood, A. M., Bowes, D. R. & Addison, J. 1976.** Structural development of migmatites near Skäldö, southwest Finland. *Geologische Rundschau* 67, 313–330.
- Hopgood, A., Bowes, D., Kouvo, O. & Halliday, A. 1983.** U-Pb and Rb-Sr isotopic study of polyphase deformed migmatites in the Svecokareliides, southern Finland. In: Atherton, M. & Gribble, C. (eds.) *Migmatites, melting and metamorphism*. Nantwich: Shiva, 80–92.
- Huhma, A. 1981.** Youngest Precambrian dyke rocks in North Karelia, East Finland. *Bulletin of the Geological Society of Finland* 53, 67–82.
- Huhma, H. 1986.** Sm-Nd, U-Pb and Pb-Pb isotopic evidence for the origin of the Early Proterozoic Svecokarelian crust in Finland. Geological Survey of Finland, Bulletin 337. 48 p.
- Huhma, H., Claesson, S., Kinny, P. D. & Williams, I. S. 1991.** The growth of Early Proterozoic crust: new evidence from Svecofennian detrital zircons. *Terra Nova* 3 (2), 175–178.

- Jacobs, J. & Thomas, R. J. 2004.** Himalayan-type indenter-escape tectonics model for the southern part of the late Neoproterozoic-early Proterozoic East-African-Antarctic orogen. *Geology* 32 (8), 721–724.
- Kähkönen, Y. 1987.** Geochemistry and tectonomagmatic affinities of the metavolcanic rocks of the early Proterozoic Tampere schist belt, southern Finland. *Precambrian Research* 35, 295–311.
- Kähkönen, Y. 1989.** Geochemistry and petrology of the metavolcanic rocks of the early Proterozoic Tampere Schist Belt, southern Finland. *Geological Survey of Finland, Bulletin* 345. 107 p.
- Kähkönen, Y., Huhma, H. & Aro, K. 1989.** U-Pb zircon ages and Rb-Sr whole rock isotope studies of Early Proterozoic volcanic and plutonic rocks near Tampere, southern Finland. *Precambrian Research* 45, 27–43.
- Kaitaro, S. 1956.** Riihimäki. Geological Map of Finland 1:100 000, Pre-Quaternary Rocks, Sheet 2044. Geological Survey of Finland.
- Kärki, A. 1995.** Palaeoproterozoic shear Tectonics in the Central Fennoscandian Shield, Finland. Department of Geosciences and Astronomy, University of Oulu, Res. Terrae Ser. A vol 10.
- Kearey, P. & Vine, F. J. 1996.** Global tectonics. London: Blackwell Science Ltd. 333 p.
- Kilpeläinen, T. 1988.** Evolution of deformation and metamorphism as a function of time in the Rantasalmi-Sulkava area, southeastern Finland. In: Korsman, K. (ed.) *Tectono-metamorphic evolution of the Raaheladoga zone*. Geological Survey of Finland. *Bulletin* 343, 77–87.
- Kilpeläinen, T. 1998.** Evolution and 3D modelling of structural and metamorphic patterns of the Palaeoproterozoic crust in the Tampere-Vammala area, southern Finland. *Geological Survey of Finland, Bulletin* 397. 124 p.
- Kilpeläinen, T. 2007.** Elämänjärven hiertovyöhyke – loiva-asetoinen makrorakenne Keski-Suomen graniitidikompleksin ja Savon vyöhykkeen rajalla. *Geologi* 59, 35–38.
- Kilpeläinen, T. & Rastas, J. 1990.** Etelä-Suomen lehtiittijakson tektonis-metamorfisesta kehityksestä. University of Turku, Institute of Geology and Mineralogy, Publication No 21. 37 p. (in Finnish).
- Kohonen, J., Pihlaja, P., Kujala, H. & Marmo, J. 1993.** Sedimentation of the Jotnian Satakunta sandstone, western Finland. *Geological Survey of Finland, Bulletin*, 369. 24 p.
- Koistinen, T. 1981.** Structural evolution of an early Proterozoic stratabound Cu-Co-Zn deposit, Outokumpu, Finland. *Transactions of the Royal Society of Edinburgh: Earth Sciences* 72, 115–158.
- Koistinen, T. 1992.** Lyhyt kuvaus Tammissaaren karttalueen kallioperästä. Suomen geologinen kartta 1:100 000, tilapäiskarttojen selitykset lehti 214. Geological Survey of Finland. 47 p. (in Finnish).
- Koistinen, T., Klein, V., Koppelmaa, H., Korsman, K., Lahtinen, R., Nironen, M., Puura, V., Saltykova, T., Tikhomirov, S. & Yanovskiy, A. 1996.** Paleoproterozoic Svecofennian orogenic belt in the surroundings of the Gulf of Finland. In: Koistinen, T. J. (ed.) *Explanation to the map of Precambrian basement of the Gulf of Finland and surrounding area 1:1 million*. Geological Survey of Finland, Special Paper 21, 21–57.
- Koistinen, T., Stephens, M. B., Bogatchev, V., Nordgulen, Ø., Wennerström, M. & Korhonen, J. (comp.) 2001.** Geological map of the Fennoscandian Shield, scale 1:2 000 000. Geological Survey of Finland, Special Maps 48.
- Kontinen, A. 1987.** An early Proterozoic ophiolite – the Jormua mafic-ultramafic complex, north-eastern Finland. *Precambrian Research* 35, 313–341.
- Kontinen, A., Paavola, J. & Lukkarinen, H. 1992.** K-Ar ages of hornblende and biotite from Late Archaean rocks of eastern Finland – interpretation and discussion of tectonic implications. *Geological Survey of Finland, Bulletin* 365. 31 p.
- Korhonen, J. V., Aaro, S., All, T., Nevanlinna, H., Skilbrei, J. R., Säävuori, H., Vaher, R., Zhdanova, L. & Koistinen, T. (comp.) 2002a.** Magnetic anomaly map of the Fennoscandian Shield: DGRF–65 anomaly of total field. Anomaly continued upwards to 500 m above ground: scale 1:2 000 000. Geological Survey of Finland, Special Maps 54.
- Korhonen, J. V., Aaro, S., All, T., Elo, S., Haller, L. Å., Kääriäinen, J., Kulinich, A., Skilbrei, J. R., Solheim, D., Säävuori, H., Vaher, R., Zhdanova, L. & Koistinen, T. (comp.) 2002b.** Bouguer anomaly map of the Fennoscandian Shield: IGSN 71 gravity system, GRS80 normal gravity formula. Bouguer density 2670 kg/m³, terrain correction applied. Anomaly continued upwards to 500 m above ground: scale 1:2 000 000. Geological Survey of Finland, Special Maps 53.
- Korja, A., Korja, T., Luosto, U. & Heikkinen, P. 1993.** Seismic and geoelectric evidence for collisional and extensional events in the Fennoscandian Shield – implications for Precambrian crustal evolution. *Tectonophysics* 219, 129–152.
- Korja, A. & Heikkinen, P. 1995.** Proterozoic extensional tectonics of central Fennoscandian Shield: results from the Baltic and Bothnian echoes from the Lithosphere experiment. *Tectonics* 14, 504–517.
- Korja, A. & Heikkinen, P. 2005.** The accretionary orogen – insight from BABEL profiles. *Precambrian Research* 136, 241–268.
- Korja, T. 1990.** Electrical conductivity of the lithosphere. Magnetotelluric studies in the Fennoscandian Shield, Finland. *Acta Univ. Oulu*, v. A215. 55 p.
- Korsman, K. 1977.** Progressive metamorphism of the metapelites in the Rantasalmi-Sulkava area, southeastern Finland. *Geological Survey of Finland, Bulletin* 290. 82 p.
- Korsman, K., Hölttä, P., Hautala, T. & Wasenius, P. 1984.** Metamorphism as an indicator of evolution and structure of the crust in Eastern Finland. *Geological Survey of Finland, Bulletin* 328. 40 p.
- Korsman, K. & Kilpeläinen, T. 1986.** Relationship between zonal metamorphism and deformation in the Rantasalmi-Sulkava area, southeastern Finland. In: Korsman, K. (ed.) *Development of deformation,*

- metamorphism and metamorphic blocks in eastern and southern Finland. Geological Survey of Finland, Bulletin 339, 33–42.
- Korsman, K., Niemelä, R. & Wasenius, P. 1988.** Multi-stage evolution of the Proterozoic crust in the Savo schist belt, Eastern Finland. Geological Survey of Finland, Bulletin 343, 89–96.
- Korsman, K., Koistinen, T., Kohonen, J., Wennerström, M., Ekdahl, E., Honkamo, M., Idman, H. & Pekkala, Y. (eds.) 1997.** Bedrock map of Finland 1:1 000 000. Geological Survey of Finland, Special Maps 37.
- Korsman, K., Korja, T., Pajunen, M. & Virransalo, P. 1999.** The GGT/SVEKA transect: structure and evolution of the continental crust in the Paleoproterozoic Svecofennian orogen in Finland. *International Geology Review* 41, 287–333.
- Korsman, K. & Lestinen, P. (eds.) 2002.** Raahe-Laatoka – symposio. Kuopio 20.–21.3.2001. Laajat abstraktit. Geological Survey of Finland, unpublished report K 21.42/2002/1. 121 p. (in Finnish)
- Kosunen, P. 2004.** Petrogenesis of mid-Proterozoic A-type granites: Case studies from Fennoscandia (Finland) and Laurentia (New Mexico). PhD thesis, University of Helsinki, Department of Geology. 21 p.
- Kousa, J., Marttila, E. & Vaasjoki, M. 1994.** Petrology, geochemistry and dating of Paleoproterozoic metavolcanic rocks in the Pyhäjärvi area, central Finland. In: Nironen, M. & Kähkönen, Y. (eds.) *Geochemistry of Proterozoic supracrustal rocks in Finland*. IGCP Project 179 Stratigraphic methods as applied to the Proterozoic record and IGCP Project 217 Proterozoic geochemistry. Geological Survey of Finland, Special Paper 19, 7–27.
- Krogh, T. E. 1973.** A low-contamination method for hydrothermal decomposition of U and Pb for isotopic age determinations. *Geochimica et Cosmochimica Acta* 37, 485–494.
- Krogh, T. E. 1982.** Improved accuracy of U-Pb zircon ages by the creation of more concordant systems using an air abrasion technique. *Geochimica et Cosmochimica Acta* 46, 637–649.
- Kuivamäki, A., Vuorela, P. & Paananen, M. 1998.** Indications of postglacial and recent bedrock movements in Finland and Russian Karelia. Nuclear Waste Disposal Research, Geological Survey of Finland, Report YST-99. 92 p.
- Kukkonen, I. & Lahtinen, R. (eds.) 2006.** Finnish Reflection Experiment FIRE 2001–2005. Geological Survey of Finland, Special Paper 43, 247 p.
- Kurhila, M., Vaasjoki, M., Mänttari, I., Rämö, T. & Nironen, M. 2005.** U-Pb ages and Nd isotope characteristics of the lateorogenic, migmatizing microcline granites in southwestern Finland. *Bulletin of the Geological Society of Finland* 77 (2), 105–128.
- Lahtinen, R. 1994.** Crustal evolution of the Svecofennian and Karelian domains during 2.1–1.79 Ga, with special emphasis on the geochemistry and origin of 1.93–1.91 Ga gneissic tonalites and associated supracrustal rocks in the Rautalampi area, central Finland. Geological Survey of Finland, Bulletin 378. 128 p.
- Lahtinen, R. & Huhma, H. 1997.** Isotopic and geochemical constraints on the evolution of the 1.93–1.79 Ga Svecofennian crust and mantle in Finland. *Precambrian Research* 82, 13–34.
- Lahtinen, R., Huhma, H. & Kousa, J. 2002.** Contrasting source components of the Paleoproterozoic Svecofennian metasediments: detrital zircon U-Pb, Sm-Nd and geochemical data. *Precambrian Research* 116 (1–2), 81–109.
- Lahtinen, R., Korja, A. & Nironen, M. 2005.** Paleoproterozoic tectonic evolution. In: Lehtinen, M., Nurmi, P. A. & Rämö, O. T. (eds.) *Precambrian Geology of Finland. Key to the Evolution of the Fennoscandian Shield*. Amsterdam: Elsevier Science B.V., 481–531.
- Laitakari, I. & Simonen, A. 1962.** Lapinjärvi. Geological Map of Finland 1:100 000, Pre-Quaternary Rocks, Sheet 3022. Geological Survey of Finland.
- Laitakari, I. & Simonen, A. 1963.** Pre-Quaternary Rocks of the Lapinjärvi Map-Sheet area. Geological Map of Finland 1:100 000, Explanation to the Maps of Pre-Quaternary Rocks, Sheet 3022. Geological Survey of Finland. 48 p. (with English summary).
- Laitala, M. 1960.** Siuntio. Geological Map of Finland 1:100 000, Pre-Quaternary Rocks, Sheet 2032. Geological Survey of Finland.
- Laitala, M. 1961.** Pre-Quaternary Rocks of the Siuntio Map-Sheet area. Geological Map of Finland 1:100 000, Explanation to the Maps of Pre-Quaternary Rocks, Sheet 2032. Geological Survey of Finland. 32p. (with English summary).
- Laitala, M. 1964.** Porvoo. Geological Map of Finland 1:100 000, Pre-Quaternary Rocks, Sheet 2021. Geological Survey of Finland.
- Laitala, M. 1965.** Pellinki. Geological Map of Finland 1:100 000, Pre-Quaternary Rocks, Sheet 2012. Geological Survey of Finland.
- Laitala, M. 1967.** Helsinki. Geological Map of Finland 1:100 000, Pre-Quaternary Rocks, Sheet 2034. Geological Survey of Finland.
- Laitala, M. 1973a.** On the Precambrian bedrock and its structure in the Pelling region, South Finland. Geological Survey of Finland, Bulletin 264. 76 p.
- Laitala, M. 1973b.** Jussarö. Geological Map of Finland 1:100 000, Pre-Quaternary Rocks, Sheet 2013. Geological Survey of Finland.
- Laitala, M. 1984.** Pre-Quaternary Rocks of the Pellinki and Porvoo Map-Sheet areas. Geological Map of Finland 1:100 000, Explanation to the Maps of Pre-Quaternary Rocks, Sheets 3012 and 3021. Geological Survey of Finland. 53 p. (with English summary).
- Laitala, M. 1991.** Pre-Quaternary rocks of Helsinki Map-Sheet area. Geological Map of Finland 1:100 000, Explanation to the Maps of Pre-Quaternary Rocks, Sheet 2034. Geological Survey of Finland. 47 p. (with English summary).
- Laitala, M. 1994.** Lohja. Geological Map of Finland 1:100 000, Pre-Quaternary Rocks, Sheet 2041. Geological Survey of Finland.
- Latvalahti, U. 1979.** Cu-Zn-Pb ores in the Aijala-Orijärvi area, Southwest Finland. *Economic Geology* 75, 1035–1059.

- Lehijärvi, M. 1961.** Kärkölä. Geological Map of Finland 1:100 000, Pre-Quaternary Rocks, Sheet 2133. Geological Survey of Finland.
- Lehijärvi, M. 1964.** Lahti. Geological Map of Finland 1:100 000, Pre-Quaternary Rocks, Sheet 3111. Geological Survey of Finland.
- Lehtonen, M. I., Kujala, H., Kärkkäinen, N., Lehtonen, A., Mäkitie, H., Mänttari, I., Virransalo, P. & Vuokko, J. 2005.** Etelä-Pohjanmaan liuskealueen kallioperä. Summary: Pre-Quaternary rocks of the South Ostrobothnian Schist Belt area. Geological Survey of Finland, Report of Investigation 158. 155 p.
- Lindberg, B. & Eklund, O. 1988.** Interactions between basaltic and granitic magmas in a Svecofennian post-orogenic granitoid intrusion, Åland, southwest Finland. *Lithos*, 22, 13–23.
- Lindroos, A., Romer, R. L., Ehlers, C. & Alviola, R. 1996.** Late-orogenic Svecofennian deformation in SW Finland constrained by pegmatite emplacement ages. *Terra Nova* 8 (6), 567–574.
- Ludwig, K. R. 2001.** Isoplot/Ex rev. 2.49. A geochronological toolkit for Microsoft Excel. Berkeley Geochronology Center.
- Ludwig, K. R. 2001.** PbDat 1.21 for MS-dos: A computer program for IBM-PC Compatibles for processing raw Pb-U-Th isotope data. Version 1.07.
- Ludwig, K. R. 2003.** Isoplot/Ex 3. A geochronological toolkit for Microsoft Excel. Berkeley Geochronology Center, Special publication No. 4.
- Luosto, U., Lanne, E., Korhonen, H., Guterch, A., Grad, M., Materzok, R. & Perchuk, E. 1984.** Deep structure of the Earth's crust on the Sveka profile in central Finland. *Ann. Geophys.* 2, 559–570.
- Luosto, U., Tiira, T., Korhonen, H., Azbel, I., Burmin, V., Buyanov, A., Kosminskaya, I., Ionkis, V. & Sharov, V. 1990.** Crust and upper mantle structure along the DSS Baltic profile in SE Finland: *Gephys. Jour. Int.*, 101, 89–110.
- Mäkitie, H. & Lahti, S. I. 2001.** The fayalite-augite quartz monzonite (1.87 Ga) of Luopa, western Finland, and its contact aureole. In: Mäkitie, H. (ed.) Svecofennian granitic pegmatites (1.86–1.79 Ga) and quartz monzonite (1.87 Ga), and their metamorphic environment in the Seinäjoki region, western Finland. Geological Survey of Finland, Special Paper 30, 61–98.
- Marrett, R. & Peacock, D. C. P. 1999.** Stress and strain. *Journal of Structural Geology* 21, 1057–1063.
- Mertanen, S. 2001.** Sekudääriset remanenssit kallioperän geologisten prosessien ilmentäjänä. In: Airo, M.-L. & Mertanen, S. (eds.) XX Geofysiikan päivät Helsingissä 15.–16.5.2001. Geofysiikan Seura, Geophysical Society of Finland, 129–134. (in Finnish)
- Mertanen, S., Pajunen, M. & Elminen, T. 2001.** Applying palaeomagnetic method for dating young geological events. In: Autio, S. (ed.) Geological Survey of Finland, Special Paper 31, 123–129.
- Mertanen, S., Pajunen, M. & Elminen, T. 2004.** Multiple remagnetization events of shear zones in southern Finland. In: Mertanen, S. (ed.) Supercontinents, remagnetizations and geomagnetic modelling. 5th Nordic Paleomagnetic Workshop, Suitia-Helsinki, Finland, September 25–30, 2004, 39–44.
- Mertanen, S., Airo, M.-L., Elminen, T., Niemelä, R., Pajunen, M., Wasenius, P. & Wennerström, M. 2008.** Paleomagnetic evidence for Mesoproterozoic – Paleozoic reactivation of the Paleoproterozoic crust in southern Finland. In: Pajunen, M. (ed.) Tectonic evolution of the Svecofennian crust in southern Finland – a basis for characterizing bedrock technical properties. Geological Survey of Finland, Special Paper 47, 215–252.
- Mikkola, T. 1955.** Origin of ultrabasics in the Orijärvi region. *Extrait des Comptes Rendus de la Société géologique de Finlande* N:o XXVIII, 39–51.
- Mouri, H., Korsman, K. & Huhma, H. 1999.** Tectono-metamorphic evolution and timing of the melting processes in the Svecofennian tonalite-trondhjemite migmatite belt: An example from Luopioinen, Tampere area, southern Finland. *Bulletin of the Geological Society of Finland* 71, 31–56.
- Murphy, M. A. 2002.** Orogen-parallel extension as expressed by the development of gneiss domes: an example from the Himalaya. 2002 Denver Annual Meeting (October 27–30, 2002), Session No 50, Thermal and Mechanical Significance of Gneiss Domes in the Evolution of Orogens, Paper No. 50–4, Geological Society of America. http://gsa.confex.com/gsa/2002AM/finalprogram/abstract_42867.htm.
- Neuvonen, K. J. 1954.** Forssa. Geological Map of Finland 1:100 000, Pre-Quaternary Rocks, Sheet 2113. Geological Survey of Finland.
- Neuvonen, K. J., Korsman, K., Kouvo, O. & Paavola, J. 1981.** Paleomagnetism and age relations of the rocks in the Main Sulphide Ore Belt in central Finland. *Bulletin of the Geological Society of Finland* 53 (2), 109–133.
- Nironen, M. 1989.** Emplacement and structural setting of granitoids in the early Proterozoic Tampere and Savo Schist Belts, Finland – implications for contrasting crustal evolution. Geological Survey of Finland, *Bulletin* 346. 83 p.
- Nironen, M. 1997.** The Svecofennian Orogen: a tectonic model. *Precambrian Research* 86 (1–2), 21–44.
- Nironen, M. 1999.** Structural and magmatic evolution in the Loimaa area, southwestern Finland. *Bulletin of the Geological Society of Finland* 71, 57–71.
- Nironen, M. 2003.** Keski-Suomen granitoidikompleksi, Karttaselitys. English summary: Central Finland Garnitoid Complex – Explanation to a map. Geological Survey of Finland, Report of Investigation 157. 45 p.
- Nironen, M. & Lahtinen, R. 2006.** Late Svecofennian sedimentary-volcanic association at Pyhäntaka. *Bulletin of the Geological Society of Finland, Special Issue* 1, 109.
- Nurmi, P. & Haapala, I. 1986.** The Proterozoic granitoids of Finland; granite types, metallogeny and related crustal evolution. *Bulletin of the Geological Society of Finland* 58, 241–261.
- Pääjärvi, A. 1991.** Pre-Quaternary Rocks of the Vesanto Map-Sheet area. Geological Map of Finland 1:100 000, Explanation to the Maps of Pre-Quaternary Rocks,

- Sheet 3313. Geological Survey of Finland. 64 p. (with English summary).
- Pajunen, M. 1986.** Deformation analysis of cataclastic structures and faults in the Tervo area, central Finland. Geological Survey of Finland, Bulletin 339, 16–31.
- Pajunen, M. 1988.** Tectono-metamorphic evolution of the Hallaperä pyrrhotite-pyrite ore deposit, Central Finland. Geological Survey of Finland, Bulletin 343, 51–76.
- Pajunen, M. & Poutiainen, M. 1999.** Palaeoproterozoic prograde metasomatic-metamorphic overprint zones in Archaean tonalitic gneisses, eastern Finland. Bulletin of the Geological Society of Finland 71, 73–132.
- Pajunen, M., Airo, M.-L., Wennerström, M., Niemelä, R. & Wasenius, P. 2001a.** Preliminary report: The “Shear zone research and rock engineering” project, Pori area, south-western Finland. Geological Survey of Finland, Special Paper 31, 7–16.
- Pajunen, M., Elminen, T., Airo, M.-L. & Wennerström, M. 2001b.** Structural evolution of bedrock as a key to rock mechanical properties. In: Rock Mechanics. A Challenge for Society. Proceeding of Regional Symposium EUROCK 2001. Rotterdam: A. A. Balkema, 143–148.
- Pajunen, M., Airo, M.-L., Elminen, T., Niemelä, R., Vaarma, M., Wasenius, P. & Wennerström, M. 2002.** Kallioperän rakennettavuusmalli taajamiin. Menetelmänkehitys ja ohjeistus. Geological Survey of Finland, unpublished report K 21.42/2002/5. 95 s. (in Finnish).
- Pajunen, M., Elminen, T., Airo, M.-L. & Wennerström, M. 2004.** Structural evolution of Svecofennian crust in southern Finland. The 26th Nordic Geological Winter Meeting, January 6th–9th 2004, Uppsala Sweden. GFF 126, (1), 32–33.
- Pajunen, M., Hopgood, A., Huhma, H. & Koistinen, T. 2008.** Integrated structural succession and age constraints on a Svecofennian key outcrop in Västerviken, southern Finland. In: Pajunen, M. (ed.) Tectonic evolution of the Svecofennian crust in southern Finland – a basis for characterizing bedrock technical properties. Geological Survey of Finland, Special Paper 47, 161–184.
- Parras, K. 1958.** On the charnockites in the light of highly metamorphic rock complex in Southwestern Finland. Bulletin de la Commission Géologique de Finlande 181. 137 p.
- Patchett, P. J., Kouvo, O., Hedge, C. E. & Tatsumoto, M. 1981.** Evolution of continental crust and mantle heterogeneity: evidence from Hf isotopes. Contributions to Mineralogy and Petrology 78 (3), 279–297.
- Patchett, J. & Kouvo, O. 1986.** Origin of continental crust of 1.9–1.7 Ga age: Nd isotopes and U-Pb zircon ages in the Svecokarelian terrain of South Finland. Contributions to Mineralogy and Petrology 92 (1), 1–12.
- Pietikäinen, K. 1994.** The geology of the Paleoproterozoic Pori shear zone, southwestern Finland, with special reference to the evolution of veined gneisses from tonalitic protoliths. PhD thesis, Michigan Technological University. 130 p.
- Peltonen, P., Mänttari, I., Huhma, H. & Whitehouse, M. J. 2006.** Multi-stage origin of the lower crust of the Karelian craton from 3.5 to 1.7 Ga based on isotopic ages of kimberlite-derived mafic granulite xenoliths. Precambrian Research 147, 107–123.
- Pihlaja, P. & Kujala, H. 2005.** Kankaanpää. Geological Map of Finland 1:100 000, Pre-Quaternary Rocks, Sheet 1144. Geological Survey of Finland.
- Platt, J. P. & England, P. C. 1993.** Convective removal of lithosphere beneath mountain belts: Thermal and mechanical consequences. American Journal of Sciences 293, 307–336.
- Ploegsma, M. & Westra, L. 1990.** The Early Proterozoic Orijärvi triangle (southwest Finland): a key area of the tectonic evolution of the Svecofennides. Precambrian Research 47, 51–69.
- Puura, V., Hints, R., Huhma, H., Klein, V., Konsa, M., Kuldkepp, R., Mänttari, I. & Soesoo, A. 2004.** Svecofennian metamorphic zones in the basement of Estonia. Proceedings of the Estonian academy of Sciences 53, 3, 190–209.
- Rämö, O. T. 1991.** Petrogenesis of the Proterozoic rapakivi granites and related basic rocks of southeastern Fennoscandia: Nd and Pb isotopic and general geochemical constraints. Geological Survey of Finland, Bulletin 355. 161 p.
- Rämö, O. T., Kurhila, M., Nironen, M., Mänttari, I. & Elliot, B. A. 2004.** Nd isotope variation in the lateorogenic microcline granites and their synorogenic country rock granitoids in southern Finland. The 26th Nordic Geological Winter Meeting, January 6th–9th 2004, Uppsala, Sweden. GFF 126, (1), 34.
- Ramsay, J. G. & Huber, M. I. 1983.** The techniques of modern structural geology, volume 1: Strain Analysis. 307 p.
- Rastas, J. 1990.** Savonlinnan Pihlajaveden intruusiobreaksiasta. Pro gradu-tutkielma, Turun yliopisto. 72 p. (in Finnish).
- Reinikainen, J. 2001.** Petrogenesis of Paleoproterozoic marbles in the Svecofennian Domain, Finland. Geological Survey of Finland, Report of Investigation 154. 84 p.
- Ruotoistenmäki, T. 1996.** A schematic model of the plate tectonic evolution of Finnish bedrock. Geological Survey of Finland, Report of Investigation 133. 23 p.
- Rutland, R. W. R., Williams, I. S. & Korsman, K. 2004.** Pre-1.91 Ga deformation and metamorphism in the Paleoproterozoic Vammala Migmatite Belt, southern Finland, and implications for Svecofennian tectonics. Bulletin of the Geological Society of Finland 76, 93–140.
- Saalmann, K., Tessensohn, F., Piepjohn, K., von Gosen, W. & Mayr, U. 2005.** Structure of Palaeogene sediments in east Ellesmere Island: Constraints on Eureka tectonic evolution and implications for Nares Strait problem. Tectonophysics 406, 81–113.
- Salli, I. 1955.** Suomusjärvi. Geological Map of Finland 1:100 000, Pre-Quaternary Rocks, Sheet 2023. Geological Survey of Finland.

- Saltikoff, B., Tontti, M. & Puustinen, K. (comp.) 2002.** Metallogenic map of Finland 1:1 000 000. Geological Survey of Finland.
- Scheinin, B. & Korsman, K. 2007.** Jakob Johannes Sederholm. Geolog, humanist och sanningsökare (Jakob Johannes Sederholm. A geologist, humanist and a seeker after truth). Bidrag till kännedom av Finlands natur of folk 170. Helsinki: Finska Vetenskaps-Societen – Suomen Tiedeseura – Finnish Society of Science and Letters. 95 p.
- Schreurs, J. & Westra, L. 1986.** The thermotectonic evolution of a Proterozoic, low pressure, granulite dome, West Uusimaa, SW Finland. *Contributions to Mineralogy and Petrology* 93, 236–250.
- Sederholm, J. J. 1907.** Om granit och gneis, deras uppkomst, uppträdande och utbredning inom urberget i Fennoskandia. *Bulletin de la Commission Géologique de Finlande* 23 u. *Fennia* 26 (2). 90 p. English summary of the contents: On granite and gneiss, their origin, relations and occurrence in the pre-cambrian complex of Fenno-Scandia. 20 p.
- Sederholm, J. J. 1923.** On migmatites and associated pre-Cambrian rocks of southwestern Finland. Part 1. The Pelling region. *Bulletin de la Commission Géologique de Finlande* 58. 153 p.
- Sederholm, J. J. 1926.** On migmatites and associated pre-Cambrian rocks of southwestern Finland. II. The region around the Barösundsfjärd W. of Helsingfors and neighbouring areas. *Bulletin de la Commission Géologique de Finlande*, 77. 143 p.
- Sederholm, J. J. 1927.** Precambrian of Fennoscandia with special reference to Finland. *Bull. Geol. Soc. Amer.* vol. 38, 1927, 13–836.
- Sederholm, J. J. 1931.** On the Sub-Bothnian unconformity and on Archaean rocks formed by secular weathering. *Bulletin de la Commission Géologique de Finlande* 95, 1–79.
- Sederholm, J. J. 1932a.** On the geology of Fennoscandia with special reference to the Pre-Cambrian. Explanatory notes to accompany a General geological map of Fennoscandia. *Bulletin de la Commission Géologique de Finlande* 98. 30 p.
- Sederholm, J. J. 1932b.** Über die Bodenkonfigurationen des Päijänne-Sees. *Bulletin de la Commission Géologique de Finlande* 100. 23 p.
- Sederholm, J. J. 1967.** Selected Works; Granites and migmatites. Edinburgh-London: Oliver & Boyd. 608 p.
- Shomali, H. Z., Roberts, R. G., Pedersen, L. B. & the TOR Working Group 2006.** Lithospheric structure on the Tornquist Zone resolved by nonlinear P and S teleseismic tomography along the TOR array. *Tectonophysics* 416, 133–149.
- Simonen, A. 1949.** Hämeenlinna. Geological Map of Finland 1:100 000, Pre-Quaternary Rocks, Sheet 2131. Geological Survey of Finland.
- Simonen, A. 1955.** Somero. Geological Map of Finland 1:100 000, Pre-Quaternary Rocks, Sheet 2024. Geological Survey of Finland.
- Simonen, A. 1956.** Pre-Quaternary rocks of the Somero Map-Sheet area. Geological Map of Finland 1:100 000, Explanation to the Maps of Pre-Quaternary Rocks, Sheet 2024. Geological Survey of Finland. 31 p. (with English summary).
- Simonen, A. 1965.** Karhula. Geological Map of Finland 1:100 000, Pre-Quaternary Rocks, Sheet 3024. Geological Survey of Finland.
- Simonen, A. 1987.** Pre-Quaternary Rocks of Map-Sheet areas of the rapakivi massif in SE Finland. Geological Map of Finland 1:100 000, Explanation to the Maps of Pre-Quaternary Rocks, Sheets 3023+3014, 3024, 3041, 3042, 3044, 3113, 3131, 3133. Geological Survey of Finland. 49 p. (with English summary).
- Simonen, A. & Leijärvi, M. 1963.** Kouvola. Geological Map of Finland 1:100 000, Pre-Quaternary Rocks, Sheet 3113. Geological Survey of Finland.
- Simonen, A. & Laitala, M. 1970.** Kotka. Geological Map of Finland 1:100 000, Pre-Quaternary Rocks, Sheets 3023+3014. Geological Survey of Finland.
- Skyttä, P., Väisänen, M. & Mänttari, M. 2006.** U-Pb zircon SIMS dating of deformation in the Orijärvi area, southern Finland. *Bulletin of the Geological Society of Finland, Special Issue 1*, 184.
- Sorjonen-Ward, P. 2006.** Geological and structural framework and preliminary interpretation of the FIRE 3 and FIRE 3A reflection seismic profiles, central Finland. Geological Survey of Finland, Special Paper 43, 105–159.
- Stacey, J. S. & Kramers, J. D. 1975.** Approximation of terrestrial lead isotope evolution by a two-stage model. *Earth and Planetary Science Letters*, 26, 207–221.
- Stephansson, O., Särkkä, P. & Myrvang, A. 1986.** State of stress in Fennoscandia. *Proc. Int. Symp. on Rock Stress Measurements, Stockholm* (Stephansson, O. ed). Luleå: Centek Publishers, 21–32.
- Suominen, V. 1988.** Radiometric ages on zircons from a cogenetic gabbro and plagioclase porphyrite suite in Hyvinkää, southern Finland. *Bulletin of the Geological Society of Finland* 60 (2), 135–140.
- Suominen, V. 1991.** The chronostratigraphy of southwestern Finland with special reference to Postjotnian and Subjotnian diabases. Geological Survey of Finland, *Bulletin* 356. 100 p.
- Suominen, V. 1997.** Smectite alteration in a lamprophyre dyke; a case study. *GFF* 119, 149–150.
- Talvitie, J. 1971.** Seismotectonics of the Kuopio region, Finland. *Bulletin de la Commission Géologique de Finlande* 248. 41 p.
- Tapponier, P., Peltzer, G., Le Dain, A.Y., Armijo, R. & Cobbing, P. 1982.** Propagating extrusion tectonics in Asia: new insights from simple experiments with plasticine. *Geology* 10, 611–616.
- Torvela, T., Mänttari, I. & Hermansson, T. 2008.** Timing of deformation phases within the South Finland shear zone, SW Finland. *Precambrian Research* 160, 277–298.
- Tuisku, P. & Laajoki, K. 1990.** Metamorphic and structural evolution of the Early Proterozoic Puolankajärvi formation, Finland – II. The pressure-temperature-deformation-composition path. *J. Metamorphic Geol.* 8, 375–391.

- Tuominen, H. V. 1957.** The structure of an Archean area: Orijärvi, Finland. *Bulletin de la Commission Géologique de Finlande* 177, 1–31.
- Vaasjoki, M. 1977a.** Rapakivi granites and other post-orogenic rocks in Finland: their age and the lead isotopic composition of certain associated galena mineralizations. *Geological Survey of Finland, Bulletin* 294, 64 p.
- Vaasjoki, M. 1977b.** Phanerozoic resetting of U- Pb ages in some South-Finnish uraninites. In: *ECOG V. Fifth European Colloquium of Geochronology, Cosmochronology and Isotope Geology, Pisa, September 5.10.1977.* 2 p.
- Vaasjoki, M. 1995.** Rengon Rouvinmäen kvartsimont-sodioriitti: uusi posttektoninen granitoidi. Summary: The Rouvinmäki quartzmonzodiorite at Renko: a new posttectonic granitoid. *Geologi* 47 (6), 79–81.
- Vaasjoki, M. & Sakko, M. 1988.** The evolution of the Raahe-Ladoga zone in Finland: isotopic constraints. In: *Korsman, K. (ed.) Tectono-metamorphic evolution of the Raahe-Ladoga zone.* Geological Survey of Finland, *Bulletin* 343, 7–32.
- Väisänen, M. 2002.** Tectonic evolution of the palaeoproterozoic Svecofennian orogen in Southwestern Finland. *Annales Universitatis Turkuensis, A II*, 154, 143 p.
- Väisänen, M. & Hölttä, P. 1999.** Structural and metamorphic evolution of the Turku migmatite complex, southwestern Finland. *Bulletin of the Geological Society of Finland* 71, 177–218.
- Väisänen, M. & Mänttari, I. 2002.** 1.90–1.88 Ga back arc basin in the Orijärvi area, SW Finland. *Bulletin of the Geological Society of Finland* 74, 185–214.
- Väisänen, M., Mänttari, I. & Hölttä, P. 2002.** Svecofennian magmatic and metamorphic evolution in southern Finland as revealed by U-Pb zircon SIMS geochronology. *Precambrian Research* 116, 111–127.
- Väisänen, M., Andersson, U. B., Huhma, H. & Mouri, H. 2004.** Age of late Svecofennian regional metamorphism in southern Finland and south-central Sweden. The 26th Nordic Geological Winter Meeting, 6.–9.1.2004, Uppsala, Sweden, abstract volume. *GFF* 126, 40.
- Wegmann, C. E. 1928.** Über die Tektonik der jüngeren Faltung in Ostfinnland. *Fennia* 50, 1–22.
- Wennerström, M., Airo, M.-L., Elminen, T., Niemelä, R., Pajunen, M., Vaarma, M. & Wasenius, P. 2008.** Orientation and properties of jointing in Helsinki area, southern Finland. In: *Pajunen, M. (ed.) Tectonic evolution of the Svecofennian crust in southern Finland – a basis for characterizing bedrock technical properties.* Geological Survey of Finland, Special Paper 47, 253–282.
- Whitehouse, M. J., Claesson, S., Sunde, T. & Vestin, J. 1997.** Ion microprobe U-Pb zircon geochronology and correlation of Archaean gneisses from the Lewisian complex of Gruinard Bay, northwestern Scotland. *Geochimica et Cosmochimica Acta*, 61, 4429–4438.
- Whitehouse, M. J., Kamber, B. & Moorbath, S. 1999.** Age significance of U-Th-Pb zircon data from early Archaean rocks of west Greenland – a reassessment based on combined ion-microprobe and imaging studies. *Chemical Geology*, 160, 201–224.
- Wiedenbeck, M., Allé, P., Corfu, F., Griffin, W. L., Meier, M., Oberli, F., von Quadt, A., Roddick, J. C. & Spiegel, W. 1995.** Three natural zircon standards for U-Th-Pb, Lu-Hf, trace element and REE analysis. *Geostandards Newsletter*, 19, 1–23.
- Zhang, J., Ding, L., Zhong, D. & Zhou, Y. 2000.** Orogen-parallel extension in Himalaya: Is it the indicator of collapse or the product in process of compressive uplift? *Chinese Science Bulletin* 45, 2, 114–119.

APPENDICES

Appendix 1. Structural relationships in the Tonalite Migmatite Belt

The Tampere Schist Belt (TSB), Vammala Migmatite Belt (VMB) and Hämeenlinna Volcanic Belt (HVB) form a key area for the correlations of the early tectonic history of the Tonalite Migmatite Belt (TMB) and Granite Migmatite Belt (GMB) (Figure 9). Their tectono-metamorphic evolution has been under intense research (e.g. Korsman et al. 1984, Pietikäinen 1994, Koistinen et al. 1996, Kilpeläinen 1998, Korsman et al. 1999, Nironen 1999, Pajunen et al. 2001a and Rutland et al. 2004) since the early studies published in several papers by Sederholm (e.g. 1931).

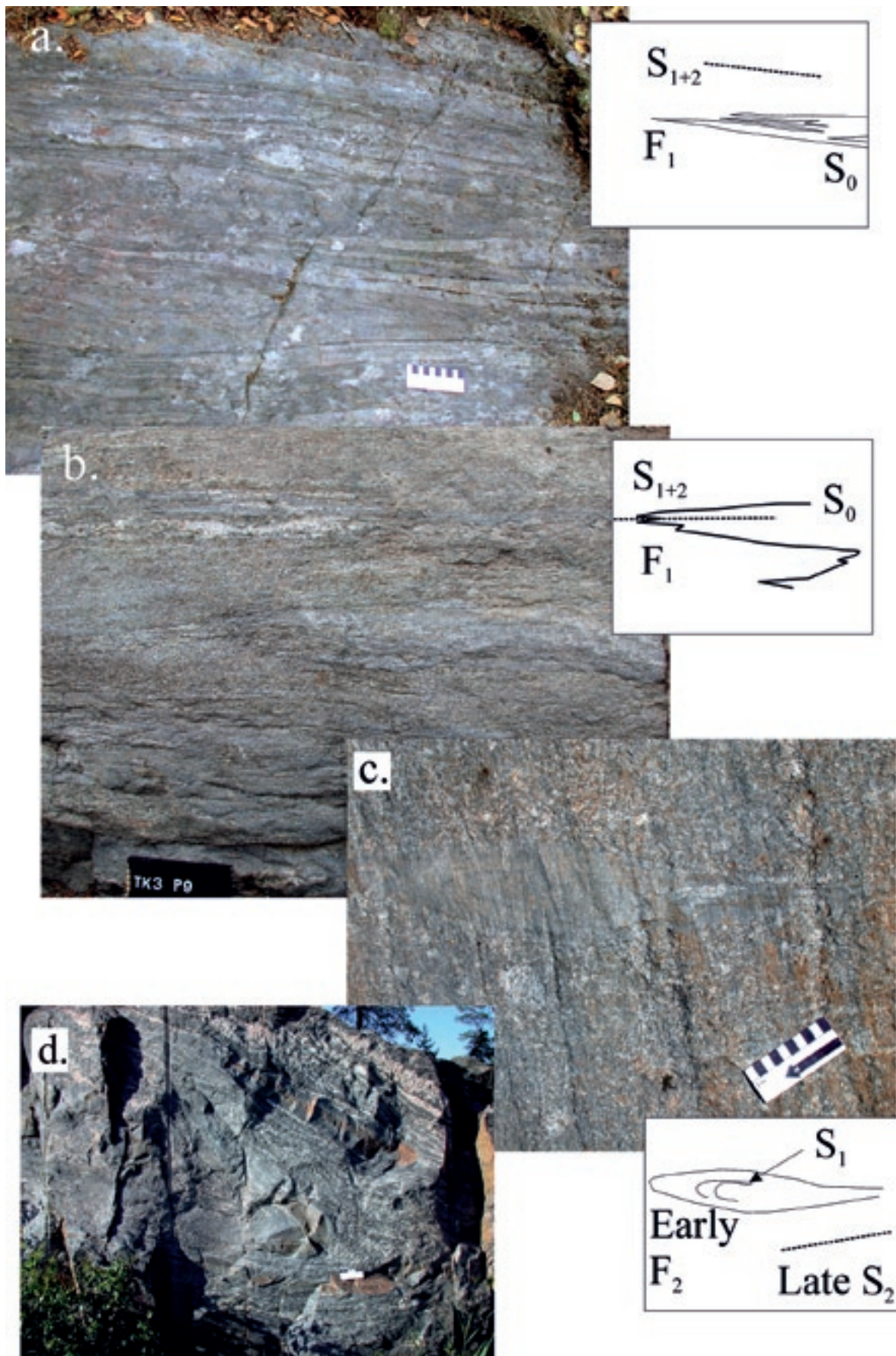
The earliest tectonic D_1 structures are identified from sedimentary and volcanic rocks. S_1 is nearly bedding-parallel, weak, penetrative foliation, and F_1 folds (Appendix-Fig. 1-1a) are strongly strained and flame-hinged (Appendix-Figs. 1-1a and b). In the strongly migmatitic areas, such as the Vammala Migmatite Belt (VMB), S_1 is preserved in competent felsic rocks; in metapelitic rocks it is represented by an internal biotite foliation in the early potassium feldspar porphyroblasts (Kilpeläinen 1998 and Nironen 1999). Corresponding F_1 folds (Appendix-Fig. 1-1b) also exist further south in the Eurajoki area to the SW of Pori, close the TMB-GMB border. According to Kilpeläinen (1998), the D_1 structures are absent in the lower-grade Tampere Schist Belt (TSB). He concluded that in the deeper part of the crust, represented by the VMB, metamorphism and deformation began earlier. Rutland et al. (2004) supposed time discordance between the TSB and VMB. The stacked northern border zone of the Granite Migmatite Belt (GMB) and the Hämeenlinna Volcanic Belt (HVB) (Figures 9 and 10) show isoclinal F_1 folding with sharp hinges in non-migmatitic andalusite-bearing metapelites (Appendix-Fig. 1-1a). Thus, the early structural succession of the HVB differs from that of the low-grade TSB. Instead, it resembles the early D_A structures (the volcanic Series I) in the detail study area, e.g. in the Southern Volcanic-Sedimentary Belt (SVB).

In the Tampere Schist Belt (TSB) the age of volcanism is c. 1.90–1.89 Ga (Kähkönen et al. 1989). The youngest age of detrital zircons in metaturbidites in the TSB is c. 1.91 Ga (Huhma et al. 1991); the metaturbidite age determines the maximum age of D_1 (Kilpeläinen 1998). This presupposes, however, that sediments of the Vammala Migmatite Belt (VMB) and Tampere Schist Belt (TSB) represent the same supra-crustal sequence.

Progressive metamorphism and partial melting of rocks, concurrently with deformation D_2 , penetratively modified the Vammala Migmatite Belt (VMB). In the turbiditic metasediments the early migmatite neosomes are trondhjemitic in composition. Strong vertical shortening is indicated by originally recumbent isoclinal to tight F_2 folds with strong mineral growth in the axial planes, S_2 , and by intense boudinage of competent layers. The S_2 was originally horizontal. Koistinen et al. (1996) described chocolate tablet boudinage of competent layers of sedimentary rocks; this suggests flattening strain. Often the deformation was strong, causing gneissic to mylonite gneissic structures and shearing/transposition along the fold limbs. In the most intensive high-strain zones, schollen migmatites developed (e.g. Pietikäinen 1994). Their boudinaged fragments contain preserved fragments of early F_2 folds indicating effective deformation during the progression of D_2 . The schollen migmatitic mica gneiss from Eurajoki, with fragments including F_2 folds (Appendix-Fig. 1-1c), is similar to those in the Pori study area. In contrast to this, such schollen migmatites do not occur in the southernmost part of the GMB. The metamorphic peak indicating high heat flow over wide areas was achieved under a rather constant pressure of c. 5 kbar (Korsman et al. 1999). Mouri et al. (1999) determined from Luopioinen in the Vammala Migmatite Belt (VMB) peak metamorphic conditions of 700–750 °C at 4–5 kbar and $a_{H_2O} = 0.4–0.7$, which was followed by decompressional cooling. Vertical flattening strain, in addition to high heat flow under rather constant pressure over wide areas (up to now no evidence or relics of progressive high-pressure assemblages have been found), indicates an extensional tectono-thermal event during D_2 . It is very similar to the D_B in the southern study area.

In the Vammala Migmatite Belt (VMB) D_3 structures, formed due to N-S shortening, deformed the originally horizontal D_{1+2} structures, the schollen migmatites included, to a more or less upright position by F_3 folding (e.g. Pietikäinen 1994, Koistinen et al. 1996, Kilpeläinen 1998, Korsman et al. 1999, Nironen 1999 and Pajunen et al. 2001a). The D_2 isotherms along with the D_3 ones form a complicated interference pattern with decreasing metamorphic grade towards the north to the Tampere Schist Belt (TSB) (Kilpeläinen 1998).

Due to the complex tectonic pattern in the Tonalite Migmatite Belt – Granite Migmatite Belt border zone described by Kilpeläinen (1998), it is difficult to bind the intrusive events to a certain deformation phase. The continuing character of magmatism (see the main text) further complicates this approach. According to



Appendix-Fig. 1-1. (a.) F_1 fold in mica schist. Scale bar is 10 cm in length. Taljala, Kalvola (Finnish grid coordinates KkJ2 2503.04E 6777.70N). (b.) F_1 fold in mica gneiss. Scale bar is 10 cm in length. Olkiluoto, Eurajoki (Finnish grid coordinates KkJ1 1525.57E 6792.75N). (c.) A fragment showing early F_2 fold (+ F_1 ?) surrounded by the late S_1 in schollen migmatitic mica gneiss. Scale bar is 10 cm in length. Olkiluoto, Eurajoki (Finnish grid coordinates KkJ1 1524.28E 6792.20N). (d.) Northwestwards-overturned folding deforms strongly-sheared migmatite foliation corresponding the S_e and F_H relationships in the detailed study area. Scale bar is 15 cm in length. Heikkilä, Eurajoki (Finnish grid coordinates KkJ1 1530.31E 6789.19N). Photos by M. Pajunen.

Nironen (1989), the weakly-deformed Hämeenkyrö D_2 tonalite intrusion in the TSB is 1885 ± 2 Ma in age, while the sphene age is 1864 ± 1 Ma; the corresponding Värmlä intrusion has an age of 1878 ± 3 Ma. The metamorphosed Järvenpää quartz diorite in the Vammala Migmatite Belt (VMB) has an age of 1881 ± 4 Ma and is D_{2+3} deformed; it was interpreted as syn- D_2 by Kilpeläinen (op. cit.). Further south, in the Granite Migmatite Belt, the syn- D_3 Pöytyä granodiorite in the Hämeenlinna Volcanic Belt (HVB) is dated at 1870 ± 12 Ma, representing the main intrusive phase, and at 1869 ± 8 Ma for a porphyritic phase (Nironen 1999). These results mean that D_3 started about 10 Ma later or it continued longer in the southern Granitic Migmatite Belt (GMB) than in the Vammala Migmatite Belt (VMB). The emplacement of the Värmlä and Pöytyä intrusions are concomitant with the syn-/late D_B tonalites in the southern Espoo Granitoid Complex (EGC). The observations from the Vammala Migmatite Belt (VMB) and Hämeenlinna Volcanic Belt (HVB) suggest their co-existence during D_2 , and suppose that D_1 was the major collisional/overthrusting phase juxtaposing the units.

Plutonic clasts in the Veittijärvi intraformational conglomerate, in Ylöjärvi in the Tampere Schist Belt (TSB), show typical synkinematic ages of 1.89–1.88 Ga (Nironen 1989). This means that the Tampere Schist Belt (TSB) underwent deformation that formed the basin for the deposition of the conglomerate and related sediments after that age. According to Kilpeläinen (op. cit.), D_2 in the VMB is c. 1.88 Ga old. The extensional D_2 evolution was able to form sedimentary basins with rapid deposition of the supracrustal sequences of the TSB. The conglomerate clasts foliated moderately during continuing subsidence and heating under D_2 extension. Extensional D_2 process explains the subsidence of the schists of TSB from the upper crustal levels next to the high-grade gneisses, the absence of D_1 from TSB schists and the progressive increase in metamorphic grade towards south from the non-migmatitic rocks of the TSB to the migmatites of the VMB (cf. Kilpeläinen 1988 and Korsman et al. 1999). Corresponding subsidence of much later sedimentary-volcanic sequences of the Jokela supracrustal association into a higher-grade environment is described in Appendix 5. The Haukivuori conglomerate with 1885 ± 6 Ma old plutonic clasts is located in the Rantasalmi-Sulkava area (RSB), which is overthrust upon the southern part of Savo Schist Belt (SSB) (Korsman et al. 1988). Korsman et al. (op. cit.) related the conglomerate to the evolution of the tectono-metamorphic discordance between the northern the SSB and southern RSB. The northern part of SSB was eroding simultaneously with a high-temperature metamorphic event in the southern unit. Thus, the overthrusting is younger than 1885 Ma; intrusion of 1836 ± 20 Ma lamprophyre dykes (Neuvonen et al. 1981) sharply cut the SSB, but they are metamorphosed in the RSB (K. Korsman pers. comm. 2006).

The young ages, e.g. the sphene age in Hämeenkyrö, indicates that the later deformations and heating effectively acted as far north as the Tampere Schist Belt (TSB). The ages are compatible with ages of the D_E thermal evolution in the study area, e.g. in the Espoo Granitoid Complex (EGC) and West Uusimaa granulite Complex (WUC). The late structures, such as shearing and fragmentation of the early D_B neosome, in migmatitic mica gneiss from Eurajoki (Appendix-Fig. 1-1d) are similar to the D_E - D_H structures in the detailed study area. This suggests that D_E and D_H deformations occurred quite similarly in southwestern Finland (Eurajoki). The wide-scale F_1 folding (Figure 11) bends the Granite Migmatite Belt (GMB) towards the north in southwestern Finland and in the southwestern archipelago (Figure 9).

Appendix 2. West Uusimaa granulite Complex characteristics

The traditional granulite-facies West Uusimaa granulite Complex (WUC) (Eskola 1914, 1915, Tuominen 1957 and Parras 1958) forms a complex structure exposed between amphibolite-facies units and granitoid complexes. Väisänen and Hölttä (1999) described corresponding granulites from the Turku area (Figures 9 and 10). The granulites are gneissic orthopyroxene-bearing granitoids, often tonalitic, migmatitic garnet-cordierite gneisses and variable pyroxene-bearing felsic, intermediate and basic gneisses (Parras 1958). Principally, the supracrustal rocks represent high-T/low-p variants of the lower-grade sequences further south in the Southern Volcanic-sedimentary Belt (SVB), such as in the Orijärvi area (e.g. Eskola 1914, 1915, Parras 1958, Schreurs & Westra 1986 and Kilpeläinen & Rastas 1990). Our field observations are from the northeastern part of the WUC between the border zone of the Hyvinkää Gabbroic-volcanic Belt (HGB) and the Espoo Granitoid Complex (EGC).

The contact of the WUC with the overlying EGC is characterized by shearing described in detail from Klaukkala (Figure 35). The contact is a low-angle extensional shear zone with top-to-SE movement; the deformation is related to the D_E extension. The border with the Perniö Granitoid Complex (PGC), interpreted using the magnetic maps and tectonic observations, is a similar low-angle zone dipping SE; the zone was deformed by the F_{G-H} interference folding, thus, evidencing its pre- D_{G-H} generation (Figure 16). The sharp Kisko fault (Figures 10 and 16) was oriented by this old structure. In the north the WUC is bordered against the Hyvinkää Gabbroic-volcanic Belt (HGB) along the complex Hyvinkää shear/fault zone (Figures 9 and 10), and the D_H structures were bent due to progressive SE-NW D_H transpression into a E-W direction in the vicinity of the shear/fault zone. In the east the Vuosaari-Korso shear/fault zone cuts the WUC; only small areas of corresponding high-grade rocks are exposed in antiformal structures in the Sipoo area. A small granitic window is also exposed in the Nuksio (Nu in Figure 9) granite area.

The West Uusimaa granulite Complex (WUC) forms a wide antiformal fold interference dome (Figure 11) showing a complex internal tectonic pattern (Figure 41); granulites in Turku are situated in a corresponding tectonic dome setting (Figure 9 and 11). The westernmost part of the WUC is characterized by dome-and-basin interferences, c. 8 km in diameter with ENE-trending high-strain zones between the dome-and-basin chains (Figures 16 and 41). The structural pattern is exposed between the Orijärvi area and the NW-trending Hiidenvesi shear zone (Figure 10). We interpret these as reflections of D_{G+H+I} interferences (cf. D_{3+4} interferences by Kilpeläinen & Rastas 1990) corresponding to the structure described from the Askola area (Appendix-Fig. 3-4).

The northeastern parts of the West Uusimaa granulite Complex (WUC) comprise large areas that show a simple tectonic geometry with exceptionally well-developed straight foliation (Appendix-Fig. 2-1). The foliation is nearly horizontal and is deformed into open F_{G+H+I} fold interferences. Between the horizontal areas are complexly folded units; their forms are determined by the F_{G+H+I} interferences (Figure 41). The borders between the complexly-deformed horizontal tectonic units and the units showing the straight foliation are low-angle, extensional D_E shear zones. Our interpretation is that the straight foliation was formed during a penetrative extensional D_E event under granulite facies conditions; large-scale crustal shearing under granulite-facies conditions produced a granoblastic microstructure in the one- or two-pyroxene rocks. In the upper crustal levels and lower temperatures the ductile deformation was more zoned, and close to the erosion level sharp faults occur (cf. Figure 4). Carbonate was often precipitated into extensional fractures or along the foliation planes of the pyroxene-gneisses. Some carbonate was precipitated still later, as indicated by the c. 10-m-wide fracture-controlled impure carbonate filling in the Porkkala-Mäntsälä zone (Hämeenkylä, Vantaa, Finnish grid coordinates KKJ2 2544.61E 6684.73N). These carbonates are products of remobilization of the primary sedimentary and volcanic carbonates that are typical in the corresponding lower-grade units (Southern Volcanic-sedimentary Belt, SVB), and of possible additive CO_2 influx that, according to Schreurs & Westra (1986), caused the granulite metamorphism. Those parts of the crust that were not deformed penetratively by the D_E show the complex preserved pattern formed during the pre-existing D_{A-D} tectonic history.

The granulite-facies rocks occur in a c. E-ENE-trending zone. In the east it continues below the Askola area (As in Figure 9), where this hot crustal "slice" caused the ductility of the overlying crust during their deformation into D_{G+H+I} dome-and-basins corresponding to those in the western WUC. This interpretation is supported by the pattern of the upwards-continued magnetic field that represents the deeper and wider magnetic anomalies of the crust (Figure 12a). The anomaly pattern characteristic for the WUC continues east to the western parts of the Vyborg rapakivi batholith (1 in Figure 1), up to the crustal-scale N-trending Riga Bay-Karelia Zone (RKZ) (Figures 8 and 10). This zone shows the lowest magnetic and gravity anomalies, indicating the deepest extension of the Vyborg rapakivi granite in the zone.



Appendix-Fig. 2-1. Well-developed and straight S_E -foliated pyroxene-bearing felsic gneiss in the West Uusimaa granulite Complex (WUC). Compass is 12 cm in length. Röykkä, Nurmijärvi (Finnish grid coordinates KKJ2 2534.02E 6715.41N). Photo by N. Nordbäck.

The orthopyroxene-bearing tonalite (charnockite) from Lohja, Maikkala that was preserved “untouched” in the D_E penetrative shearing, was dated by conventional U-Pb at 1860 ± 4 Ma based on zircon and 1837 ± 3 Ma based on monazite. The U-Pb zircon ages obtained with SIMS from the same sample give a concordia age of 1862 ± 4 Ma for the rock (Appendix 8). The penetrative D_E shearing sharply cuts the tonalite areas. Therefore, the intrusion age of the tonalite determines that the major penetrative horizontal D_E deformation occurred later than c. 1.86 Ga. The age is similar to those obtained from corresponding pyroxene granitoids from Kakkskerta, near Turku, and from Houtskär, from the Turku archipelago (Suominen 1991).

Granulite mineral assemblages formed during progressive metamorphism are often later affected by retrograde metamorphism; decomposition of pyroxenes to clinoamphibole is typical, for example in the northern Espoo Granitoid Complex (EGC). The Maikkala tonalite also contains metamorphic mineral assemblages suggesting later high-temperature metamorphism, presumably represented by the monazite and homogeneous core ages of c. 1.84–1.83 Ga (Appendix 8). The c. 1.82 Ga ages of migmatite neosomes in granulitic metapelites (Väisänen et al. 2004) indicate a continued high-T event. According to our observations, these late granitic neosomes are related to the evolution of D_H , which is also characterized by large amounts of granitic melt elsewhere. Locally, particularly in the areas of lower metamorphic grade, there was a cooling stage between the events. At deeper crustal depths, high heat flow was more continuous from the early- D_E tonalites at 1.86 Ga to the D_H phases evolving at c. 1.83–1.81 Ga. The temperature remained quite high, because granitic melts, like the 1804 ± 2 Ma pegmatitic granite dykes (Pajunen et al. 2008), still intruded the latest-identified Svecofennian D_1 folds.

Appendix 3. Structural relationships in Hyvinkää Gabbroic-volcanic Belt

The structurally-complex Hyvinkää Gabbroic-Volcanic Belt (HGB) is located between the Hyvinkää shear/fault zone and strong shear zones bordering it in the north to the Renko area (Figures 9 and 41). The NNE-trending Hyvinkää-Lahti shear/fault zone divides the HGB into Hyvinkää (Hy in Figure 9) and Askola (As in Figure 9) areas. Large c. 1.88 Ga old (Patchett et al. 1981) layered gabbro massifs surrounded by supracrustal sequences characterize the Hyvinkää-part of the HGB. The Askola area is characterized by roundish dome-and-basin structures; gabbroic-volcanic rock associations are squeezed between the domes.

Setting of gabbros of the Hyvinkää Gabbroic-volcanic Belt

The central parts of the gabbroic massifs are weakly deformed (Appendix-Fig. 3-1a), but their border zones are strongly deformed and show ductile shearing, and locally the gabbros are semi-brittle faulted. Volcanic rocks and mica gneisses that surround the gabbros locally show primary structures such as bedding, fragmentary (Appendix-Fig. 3-2a), agglomerate and pillow lava structures. The paragneisses often show a complex polyphase deformation that is very similar to that described from the Espoo Granitoid Complex (EGC) and Southern Volcanic-sedimentary Belt (SVB), like the D_{C-D} dome-and-basin structure shown in Appendix-Fig. 3-2b, but no F_A fold observations currently exist. In the supracrustal rocks, especially in amphibolites, a lineation dips steeply E or SE (Appendix-Fig. 3-2c); correspondingly to that described from the SVB (Figure 14e).

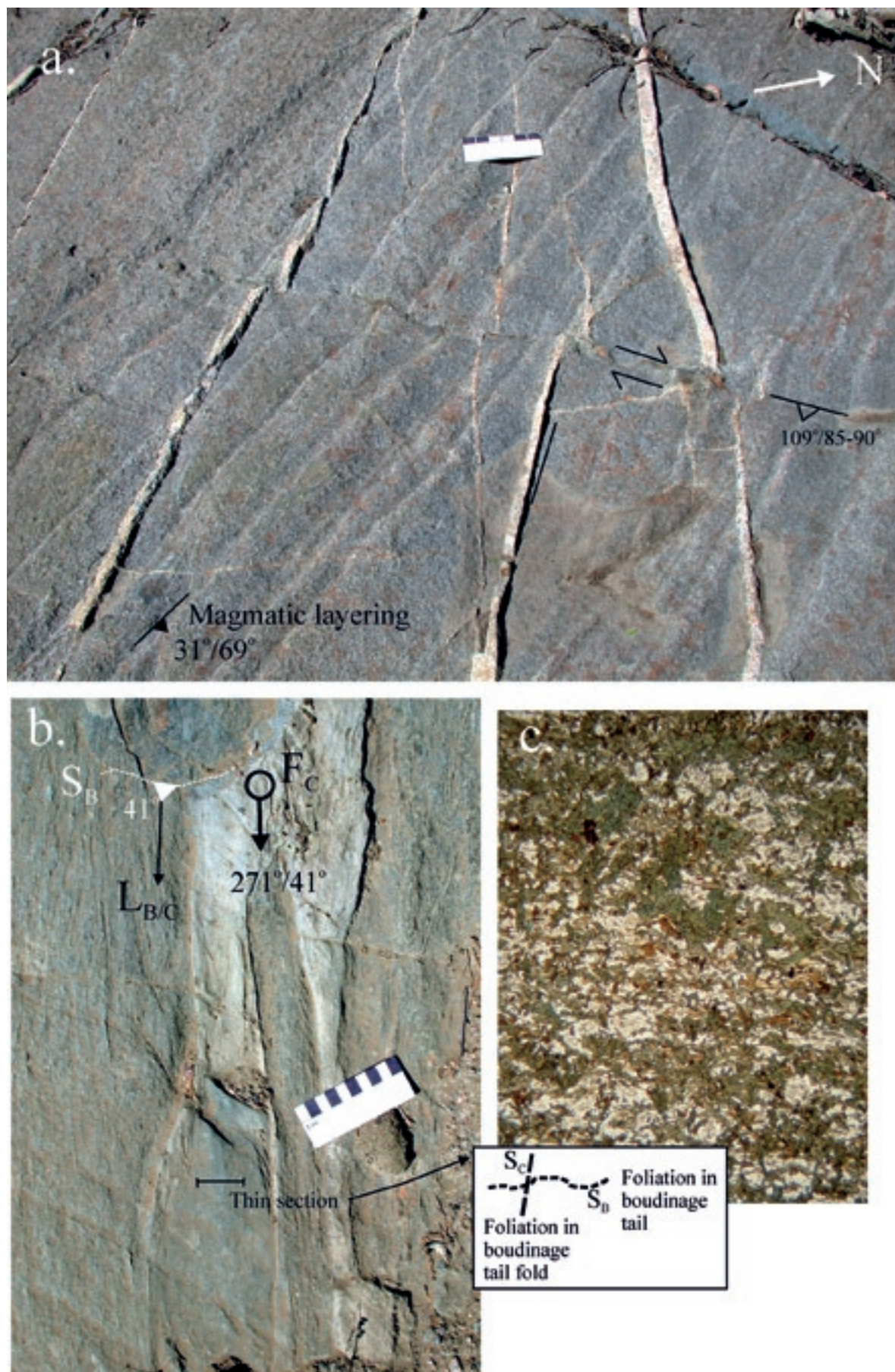
Often the primary magmatic layers of the Hyvinkää gabbro are folded to an upright position. Open folds with NW-trending steep axial planes of the magmatic layers indicate ductile deformation even in the well-preserved parts. The recent setting of magmatic layers becomes evident as variation in the magnetic anomaly pattern (Appendix-Fig. 3-3a). At the southwestern end of the Hyvinkää gabbro massif a folded “tail” of deformed layered mafic rock (Appendix-Figs. 3-3 and 3-1b and c) is interpreted as a layered gabbro that thins and dies out towards the attenuated NE-end of the western massif. The western massif has a corresponding tail in its NE-part, and there are drag folds in the SE and NE corner of the western massif – the structures indicate their dextral rotation. The folded “tail” shows a fold axis paralleling the lineation observed in the amphibolites elsewhere in the HGB (Appendix-Fig. 3-2c). We interpret this as $L_{B/C}$, corresponding to $L_{A+B/C}$ of the Southern Volcanic-sedimentary Belt (SVB).

The supracrustal sequences, intensely folded between the gabbros, exhibit corresponding dextral rotation drags. The “tail” structures suggest D_B boudinage that was later refolded by D_C and rotated during continuing deformations. The volcanic belt between the major gabbro bodies forms D_{C+D} dome-and-basin structures that were subsequently bent by later deformations (Appendix-Fig. 3-2b). The structures suggest that the gabbros represented originally widespread layered massifs that were fragmented and boudinaged during D_B flattening, and were folded by D_{C+D} and dextrally rotated by D_H . The interpretation is supported by the folded pattern of occurrence of gabbroic “fragments” in the Granite Migmatite Belt (GMB) (Figures 7 and Appendix-Fig. 3-3). The structural evolution of the gabbros is summarized in Appendix-Fig. 3-3b; the complexly folded gabbros represent originally nearly horizontal magma bodies and their exposure is determined by the late wide-scale folding phases D_G , D_H and D_I . In the Askola area (see below), gabbroic rocks are sometimes preserved as remnants in metamorphic amphibolites; therefore, it is likely that gabbros were originally more widespread than can be estimated from the map shown in Appendix-Fig. 3-4.

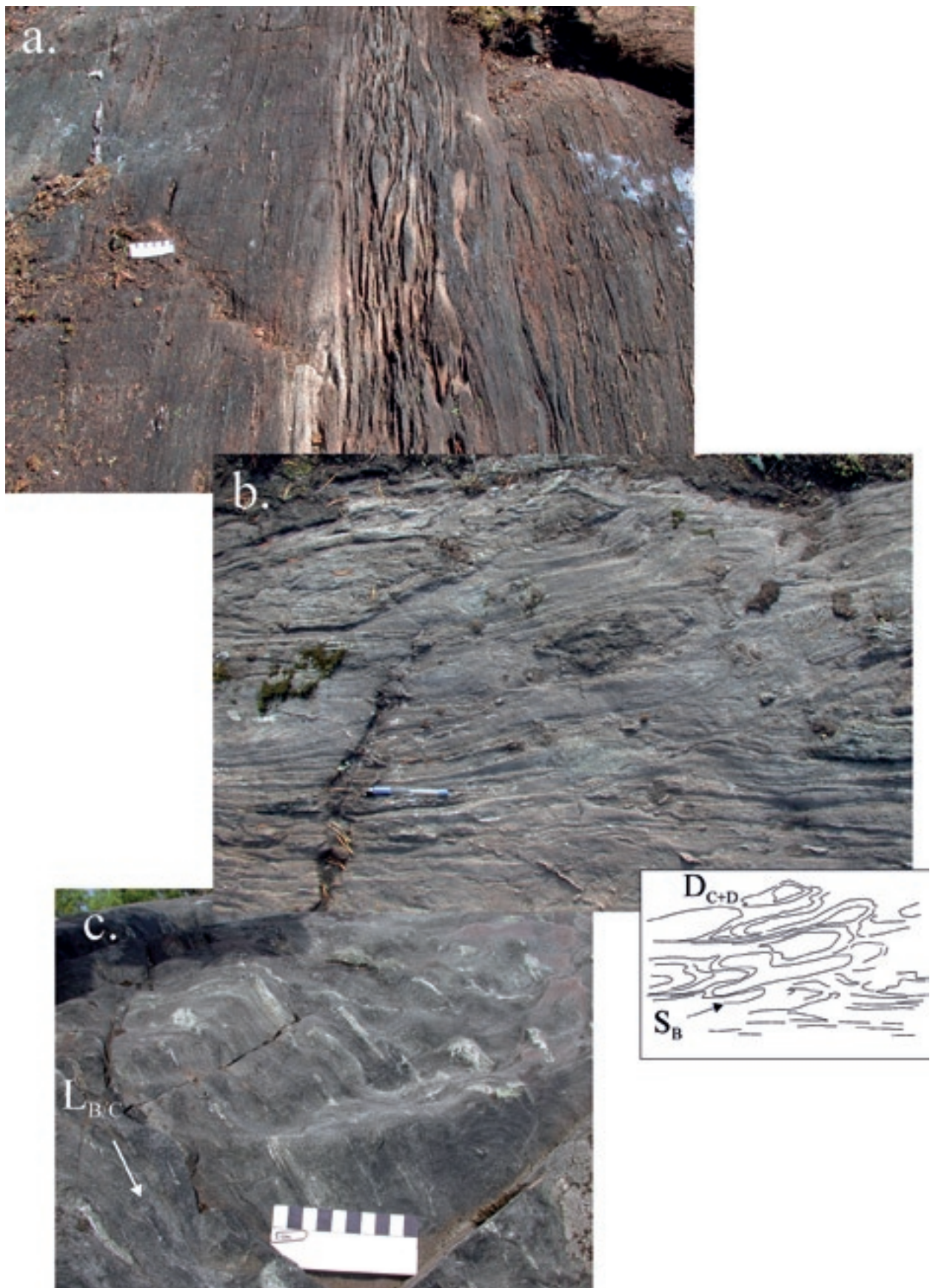
The gabbro massifs are cut by straight NE-trending structures that were formed by dextral movement. Some linear ESE- and SE-trending structures also occur. In the Hyvinkää massif NW-trending structures also cut the massif: they are parallel to the axes of open-folding F_H cont. On an outcrop, in the interior of the Hyvinkää massif, semi-brittle faulting and granite-filled fractures show an en échelon pattern, suggesting competent behavior of the gabbros during the NW-SE-directional shortening. These structures coincide with the clockwise rotation and dextral movements along the E-W-trending shear zones, and the overall SE-NW transpression during the D_H deformation.

Dome structures in the Askola area of the Hyvinkää Gabbroic-volcanic Belt

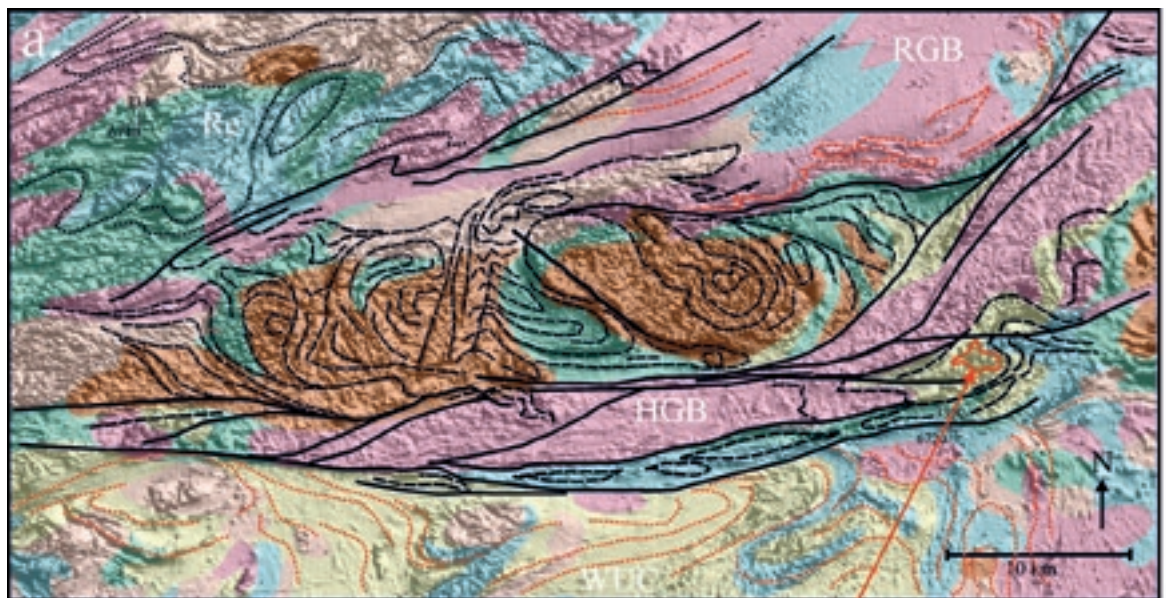
The Askola area (As in Figure 9) of the Hyvinkää Gabbroic-volcanic Belt (HGB) is separated from the Hyvinkää area (Hy in Figure 9) by the sinistral Hyvinkää-Lahti shear/fault zone (Figures 10 and 41), which is related to the N-NNE-trending D_1 deformation; the shear/fault zone is located in the northern continuation of the Vuosaari-Korso shear/fault zone (Figures 10 and 41). The axial plane of the open semi-ductile crustal



Appendix-Fig. 3-1. (a.) Layered Hyvinkää gabbro is cut by granite dykes and semi-brittle faults. Scale bar is 15 cm in length. Lähdemäki, Hyvinkää (Finnish grid coordinates KKKJ2 2535.59E 6723.69N). (b.) Detail from the folded tail in the SE-side of the Hyvinkää gabbro and (c.) a microphoto from the fold. The new mineral growth in the folded tail indicates medium-grade metamorphic conditions. Scale bar is 10 cm in length in (b.). Rantalanhaka, Hyvinkää (Finnish grid coordinates KKKJ2 2534.50E 6722.85N). Photos by M. Pajunen.



Appendix-Fig. 3-2. (a.) Mafic, partly fragmentary volcanic rock in the Hyvinkää Gabbroic-volcanic Belt (HGB). Scale bar is 10 cm in length. Konnuunmäki, Hyvinkää (Finnish grid coordinates KKJ2 2528.20E 6723.31N). (b.) D_{C+D} dome-and-basin structure in non-migmatitic mica gneiss in the border zone of the Hyvinkää Gabbroic-volcanic Belt (HGB) and the West Uusimaa granulite Complex (WUC). Pencil is 14 cm in length. Karhulampi, Hyvinkää (Finnish grid coordinates KKJ2 2537.04E 6714.43N). (c.) Strong lineation ($L_{B/C}$) in amphibolite in the HGB. Scale bar is 10 cm in length. Palosenkallio, Hyvinkää (Finnish grid coordinates KKJ2 2542.97E 6718.08N). Photos by M. Pajunen.



Legend

- Gabbro
- Amphibolite
- Intermediate granitoids
- Mica gneisses
- Felsic granitoids
- Felsic and pyroxene gneisses

Jokela supracrustal association

b.

D_8 - D_0 deformations:

Intrusion of layered gabbros - pre-syn- D_8
Vertical section



D_8 flattening and boudinage of gabbros
Vertical section

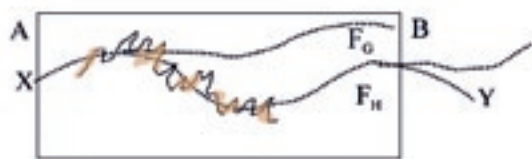


D_{C-D} folding
Vertical section

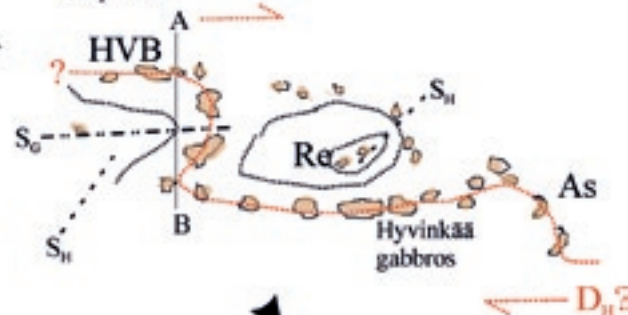


F_C - F_1 fold structures:

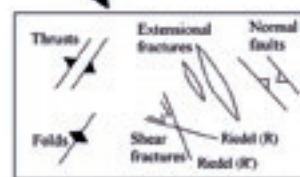
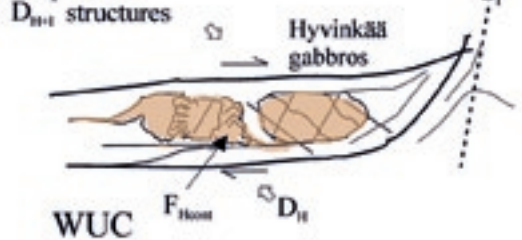
Vertical section



Map view



Map view



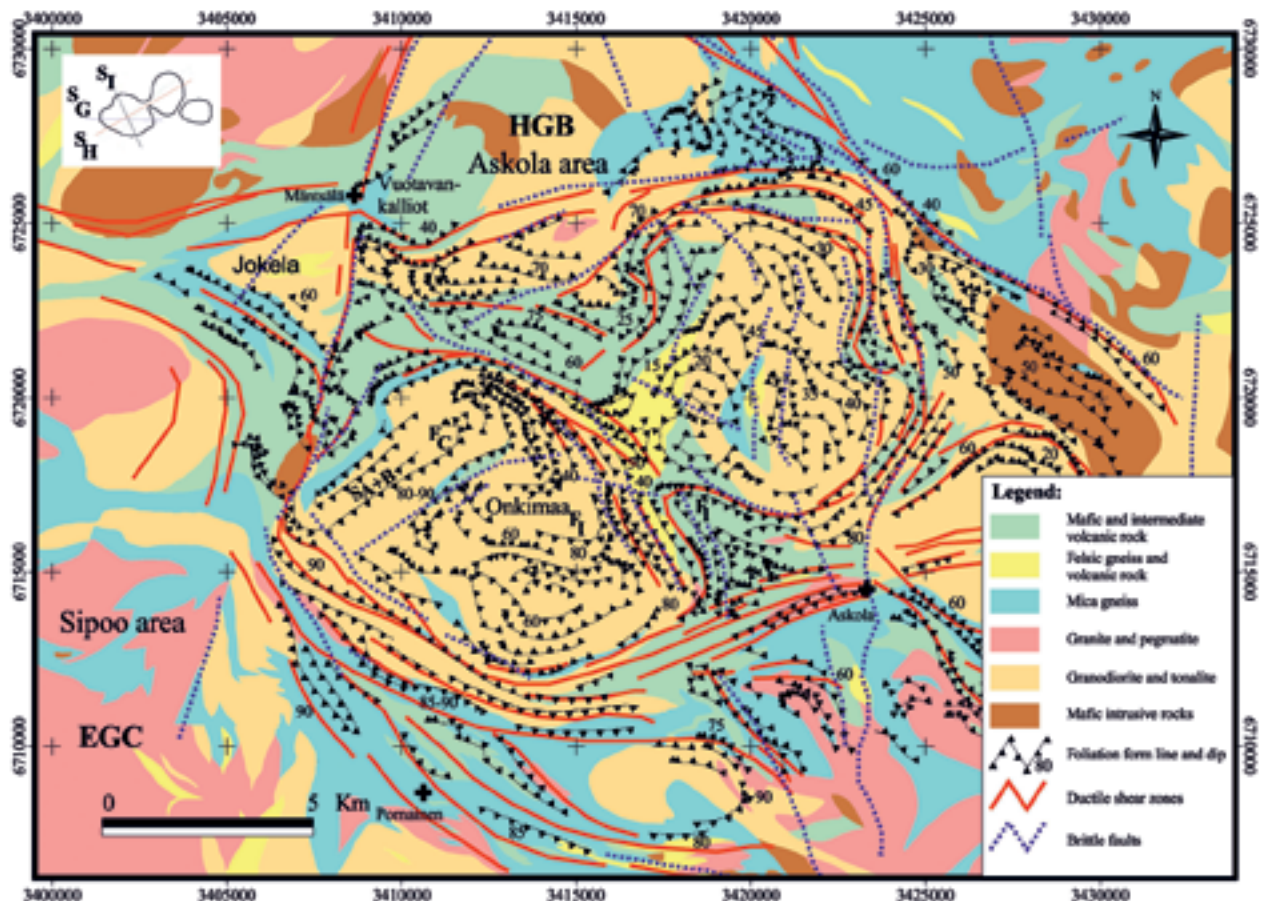
Appendix-Fig. 3-3. (a.) Tectonic structure of the Hyvinkää gabbro and (b.) schematic model of its tectonic evolution on a combined magnetic (shading) and lithological (colours) map. The location of the Jokela supracrustal association (Jo) is shown.

bend F_1 parallels the Hyvinkää-Lahti shear/fault zone, which further north changes in character to the Lake Päijänne fracture pattern already described by Sederholm (1932b) (Figure 10).

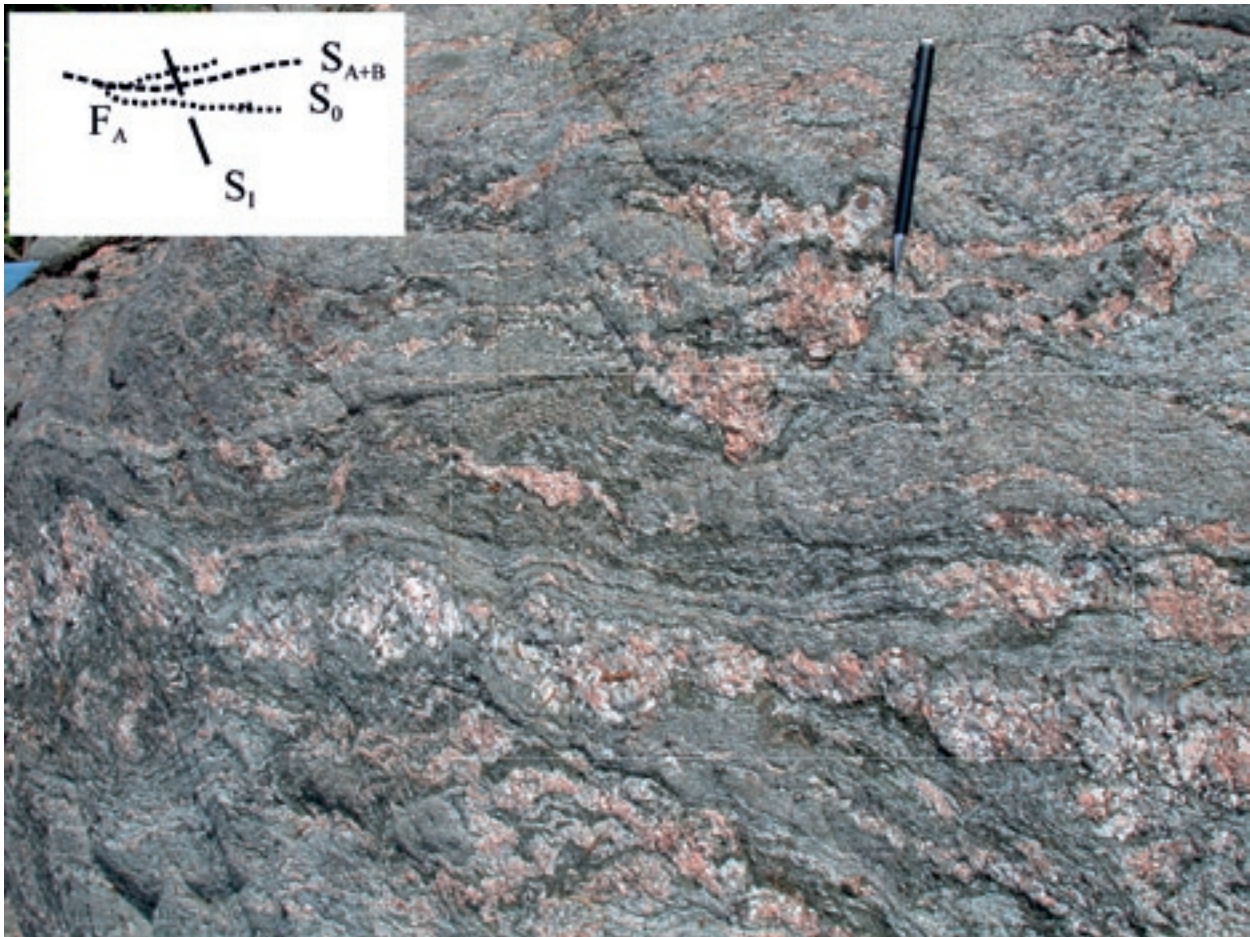
The Askola area differs structurally from the western part of the Hyvinkää Gabbroic-Volcanic Belt (HGB). It shows systematic dome-and-basin structures with zones of gabbros and amphibolites and lesser mica gneisses squeezed between the dome structures (Figure 9 and Appendix-Fig. 3-4). The internal parts of the domes are composed of granodioritic to tonalitic intrusives and migmatitic garnet-cordierite gneisses. The structural pattern of the foliations, shown in Appendix-Fig. 3-4, suggests that the lower tectonic slices of crust are exposed in the dome windows and the rocks of the upper tectonic slice, typical rocks of the HGB, are compressed between the domes (Appendix-Fig. 3-4).

Migmatitic mica gneisses in the Onkimaa dome centre provide evidence of several folding generations prior to the formation of the open rounded dome structure. Isoclinal early flame-crested folds (F_A) underwent additional flattening with contemporaneous granitic melting during D_B (Appendix-Fig. 3-5). Isoclinal folds (F_C) with steep NE-trending axial planes refold these structures. The early D_{C-D} dome-and-basin interference structures typical in the southern units, like in the Southern Finland Sedimentary-volcanic Belt (SVB), are not identified here (due to restricted observations by us).

Intermediate microtonalite dykes (observed up to 0.5 m wide) cut the structures, suggesting a cooling stage after the $D_{A-C(D)}$ and a new pulse of magmatism. We relate the dykes to the D_E (see main text). A model shown in Figure 4 can explain the contrasts between the steeply and gently dipping foliations in the dome interior contra margin settings. The borders of the internal dome and overlying rocks were interpreted as an extensional D_E shear structure corresponding to that described from the Espoo Granitoid Complex (EGC) in Klaukkala (Figure 35). The open fold structure F_1 with NW-SE-trending axial planes deforms the strong S_{A-B} foliation, appearing as macro-crenulation on the outcrop (Appendix-Fig. 3-5). It also deforms the microtonalite dykes. This folding has map-scale amplitude. Although some overprinting occurred due to shearing along eastern low-angle border faults of the Onkimaa dome, it is evident that the folds are related to dome formation. This is supported by a similar NW-trending fold pattern in the overlying tectonic slice



Appendix-Fig. 3-4. Tectonic structure in the Askola dome-and-basin area. (Finnish grid coordinates KKI3).



Appendix-Fig. 3-5. F_A folding intensified and migmatized by D_B and refolded by F_1 in migmatitic garnet-bearing mica gneiss inside the Onkimaa dome. Pencil is 14 cm in length. Palosenkallio, Pornainen (Finnish grid coordinates KKKJ2 2756.81E 6716.42N). Photo by M. Pajunen

that was compressed between the domes to the northwest of Askola. The dome series suggests a complex fold interference pattern formed during D_{G+H+I} (Appendix-Fig. 3-4).

The structural pattern is fragmented by predominantly N-trending brittle faults that partly follow the ductile shear zones; observations further west in the Sipoo area suggest late (post-Svecofennian) low-angle overthrust faults with east-side-up movement.

The relations of the Onkimaa granodiorite in the northern part of the dome have not been studied here, but structurally (e.g. strongly foliated and showing a complex pattern of shear bands) it is quite similar to the tonalites in the Sipoo area, e.g. the Hindsby tonalite (main text). The cutting intermediate microtonalite dykes are also quite similar and we can suppose that the dome windows represent antiforms of the same tectonic slice exposed in the eastern Espoo Granitoid Complex (EGC) in Sipoo (Si in Figure 9). The Askola area is bordered to the southwest and south along steep strong shear zones against the Sipoo area.

Appendix 4. Structural succession in non-migmatitic Orijärvi area

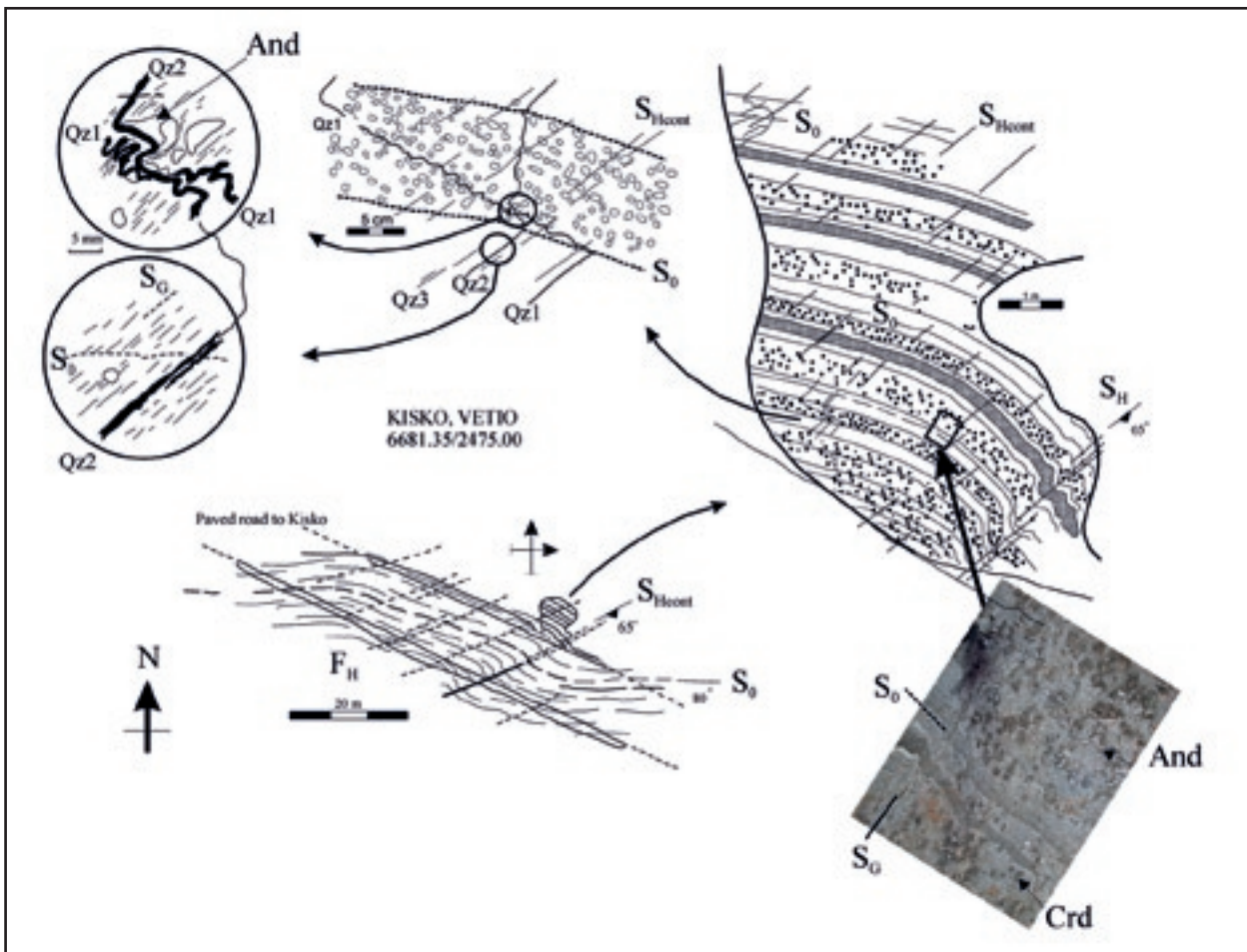
The lower amphibolite facies Orijärvi area (Or in Figure 9) have been extensively studied since the detailed metamorphic studies of Eskola (1914 and 1915) because of its ore potential (e.g. Latvalahti 1979) and scientific value (e.g. Eskola ops. cit., Tuominen 1957, Schreurs & Westra 1986, Ploegsma & Westra 1990, Kilpeläinen & Rastas 1990, Skyttä et al. 2006 and Pajunen et al. 2008). In the Orijärvi area the primary structures of supracrustal rocks are well preserved. The Zn-Cu-Pb ores associated with altered rocks, such as coarse-grained cordierite-anthophyllite rocks (Eskola 1914 and 1915), skarn-iron ores, iron formations (e.g. Eskola 1914, Latvalahti 1979 and Saltikoff et al. 2002) and carbonate rock horizons (Bleeker & Westra 1987 and Reinikainen 2001) in the Orijärvi area indicate a shallow-water deposition. According to Lahtinen et al. (2002), the depositional age of mica gneisses in Orijärvi belongs to the Svecofennian age group of c. 1.9 Ga. Väisänen & Mänttari (2002) proposed a back-arc basin origin for the volcanogenic rocks. Volcanic rocks are divided into two series according to their structural relationships (the early Series I and the later Series II; see main text) and to their geochemical characteristics and ages (cf. Väisänen & Mänttari 2002). The 1998 ± 2 Ma Orijärvi granodiorite was interpreted as syngenetic with the early volcanic sequence (Väisänen & Mänttari 2002). The gabbroic associations described by Hopgood et al. (1976 and 1983) and Hopgood (1984) from the Jussarö-Skåldö area (Ju in Figure 9) are also related to the early volcanism.

The Orijärvi area is characterized by F_G folds with E-trending axial planes and nearly horizontal axes (Figure 16). In the central part of the area the axial planes are openly warped, but folding intensified to tight in the N-trending deformation zone in the east (reactivated by ductile Jyly shearing); we have interpreted this N-trending zone as a D_1 structure by comparing it to the structures in the Vuosaari-Korso zone in the Espoo Granitoid Complex, EGC (Figure 11). The minimum age of D_1 folding can be estimated with pegmatitic granite at c. 1.804 ± 2 Ga (I_g granitoid in Pajunen et al. 2008). The D_H folds with NE-trending axial planes that characterize the West Uusimaa granulite Complex (WUC) and the Espoo Granitoid Complex (EGC) as large-scale folds can also be seen on outcrops as gentle to open, sometimes north-westwards overturned folds; they form complex dome-and-basin structures with F_G and F_I . In the high-grade areas some granitic melt fraction intruded into the S_H axial planes (Figures 29 and 30a), or a new mineral foliation formed in the D_E granitoids. The D_H folding is the main structure seen in the *Vetio outcrop* (site shown in Figure 16) at Kisko, in the Orijärvi area (Appendix-Fig. 4-1). The outcrop illustrates well the principal features of metamorphic mineral growth and deformation in the lower-grade mica schists. Granitoids related to D_E are absent from this lower-grade outcrop.

The mica schist shows well-preserved primary layering S_0 , which gives a good reference point for analyzing the structural succession on the *Vetio outcrop*. Large, long andalusite₁ porphyroblasts have crystallized sub-parallel to primary layering. Andalusite contains an early foliation parallel to the bedding S_0 . The foliation is preserved as fine-grained internal S_1 biotite foliation; locally, the same foliation is also preserved in the pressure shadows of andalusite. The andalusite growth resembles that of the Tampere Schist Belt (TSB) (cf. Kilpeläinen 1998) and the Rantasalmi-Sulkava area (RSB) (Korsman 1977 and Korsman & Kilpeläinen 1986). The early cordierite₁, possibly formed by breakdown of chlorite, overgrew S_0 and the nearly bedding-parallel foliation; it was penetratively retrogressed to pinitite. The foliation, sub-parallel to S_0 , indicates nearly horizontal generation of this early foliation. An intermediate dyke including recrystallized (grains are entirely mortar-textured or on grain rims) plagioclase laths has also intruded into the direction of S_0 . The dyke has weak dyke-parallel foliation and was folded by F_H ; the most intense penetrative biotite foliation is S_H .

D_H deforms the early foliation, andalusite₁ and cordierite₁ porphyroblasts, and the penetrative S_H biotite foliation curves around the porphyroblasts. Idioblastic andalusite₂ grew onto the edges of andalusite₁ and overgrows the S_H foliation. The increased temperature is shown by fibrolitic sillimanite that was crystallized in S_H foliation plane, especially close to the andalusite grains in the intensely D_H -deformed parts of the rock. Cordierite₂ grew as syntectonic poikiloblasts, and its latest phase is idioblastic and overgrew S_H . On the outcrop scale the large cordierite porphyroblasts were aligned in the S_H planes. The early generation of quartz veins was formed into dilatational fractures during the early D_H into the S_H direction. The veins were deformed to become pinch-and-swell-structured and folded during the continuing D_H . Late idioblastic garnet poikiloblasts overgrow S_H . Late muscovite porphyroblasts overgrow all the described structures and indicate a late potassium-rich fluid infiltration. This is also supported by some late alteration on the edges of cordierite₂.

The occurrence of retrograde phases (e.g. in cordierite₁) predating D_H and the existence of low-temperature quartz₁ veins suggests a cooling stage between the early andalusite-cordierite deformation and later



Appendix-Fig. 4-1. Detailed structures of andalusite-cordierite-bearing mica schist (photo; width of the area of the figure is c. 0.5 m) in the Orijärvi area. Vetio, Kisko (Finnish grid coordinates KKJ2 2475.00E 6681.35N). Primary drawing by T. Koistinen reinterpreted here. Photo by M. Pajunen.

D_H with peak metamorphism in the sillimanite stability field. Thus, the bedding-parallel dykes may be correlative with the pre- D_B volcanogenic dykes that are boudinaged and S_H foliated, e.g. in Rövaren (Figure 40a). The foliation in the early andalusite₁ and cordierite₁ resembles that observed in the early K-feldspar porphyroblasts of the mica gneisses in the upper tectonic slices of the Hyvinkää Gabbroic-volcanic Belt (HGB), but we have no observations on relics of early andalusite from them, even though primary layering is often well preserved. No pseudomorphs of the early andalusite have been found in the higher-grade gneisses, either.

Appendix 5. Jokela supracrustal association

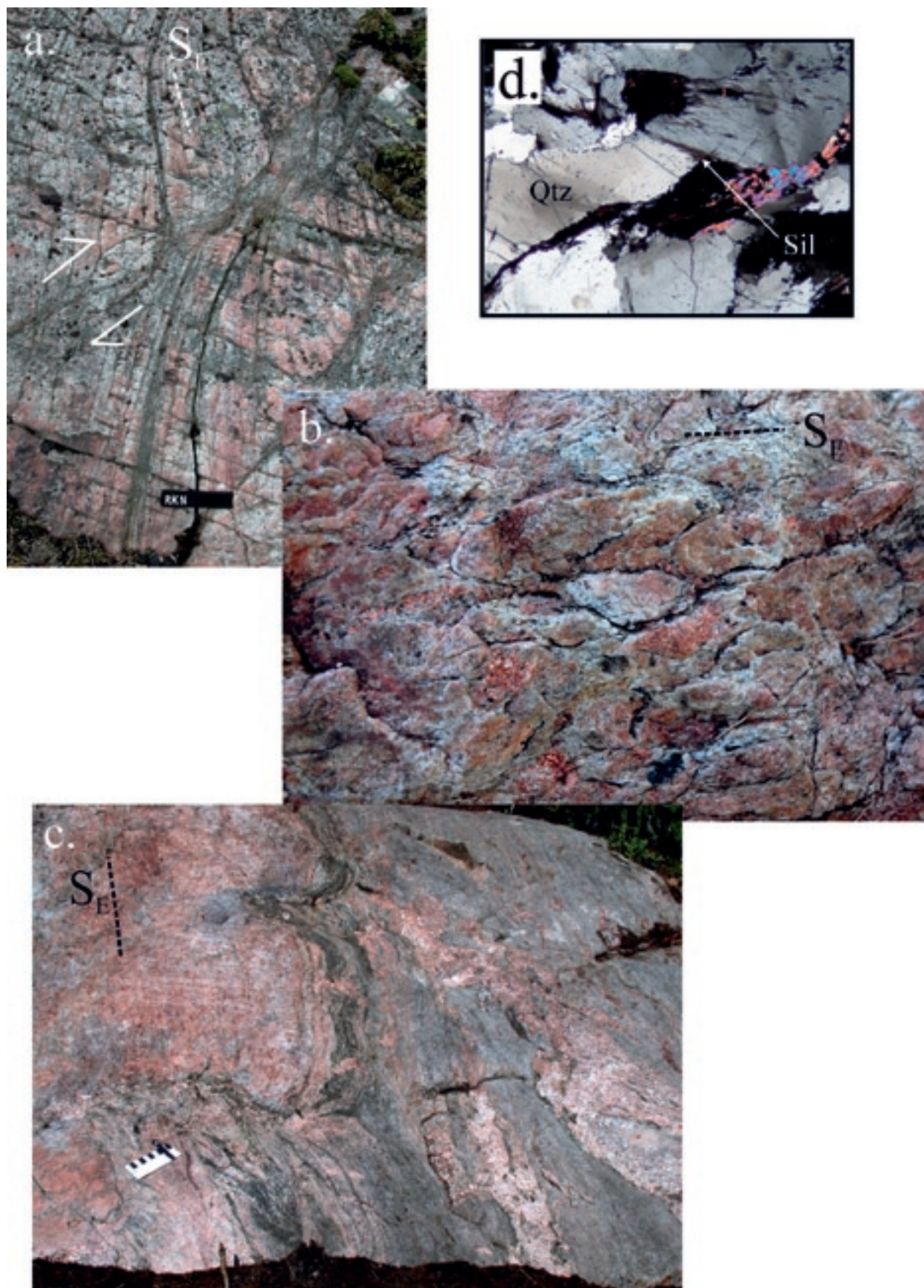
The supracrustal Jokela association (Figure 9 and Appendix-Fig. 3-4) is situated at the eastern end of the Hyvinkää shear/fault zone, in the intersection with the Hyvinkää-Lahti shear/fault zone. It stands out from its surroundings as a highly magnetized synformal association between branches of the Hyvinkää shear/fault zone. Scattered quartzite exposures also occur outside of the coherent Jokela formation.

The association is composed of polydeformed supracrustal rocks showing primary depositional structures, which, however, are often destroyed by penetrative shearing or transposition. The reddish to grey quartzite, e.g. in the Jokela open pit (Appendix-Fig. 5-1a), shows primary layering and beds are locally laminated and cross-bedded. The rock is fractured and foliated with flattened quartz surrounded by weakly recrystallized fine-grained grains. Minor phases, tourmaline, magnetite and sillimanite formed by breakdown reaction of muscovite, refer to some clay content in the quartzite. The quartzite is in close association with less mature feldspathic arenites and intraformational conglomerates. The sedimentary structure of the conglomerate, with clasts of up to 2–3 cm scattered in a sandy matrix, is still identifiable after deformation (Appendix-Fig. 5-1b). The only observed contact of quartzite against non-mature sediments is primarily depositional and only weakly tectonic (Appendix-Fig. 5-1c). The succession also contains calcareous interlayers, and in places the rock is penetratively silicified and tourmalinized due to later fluidization events. Intermediate clinoamphibole-bearing volcanogenic gneisses, presumably tuffitic in origin, and bedding-parallel, weakly plagioclase porphyritic mafic dykes are in close association with the sediments (Appendix-Fig. 5-2a). Locally, they occur as interlayers in impure sediments (Appendix-Fig. 5-4c); such interlayers are not met in quartzite. Pegmatitic granites intrude the supracrustal association. It locally contains fragments of complexly-folded quartzite (Appendix-Fig. 5-3d) that is strongly assimilated into granite (Appendix-Fig. 5-3c). However, the granite dyke sharply cuts the volcanogenic rock, which does not show such complex folding as in quartzite, indicating that the volcanogenic series post-dates the quartzite accumulation. The volcanogenic rocks are mostly associated with the less mature sediments, suggesting that the impure sedimentation was also later than the deposition of the quartzite. The pelitic layers with sillimanite (Appendix-Fig. 5-3a) show feldspar porphyroblasts and some melting, and display a simpler folding pattern than quartzite (Appendix-Fig. 5-3d). The lithology and primary structures suggest that the deposition of quartzite and its associates occurred in a sub-aquatic, high-energy environment accompanied by volcanic activity. Transition from clastic sediments, quartzites, conglomerates and arenites to calcareous sedimentary rocks (Appendix-Fig. 5-3b) and pelitic gneisses refers to the change in deposition to a tranquil deeper-water environment.

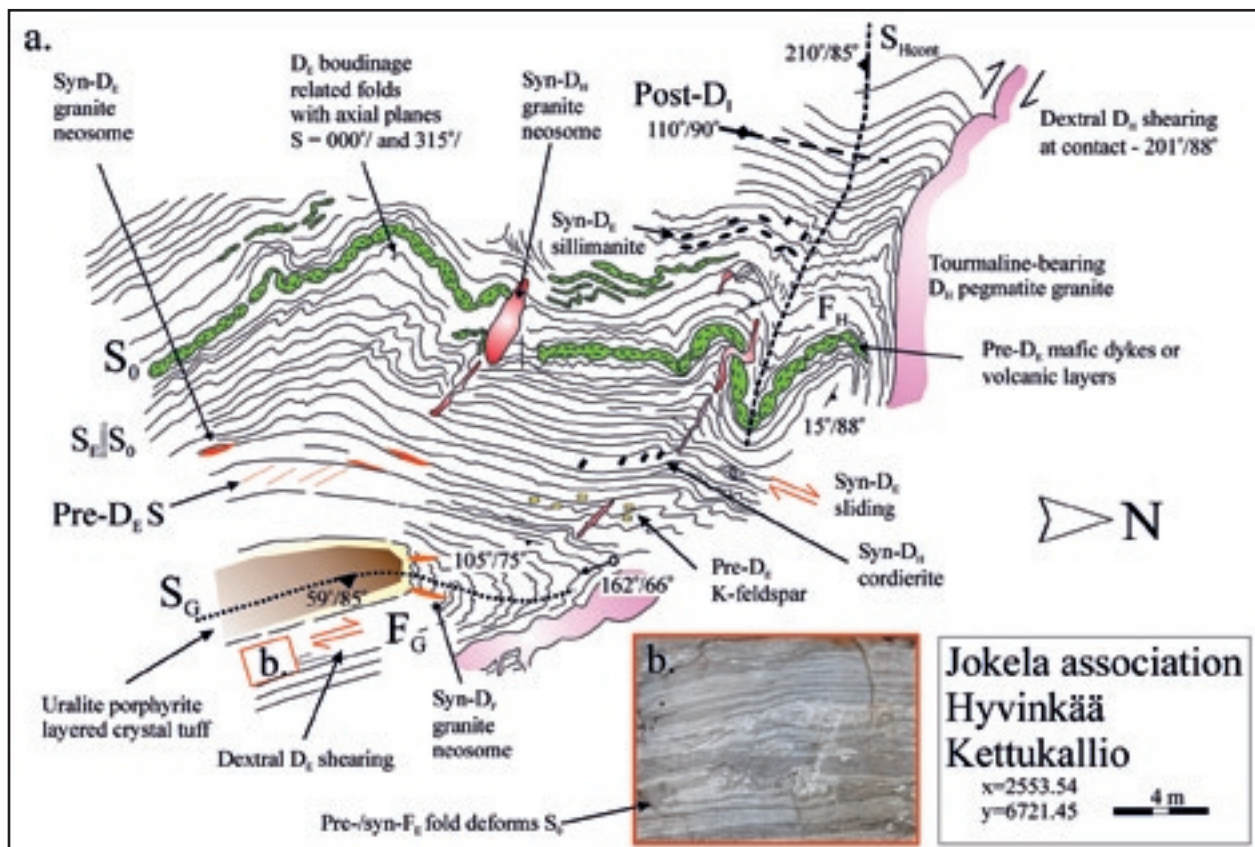
In Tiirismaa the detrital zircon population of 1.87–1.86 Ga indicates the maximum age of deposition of the quartzite (Lahtinen et al. 2002). According to the close resemblance to Tiirismaa in lithology, metamorphism and tectonic setting, we conclude that the Jokela association also represents a young deposition and volcanism. It is a good fixing point for structural analysis of the post-sedimentation (post–1.87–1.86 Ga) evolution.

The outcrop in Mäntsälä, Jokela, at the Kettukallio site in Appendix-Fig. 5-2 exemplifies the tectono-metamorphic history of the association. The strongest penetrative structure on outcrops is a spaced biotite foliation; we relate it to D_E based on the combination of the information from surrounding areas and on the age data. Early quartz veins precede the main foliation S_E . Under the microscope, an openly-folded internal biotite foliation, S_{i1} , exists in the early K-feldspar₁ porphyroblasts. A penetrative schistosity S_{i2} in the axial plane of the open folds also appears as a weak biotite growth in the pressure shadows of K-feldspar₁ porphyroblasts (Appendix-Fig. 5-4a). This kind of pre- D_E foliation also exists in the gneisses of so-called Upper Tectonic Unit, UTU (cf. Appendix 6). We are not able to relate the early foliations, S_{i1} and S_{i2} , to the structural successions described from the other units. The earliest fold structure deforming the primary layering and lamination, S_0 , are isoclinal, round-hinged intrafolial folds (Appendix-Fig. 5-2b). The polyphase folding in the quartzite fragment (Appendix-Fig. 5-3d) does not show the intense S_E foliation, and we suppose the folding to be related to the early, low-T evolution of the sedimentary-volcanic pile.

The spaced biotite foliation S_E deforms the weak penetrative S_{i2} biotite foliation. S_E curves around the K-feldspar₁ porphyroblasts. Early granitic melts with K-feldspar₂, on the one hand, cut the S_E foliation; on the other hand, S_E curves around the melt patches (Appendix-Fig. 5-4a). On the outcrop these melt patches are S_E -parallel, boudinaged granite veins, considered to be syntectonic with D_E . The D_E is characterized by intense boudinage of competent layers (Appendix-Figs. 5–2a and 5–4c). C. 50% shortening during D_E can roughly be estimated from bent primary layers surrounding a rotated, pre-early D_E , extensional quartz vein (Appendix-Fig. 5-4b). Isoclinal intrafolial folds parallel to bedding in quartzite that show a very weak axial



Appendix-Fig. 5-1. (a.) D_E deformed and sheared quartzite of the Jokela supracrustal association; microphoto in (d.). Scale bar is 12 cm in length in (a.). Junninkallio, Hyvinkää (Finnish grid coordinates KKJ2 2554.34E 6721.44N). (b.) Intraformational conglomerate of the Jokela supracrustal association. Width of the area of the figure is c. 0.5 m. Junninkallio NE, Hyvinkää (Finnish grid coordinates KKJ2 2554.70E 6721.70N). (c.) Primary depositional contact between Jokela quartzite and mica gneiss. Scale bar is 10 cm in length. (d.) Microphoto of Jokela quartzite; Qtz = quartz and Sil = sillimanite. Width of the area of the figure is c. 3 mm. Junninkallio, Hyvinkää (Finnish grid coordinates KKJ2 2554.76E 6721.73N). Photo (a.) by R. Niemelä and photos (b.)-(d.) by M. Pajunen.

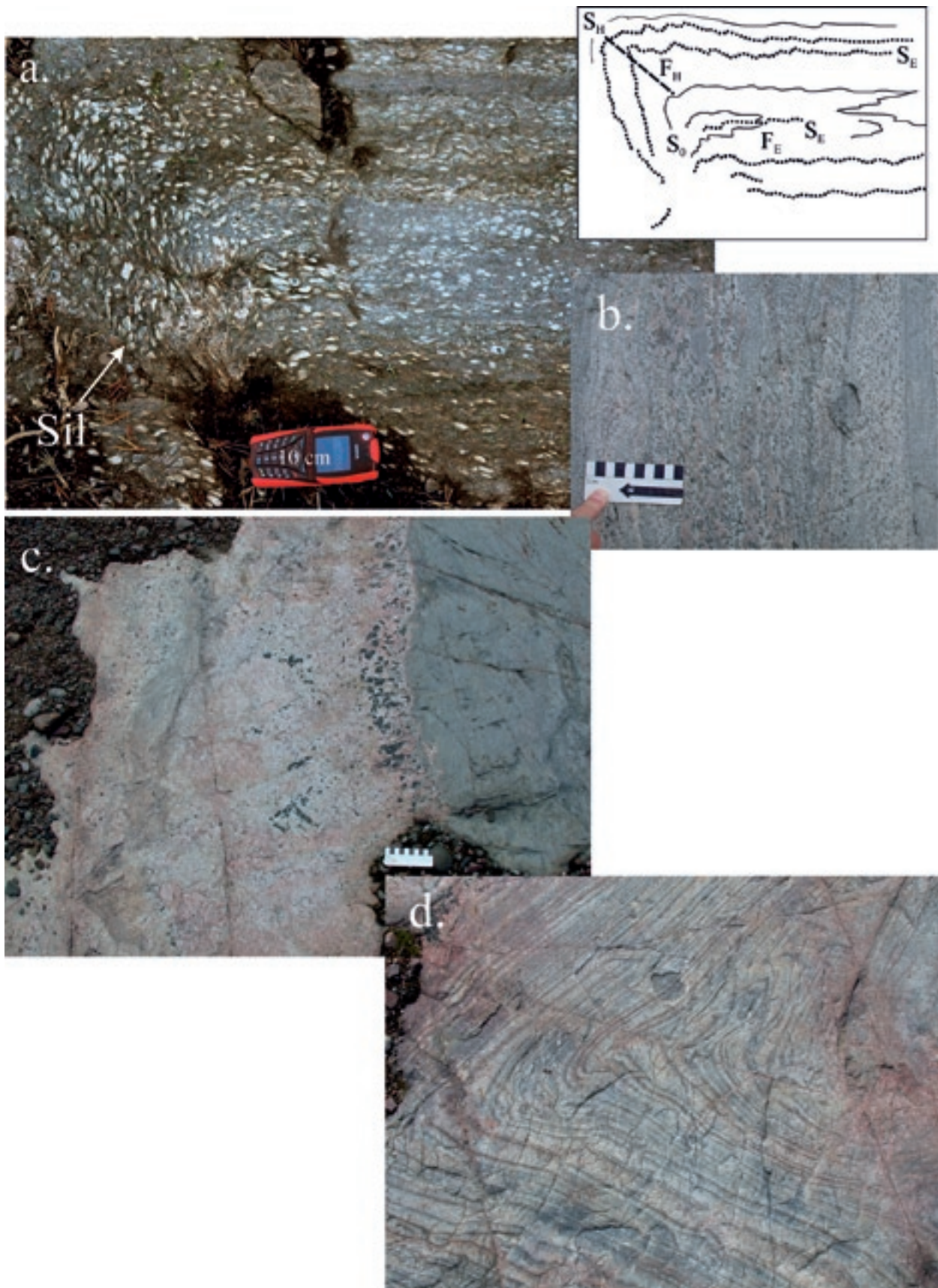


Appendix-Fig. 5-2. (a.) Detailed structures of the Jokela supracrustal association on the Kettukallio key outcrop in Hyvinkää (Finnish grid coordinates KKJ2 2553.54E 6721.45N). (b.) Pre-/syn- D_E folds deforming S_0 layering at Kettukallio. Width of the area of the figure is c. 0.5 m. Photo by M. Pajunen.

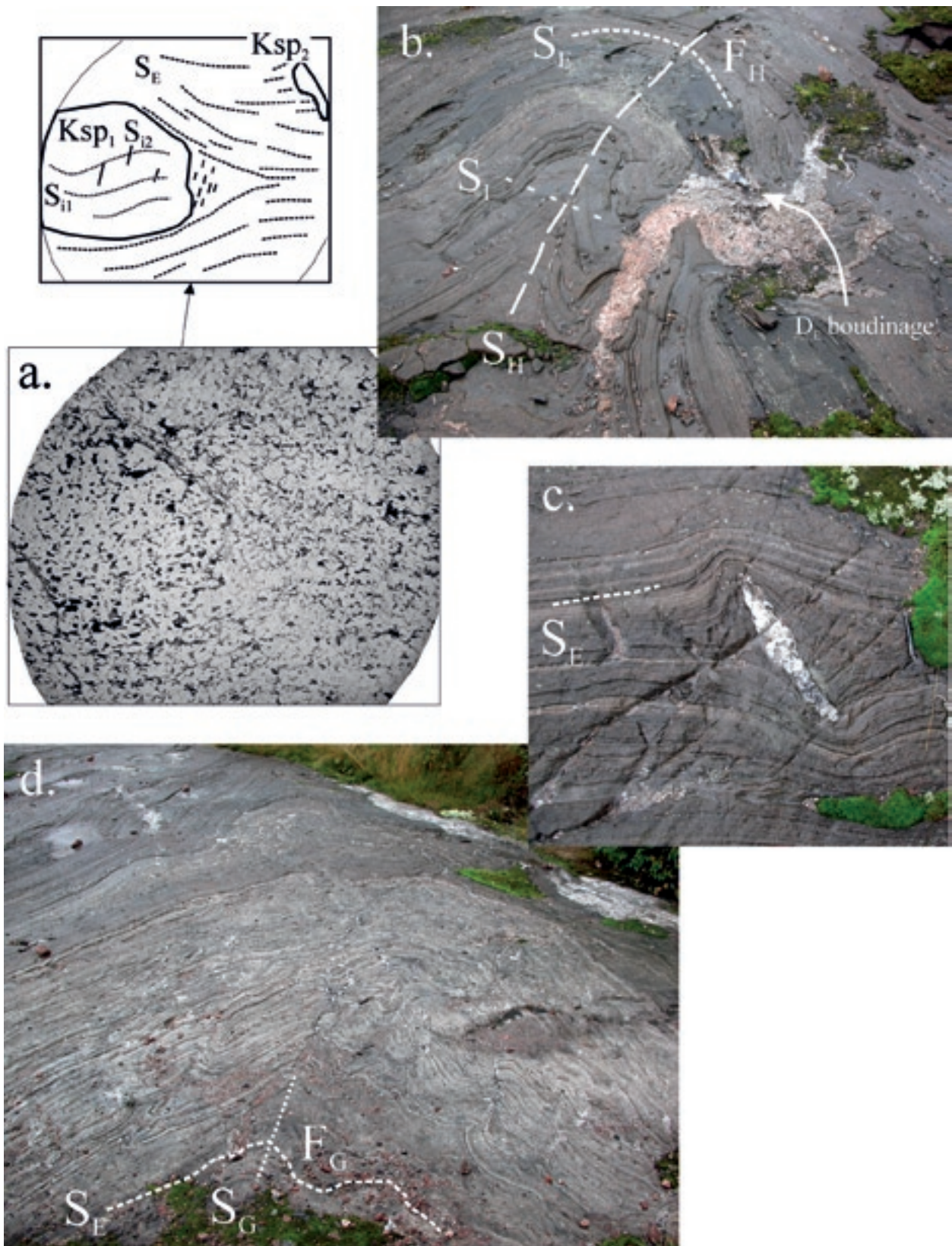
plane foliation are related to D_E (Appendix-Fig. 5-2a and b). In the pelitic sillimanite gneiss, sillimanite predominantly grew in the S_E plane (Appendix-Fig. 5-3a). An increase in temperature caused instability of biotite-sillimanite paragenesis, forming cordierite and melt. It is plausible that the early K-feldspar₁ was formed due to the breakdown of early muscovite.

The S_0 and S_E are folded by tight F_G with c. N-trending axial planes (Appendix-Figs. 5-2 and 5-4d). The S_G is a macro-crenulation with some granitic segregation in the foliation planes. The D_G synform structure in Appendix-Fig. 5-2a dips moderately towards the south, but no reliable observation of the top direction of bedding has been made. Dextral, tight F_H folds with NNW-trending axial planes refold the earlier structures (Appendix-Fig. 5-4b); S_H foliation is weak. In the pelitic layers, cordierite and some granitic melt was formed in the S_H plane; this indicates peak metamorphism during F_H folding. The intrusion of the pegmatitic granite dykes occurred during or after D_H . In places the previous structures are almost totally assimilated into granite (Appendix-Fig. 5-3c). The whole outcrop was openly refolded by c. E-W contraction during D_1 , which also caused dextral sliding along the granite contact. Localized dextral folds deforming the axial plane granite of D_H or S_{0+E} may belong to D_1 . The pegmatitic granite dykes show the same position in the structural sequence as the 1.8 Ga pegmatitic granite dyke described by Pajunen et al. (2008). When correlating the directions of structures to the surrounding areas, the D_{G-H} structures were rotated c. 90° anticlockwise. This rotation is considered to be caused by the D_1 deformation; the Jokela association is located in close association with the strong F_1 axial zone (Figure 11).

The tectono-metamorphic evolution in Jokela shows a one-stage prograde metamorphic event in the sillimanite and cordierite stability fields under low-pressure amphibolite facies conditions. It corresponds to that described from the Upper Tectonic Unit (Appendix 6), even though metamorphic mineral parageneses there indicate a higher grade. In the southern Svecofennian domain, corresponding supracrustal associations (yellow triangles in Figures 9) have undergone a similar tectonic-metamorphic evolution; they are closely associated with major crustal high-strain zones, especially their intersections, such as between the



Appendix-Fig. 5-3. (a.) Sillimanite-bearing mica schist in the Jokela supracrustal association. Junninkallio NE, Hyvinkää (Finnish grid coordinates KKJ2 2554.80E 6721.62N). (b.) Calcareous sediment within the Jokela supracrustal association. Scale bar is 10 cm in length. (c.) Jokela quartzite as a strongly assimilated fragment in the D_G pegmatitic granite dyke, which sharply cuts the volcanic rock of the same association. The relations with granite provide evidence that the quartzite predates the volcanic rock. Scale bar is 10 cm in length. (d.) A better-preserved part of the same quartzite as in the fragment shown in (c.). Polyphase folding of the primary layering, S_0 , predates the pegmatitic granite related to the D_H . Width of the area of the figure is c. 1 m. Figures (b-d.) = Latostenmaanmäki, Hyvinkää (Finnish grid coordinates KKJ2 2554.83E 6722.63). Photos by M. Pajunen.



Appendix-Fig. 5-4. Detailed structures on the Kettukallio key outcrop. Kettukallio, Hyvinkää (Finnish grid coordinates KKJ2 2553.54E 6721.45N). (a.) A microphoto showing the early internal foliation structures, S_{11} and S_{12} , in potassium feldspar, Ksp_1 , and their relations with S_E and syn- D_E neosome, Ksp_2 . Width of the area of the figure is c. 10mm. (b.) An S_E boudinage structure refolded by F_H . Width of the area of the figure is c. 1.5 m. (c.) A pre- D_E quartz vein surrounded by the bent S_E indicating c. 50% vertical shortening; some shear had occurred, as indicated by rotation of the quartz vein. Width of the area of the figure is c. 0.5 m. (d.) An F_G fold in felsic gneiss (impure sediment). Width of the area of the figure is c. 2 m. Photos by M. Pajunen.

Hyvinkää, Southern Finland or Hämeenlinna high-strain/shear zones and the major D_1 axial zones. Simonen (1987; also in Korsman et al. 1997) related the origin of supracrustal sedimentary-volcanic rocks of the Taalikkala inclusion in Vybörg rapakivi at Lappeenranta (Ta in Figure 8) to the rapakivi stage. We re-examined the samples collected during the regional mapping of GTK (Simonen 1987), because Simonen (op. cit.) described depositional discordance between the arkosic sediments overlain by volcanic sequences and Svecofennian granitoid of unknown age. According to the tectonic-metamorphic correlation the rocks correspond to the one-stage association in Jokela. Unfortunately, we were not able to re-investigate the depositional relationships in the field but, if the discordance observation is correct, further studies on the Taalikkala “roof pendant” could be helpful in understanding the stratigraphic position and depositional environment of these rocks.

Nironen and Lahtinen (2006) suggested an extensional rift-related shallow basin for the formation of the corresponding Pyhäntaka formation. Corresponding quartzites also exists in Sweden. The evolution from the D_D to D_{E-H} and finally to D_1 shows a very continued character. We suggest a rapid evolution of the supracrustal association and a tectonically-active, high-energy depositional environment as indicated by the intraformational conglomerates within the quartzite beds. We suggest that the depositional evolution of the whole Jokela sequence was related to the oblique dilatational events during the SW-NE transpression in the $D_{(D-)E}$ and SE-NW transpression in the D_H . The process was accompanied by crustal thinning and high heat flow, which culminated c. 1.85–1.84 Ga ago. Contractional $D_{E,cont}$ and $D_{H,cont}$ caused rapid folding during the progressive deformation. Extension caused upper crustal subsidence with rapid evolution of basins for sedimentation of high-energy sedimentary sequences. Quartzites were originally rather thin formations, which were thickened by the complex deformation multiplying the thickness of the quartzite sequence. These sediments were already folded when the later-stage volcanic sequences were generated (Appendix-Figs. 5-3c and d). The rapid subsidence was stepwise, which is evidenced by a rapid change from quartzite to impure sediment sedimentation (Appendix-Fig. 5-1c).

Pull-apart basins form restricted structures in transcurrent zones appropriate for the rapid accumulation of thick sediment deposits and contemporaneous volcanism (e.g. Kearey & Vine 1996 and Saalman et al. 2005). Such basins form during continuous tectonic evolution. In the study area they were related to thinning of the crust and increased the heat flow that may be related to the magmatic rocks of D_E in the deeper crustal levels. Suitable structures bordering such pull-apart basins include major crustal structures, like the E-W-trending Hämeenlinna, Hyvinkää and the southern Finland shear zones showing complex deformation histories. This large, originally ESE-trending pull-apart basin was formed between the major crustal deformation zones of the Riga Bay-Karelia Zone (RKZ) and Baltic Sea-Bothnian Bay Zone (BBZ), or the Transscandinavian Igneous Belt (TIB) (Figure 8).

Appendix 6. Structural characteristics of high-grade gneisses of the Upper Tectonic Unit (UTU) of the southern Svecofennian domain

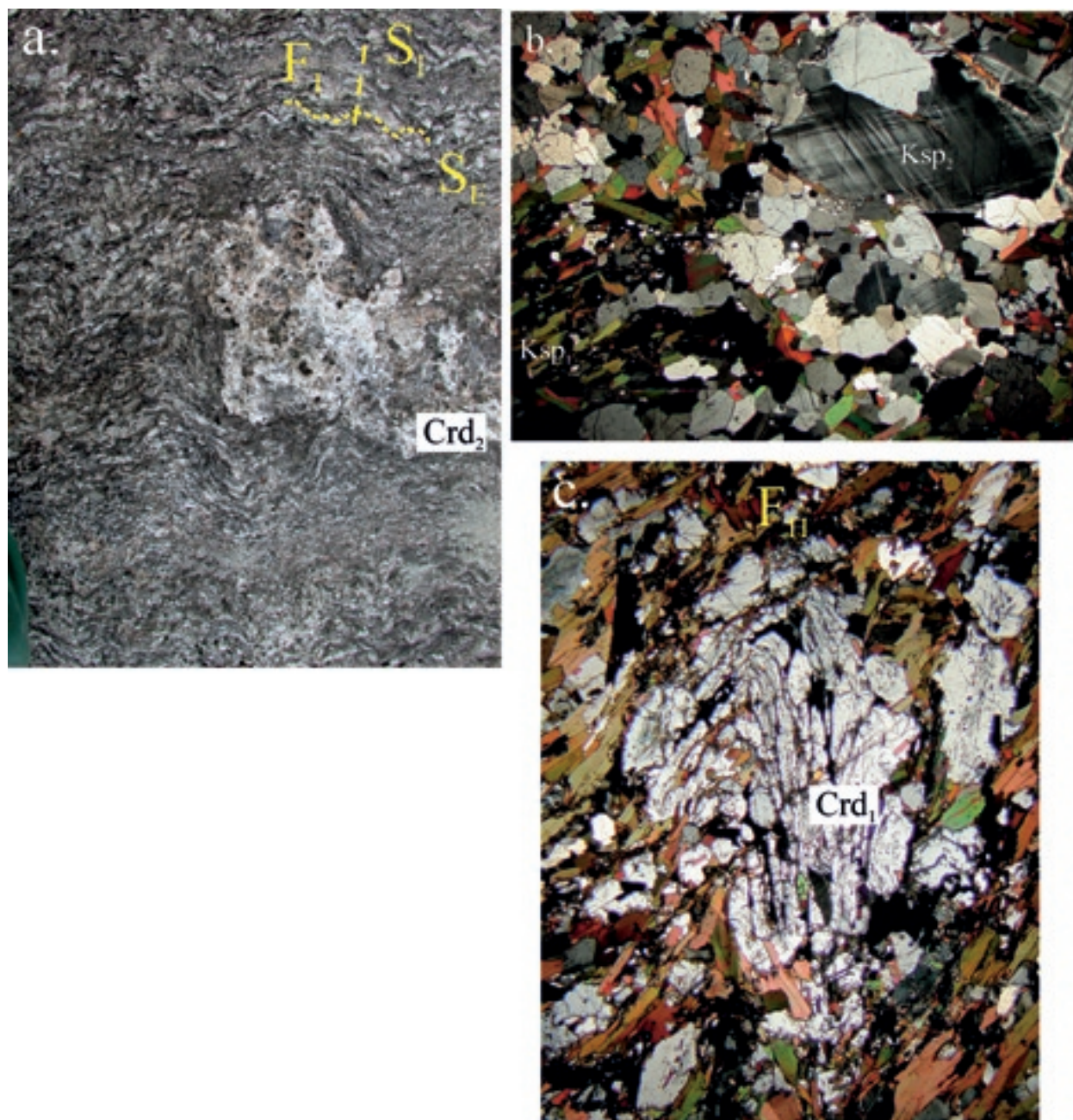
The rocks of the Hyvinkää Gabbroic-volcanic Belt (HGB) are squeezed between the large-scale D_{G+H+I} dome-and-basin structures in the Askola area. The volcanic and closely related sedimentary rocks of the HGB show structures that were already formed during the early stages of the Svecofennian orogeny; they show at least the D_B structures. However, there are also high-grade migmatitic metapelitic gneisses that do not show signatures of these early deformations in the study area, for example the Jokela supracrustal association. Structural evolutions of these rocks are exemplified from the Vuotavankalliot site in Mäntsälä (HGB) and the Matinojankallio site in Sipoo (EGC) (Appendix-Fig. 3-4).

Garnet-cordierite gneiss (Appendix-Fig. 6-1a) in the Vuotavankalliot site in Mäntsälä (Appendix-Fig. 3-4), to the north of the Askola dome area, is located within the gabbroic and volcanic rocks in the vicinity of the Hyvinkää-Lahti shear zone. The migmatitic gneiss is characterized by a spaced biotite foliation that overprints an earlier weak penetrative biotite foliation. The gneiss shows open to tight folds with NNE-trending axial planes, which deform both foliations and also the garnet- and cordierite-bearing melt patches in the gneiss. According to correlation with neighbouring areas, these folds are related to the F_1 folds. Early K-feldspar₁ that was formed by progressive metamorphism (by breakdown of muscovite?) includes two biotite generations, inclined towards each other, as an internal S_1 structure. The later foliation represents the main spaced foliation in the gneiss. During progressive metamorphism, biotite and sillimanite became unstable; cordierite₁ with sillimanite and spinel inclusions and K-feldspar₂ (Appendix-Fig. 6-1b) were formed. The cordierite₁ crystallized in the direction of the spaced foliation, which, however, curves around the porphyroblasts. Large melt patches including fresh cordierite₂, without sillimanite inclusions, garnet and a new K-feldspar₂ are also surrounded by the spaced cleavage, but their development continued after the active phase of that deformation because melt patches partly overgrew it. The K-feldspar₁ is slightly altered to sericite (K-feldspar₂ is not altered). The macro-crenulation in Appendix-Fig. 6-1a refolds all the structures described (Appendix-Fig. 6-1c) and is related to D_1 according to the orientation of the axial plane in a NNE direction. It shows a high-T and ductile character. The latest deformation is a semi-brittle shearing, which occurred in the andalusite stability field as indicated by small andalusite grains in these seams.

In general, the tectonic evolution of these gneisses is simpler than that described from migmatitic mica gneisses of the Southern Volcanic-sedimentary Belt (SVB) or the Espoo Granitoid Complex (EGC). The rock experienced only one important migmatization phase related to its continuous progressive mineral growth history, whereas several observations indicate at least two migmatization events occurring widely in the southern Svecofennian (cf. Pajunen et al. 2008 and Figures 22 and 36). We have not identified D_C and D_D fold patterns from the Vuotavankalliot gneiss. Often the spaced S_E foliation parallels S_0 referring to horizontal event. Due to correlation with neighbouring areas like the Espoo Granitoid Complex (EGC) and West Uusimaa Complex (WUC), we relate the spaced foliation, the strongest foliation in the rock, to the extensional deformation D_E . This interpretation is supported by progressive high-T/low-p metamorphism accompanied by granitic melts. There is only one weak deformation predating the D_E ; it has not been established whether it represents the early D_E or very weak deformation during the earliest stages (e.g. D_B ?) of crustal evolution, because the deposition age of the rock is not known. The original position of D_E structures was generally nearly horizontal; the steep position of D_E before F_1 folding indicates folding events (D_{G-H}) between the D_E and D_1 .

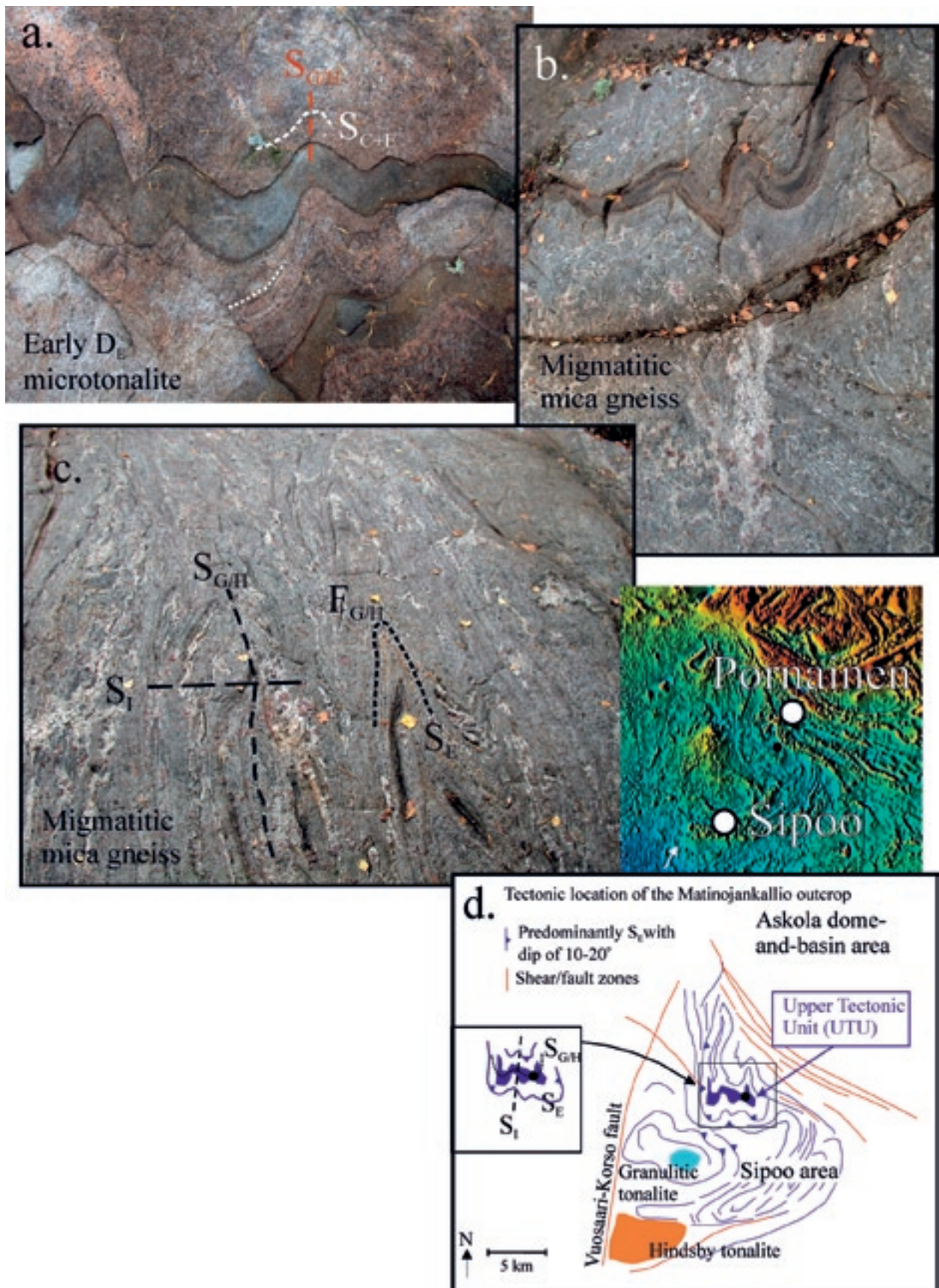
In Sipoo, at the Matinojankallio site, migmatitic garnet-cordierite gneisses (Appendix-Figs. 6-2b and c) are in close association with a syn-/late D_B tonalite (Appendix-Fig. 6-2a). Unfortunately, their contact was not exposed during mapping. The outcrop is located in the folded E-trending synformal structure. According to tectonic interpretation, the synform is overlying the high-grade tonalitic rocks exposed in an antiformal setting in the west (Appendix-Fig. 6-2d), in northern Sipoo (Si in Figure 9). Intermediate microtonalite dykes cut the tonalite and migmatitic gneiss and the rocks show a major tight folding phase with E-trending axial planes. The dyke contacts of the tonalite indicate intrusion into cooled rock with indistinct altered chilled margins (Appendix-Fig. 6-2a); the structures and relationships between the dyke and tonalite are quite similar to those described before, e.g. at Hindsby (Figure 24). A wide altered zone surrounds the dyke in the mica gneiss (Appendix-Fig. 6-2b) and its composition changes close to the dyke borders to garnet-rich. In the mica gneiss the wall rock-dyke reactions were strong and are interpreted to have resulted in intrusion into a lower-grade and more reactive rock.

The tectonic succession in mica gneiss (Appendix-Fig. 6-2c) resembles that in Vuotavankalliot (above). The mica gneiss has rather well preserved primary bedding and a strong prograde mineral foliation parallel



Appendix-Fig. 6-1. (a.) F_1 folds in S_E foliated garnet-cordierite gneiss from the Upper Tectonic Unit (UTU). Width of the area of the figure is c. 0.5 m. (b.) and (c.) show the microstructures of the gneiss; see text for details. Crd = cordierite and Ksp = potassium feldspar. Width of the area of the figure is (b.) is c. 4 mm and (c.) is c. 3 mm. Vuotavankalliot, Mäntsälä (Finnish grid coordinates KKJ2 2569.22E 6736.67N)). Photos by M. Pajunen.

to it. We relate the main foliation to the D_E deformation. The intermediate dyke intruded nearly parallel to the bedding planes, but the alteration zone surrounding the dyke overprints S_0 . The dyke has a S_E penetrative mineral foliation. Thus, we interpret the dyke to be intruded during early D_E . The main foliation S_E intensified during a continuing temperature increase that also caused progressive migmatization. Only one prograde migmatization pulse finally producing garnet-bearing melt can be detected. At least three post- D_E fold generations occurred. We relate the folds with E-trending axial planes to D_G , which was refolded by F_H forming the D_{G+H} synform; the synform was openly bent by later F_1 folding with NNW-trending axial planes. Migmatization began to develop in the S_E planes and achieved its peak during D_H ; the coarse melt fractions were intruded into the S_H axial planes. The contact between the tonalite and gneiss must be in this case tectonic and formed pre-/early D_E .



Appendix-Fig. 6-2. (a.) An intermediate D_E microtonalite dyke cutting the syn-/late D_B tonalite. Width of the area of the figure is c. 1.5 m. (b.) The same dyke is cutting the migmatitic garnet-bearing mica gneiss (Upper Tectonic Unit, UTU), showing a wide alteration rim and garnet-bearing contact zone; width of the area of the figure is c. 1.5 m. The folding pattern in the outcrop (c.) is interpreted from the tectonic data and aeromagnetic map (inset) as a part of regional tectonic pattern in (d.). Width of the area of the figure is c. 2 m. Matinojankallio, Sipoo (Finnish grid coordinates KKKJ2 2572.72E 6703.64N). Photos by M. Pajunen.

In summary, these high-grade gneisses show only one strong metamorphic event, without signs of pre-existing coarse-grained andalusite-metamorphism that characterizes the Vetio outcrop in the Orijärvi area (Appendix 4). The early tectonic history of these gneisses occurred in upper crustal level low-grade conditions and the peak of the progressive high-grade metamorphism was achieved during the late Svecofennian period. Tectonically, these mica gneisses are located in the large-scale F_{G+H+I} synforms. However, the high-grade mica gneisses in the D_{G+H+I} antiformal settings show a two-stage metamorphic character with two neosome phases (e.g. Pajunen et al. 2008). We include these gneisses into so-called Uppet Tectonic Unit (UTU). The UTU tectonic succession is very similar to that observed in the Jokela association (Appendix 5), which has a young deposition age. The age of the deposition of the mica gneisses is not known. The similarity to the Jokela association may support their coherent origins. This interpretation suggests that the late deep-water sediments were more widespread than was previously known, and these mica gneisses thus represent the later stage of the pull-apart basin sedimentation described from Jokela (Appendix 5).

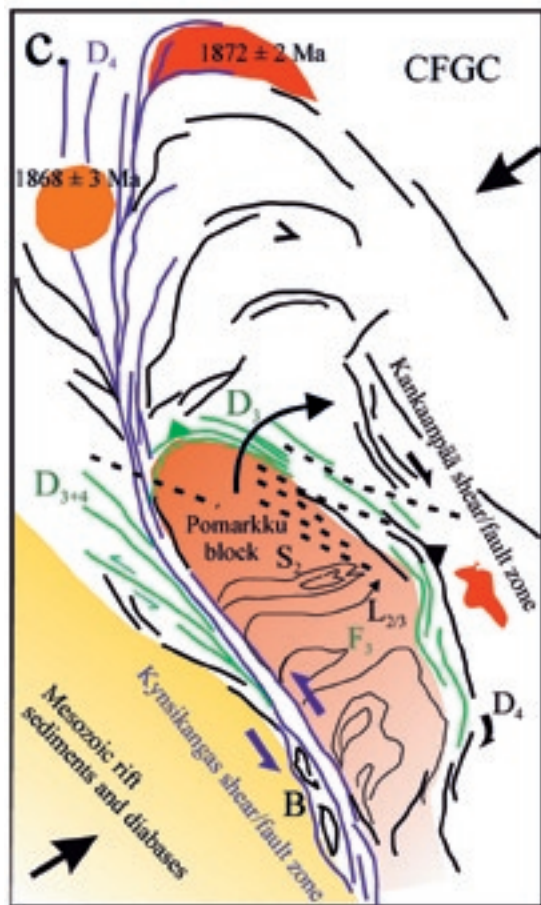
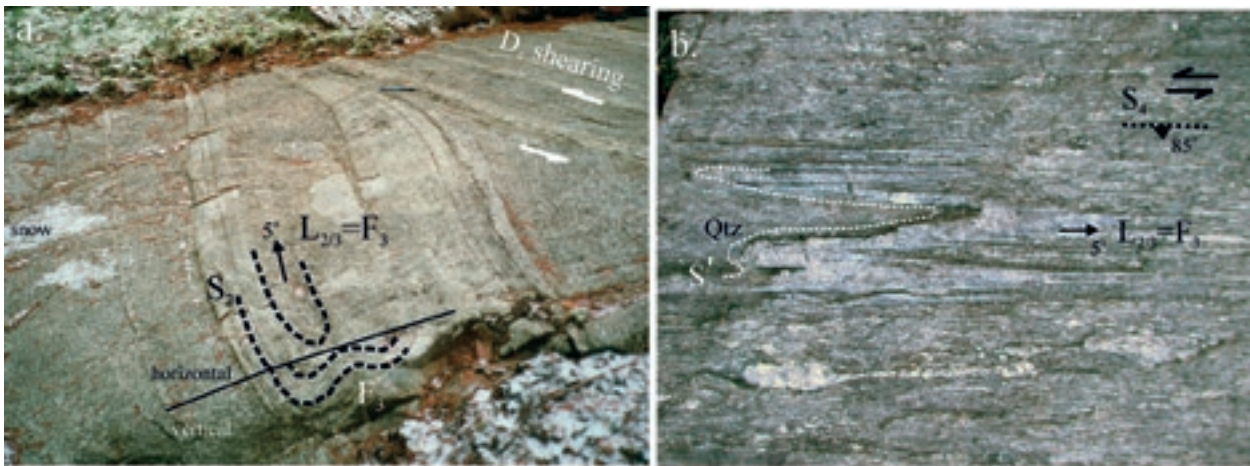
Appendix 7. Pomarkku block – key to the generation of stacked structures in central and eastern Finland

The tectonic setting of the Pomarkku block in the Pori area (Po in Figure 9; cf. Pietikäinen 1994 and Pajunen et al. 2001a), bordered by high-strain zones, is of key importance in analyzing the development of the NW-stacking and block structures of Central Finland; the Central Finland Granitoid Complex (CFGC) and the Savo Schist Belt (SSB). Similar characteristics can also be found in the geometries of the N-directional blocks in the Archaean domain (Figure 8).

The internal structure of the Pomarkku block is characterized by F_3 folding with E-trending axial planes (naming after Pajunen et al. 2001a) that deforms the subhorizontal D_2 structures. In the tonalite-dominant parts the F_3 folds are generally open with a weak upright S_3 foliation/crenulation. S_2 and S_3 intersection forms approximately horizontal, E-W-trending intersection lineation $L_{2/3}$. In the central part of the Pomarkku block, southwards-overtured F_3 folds indicate overthrusting towards the south along c. E-W trending shear zones (Pajunen et al. 2001a). At the southwestern edge of the Pomarkku block the D_3 structures are bent and crosscut by the steep 1–2 km wide Kynsikangas shear zone (Appendix-Fig. 7-1a) that turns from a NW to a N trend near the Bothnian coast. Rotation of porphyroblasts, drag folds and a strong horizontal stretching lineation (Appendix-Fig. 7-1b) in the amphibolite facies protomylonitic to mylonitic rocks indicate sinistral strike-slip movement (Pietikäinen 1994 and Pajunen et al. 2001a); Pajunen et al. (op. cit.) named the shearing phase as D_{3-late} . The Kynsikangas structure shows less prominent recrystallization and neomineralization than the earlier D_3 shear structures trending WNW in the Pori area, southwest of Kynsikangas. The zone shows polyphase deformation; it was still reactivated during the 1.5–1.6 Ga rapakivi granite event and the formation of the Satakunta sandstone basin. In the E-W-trending northern edge of the Pomarkku block the observations on drag folds and lineations dipping NE (cf. Pihlaja & Kujala 2005) indicate ductile sinistral oblique reverse top-to-SW movement. At the eastern margin of the Pomarkku block the E-W-trending D_3 structures are bent into the direction of the NW-trending Kankaanpää shear zone. This eastwards-bulging eastern border of the Pomarkku block (Appendix-Fig. 7-1c) shows drag folds and a moderate lineation plunging c. NE (Pajunen et al. 2001a), as well as oblique dextral movement in the zone.

The age of block forming deformation can be fixed by the quartz monzonites to north of the Pori area. The granitoid set into an arched structure, imitating the form of the northern edge of the Pomarkku block, (Figures 9 and Appendix-Fig. 7-1c) was dated at 1872 ± 2 Ma (Mäkitie & Lahti 2001); it is penetrating the earlier structure, but showing some signatures of deformation in the zone. However, the practically non-deformed Härkmeri quartz-monzonite dated at 1868 ± 3 Ma (Lehtonen et al. 2005) is cutting the Kynsikangas structure and causes a metamorphic contact aureole upon regional metamorphic parageneses, and fixes the end of the major deformation in the Tonalite Migmatite Belt (TMB). This intrusive, marking the end of the deformation in the north, gives approximately the same age as is obtained from the garnet-bearing tonalites that originated in the Southern Finland Granitoid Zone in the south, in the Espoo Granitoid Complex (EGC) (see the main text). Using structural and age correlation with the detailed study area we relate the strongest ductile phase shearing in the Kynsikangas zone to D_D deformation, D_4 in the north in the following (D_{3-late} of Pajunen et al. 2001a), which appears in the south as ductile folding with N-trending axial planes forming the D_{C+D} dome-and-basin structures. The sinistral sliding along the Kynsikangas and concomitant overthrusting of the Central Finland Granitoid Complex (CFGC) upon the Pomarkku block at its northern and eastern edges indicate c. SW-NE shortening during the D_D . Sinistral strike-slip movement in the Kynsikangas zone and sinistral oblique dip-slip movement at the northern edge and dextral oblique movement in the Kankaanpää zone refer to clockwise rotation of the Pomarkku block (Appendix-Fig. 7-1c). The model of clockwise rotation during dextral transpression along the major N-trending deformation zones, the Baltic Sea-Bothnian Bay Zone (BBZ) and Riga Bay-Karelia Zone (RKZ) (Figure 8) explains the tectonic development of the Pomarkku Block. It also accounts for the SW-trending dextral movement causing the bulbous structure of the Pomarkku block and the boudinage-like structures (B in Appendix-Fig. 7-1c) in the western side of the N-trending part of the Kynsikangas zone. The arched, 1872 ± 2 Ma intrusion was intruded into oblique dilatational settings during this transpressional deformation $D_{4/D}$.

Later movements were more concentrated in zones. To the south of the Pomarkku block, local zones of symmetrical to dextral asymmetrical folds with N-S-trending axial planes show some shearing in the axial direction (F_4 of Pajunen et al. 2001a). Correlation of these sporadic folds is uncertain: they may represent the F_D , F_F or even the F_1 folds. Open warps with N-S-trending axial planes, deforming the described structures and causing ovoidal interference structures, were named by Pajunen et al. (2001a) as F_x ; this interference pattern is similar to the D_{F-H} structures in the detailed study area. The final products of faulting,



Appendix-Fig. 7-1. (a.) Sinistral shearing bends the pre-existing structure, e.g. F_3 , into the direction of the Kynsikangas shear/fault zone. Pencil is 14 cm in length. (b.) Strong stretching lineation in the direction of the zone. Width of the area of the figure is c. 0.5 m. Levanpelto, Kullaa (Finnish grid coordinates KKJ1 1566.89E 6809.60N). (c.) A schematic model of the generation of the Pomarkku block in a SW-NE transpressional event that caused clockwise rotation of the Pomarkku block. The 1872 ± 2 Ma granitoid (Mäkitie & Lahti 2001) shows signatures of deformation in the Kynsikangas structure, but the 1868 ± 3 Ma granitoid (Lehtonen et al. 2005) cuts it.

especially close to the sandstone basin, are brittle pseudotachylites that sometimes have “vesicle” microstructures (Pajunen et al. 2001a).

Correlations with central and eastern Finland

The Archaean-Svecofennian border is characterized by major crustal NW- and N-trending shear zones of the Ladoga-Bothnia Bay zone (e.g. Talvitie 1971 and Korsman & Lestinen 2002). The major NW-trending zone is determined as a linear gravity low (Korhonen et al. 2002b) caused by shearing, granitization and granite magmatism (e.g. Pajunen 1986 and Pääjärvi 1991). The zone shows polyphase cataclastic characteristics. NW-trending zones are generally ductile dextral shear zones (e.g. Talvitie 1971); sometimes they also show sinistral strike-slip movement (D_c in Pajunen 1986). N-trending semi-ductile east-side-up dextral oblique shear/fault zones (D_d in Pajunen 1986) overprint the NW-trending shear zones. These NW- and N-trending shear zones overprint shear zones dipping with a low angle towards the SE (see also Kilpeläinen

2007) and cause the nearly-horizontal sliced structure that characterizes the Central Finland Granitoid Complex (CFGC) and the Savo Schist Belt (SSB). This structure is well defined in the magnetic anomaly pattern, especially near the Archaean-Proterozoic suture zone, but become less evident in the central parts of the CFGC. This stacked structure is also supported by the tectonic pattern of supracrustal remnants in the granitoid unit; the WNW-trend of the western extensions of the SSB, for example in the Rautalampi district (Ra in Figure 9) and in the Pyhäsalmi area towards the west, which are bent by the $D_{4/D}$ deformation.

The stacked and sheared structures in the Central Finland Granitoid Complex (CFGC) and further east show similarities to the structure of the Pomarkku block. The NW-trending dextral shearing structures can be explained by more N-S-oriented shortening than in the west, but the stress field later turned close to a NE-SW direction, as indicated by the dextral N-S faults (D_d of Pajunen 1986). The more brittle character of the N-S faults in Central Finland with respect to that in the west indicates earlier cooling and stabilization in Central Finland. We suppose that the NW-stacked, low-angle structure was formed by overthrusting towards the north during the collisional event corresponding to the D_3 deformation in the Pomarkku Block; the NW-trending shear zones could have formed contemporaneously. Lahtinen and Huhma (1997) separated two different magmatic series due to their Sm-Nd characteristics: the earlier, ca 1.888 Ga old granitoids show more primitive characteristics, whereas the later pulse show signatures from re-melted pre-existing crust. The later granitoids in the CFGC follow the arced structures: the post-/late orogenic granitic intrusion in Figure 9 (see also Nironen 2003). We proposed their emplacement into oblique dilatation zones related to the overall SW-NE-trending $D_{4/D}$ transpression. They were intruded especially into the E-W-trending, originally contractional low-angle zones (D_c) that turned to extensional during the later evolution ($D_{4/D}$). These granitoids were effectively destroying the earlier low-angle SE-dipping features of the CFGC. The collisional stage in areas close to the Archaean-Proterozoic boundary zone had already proceeded far before the intrusion of 1884 ± 5 Ma orthopyroxene-bearing granitoids (Hölttä 1988), because their contact cut the regional metamorphic parageneses and contractional F_3 folding (Hölttä et al. 1988 and Korsman et al. 1999); these granitoids represent the end of the main thermal events near the craton boundary. However, in western Finland, corresponding orthopyroxene-bearing granitoids have ages of 1871 ± 2 to 1868 ± 3 Ma. As noted, the later magma phase determines the major stacking and folding structures in this area, and indicates c. 10–15 Ma later stabilization with respect to the craton boundary. According to Koistinen (1981), the N-trending D_3 , labelled later as syn- D_4 (Koistinen et al. 1996) (D_f of this paper), was dated in eastern Finland with the syn- D_4 Maarianvaara granite at c. 1857 ± 8 Ma old (Huhma 1986). The development of these structures, and magma and metasomatic pulses in these times (cf. Pajunen & Poutiainen 1999) establishes the continuity of deformation and heat flow. However, in the northern units it was more divided and local at this stage.

Appendix 8. Multigrain TIMS U-Pb isotopic dating of zircon and monazite, and SIMS dating of zircon

SAMPLES

Samples A1738 Staffas (syn-/late D_B tonalite, Hindsby intrusion; SIMS), A1676 Bollstad (syn-/late D_B tonalite; TIMS & SIMS), A1785 Hakkila (early D_E garnet-bearing tonalite), A1784 Hyrylä (early D_E garnet-bearing tonalite/granite), A1335 Maikkala (pyroxene-bearing tonalite, charnockite), A1745 Jyskelä (late D_E gabbro; TIMS & SIMS), A1677 Bollstad (D_H pegmatitic granite; TIMS) and A1678 Kopparnäs (D_H diabase; TIMS & SIMS). The Samples were collected in the project “Construction potential modeling of bedrock in urban areas” during 1999–2002, except for the sample A1335 Maikkala, which was collected by K. Korsman (unpublished report by H. Huhma 3.2.94/GSF/Petrological Department/Isotope Geology Division); the original data have been recalculated here.

ANALYTICAL METHODS

The digestion of zircon and extraction of U and Pb for TIMS isotopic age determinations mainly follows the procedure described by Krogh (1973). ²³⁵U–²⁰⁸Pb (zircon) or ²³⁵U–²⁰⁶Pb (monazite) spiked and non-spiked isotopic ratios were measured using a VG Sector 54 TIMS (Thermal Ionization multicollector Mass Spectrometer). The measured lead and uranium isotopic ratios were normalized to the accepted ratios of SRM 981 and U500 standards. The U-Pb age calculations were done using the PbDat-program (Ludwig 1991) and the fitting of the discordia lines using the Isoplot/Ex program (Ludwig 2001). Further information is given in App-Table 1.

For ion microprobe dating (NORDSIM Project#: N04-FI-12), the selected zircon grains were mounted in epoxy, polished, and coated with gold. The ion microprobe U-Pb analyses were carried out using the Nordic Cameca IMS 1270 at the Swedish Museum of Natural History, Stockholm, Sweden. The spot-diameter for the 4nA primary O₂⁻ ion beam was c. 25 µm and oxygen flooding in the sample chamber was used to increase the production of Pb⁺ ions. Three counting blocks, each including four cycles of the Zr, Pb, Th, and U species of interest, were measured from each spot. The mass resolution (M/ΔM) was 5400 (10%). The raw data were calibrated against a zircon standard (91500; Wiedenbeck et al. 1995) and corrected for background at mass 204.2 and modern common lead (T = 0; Stacey and Kramers 1975). For the detailed analytical procedure see Whitehouse et al. (1997 and 1999). The plotting of the U-Pb data and calculating of the concordia and intercept ages were performed using the Isoplot/Ex 3 program (Ludwig 2003). The data-point error ellipses in the concordia diagrams are 2 sigma. All the errors in age results are 2 sigma and calculated ignoring the decay constant errors. The results are compiled in App-Table 2.

SAMPLES, ZIRCON DESCRIPTIONS AND U-PB AGE RESULTS

A1738 Staffas, Sipoo – syn-/late D_B tonalite

Finnish grid coordinates KJ2 2568.79E 6694.48N

SIMS, zircon, NORDSIM sample number n1660, mount number M561 (large grains)

Sample information

Sample A1738 from Staffas in Sipoo, from the wide and homogeneous Hindsby intrusion (Figures 24 and 25), was analyzed to establish the isotopic age of the typical, structurally-fixed syn-/late D_B tonalite intrusion. The tectonic antiformal setting of the Hindsby intrusion is presented in Appendix-Fig. 6-2d, and the details of its structural evolution are discussed in the main text. The tonalite is metamorphosed with the main mineral assemblage plagioclase, quartz, biotite with minor garnet and pyroxene. Pyroxene is decomposed to clinoamphibole, and biotite is locally chloritized.

App-Table 1. Multigrain TIMS U-Pb isotopic data on zircons and monazites. Samples A1676 Bollstad tonalite, A1335 Maikkala charnockite, A1745 Jyskelä gabbro, A1677 Bollstad pegmatite and A1678 Kopparnäs diabase.

Sample information	Sample weight/mg	U ppm	Pb ppm	$^{206}\text{Pb}/^{204}\text{Pb}$ measured	$^{206}\text{Pb}/^{206}\text{Pb}$ radiogenic	$^{206}\text{Pb}/^{238}\text{U}$	2SE-%	ISOTOPIC RATIOS ¹⁾	2SE-%	$^{207}\text{Pb}/^{235}\text{U}$	Rho ²⁾	2SE-%	APPARENT AGES / Ma±2 sigma	$^{206}\text{Pb}/^{238}\text{U}$	$^{207}\text{Pb}/^{235}\text{U}$	$^{207}\text{Pb}/^{206}\text{Pb}$
A1676 Bollstad tonalite																
A) Zircon d>4.3 g cm ⁻³ , >75µm, short prismatic, l:w=2.5-5, light coloured, abraded 7h	0.61	299	91	3994	0.06	0.2969	0.65	4.619	0.65	0.1128	0.97	0.15	1753	1676	1753	1846±3
B) Zircon d>4.3 g cm ⁻³ , >75µm, short prismatic, l:w=2.5-5, light coloured	0.55	479	137	1516	0.06	0.2755	0.65	4.264	0.65	0.1123	0.97	0.15	1687	1569	1687	1837±3
C) Zircon d>4.3 g cm ⁻³ , <75µm, short prismatic, l:w=2.5-5, light coloured, abraded 6h	0.49	473	145	5293	0.05	0.3027	0.65	4.708	0.65	0.1128	0.97	0.15	1769	1705	1769	1845±3
D) Zircon d>4.3 g cm ⁻³ , <75µm, short prismatic, l:w=2.5-5, light coloured	0.41	530	156	1641	0.05	0.2855	0.65	4.436	0.65	0.1127	0.97	0.15	1719	1619	1719	1843±3
E) Monazite: fine-grained, oval-shaped, abraded 1/4 h	0.17	3506	4788	21173	3.68	0.3291	0.95	5.072	0.96	0.1118	0.99	0.15	1832	1834	1832	1829±3
A1335 Maikkala charnockite³⁾																
A) Zircon d: 4.3-4.5 g cm ⁻³ , >75 µm, abraded	7.6	541	169	9660	0.05	0.3117	0.65	4.863	0.65	0.1131	0.97	0.15	1795	1749	1795	1850±3
B) Zircon d: 4.3-4.5 g cm ⁻³	6.3	498	159	10250	0.05	0.3195	0.65	4.988	0.65	0.1133	0.97	0.15	1817	1787	1817	1852±3
C) Zircon d: 4.2-4.3 g cm ⁻³	8.1	626	196	7001	0.05	0.3103	0.65	4.824	0.65	0.1128	0.97	0.15	1789	1742	1789	1844±3
D) Zircon d: 4.3-4.5 g cm ⁻³ , <75 µm, abraded 5h	6.7	534	171	7622	0.05	0.3182	0.65	4.972	0.65	0.1133	0.97	0.15	1814	1781	1814	1853±3
F) Zircon d: 4.3-4.5 g cm ⁻³ , >75 µm, abraded	6.7	536	168	10447	0.05	0.3125	0.65	4.878	0.65	0.1132	0.97	0.15	1798	1753	1798	1851±3
G) Zircon d: 4.0-4.2 g cm ⁻³ , >75 µm	7.8	905	242	3613	0.06	0.2645	0.65	4.061	0.65	0.1114	0.97	0.15	1646	1512	1646	1821±3
E) Monazite	1.9	896	5207	10811	19.44	0.3258	0.65	5.045	0.65	0.1123	0.97	0.15	1826	1818	1826	1837±3
A1745 Jyskelä gabbro																
A) Zircon d>4.2 g cm ⁻³ , >75 µm, brown, transparent, subhedral-anhedral, elongated, abraded 8 h	0.42	951	330	8990	0.13	0.3223	0.65	4.984	0.65	0.1122	1	0.15	1801	1801	1817	1835±3
B) Zircon d>4.2 g cm ⁻³ , <75 µm, brown, transparent, subhedral-anhedral, elongated, abraded 1 h	0.32	830	285	5291	0.13	0.3180	0.65	4.896	0.65	0.1117	1	0.15	1802	1780	1802	1827±3
C) Zircon d: 4.2-4.0 g cm ⁻³ , >75 µm, brown, transparent, subhedral-anhedral, elongated, abraded 8 h	0.35	1393	464	4181	0.12	0.3120	0.65	4.793	0.65	0.1114	1	0.15	1784	1750	1784	1823±3
D) Zircon d: 4.2-4.0 g cm ⁻³ , <75 µm, brown, transparent, subhedral-anhedral, elongated, abraded 1 h	0.40	1340	447	4392	0.12	0.3109	0.65	4.778	0.65	0.1114	1	0.15	1781	1745	1781	1823±3

Sample information		Sample weight/mg	U ppm	Pb ppm	$^{206}\text{Pb}/^{204}\text{Pb}$ measured	$^{206}\text{Pb}/^{206}\text{Pb}$ radiogenic	$^{206}\text{Pb}/^{238}\text{U}$	ISOTOPIIC RATIOS ¹⁾		APPARENT AGES / $\text{Ma} \pm 2 \text{ sigma}$					
Analysed mineral and fraction								$^{207}\text{Pb}/^{235}\text{U}$	2SE%	$^{206}\text{Pb}/^{238}\text{U}$	2SE%	Rho ²⁾	$^{206}\text{Pb}/^{238}\text{U}$	$^{207}\text{Pb}/^{235}\text{U}$	$^{207}\text{Pb}/^{206}\text{Pb}$
A1677 Bollstad pegmatite															
A) Zircon d: 4.0–3.8 g cm ⁻³ , >150 µm, prismatic, dark brown, abraded 2 lh	0.48	3693	951	7952	0.01	0.2648	0.65	3.990	0.65	0.1093	0.15	0.97	1514	1632	1789±3
B) Zircon d: 4.0–3.8 g cm ⁻³ , 150–75 µm, prismatic, dark brown, abraded 18h	0.42	3443	882	9011	0.01	0.2642	0.65	3.987	0.65	0.1094	0.15	0.97	1512	1632	1790±3
C) Zircon d: 4.0–3.8 g cm ⁻³ , <75 µm, prismatic, dark brown, abraded 12h	0.52	3721	964	4324	0.01	0.2651	0.65	4.003	0.65	0.1095	0.15	0.97	1516	1635	1792±3
D) Zircon d>4.0 g cm ⁻³ , >75 µm, prismatic, dark brown, abraded 4h	0.17	5116	1305	4711	0.01	0.2612	0.65	3.935	0.65	0.1093	0.15	0.97	1496	1621	1788±3
E) Zircon d>4.0 g cm ⁻³ , >75 µm, prismatic, dark brown	0.24	3249	832	2561	0.02	0.2585	0.65	3.889	0.65	0.1091	0.15	0.97	1482	1611	1785±3
F) Zircon d: 4.0–3.8 g cm ⁻³ , <75 µm, prismatic, dark brown	0.42	3255	820	1750	0.02	0.2516	0.65	3.781	0.65	0.1090	0.15	0.97	1447	1589	1782±3
G) Monazite: coarse-grained, euhedral-subhedral, abraded 1/4 h	0.22	6273	1.07 %	47968	4.87	0.3298	0.97	5.081	0.97	0.1117	0.06	0.99	1838	1833	1828±1
A1678 Kopparnäs diabase															
A) Zircon d>4.0 g cm ⁻³ , <75 µm, elongated, bright, light coloured, abraded 4h	0.48	443	144	2188	0.14	0.2956	0.65	4.508	0.65	0.1106	0.15	1	1669	1733	1810±3
B) Zircon d>4.0 g cm ⁻³ , <75 µm, elongated, bright, light coloured, abraded 3h	0.07	614	204	1283	0.13	0.3006	0.65	4.602	0.65	0.1110	0.15	1	1694	1750	1816±3
C) Zircon d>4.0 g cm ⁻³ , >75 µm, elongated, bright, light coloured, abraded 3h	0.05	511	180	634	0.15	0.3027	0.65	4.632	0.65	0.1110	0.15	1	1705	1755	1816±3

¹⁾ Isotopic ratios corrected for fractionation, blank (30–50 pg), and age related common lead (Stacey and Kramers, 1975; $^{206}\text{Pb}/^{204}\text{Pb} \pm 0.2$; $^{207}\text{Pb}/^{206}\text{Pb} \pm 0.1$; $^{206}\text{Pb}/^{206}\text{Pb} \pm 0.2$). ²⁾ Rho=Error correlation between $^{207}\text{Pb}/^{235}\text{U}$ and $^{206}\text{Pb}/^{238}\text{U}$ ratios. ³⁾ Analyses by H.Huhma; blank 0.5 ng.

App-Table 2. SIMS U-Pb isotopic data on zircons. Samples from Uusimaa area, southern Finland.

Sample/ spot #	Spot site on zircon, zircon type	²⁰⁷ Pb ²⁰⁶ Pb	±s	²⁰⁷ Pb ²³⁸ U	±s	²⁰⁶ Pb ²³⁸ U	±s	²⁰⁷ Pb ²⁰⁶ Pb	±s	²⁰⁷ Pb ²³⁵ U	±s	²⁰⁶ Pb ²³⁸ U	±s	²⁰⁷ Pb ²³⁵ U	±s	r	Disc. %	[U] ppm	[Th] ppm	[Pb] ppm	Th/U meas	²⁰⁶ Pb/ ²⁰⁴ Pb measured	
A1738 Staffas tonalite (n1660)																							
n1660-01a	quite homog, long prismatic	1879	4	1892	12	1904	22	0.1149	0.2	5.445	1.3	0.3436	1.3	0.99	0.99	1453	282	585	0.19			1.79E+05	
n1660-02a	weakly zoned, short prismatic	1836	3	1842	11	1847	21	0.1122	0.2	5.134	1.3	0.3317	1.3	0.99	0.99	832	54	312	0.06			2.98E+04	
n1660-03a	quite homog, long prismatic	1837	4	1835	12	1838	21	0.1120	0.2	5.096	1.4	0.3300	1.3	0.98	0.98	522	29	194	0.06			8.54E+05	
n1660-04a	weakly zoned, short prismatic, healthy	1797	4	1802	11	1807	21	0.1098	0.2	4.898	1.3	0.3234	1.3	0.99	0.99	719	105	268	0.15			1.35E+03	
n1660-05a	zoned, short prismatic	1851	6	1842	12	1834	21	0.1132	0.3	5.134	1.4	0.3291	1.3	0.97	0.97	401	47	151	0.12			7.21E+03	
n1660-06a	weakly zoned, short prismatic	1839	8	1854	12	1867	22	0.1124	0.5	5.207	1.4	0.3358	1.3	0.94	0.94	486	70	188	0.14			1.04E+03	
n1660-07a	quite homog(dark), prismatic	1849	5	1843	12	1839	21	0.1130	0.3	5.144	1.4	0.3301	1.3	0.98	0.98	549	57	207	0.10			3.69E+03	
n1660-08a	(incl. secondary zr phase) <i>zoned, prismatic</i>	1851	19	1808	15	1771	21	0.1132	1.1	4.934	1.7	0.3161	1.3	0.78	0.78	614	71	222	0.12			8.23E+02	
n1660-09a	quite homog, pale outer domain, short prismatic	1806	6	1824	12	1839	21	0.1104	0.3	5.025	1.4	0.3300	1.3	0.97	0.97	484	73	184	0.15			1.94E+03	
n1660-09b	<i>dark inner domain, short prismatic</i>	1927	32	1897	19	1870	22	0.1180	1.8	5.478	2.2	0.3365	1.3	0.60	0.60	81	28	33	0.34			4.39E+02	
n1660-10a	quite homog., prismatic	1851	5	1856	12	1860	21	0.1132	0.3	5.221	1.4	0.3345	1.3	0.98	0.98	422	47	162	0.11			7.24E+04	
n1660-11a	quite homog, pale outer domain, prismatic	1867	7	1845	12	1825	21	0.1142	0.4	5.152	1.4	0.3271	1.3	0.96	0.96	693	78	260	0.11			1.05E+03	
n1660-11b	dark, zoned inner domain (dark), prismatic	1960	9	1947	13	1935	22	0.1202	0.5	5.804	1.4	0.3501	1.3	0.93	0.93	145	68	63	0.47			9.28E+03	
n1660-12a	weakly zoned, prismatic	1868	5	1864	12	1861	21	0.1143	0.3	5.272	1.4	0.3347	1.3	0.98	0.98	438	31	167	0.07			6.69E+04	
n1660-13a	<i>quite homog, pale tip domain, prismatic</i>	1864	21	1883	16	1904	24	0.1140	1.2	5.399	1.9	0.3436	1.4	0.78	0.78	547	30	210	0.05			2.71E+02	
n1660-13b	<i>quite homog, dark inner domain, prismatic</i>	1866	11	1844	12	1825	21	0.1141	0.6	5.148	1.5	0.3272	1.3	0.91	0.91	425	52	158	0.12			4.56E+02	
n1660-14a	quite homog, prismatic	1880	4	1886	12	1891	22	0.1150	0.2	5.405	1.3	0.3409	1.3	0.99	0.99	940	188	377	0.20			6.89E+04	
n1660-15a	zoned, prismatic	1838	5	1830	12	1823	21	0.1124	0.3	5.065	1.4	0.3269	1.3	0.98	0.98	450	47	168	0.10			9.78E+03	
n1660-16a	weakly zoned, prismatic	1865	3	1921	12	1973	23	0.1141	0.2	5.631	1.3	0.3581	1.3	0.99	0.99	1561	119	634	0.08			2.48E+05	
n1660-17a	<i>zoned (hit on fracture), prismatic</i>	1802	18	1631	14	1502	18	0.1101	1.0	3.985	1.7	0.2624	1.3	0.80	0.80	180	36	55	0.20			4.00E+02	
n1660-18a	<i>weakly zoned, dark, prismatic</i>	1838	17	1808	14	1782	21	0.1123	0.9	4.933	1.6	0.3185	1.3	0.82	0.82	382	39	138	0.10			4.13E+02	
A1784 Hyrylä granite dyke (n1661)																							
n1661-01a	quite homog, short prismatic	1852	7	1849	12	1847	21	0.1132	0.4	5.179	1.4	0.3317	1.3	0.96	0.96	381	227	162	0.60			3.21E+04	
n1661-02a	quite homog, prismatic	1862	5	1860	12	1859	22	0.1138	0.3	5.247	1.4	0.3343	1.3	0.98	0.98	314	94	126	0.30			6.37E+04	
n1661-03a	quite homog, prismatic	1864	6	1852	12	1841	21	0.1140	0.3	5.194	1.4	0.3306	1.3	0.97	0.97	275	124	113	0.45			1.90E+05	
n1661-04a	homog pale outer domain/rim, prismatic	1860	4	1771	11	1696	20	0.1137	0.2	4.720	1.3	0.3009	1.3	0.99	0.99	1423	261	500	0.18			6.72E+03	
n1661-04b	quite homog dark inner domain/core, prismatic	1921	7	1852	12	1791	21	0.1176	0.4	5.194	1.4	0.3202	1.3	0.96	0.96	210	60	80	0.28			1.00E+04	
n1661-05a	quite homog, prismatic	1863	4	1867	12	1871	22	0.1139	0.2	5.289	1.3	0.3367	1.3	0.99	0.99	524	289	224	0.55			5.58E+04	
n1661-06a	homog, long prismatic	1865	5	1864	12	1864	22	0.1141	0.3	5.272	1.4	0.3352	1.3	0.98	0.98	438	229	185	0.52			6.74E+04	
n1661-07a	homog darker inner domain, stubby rounded grain with paler outer domain	1840	7	1846	12	1851	22	0.1125	0.4	5.158	1.4	0.3326	1.3	0.96	0.96	189	129	82	0.68			4.23E+04	
n1661-08a	homog darker inner domain, stubby rounded grain with paler outer domain	1857	8	1852	12	1848	21	0.1136	0.4	5.197	1.4	0.3319	1.3	0.95	0.95	243	78	97	0.32			1.12E+05	
n1661-09a	homog darker inner domain, stubby rounded grain with paler outer domain	1861	6	1861	12	1861	22	0.1138	0.4	5.253	1.4	0.3347	1.3	0.97	0.97	266	113	110	0.43			1.04E+05	
n1661-10a	quite homog dark, short prismatic	1854	6	1859	14	1864	27	0.1134	0.3	5.241	1.7	0.3353	1.6	0.98	0.98	291	179	126	0.62			2.54E+04	
n1661-11a	quite homog dark, long prismatic	1857	5	1846	14	1836	26	0.1136	0.3	5.160	1.7	0.3295	1.6	0.98	0.98	606	242	245	0.40			4.71E+03	
n1661-12a	weakly zoned dark, prismatic	1944	9	1932	15	1921	27	0.1192	0.5	5.706	1.7	0.3472	1.6	0.95	0.95	155	88	69	0.57			5.88E+03	
n1661-13a	quite homog dark, prismatic	1852	6	1808	14	1770	25	0.1132	0.4	4.933	1.7	0.3160	1.6	0.98	0.98	421	198	166	0.47			5.23E+03	
n1661-14a	weakly zoned dark, prismatic	1861	4	1855	14	1849	26	0.1138	0.2	5.213	1.6	0.3323	1.6	0.99	0.99	537	316	229	0.59			9.69E+04	
n1661-15a	homog, round grain	1872	6	1870	14	1869	27	0.1145	0.3	5.308	1.7	0.3363	1.6	0.98	0.98	257	90	105	0.35			8.88E+04	
n1661-16a	homog paler outer domain, short prismatic	1862	3	1888	14	1912	27	0.1139	0.1	5.420	1.6	0.3452	1.6	1.00	1.00	1595	132	635	0.08			5.84E+04	
n1661-16b	homog darker inner domain, short prismatic	1975	4	2025	15	2074	29	0.1213	0.2	6.345	1.6	0.3794	1.6	0.99	0.99	2.2	2.2	330	279	0.59		1.37E+04	

Sample/ spot #	Spot site on zircon, zircon type	^{207}Pb ^{206}Pb	$\pm s$	^{207}Pb ^{235}U	$\pm s$	^{206}Pb ^{238}U	$\pm s$	^{207}Pb ^{206}Pb	$\pm s$	^{207}Pb ^{235}U	$\pm s$	^{206}Pb ^{238}U	$\pm s$	r	Disc. % 2s lim.	[U] ppm	[Th] ppm	[Pb] ppm	Th/U meas	$^{206}\text{Pb}/^{204}\text{Pb}$ measured
A1785 Hakikila tonalite (n1662)																				
n1662-01c	homog pale rim, stubby grain	1545	113	722	34	487	7	0.0958	6.3	1.036	6.4	0.0784	1.5	0.23	-36.0	2798	532	249	0.19	6.54E+02
n1662-01b	homog darker inner domain/core, stubby grain	1878	8	1900	12	1920	22	0.1149	0.4	5.497	1.4	0.3469	1.3	0.95		222	58	92	0.26	4.23E+03
n1662-01a	quite homog dark inner domain,																			
n1662-02a	stubby grain (+thin outer rim)	3298	4	3275	13	3237	34	0.2686	0.2	24.164	1.3	0.6524	1.3	0.98		184	107	172	0.58	1.94E+05
n1662-03a	homog outer rim, stubby grain	1863	4	1811	11	1767	21	0.1139	0.2	4.953	1.3	0.3154	1.3	0.99	-3.2	944	31	335	0.03	7.07E+03
n1662-03b	homog paler inner domain, stubby grain	1871	3	1867	11	1864	21	0.1144	0.2	5.291	1.3	0.3553	1.3	0.98		1075	111	412	0.10	1.44E+05
n1662-04a	homogenized?, long crystal	1848	5	1827	12	1808	21	0.1130	0.3	5.043	1.4	0.3238	1.3	0.98		646	300	259	0.46	2.75E+03
n1662-05a	zoned, long crystal	1869	7	1849	12	1831	21	0.1143	0.4	5.176	1.4	0.3285	1.3	0.96		209	108	87	0.52	1.87E+04
n1662-06a	zoned, long crystal	1873	5	1865	12	1858	22	0.1145	0.3	5.275	1.4	0.3340	1.3	0.98		412	166	170	0.40	1.48E+05
n1662-07a	zoned, long crystal	1865	5	1851	12	1838	21	0.1140	0.3	5.188	1.3	0.3300	1.3	0.98		412	34	155	0.08	9.71E+04
n1662-08a	zoned, long crystal	1860	6	1832	12	1808	21	0.1137	0.3	5.075	1.4	0.3237	1.3	0.97	-0.2	576	185	226	0.32	1.22E+04
n1662-09a	zoned, long crystal	1870	4	1877	14	1883	27	0.1144	0.2	5.348	1.6	0.3392	1.6	0.99		587	55	227	0.09	6.81E+04
n1662-10a	zoned, long crystal	1872	4	1869	14	1865	27	0.1145	0.2	5.299	1.6	0.3356	1.6	0.99		736	447	319	0.61	6.28E+04
n1662-11a	zoned, long crystal	1864	6	1874	14	1883	27	0.1140	0.3	5.329	1.7	0.3391	1.6	0.98		302	81	122	0.27	2.07E+04
n1662-12a	zoned, long crystal	1870	3	1878	14	1884	27	0.1144	0.2	5.355	1.6	0.3395	1.6	1.00		1216	18	462	0.01	1.60E+05
n1662-13a	quite homog, long crystal	1869	4	1872	14	1875	27	0.1143	0.2	5.321	1.6	0.3377	1.6	0.99		819	668	374	0.82	9.63E+04
n1662-14a	quite homog, long crystal	1858	5	1866	14	1873	27	0.1136	0.3	5.282	1.6	0.3372	1.6	0.99		847	37	322	0.04	3.86E+04
n1662-15a	zoned, long crystal	1871	4	1881	14	1891	27	0.1144	0.2	5.378	1.6	0.3409	1.6	0.99		681	489	307	0.72	1.42E+05
A1335 Maikkala charnockite (n1663)																				
n1663-01a	weakly zoned (dark domain), long prismatic	1853	11	1860	13	1867	22	0.1133	0.6	5.247	1.5	0.3359	1.3	0.90		224	46	88	0.21	2.65E+03
n1663-01b	weakly zoned (pale domain), long prismatic	1862	5	1859	12	1857	21	0.1139	0.3	5.240	1.4	0.3338	1.3	0.98		544	84	210	0.15	3.62E+04
n1663-02a	weakly zoned, long prismatic	1865	6	1855	12	1845	21	0.1141	0.3	5.212	1.4	0.3314	1.3	0.97		279	63	109	0.23	5.95E+04
n1663-03a	quite homog, long prismatic	1861	4	1856	12	1852	21	0.1138	0.2	5.221	1.3	0.3328	1.3	0.98		485	28	182	0.06	1.94E+04
n1663-04a	weakly zoned, short prismatic	1867	4	1855	12	1845	21	0.1142	0.2	5.217	1.3	0.3313	1.3	0.99		531	88	204	0.17	8.50E+04
n1663-05a	zoned, long prismatic	1860	9	1821	12	1788	21	0.1137	0.5	5.011	1.4	0.3196	1.3	0.93	-1.0	100	18	37	0.18	3.12E+04
n1663-06a	zoned, short prismatic	1870	6	1871	12	1871	22	0.1144	0.4	5.312	1.4	0.3368	1.3	0.97		295	82	119	0.28	7.16E+04
n1663-07a	homogenized, pale core, prismatic	1830	3	1813	11	1797	21	0.1119	0.2	4.960	1.3	0.3215	1.3	0.99		1239	32	444	0.03	7.20E+03
n1663-07b	darker tip domain	1859	4	1862	12	1864	21	0.1137	0.2	5.256	1.3	0.3353	1.3	0.98		530	147	212	0.28	1.12E+04
n1663-08a	zoned, short prismatic	1864	7	1853	12	1843	21	0.1140	0.4	5.201	1.4	0.3310	1.3	0.96		228	46	88	0.20	3.88E+04
A1676 Bollstad tonalite (n1665)																				
n1665-01a	quite homog, dark inner domain, prismatic	1856	94	1776	48	1708	25	0.1135	5.4	4.748	5.6	0.3035	1.6	0.29		284	34	98	0.12	2.72E+02
n1665-02a	zoned, short prismatic	1857	7	1894	15	1928	27	0.1135	0.4	5.459	1.7	0.3487	1.6	0.97	0.5	191	39	78	0.20	3.80E+04
n1665-03a	quite homog, dark inner domain, short prismatic	1858	10	1857	15	1856	27	0.1136	0.5	5.226	1.7	0.3337	1.6	0.95		173	70	71	0.40	8.90E+03
n1665-04a	weakly zoned, short prismatic	1888	9	1873	15	1860	27	0.1155	0.5	5.328	1.7	0.3345	1.6	0.95		137	52	56	0.38	1.26E+05
n1665-05a	zoned, short prismatic	1879	7	1886	15	1892	27	0.1150	0.4	5.406	1.7	0.3410	1.6	0.97		202	76	84	0.38	3.09E+04
n1665-06a	quite homog, dark, short prismatic	1874	11	1867	15	1862	27	0.1146	0.6	5.290	1.8	0.3348	1.7	0.94		120	43	49	0.36	4.69E+03
n1665-07a	pale inner domain/core	1868	7	1815	14	1769	25	0.1142	0.4	4.973	1.7	0.3157	1.6	0.97	-2.5	340	159	133	0.47	4.34E+03
n1665-08a	weakly zoned, short prismatic	1879	7	1883	15	1886	27	0.1149	0.4	5.386	1.7	0.3399	1.6	0.97		195	78	82	0.40	1.23E+04
A1745 Jyskelä gabbro (n1666)																				
n1666-01a	quite homog	1836	3	1834	14	1832	26	0.1123	0.2	5.087	1.6	0.3286	1.6	0.99		1097	223	422	0.20	3.90E+04
n1666-02a	quite homog	1830	4	1816	14	1803	26	0.1119	0.2	4.979	1.7	0.3228	1.6	0.99		466	133	180	0.28	1.00E+05
n1666-03a	quite homog	1847	4	1832	14	1818	26	0.1129	0.2	5.073	1.6	0.3258	1.6	0.99		669	186	260	0.28	1.07E+05
n1666-04a	quite homog	1841	2	1834	14	1828	26	0.1125	0.1	5.089	1.6	0.3280	1.6	1.00		1622	1282	711	0.79	2.05E+05
n1666-05a	quite homog	1824	6	1815	14	1807	26	0.1115	0.3	4.975	1.7	0.3236	1.6	0.98		287	46	108	0.16	3.00E+04
n1666-06a	quite homog	1838	3	1837	14	1837	26	0.1123	0.1	5.106	1.6	0.3296	1.6	1.00		1540	164	581	0.11	2.18E+05
n1666-07a	quite homog	1821	10	1766	15	1721	25	0.1113	0.5	4.695	1.7	0.3059	1.6	0.95	-2.3	270	48	96	0.18	3.38E+03

Sample/ spot #	Spot site on zircon, zircon type	^{207}Pb ^{206}Pb	$\pm s$	^{207}Pb ^{235}U	$\pm s$	^{206}Pb ^{238}U	$\pm s$	^{207}Pb ^{206}Pb	$\pm s$	^{207}Pb ^{235}U	$\pm s$	^{206}Pb ^{238}U	$\pm s$	r	Disc. % 2 σ lim.	[U] ppm	[Th] ppm	[Pb] ppm	Th/U meas	$^{206}\text{Pb}/^{204}\text{Pb}$ measured
A1678 Kopparnäs diabase (n1664)																				
n1664-01a	homog, elongated formless large grain	1827	3	1840	11	1851	21	0.1117	0.2	5.122	1.3	0.3326	1.3	0.99		1497	137	566	0.09	1.98E+05
n1664-02a	homog, long prismatic large crystal	1832	3	1842	11	1851	21	0.1120	0.2	5.135	1.3	0.3325	1.3	0.99		1144	123	434	0.11	1.08E+05
n1664-03a	homog, long prismatic large crystal	1833	3	1846	11	1859	21	0.1120	0.2	5.162	1.3	0.3342	1.3	0.99		1041	77	394	0.07	1.68E+05
n1664-04a	homog, short large grain	1831	2	1862	11	1890	22	0.1119	0.1	5.258	1.3	0.3407	1.3	1.00	0.9	1981	170	766	0.09	1.33E+05
n1664-05a	homog, short large grain	1831	6	1847	12	1861	21	0.1120	0.3	5.166	1.4	0.3347	1.3	0.97		592	85	228	0.14	6.01E+04
n1664-06a	homog, round bright	1832	3	1854	14	1873	27	0.1120	0.2	5.206	1.6	0.3371	1.6	0.99		868	131	338	0.15	8.13E+04
n1664-07a	homog, round bright	1831	8	1834	15	1836	26	0.1119	0.5	5.086	1.7	0.3296	1.6	0.96		163	95	69	0.58	2.80E+04
n1664-08a	homog, round bright	1830	3	1843	14	1854	26	0.1118	0.2	5.140	1.6	0.3333	1.6	0.99		746	98	286	0.13	1.33E+05
n1664-09a	quite homog, dark, prismatic	1680	22	998	13	717	11	0.1030	1.2	1.672	2.0	0.1177	1.6	0.81	-54.0	215	81	31	0.37	9.16E+02
n1664-10a	dark tip, prismatic	1752	11	1511	14	1345	20	0.1072	0.6	3.429	1.7	0.2320	1.6	0.94	-22.1	240	243	81	1.01	2.88E+03
n1664-11a	quite homog, dark, elongated	1832	9	1819	14	1808	26	0.1120	0.5	5.000	1.7	0.3238	1.6	0.96		177	133	76	0.75	1.05E+04
n1664-12a	weakly zoned, prismatic	1845	2	1867	14	1886	27	0.1128	0.1	5.287	1.6	0.3399	1.6	1.00		1977	73	755	0.04	2.05E+04
n1664-13a	weakly zoned, long prismatic	1819	6	1836	14	1851	26	0.1112	0.4	5.101	1.7	0.3327	1.6	0.98		258	130	108	0.50	1.49E+04
n1664-14a	quite homog, elongated	1838	5	1844	14	1850	26	0.1124	0.3	5.150	1.7	0.3324	1.6	0.99		793	113	304	0.14	2.77E+03
n1664-15a	quite homog, dark, prismatic(fractured)	1773	26	1693	18	1629	24	0.1084	1.4	4.299	2.2	0.2875	1.6	0.76	-1.9	188	129	70	0.69	3.66E+02
n1664-16a	quite homog, dark, prismatic(fractured)	1795	17	1700	16	1624	24	0.1098	0.9	4.334	1.9	0.2864	1.6	0.87	-5.6	137	133	52	0.97	8.95E+02
n1664-17a	dark outer domain, prismatic(fractured)	1699	83	1258	36	1017	15	0.1041	4.6	2.453	4.9	0.1708	1.6	0.34	-21.0	309	76	62	0.25	1.73E+02

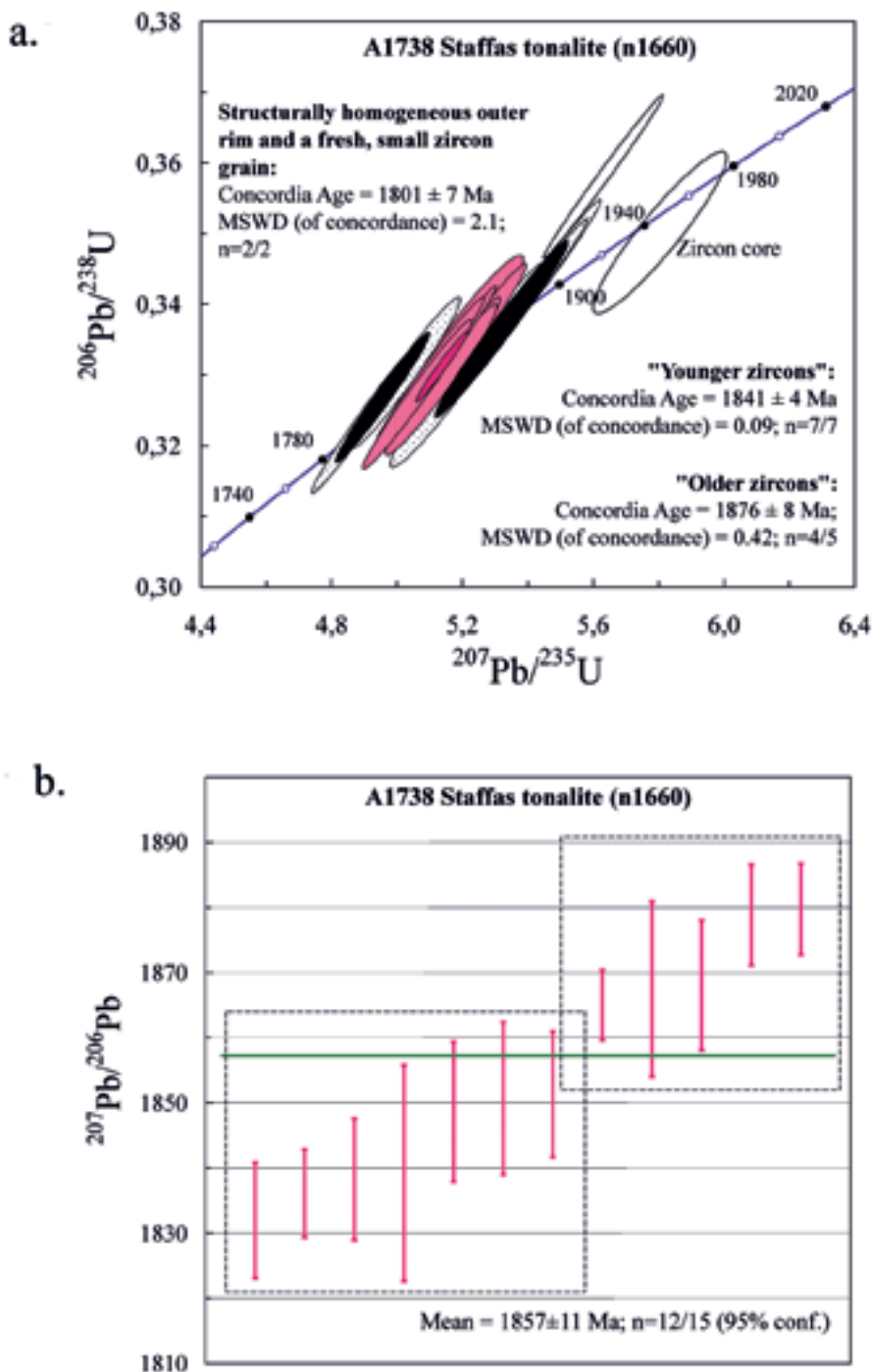
All errors are at 1 sigma level. Degree of discordance is calculated at the closest 2 sigma limit. Rejected data are indicated in italics.
*) Internal structure of the dated zircon domains on BSE-images: zoned = magmatic compositional zoning (oscillatory, banded, etc.); homog= quite homogeneous zircon domain.

Zircon description

The tonalite sample A1738 Staffas has a homogeneous zircon population. The grain-size differences are also quite small. The zircon is mostly pale brown, transparent to translucent, and prismatic with a length to width ratio of 3–5.

SIMS U-Pb age results

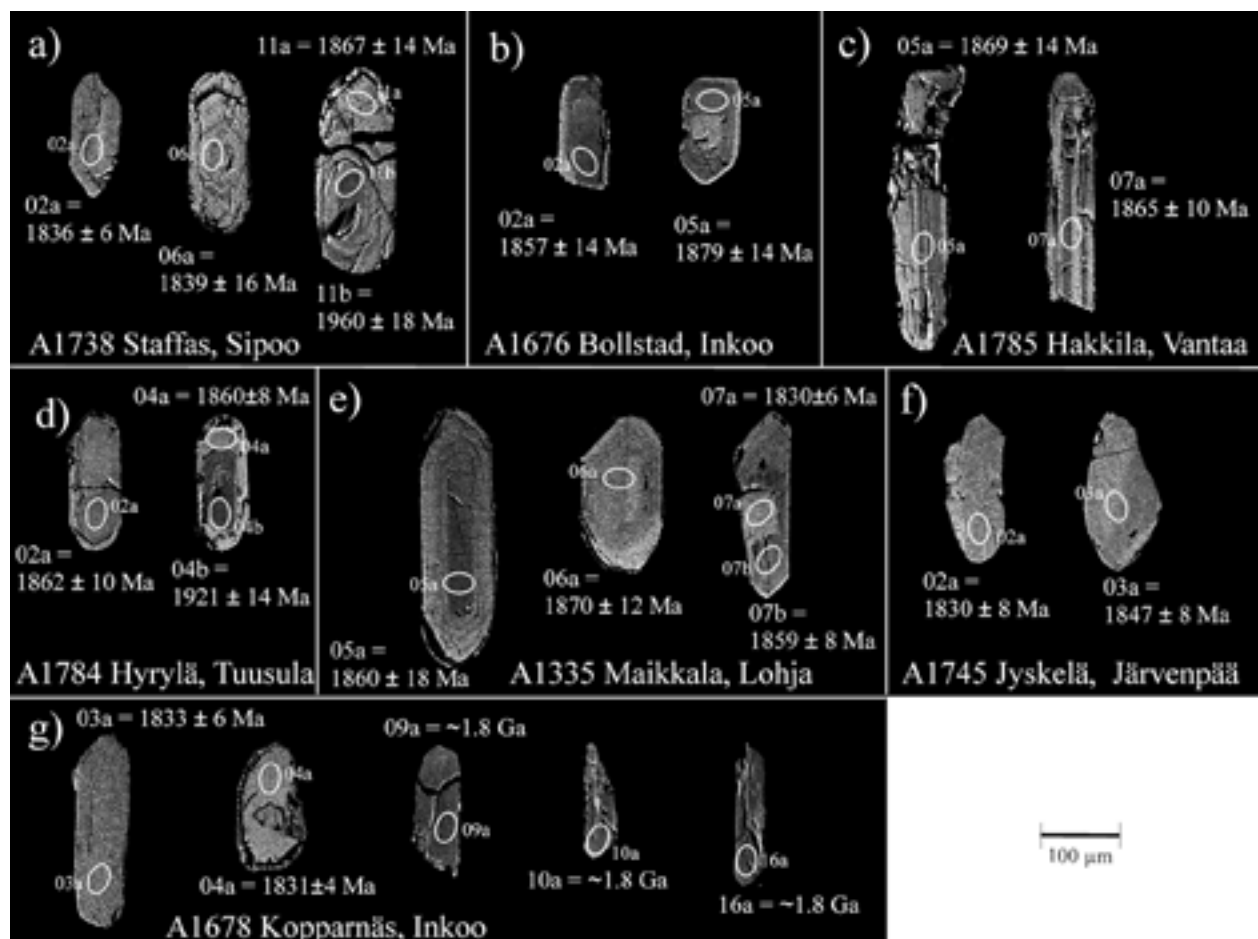
From the Staffas tonalite we dated 21 zircon domains and rejected six analyses because of the low $^{206}\text{Pb}/^{204}\text{Pb}$ ratios (App-Table. 2). In BSE images the zircons show mostly either weak zoning and/or homogeneous internal structure and frequent fractures. The U-Pb data are mostly concordant and show a wide range of ages (Appendix-Fig. 8-1a).



Appendix-Fig. 8-1. Ion microprobe age data on zircons; sample A1738 Staffas tonalite. A) Concordia plot. B) Weighted average of $^{207}\text{Pb}/^{206}\text{Pb}$ ages. The two youngest and the oldest data points are not shown in figure.

The oldest age of 1.96 Ga was measured from a BSE-darker core domain (11b) that is surrounded by younger zircon phase (1.87 Ga) (Appendix-Fig. 2). Additionally it has a thin rim growth on the other end of the grain (Appendix-Fig. 8-2a). A BSE-pale, homogeneous rim domain of zircon 09 has a $^{207}\text{Pb}/^{206}\text{Pb}$ age of 1.81 Ga. Its BSE-darker core has a clearly older age (ca. 1.93 Ga) but the analysis was rejected because of high common lead content. A 1.80 Ga age was measured from a small, euhedral, and weakly zoned zircon with an anomalous outlook. Thus, it is unsure if it is contamination from rock-crushing or mineral separation processes. The other possibility is that it is from some tiny vein connected with metamorphism. The concordia age for the two young zircons is 1801 ± 7 Ma (Appendix-Fig. 8-1a).

The majority of the U-Pb data plot between 1880 Ma and 1840 Ma. The weighted average of the $^{207}\text{Pb}/^{206}\text{Pb}$ ages is 1857 ± 11 Ma (Appendix-Fig. 8-1b). However, the data seem to form two separate age populations (Appendix-Fig. 8-1a) although evidence from the dated zircon domains is totally absent. Younger and older ages have been dated both from BSE-darker domains with weak internal structure and internally quite homogeneous domains. The concordia ages for the two apparent age groups are 1841 ± 4 Ma ($n=7/7$) and 1876 ± 8 Ma ($n=4/5$) (Fig. 3a). Based on field evidence, the older age of $\sim 1.88\text{--}1.87$ Ga is considered as better alternative for the tonalite age and then, the ~ 1.84 Ga zircon may indicate metamorphism related lead loss.



Appendix-Fig. 8-2. Selected BSE images of zircons: a) A1738 Staffas, syn-/late D_B tonalite – Hindsby intrusion; b) A1676 Bollstad, syn-/late D_B tonalite; c) A1785 Hakkila, early D_E garnet-bearing tonalite; d) A1784 Hyrylä, early D_E garnet-bearing tonalite; e) A1335 Maikkala, pyroxene-bearing tonalite, charnockite; f) A1745 Jyskelä, late D_E gabbro; A1678 Kopparnäs, D_H diabase.

A1676 Bollstad 1, Inkoo – syn-/late DB tonalite

Finnish grid coordinates KJ2 2497.78E 6662.16N

TIMS, zircon and monazite

SIMS, zircon, NORDSIM sample number n1665, mount number M562 (small grains)

Sample information

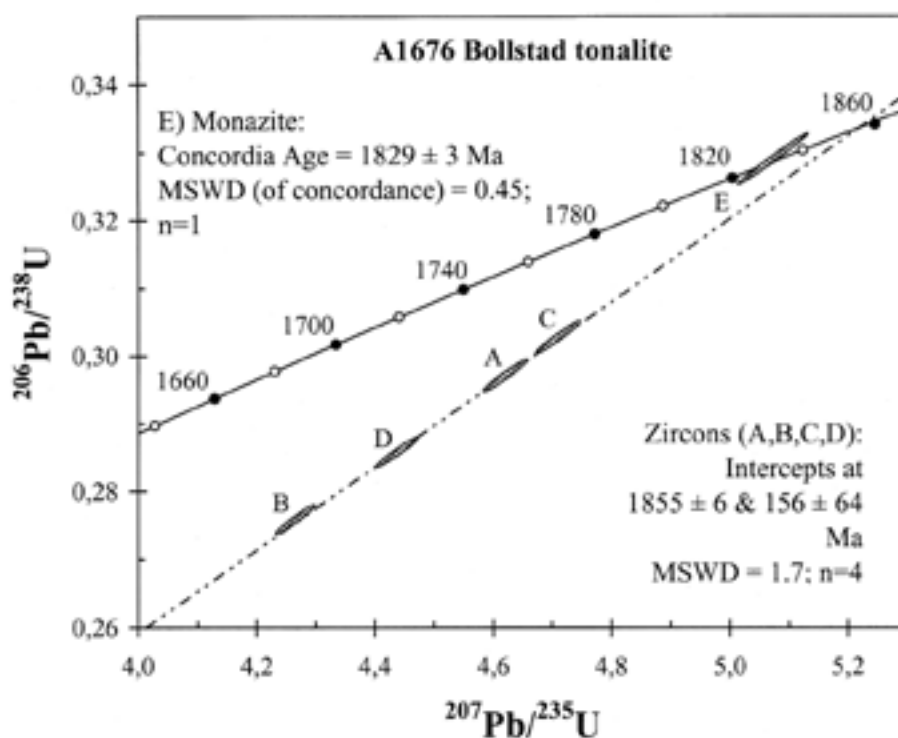
The sample A1676 Bollstad from Inkoo was taken to establish the age of a tonalite that was intruded by granitic pegmatite dykes (sample A1677 Bollstad 2) that structurally evidences the beginning of the D_H extensional deformation in the Inkoo area. The tonalite is strongly deformed by D_H and shows new progression overprinting the early magmatic structure. The dated tonalite, with the main mineral composition plagioclase, biotite, quartz, is shown in Figure 39. The purpose was to determine the length of the discordance that is evident based on structure (cf. Sederholm 1926 and Pajunen et al. 2008).

Zircon and monazite descriptions

The sample included very fine-grained, pale yellow, ellipsoidal to round monazite without developed crystal faces. Zircon population is quite homogeneous and fine-grained ($<75 \mu\text{m}$). Typically zircon is brownish, translucent and prismatic or shorter, partly without crystal faces. More ellipsoidal and rounded, bright, possibly metamorphic zircon also exists (not included in the TIMS analysis).

TIMS U-Pb age result

The TIMS age was analyzed from rather fine-grained, reddish and long zircon grains. The Pb/U ratios scatter evenly on the regression line, giving the upper intercept age of $1855 \pm 6 \text{ Ma}$ ($n=4$; $\text{MSWD}=1.7$). The concordant monazite age of $1829 \pm 3 \text{ Ma}$ was obtained by TIMS. The TIMS U-Pb data are shown in Appendix-Table 1 and Appendix-Fig. 8-3.



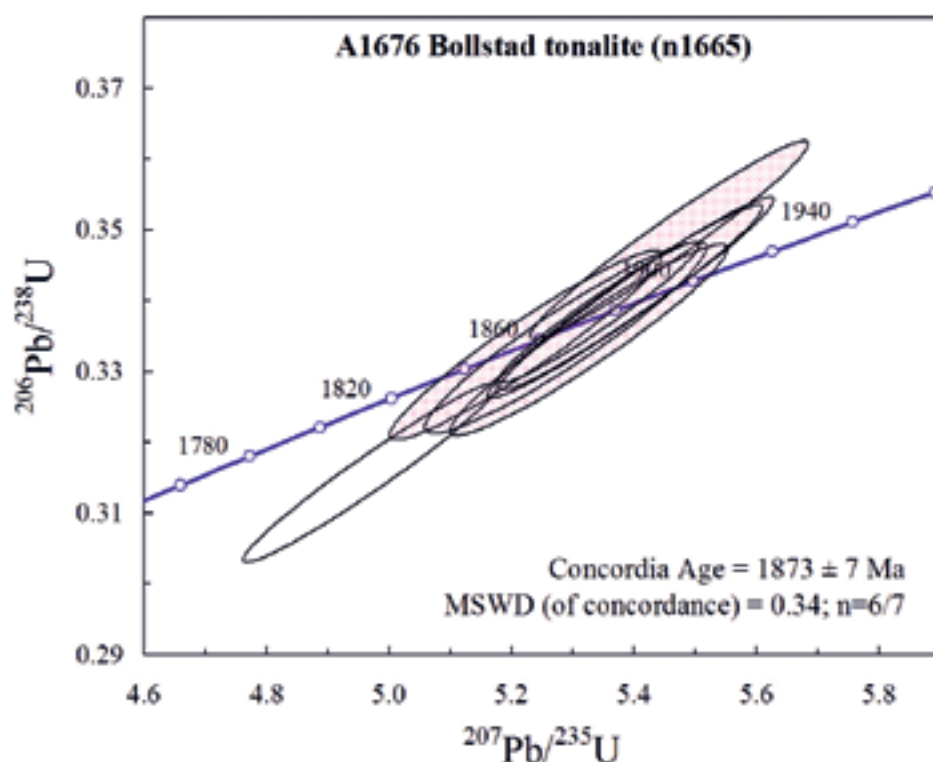
Appendix-Fig. 8-3. A concordia plot for TIMS U-Pb data on zircon and monazite; sample A1676 Bollstad tonalite (see also Appendix-Table 1), Inkoo.

SIMS U-Pb age results

From the tonalite sample A1676 Bollstad 1, only eight dates were determined (App-Table 2), and one of these was rejected because of the high common lead content. Zircon is mostly quite stubby, shows only a weak internal structure and frequently has a very thin BSE-pale rim around it (Appendix-Fig. 8-2b).

All data plot in a cluster on a concordia diagram (Appendix-Fig. 8-4). A concordia age of 1873 ± 7 Ma for six of the seven data points can be calculated. The slightly discordant data (06a) are from an internally homogeneous core.

1873 ± 7 Ma is an unambiguous age for the syn-/late D_B tonalite. Although no direct age data are available, the thin BSE-pale rims are suggested to represent metamorphic zircon growth at 1.83 Ga, which is defined by the monazite from the rock. The TIMS U-Pb age of 1855 ± 6 Ma is slightly younger than that from the ion microprobe analyses. It is considered that the upper intercept defined by the discordant data has shifted slightly down because of 1.83 Ga metamorphism.



Appendix-Fig. 8-4. A concordia plot for SIMS U-Pb data on zircons; sample A1676 Bollstad tonalite, Inkoö.

A1785 Hakkila, Vantaa – an early D_E garnet-bearing tonalite dyke

Finnish grid coordinates KKJ2 2560.63E 6687.710

SIMS, zircon, NORDSIM sample number n1662, mount number M561 (large grains) and M562 (small grains)

Sample information

The sample A1785 Hakkila from Vantaa, a garnet-bearing tonalite dyke (Figure 29), represents a tonalitic magma event that cuts the early deformation phases, especially the tectonic D_{C+D} dome-and-basin structures. It is strongly metamorphosed and migmatized by the D_H granitic neosomes. According to structural analysis it is related to the early phase of the D_E magmatism. The age was determined to establish the start of the D_E evolution in the detailed study area. The sample location is shown in Figure 13 with the rectangle indicating the site of the tonalite in Figure 29.

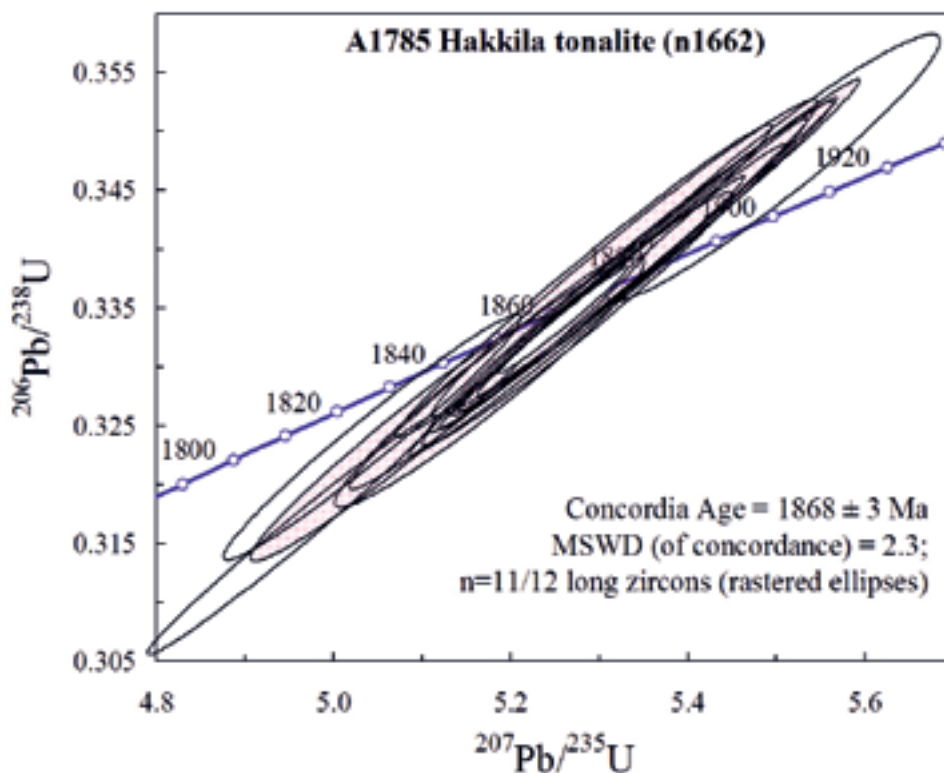
Zircon description

The zircon population in tonalite sample A1785 Hakkila is quite homogeneous. It mainly consists of very long, pale brownish, transparent to translucent, principally quite tabular crystals. In addition to these, more brownish, short stubby grains with or without clear crystal faces also exist.

U-Pb age results

A total of 17 zircon domains were dated using an ion microprobe (App-Table 2). One data point (n1662–01c) was rejected, as its $^{206}\text{Pb}/^{204}\text{Pb}$ ratio was very low. The long zircon crystals mainly showing clear zoning determine the age for the tonalite; 11 of 12 analyses yield a concordia age of 1868 ± 3 Ma (Appendix-Fig. 8-5). Only one apparently younger data (n1662–04a) from an internally-homogenized domain was not included in the tonalite age calculation. The BSE images of typical analyzed zircons are presented in Appendix-Fig. 8-2c.

Only four domains were dated from the stubby zircons. An inner domain/core of one grain shows an extremely old age of 3.30 Ga. The other three ages from internally structureless inner and outer domains (cores and rims?) plot in the same cluster with the age data from the long magmatic crystals. As these zircons are considered as inherited ones, their U-Pb system must have been homogenized during the tonalite intrusion. The age of 1868 ± 3 Ma is interpreted as the intrusion age of the Hakkila early D_E garnet-bearing tonalite dyke.



Appendix-Fig. 8-5. A concordia plot for SIMS U-Pb data on zircons; sample A1785 Hakkila tonalite, Vantaa.

A1784 Hyrylä, Tuusula – early D_E garnet-bearing tonalite dyke

Finnish grid coordinates KJ2 2557.23E 6697.25N

SIMS, zircon, NORDSIM sample number n1661, mount number M561 (large grains) and M562 (small grains)

Sample information

The sample A1784 Hyrylä from Tuusula is a structurally similar tonalitic dyke (Figure 30a) to the Hakkila dyke, but it cuts slightly more deformed gneissic country rock. According to structural analysis it is also early D_E intrusive dyke that close by also forms larger intrusions showing lamination related to extensional SE-opening during emplacement (Figures 30b ad c). The dyke age was proposed to establish the age for the extensional opening phase.

Zircon description

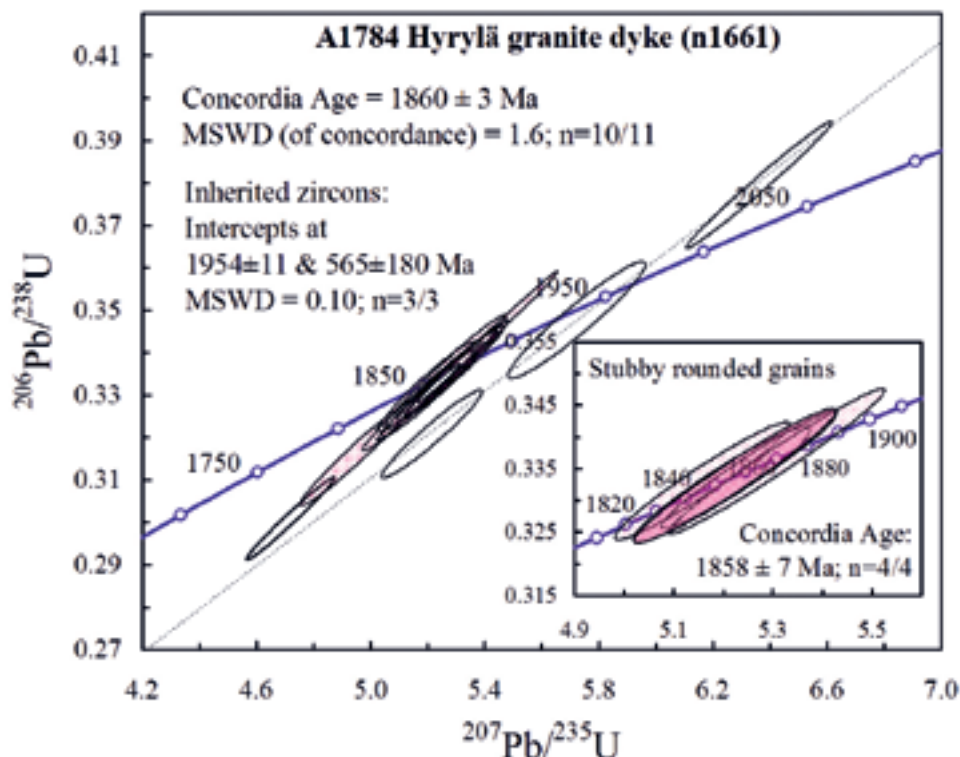
The granitic dyke A1784 Hyrylä contains only a tiny amount of zircon. The population is heterogeneous, consisting of long and short prismatic crystals, very bright, equidimensional crystals as well as oval grains without crystal faces. The majority of the grains are transparent to translucent. It is also possible that all the zircons are inherited ones.

SIMS U-Pb age results

Eighteen zircon domains were dated using an ion microprobe (App-Table 2). Of these, four were dated from internally-homogeneous, stubby, round zircons and the rest from prismatic grains that do not show clear magmatic zoning but have quite homogeneous internal structures in BSE images. No correlation between the U and Th concentrations and zircon types existed (see App-Table 2).

The U-Pb data from the majority (10/14) of the prismatic zircons plot in a cluster defining a concordia age of 1860 ± 3 Ma (Appendix-Fig. 8-6). Three of the prismatic zircons are certainly inherited, showing a discordia age of c. 1.95 Ga. Two of these were measured from inner domains enveloped by younger rim phases (n1661-04b, n1661-16b). However, in the BSE images (Appendix-Fig. 8-2d), the inner darker older domains and the pale younger domains do not have any clear boundaries. It is thus suggested that the outer domains of the grains have suffered homogenization of their U-Pb system.

The rounded, stubby grains considered as metamorphic zircons give the same age as the prismatic crystals. The concordia age for these is 1858 ± 7 Ma (Appendix-Fig. 8-6). These zircons can be considered initially as inherited ones.



Appendix-Fig. 8-6. A concordia plot for SIMS U-Pb data on zircons; sample A1784 Hyrylä granite dyke, Tuusula.

A1335 Maikkala, Lohja – mid- D_E pyroxene-bearing tonalite, charnockite

Finnish grid coordinates KJ2 2500.50E 6690.60N

TIMS, zircon and monazite

NORDSIM, zircon, mount number n1663, large grains = M561

SIMS, zircon, NORDSIM sample number n1663, mount number M561 (large grains)

Sample information

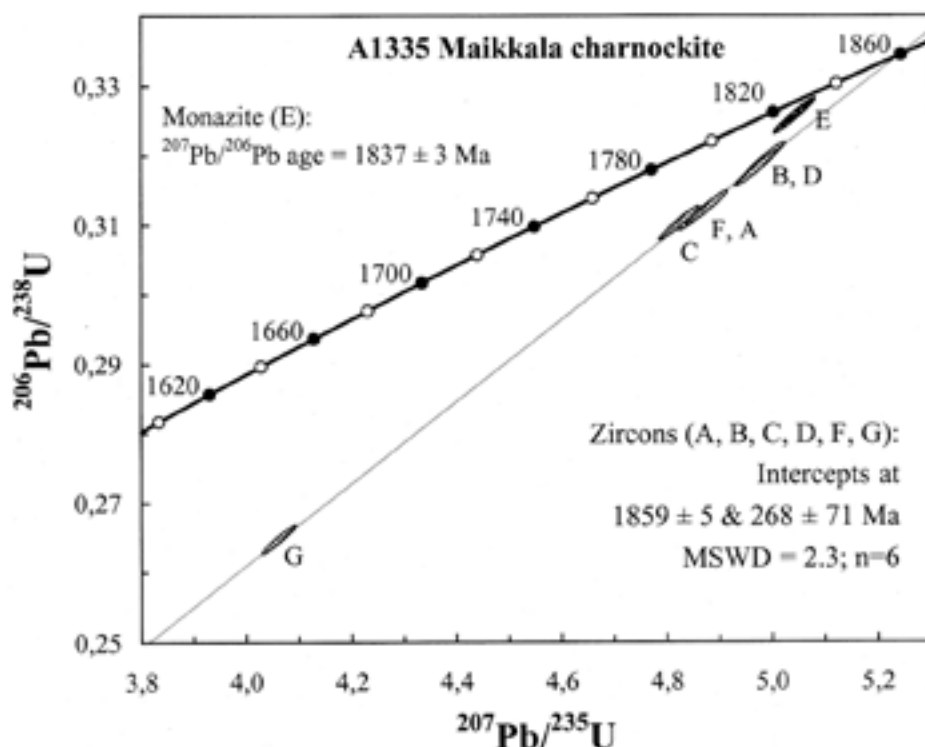
K. Korsman originally gathered this sample for dating the tectono-metamorphic evolution of the granulites in the West Uusimaa granulite Complex; the TIMS analysis was carried out by H. Huhma. The sample A1335 Maikkala from Lohja represents a high-grade tonalitic rock (charnockite) form. It is pyroxene-bearing, medium-grained, rather homogeneous rock and represents a rock preserved from the penetrative D_E deformation in the granulite area. Thus, in addition to the intrusion age for the tonalite it also established the upper limit for the penetrative extensional D_E deformation age.

Monazite and zircon descriptions

The sample included enough monazite for two fractions for TIMS. It included a lot of homogeneously pale brownish, translucent zircon varying from very long or shorter (length-width ratio = 3–7) prismatic grains to short, roundish grains. The zircon grains are zonal with well-developed crystal-faces referring to their magmatic origin. Only a few clear cores still having crystal structures preserved were detected.

TIMS U-Pb age result and zircon description

Six fractions of zircon were analyzed by TIMS. The U-Pb data (App-Table 1) give an upper intercept age of 1860 ± 5 Ma (Appendix-Fig. 8-7), predominantly based on the light fraction. The age is regarded as the magmatic age. A concordant monazite age of 1837 ± 3 Ma is interpreted as metamorphic (App-Table 1).

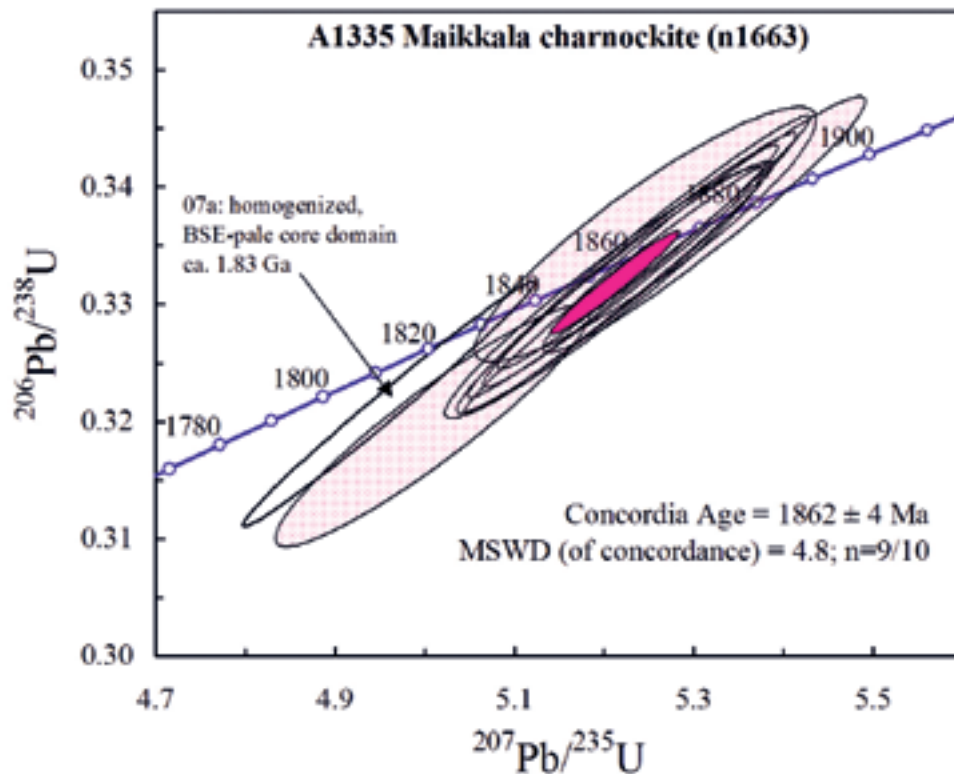


Appendix-Fig. 8-7. A concordia plot for TIMS U-Pb data on zircon and monazite; sample A1335 Maikkala pyroxene-tonalite (charnockite), Lohja.

U-Pb age results

From the charnockite sample A1335 from Maikkala, a total of ten zircon domains were dated using an ion microprobe (App-Table 2). All the data are concordant and nine of them define a concordia age of 1862 ± 4 Ma for the rock (Appendix-Fig. 8-8). All these were dated from magmatically-zoned zircons. A slightly younger age of c. 1.83 Ga is from a BSE-pale, homogeneous, low Th/U core domain (07a) with a 1.86 Ga BSE-darker main phase of the zircon (07b) (Appendix-Fig. 8-2e).

The TIMS U-Pb age and ion microprobe age are consistent. The homogenized core of the zircon 07 gives the same metamorphic age as the monazite. It thus seems probable that the previously metamict core was healed during the metamorphism.



Appendix-Fig. 8-8. A concordia plot for SIMS U-Pb data on zircons; sample A1335 Maikkala pyroxene-bearing tonalite (charnockite), Lohja.

A1745 Jyskelä, Järvenpää – D_E gabbro

Finnish grid coordinates KKJ2 2562.56E 6711.55N

TIMS, zircon

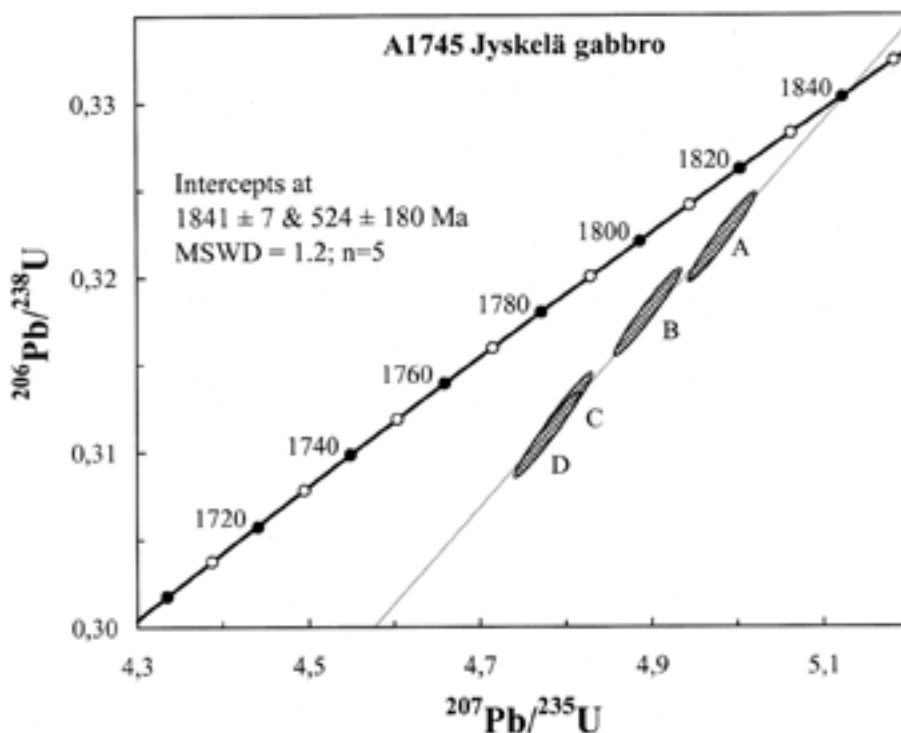
SIMS, zircon, NORDSIM sample number n1666, mount number M562 (small grains)

Sample information

The gabbroic rocks are rare in the central parts of the granitoid-dominant units like the Espoo Granitoid Complex (EGC); the sample A1745 Jyskelä from Järvenpää is a gabbro from such an area. It was emplaced according to structural analysis into a low-angle structure that is interpreted as extensional S_E foliation exemplified in Figure 34b and c. The gabbro's structural setting is illustrated in Figure 34a and its relations to the later D_H granites are shown in Figure 34d.

TIMS U-Pb age result and zircon description

The A1745 Jyskelä gabbro was dated using the conventional U-Pb method (App-Table 1). The four analyzed fractions give an upper intercept age of 1841 ± 7 Ma (MSWD=1.2) for the gabbro (Appendix-Fig. 8-9). The zircons in sample are quite odd-looking (EDS: Zr, Si, O). They are dark brown, transparent to translucent, elongated, and often flat with only rare crystal faces. Actually, the margins can be quite shapeless. However, dark brown zircons are quite usual in mafic igneous rocks.



Appendix-Fig. 8-9. A concordia plot for TIMS U-Pb data on zircons; sample A1745 Jyskelä gabbro, Mäntsälä.

SIMS U-Pb age results

From the A1745 Jyskelä gabbro, seven zircon domains were dated using an ion microprobe (App-Table 2). The zircons show no clear zoning and some domains show tiny BSE-white heavy spots (phase separation?) (Appendix-Fig. 8-2f). The dated zircon domains are all unaltered, preferably dark in BSE images. The six concordant U-Pb analyses give an unambiguous age of 1838 ± 4 Ma (Appendix-Fig. 8-10) for the gabbro. This age is identical within the error limits with the conventional U-Pb age of 1841 ± 7 Ma.

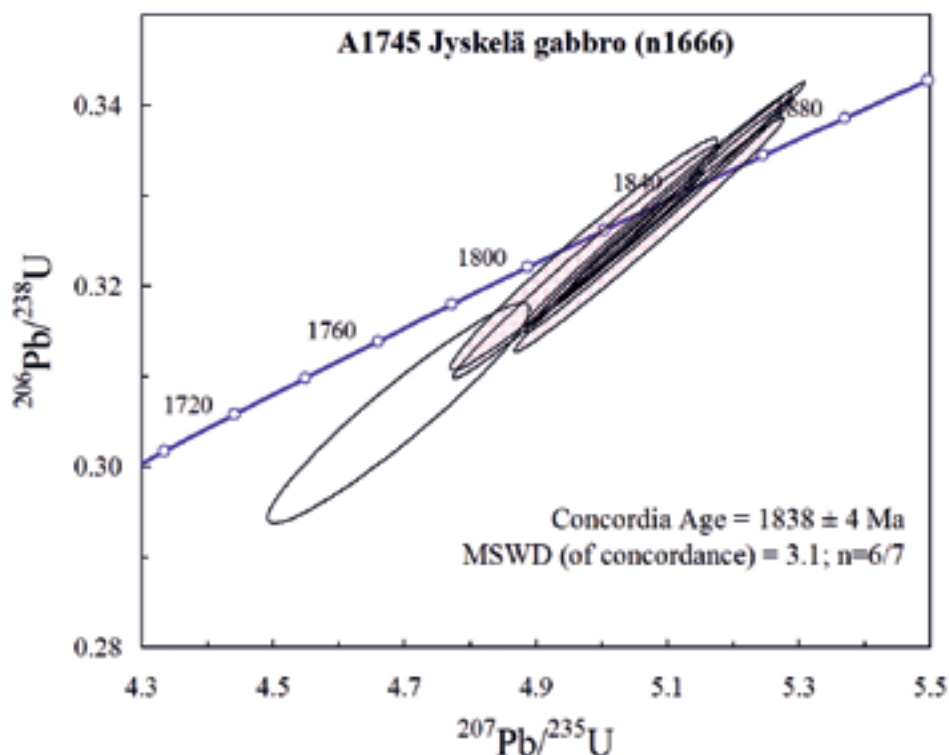
A1677 Bollstad 2, Inkoo –D_H pegmatitic granite

Finnish grid coordinates KKJ2 2497.78E 6662.16N

TIMS, zircon and monazite

Sample information

The pegmatitic granite, sample A1677 Bollstad 2 from Inkoo, represents a D_H granite dyke that was emplaced into a cooled syn-/late D_B tonalite (sample A1676 Bollstad 1). The D_H granites characterize the Southern Finland Granitoid Zone (SFGZ). The dyke was originally set into an upright position, but due to continued flattening and heating it deformed into isoclinal folds. The structural relationships of the



Appendix-Fig. 8-10. A concordia plot for SIMS U-Pb age data on zircons; sample A1745 Jyskelä gabbro, Mäntsälä.

dyke are illustrated in Figure 39. The age of the dyke establishes the beginning of the D_H phase in the Inkoo area.

Monazite and zircon descriptions

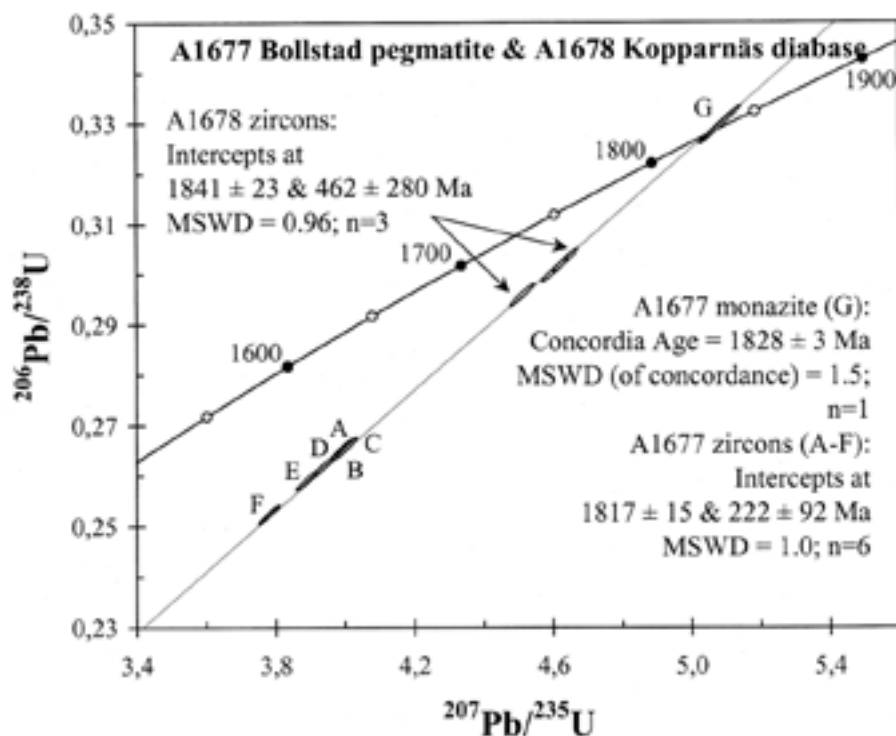
The sample included much brownish orange, pigmented (Fe?) monazite, and some bright yellow crystals with well-developed crystal face. Monazite is coarse-grained, referring to its magmatic origin. There are only a few mixed-like zircons in the density fraction $>4.2 \text{ g/cm}^3$. The fraction $4.2\text{--}4.0 \text{ g/cm}^3$ had enough zircon for only a few age determination fractions. The majority of the prismatic (length-width ratio = 2.5–5) zircons are very light, $<4.0 \text{ g/cm}^3$, dark brownish and metamict in character. These zircons are typical for pegmatite granites.

TIMS U-Pb age results

Monazite gives a concordant $^{207}\text{Pb}/^{206}\text{Pb}$ age of $1828 \pm 1 \text{ Ma}$; the age taking into account the concordancy is $1828 \pm 3 \text{ Ma}$ (Appendix-Fig. 8-11). The age is exactly consistent with the monazite age from the Bollstad tonalite (sample A1676 Bollstad 1).

Six fractions of zircon were analyzed (App-Table 1). The zircons were light and high in uranium, and the analyze points scattered far from the concordia. The upper intercept age for zircons gives an age of $1817 \pm 15 \text{ Ma}$ (MSWD = 1.6 ($n = 6$)) (Figure Appendix-Fig. 8-11). Even though the error is large it can be assumed that the zircon is not much older than the monazite in the rock. When combined with the monazite analyses the value describing the quality of regression is 1.1 (MSWD). Because it is close to 1, are the zircon and monazite quite similar in age.

The age of monazite is interpreted to represent the pegmatitic granite dyke age. The dyke emplacement establishes the initiation of the late D_H granite event in the border zone of the most intense granitoid areas, such as the Espoo Granitoid Complex (EGC).



Appendix-Fig. 8-11. A concordia plot for TIMS U-Pb data on zircon and monazite; sample A1677 Bollstad pegmatite granite, Inkoo; sample A1678 Kopparnäs diabase, Inkoo.

A1678 Kopparnäs diabase

Finnish grid coordinates KJ2 2514.13E 6659.09N

TIMS, zircon

SIMS, zircon, NORDSIM sample number n1664, mount number M561 (large grains) and M562 (small grains)

TIMS U-Pb age result and zircon description

From the A1678 Kopparnäs diabase, three zircon fractions have previously been dated using TIMS (App-Table 1). For the analyses, only extremely fine-grained, pale, transparent, and elongated zircons, which do not often show clear crystal faces, were selected. The larger grains were not dated as it is extremely implausible that a very fine-grained rock contains large or medium-sized co-magmatic zircons. In addition to these fine-grained dated zircons the sample contains large, dark brown and pale zircons with mixed shapes. As the zircon amount in the sample is very small and the quality is rather heterogeneous, it could be considered that all the zircons are inherited.

The age results (App-Table 1) are highly discordant and give an upper intercept age of 1841 ± 23 Ma (MSWD=0.96; n=3) (Appendix-Fig. 8-11). However, it should be kept in mind that three point isochrones defined by highly discordant data are certainly doubtful. The data points plot on the same discordia line with the highly discordant zircon data from Bollstad pegmatite.

For ion microprobe dating, various zircon types were selected: the large grains are mostly turbid to translucent, long and short crystals and the majority of the smaller zircons are brownish, transparent to translucent, long and short grains as well as roundish ones.

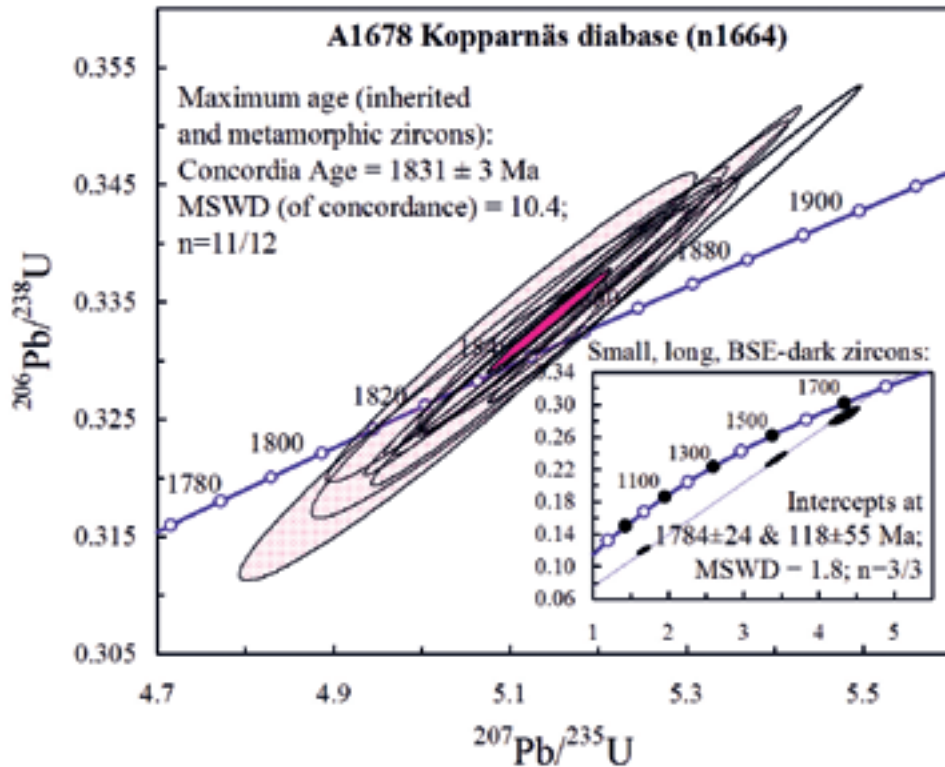
SIMS U-Pb age results

From diabase sample A1678 Kopparnäs, a total of 17 zircon domains were dated using an ion microprobe (App-Table 2). Two of these were rejected because of high common lead contents. Twelve analyses plot in a tight cluster on a concordia diagram (Appendix-Fig. 8-12). Eleven of the 12 confirm an age of 1831 ± 3

Ma for these zircons, which include large and small euhedral to round grains with mainly homogeneous internal structures.

Three small, brownish, long BSE-dark zircon grains (9a, 10a, and 16a) show younger $^{207}\text{Pb}/^{206}\text{Pb}$ ages with an upper intercept age of 1784 ± 24 Ma (the two rejected data with low $^{206}\text{Pb}/^{204}\text{Pb}$ (15a and 17a) from a similar zircon type would also plot on the same discordia line) (Appendix-Fig. 8-2g). These zircons also have the lowest U contents in the data.

In our opinion the maximum age for the diabase preferably is determined according to those 1.78 Ga small, long, brownish, low-U grains, as a very fine-grained mafic rock normally does not include much co-magmatic zircon. Thus, the c. 1.83Ga zircons are all inherited.



Appendix-Fig. 8-12. A concordia plot for SIMS U-Pb data on zircons; sample A1678 Kopparnäs diabase, Inkoo.

SUMMARY

The ages of rocks discussed in the main text are summarized in App-Table 3.

App-Table 3. Summary of the age results (see Appendix 8 for further information).

Sample name Rock type	Anal. no.	TIMS U-Pb age results	NORDSIM U-Pb age results
A1785 HAKKILA TONALITE	n1662	-	1868 ± 3 Ma (n=11/12; concordia age)
A1784 HYRYLÄ GRANITE DYKE	n1661	-	1860 ± 3 Ma (n=10/11; concordia age) Metamorphic ages 1858 ± 7 Ma; n=4/4; Inherited ~1.95 Ga
A1738 STAFFAS TONALITE	n1660	-	AVE=1857 ± 11 Ma (n=12) “Younger?” 1841 ± 4 Ma (n=7/7) “Older?” 1876 ± 8 Ma (n=4/5) Metamorphic zircon phases 1801±7 Ma (n=2/2)
A1745 JYSKELÄ GABBRO	n1666	1841 ± 7 Ma / zircon	1838 ± 4 Ma (n=6/7)
A1678 KOPPARNÄS DIABASE	n1664	1841 ± 23 Ma (n=3) Three highly discordant fractions / tiny zircons). Fractions plot on a discordia line with the pegmatite zircons from Bollstad	1831 ± 3 Ma (n=11/12) inherited grains 1784 ± 24 Ma (n=3/3) a few small grains. This age is considered as maximum age for the Kopparnäs diabase.
A1676 BOLLSTAD TONALITE	n1665	1855 ± 6 Ma / zircon (n=4) 1829 ± 3 Ma / monazite (n=1)	1873 ± 7 Ma (n=6/7)
A1677 BOLLSTAD PEGMATITIC GRANITE		1828 ± 3 Ma / monazite ~1.82 Ga / zircon (n=6) Highly discordant zircon U-Pb data	
A1335 MAIKKALA PYROXENE-TONALITE (CHARNOCKITE)	n1663	1860 ± 5 Ma / zircon 1837 ± 3 Ma / monazite	1862 ± 4 Ma (n=9/10) ~1.83 Ga metamorphic zircon phase (n=1)

Appendix 9. Tectono-metamorphic evolution of the Svecofennian domain in the study area is compiled in App-Table 4.

App-Table 4. Summary of the tectonic evolution of the Svecofennian domain in southern Finland. Abbreviations: VMB = Vammala Migmatite Belt, SVB = Southern Finland Volcanic-Sedimentary Belt, EGC = Espoo Granitoid Complex, HGB = Hyvinkää Gabbroic-volcanic Belt, WUC = West Uusimaa granulite Complex, GMB = Granitic Migmatite Belt, TMB Tonalite Migmatite Belt, SFGZ = Southern Finland Granitoid Zone, BBZ = Baltic Sea-Bothnian Bay Zone, RKZ = Riga Bay Karelia Zone and TIB = Transscandinavian Igneous Belt.

MAJOR GEOTECTONIC EVENT		DEFORMATION PHASE		AGE (Ga)		LITHOLOGY		RELATIONSHIPS OF STRUCTURES AND METAMORPHISM		STRESS FIELD		GEOTECTONIC INTERPRETATION		DISCUSSION AND APPLICATIONAL ASPECTS	
SVECOFENNIAN EVENTS															
EARLY SEDIMENTATION AND VOLCANISM															
Pre-E ₁	Pre-D _A	1.95- (?)	Ultramafic and mafic rocks (e.g. cortlandites in VMB) ⁽¹⁾ ; psammitic-dominant metasedimentary rocks ⁽¹⁾							Early ocean floor magmatism?			Similar psammitic metasediments locally occur in the GMB		
		1.9-1.89	Series I volcanism: mafic-intermediate-felsic volcanic rocks ⁽²⁾ in the SVB and EGC; Orjäärvi granodiorite ⁽²⁾ ; there are also other early granitoids in the SVB (e.g. Algersö granodiorite in Föglö ⁽⁵⁾), but their relations to volcanism are not known	Early volcanic and sedimentary sequences are folded by F _A structures in Orjäärvi granodiorite not known			Island arc volcanism and magmatism		In the SVB and EGC mafic-intermediate dykes cut the S _A of the early sedimentary-volcanic sequences; two volcanic series can be distinguished on a structural basis						
		1.9	Psammitic-pelitic metaturbiditic metasedimentary rocks, sulphide and iron ore formations, calcareous rocks and limestones in the SVB	F _A -folded limestone in Kalkkiranta Sipoo is in association with F _A -folded volcanogenic felsic gneisses			Limestones, sulphide ores and iron formations indicate a low-water environment; metapsammitic and metapelitic sediments deposited in deep water environment		Psammitic-pelitic sedimentary rocks occur in close association with the pre-D _A felsic gneisses (volcanic rocks) and shallow water sediments due to later deformations (especially D _A)						
EARLY COLLISIONAL EVENT BETWEEN THE ARCHAIC CONTINENT AND SVECOFENNIAN ISLAND ARC															
E ₁	D _A	ca. 1.9-1.88		Isoclinal, often rootless folds, and weak penetrative foliation, probably major thrust faults	C. N-S contraction according to F _A observations	Early crustal thickening (possibly in island arc environment)		Strong rearrangement of rocks from different geotectonic environments close to each other; a change from lithostratigraphy to tectonic stratigraphy; relations of D _A to the D ₁ in the northern terranes is not determined							
COLLAPSE OF ISLAND ARC AND LATER SEDIMENTATION AND VOLCANISM															
E ₂	Post-D _A and pre-early syn-D _B	1.88-1.87 ⁽²⁾	Series II volcanism: mafic to intermediate early/syn-D _B volcanism and mafic to intermediate dykes	The earliest identified structure S _B ; no F _A folds detected; mafic dykes cut the S _A		Possible intra-arc volcanism		Related to collapse and sinking of oceanic slab into the mantle							
		1.88-1.87 ⁽³⁾	Gabbroic-tonalitic association in the SVB and gabbros in the HGB	Strongly S _B -foliated and boudinaged - relationships with D _A in the volcanic series not known		Possible intra-arc magmatism syngenetic to the intra-arc volcanic rocks		Mafic rocks are sometimes suggested as synvolcanic with the early volcanic sequences ⁽⁵⁾ ; further study is needed to determine their structural relationships							
		D _B	Thronhjemitic to granitic migmatization	Isoclinal (to tight) recumbent folding with strong penetrative foliation, lineation weak - intersection between S _{(A)-B-C} , boudinage of competent layers with local shearing, prograde metamorphism to medium- to high-grade conditions	Strong vertical shortening due to crustal extension	Extensional event related to collapse of the island arc due to sinking of the oceanic slab into the mantle		Subduction is interpreted to be away from the Archaean craton; the distribution of the gabbroic rocks in the HGB and HVB (App-Fig. 3-3b) estimates approximately SSW-NNE minimum principal stress; becomes diachronically younger towards the south from the TMB to GMB							
	Syn- to late D _B	1.88-1.87	Gneissic tonalites, locally pyroxene-bearing in the EGC, WUC and SVB	S _C foliated showing a complex pattern of later shear band structures, all the D _{E-H} granitoids and dykes cut the tonalite			Forms large homogeneous intrusions (e.g. Hindby intrusion)								
N-S COLLISION - A NEW CONTINENTAL CRUST FORMED															
E ₃	D _C	1.88-1.87	Granitic neosomes to a in decreasing extent after D _B	Moderate to tight folding with weak E-trending axial plane foliation or crenulation deforming the D _{(A)-B} structures; the first penetrative deformation in the syn-/late D _B tonalites	N-S contraction	Collisional event in the ductile stage causing crustal shortening		C. similar ages of the D _C and D _B suggest continuous overall D _C collision and local D _B extension, both becoming diachronically younger southwards							
SW-NW TRANSPRESSIONAL COLLISION															
Transition from E ₃ to E ₄	D _D	1.88-1.87	Pyroxene-bearing quartz-monzonites in the CFGC	Open to tight folding causing ellipsoidal D _{(C)-D} dome-and-basin structures especially in the SVB, no significant foliation identified; developed into intensive D ₄ shearing causing block structures in the northern terranes (e.g. CFGC and TMB); deformation was more zonal in the north than in the south	NE-SW transpression; related SE-NW oblique extension (e.g. in the CFGC)	Ductile oblique collisional event causing crustal shortening; intense movements of crustal blocks indicating escape tectonics model of deformation		The quartz-monzonites of 1.87-1.86 Ga ^(14 and 15) establish the closing of D _D in the northern terranes							
COOLING STAGE															
The cooling stage after the D _D varied in duration in different areas. In the northern terranes cooling began after D ₄ and deformation developed to become more zoned in character. In the south (SFGZ) thermal activity was in places nearly continuous, but local cooling stages of c. 30 Ma occurred.															
FORMATION OF THE SOUTHERN FINLAND GRANITOID ZONE (SFGZ) IN OBLIQUE EXTENSIONAL TECTONIC REGIMES															
E ₄	D _E	c. 1.87-1.84	Strong tonalitic to granitic magmatism with minor gabbros; pull-apart-basin supracrustal rocks (see details below)	Strong horizontal S _{ECI} foliation with top-to-SE movement in the SFGZ; often totally destroyed the previous D _{(A)-D} structures; complex D _E shear band structures in previous rocks	C. NW-SE oblique extension during overall NE-SW transpression	Oblique extensional zones developed under NE-SW transpression between the the major N-trending shear zones (BBZ, RKZ and TIB)									
		1.87-1.84 ⁽¹³⁾	Garnet-bearing tonalites and contemporaneous pegmatitic granites predominantly in the EGC; microtonalite dykes	Metamorphosed intrusions and dykes, often garnet bearing; cut the syn-/late D _B tonalites; remelt by the later metamorphic events, e.g. during D _H	NE-SW to E-W dilatation		Early pegmatitic granite borders of the early tonalitic dykes indicate increasing temperature during their emplacement								
		After 1.87-1.86 ⁽⁷⁾	Jokela sedimentary-volcanic association: quartzites, conglomerates, pelitic metasediments and volcanic rocks	Shows one prograde metamorphism to medium-grade and low pressure, strong S _E and later deformations, very weak foliation preceeding S _E ; cut by D _{E-H} granitic magmas	Upper crustal oblique NW-SE extension	Sedimentation and volcanism in a pull-apart-basin in a high-energy environment; later change to deep water sedimentation and volcanism		Corresponding associations occur and are generally preserved in the intersections of the major E-trending shear zones (predominantly D _H) and D ₁ structures.							
		c. 1.86-1.84	Tonalites, granites and gabbros	Show only weak contractional D _E deformation structures and are cut by the late D _E granitic dykes; also composite dykes with pegmatitic granites; often emplaced along S _{ECI} planes				Lower-crustal intrusive magmatism is possibly related to upper-crustal volcanism e.g. in the D _E pull-apart-basins							
		c. 1.86-1.85 ⁽¹⁷⁾	Granitic intrusions in eastern Finland (Maarianvaara)	Zones of folding with N-trending axial planes in eastern Finland ⁽¹⁶⁾ ; shear zones bordering the Central Finland block; Hiidenvesi shear zone in the WUC	E-W contraction	Related to escape tectonics causing eastwards movement of crustal blocks in central Finland		D _E structures are local and not significantly developed in southern Finland; stress probably released along the major E-trending shear zones in the south							
		c. 1.84	Minute granitic veining	Open to moderate large-scale folding locally with granitic veining in the axial plane; shearing especially along the early shear zones between granitoid and supracrustal terranes	N-S contraction	Collisional crustal shortening		Deformation D _E occurred simultaneously with the D _E , suggesting different local stress fields in different parts of the Svecofennian domain; situations of this kind are characteristic of escape tectonics							
		1.83-1.80	Granodiorites, granite and pegmatitic granite dykes	Extensional recumbent folding F _{HECI} with strong horizontal S _{HECI} and contractional folding with NE-SW-trending axial planes, medium- to high-grade metamorphism at low pressure and strong partial melting of earlier granitoids and gneisses	NW-SE transpression	Rotation of the stress field into NW-SE caused oblique contraction in the SFGZ and closing of the D _E pull-apart-basins		In high-grade areas (e.g. WUC and EGC) the change from D _E to D _H magmatism was transitional; patchy occurrence of the D _H granites refers to local oblique extensional zones during continued transpression							
		1.83-1.78	Diabase dykes	Weakly deformed amphibolite facies N-S- and E-W-trending diabase dykes	Oblique dilatational zones during the overall NW-SE transpression		There are also gabbroic rocks (D _H ?) within D _H granites, indicating wider deep-seated magmatism and heat flow during D _H								
POST-TECTONIC MAGMATISM AND FADING OF THE SVECOFENNIAN OROGENY															
E ₅	D ₁	c. 1.8	Late deformation in the N-S-trending major deformation zones (BBZ, RKZ and TIB); large-scale folding with N-trending axial plane forming open D _{(G)-H-I} dome-and-basin structures		C. ESE-WNW contraction	Crustal shortening and shearing along the major shear/fault zones									
		1.8-	Homogeneous granitic intrusions (stocks)	Post-tectonic to the major Svecofennian deformation phases, but are often sitting close to the intense D ₁ zones, like in the BBZ or RKZ				The BBZ, RKZ and TIB evolution initiated during the D _D transpression and continued during the D _{E-H} ; the D ₁ structures deform the SZGZ; the deformation style was brittle in the north and ductile in the south until the fade of the Svecofennian orogeny Post-tectonic or late tectonic to the D ₁ (?)							
POST-SVECOFENNIAN EVENTS															
	D _p	RAPAKIVI STAGE													
		1.65-1.52	Rapakivi granites, quartz-porphry and diabase dykes	Drag folding, zonal semi-ductile dextral shear zones, jointing in the direction of diabase dykes; large-scale listric faulting ⁽⁸⁾		Crustal extension		Rapakivi were set into the intersections of the late Svecofennian high-strain zones (D _E , D _G , D _H and D _I); the diabase dykes are at least partly controlled by ductile shearing structures like the Hiidenvesi shear zone in the WUC and jointing							
		RIFTING STAGE													
		c. 1.25	Sandstone and mafic diabase	Open dragfolds, weak fractural cleavage, brittle faults		Upper crustal extension									
		CALEDONIAN OROGENY													
c. 450 Ma		Brittle faults, reactivation of pre-existing structures and possibly low-angle brittle thrusting faults; fluid activity in preexisting faults; U-mobilization ⁽¹²⁾ and remagnetization ⁽¹³⁾		Reflections of Caledonian orogeny											
POST-GLACIAL EVENTS															
		<10 000 a	Minor faults deforming glaciogenic sediments and recent earthquakes ⁽¹⁰⁾		Present-day c. NW-SE stress field ⁽¹¹⁾	Post-glacial isostasy and modern plate-tectonics(?)		Reactivation along pre-existing brittle structures, joints and faults							

(1) Korsman et al. (1999, and references therein), (2) Väisänen & Mänttari (2002), (3) Hopgood et al. (1983), (4) Patchett et al. (1981), (5) Suominen (1991), (6) Pajunen et al. (2006), (7) Lahtinen et al. (2002), (8) Korja & Heikkinen (1995), (9) Elminen et al. (2008), (10) Kuivamäki et al. (1988), (11) Stephansson et al. (1986), (12) Vaasjoki (1977b), (13) Mertenan et al. (2008), (14) Mäkitie & Lahti (2001), (15) Lehtonen et al. (2005), (16) Koistinen 1981 and (17) Huhma (1986).

INTEGRATED STRUCTURAL SUCCESSION AND AGE CONSTRAINTS ON A SVECOFENNIAN KEY OUTCROP IN VÄSTERVIKEN, SOUTHERN FINLAND

by

Matti Pajunen¹, Alaric Hopgood², Hannu Huhma¹ and Tapio Koistinen³

Pajunen, M., Hopgood, A., Huhma, H. & Koistinen, T. 2008. Integrated structural succession and age constraints on a Svecofennian key outcrop in Västerviken, southern Finland. *Geological Survey of Finland, Special Paper 47*, 161–184, 21 figures and 2 tables.

The Västerviken outcrop in Karjalohja, southwestern Finland, represents an example of polyphase migmatitic rocks of the Svecofennian amphibolite facies supracrustal gneiss terrain, southeast of the non-migmatitic rocks in the Orijärvi area. The structural sequence on the outcrop yields two major groups of ductile deformation events, E_a - E_b and E_d - E_g , with a cooling stage in between them and later wide-scale open warping structures, D_h - D_i , of the earlier structures. The structural succession at Västerviken is correlated to the regional structural scheme in the southern Svecofennian domain.

The primary features of the felsic gneiss suggest a volcanic or volcano-clastic origin at c. 1.9 Ga. The earliest structures identified are isoclinal, intrafolial folds, F_a , in layered felsic gneisses, but they were not identified in the D_b -deformed gneissic tonalites. The first strong metamorphic pulse was accompanied by structures that provide evidence of an intense shortening event, E_b , that caused isoclinal F_b folding of the polyphase neosome veins at c. 1.88 Ga. Discordant relations of mafic dykes to the host rock and to E_b neosome veins, prove that the crust was rigid and cool prior to mafic dyke intrusion; this dilatational event is named as E_c . The mafic dykes were metamorphosed and altered in a potassium-metasomatic event, E_d , that was progressively developed to high-temperature, penetrative shortening accompanied by production of garnet-bearing granitic veins and dykes. The E_c - E_d events are related to an progressive extension that was followed by contractional steep folding events. Isoclinal F_c characterizes the outcrop and surrounding area. Large-scale asymmetric transpressional folding, F_f with a NE-SW-trending axial plane deformed the earlier structures. The E_f event was followed by angular F_g folding with N-trending axial planes suggests c. E-W contraction. An ESE-WNW-trending coarse-grained pegmatitic granite dyke, which yielded a U-Pb monazite age of 1804 ± 2 Ma, cuts the D_g structures as shown by gneiss fragments including F_g folds in the dyke. A pegmatitic granite dyke was intruded into a dilatational fracture after or during the latest stage of the E_g event, partly regulated by ductile sinistral N-S shearing near the dyke contacts. The latest structures, D_h - D_i , are open warps of the early structures. F_h folds are recumbent warps that were refolded by the open F_i folds formed under N-S compression. These deformations did not markedly affect the pre-existing structures on outcrop scale, but they are important when interpreting the regional variations in metamorphic grade, geophysical anomaly patterns or continuation of lithological sequences on the present-day erosion surface.

Key words (GeoRef Thesaurus, AGI): structural geology, gneisses, granites, dikes, structural analysis, deformation, absolute age, U/Pb, Proterozoic, Paleoproterozoic, Västerviken, Karjalohja, Finland

¹ *Geological Survey of Finland, P.O. Box 96, FI-02151 Espoo, Finland*

² *School of Geography and Geology, University of St Andrews, St Andrews, Fife KY16 9ST, Scotland*

³ *Koskelantie 29 B 24, FI-00610 Helsinki, Finland*

¹ *E-mail: matti.pajunen@gtk.fi*

INTRODUCTION

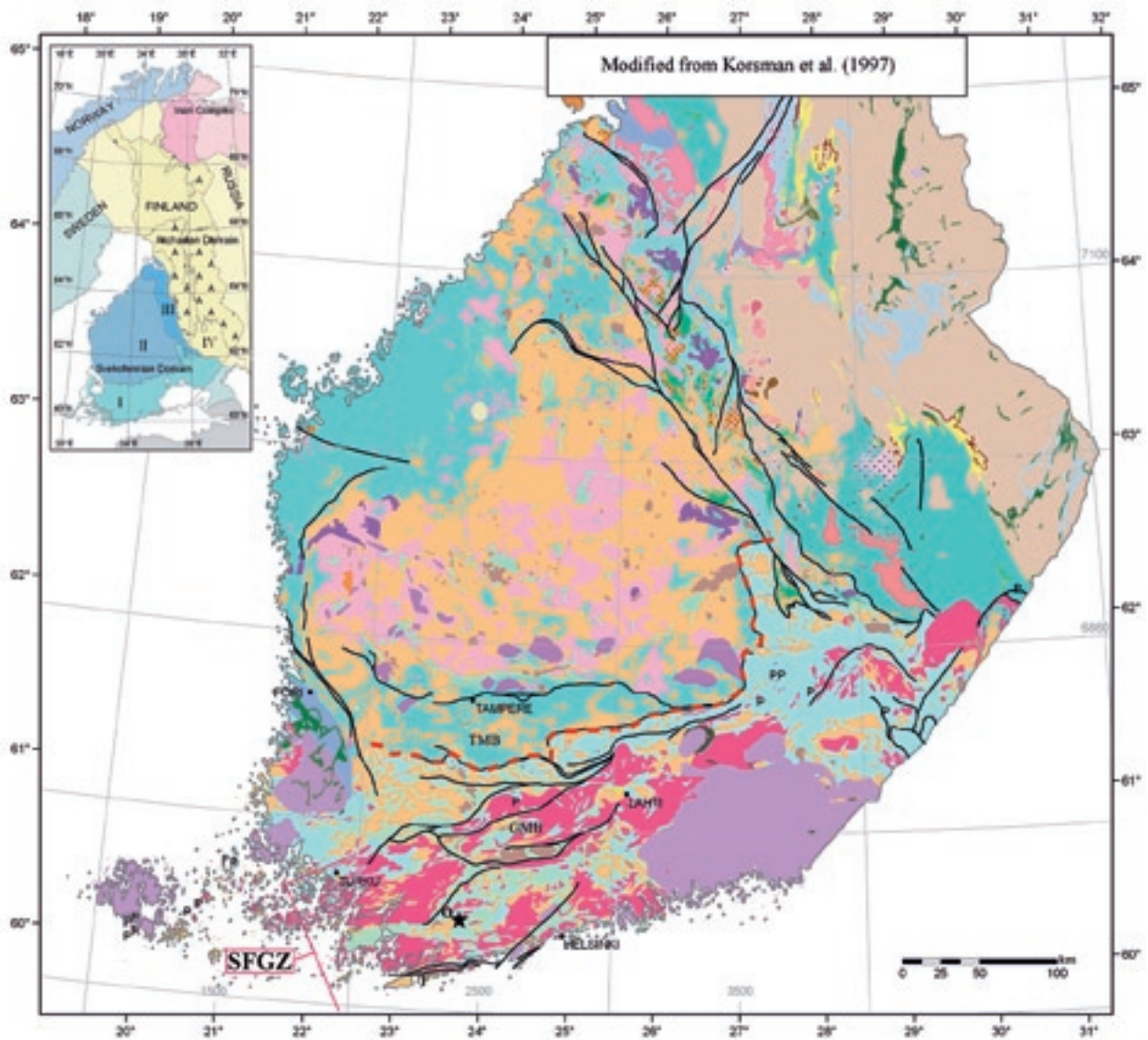
The c. 1.9 Ga old Svecofennian domain in the central part of the Fennoscandian Shield collided with the Archaean continent in the east at 1.89–1.885 Ga ago (Wegmann 1928, Koistinen 1981 and Korsman et al. 1999) (Figure 1). The multi-phase accretion, collision and extension history (Koistinen 1981, Lahtinen 1994, Korsman et al. 1999, Kilpeläinen 1998, Pajunen et al. 2004 and 2008) led to the recent re-constructions of geotectonic terranes each with individual characteristics representing different primary formation environments, timing and tectono-magmatic histories. The 1.93–1.92 Ga primitive Pyhäsalmi island arc (Korsman et al. 1984, Lahtinen 1994 and Korsman et al. 1999) was fragmented during collision against the craton boundary (Koistinen 1981 and Koistinen et al. 1996). The central Finland granitoid complex (cf. Nironen 2003) covers a wide area and is composed of tectonic slices stacked towards the N-NW (Pajunen et al. 2008) between the primary arc and the more mature arcs in the west and south. It shows a polyphase magmatic history with large amounts of syntectonic, mostly I-type granitoids (Nurmi & Haapala 1986) that were then intruded by post-kinematic granites that are younger towards the west (Rämö et al. 2001). In the south younger, c. 1.9–1.88 Ga old (Vaasjoki & Sakko 1988 and Väisänen & Mänttari 2002), volcanic-sedimentary belts trend roughly E-W and show a primary accumulation environment with more deep-water characteristics towards the north (Kähkönen 1987 and Ehlers & Lindroos 1990). Southern sequences were intruded by huge amounts of felsic granitoids that form the c. 100 km wide ENE-trending Southern Finland Granite Zone, SFGZ (Figure 1). Major high-strain or polyphase shear and fault zones separate the terrains (Pajunen et al. 2008).

As early as 1926 J. J. Sederholm described a tectono-magmatic discordance with cooling stages between the magmatic and migmatitic pulses in migmatitic granitoids in the southernmost Svecofennian terrain in the Tammisaari archipelago. Korsman et al. (1984 and 1988) established a corresponding tectono-metamorphic discordance between the Trondhjemite Migmatite Belt (TMB) and Granite Migmatite Belt (GMB) (Korsman et al. 1997 and Figure 1). The crust largely stabilized in the north c. 1.875 Ga ago, whereas in the south thermal heat flow remained high still later at c. 1.86–1.80 Ga ago (e.g. Korsman et al. 1999 and Pajunen et al. 2008). Several detailed or regional structural analyses to determine the complex evolution of the Svecofennian domain have been published during the last 30 years (e.g. Laitala 1973, Hopgood et al. 1976, Verhoef & Dietvorst 1980, Koistinen 1981, Hopgood 1984, Ehlers

et al. 1993, Koistinen et al. 1996, Korsman et al. 1984, 1988 and 1999, Kilpeläinen 1988 and 1998, Kilpeläinen & Rastas 1990, Pietikäinen 1994, Nironen 1999, Pajunen et al. 2001, Väisänen et al. 1994, Väisänen 2002, Väisänen & Hölttä 1999, Pajunen et al. 2004 and 2008). These analyses give a blanket overview of the evolution in the domain, but there are many contradictions in details, especially, in the southernmost parts. Correlation of deformation events over the major tectono-metamorphic discordances (e.g. Korsman et al. 1984) has been difficult. Correlation problems arise, because different tectono-thermal terranes display dissimilar "steps" in the deformation succession (Hopgood et al. 1976 and Pajunen et al. 2008). On the present-day erosion level slices from different crustal depths are exposed, for instance the Orijärvi area (Eskola 1914 and Kilpeläinen & Rastas 1990) contrasts with the neighbouring granulite facies West Uusimaa Complex (Parras 1958, Shreurs & Westra 1986 and Kilpeläinen & Rastas 1990). Accordingly, structures developed simultaneously in various depths exist in a close association to each other. In many cases they differ in appearance and tectonic style due to different ductility contrasts at various depths. Kilpeläinen (1998) evidenced that some early structures are totally missing from the tectonic slices representing the upper crustal levels during deformation.

The main goal of this paper is to provide data from a well-studied structural succession integrated with two new age determinations from a key outcrop as a contribution to current attempts to better establish the tectonic evolution of the southern Svecofennian crust. The key outcrop, in the Västerviken, Karjalohja (Figures 2 and 3), is situated in a migmatitic terrane, to the southeast of the Orijärvi area that was described in the classical papers of Eskola (1914 and 1915). Felsic gneisses, the origin of which has been under debate since Eskola's time, characterize the terrane. Between felsic gneisses there are zones of intermediate to mafic volcanic rocks and pelitic to psammitic metasedimentary gneisses and calc-silicate rocks. Several pulses of intrusive rocks and migmatization veins intrude the supracrustal successions (Sederholm 1926 and Hopgood et al. 1983).

For the present study T. Koistinen and A. Hopgood carried out the primary fieldwork on the outcrop in the early 1990's. Samples for isotopic dating, carried out by H. Huhma, were collected at 1991. The authors collaborated in the spring of 2004 to review the data, in thin section and on the outcrop, and integrated this with the current knowledge on the tectonic evolution of the Svecofennian domain.



LEGEND

NEOPROTEROZOIC ROCKS

Siltstone, sandstone and conglomerate

MESOPROTEROZOIC ROCKS

Siltstone, sandstone and conglomerate
 Olivine diabase (1.27 Ga)
 Rapakivi granite (1.65-1.57 Ga)
 Gabbro-anorthosite (1.65-1.57 Ga)

PALEOPROTEROZOIC ROCKS

Granite and associated rocks; southern Finland (1.81-1.77 Ga)

SVECOFENNIAN DOMAIN

I Accretionary arc complex of southern Finland (1.90-1.82 Ga)
 Microcline granite (1.84-1.82 Ga)
 Granodiorite, tonalite and quartz diorite (1.89-1.87 Ga)
 Gabbro and diorite (1.89-1.87 Ga)
 Quartzite
 Mica schist and mica gneiss
 Volcanic rocks

II Accretionary arc complex of central and western Finland (1.90-1.87 Ga)

Pyroxene granitoid (1.88-1.87 Ga)
 Granite (1.88-1.87 Ga)
 Granite (~1.88 Ga)
 Granodiorite, tonalite and quartz diorite (1.89-1.87 Ga)
 Gabbro and diorite (1.89-1.87 Ga)
 Mica gneiss and mica schist
 Volcanic rocks (~1.90-1.88 Ga)

III Primitive arc complex of central Finland (1.93-1.87 Ga)

Granite (~1.88 Ga)
 Pyroxene granitoid and mafic dykes (1.885 Ga)
 Granodiorite, tonalite and quartz diorite (1.89-1.87 Ga)
 Gabbro and diorite (1.89-1.87 Ga)
 Mica gneiss and mica schist with intercalated carbonate rocks
 Volcanic rocks (~1.92-1.88 Ga)
 Gneissic tonalite and granodiorite (1.93-1.91 Ga)

IV KARELIAN DOMAIN

Granite and granodiorite with gneissic inclusions
 Granite and granodiorite (~1.86 Ga)
 Granite (1.87 Ga)
 Granite (1.89-1.88 Ga)
 Granodiorite, tonalite and quartz diorite (1.89-1.87 Ga)
 Gabbro
 Mica schist, black schist, arkosite, conglomerate, carbonate- and calc-silicate rocks, metavolcanic rocks, BIF
 Gneissic alkaline granite
 Serpentinites and other rocks of ophiolitic origin
 Gabbro (2.15-2.00 Ga)
 Volcanic rocks, ultramafic to felsic
 Quartzite
 Gabbro (2.2 Ga)
 Granite (2.45-2.3 Ga)

ARCHEAN ROCKS

Granitoids
 Metavolcanic rocks
 Metasedimentary rocks
 Carbonatite
 Impact rocks

Major deformation zone, unspecified
 Boundary between tonchjemite and granite migmatite belts

Figure 1. Study area (star) in Västerviken Karjalohja (Finnish grid coordinates KKJ2 x= 6674300 and y = 24860900) on the geological map of southern Finland. Simplified from Korsman et al. (1997). SFGZ = Southern Finland Granite Zone, O = Orijärvi area, T = Tammisaari area, TMB = Tonalite Migmatite Belt (trondhjemite migmatite belt) and GMB = Granite Migmatite Belt.

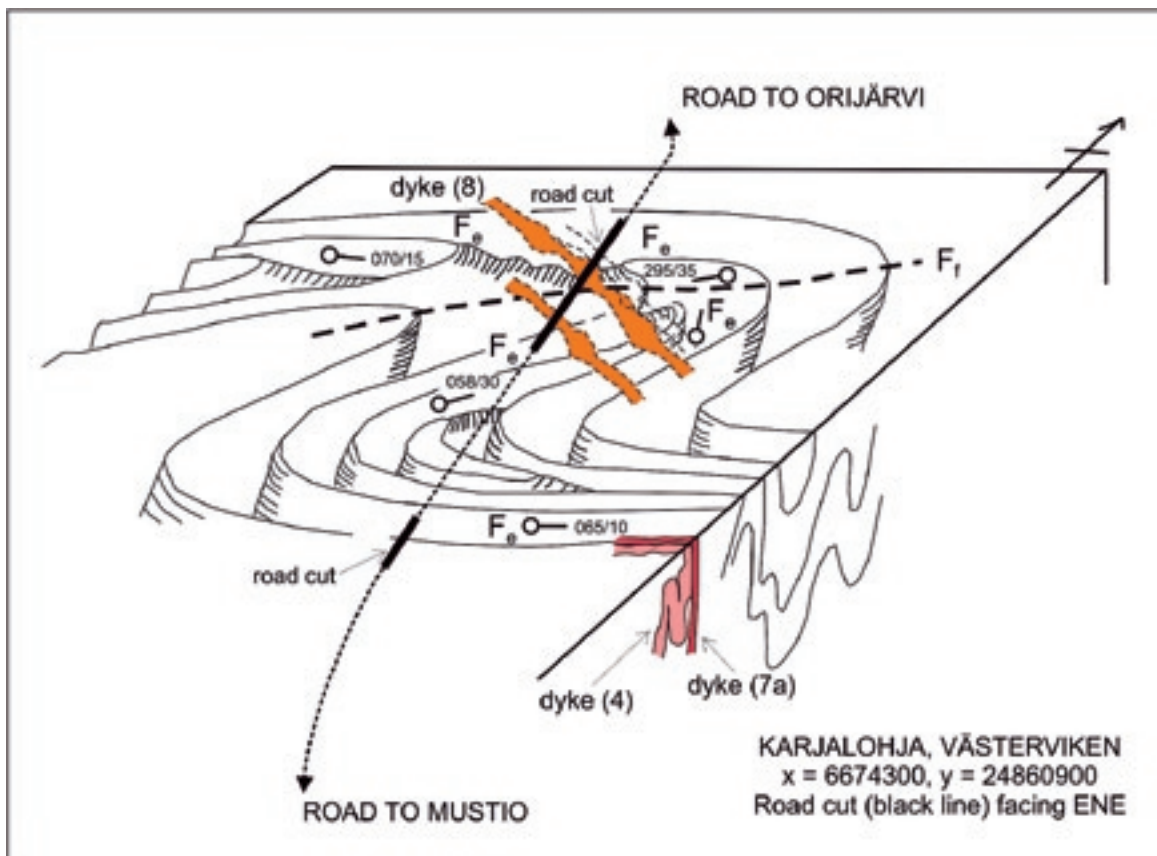


Figure 2. Tectonic setting of the studied Västerviken outcrop.

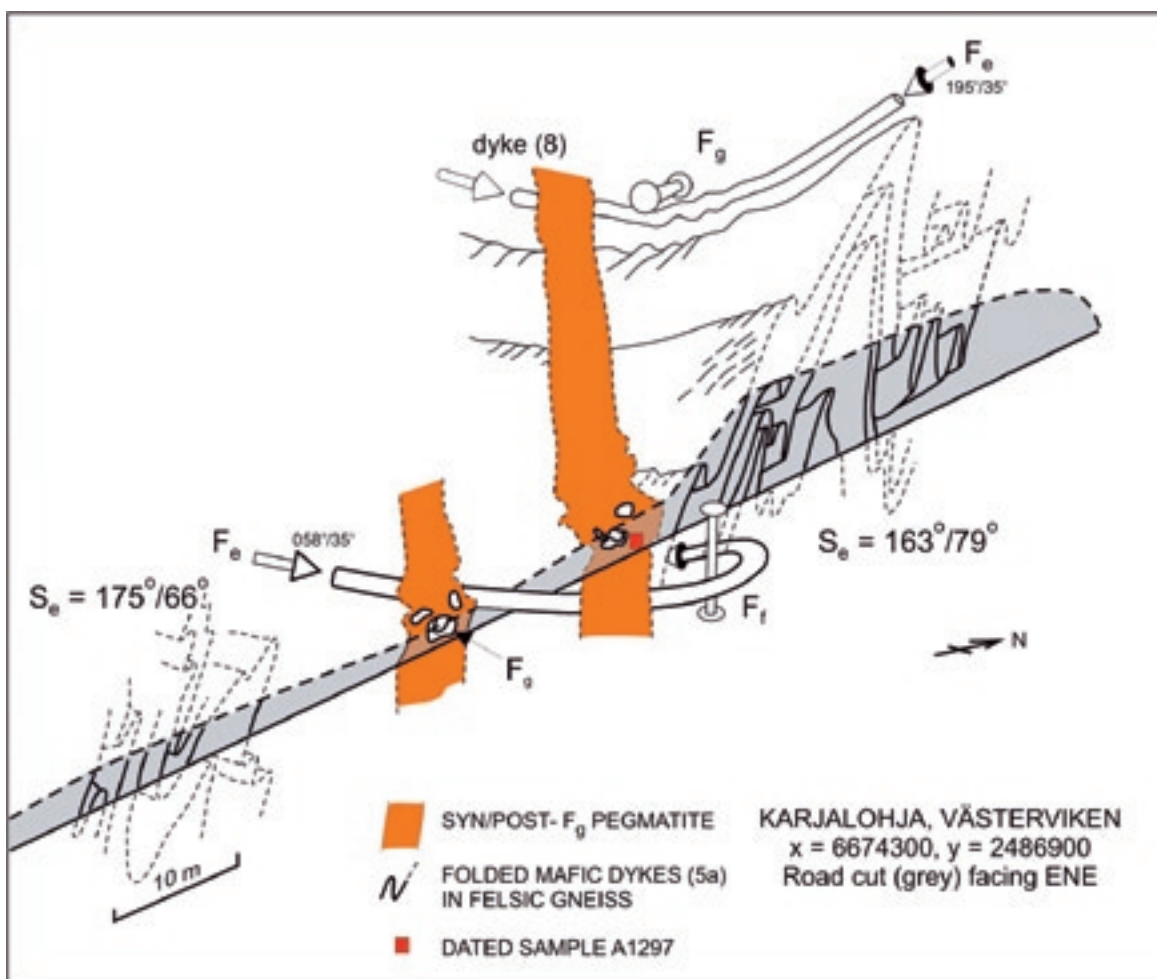


Figure 3. Detailed tectonic structure of the Västerviken outcrop.

METHODS AND DATA

Structural mapping in Västerviken was made on an outcrop (Finnish grid coordinates KJ2 x = 6674300 and y = 2486900) that clearly shows the major structural elements of the complex polyphase tectonic history known to characterize the area (Hopgood 1984). The analysis is based on the simple principle of overprinting between tectonic, magmatic and metamorphic events – the younger event affecting the earlier one. The successive sequence of events, E_a , E_b , E_c etc. was established using methods described by Hopgood (1980 and 1999). The structures are named from older to younger as follows: the primary bedding = S_0 , the first identified deformation = D_a , related folding = F_a , related axial foliation/surface/plane = S_a , lineation = L_a , magmatism = I_a and metamorphism = M_a ; the second, respectively, D_b , F_b , S_b , L_b , I_b and M_b ; the third D_c , F_c , S_c , L_c , I_c and M_c etc.

The U-Pb analyses on monazite and zircon were made at the Geological Survey of Finland, following procedures by Krogh (1973). The handpicked mineral concentrates were washed in HNO_3 in an ultrasonic bath, rinsed several times with H_2O and dissolved in HF and HNO_3 at 200°C for several days in steel jacketed teflon capsules. After evaporation of the fluorides the sample in HCl solution was aliquoted and a mixed $^{206}Pb/^{235}U$ (for monazite) or $^{208}Pb/^{235}U$ (for zircon) isotopic tracer was added. For isotopic measurements Pb was loaded on a single Re filament with Si-gel and H_3PO_4 and U on Ta-side filament using H_3PO_4 . Measurements were made using a VG Sector 54 mass spectrometer. The performance of the ion counter was checked by repeated measurements of a NBS 982 standard. Programs by Ludwig (1991, 2001) were used for age calculations.

DESCRIPTION OF THE VÄSTERVIKEN OUTCROP

Lithology

The main rock type on the Västerviken outcrop is felsic gneiss (Figures 4 and 5) that was intruded by intermediate to mafic dykes and several pulses of felsic veins and dykes. The felsic gneiss shows variably distinguishable banding that at least partly represents the original bedding, S_0 . Often S_0 is destroyed by polyphase deformation and concomitant metamorphic recrystallization, but when visible, it exhibits as minute variation of grain-size or composition. Compositional layering appears as biotite-, biotite-green hornblende-rich, amphibolitic and calc-silicate-bearing layers. Intermediate to mafic layers in the felsic gneiss imply a volcanic or volcanic-sedimentary origin for the rocks of the Västerviken outcrop. Under the microscope the layered felsic gneiss is fine-grained, the grain size being on average less than 1mm, and granoblastic composed of plagioclase, quartz and biotite, with opaque minerals, apatite and zircon as minor minerals. Small amounts of up to 1.0 cm subidioblastic or xenoblastic garnet grains exist in the biotite-rich layers (Figure 6a) or in flattened biotite patches in the more homogeneous parts. Some garnets show a two-stage growth with quartz and some biotite inclusions with vague internal foliation in their cores (I in Figures 6b and c) that are overgrown by rims including relic biotite inclusions (II in Figure 6c). The primary origin of the homogeneous felsic gneisses has been under debate for years and at present there exists no widely accepted consensus. The host gneiss is bor-

dered by more homogeneous tonalitic gneiss along tectonic zones (1 in Table 1). In contrast to the banded gneiss, some potassium feldspar occurs in homogeneous parts of the rock. A sample of the layered felsic gneiss was chosen for isotopic study (sample A1295, Table 2).

The felsic gneiss is cut by intermediate to mafic dykes (5a in Table 1) up to 0.5 m wide (Figure 7) that are strongly deformed and altered by later events. Isoclinally folded felsic segregation veins (6 in Table 1) indicate intense shortening in the dykes (Figure 8). Rarely, in the least deformed parts near fold hinges, a vague ophitic structure can be identified; one dyke shows plagioclase-porphyritic structure (5b in Table 1). The dyke cuts sharply across the felsic gneiss and the early phase of felsic neosome and pegmatitic veining (Figure 7); thus it post-dates the early migmatization pulses and boudinage of the felsic segregation veins. In the better-preserved parts the dyke is composed of hornblende, plagioclase and quartz with minor opaque minerals. Mostly the dykes are penetratively altered and granitized resulting in breakdown of almost all the hornblende to biotite; alteration occurs in zones parallel to the dyke. In these tightly folded dykes quartz often shows undulose extinction and biotite shows intense crenulation cleavage.

Several generations of neosome-forming felsic vein and dyke material can be distinguished on the outcrop. The early narrow quartz-feldspar segregation veins (2 in Table 1) and the isoclinally or ptygmatically folded, fine- to medium-grained trochjemitic

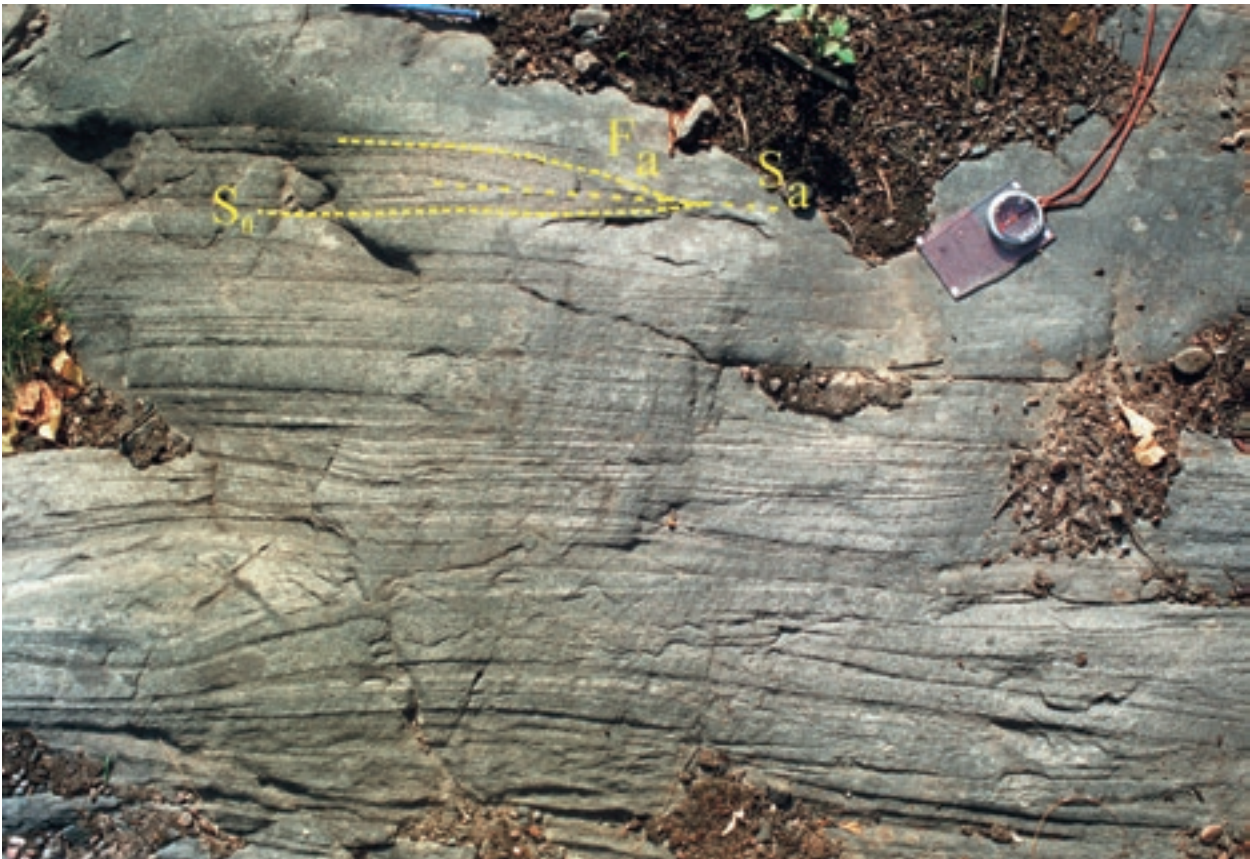


Figure 4. F_a folding in felsic banded gneiss. Photo by T. Koistinen.

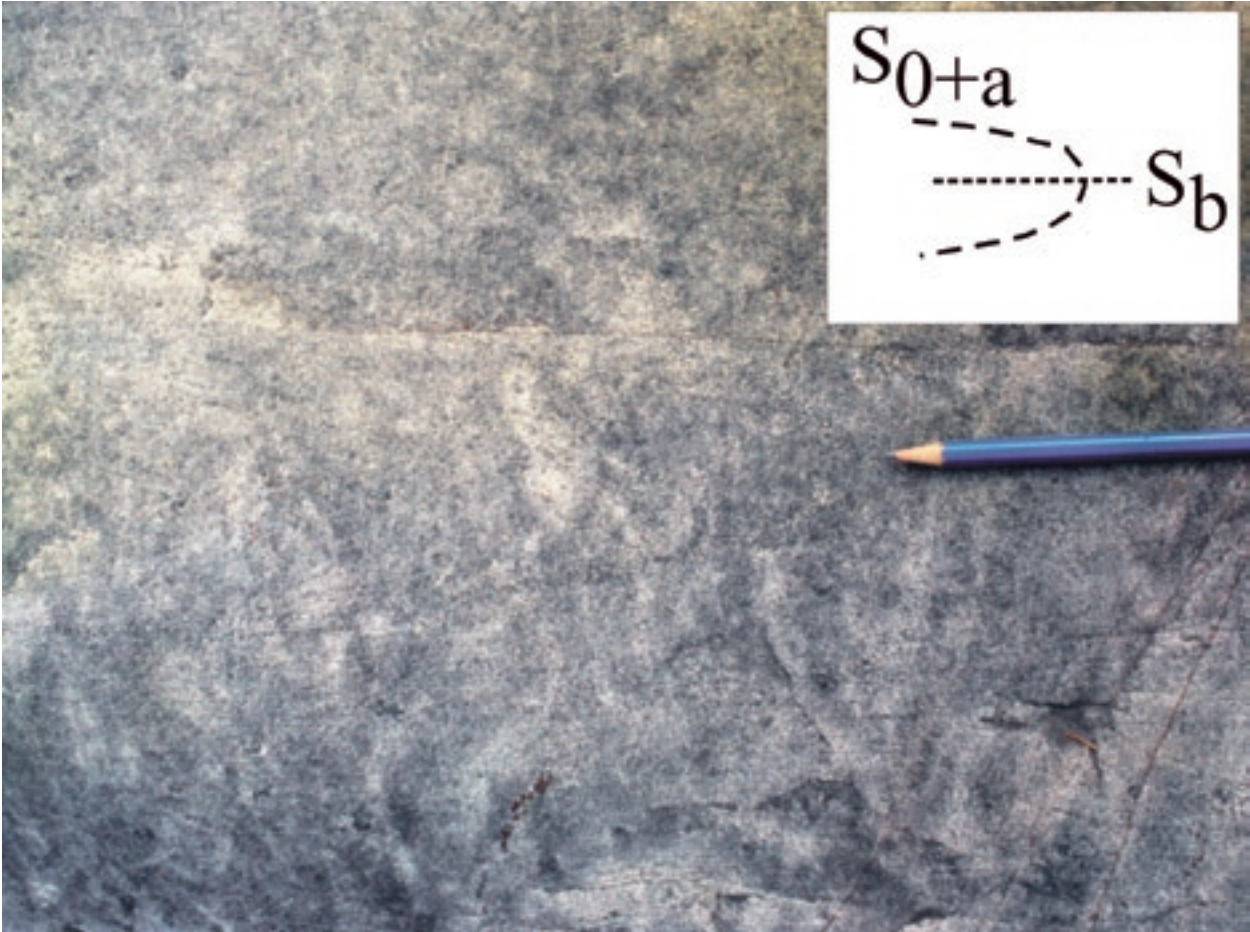


Figure 5. S_a foliation deformed by F_b folding in homogeneous weakly banded felsic gneiss. Photo by T. Koistinen.

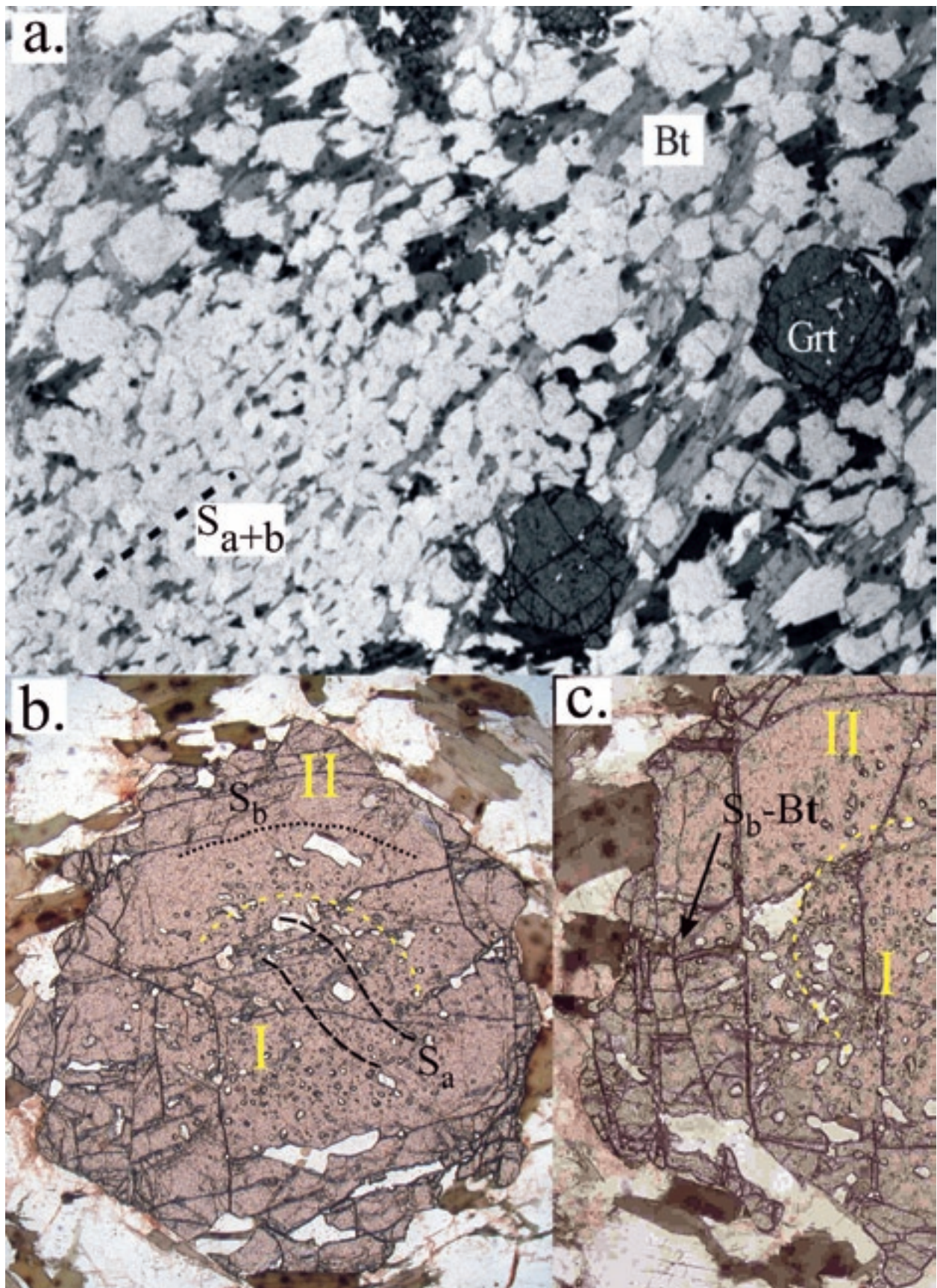


Figure 6. a. Two-stage garnet grains in banded and folded felsic gneiss. Rims of the grains overgrow S_b foliation. Photo T. Koistinen. b. Two-stage garnet with a vague internal S_a foliation in the core (I) and nearly inclusion-free rim (II) overgrowing the S_b . c. Garnet rim (II) overgrowing the S_b biotite. Photos by M. Pajunen.

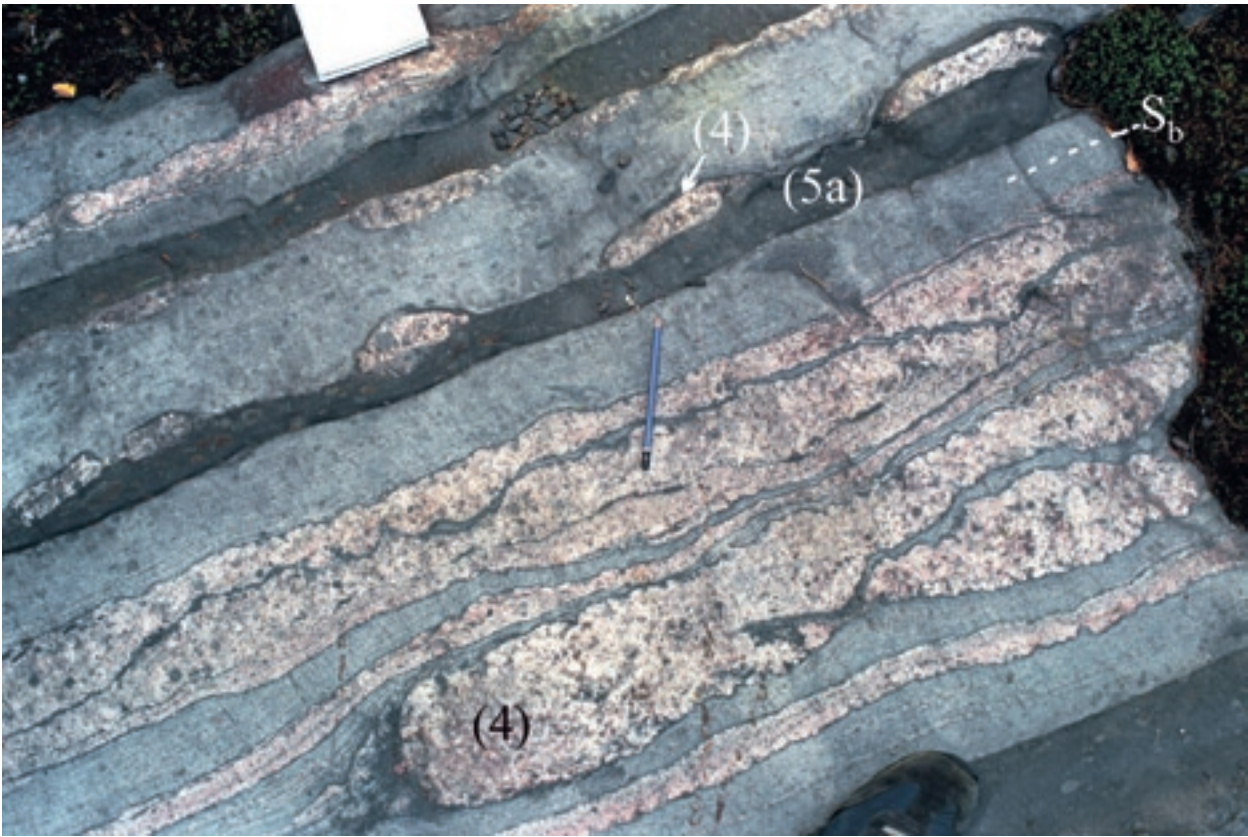


Figure 7. Mafic dyke cutting a pinch and swell structured, D_b boudinaged, pegmatitic granite dyke (4 in Table 1). The cutting relationships indicate cooling after D_b . Photo by T. Koistinen.

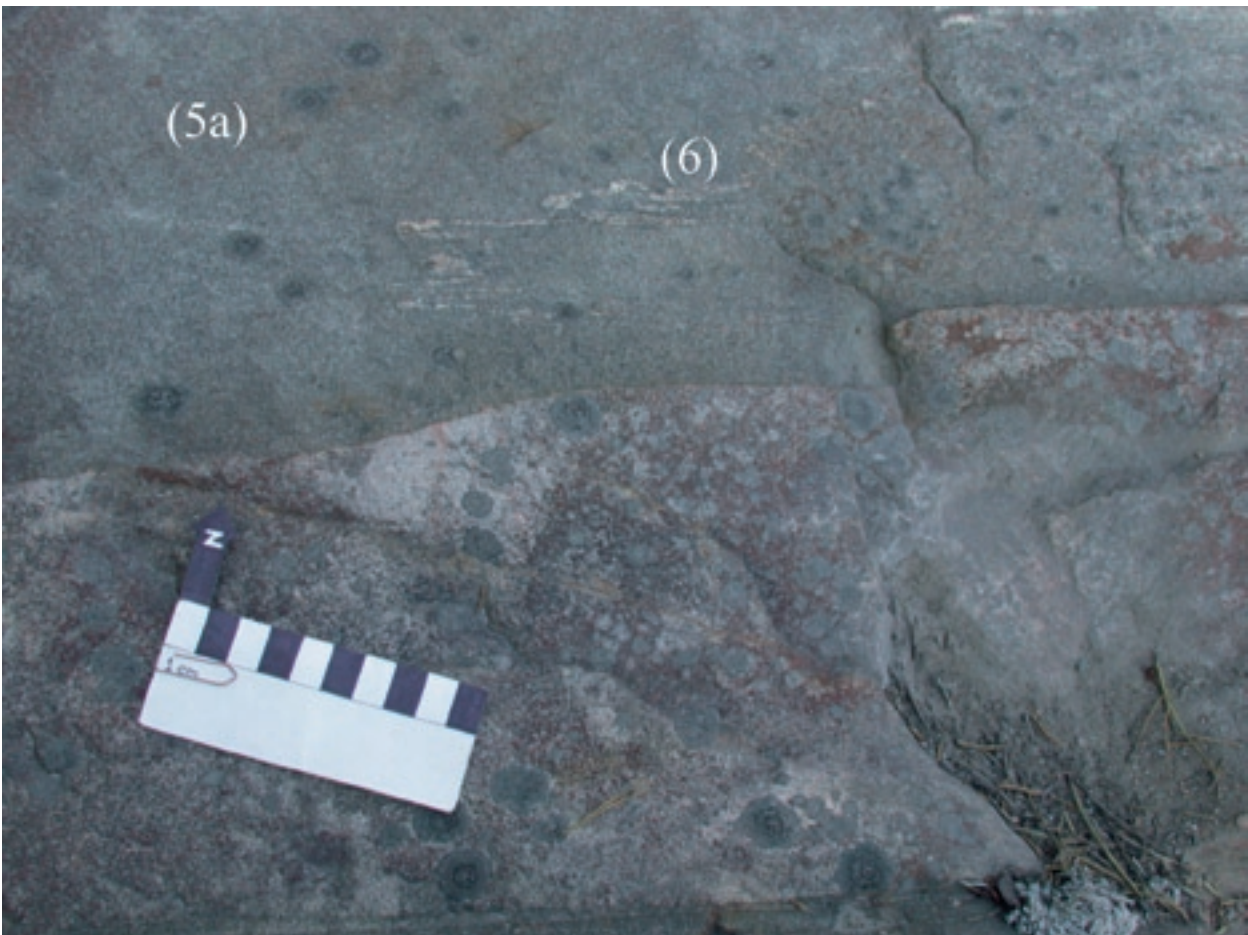


Figure 8. Isoclinally folded felsic segregation vein (6 in Table 1) in a mafic dyke (5a in Table 1) indicating strong shortening, D_d , of the dyke. Photo by M. Pajunen.

veins (3 in Table 1) migmatize the host gneiss (Figure 9). Narrow biotitic selvages with minute garnet grains border the veins; garnet has not been found in the veins themselves.

A later generation of more coarse-grained veining (4 in Table 1) is also isoclinally folded and changes from trondhjemitic to granitic in composition (Figure 7 and 10). No garnet was found in the veins. They show biotite-rich rims against the host rock. These dykes form ductile pinch and swell structures that locally form totally isolated swells; in places, only the border zone of the dykes shows pinch and swell structure. The spaced foliation of surrounding gneiss parallels the contacts of the pinch and swell structured pegmatite veins. The mafic dykes described above cut these felsic veins (2–4 in Table 1).

Foliated pegmatitic granite dykes (7a in Table 1) overprint the early felsic veining (2–4 in Table 1) (Figure 10). In contrast to the previous ones they include sparse, up to 1 cm garnet grains. The pegmatitic granite dykes show tight folding and bulging of the borders with some quartz in the shallow boudinage necks. However, strain including boudinage was not as intense as in the pinch and swell dykes (4

in Table 1). There are weak biotite melanosomes on the dyke borders, but between the isoclinally folded limbs of folded dykes, biotite was coarsened and indicates metasomatic potassium segregation during the flattening process. The borders of the dykes vary between being sharply penetrating to more or less gradational against the earlier vein generations. In detail these garnet-bearing dykes cut the pre-existing veins (2–4 in Table 1) and the foliation related to them (Figure 11). Vague coarse-grained granitic patching and narrow, ptygmatically folded veining (7b in Table 1) of granitic composition similarly overprint the earlier felsic migmatization veins.

The latest coarse-grained pegmatitic granite dykes (8 in Table 1) (Figure 12) cut all the described structures except for those classed as E_h and E_i (Table 1). The dykes are up to five metres wide and c. ESE-WNW-trending, dipping 65° to the south. In the northern contact zone of the widest dyke the granite is medium-grained and changes to coarse-grained towards the central part; in the southern contact the rock is coarse-grained. The contacts of the dykes are quite sharp, but showing slight pinch and swell, indicating some ductile to semi-ductile deformation during their intrusion. Their tectonic



Figure 9. Early D_b trondhjemitic neosome (3 in Table 1) in F_d folded felsic gneiss. The stretching and ptygmatic folding of these early dykes indicate strong flattening. The later pegmatitic granite dyke (7a in Table 1) cuts both S_0 and early neosome veins (2 and 3 in Table 1). Photo by M. Pajunen.



Figure 10. Relationships between pinch and swell structured granitic (4 in Table 1) and garnet-bearing granite dykes (7 in Table 1). Spaced S_b parallel with the pinch and swell structured granite dykes that show stronger deformation than the garnet-bearing granite dyke that is compressed to follow the pinch and swell structure of the early dykes. See also Figure 11. Photo by M. Pajunen.

setting can be placed from enclaves up to 0.5 m of the deformed country rock that contain pre-existing F_g folds (Table 1). Locally, the contacts are sinistrally sheared in a N-S direction. However, the coarse biotite shows no determinable foliation in the central parts (Figure 13). The dykes are potassium feldspar-rich, quartz occurs up to 20 cm wide patches and patchy biotites have grown up to 15 cm grains; no garnet was found. The dykes are widespread in the surrounding outcrops indicating an important magmatic pulse. This rock was chosen for isotopic dating (sample A1297, Table 2).

Deformation succession and its regional correlation

The following description of the deformation succession (Table 1) exposed at Västerviken concentrates on the local major structures that can be identified on the outcrop (Figures 2 and 3). Not all of the minor features of the detailed field study are described here, because their regional significance has not yet been ascertained, and some structures ob-

served in regional scale are not represented in the studied outcrop (cf. Pajunen et al. 2008).

E_a event

The earliest deformation structures identified on the outcrop are small isoclinal, intrafolial folds F_a that deform the primary layering S_0 . The fold limbs have become intensely thinned and their hinges are sharp and attenuated (Figure 4). Relict S_a is identified as a weak biotite foliation bending around F_b fold hinges in the felsic gneiss and weak felsic segregation (Figure 5). Elsewhere its identification is uncertain. The early folds are not identified in the non-layered tonalitic gneisses (1 in Table 1). There are also some quartz-(feldspar) veins (2 in Table 1) post-dating S_a (Figure 9). Metamorphic assemblages during D_a cannot be established with certainty, because later higher-grade events have overprinted them; S_a biotite/hornblende foliation was accentuated by D_b mineral growth where S_b is parallel to it (Figure 14) and there is a mineral lineation, L_a , parallel to F_a fold axes. The establishment of early garnet growth

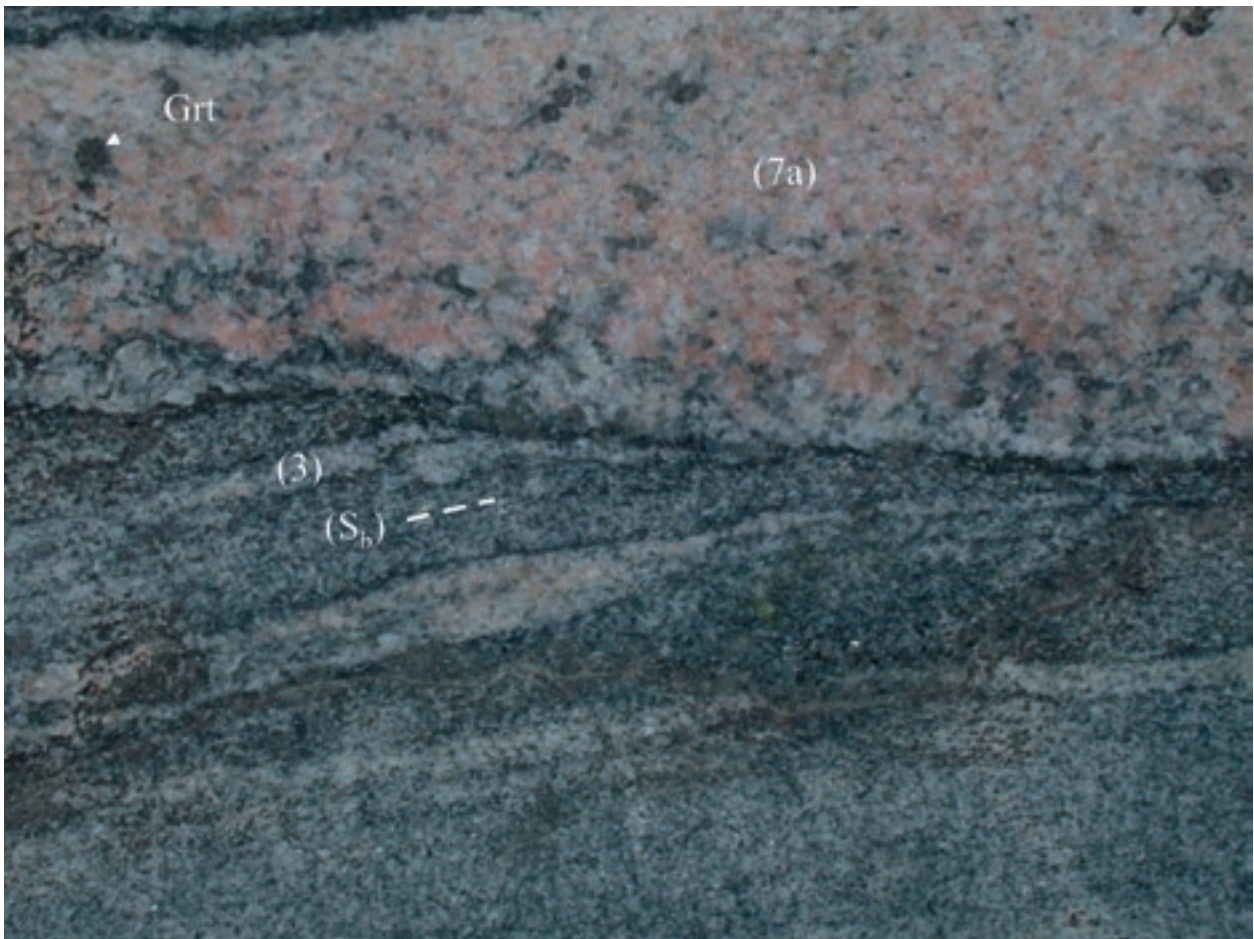


Figure 11. Detail from the contact of a garnet-bearing granite dyke (7 in Table 1). The dyke cuts both the veins of earlier migmatization pulses and the S_b foliation. Photo by M. Pajunen.

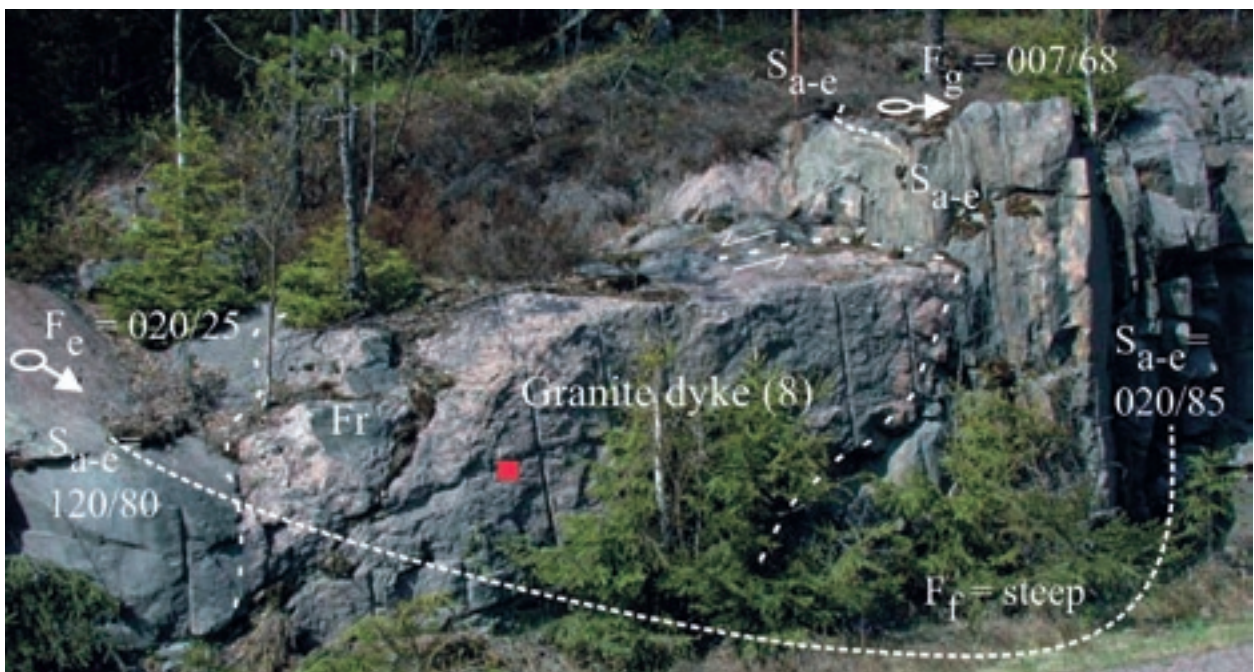


Figure 12. Pegmatitic granite dyke (8 in Table 1) cutting across a large F_f fold, which shows as a bend in the S_b foliation and the F_e fold axes. Fr = fragment of country rock and red box = sample A1297. Photo by M. Pajunen.



Figure 13. Detail of the dated (A1297), undeformed, coarse-grained part of the pegmatitic granite dyke (8 in Table 1). Biotite shows as large non-oriented plates. Photo by M. Pajunen.

with respect to deformation is tentative, but some curved inclusion trails in garnet cores implies early growth (Figure 6b). If the vague internal foliation in garnet cores is a relic S_a , then the biotite-quartz-garnet assemblage is a result of the early prograde metamorphism, M_a , to amphibolite facies during E_a similar to that described by Hopgood et al. (1976) from c. 30 km southwest of the study area, in Skåldö, Tammissaari. The F_a fold axis is nearly horizontal, plunging gently east on the outcrop; estimation of tectonic transport direction is only tentative due to reorientation of F_a by later deformation.

E_b event

D_b deformation was associated with the tectonic episode that produced the regional foliation, segregation and migmatization that characterizes the outcrop. D_b was accompanied by intense shortening as shown by small-amplitude, isoclinal to tight, intra-folial folds, F_b , that refold the S_a foliation (Figure 5). S_b is axial planar mineral foliation, penetrative biotite foliation or spaced crenulation and segregation

of coarse- and fine-grained bands in felsic gneisses. F_b hinges are typically round and locally shearing occurred along the fold limbs promoted by the increased ductility resulting from continuing melting. In the layered gneiss the F_b folds are generally tight and less than 1 m in amplitude and F_b fold axes plunge gently approximately E or W. S_a and S_b form an intersection lineation ($L_{a,b}$) that is best seen in the felsic gneiss when S_b forms a strongly recrystallized spaced biotite crenulation intersecting the S_a segregation foliation. The early plagioclase-quartz segregation veining (2 in Table 1) was produced along S_b planes and anatectic pulses progressed to more intense trondhjemitic neosome (3 in Table 1) formation. These early veins are isoclinally folded and attenuated indicating intense flattening strain (Figure 9). The later, more coarse-grained granite veins (4 in Table 1) have spaced S_b foliation lying parallel to the vein contacts (Figure 10) and were deformed into boudins and pinch and swell structures (Figure 7). Garnet rims (II in Figures 6a and 6b) overgrow S_b that is preserved as some M_b biotite relics (Figure 6c), but S_b is curved to surround the garnet core (I in Figure 6b).

Table 1. Succession of structural elements on the Västerviken outcrop.

Event	Structure	Description	Process
E ₀	S ₀	Primary layering, sedimentary or volcanic (Figure 4).	
E _a	F _a	Intrafolial, isoclinal, sharp-hinged folds with E-trending axis (Figure 4).	Folding of indurated sedimentary layers.
	S _a	Axial plane penetrative mineral foliation (strengthened by M _b) or vague internal foliation in garnet (Figure 6b).	
	L _a	Mineral lineation (predominantly Hbl at present, Figure 14), intersection between S ₀ and S _a ?	
		Tonalites (1), approximately concordant to S _a , includes S _b .	Intrusion into the supracrustal gneisses.
E _b	F _b	Intrafolial, tight to isoclinal, round hinge, refolds S _a (Figure 5).	Onset of T increase.
	S _b	Axial plane penetrative mineral foliation (Hbl, Bt) (e.g. Figures 5, 6 and 7).	Low-grade metamorphism up to amphibolite facies.
	I _b ?	Qtz-Fsp segregation veins (2, Figure 9), parallel to S _a , cut by veins (3); relation to tonalite (1) not seen.	
	I _b	Trondhjemitic veins (3), strongly folded and boudinaged (Figure 9).	Early-D _b segregation veining – low-T (cf. Mouri et al. 1999).
	I _b	Granitic veins (4), folded, pinch and swell structured and boudinaged, compositional difference between veins (3) and (4), folds rounder in vein (4) than in vein (3) (Figures 7 and 10).	
			Cooling. Crust becomes rigid.
E _c	I _c	Mafic dyke (5a) in brittle host. Cuts boudins of veins (4) with sharp contacts (Figure 7), vague blasto-ophitic texture.	Extension perpendicular to foliation. Mafic dykes (5) intruded into rigid, cool crust.
	I _c	Plagioclase-porphyritic dyke (5b) with sharp contacts and finer-grained margins.	
E _d	F _d	Intrafolial, small, tight angular folds with sharp hinges in altered dyke (Figure 15) isoclinal round hinges in folded segregation veins (6) (Figure 8).	T increase. Flattening perpendicular to foliation. Low-T biotitic alteration in some mafic dykes (5).
	S _d	Spaced foliation.	
	L _d	Intersection lineation L _d near the dyke (5a) contact folded by F _e (Figure 18).	
	I _d	Granite dykes (7a), garnet-bearing, cuts veins (3) and (4) (Figures 10 and 11), less deformed (flattened) than dykes (3) and (4). Ptygmatic granite veins and melt patches (7b).	T increase and partial melting. Coarsening and granitization of pre-existing granite dykes causing gradational boundaries (Figure 9).
E _e	F _e	Large amplitude (more than 5 m) isoclinal folds (Figure 16). Refolds S _d . Thinned limbs. Relation to dykes (7a) not seen.	Intense compression.
	S _e	Axial plane crenulation cleavage – S _d /S _e .	Some biotite growth into S _e axial plane (Figure 17).
	L _e	Intersection lineation between S _d and S _f parallel to hinges (Figure 18).	
E _f	F _f	Large (amplitude tens of metres) moderate folds (Figures 2, 3 and 12). Axial planar trend of F _f is c. NE (Figures 2 and 3). Steep fold axis.	Moderate horizontal SE-NW compression.
	S _f	Weak local spaced axial planar cleavage approximately 160/90 (Figure 19).	
E _g	F _g	Sub-angular moderate folds (Figure 20).	Moderate horizontal E-W compression.
	S _g	Axial plane approximately 090/90.	
	I _g	Coarse-grained pegmatitic granite dykes (8) dated at 1804 ± 2 Ma. Contacts c. 180/65. Local N-S-shearing in the contacts. Includes enclave of F _g fold.	
E _h	F _h	Open recumbent folds (Figure 16) refold S _e axial plane.	
	S _h	No axial plane structure observed. Axial plane dips gently north.	
	L _h	Wrinkling of pre-existing biotitized zones along the fold hinge (approximately 270/10).	
E _i	F _i	Open warps refold S _h (Figure 16).	Weak horizontal N-S compression.
	S _i	Axial plane approximately 000/90.	

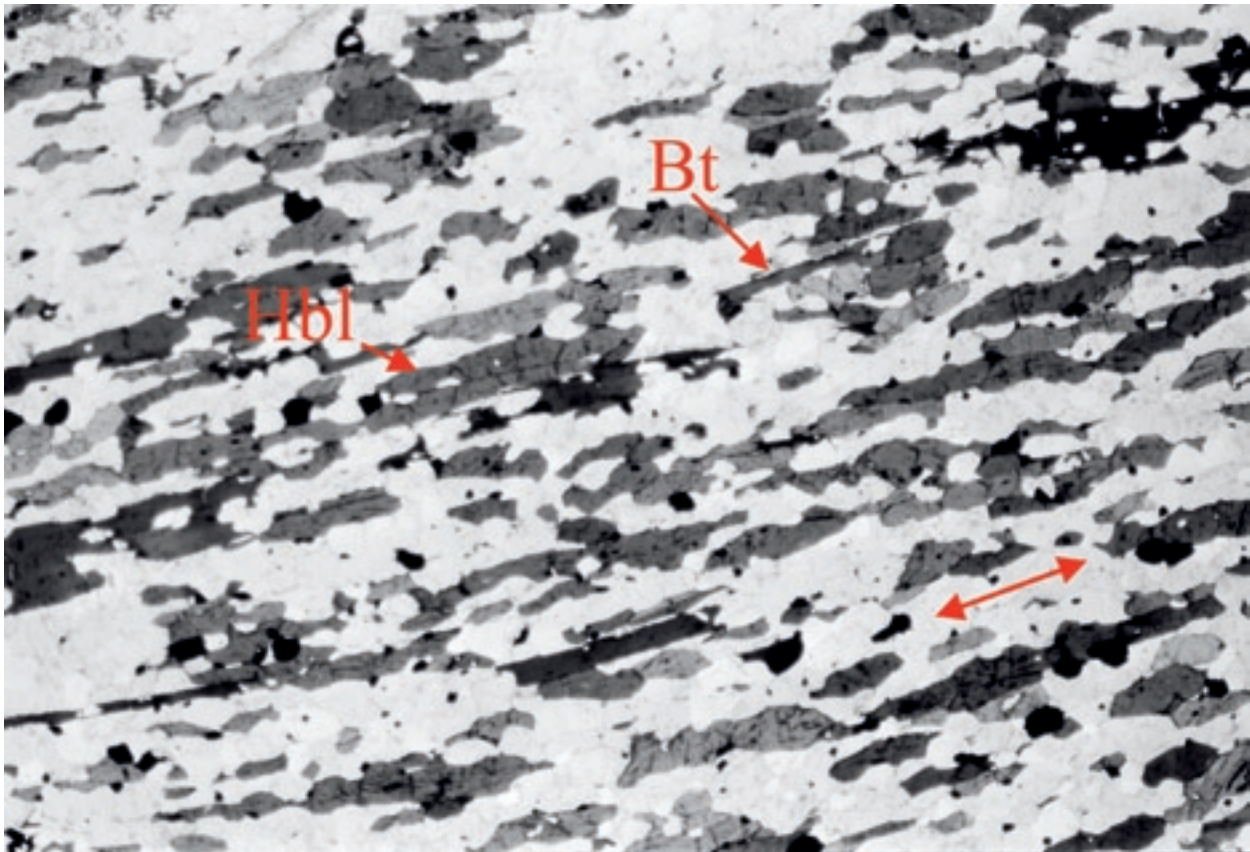


Figure 14. L_a mineral lineation in an intermediate biotite (Bi)-hornblende (Hbl) gneiss layer. Photo by T. Koistinen.

E_c event

The E_c mafic dykes (5a in Table 1) cut the foliation, trondhjemitic veining (3 in Table 1) and also split the pinch and swell structure of the early pegmatite dykes (4 in Table 1). Some faulting occurred during the dyke emplacement because of non-continuation of the pinch and swell structure on the opposite side of dyke (Figure 7). Their sharp and originally planar contacts suggest intrusion into cooled, rigid crust indicating a stabilizing and cooling stage after the E_b event. The plagioclase-porphyritic dyke (5b in Table 1) shows a similarly retrogressed (see below) mineral assemblage suggesting its emplacement corresponded to the mafic dyke. The deformation structures in the dykes show post- E_c structural history.

E_d event

Retrograde, spaced foliation (Figure 15) in the mafic dykes is F_c -folded (Figure 15 and 16); under the microscope some remnants of small tight angular F_d folds are crenulated by D_c . Locally the hornblende-plagioclase assemblage of the dyke was altered to almost monomineralic coarser-grained (3 mm) biotite (Figure 17). This type of alteration implies metasomatic potassium enrichment during the develop-

ment of the foliation. In the strongly altered dyke contacts composite foliation S_{a+b} and the spaced foliation S_d formed an intersection lineation L_d ($L_{(a+b)/d}$ in Figure 18).

Narrow, isoclinally-folded feldspathic segregation veins (6 in Table 1) cut the mafic dyke (Figure 8); originally the veins formed approximately perpendicular to the dyke. The shortening in the garnet-bearing granite dykes (7a in Table 1) (Figures 10 and 11) corresponds to that in the mafic dykes; they intruded prior to E_c . Isoclinal folding in these dykes (7a in Table 1) (Figure 2) and tight folds in felsic gneiss (Figure 9) indicate that the continuing D_d deformation under increasing temperature affected the rock more thoroughly. Deformation occurred under changing conditions of potassium-rich fluidal activity during the granitic anatexis event. The formation of these garnet-bearing granite dykes, more irregular granitic melt patches and pygmatic veins (7b in Table 1) indicates a new thermal pulse with temperature increase to high-grade conditions related to flattening strain.

E_e event

Ductile F_c folds in the mafic dykes are tight with amplitudes of several metres (Figures 2, 3 and 16). Their hinges are relatively thicker than their limbs.

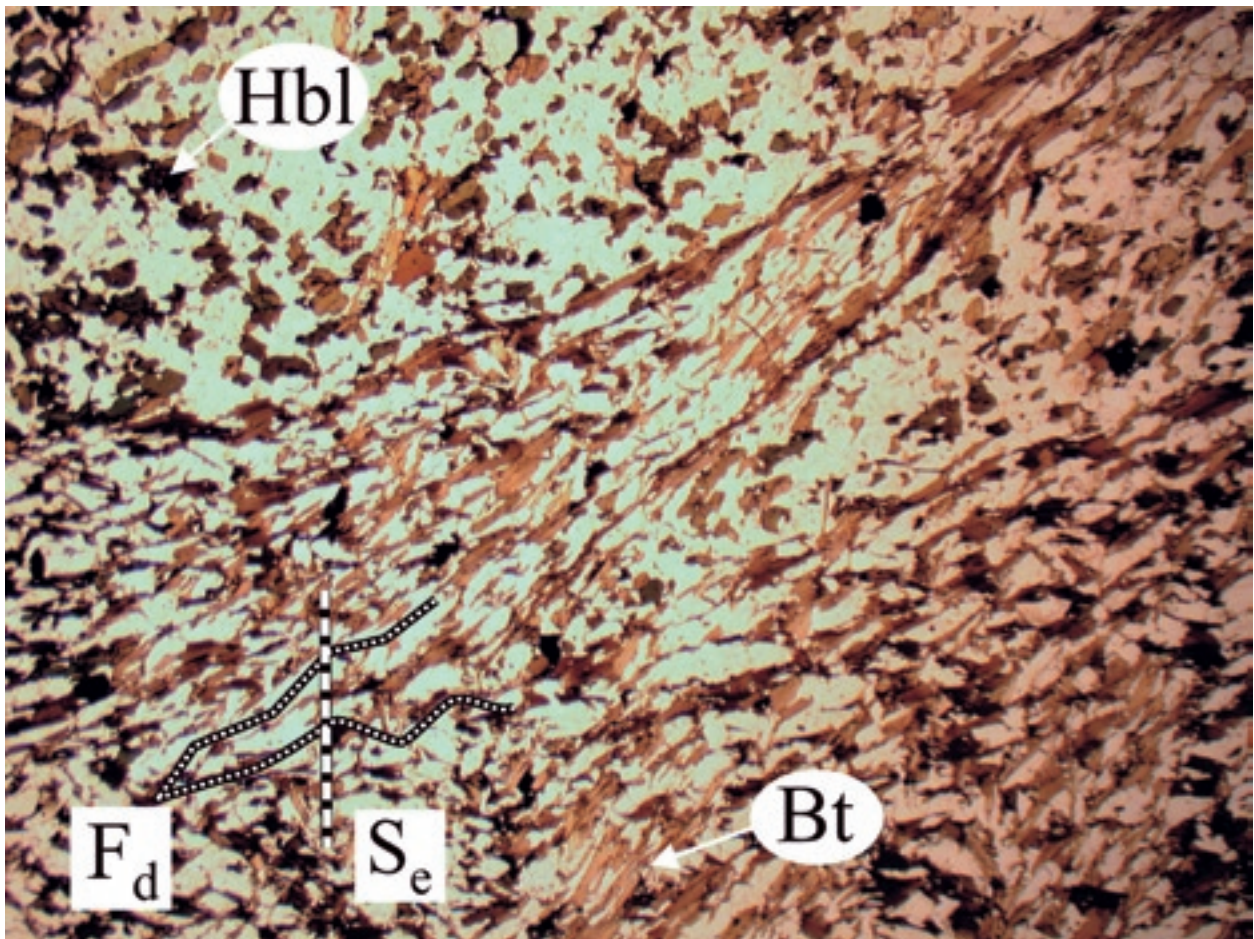


Figure 15. Photomicrograph of an intermediate dyke showing zoned alteration of hornblende (Hbl) to biotite (Bi). The altered zones are isoclinally F_d folded and they are further crenulated in D_c . Photo by M. Pajunen.

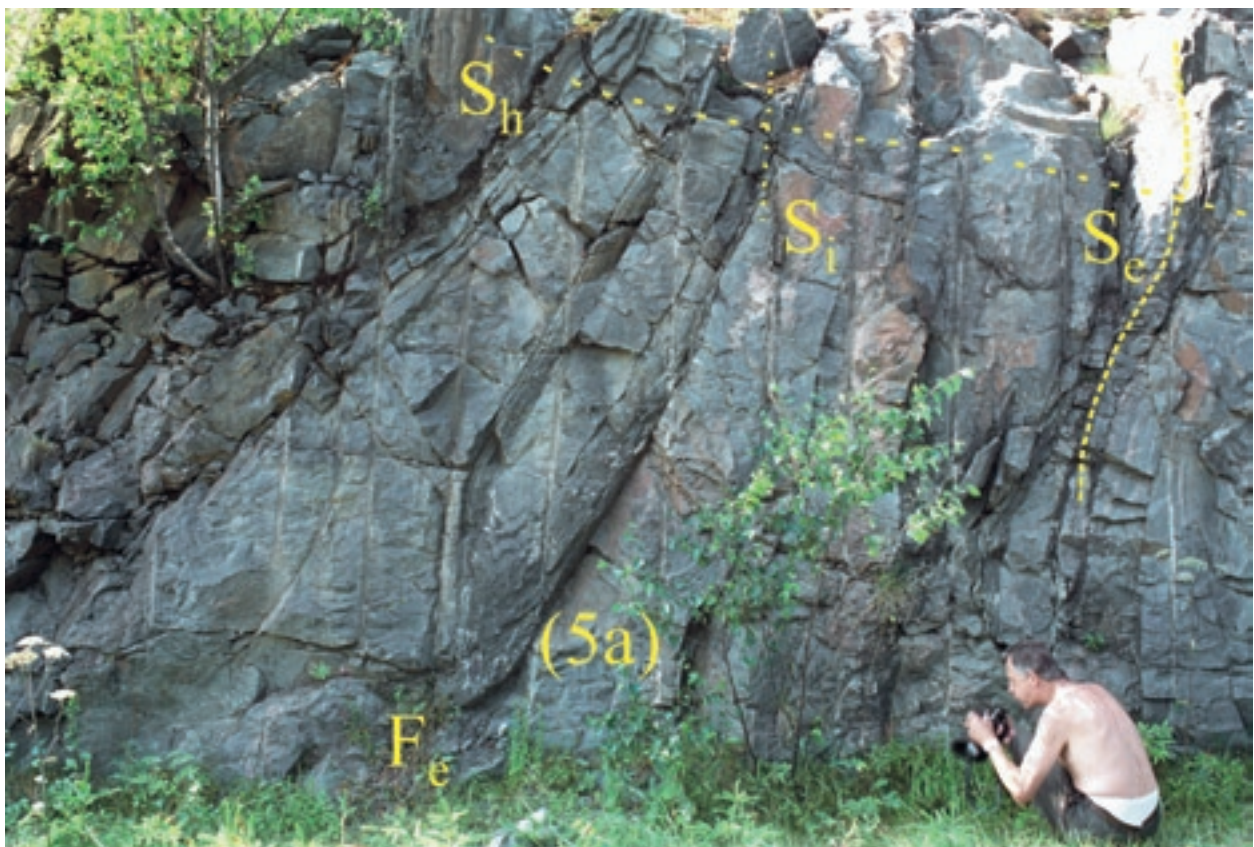


Figure 16. Isoclinally F_e folded mafic dykes (5a in Table 1). The axial plane S_e was bent by later open recumbent folding F_h (axial planar attitude $000^\circ/45^\circ$) and c. N-S trending compression D_i . Photo by T. Koistinen.

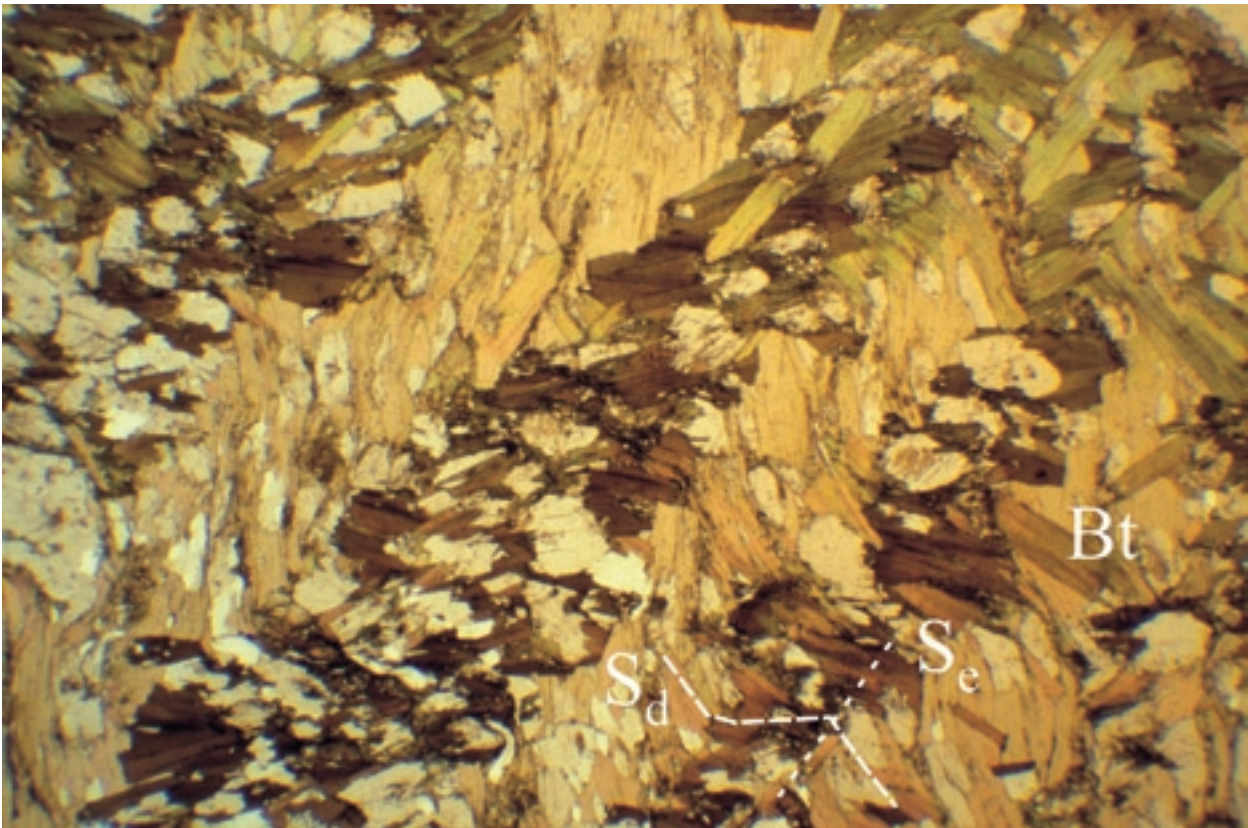


Figure 17. Microphoto of S_c crenulation in penetratively biotitized (D_d) mafic dyke. Photo by T. Koistinen.

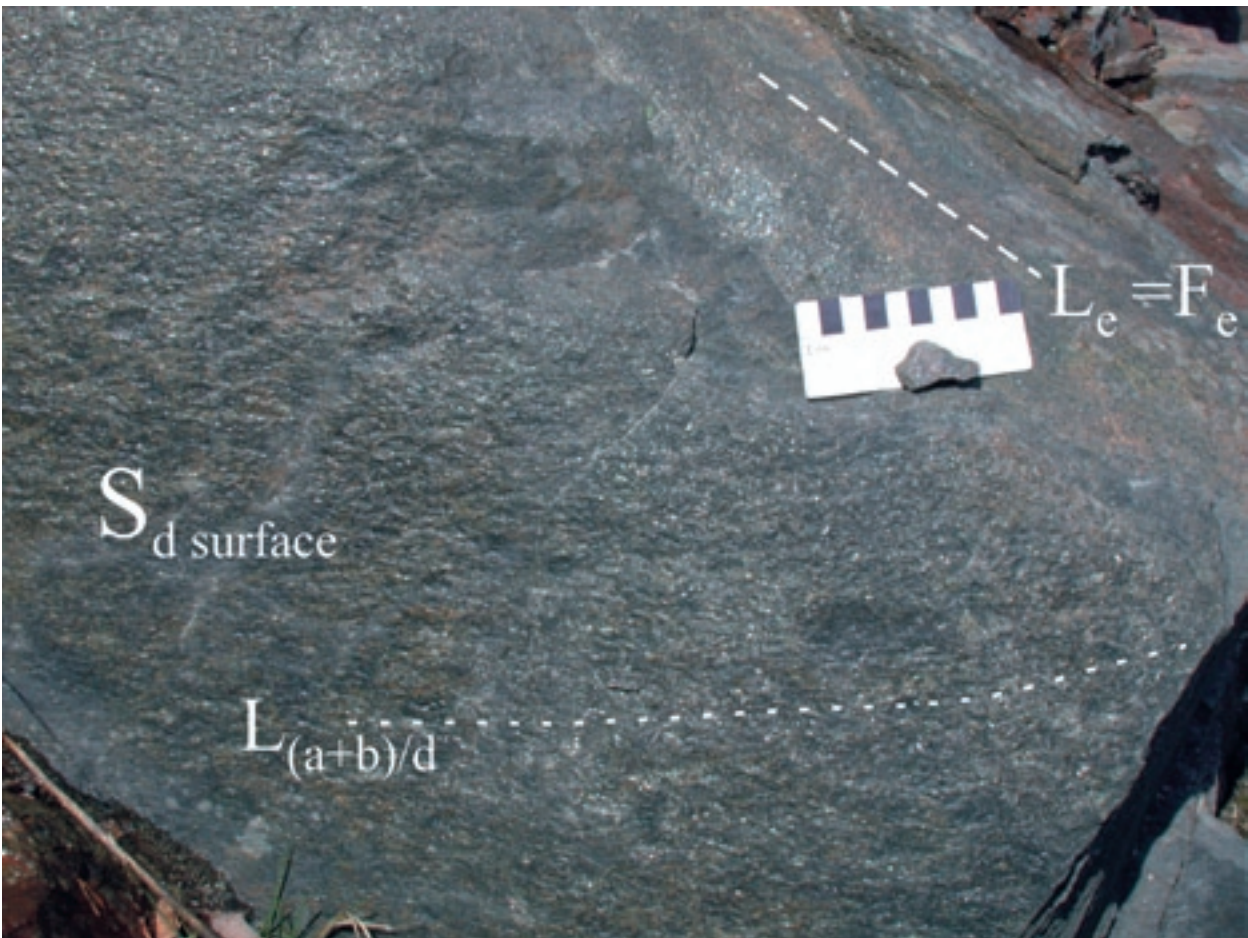


Figure 18. L_d intersection lineation folded around an F_e fold. The intersection lineation L_e between the biotitic alteration-segregation foliation S_d and S_c is parallel to the F_e fold axis. Photo by M. Pajunen.

In the felsic gneiss F_c are rounder and fragmented reflecting competence contrast between the dyke and gneiss. S_c foliation dips steeply south. F_c fold axes are bent by later deformation and have a shallow plunge. S_c biotite foliation was generated in the most intensely folded hinges. Generally, in the mafic dykes, S_c is a crenulation cleavage with some biotite in the axial plane (Figures 15 and 17). The intersection lineation, L_d , was bent around the F_c hinge (Figure 18). The angular disparity between F_c hinges and the lineation serves to separate them as products of different deformation episodes, indicating different tectonic transport directions with respect to the early deformation. In the dykes themselves the S_d alteration segregation foliation bends around the F_c fold hinges. The S_d and S_c form a weaker intersection lineation L_c that is parallel to the F_c fold axis. The two intersection lineations can be clearly distinguished on the outcrop (Figure 18).

E_f event

D_f deformed the S_c axial surfaces into semi-open, dextral, asymmetric folds with c. NE-trending axial planes, S_f (Figures 2 and 3). On the outcrop F_f axes

can be seen to plunge steeply (Figure 12), but in areas characterized by horizontal earlier structures, the plunge is typically shallow (Pajunen et al. 2008). The amplitude of F_f folds ranges between tens of metres and kilometres, and the folds are clearly visible at map scale, for example on aeromagnetic and lithological maps (1:100 000). On the Västerviken outcrop weak, spaced S_f cleavage deforming the main foliation in the limbs of F_f folds can sometimes be observed (Figure 19).

E_g event

Sub-angular moderate folds F_g (Figure 20) with N-trending steep axial planes refold the F_f fold limbs and suggests E-W contraction. No S_g axial plane foliation was observed, but local N-trending sinistral shearing along the granite pegmatite dyke (8 in Table 1) occurred.

The granite pegmatite dyke (8 in Table 1) cuts all the structures described above (Figures 2, 3 and 12). It includes fragments of F_g -folded country rock. The dyke intruded into a dilatational fracture in c. ESE-WNW direction and is related to the latest phase of E_g or shortly post-dating it.



Figure 19. S_f crenulation cleavage crosscutting S_c . Photo by M. Pajunen.



Figure 20. Sub-angular F_g folding on the limb of large F_f fold in felsic gneiss. Photo by M. Pajunen.

E_h , E_i and other late events

S_c axial planes are curved to form open recumbent folds with shallow S_h axial planes dipping north (Figure 16). No axial planar foliation was observed, but there are F_h wrinkles in the pre-existing biotitized zones with approximately $270^\circ/10^\circ$ axes.

Very open F_i warps re-fold the S_h axial surface (Figure 16). The S_i axial plane is steep and approximately E-trending indicating N-S contraction. In the studied outcrop it cannot be established whether the lower-grade, semi-ductile deformation zones with fine-grained, neomineralized biotite and deformed quartz, overprinting the higher-grade E_c kinking in biotite, is related to these late open warps. These microstructures indicate that deformation took place under semi-brittle conditions, characteristics that are related to the latest Svecofennian, and at least partly, to post-Svecofennian events by Elminen et al. (2008) and Mertanen et al. (2001 and 2008).

Isotopic results

Mineral separation of the felsic gneiss A1295 yielded a small amount of small, short, nearly colourless and transparent crystals of zircon. Many grains have slightly rounded edges due to resorption. The zircon population appears to be homogeneous, and consistent with a felsic metavolcanic rock. The U-Pb data are shown in Table 2 and Figure 21. The two U-Pb analyses on zircon from the felsic gneiss sample A1295 are discordant and do not allow a reliable age determination. The analyses plot on the chord with intercepts at 1881 and 291 Ma.

The pegmatitic granite (8 in Table 1) A1297 contains monazite, which in the extracted fraction occurs mostly as turbid and reddish fragments. The heavy minerals also contain a small amount of low-density zircon, which was not analysed in this study. In spite of the high content of U, the U-Pb analysis on monazite from the pegmatite A1297 is nearly concordant and provides an age of 1804 ± 2 Ma (Figure 21). This is considered to be an intrusive age for the pegmatite generation, which postdates the major ductile folding deformations (F_{a-g}) observed in the outcrop.

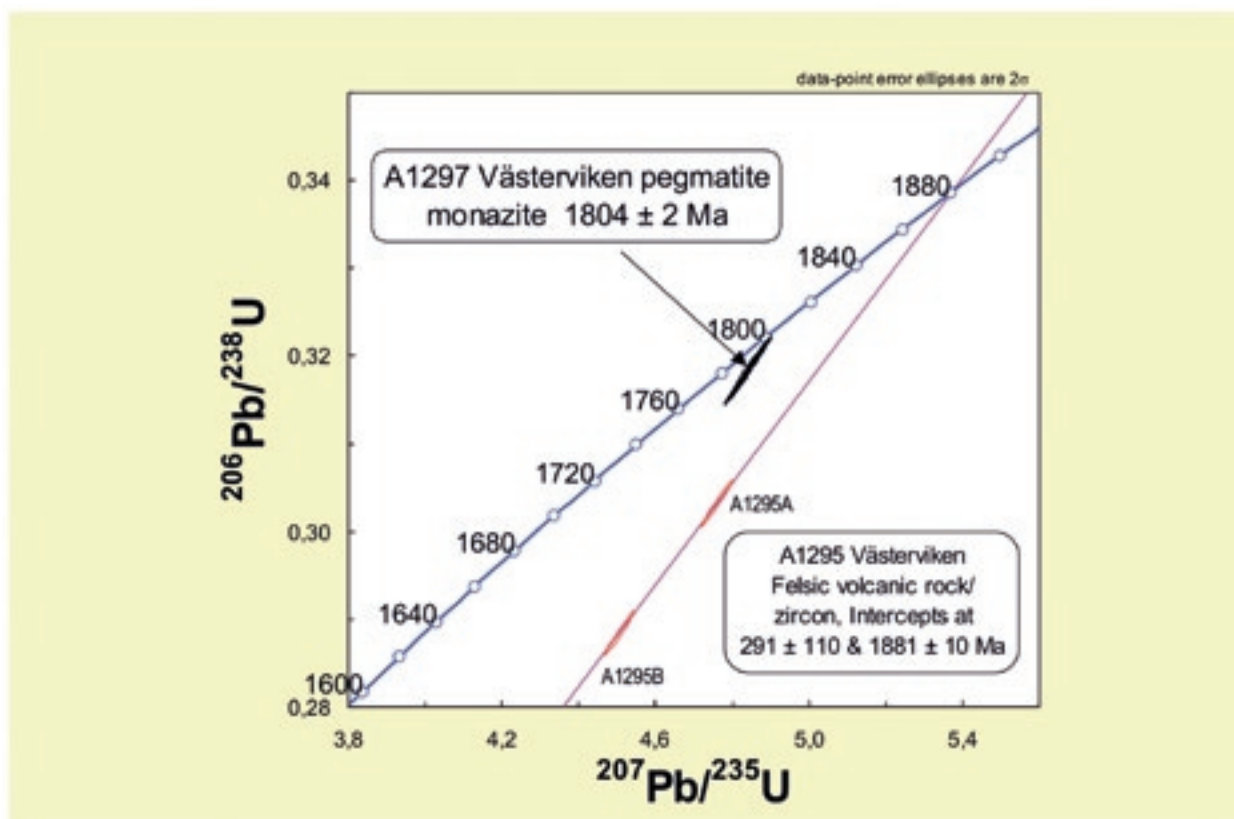


Figure 21. Concordia diagram of zircon and monazite analyses from the Västerviken samples.

Table 2. Mineral U-Pb data from the Västerviken samples.

Sample information	Sample	U	Pb	206Pb/204Pb	208Pb/206Pb	ISOTOPIC RATIOS*						Rho**	APPARENT AGES / Ma		
						measured	radio-genic	206Pb/238U	2s %	207Pb/235U	2s %		207Pb/206Pb	2s %	206Pb/238U
A1295 felsic metavolcanic rock:															
A1295A +4.3 a5h zircon	6	499	167	12423	0.161	0.303	0.7	4.761	0.7	0.114	0.12	0.99	1707	1778	1862
A1295B +4.3 zircon	9	555	182	12779	0.206	0.288	0.7	4.507	0.7	0.113	0.12	0.99	1633	1732	1853
A1297 pegmatitic granite (8 in Table 1):															
A1297A Monazite	0.3	10920	9477	11641	2.04	0.318	1	4.84	1	0.110	0.12	0.99	1781	1791	1804

*)Corrected for blank (Pb=0.5 ng, U=0.2 ng), mass fractionation and initial age related common lead (Stacey & Kramers, 1975).

**)Error correlation

Zircon in A1295: small, short, light, translucent

DISCUSSION

The structural succession described from the migmatites of the Västerviken outcrop demonstrates their complicated deformational history. This description of one key outcrop by no means tells the whole tectonic history of the area, but it can be used for correlative analyses of deformation structures in the neighbouring areas.

Primary association

The rocks of the southern Finnish coast and archipelago show evidence of a primary depositional environment characterized by felsic to mafic volcanic rocks, e.g. pillow lavas, metaturbiditic rocks and layers of shallow-marine carbonate rocks and silicate-facies iron formations (e.g. Sederholm 1926 and Ehlers & Lindroos 1990). The volume of carbonate rocks and pillow lavas diminishes towards the north, and volcanism changes to intermediate, pyroclastic and epiclastic in character (Kähkönen 1987). Deep-water turbiditic sedimentation with intermediate to mafic volcanism characterizes terranes further north such as the tonalitic migmatite belt (Korsman et al. 1984 and Kähkönen 1987). Mafic and calc-silicate layers are the primary features providing evidence for a volcanic or volcano-clastic origin for the felsic gneiss in the outcrop studied here.

Although the U-Pb zircon analyses of the felsic gneiss are discordant, they, however, plot on the chord with intercepts at 1881 and 291 Ma, and suggest that the age is compatible with many Svecofennian volcanic rocks. The lowermost rhyolitic lava flow in the Orijärvi area shows a conventional age of 1895 ± 2 Ga and dacite representing an upper stratigraphic level is 1878 ± 4 Ma old (Väisänen & Mänttari 2002). The Orijärvi granodiorite that yielded an age of 1898 ± 9 Ma was regarded as comagmatic with the surrounding volcanic rocks (Väisänen et al. 2002). Hopgood et al. (1983) reported a conventional U-Pb zircon age of 1895 ± 13 Ma for the banded dioritic gneiss in Baggö in the Tammissaari area, which they considered to be an age estimate for the protolith of volcanogenic sedimentary assemblage. Garnetiferous gneiss from Björkholmen, also in the Tammissaari area, gave a conventional U-Pb zircon age of 1896 ± 3 Ma and this was suggested as the source age of the volcanic-volcanogenic assemblage with associated marbles, calc-silicate rocks and amphibolites (Hopgood et al. 1983).

Deformation

The Västerviken outcrop represents a polyphase and migmatitic equivalent of the Svecofennian amphibolite facies supracrustal gneiss terrane southeast of the Orijärvi area. The structural sequence on the outcrop yields two major ductile events, E_a - E_b and E_d - E_g . Semi-brittle to brittle fracturing channeling the mafic dyke magmatism, D_c , indicates a cooling stage between the ductile events. Late ductile to semi-ductile open folding phases E_h - E_i do not show any marked effects on the outcrop scale, but they are important when in the context of map-scale structures and variations in regional metamorphic assemblages (cf. Pajunen et al. 2008).

U-Pb analyses on zircons from mafic pegmatoids from the Tammissaari area, c. 30 km to the southeast of Västerviken, define a chord with an upper intercept age of 1885 ± 7 Ma (Hopgood et al. 1983). According to Hopgood et al. (op. cit.) the dating establishes the crystallization age of the mafic magma. This magmatism post-dates the sedimentary-volcanogenic pile, but pre-dates the first recognized deformational phase and associated penetrative metamorphic fabric. This can be postulated as a maximum age of the non-migmatitic D_a in the present study area.

D_b was a strong vertical shortening event with concurrent felsic neosome formation; trondhjemite veins (3 in Table 1) and pinch and swell structured veins (4 in Table 1). The D_b structures were deformed into steep position during later deformation events (e.g. Pajunen et al. 2008). Pajunen et al. (2004) related the corresponding structures to a crustal collapse, and later, to an island arc collapse (Pajunen et al. 2008). Unfortunately, no acceptable material was obtainable for conventional U-Pb analyses from the granitic pinch and swell veins in Västerviken (sample A1296). Many age determinations provide evidence for an early migmatitic-metamorphic history in the vicinity of Västerviken. According to Hopgood et al. (1983) large euhedral sphenes from a quartzofeldspathic vein (A798 Kurö) crosscutting banded dioritic gneiss provide concordant analysis with an age of 1882 ± 9 Ma. This vein shows weak effects of F_c folding of Hopgood et al. (op. cit.) and the date is supported by concordant 1877 ± 6 Ma old monazite from garnetiferous gneiss (A806). Pink aplite veins containing monazite with a concordant age of 1871 ± 3 Ma (A797-Orrholmar-na) cut the quartzofeldspathic veins. An example from trondhjemite migmatites (cf. Korsman et al. 1984) is provided by the study of Mouri et al. (1999), who report ages of c. 1.88 Ga for monazite and

garnet in Luopioinen, c. 50 km ESE from Tampere. In the present outcrop, the main garnet growth (inclusion-free rims) post-dated D_b , but the S_b foliation bends around the garnet core with inclusion trails. Correlation between the ages and structures described indicate that D_b occurred c. 1.88 Ga ago, at about the same time as the youngest volcanic rocks in the Orijärvi area were emplaced. Thus, several pulses of felsic vein formation occurred over a very short time indicating a c. 1.88 Ga migmatitic event with concomitant volcanism (cf. Väisänen & Mänttari 2002) in the Southern Finland Granite Zone (Figure 1).

In Västerviken the cooling stage after E_b is evidenced by the intrusion of the mafic dykes, M_c , into a semi-brittle to brittle fractures of the E_b -migmatized host rock, and by the formation of the retrograde, metasomatic segregation foliation S_d into the mafic dykes. Earlier in 1926 Sederholm described a similar discordance from the Tammissaari archipelago. Several studies (e.g. Korsman et al. 1984) divided the crustal evolution in the southernmost Svecofennian into two major tectono-thermal stages, the c. 1.9–1.88 Ga and c. 1.83–1.80 Ga events. The earlier stage was followed by felsic magmatism and fluidization over wide areas of the Svecofennian domain, and even in the eastern part of the Archaean terrain at c. 1.85 Ga ago (compiled in Pajunen & Poutiainen 1999). Recently, several age determinations of magmatic rocks (e.g. Kurhila et al. 2005) and of tectono-metamorphic processes have widened the age range of magmatic and metamorphic processes to cover the whole 1.86–1.80 Ga evolution (e.g. Pajunen et al. 2008). The E_c mafic dykes marking the tectonic break in Västerviken were not dated but the granitic neosome veins (7a-b in Table 1) postdating the E_c dykes provide evidence of new metamorphic progression. Intermediate dykes in a corresponding setting to the mafic dykes are common in the southern Svecofennian area (e.g. D_E microtonalite dykes of Pajunen et al. 2008). They indicate intrusion into cooled crust and were later migmatized by a granitic migmatization pulse, except for in the granulite areas, where heat flow remained continuously high during these late stages of the Svecofennian evolution.

The granitic veins (7a in Table 1) are F_c -folded, but are not as strongly deformed as the typical D_b veins (3 and 4 in Table 1). The structural setting of the granitic dykes (7a in Table 1), patchy pegmatitic granite neosome and narrow pygmatic granite veins (7b in Table 1) corresponds to the granite-pegmatite dykes and contemporaneous veining (D_H) described by Pajunen et al. (2008) from Bollstad, Inkoo, c. 18 km SE from Västerviken, but are deformed into steep position. In Bollstad the pegmatitic granite

dyke intruded into a brittle fracture that is related to the onset of oblique extension (D_H). Thus, the age of the pegmatitic dyke fixes the beginning of the episode in the area at 1828 ± 3 Ma ago (Pajunen et al. 2008). As the extension evolved, granitic migmatization increased and finally large amounts of late-Svecofennian granites were intruded. Continuing vertical shortening with increasing heat flow signified the extensional deformation (D_H of Pajunen et al. 2008).

The latest data on tectonic and magmatic events establish the Svecofennian evolution as a more continuous process under regional transpressional deformations that began at c. 1.87–1.86 Ga ago and continued under varying stress field to c. 1.8 Ga (Pajunen et al. 2008). Earlier Ehlers et al. (1993) represented the first postulations on transpressional evolution in the Svecofennian domain; they interpreted the intrusion of the 1.84–1.83 Ga granites as synkinematic to the transpressional event at 1.83 Ga. These transpressional deformations caused alternating oblique extensional and contractional structures that caused varying structural sequences in different tectonic units or crustal depths. According to Pajunen et al. (2008), the SE-NW extensional process (D_E) was closely followed by N-S contraction causing wide-scale folding with E-W-trending axial planes (D_G). It was followed by transpression in a NE-SW direction (D_H), and during the latest Svecofennian stages the stress field turned to c. E-W-directed (D_I). The high thermal activity related to these transpressional processes show the most continuous character in the granulite areas of southernmost Finland. The U-Pb results on monazites from the West-Uusimaa granulites c. 10 km north from Västerviken also provide ages of 1.83–1.82 Ga, whereas Sm-Nd analyses on garnet suggest that the granulites cooled to garnet Nd-blocking temperature (c. 650–700 °C) at about 1.8 Ga ago (Väisänen et al. 2004). Väisänen et al. (2002) have reported U-Pb sims results on zircons from the Turku area. These include an age of 1826 ± 5 Ma for the leucosome of the Lemu garnet-cordierite gneiss, and ages of c. 1.8 Ga for the leucosome of the Masku tonalite and for the metamorphic zircon rims in the 1878 ± 19 -Ma-old Kakskerta enderbite.

In the Västerviken outcrop the coarse-grained 1804 ± 2 Ma old pegmatitic granite (8 in Table 1) (A1297) post-dates the major ductile deformation fabrics. It contains fragments of the host rock with F_g folds that exhibit c. E-W contraction. The dyke contact shows a sinistral N-S shear component implying local (?) rotation of the stress field after the E-W-contractional E_g event into a more NW-SE trend. Rotations of stress field during the late deformations, D_{f-g} (D_{G-I} of Pajunen et al. 2008), postulate

variations in setting of the extensional granitic magmas during the heterogeneous heat flow and deformation from c. 1.84 to 1.80 Ga. The age of 1.8 Ga is common throughout the Shield. The two medium-grained pink aplogranites in Tammisaari (see Hopgood et al. 1983), which post-date folds of F_E generation of Hopgood et al. (op. cit.) gave discordant U-Pb analyses on zircon with upper intercept ages of c. 1.84 and 1.8 Ga. Monazites from both samples gave ages of c. 1.8 Ga (A947 Trekobb, A948 Dyneskär). It is conceivable that these anatectic aplogranites crystallized at c. 1.8 Ga, and some zircon may be inherited from their source rocks. The Rb-Sr muscovite ages for discordant coarse-grained pegmatites also give ages of c. 1.8 Ga. The pegmatite (8 in Table 1) in Västerviken may well be correlated temporally with the 1.8 Ga pegmatites in the Tammisaari area (Hopgood et al. 1983), as well as with pegmatites in Kemiö in southern Finland (Lindroos et al. 1996). Mafic diabase dykes that are as-

sociated with pegmatitic granite dykes also represent a late magmatism in the area (Pajunen et al. 2008); it relates to a deep source of the heat flow continuing into the latest Svecofennian evolution. Alviola et al. (2001) described c. 1.79 Ga pegmatitic granite pulses from the Bothnian area in western Finland.

Stabilization of the crust in the south took place shortly after 1.8–1.79 Ga (e.g. Suominen 1991), which represents the age of post-tectonic granites in the southern Svecofennian terrane.

ACKNOWLEDGEMENTS

We want to thank the official reviewers of the paper, Timo Kilpeläinen and Mikko Nironen, for their suggestions for revisions to improve the paper.

REFERENCES

- Alviola, R., Mänttari, I., Mäkitie, H. & Vaasjoki, M. 2001.** Svecofennian rare-element granitic pegmatites of the Ostrobothnia region, western Finland: their metamorphic environment and time of intrusion. In: Mäkitie, H. (ed.) Svecofennian granitic pegmatites (1.86–1.79 Ga) and quartz monzonite (1.87 Ga), and their metamorphic environment in the Seinäjoki region, western Finland. Geological Survey of Finland, Special Paper 30, 9–29.
- Ehlers, C. & Lindroos, A. 1990.** Early Proterozoic Svecofennian volcanism and associated plutonism in Enklinge, SW Finland. *Precambrian Research* 47, 307–318.
- Ehlers, C., Lindroos, A. & Selonen, O. 1993.** The late Svecofennian granite-migmatite zone of southern Finland – a belt of transpressive deformation and granite emplacement. *Precambrian research* 64, 295–309.
- Elminen, T., Airo, M.-L., Niemelä, R., Pajunen, M., Vaarma, M., Wasenius, P. & Wennerström, M. 2008.** Fault structures in the Helsinki Area, southern Finland. In: Pajunen, M. (ed.) Tectonic evolution of the Svecofennian crust in southern Finland – a basis for characterizing bedrock technical properties. Geological Survey of Finland, Special Paper 47, 185–213.
- Eskola, P. 1914.** On the petrology of the Orijärvi region in southwestern Finland. *Bulletin de la Commission Géologique de Finlande* 40, 277 p.
- Eskola, P. E. 1915.** Om sambandet mellan kemisk och mineralogisk sammansättning hos Orijärvi traktens metamorfa bergarter. Summary of the contents: On the Relations between the Chemical and Mineralogical Composition in the Metamorphic Rocks of the Orijärvi Region, 109–145. *Bull. Comm. Géol. Finlande* 44, 1–107.
- Hopgood, A. M. 1980.** Polyphase fold analysis of gneisses and migmatites. *Transactions of the Royal Society of Edinburgh, Earth Sciences* 71, 55–68.
- Hopgood, A. M. 1984.** Structural evolution of Svecokarelian migmatites, southern Finland: a study of Proterozoic crustal development. *Transactions of the Royal Society of Edinburgh, Earth Sciences* 74, 229–264.
- Hopgood, A. M. 1999.** Determination of structural successions in migmatites and gneisses. Dordrecht: Kluwer Academic Press. 346 p.
- Hopgood, A. M., Bowes, D. R. & Addison, J. 1976.** Structural development of migmatites near Skåldö, southwest Finland. *Geologische Rundschau* 67, 313–330.
- Hopgood, A., Bowes, D., Kouvo, O. & Halliday, A. 1983.** U-Pb and Rb-Sr isotopic study of polyphase deformed migmatites in the Svecokareliides, southern Finland. In: Atherton, M. & Gribble, C. (eds.) *Migmatites, melting and metamorphism*. Nantwich: Shiva, 80–92.
- Kähkönen, Y. 1987.** Geochemistry and tectonomagmatic affinities of the metavolcanic rocks of the early Proterozoic Tampere schist belt, southern Finland. *Precambrian Research* 35, 295–311.
- Kilpeläinen, T. 1988.** Evolution of deformation and metamorphism as a function of time in the Rantasalmi-Sulkava area, Southeastern Finland. *Geol. Surv. Finland Bull.* 343, 77–87.
- Kilpeläinen, T. 1998.** Evolution and 3D modelling of structural and metamorphic patterns of the Palaeoproterozoic crust in the Tampere-Vammala area, southern Finland. Geological Survey of Finland, *Bulletin* 397, 124 p.

- Kilpeläinen, T. & Rastas, J. 1990.** Etelä-Suomen lehtiittijakson tektonis-metamorfisesta kehityksestä. University of Turku, Institute of Geology and Mineralogy, Publication No 21. 37 p. (in Finnish)
- Koistinen, T. J. 1981.** Structural evolution of an early Proterozoic stratabound Cu-Co-Zn deposit, Outokumpu, Finland. Transactions of the Royal Society of Edinburgh, Earth Sciences 72, 115–158.
- Koistinen, T., Klein, V., Koppelmaa, H., Korsman, K., Lahtinen, R., Nironen, M., Puura, V., Saltikova, T., Tikhomirov, S. & Yanovskiy, A. 1996.** Paleoproterozoic Svecofennian orogenic belt in the surroundings of the Gulf in Finland In: Koistinen, T. (ed.) Explanation to the Map of Precambrian basement of the Gulf of Finland and surrounding area 1:1 million. Geological Survey of Finland, Special Paper 21, 21–57.
- Korsman, K., Hölttä, P., Hautala, T. & Wasenius, P. 1984.** Metamorphism as an indicator of evolution and structure of the crust in Eastern Finland. Geological Survey of Finland, Bulletin 328. 40 p.
- Korsman, K., Niemelä, R. & Wasenius, P. 1988.** Multi-stage evolution of the Proterozoic crust in the Savo schist belt, Eastern Finland. Geological Survey of Finland, Bulletin 343, 89–96.
- Korsman, K., Koistinen, T., Kohonen, J., Wennerström, M., Ekdahl, E., Honkamo, M., Idman, H. & Pekkala, Y. (eds.) 1997.** Bedrock map of Finland 1:1 000 000. Geological Survey of Finland.
- Korsman, K., Korja, T., Pajunen, M. & Virransalo, P. 1999.** The GGT/SVEKA transect: structure and evolution of the continental crust in the Paleoproterozoic Svecofennian orogen in Finland. International Geology Review 41, 287–333.
- Krogh, T. 1973.** A low-contamination method for hydrothermal decomposition of zircon and extraction of U and Pb for isotopic age determinations. *Geochimica and Cosmochimica Acta* 37, 485–494.
- Kurhila, M., Vaasjoki, M., Mänttari, I., Rämö, T. & Nironen, M. 2005.** U-Pb ages and Nd isotope characteristics of the lateorogenic, migmatizing microcline granites in southwestern Finland. *Bulletin of the Geological Society of Finland* 77 (2), 105–128.
- Lahtinen, R. 1994.** Crustal evolution of the Svecofennian and Karelian domains during 2.1–1.79 Ga, with special emphasis on the geochemistry and origin of 1.93–1.91 Ga gneissic tonalites and associated supra-crustal rocks in the Rautalampi area, central Finland. Geological Survey of Finland, Bulletin 378. 128 p.
- Laitala, M. 1973.** On the Precambrian bedrock and its structure in the Pellinge region, South Finland. Geological Survey of Finland, Bulletin 264. 76 p.
- Lindroos, A., Romer, R. L., Ehlers, C. & Alviola, R. 1996.** Late-orogenic Svecofennian deformation in SW Finland constrained by pegmatite emplacement ages. *Terra Nova* 8 (6), 567–574.
- Ludwig, K. R. 1991.** PbDat 1.21 for MS-dos: A computer program for IBM-PC Compatibles for processing raw Pb-U-Th isotope data. Version 1.07. U.S. Geological Survey, Open File Report 88–542. 35 p.
- Ludwig, K. R. 2001.** Isoplot/Ex rev. 2.49. A Geochronological Toolkit for Microsoft Excel. Berkeley Geochronology Center, Special Publication No. 1a. 55 p.
- Mertanen, S., Pajunen, M. & Elminen, T. 2001.** Applying palaeomagnetic method for dating young geological events. In: Autio, S. (ed.) Geological Survey of Finland, Current Research 1999–2000. Geological Survey of Finland, Special Paper 31, 123–129.
- Mertanen, S., Airo, M.-L., Elminen, T., Niemelä, R., Pajunen, M., Wasenius, P. & Wennerström, M. 2008.** Paleomagnetic evidence for Mesoproterozoic – Paleozoic reactivation of the Paleoproterozoic crust in southern Finland. In: Pajunen, M. (ed.) Tectonic evolution of the Svecofennian crust in southern Finland – a basis for characterizing bedrock technical properties. Geological Survey of Finland, Special Paper 47, 215–252.
- Mouri, H., Korsman, K. & Huhma, H. 1999.** Tectono-metamorphic evolution and timing of the melting processes in the Svecofennian Tonalite-Trondhjemite Migmatite Belt: An example from Luopioinen, Tampere area, southern Finland. *Bulletin of the Geological Society of Finland* 71, 31–56.
- Nironen, M. 1999.** Structural and magmatic evolution in the Loimaa area, southwestern Finland. *Bulletin of the Geological Society of Finland* 71, 57–71.
- Nironen, M. 2003.** Keski-Suomen granitoidikompleksi, Karttaselitys. English summary: Central Finland Garnitoid Complex – Explanation to a map. Geological Survey of Finland, Report of Investigation 157. 45 p.
- Nurmi, P. & Haapala, I. 1986.** The Proterozoic granitoids of Finland; granite types, metallogeny and related crustal evolution. *Bulletin of the Geological Society of Finland* 58, 241–261.
- Pajunen, M. & Poutiainen, M. 1999.** Palaeoproterozoic prograde metasomatic-metamorphic overprint zones in Archaean tonalitic gneisses, eastern Finland. *Bulletin of the Geological Society of Finland* 71, 73–132.
- Pajunen, M., Airo, M.-L., Wennerström, M., Niemelä, R. & Wasenius, P. 2001.** Preliminary report: The “Shear zone research and rock engineering” project, Pori area, south-western Finland. Geological Survey of Finland, Special Paper 31, 7–16.
- Pajunen, M., Airo, M.-L., Elminen, T. & Wennerström, M. 2004.** Structural evolution of Svecofennian crust in southern Finland. The 26th Nordic Geological Winter Meeting, January 6th–9th 2004, Uppsala, Sweden. Abstract Volume. GFF 126 (1), 32.
- Pajunen, M., Airo, M.-L., Elminen, T., Mänttari, I., Niemelä, R., Vaarma, M., Wasenius, P. & Wennerström, M. 2008.** Tectonic evolution of the Svecofennian crust in southern Finland. In: Pajunen, M. (ed.) Tectonic evolution of the Svecofennian crust in southern Finland – a basis for characterizing bedrock technical properties. Geological Survey of Finland, Special Paper 47, 15–160.
- Parras, K. 1958.** On the charnockites in the light of highly metamorphic rock complex in Southwestern Finland. *Bulletin de la Commission Géologique de Finlande* 181. 137 p.

- Pietikäinen, K. 1994.** The geology of the Paleoproterozoic Pori shear zone, southwestern Finland, with special reference to the evolution of veined gneisses from tonalitic protoliths. PhD thesis, Michigan Technological University. 130 p.
- Rämö, O. T., Vaasjoki, M., Mänttari, I., Elliot, B. A. & Nironen, M. 2001.** Petrogenesis of the Post-kinematic magmatism of the Central Finland Granitoid Complex I; radiogenic isotope constraints and implications for crustal evolution. *Journal of Petrology* 42, 1971–1993.
- Sederholm, J. J. 1926.** On migmatites and associated Pre-Cambrian rocks of South-Western Finland. Part II. The region around the Barösundsfjärd W. of Helsingfors and neighbouring areas. *Bulletin de la Commission Géologique de Finlande* 77. 143 p.
- Shreurs, J. & Westra, L. 1986.** The tectonic evolution of a Proterozoic, low-pressure, granulite dome, West Uusimaa, SW-Finland. *Contrib. Mineral. Petrol.* 92, 236–250.
- Stacey, J. S. & Kramers, J. D. 1975.** Approximation of terrestrial lead isotope evolution by a two-stage model. *Earth and Planetary Science Letters* 26, 207–221.
- Suominen, V. 1991.** The chronostratigraphy of southwestern Finland with special reference to Postjotnian and Subjotnian diabases. *Geological Survey of Finland, Bulletin* 356. 100 p.
- Vaasjoki, M. & Sakko, M. 1988.** The evolution of the Raahe-Ladoga zone in Finland: isotopic constraints. In: Korsman, K. (ed.) *Tectono-metamorphic evolution of the Raahe-Ladoga zone*. Geological Survey of Finland, *Bulletin* 343, 7–32.
- Väisänen, M. 2002.** Tectonic evolution of the palaeoproterozoic Svecofennian orogen in Southwestern Finland. *Annales Universitatis Turkuensis, A II*, 154. 143 p.
- Väisänen, M., Hölttä, P., Rastas, J., Korja, A. & Heikkinen, P. 1994.** Deformation, metamorphism and the deep structure of the crust in the Turku area, southwestern Finland. In: Pajunen, M. (ed.) *High temperature-low pressure metamorphism and deep crustal structures: meeting of IGCP project 304 'Deep Crustal Processes' in Finland, September 16–20, 1994*. Geological Survey of Finland, *Guide* 37, 35–41.
- Väisänen, M. & Hölttä, P. 1999.** Structural and metamorphic evolution of the Turku migmatite complex, southwestern Finland. *Bulletin of the Geological Society of Finland* 71, 177–218.
- Väisänen, M. & Mänttari, I. 2002.** 1.90–1.88 Ga arc backarc basin in the Orijärvi area, SW Finland. *Bulletin of the Geological Society of Finland* 74, 185–214.
- Väisänen, M., Mänttari, I. & Hölttä, P. 2002.** Svecofennian magmatic and metamorphic evolution in southwestern Finland as revealed by U-Pb zircon SIMS geochronology. *Precambrian Research* 116, 111–127.
- Väisänen, M., Andersson, U. B., Huhma, H. & Mouri, H. 2004.** Age of late Svecofennian regional metamorphism in southern Finland and south-central Sweden. The 26th Nordic Geological Winter Meeting, January 6th–9th 2004, Uppsala, Sweden. Abstract volume. *GFF* 126, 40.
- Verhoef, P. N. W. & Dietvorst, E. J. L. 1980.** Structural analysis of differentiated schists and gneisses in the Taalintehdas area, Kemiö island, southwest Finland. *Bulletin of the Geological Society of Finland* 52, 147–164.
- Wegmann, C. E. 1928.** Über die Tektonik der jüngeren Faltung in Ostfinnland. *Fennia* 50, 1–22.

FAULT STRUCTURES IN THE HELSINKI AREA, SOUTHERN FINLAND

by

Tuija Elminen, Meri-Liisa Airo, Reijo Niemelä, Matti Pajunen,
Markus Vaarma, Pekka Wasenius and Marit Wennerström*

Elminen, T., Airo, M.-L., Niemelä, R., Pajunen, M., Vaarma, M., Wasenius, P. & Wennerström, M. 2008. Fault structures in the Helsinki Area, southern Finland. *Geological Survey of Finland, Special Paper 47*, 185–213, 32 figures and 2 tables.

The purpose of the study was to work out the origin and characteristics of bedrock faults and to classify faults for applied geology, particularly for constructional purposes in the Helsinki area in southern Finland.

The study area is located within the Paleoproterozoic Svecofennian domain. The prolonged Svecofennian orogeny (1.9–1.8 Ga) led to complicated deformation patterns. Three distinctively different fault systems crosscutting these structures were recognized. They were well defined by kinematics and crosscutting relationships but some other fault structures could not with certainty be tied to any of these systems. The earliest set of the defined fault zones shows strongly localized deformation and was formed at the end of the latest Svecofennian events. These steep NE-trending zones crosscut all the ductile structures and are characterized by a sinistral east side up reverse movement. They were formed within a compressional stress field under retrograde amphibolite to greenschist facies conditions. The next major crustal movements identified were accompanied by A-type granite magmatism at 1650–1620 Ma. The exhumation after the Svecofennian orogeny had already progressed far. Brittle NW-SE-oriented normal faults were formed and the older NE-trending faults were reactivated in a strike-slip regime. The movements continued after the magma emplacement. Later, long N-S-oriented brittle faults with different patterns and kinematics crosscut the pre-existing structures. Brittle low-angle thrust faults of different orientations make up one of the less defined groups and may partly belong to some of the above-mentioned systems.

Key words (GeoRef Thesaurus, AGI): structural geology, fault zones, faults, classification, mineralogy, ultrastructure, reactivation, urban environment, Paleoproterozoic, Helsinki, Espoo, Vantaa, Finland

* *Geological Survey of Finland, P.O. Box 96, FI-02151 Espoo, Finland*

* *E-mail: tuija.elminen@gtk.fi*

INTRODUCTION

The study of the ductile deformation history of the Svecofennian orogeny in Southern Finland has been done since the end of 1800s. The localization of bedrock units and structures is therefore well-known and ductile structures with some major ductile high strain zones have been presented in bedrock maps (Korsman et al. 1997). In contrast, post-Svecofennian faults that clearly crosscut the Paleoproterozoic structures have been sparsely studied even though they are frequently exposed in outcrops and bedrock construction has revealed zones of considerable faulting and fracturing.

Lineaments in southern Finland have been interpreted mainly from the topography (Sederholm 1910 and Härme 1961), and most classifications have been based on their dimensions. Additional detailed geological studies on shear zones with varying methods have been done in other parts of Finland (Talvitie 1971, Parkkinen 1975, Aarnisalo 1978 and Pajunen 1986). In the south, the movements and tectonic relationships at the Porkkala-Mäntsälä shear zone that crosscuts the study area have been studied by Heeremans et al. (1996). Similar structures have been described in the Johannislund, Kisko and Suomusjärvi shear zones, a hundred kilometres west of Helsinki (Ploegsma & Westra 1990 and Ploegsma 1991).

There are only a few studies on the structural and microstructural characteristics, kinematics and age relations of fault structures in Finland (for example Pajunen 1986, Pietikäinen 1994 and Pajunen et al. 2001). However, fault zones represent an important contribution to the geological information in many respects. Often acting as zones of weakness in the bedrock, they are vital to diverse geological applications like ground water studies, construction work, waste disposal and ore prospecting.

Temperature, confining pressure, differential stress, strain rate, fluids and the properties of the deforming material are important factors during faulting. The stressfield and crustal conditions have varied in the Svecofennian bedrock still in late- and post-orogenic times and thus the characteristics of fault systems also vary as they represent different crustal levels and different periods of deformation.

The movements have often occurred repeatedly along pre-existing fault systems, even if the stress field orientation has changed. Mineralogical alteration due to strong hydrothermal activity is common in fault zones and often characterizes different fault generations. Consequently, polyphase reactivation of fault zones with fault structures varying from ductile to brittle and with plentiful overprinting can be observed. In summary, not only macroscopic characteristics like dimensions and geometry of the fault systems, but also microscopic features like fabrics and mineral assemblages are required to decipher the deformation history of the fault zones.

In this work, all fault structures that were identified in the study area in Espoo, Helsinki and Vantaa (Figure 1) were studied. Analyses of fault structures, kinematics and age relations were based on field observations and microscopic studies. Previous bedrock maps (Laitala 1960, Laitala 1967, Härme 1969 and Laitala 1994), aeromagnetic data (by the Geological Survey of Finland, GTK) and topographic data (by the National Land Survey of Finland) were used for regional correlation and setting of faults. The fault structures were classified by their geological character and kinematics, and fault systems of different types and origins were discovered.

METHODS

Fault structures were examined during regional structural studies in the area and thematic research was done on discovered fault areas. Lithological, structural, fault and joint data were collected in the field (Pajunen et al. 2008 and Wennerström et al. 2008). The fault data consist of structural relationships, fault plane strike and dip, dimensions, slickenline trend and plunge, sense of shear, fault type (Anderson's classification 1942), estimates of net slip, character of fault (brittle to ductile) and fault rock texture. 466 fault observations were made.

Microstructures, mineralogy and alteration were examined and estimates of the metamorphic grade

were made using mineralogy and grain-scale microstructures following Passchier and Trow (1996). Some mineralogical determinations were made by microanalysis (Cameca SX100) and XRD.

Kinematic analysis was used to estimate the paleostress conditions during faulting events. The analysis was carried out using the FaultKinWin program, version 1.2 by R.W. Allmendinger, Dept. of Geological Sciences, Cornell University, Ithaca, U.S.A.

The spatial distribution of fault structures was correlated with the distribution of lineaments in topographic and aeromagnetic data. The southern coast of Finland is well exposed and the landscape is charac-

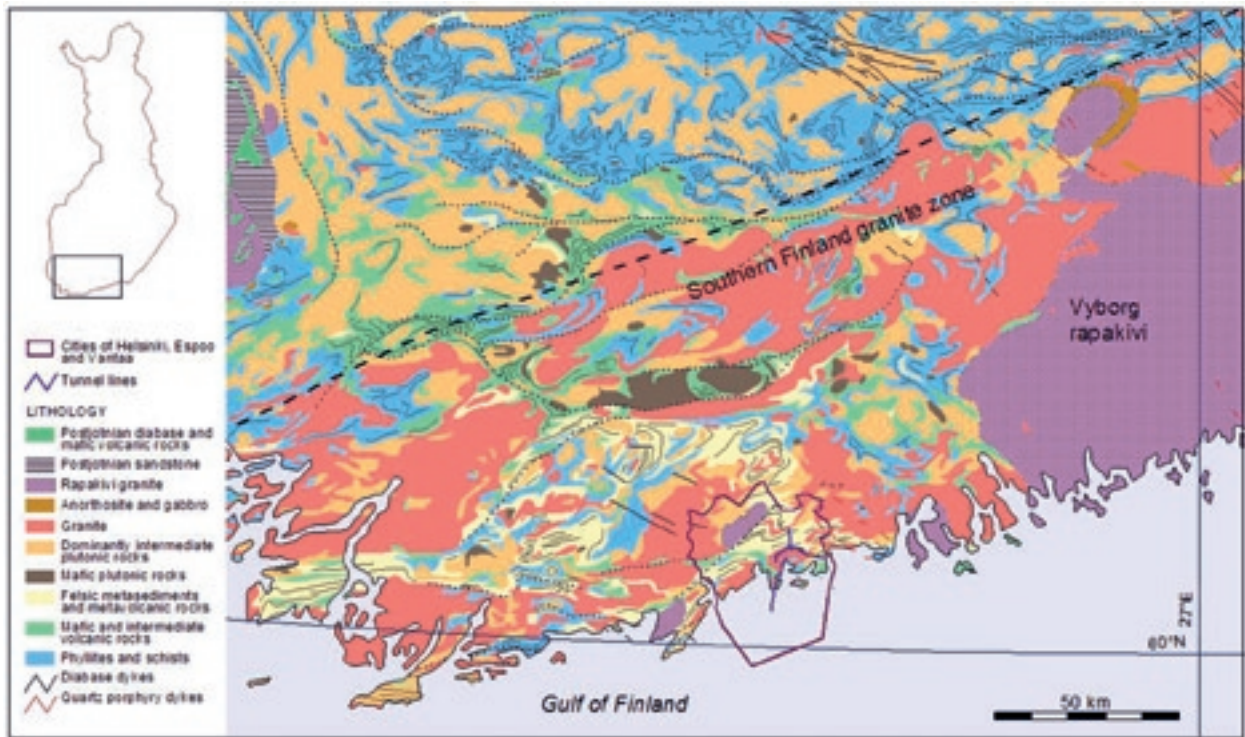


Figure 1. Bedrock of southernmost Finland. The granite zone belongs to the 1900–1800 Ma Palaeoproterozoic Svecofennian domain. Some Mesoproterozoic rapakivi-related rocks (1650–1540 Ma) crosscut the Svecofennian rocks. The study area is restricted to the Espoo, Helsinki and Vantaa areas.

terized by ice polished bedrock partially covered by glaciogenic and marine sediments. The weathered and eroded faults appear as topographic depressions, usually covered by clays. Digital topographic data were processed to view fault patterns, trends and dimensions. The aspect transformations highlighted the fault slopes so that comparisons in density and length of the differently oriented slopes could be made. Slope transformations represent the degree of slope and asymmetry of depression was used to interpret direction of the dip of an eroded fault.

The Helsinki region is covered by high-resolution airborne geophysical data, which were gathered by using 200 m (partly 100 m) flight line spacing and 35 m nominal terrain clearance (see Airo et al. 2008). In aeromagnetic data fault structures are generally seen as magnetic lineaments of varying length and often with a depression in magnetic field intensity. The magnetic lineaments and their preferred orientations were compared and related to the field and topographic data on fault structures. Specific structural features were analysed from enhanced and transformed aeromagnetic data in order to strengthen the magnetic fault structure expressions, which sometimes may be very weak due to the migmatized and deformed bedrock of the study area. In particular, in areas of poor magnetic contrast enhancement of magnetic data was necessary.

Horizontal derivatives of the magnetic field proved to be useful in defining systematic patterns and trends. Upward continuation of the magnetic field data from 35 m to 100 m or 200 m was applied to smooth out the noise caused by man-made activity in the densely populated capital area. However, it was agreed that these anomalies tend to be very local and can quite easily be separated from geological bedrock anomalies, which show continuity from one survey line to the next one.

Reference data from tunnels that have been mapped for their geotechnical properties during excavation was available from the Helsinki City Geotechnical Division. The data is from depths between 30–80 m. The tunnels are oriented N-S and E-W extending 40 km all together (Figure 1). The data include location information of so-called “zones of weakness” and their classification for engineering purposes (Gardemeister et al. 1976). The term “zone of weakness” is used by geotechnical engineers and means any fractured zone with incohesive material. The data are not geologically classified but the orientation, width and joint and fracturing properties of the zones are mentioned (Table 1). Tunnel data were used to map the continuity of the fault structures and especially to predict the properties of the faults for the application of the project (Pajunen et al. 2002a, Pajunen et al. 2002b, Pajunen

Table 1. Jointing and weathering classes from Gardemeister et al. (1976). The classification has been used to describe the weak zones in tunnels for engineering purposes.

Jointing		
RI1	planelike joints deal the rock into two or more parts	
RI2	abundant jointing	no joint filling
RI3	dense jointing	some joint filling
RI4	abundant or dense jointing	filling
RI5		abundant clay or gouge
Weathering		
Rp1	no weathering	
Rp2	some weathering	
Rp3	abundant weathering	
Rp4	totally weathered	

et al. 2008 and Wennerström et al. 2008). Although the area is densely populated and developed, some of the zones could be traced to the surface where geological observations were made.

Some additional fault observations (locality, strike and dip) were provided from Helsinki and Espoo City Geotechnical offices. Also information on soil thickness from old drilling data from Helsinki City and GTK was used.

GEOLOGICAL OUTLINE

The present-day crustal architecture in southern Finland implies a multistage accretionary and orogenic history 1900–1800 Ma ago (e.g. Korsman et al. 1999 and Lahtinen et al. 2005). The bedrock in the southernmost coastal region is part of the southern Finland granite zone (Pajunen et al. 2008) in the Svecofennian domain (Figure 1). The supracrustal rocks are dominantly migmatitic, often quartzo-feldspathic gneisses with amphibolitic layers and volcanic units. Felsic plutonic rocks are abundant and gabbroic rocks exist in small amounts. The early plutonic rocks are foliated and locally banded. Younger, less deformed granites and pegmatites crosscut these rocks in complex patterns. The tectonic evolution of the Svecofennian crust in the study area is described in detail in Pajunen et al. (2008). 1650–1540 Ma rapakivi plutons and diabase dykes crosscut the Svecofennian crust in the Gulf area (Laitakari et al. 1996).

General structures in the study area

The northwestern part of the study area consists of granitoids with weak, shallow dipping foliation

(Figure 2). From the southwestern corner of the area a steep high strain zone trends NE and bends to the east comprising an east verging dextral fold. The NE-SW oriented Porkkala-Mäntsälä fault (called PM here) follows the previous ductile structure in the SW and continues further NE, extending at least 150 km to Lahti. To the SW this structure continues another 150 km to Estonia (Koistinen 1994). The elongated Bodom rapakivi pluton, 1637.5 ± 2.2 Ma in U-Pb age (Kosunen 2004), lies adjacent to the PM zone on its western side crosscutting the Svecofennian structures. The corresponding Obbnäs pluton 1640 ± 14 Ma (Kosunen 2004) 20 km to the SW, outside the study area, is located on the eastern side of the PM zone. The rapakivi plutons are from geochemically different sources (Kosunen 2004). East of the PM, migmatized plutonic and supracrustal rocks strike NE and dip steeply, except in the southernmost part, where the general trend of the structures is E-W. In the eastern part of the study area the foliations rotate to N-S where a N-S-oriented fault zone, the Vuosaari-Korso zone (called VK here), crosscuts the structural trend.

DESCRIPTION OF FAULT STRUCTURES

Observations of fault structures were connected to the linear trends observed on the topographic and aeromagnetic maps (Figure 3). The fault types and trends correlated and faults could be divided into at least 7 different groups based on fault types and trend. These groups (A-G) were used mainly to organize the description and the division does not exclude that some of the different types could belong to the same fault system. In particular the different low-angle brittle faults ascribed to group G may not

belong to a single system but may represent different events. An interpretation of the relationships and affiliation of the faults to distinct fault systems and events will be considered in the discussion. The fault groups are:

- A) E-W- and ENE-WSW-oriented Svecofennian shear zones
- B) NE-SW-oriented steep ductile faults crosscutting the Svecofennian deformation pattern

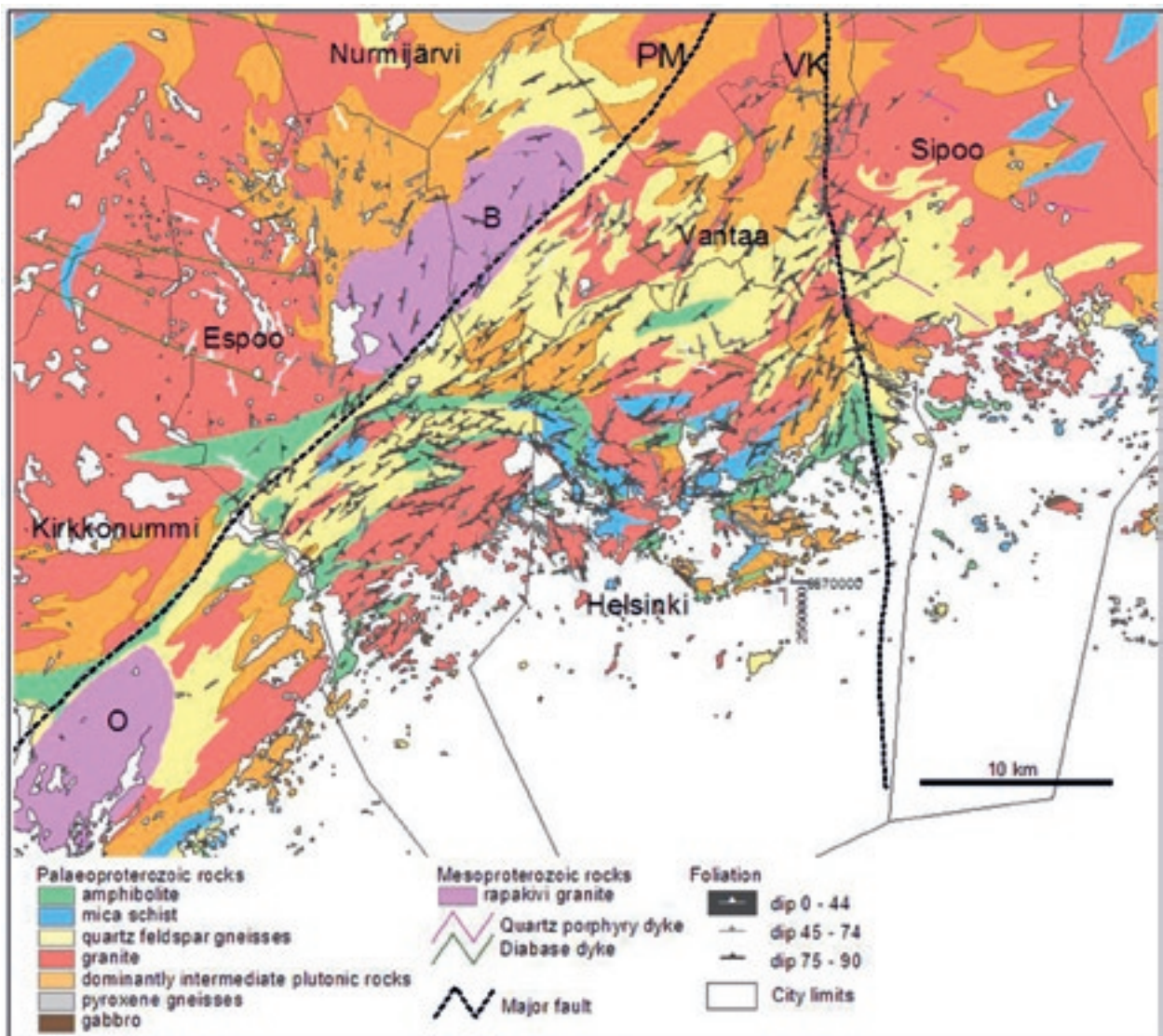


Figure 2. Lithology and ductile structures of the study area. PM=Porkkala-Mäntsälä fault, VK=Vuosaari-Korso fault, B=Bodom rapakivi, O=Obbnäs rapakivi.

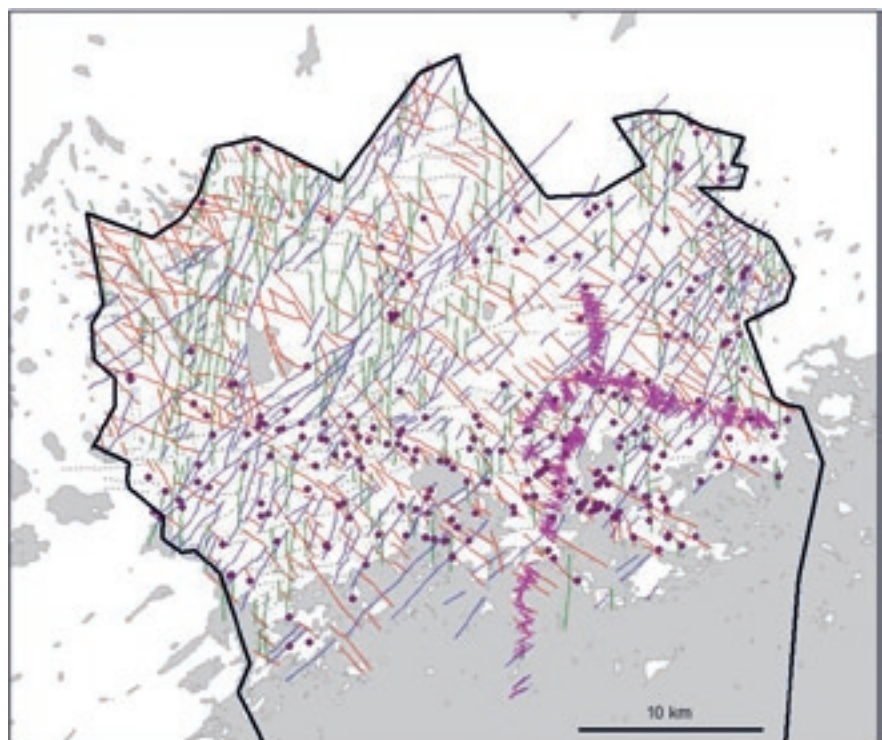


Figure 3. Lineaments interpreted from topographic maps and geophysical images. The different orientations, marked in different colours, are interpreted to represent different types of faults. Dashed line; E-W to ENE-WSW oriented, blue line; NE-SW oriented, red line; WNW-ESE and NNW-SSE oriented, green line; N-S oriented faults. Observation points marked with dots. Weak zone observations in the tunnels marked with violet lines.

- C) Brittle NE-SW faults, reactivation of group B faults, NE faults crosscutting rapakivi granites
- D) Arrays of brittle WNW-ESE- and NNW-SSE-oriented faults that crosscut rapakivi granites
- E) N-S-oriented brittle faults crosscutting faults of group D
- F) Brittle E-W-oriented narrow faults
- G) Low-angle brittle faults of different orientations, probably of various origins

Some faults from groups A to E are outlined in Figure 4. In the following, field relationships, outcrop studies, magnetic features, mineralogy and microstructures of the faults from ductile to brittle will be described. Geotechnical notes from corresponding zones of weakness from the tunnels, kinematics and paleostress estimation will also be presented.

A) Ductile shear zones; E-W and ENE-WSW

Field relationships

Mylonites parallel to the foliation occur in the southern part of the study area, in the E-W and ENE-WSW striking areas. The structures are not drawn on the maps as proper zones as there were no clear indications of continuous shear zone systems in topographic and aeromagnetic data. The gneissic and mylonitic structures may include different shear zone generations, even subsequently folded ones. The youngest mylonites (that is, the blastomylonites excluded) are described here.

The E-W shear structures are well displayed in aeromagnetic data (Figure 5). They are expressed as slightly curved zones of magnetic minima parallel

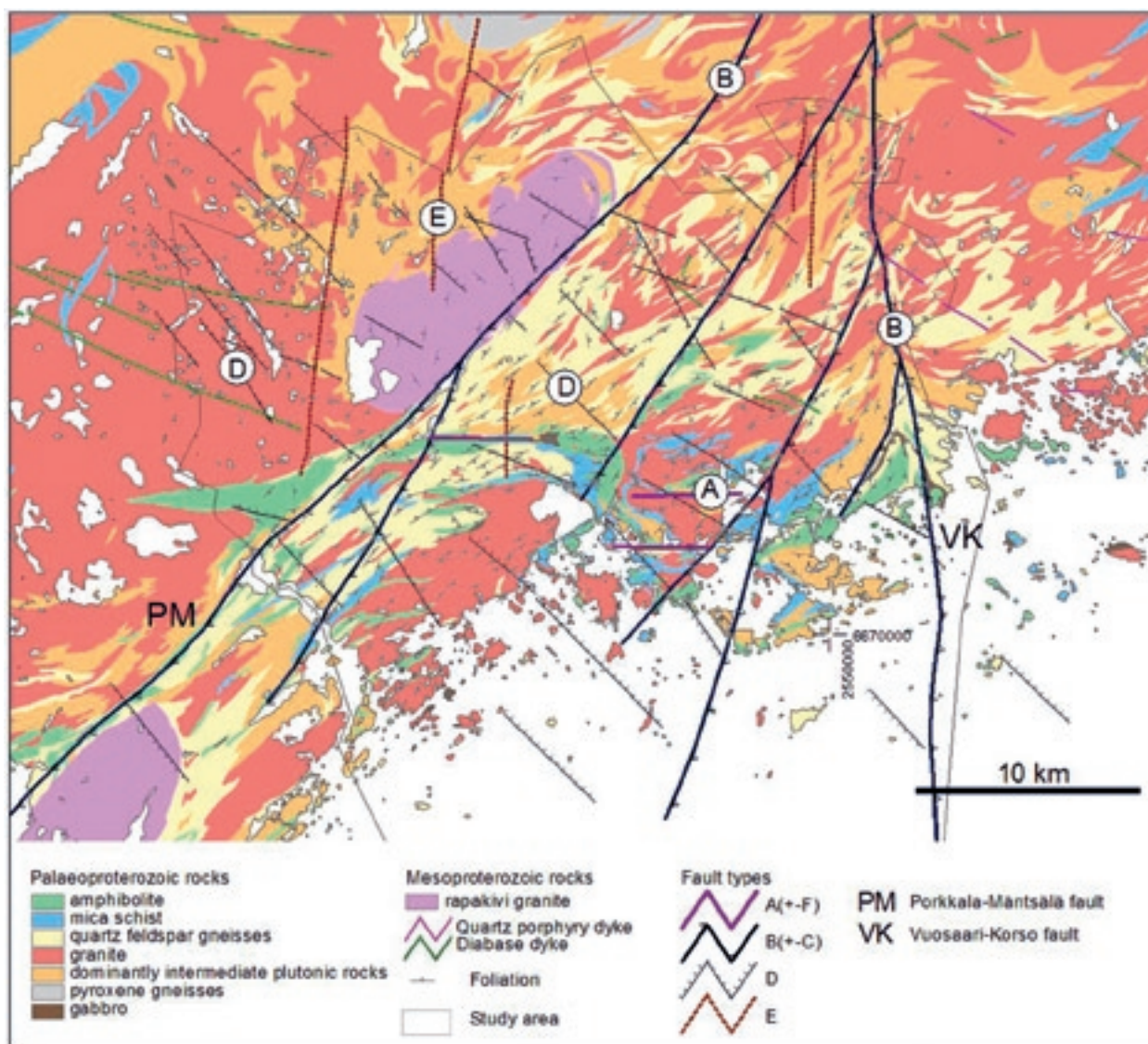
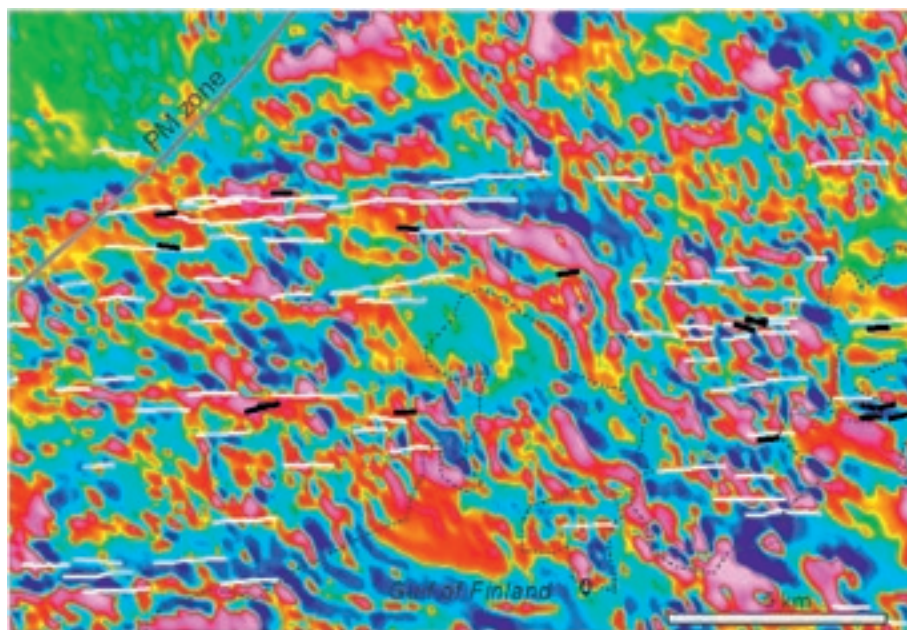


Figure 4. Some examples of the four different fault types shown on the lithological map and described in the text: A) E-W to ENE-WSW-trending Svecofennian shear zones, B) NE-SW-trending ductile steep faults crosscutting the Svecofennian deformation pattern, D) Arrays of brittle WNW-ESE- and NNW-SSE-trending faults that crosscut the ductile faults and are well distinguished in the topographic lineament network, E) N-S-trending brittle faults.

Figure 5. E-W-trending shear zones (continuous white lines) based primarily on topography represented on aeromagnetic image (100 m up elevated) that accentuates the E-W structures, in the southern Espoo and Helsinki areas. Observed E-trending mylonites with black symbols. The faults are vertical or steep.



to the ductile magnetic anomaly strikes. They appear as groups that can be followed for several kilometres. The NE-trending faults (group B) crosscut the E-W magnetic pattern.

In outcrops the E-W and ENE mylonites obliquely slightly truncate the E- or ENE foliation; also

non-foliated granite is affected by the shear zones. The host rock changes gradually to 0.5 to 5 m wide meso- and ultramylonite zones (Figure 6). The mylonite zones dip 62–90° (one dips 35°) to the south and mostly show reverse south side up sense of shear.



Figure 6. Mylonitized granite in Kivinokka, Helsinki. Water or soil covered topographic depressions and aeromagnetic E-W trending anomalies occur 10 m north and 350 m south of the site). Compass length 12.5 cm. Photo by T. Elminen.

Mineralogy and microstructures

In granitic mylonites quartz and feldspar show upper greenschist to lower amphibolite facies syntectonic recrystallization structures (Figure 7). Biotite overgrows partly the mylonitic structure.

Reactivation and alteration

Some E-W and ENE mylonite zones have been reactivated at lower grade conditions, so that parallel faults with gouge and fault breccias formed at the zones or at their margins. The fault breccias usually consist of lens shaped fragments with (altered) chloritic coatings. The slickenlines are subhorizontal.

Notes from the tunnels

The E-W zones of weakness in the tunnels are generally 1–3 metres wide but 10 % of the zones are over 10 metres wide. Weathering varies from absent to slight and abundant. Intactness in these zones is described to be mostly Ri3 and Ri4 (Table 1), meaning dense jointing/fracturing with some fillings and very dense jointing/fracturing with gouge/swelling

minerals. On average, the E-W-oriented zones of weakness are the most intensely fractured and harmful when one considers excavating. The reported zones probably represent the reactivated faults. ENE-WSW-oriented zones of weakness are rare.

B) Ductile reverse faults; NE-SW

Field relationships

Throughout the area NE-SW faults truncate the regional ductile deformation structures (Figure 8). The major faults, PM and VK belong to this group (although the orientation is N-S for the latter), and especially these faults have been reactivated also under brittle conditions (see type C).

In aeromagnetic data the faults occur as lineaments with reduced magnetization and they distinctly crosscut pre-existing E-W structures. The lineaments extend at least 5–25 km and are interpreted as continuing to at least 2–3 km in depth.

On map scale the regional ENE-WSW foliation is sinistrally bent to the fault orientation usually in an about 200 m wide zones. The bending is gradual

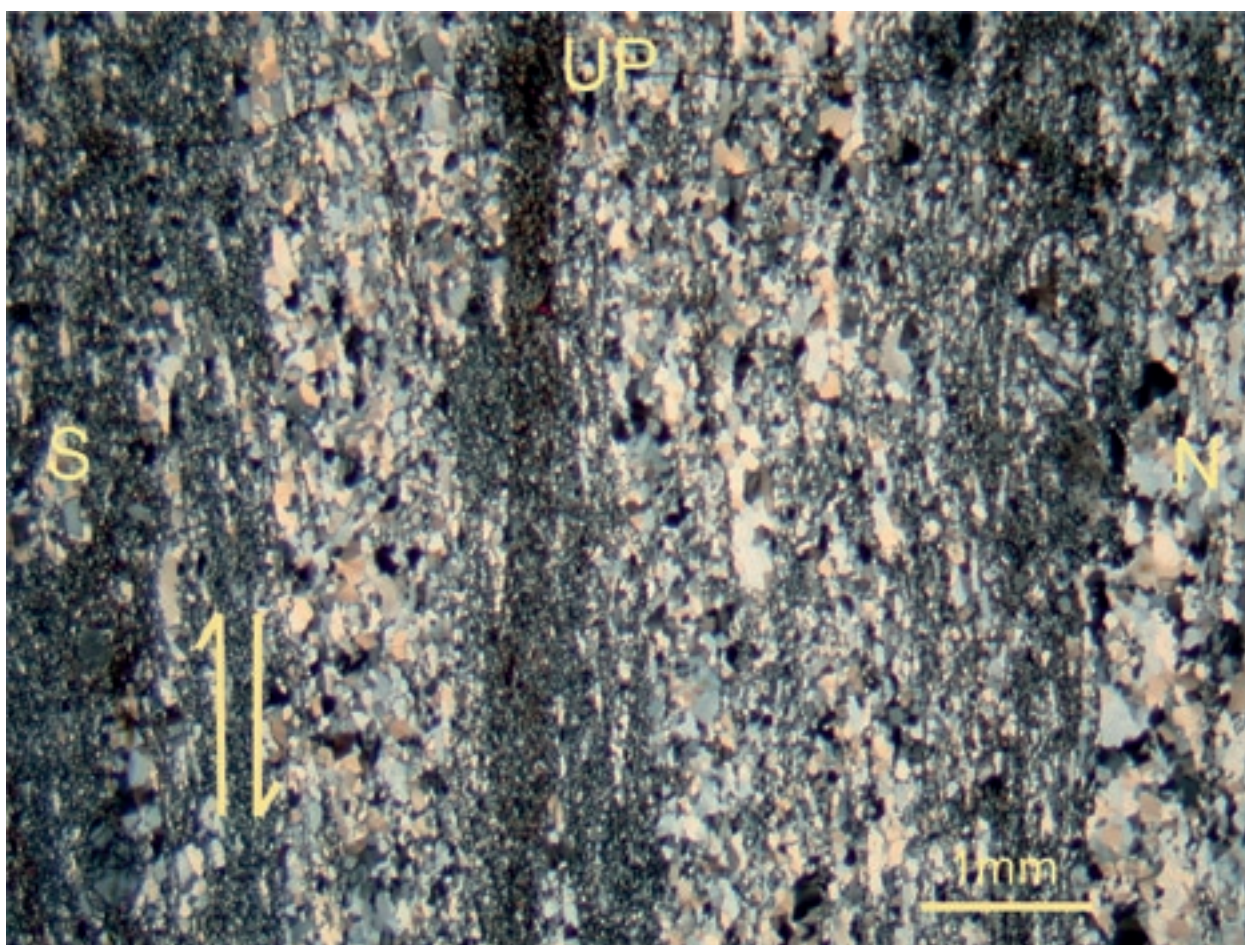


Figure 7. Mylonitized granite from Kivinokka, Helsinki. Coarser grains are quartz, fine-grained stripes consist of feldspars and some biotite. Arrows show the sense of shear defined by C/S fabric. Photo by T. Elminen.

and too large-scale to be recorded at outcrop scale. The central part of these fault zones is usually eroded showing about 100 metre wide valleys in the topography. Proto- to ultramylonitic rocks occur as 1 cm to 10 m wide zones close to the valleys (Figure

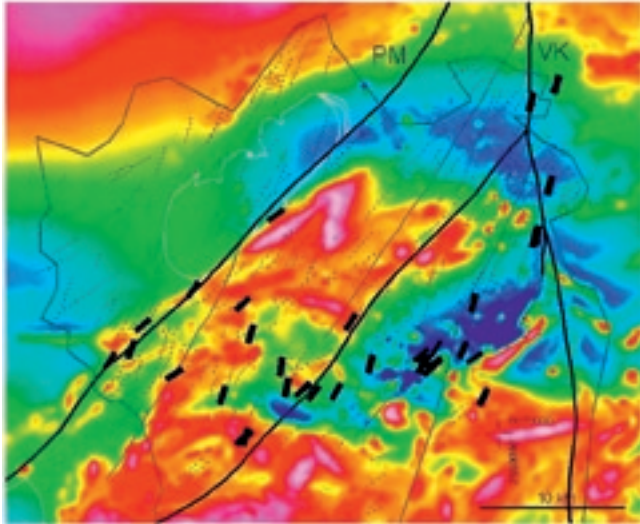


Figure 8. The ductile NE-trending fault zones are distinct in the magnetic image. The faults are interpreted from integrated field, topographic and airborne magnetic data. Field observation sites with black marks. The magnetic image is an upward continuation of the magnetic field data from 35 m to 200 m.

9). The dip varies from 70 to 90° to the east. Close to the PM fault the lithological contacts follow the same orientation and are often tectonized. At the VK zone there are some pseudotachylite-like rocks but due to recrystallization and alteration not certainly definable.

Stretching lineations in the NE-SW faults vary from weak to distinctive. They are especially well developed in narrow ultramylonitic zones. Lineations as well as microscopic kinematic indicators indicate east side up and sinistral movements, with fairly steep plunge, thus the faults represent subvertical reverse faults.

Close to the VK zone, in the Länsi-Salmi quarry, a system of east dipping faults with varying dips was exposed (later exploded). These thrust faults showed increasingly brittle characteristics with declining dip (Figure 10). Steeper faults had steep slickenlines but structures with dips of about 30° were more like joints, without slickenlines, and often filled with chlorite. Chlorite-filled subvertical en echelon joints with compatible geometry were present as well. Also formation of some irregular breccias in which matrix was replaced by chlorite was probably related to these faults.



Figure 9. Ca 30 cm wide, NE-trending mylonite fault in amphibolite in Lemissaari, Helsinki. An aeromagnetic NE-trending anomaly is located 100 m NW of the site. The topographic depression there is covered with soil and sea bays. Photo by T. Elminen.



Figure 10. Semi-brittle to brittle reverse fault in the Länsi-Salmi quarry, Helsinki. Photo towards north-east. The low-angle jointing is probably related to the faulting. Photo by T. Elminen.

Mineralogy and microstructures

The mylonites have medium-grade mineral assemblages. In granite the recrystallized material consists of quartz, K-feldspar, plagioclase and biotite. In the intensively deformed samples fine-grained biotite zones have a lattice preferred orientation (Figure 11). Mylonitized amphibolite consists mainly of hornblende and plagioclase with minor epidote and chloritized biotite (Figure 12).

Syntectonic recrystallization structures in quartz and feldspar indicate medium-grade conditions. In granite quartz shows abundant recovery and recrystallization structures that are typical at 400–700 °C (Passchier & Trow 1996). Feldspar porphyroclasts have core-and-mantle structure and micro shear zones, and some “bookself” microfracturing occurs too; the structures form typically at 400–500 °C. Garnet in the mylonitized granitic rock is mechanically crushed and biotite has grown in the interspaces.

In some thin sections semi-brittle chloritic fault seams crosscut the biotite rich mylonite. The kine-

matic indicators in both the biotite and chlorite rich parts show the similar sense of shear.

Reactivation and alteration

Subparallel breccias and joints often crosscut the mylonitic fabrics of the PM and VK faults (see type C). Smaller faults, like observation site Lemissaari (Figure 9) mostly lack reactivation structures.

Notes from the tunnels

The NE-trending zones of weakness in the tunnels are usually 1–2 metres wide, a little narrower than in the other fault orientations. Weathering is absent or slight. The intactness classes were R_{i3} – R_{i4} as in E-W-oriented zones. Water leakage was abundant in major zones comprising many faults but was absent in smaller separate ones. Probably the impact of later brittle events is remarkable and some of the zones may belong to the group C.



Figure 11. Mylonitized granite in a NNE trending fault, close to the VK zone, Sotunki, Vantaa. In the field, the mylonite zones are narrow, and also in microscale the intensity of deformation varies strongly. Here the biotite band above the diagonal of the picture is very fine grained compared to the other parts of the thin section and the grains have preferred crystallographic orientation. Photo by T. Elminen.

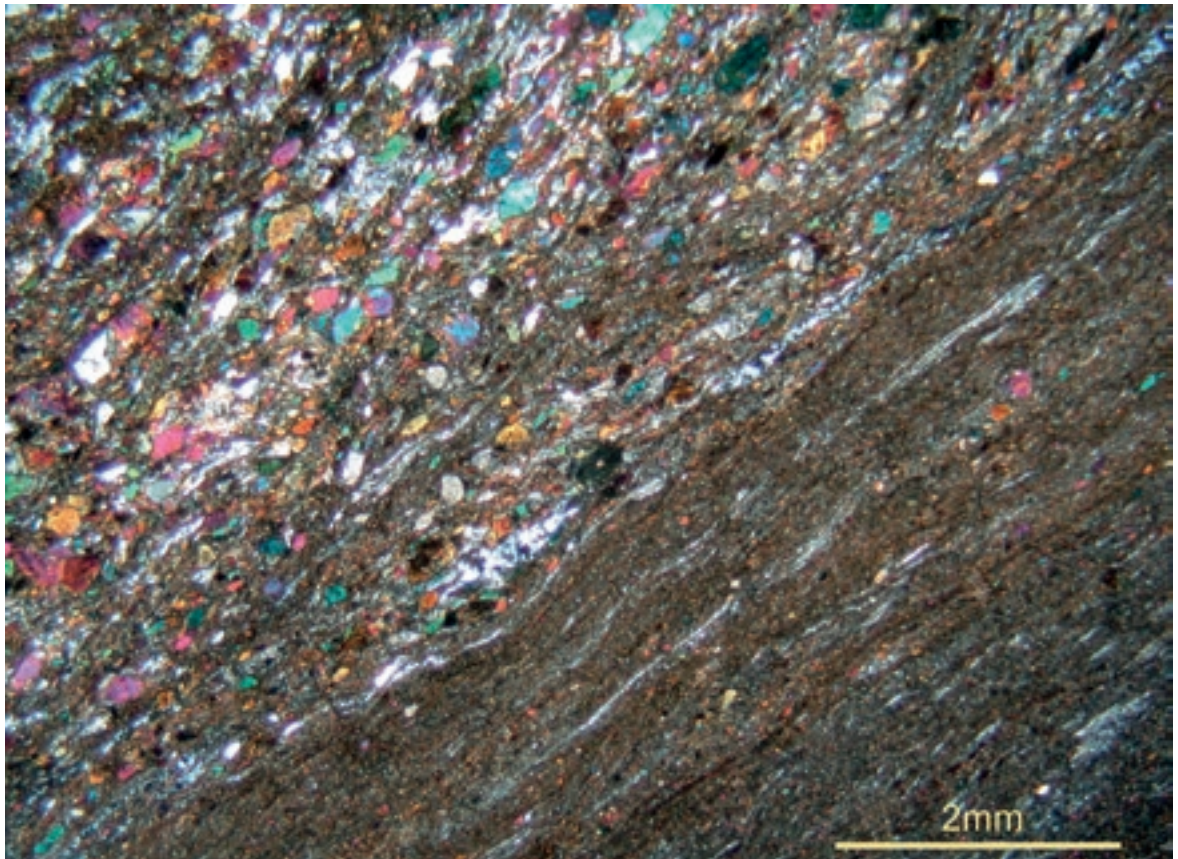


Figure 12. Mylonitized amphibolite from Lemissaari (Figure 9). The main constituents are hornblende and plagioclase. The fine-grained ultramylonitic part contains also some epidote and chloritized biotite, which were identified by microanalysis. Photo by T. Elminen.

C) Brittle NE-SW faults, reactivation of group B faults, NE faults crosscutting rapakivi granites

The NE fault structures post-dating group B are under a single group. The group consists of brittle NE faults, reactivation on pre-existing NE zones and NE faults in rapakivi, which is a special case because these granites were intruded under brittle conditions. These all share some common features. The tunnel observations on group C cannot be separated from group B.

Brittle NE faults

There are only a few observations of small NE faults with only brittle structures and they are too small to be observed in topographic or aeromagnetic data. They occur as ± 1 mm broad seams of micro breccia with quartz matrix (Figure 13) or sometimes only slickensides are exposed in roadcuts. The slickensides on the steep planes are horizontal and subhorizontal with dextral sense of shears. Dextral en echelon patterns occur as well.

Reactivation structures on pre-existing NE faults

Especially the major zones PM and VK have plenty of brittle fault structures truncating the ductile ones. Matrix in breccias is cemented by quartz, sometimes epidote, prehnite or carbonate. The slickenlines are subhorizontal and a dextral sense of shear dominates. Jointing parallel or subparallel to the fault orientation often occurs in the valley edge outcrops.

NE faults crosscutting rapakivi granites

Along the most distinctive topographic valley, the PM fault cuts a 70 m broad slice of the Bodom rapakivi pluton at its eastern contact. Close to the valley the rapakivi granite is exceptionally foliated in a few outcrops. Next to the valley the foliation parallels the PM but 400 metres away to the NW it turns almost to N-S (Figure 14). There the quartz forms up to 10 cm long narrow grains. The Obbnäs pluton is also truncated by slightly mylonitized zones, and in one outcrop at the margin the strongly mylo-



Figure 13. A brittle NE fault in Porvoo, east of the study area. The compass lies on a horizontal cross section and the vertical fault plane can be seen in the lower part of the picture. The red seams consist of micro breccia with quartz matrix and haematite pigmentation. The NE en echelon structure shows dextral movement, as do the slicken lines (SL). Photo by T. Elminen.

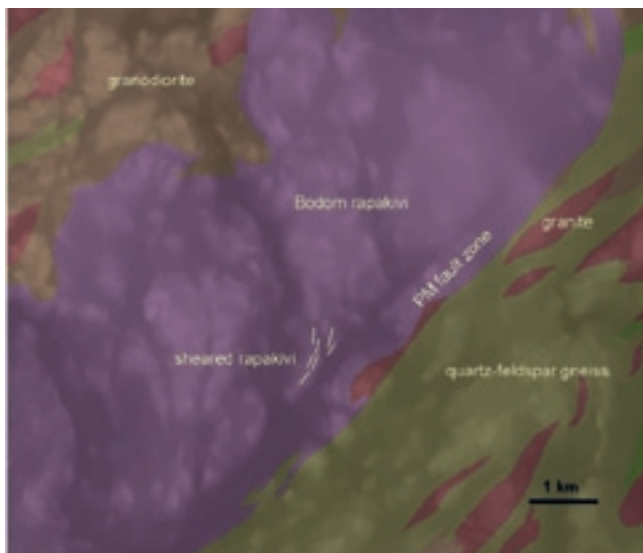


Figure 14. Rotated foliation (white lines) was measured from a few outcrops in the Bodom rapakivi pluton. This foliation with 10 cm long narrow quartz grains was not observed in other parts of the pluton. The image shows lithology with colours and the elevation by the tone value. The dark PM zone and some NW fault valleys stand out well. Digital elevation model © National Land Survey of Finland, permit No. 13/MML/08.

nitized rapakivi granite contains flattened xenoliths of country rock (Figure 15).

Mineralogy and microstructures in rapakivi NE faults

In the foliated parts of the rapakivi plutons the grain size has been reduced (Figure 16). Feldspars are generally somewhat rounded or fragmented. K-feldspars where the fragments are only slightly separated have undulose quartz, sometimes altered biotite, epidote and fluorite in the interstices. Quartz surrounds broken feldspar grains, sometimes as a single-grain, sometimes as smaller flattened grains. Quartz microstructures include deformation lamellae, weak to strong undulose extinction, subgrains and recrystallized grains. Biotite is bent and sometimes kinked. Also very fine-grained biotite with tapering tails exists. Hornblende has altered to a fine-grained non-identifiable mineral or mixture of minerals (microanalysis, XRD).

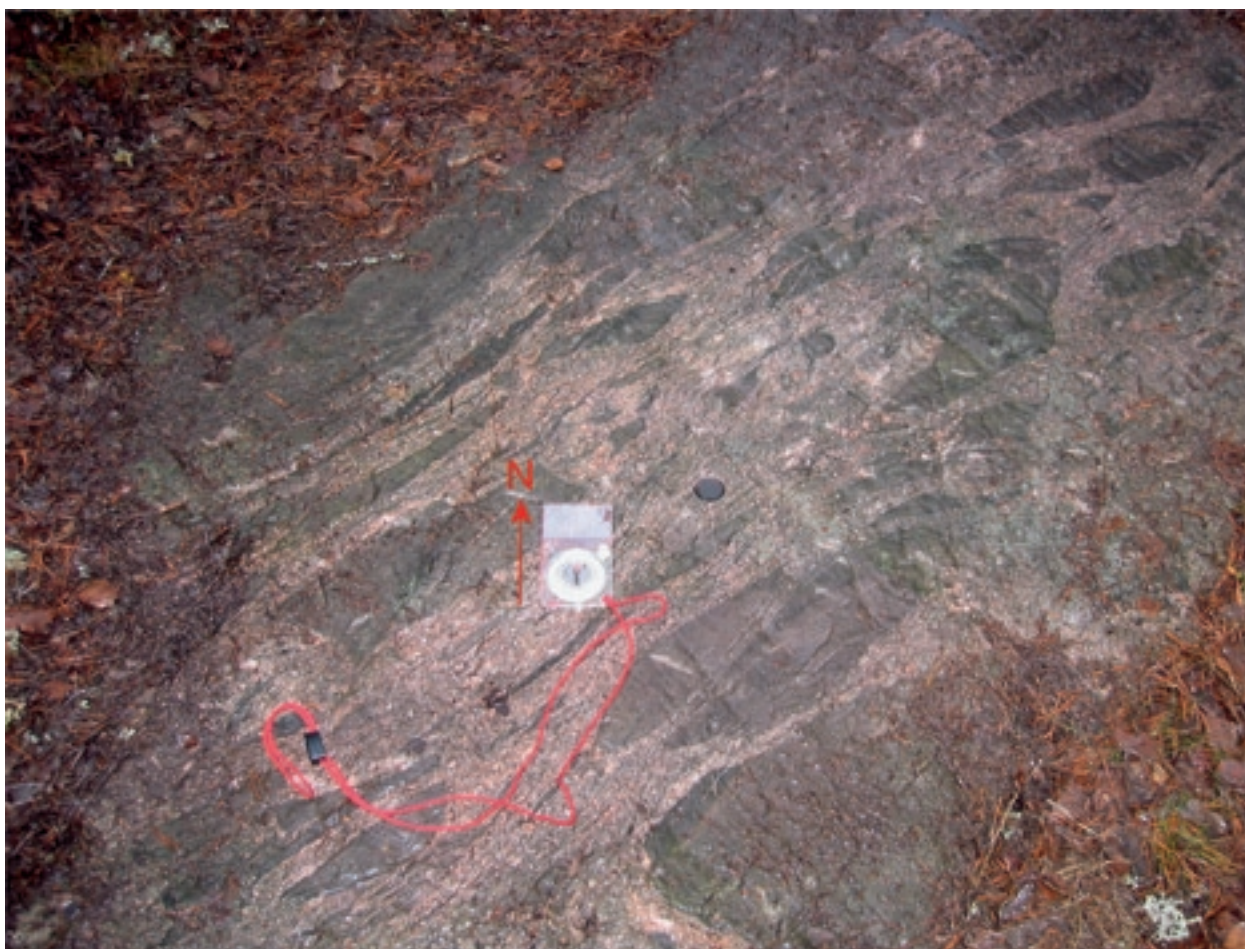


Figure 15. Xenoliths at the mylonitic Obbnäs rapakivi pluton, close to the contact in Kirkkonummi. The undeformed Svecofennian rocks are 20 m NW of the site and there is a soil-covered depression in between. Photo by T. Elminen.

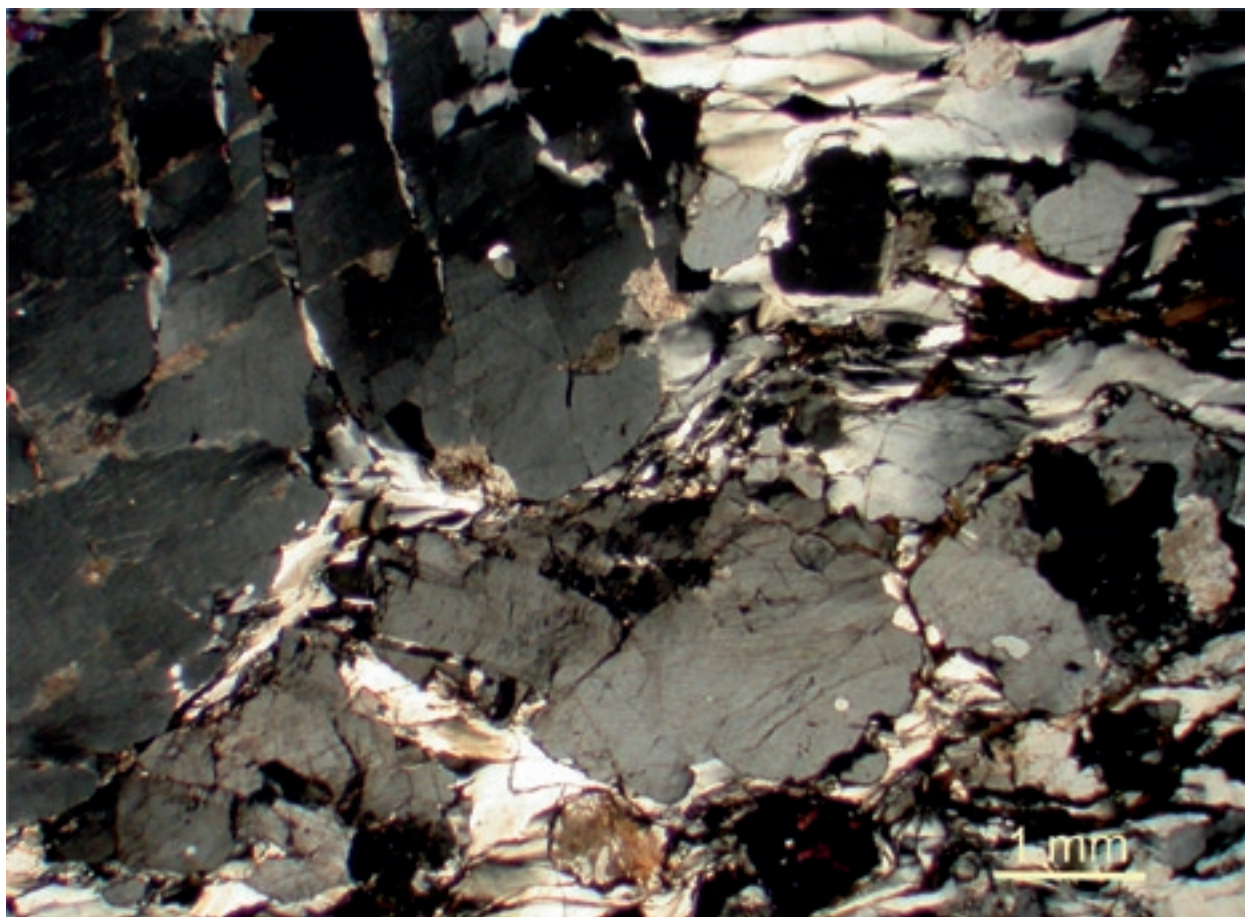


Figure 16. Sheared rapakivi texture. K-feldspar in the upper left corner has been broken and the interstices are filled with quartz. Strongly undulose quartz surrounds rounded feldspars. The grain size in undeformed rapakivi is at least 10 times larger. Photo by T. Elminen.

D) Brittle normal faults; WNW-ESE and NNW-SSE

Field relationships

The most abundant faults crosscutting the Svecofennian structures and rapakivi granites in the area are WNW- to NNW-trending straight and steep faults. They form a network pattern in the topography (Figure 17). The geometry of the fault set is orthorhombic with strike deviating roughly 30° (Figure 18) and dipping 75–90 degrees both to NE and SW. The fault valleys are 1–5 km long in general. In the northwestern part of the study area, where the homogeneous granitoids are only weakly foliated, the fault pattern is well developed. The joint data from the study area shows the same strike distribution and, in addition to the steeply dipping sets, there are also sets with gentler dips (Wennerström et al. 2008).

The faults crosscut the Bodom and Obbnäs rapakivi plutons. A microbreccia that crosscuts Obbnäs rapakivi has a WNW-ESE-oriented en echelon type sinistral geometry, comparable to some of the joint

sets. Quartz-filled joints in this orientation occur, too. Some open joints have a coating of few millimetres long quartz crystals. In the Vyborg rapakivi massif at Myrskylä (Figure 1), many NNW-trending quartz veins are observed in the granite (Laitakari & Simonen 1963) and a few WNW-trending veins exist in the Svecofennian rocks in up to one kilometre from the contact. Also some carbonate filled joints occur in this orientation. Whether some of the faults outside the rapakivi are older than the intrusion is difficult to show.

In aeromagnetic data, the similar WNW- and NNW-trending structures are expressed as faint, rectilinear, minor lineaments. Their expression can be enhanced by using processed magnetic data (Airo et al. 2008). The small magnetic gradients indicating these fault structures are related to parallel, more regional lineaments. In some places the regional lineaments are associated with a linear systematic change in magnetic field intensity on both sides of the lineament. This change may be only some nanoteslas in intensity, but is nevertheless clearly recognized in high-resolution aeromagnetic data, espe-

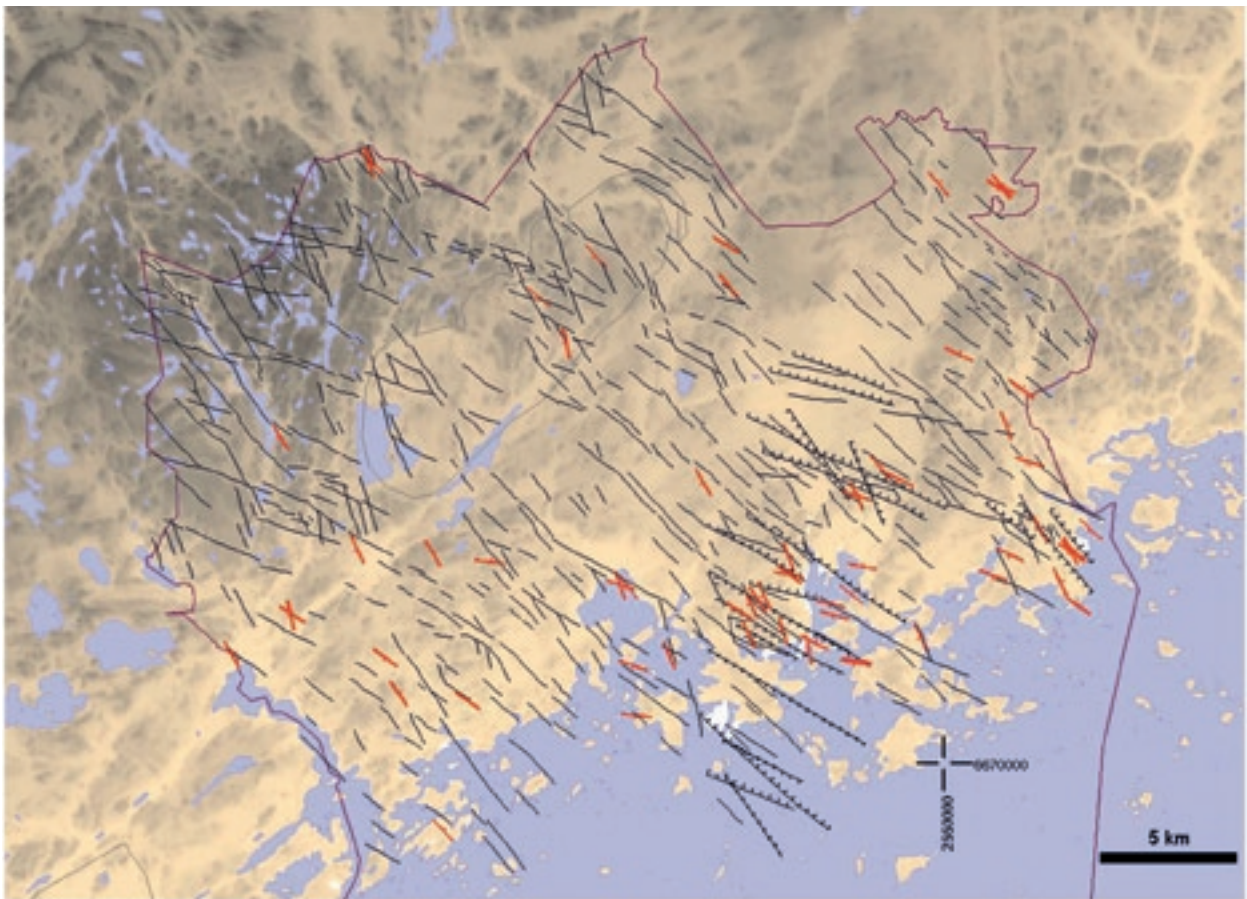


Figure 17. The brittle NW-SW oriented faults are best expressed in the topographic elevation map. Black lines are estimated NW-SE oriented fault zones from topographic and geophysical data. Red symbols mark observations on brittle faults of the same orientation with dips over 45°. Hatched lines represent extrapolated zones from tunnel weak zone data. The hatched side represents the dip direction. The broader the observed zone, the longer the line. Digital elevation model © National Land Survey of Finland, permit No. 13/MML/08.

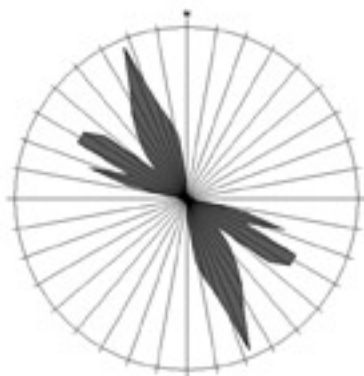


Figure 18. Rose diagram of group D brittle fault planes, which have strikes between 100–175° and dips over 45°. 70 observations in the study area.

cially in filtered or enhanced data. Such systematic linear change commonly indicates block movement. We interpret this to be connected to brittle failure of the bedrock in regional extent.

The brittle fault structures are mostly eroded, and the abrading processes during the last glacia-

tions especially favoured NW-SE-oriented valleys. However, some breccias and fault breccias are still exposed (Figure 19) and road cuts sometimes reveal reddish coarse slickensides (Figure 20).

36 slickenline observations from a total of 70 fault planes of WNW-ESE- and NNW-SSE joints and breccias have been recorded. Slip directions can be divided to steep and subhorizontal (54–75° and 1–26°, respectively). Steeply plunging lineations show normal faulting as a rule. The subhorizontal movements have usually sinistral sense of shear as well as the en echelon structures in the microbreccia.

The stress directions were interpreted by the kinematic analysis from the slickenlines on the fault planes. For the faults with steep striations the minimum principal stress, σ_3 , has a N-S direction, (N10E), and the maximum principal stress, σ_1 , is steep (Figure 21A). The result indicates extensional conditions for the normal faulting. For the gentler, sinistral slickenlines σ_3 is also in N-S direction but also σ_1 is subhorizontal, in E-W direction, which indicates strike-slip conditions (Figure 21B).



Figure 19. About one metre wide fault breccia in a road cut at Lakisto, Espoo. The incohesive fault breccias in NW-SE trending faults are usually poorly preserved, probably due to glacial processes during the last glaciations. Photo by T. Elminen.



Figure 20. Slickenside on a NW-SE normal fault plane. The dip is towards the photographer, to the SW. Lakisto, Espoo. Photo by T. Elminen.

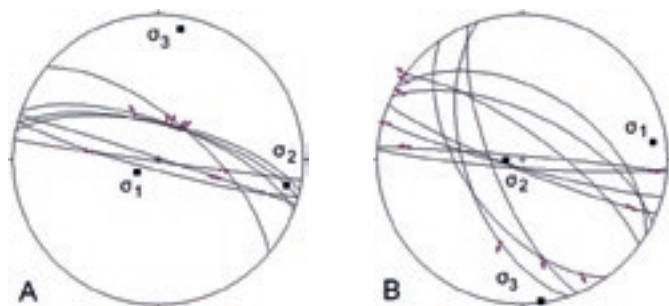


Figure 21. The paleostress directions for WNW-ESE- and NNW-SSE-oriented brittle faults by the kinematic analysis from the slickenlines on the fault planes. (a.) For the faults with steep striations the least principal stress axis, σ_3 , has a N-S direction, (N10E), and the greatest axis, σ_1 , is vertical. The result thus indicates horizontal extension during the normal faulting. (b.) For the gentler, sinistral striations, σ_3 is also in N-S direction but σ_1 is horizontal as well, which indicates strike-slip conditions.

Mineralogy and microstructures

The microstructures show brittle deformation. In breccias mineral grain fragments are angular with a large variation in size, and healed cracks and veins are abundant (Figure 22). Microstructures indicate very low-grade conditions (<300°C). The matrix is often stained with red hematite. The slickenside coatings consists of microbreccia or gouge with some Fe-oxide pigmentation.

Reactivation and alteration

It is not possible to distinguish the age relations of the different slickenside sets of these brittle structures. No overprinting relationships are seen with

the steep and gentle striations but the gentler are more frequent.

A WNW-ESE-oriented altered rapakivi-related diabase dyke has sheared contacts. The fault material is fault gouge and the striation is sub-horizontal. Also sub-horizontally striated carbonate-fillings occur in some diabase contacts.

Notes from the tunnels

In the tunnels corresponding zones of weakness are most abundant. They are usually ca 2 m wide. The weathering varies from absent to minor. Intactness is class Ri3 – Ri4. Water leakage is most common in these zones.

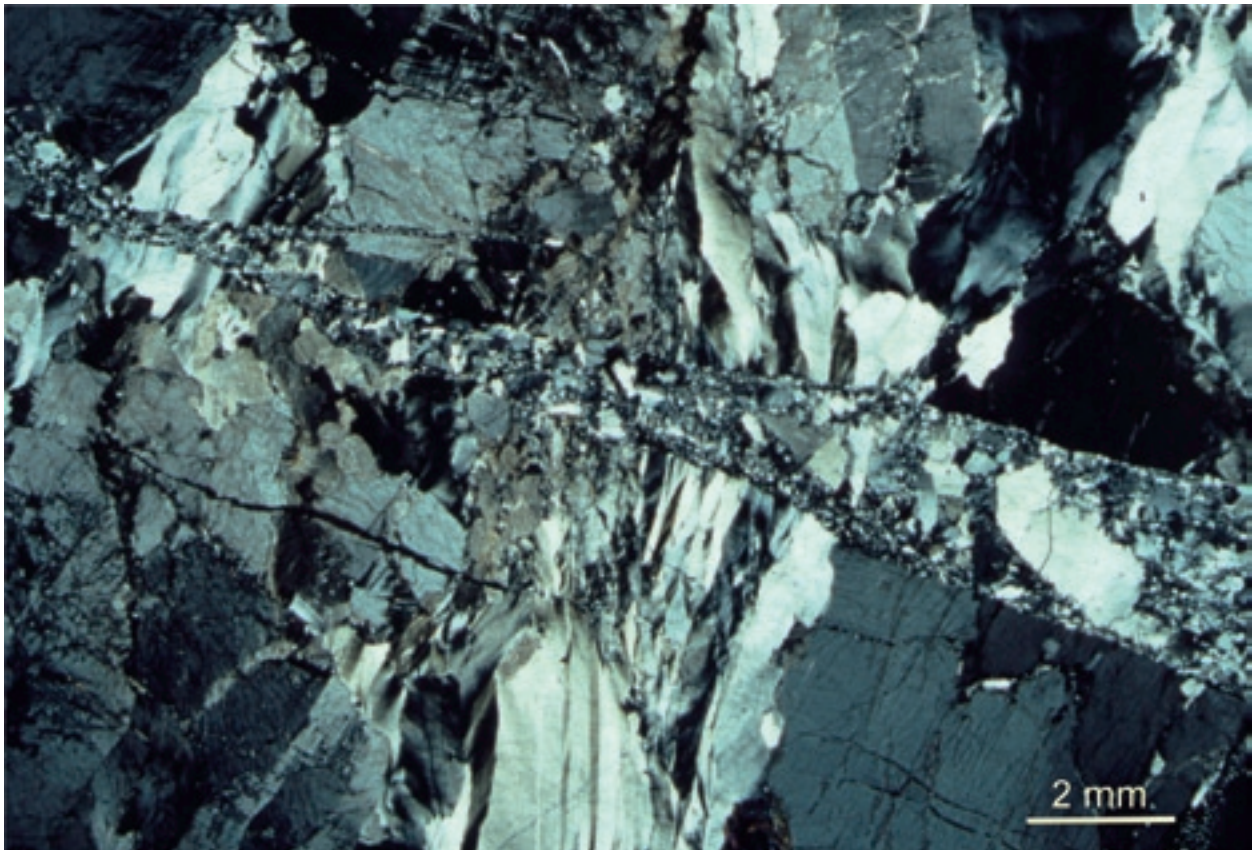


Figure 22. Microphoto showing NW-SE-oriented breccia zone within a sinistral en echelon pattern in rapakivi granite that is foliated in NE-SW direction. In addition to the quartz and feldspars in the foliated part, the breccia contains clay minerals and abundant haematite. Photo by T. Elminen.

E) Brittle strike-slip faults; N-S

Field relationships

Topographic data show narrow, commonly 5 km and a few 15 km long, N-S-oriented valleys. The lineaments occur in surface-derived aerogeophysical data as well. North of the study area, in Nurmijärvi, the map data show a displacement along the fault, which is not often recognized in the area (Figure 23). The fault crosscuts and displaces a 5 km broad Svecofennian fold structure, an E-trending lineament and a NW-SE fault, which is interpreted from topography. The apparent displacement is about 400 metres and sinistral.

All outcrop observations along these N-S trending valleys are on brittle fault structures. Long quartz and carbonate filled joints and joint swarms with some breccia occur. The slickenlines are nearly horizontal and both sinistral and dextral displacements are observed, the former being more common. Sometimes only small irregular breccia bands occur in the outcrops closest to the valleys. An outcrop in Nurmijärvi shows long N-S sinistral strike-slip faults and conjugate smaller NNW-SSE faults (Figure 24).

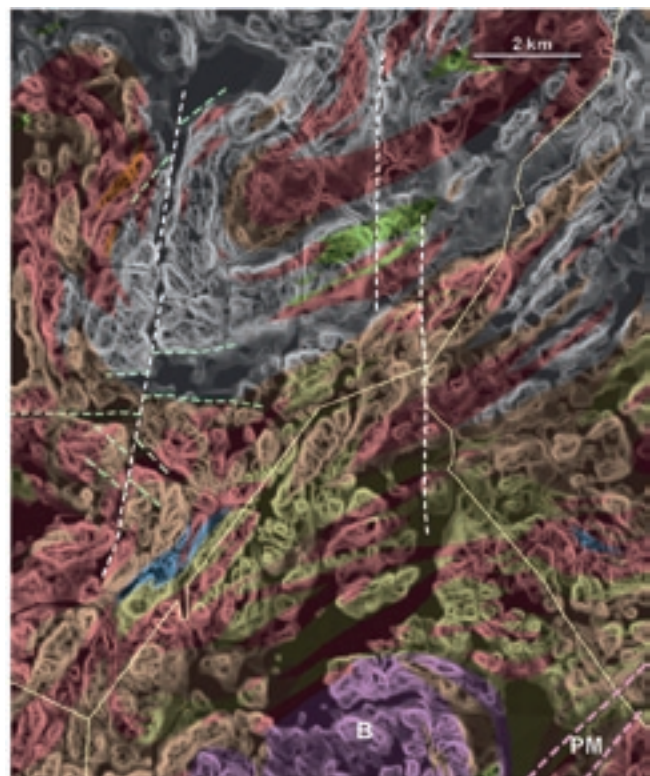


Figure 23. Fault relationships observed on a combined lithological map and slope derivation on topography data. The lighter the colour, the steeper the slope. Dashed lines represent fault lines. A N-S fault (white) displaces sinistrally earlier E-W- and NW-trending faults (light green). The location is next to the study area in Nurmijärvi. The yellow lines are city borders. Digital elevation model © National Land Survey of Finland, permit No. 13/MML/08.

The first order fault contains breccia, cavities and quartz + laumontite and separate carbonate fillings. Some other outcrops show NNW-SSE joints with an echelon pattern close to the narrow N-trending faults.

In Nummela, rapakivi-related E-W diabase dykes are crosscut by N-S trending carbonate-filled joints with horizontal slickenlines (Figure 25). Some of the joints are also partly open and partly filled with carbonate crystals.

Notes from the tunnels

In the tunnel data the N-S-oriented zones of weakness are usually 1–2 metres wide. The weathering is mostly strong. Intactness class is Ri4–Ri5, which means quite abundant fracturing with gouge/clay minerals. Water leakage, however, is rare.

F) Brittle strike-slip faults; E-W

In addition to the brittle faults in reactivated E-trending shear zones, chloritic, steep slickensides occur also separately, crosscutting earlier deformation structures. These E-W-oriented faults are often very thin usually, 0.1–1 cm, consisting of partly altered chlorite. Microscopic cracking occurs in the host rock. The faults have subhorizontal slickenlines, and both sinistral and dextral movements have been observed.

G) Low-angle reverse faults

Field relationships

Brittle low-angle faults ($\text{dip} \leq 45^\circ$) generally exist in the area; faults dipping between 45 and 75° are rare. The observations on low-angle faults (32) were made in road cuts. The fault width is usually 5–15 cm and the fault rocks consist of fault breccia and gouge that are usually weathered (Figure 26). Some chloritic slickensides occur too. Outcrop observations of low-angle faults are sparse, but considering their frequency in tunneling data, the structures should be common. A stereoplot on the low-angle faults shows some maximum in ca N, E, S, and W dip directions, which becomes more evident when low-angle fault data from tunnels (99 measurements) are added (Figure 27 a and b). The kinematic indicators in outcrops indicate thrust movements.

The chlorite filled low-angle thrusts and joints that were conjugate to steep NE faults in



Figure 24. Brittle steep N-S fault in pyroxene gneiss. The first order N-S faults are filled with quartz + laumontite and porphyroclasts. The NNW-SSE oriented faults represent second order faults in the sinistral strike-slip movement. Nurmijärvi. Photo by T. Elminen.



Figure 25. N-S fault crosscutting a WNW-trending diabase dyke. Sinistral horizontal slickenlines (SL) on carbonate filling and contact. Nummela. Photo by T. Elminen.



Figure 26. Brittle low-angle faults in a road cut. Photograph to east. Some faults follow and other truncate the gentle schistosity. The strongly weathered fault rock consists of fault breccia and gouge. Kauklahti, Espoo. Photo by M. Pajunen.

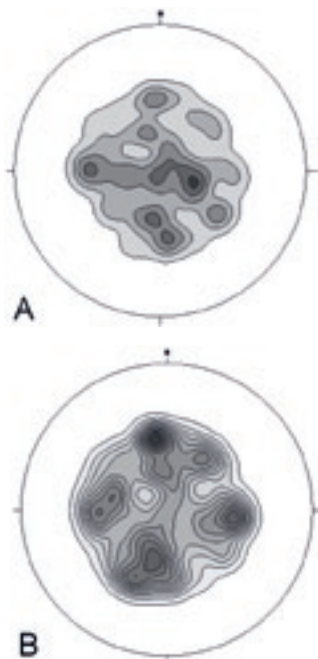


Figure 27. Contour diagram of poles to fault planes of brittle low angle ($<46^\circ$) faults, lower hemisphere projection. The dip directions are not uniform but roughly four directions can be distinguished. (a.) Measurements from outcrops, 68 fault plane observations. The number includes observations also outside, but not far, from the study area. (b.) Weak zone data from geotechnical notes from three tunnels added. 99 observations + outcrop observations, altogether 167 plane measurements.

the Länsi-Salmi quarry were described previously. There was also one 10 cm wide and weathered fault with the same dip direction, to the east, that closely resembled the weathered faults at road cuts. No other possible conjugate structures with the low-angle thrusts were observed.

Notes from the tunnels

The properties of low-angle zones of weakness in tunnels vary. The width is usually 1–3 metres. Weathering is absent or weak. The intactness class varies from Ri1 to Ri5, 1 meaning splitting of the rock and 5 meaning that all the structure consists of gouge/swelling minerals. Water leakage is reported as quite common.

DISCUSSION

NE-SW-oriented reverse faults – relations, reactivation

The earliest well specified fault system in the study area consists of NE-trending ductile mylonites (group B). They crosscut the ductile Svecofennian deformation structures and are, in turn, truncated by brittle faults and joints. Especially the major faults, PM and VK contain a variety of parallel structures from ductile to brittle. We suggest that there were two major events affecting the NE-trending faults. First they were developed during the late Svecofennian evolution and later many of them were reactivated during the rapakivi magmatism and after it.

The ductile deformation in the NE fault zones is strongly localized. The development of the mylonites started in amphibolite facies conditions and continued in retrograde conditions in greenschist facies. The kinematic indicators point to thrusting from east to south-east (Figure 28). The (possible) pseudotachylites and the semi-brittle chlorite-bearing reverse faults that grade to en echelon joints show all the same kinematics as the amphibolite facies mylonites.

The crosscutting low-grade brittle stage structures in some of the NE zones show different kinematics, namely dextral strike-slip movements. This reactivation could have formed under the same kinematic conditions like those resulting in the dextral shearing in rapakivi plutons. These strike-slip movements may also be related to NW-SE-oriented normal faulting (see below).

Age determinations have been done in the Suomusjärvi fault (Ploegsma, 1991), which is located ca 70 km west of the study area and, according to the description in Ploegsma and Westra (1990), they seem to belong to the same category of faults as the NE-trending faults in the study area. Biotite Rb-Sr ages in undeformed tonalite were 1644 ± 44 Ma and in ultramylonite 1533 ± 23 Ma. In the Porkkala-Mäntsälä fault, age determinations were made by Heeremans and Wijbrans (1999). ^{40}Ar - ^{39}Ar K-feldspar ages of the Obbnäs rapakivi granite (along the PM fault) were in the range of 1400–1550 Ma, and in the PM fault zone ages predominantly range between 1300–950 Ma. The age relationships of the Bodom and Obbnäs rapakivi plutons and the NE-trending PM fault have been discussed earlier

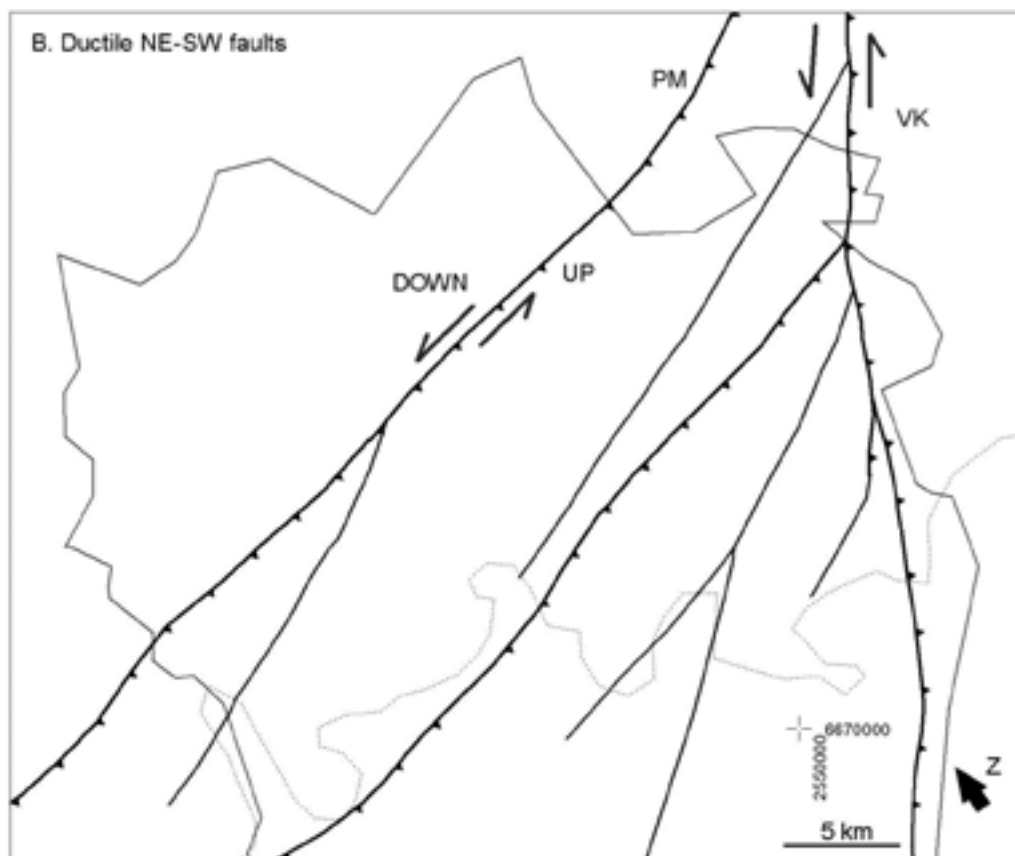


Figure 28. The earliest faults crosscutting the Svecofennian structures in the study area are NE-SW ductile faults that dip steeply to the SE. Thrusting (z) from the east – south-east caused sinistral reverse movements along these faults in the final stages of the Svecofennian deformation.

(Härme 1961, Heeremans et al. 1996 and Heeremans and Wijbrans 1999). Heeremans et al. (1996) suggested that the vertical movement within the ductile mylonites was related to the anorogenic rapakivi magmatism. Ploegsma and Westra (1990) supposed that similar structures in Johannislund, Kisko and Suomusjärvi faults, could be connected to the Gothian orogeny (1700–1550 Ma) ca 600 km southwestwards; their “D3” folding preceded the faulting.

The inferred ages of the fault zones are in the same age range and younger than those reported for rapakivi granites; however the kinematic indicators and rheology indicate two separate events for the mylonitization and the rapakivi-related faulting. The first movements along the PM zone and other NE-trending faults occurred at amphibolite facies ductile condition with a sinistral sense of shear. Rapakivi granites are estimated to have intruded at 2–5 km depth, according to the contact effects and roof pendants, a crustal level where deformation is brittle. The parallel mylonite-type structures in the rapakivi granites must have formed after magma emplacement but before cooling because the internal structures are ductile whereas in the surrounding rocks structures are brittle. In Bodom rapakivi the clock-

wise rotation of a foliation defined by flattened quartz crystals indicates dextral shear along the PM zone before the complete cooling of the pluton. The PM fault valley crosscutting the Bodom pluton suggests fault movements in brittle conditions after magma emplacement and cooling. Hence, the metamorphic and kinematic conditions in the PM zone have changed from the amphibolite facies east side up sinistral movement before rapakivi magmatism to the low-grade conditions and dextral strike-slip movements at the reactivation during the rapakivi magmatism. Thus, the 40Ar–39Ar and biotite Rb–Sr isotope ages in mylonites would then be reactivation ages. The Rb–Sr age in tonalite in Suomusjärvi was very likely reset that time as well.

The NE-trending faults are restricted to the southern part of Finland. The descriptions of Johannislund and Kisko faults close to the Suomusjärvi fault by Ploegsma and Westra (1990), suggest that they represent the same category of faults as the NE-trending faults in the study area. These and corresponding zones are sketched on the map, according to aeromagnetic data and lithological and bedrock maps (Figure 29). The faults can be traced in the southern Finland granite zone but vanish in the north. The VK fault is the easternmost zone of that type.

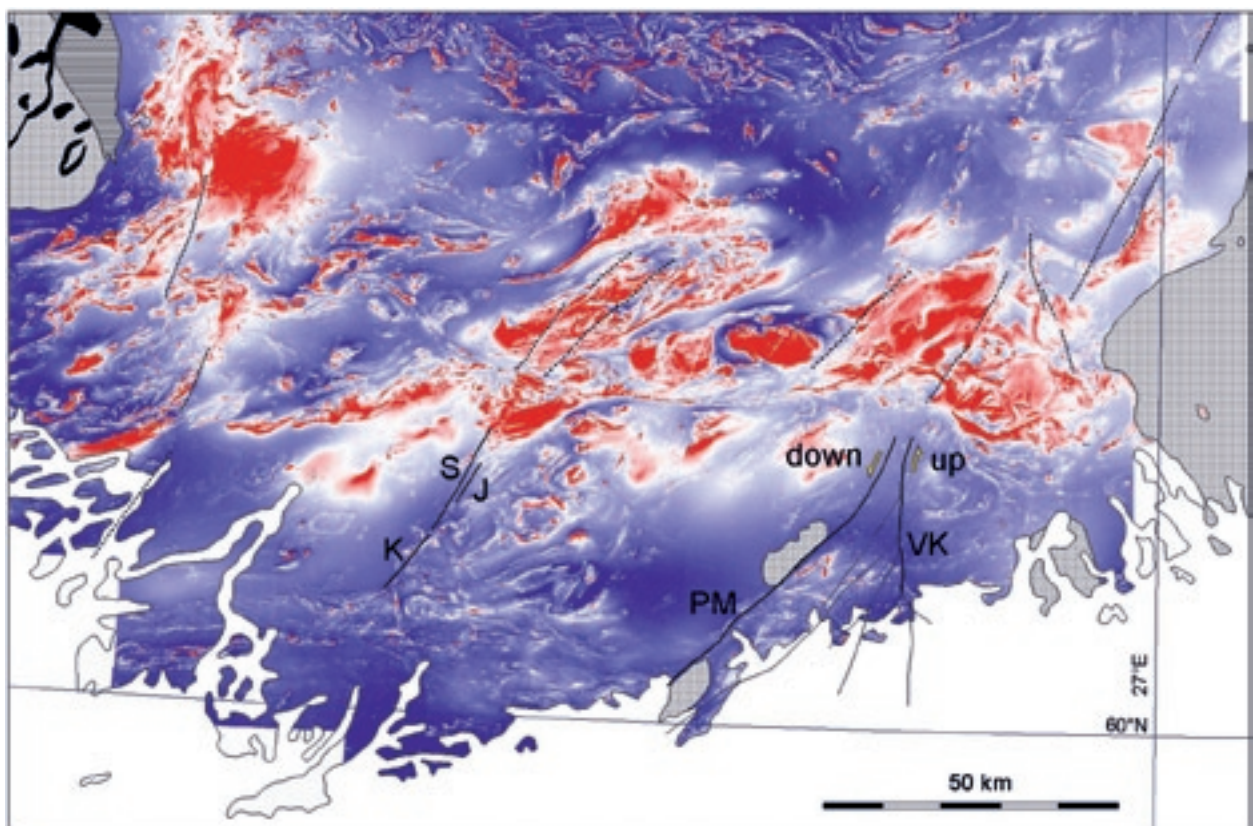


Figure 29. Some NE-trending fault lineaments in southern Finland on a magnetic image that shows strongly magnetic areas in red and weakly magnetic areas in blue. Porkkala-Mäntsälä (PM) and Vuosaari-Korso (VK) faults were formed in retrograde ductile conditions with thrusting from the east – south-east. According to Ploegsma & Westra (1990), Suomusjärvi (S), Kisko (K) and Johannislund (J) faults represent the same fault category as PM and VK. Dashed lines represent assumed faults of the same type inferred from aeromagnetic, topographic and bedrock map (1:100 000) data. Gray area: rapakivi granites, lined area: sandstone graben in Satakunta, black: 1260 Ma diabase, crosscutting the sandstone. The magnetic image is from GTK web sites.

The major zones coincide with remarkable discontinuities and negative anomalies on the gravity map, which refer to large, crustal scale structures.

Based on palaeomagnetic studies, reactivation of the PM zone was interpreted to have occurred several times: 1580 or 440 Ma, 415 Ma and 300–250 Ma ago (Mertanen et al. 2008). The samples were collected from hydrothermally altered mylonites. In Estonia some 400 Ma sedimentary rocks are crosscut by NE-trending faults (Puura et al. 1996) and remagnetization components of 300–250 Ma are recorded from Estonian sedimentary rocks, as well (Mertanen et al. 2008). This supports the supposition of activity at the PM zone also in late Paleozoic time.

Normal faults – relations to rapakivi magmatism and reactivation of NE-trending faults

The network of WNW to NNW brittle normal faults (group D) comprises another distinctive set of faults. Some faults crosscut rapakivi granites and were clearly developed after the cooling of the plutons. Probably the faulting started even earlier, during the rapakivi-related magmatism, and also the pre-existing NE faults were reactivated in the process.

The diabase dykes in the study area are not dated but can be related to the rapakivi magmatism. The 1640 Ma Obbnäs pluton (Kosunen 2004) contains a hybrid part as a result of mixing of acid and basic magmas (Kosunen 1999). Also in the c.a. 1640 Ma old Suomenniemi rapakivi association (Vaasjoki et al. 1991) in SE-Finland, the diabase and rapakivi crosscut each other (Rämö 1991). In the study area the diabase dykes and the normal faults are parallel, so it is possible for them to have been formed under similar kinds of stress conditions. Also the observed quartz joints are NW-SE-oriented. The joints being restricted to the rapakivi plutons and to their vicinity indicate formation of the joint set after cooling of the magma but still at the time with rapakivi originated fluid activity.

The geometry of the normal faults with two main trends and with dip to both sides is orthorhombic. A pattern of the four fault sets can form contemporaneously (Reches 1983). The 30 degrees difference in strike could also be due to rotation of the stress field with successive fault sets. A hundred kilometres to the north of the study area, a NW-SE-oriented diabase dyke swarm comprises two sets of different ages and their trends deviate ca 20° (Figure 1). The older set of this Häme swarm is 1665 Ma old and trends N75W, and the younger is 1645 Ma old and trends N55W (Vaasjoki & Sakko 1989). This indicates a clockwise rotation of the extensional axis at 20 Ma during the rapakivi-related magmatism.

The steep and subhorizontal striation sets on the normal fault planes cannot be mineralogically or microstructurally separated from each other but the latter are more frequent. Although not recorded we assume that the subhorizontal striations are later and overprint some of the original steeper striations. A change to more gentle plunges could occur under continuous strike-slip conditions, which would lead to more horizontal movements at the existing normal faults (Waldron 2004). The horizontal striations on diabase contacts with fault gouge refer to horizontal movements some time after the emplacement and cooling of the dykes.

The kinematic analysis on the faults with steeply plunging slickenlines demonstrates extensional conditions and on those with gently plunging slickenlines sinistral strike-slip conditions. In both stress fields subvertical NE-trending faults would show dextral strike-slip movements (Figure 30). Most of the measured slip properties of brittle NE fault planes are of that type (Figure 31), both as reactivation on pre-existing zones (group B) and as development of new brittle faults (group C). Movements concentrating easily in the old zones would release the stress and explain the small amount of merely brittle NE faults. Dextral strike-slip movements were also interpreted along NE-trending PM fault in Bodom rapakivi in its cooling time. All observations on normal faults (striations, sinistral en echelon joints and breccias) and strike-slip NE faults point to a stress field where the minimum principal stress axis is in N-S direction. The steeper striations on normal faults indicate an extensional stress field where maximum principal stress axes is vertical which could be a situation first but other structures point to a transcurrent regime where maximum principal stress axes would be close to E-W direction.

The pattern of the NW-SE faults and diabase dykes is widespread in southern Finland, with the area extending at least beyond the migmatite belt. Often they concentrate in earlier Svecofennian structures with the same trend. To define the distribution by geophysical maps data need to be processed and studied over large areas. The glacial sediments covering the bedrock forms inland also makes it difficult to define the area more precisely.

N-S strike-slip faults

N-trending brittle strike-slip faults (group E) are very long, vertical to steep and form a conjugate set with short NNW-SSE joints. The latter often form sinistral en echelon patterns. The N faults are distinctive but rarer than the normal faults (group D).

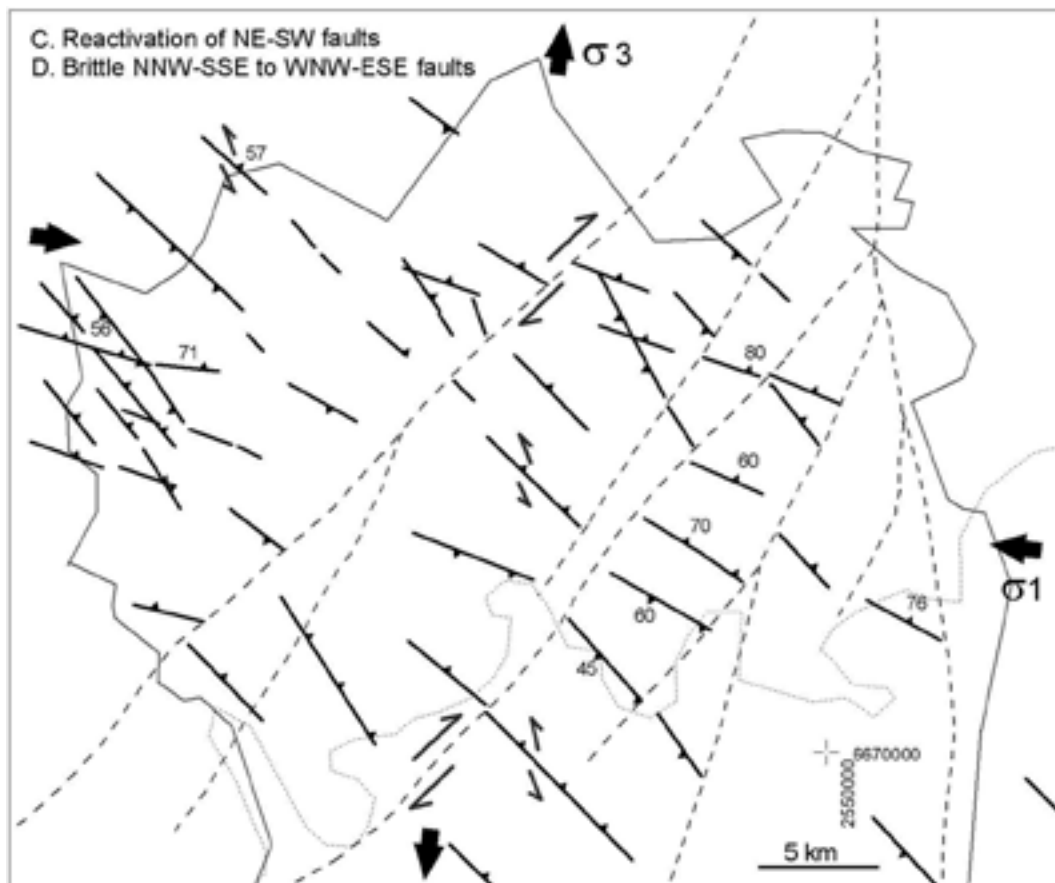


Figure 30. Brittle WNW-ESE and NNW-SSE normal faults (uniform lines) crosscut 1640 Ma old rapakivi granites. They were formed in N-S extension, and brittle sinistral strike-slip on pre-existing NE-SW-oriented faults (dashed lines) fit into the same stress field. This movement has also been observed in cooling rapakivi plutons. The movements occurred in a transcurrent regime.

A stress field that would cause sinistral movements along a N-trending strike-slip fault system would have the extensional axes, σ_3 in NE-SW orientation and NW-SE shortening axis σ_1 (Figure 32). This stress field would also cause horizontal reactivation in the previous normal faults (group D) with sense of shear depending on the orientation of the fault. Since the N-S faults crosscut the normal faults they are younger. Some time between normal faulting and the development of N-S faults must have elapsed to produce the different conditions where the N-S strike-slip type is dominant.

E-W and ENE fault structures

In the southern part of the study area there are sheared rocks subparallel to the general E-W and ENE strike of the foliation. The mylonites (group A) that slightly crosscut the foliation were examined and the reverse faulting with south side up movement indicates their formation in N-S compression. These zones were later clearly crosscut by the NE-SW mylonite faults, which offset the fault zones so that they are not continuous in map scale.

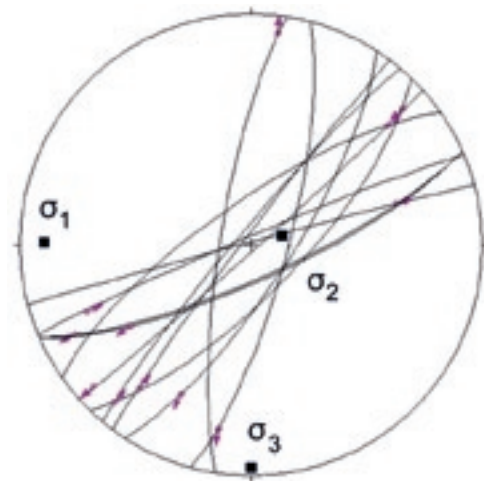


Figure 31. Paleostress directions for NE-SW faults derived by kinematic analysis from the slickenlines on the fault planes. Both brittle reactivation on older faults and new brittle faults were used. The maximum principal stress axis, σ_1 , is E-W and the minimum principal stress axis, σ_3 , is N-S, which is consistent with the normal fault paleo-stress field (Figure 21).



Figure 32. Brittle subvertical N-S sinistral strike-slip faults (uniform lines) crosscut the pre-existing NW-SE oriented normal faults (dashed lines). The N-S faults often have conjugate NNW-SSE-oriented joints with sinistral en echelon pattern (J). The N-S strike-slip faults could have been formed in a stress field where σ_3 was NE-SW and σ_1 NW-SE. This stress field would also cause horizontal movements in the previously formed NW-SE normal faults with sense of shear depending on the orientation of the original fault.

The ductile history of E-W zones is complicated (Pajunen et al. 2008) and the lower amphibolite facies structures cannot be tied to a single deformation. They may represent a retrograde phase during the Svecofennian orogeny or later reactivation during post-Svecofennian time.

The younger E-W faults (group F) are brittle with fault breccias and gouges so they postdate the mylonitization in these zones and also the ductile NE-SW ductile faults. They often occur at the E-W mylonite zones as a consequence of reactivation. Both these and the single E-W chloritic slickensides have horizontal slickenlines unlike the lineations in mylonites that are steep. With both dextral and sinistral strike-slip movements the brittle E-W faults do not fit into a single kinematic condition. The dextral movements would be compatible with the kinematics of both the system of NW normal faults and NE strike-slip and the N-S strike-slip system that were described before but the relations are not proved by field observations.

Low-angle faults

The low-angle faults (group G) can be divided into four groups based on their different dip directions. All structures were brittle and very weathered and no evidence of conjugate structures was found at the outcrops. Kinematically the four thrust faults with orthogonal dip directions cannot be formed in a singular event. The N and S dipping faults however could be conjugate as well as the pair of W and E dipping faults.

In the Länsisalmi quarry, east dipping narrow fault structures (described with group B) were connected to ductile to semi-brittle NE reverse faulting. They were not weathered, except for one 10 cm wide strongly weathered fault, which may have the same semi-brittle origin (same location, same orientation). This postulates that also some other of the east dipping weathered low-angle faults could have a more ductile origin and be related to the late Svecofennian east side up fault system.

Brittle E dipping thrusts would also fit into the later transcurrent system with NW-trending normal faults and NE-trending strike-slip faults. Still, a separate system of E and W dipping thrusts might have formed in a different event in E-W compression. S and N dipping thrusts could similarly have formed in N-S compression. As no conjugate structures were observed the interpretation remains open. The brittle low-angle thrusts clearly need more examination to define the conditions for their formation.

General remarks

The crust has been stabilized after Svecofennian deformation and exhumation has been assumed to happen rather shortly after that. The different fault sets formed in different kinematic settings show increasingly brittle structures with time. The history of ductile faults formed under metamorphic conditions and some brittle fault sets displaying distinct fault patterns is better understood, but the origin of some, probably the latest, brittle faults remains obscure. All over the study area, horizontal striations on brittle slickensides and fault gouges are more common than steep lineations; the horizontal movements probably post-date and overprint older structures.

Older, Svecofennian, bedrock structures controlled the location of younger structures. For example the E-W high strain zones contain much more E-trending mylonitic and brittle fault structures than other areas suggesting that reactivation during subsequent deformation concentrated easily in zones that had been disturbed before. Deformation during the late Svecofennian events, especially E4 of Pajunen et al. (2008), determined the locations for the major NE-SW faults zones, which as crustal scale structures were reactivated many times afterwards. Almost all the major fault zones display abundant reactivation structures in different conditions. The overprinting and hydrothermal activity makes it difficult to define different fault sets and to establish

the timing. This study showed that it is very useful to look for smaller fault structures outside the major faults because they often represent a single event. After studying them similar structures are easier to find and distinguish also in the major zones.

The brittle normal faults seem to cover the study area quite homogeneously. However, the faults are easier to interpret from topographic maps in plutonic rock areas or in shallow dipping structures than in steeply dipping metamorphic rocks. For example, in Espoo in a granitic area the lake Nuuksion Pitkäjärvi can be interpreted from the topography as a junction of a long NW-SE-oriented fault and an array of smaller NNW-trending faults, both of group D. The imprint of all of the described fault structures on present bedrock landforms is substantial.

The areal distribution of fault sets can also be defined by high-resolution aeromagnetic data, which however needs to be processed by appropriate filtering and enhancing (Airo et al. 2008).

The large amount of data, especially in the case of brittle fault structures proved to be practical. When outcrops are small and little structural relationships are visible, e.g. no conjugate faults, it is not possible to distinguish whether the fault in one outcrop represents a first order structure or second order fault structure. Statistical analysis of many observations reveals the role of the fault in a regional context and decreases the risk of misinterpretations.

Although this paper concentrates on the geological properties of the faults, the understanding and classifying the structures can provide useful information for applications. For example the chloritic slickensides are harmful in excavating and are expected especially in areas of E-trending foliation and topographic depressions. The weathering and fracturing data from the tunnels, although it is statistical, shows that certain zones tend to be more fractured than others.

The different fault types with the properties described above are classified in Table 2. Some references from the tunnels are included.

SUMMARY

The different fault zones in the study area could be separated into distinct groups based on their characteristics. The crosscutting relationships prove the assumption of decreasing temperature with exhumation and time in the area. The different fault rock types were formed by different deformation mechanisms, which act at different temperatures. It is also clear that the stress field changed with time, and dif-

ferent fault groups could be separated by the faulting types and kinematics too.

Svecofennian E-trending mylonites formed under amphibolite facies conditions may represent different deformation episodes. The youngest phase crosscut the general foliation and was formed in upper greenschist to lower amphibolite facies when the southern blocks were uplifted and/or thrust northwards.

Table 2. The different fault types and their properties summarized. The order from A to E is from older to younger event. C and D are interpreted to have formed at the same time. The relative timing of fault types F and G remains open.

Class and nature	A. Ductile E-W and ENE-SWS	B. Ductile (to semi-brittle) NE-SW	C. Brittle NE faults and reactivation of NE-SW major faults	D. Brittle WNW-ESE and NNW-SSE	E. Brittle N-S	F. Brittle E-W	G. Brittle low angle, dips to N, E, S, W
Fault rock structure	Mylonite, mylonite gneiss	Mylonite, mostly ultramylonite	Breccias	Breccias and fault breccias	Breccias, quartz and carbonate filled joints	Chloritic (altered) slickensides, fault	Fault breccias, strongly weathered
Metamorphic facies	Latest ductile shearing, upper greenschist to lower amphibolite facies	Amphibolite to greenschist, continuous retrograde faulting	(Phehnite-pumpellyite [some prehnite filled breccias])	Very low grade	Zeolite (laumontite, analcime)	Very low grade	Very low grade, some may have higher degree origin
Dip and fault type, sense of shear	Steep (some low angle), reverse	Steep, oblique reverse, sinistral. Conjugate with minor east dipping low angle faults	Steep, strike-slip, mostly dextral	Steep normal fault, oblique, sinistral	Steep strike-slip, mostly sinistral. Conjugate with minor NNW-SSW faults	Steep, strike-slip, both dextral and sinistral	Low angle, reverse
Kinematics	Thrusting from the South	Thrusting from East - South-East	N-S extension, strike-slip regime	N-S extension, extensional, later strike-slip regime	NNE-SSW oriented extension	Not interpreted. Sinistral and dextral	Probably different origins
Structural relationships	In high strain zones. Mylonites slightly crosscut foliation	Foliation bends into parallelism towards the faults which, however, crosscut it. Faults crosscut E-W zones (A).	Rapakivi related magmatism and later	Crosscut ductile structures, crosscut rapakivi. Coeval with C.	Crosscut ductile structures and diabases, displaces brittle NNW-SE faults (D)	Gouge zones parallel and crosscut ductile E-W mylonites (A)	Crosscut ductile structures, some may have semi-ductile origin (conjugates to semi-brittle NE-SW (B))
Age estimation	Svecofennian	Late Svecofennian	Rapakivi related magmatism and later	Rapakivi related magmatism and later	Later than rapakivi	Later than rapakivi	Later than rapakivi
Reactivation	Reactivation in F (may be simultaneous with D)	Reactivation in C (and D)	Reactivates B	Horizontal movements probably overprint oblique. (Reactivates A?)	Possibly reactivates D and C - not observed	Reactivates A (and D7). Or these are just products of D.	
Regional position in the study area	Areas of E-W striking foliation	Two major faults crosscut the study area, a few smaller ones	Same as B, not many observations on small faults	Cover all the study area, most dense of the fault types	All over the area, sparse	Occur mostly in southern E-W trending areas	All over the area
Length, average	4 km usually, longest 10 km	Major zones 100 km, smaller 5 -25 km	(Same as B)	1-5 km	5-15 km	(Same as A)	Not measurable
Width, from tunnel data (means zone of weakness)	Cannot be distinguished from brittle structures and reactivation	Usually 1-2 m, probably due to later activation. Narrowest zones, 63% < 2m	Usually 1-2 m. Narrowest zones: 63% < 2m	Usually 2-3 m	Usually 1-2 m	Usually 1-3 m. Widest zones: a few 10-20m	Usually 1-2 m
Geotechnical special characteristics, from tunnel data	E-W same as brittle E-W (F), due to reactivation. ENE-SWS weak zones are rare.	Same as brittle NE-SW (C), due to reactivation.	Rp1 most common, R3-4 common, R3 dominates.	Large variation between Rp0.5 and Rp2. R3-4 common, R3 dominates.	Most weathered zones. 20% of the faults Rp 2.5 and over. Mostly R3-4 however also common; 17%.	Rp0.5-1 common. Rp3 most common (5%) in these zones. R3-4 common, R3 dominates.	Large variation between Rp0.5 and Rp2. R3 5-4.5 most common.
Water leakage, from tunnel data	See F	See C	In two major zones the water leakage is abundant but in smaller faults absent.	Often water leakage. Distributed evenly in many zones.	Rare water leakage	Some water leakage	Often water leakage

Late Svecofennian NE-trending ductile reverse faults developed under retrograde conditions from amphibolite to greenschist facies during thrusting from south-east.

The brittle WNW to NNW-trending normal faults formed under very low-grade extensional conditions in a transcurrent regime. At the same time the pre-existing NE-SW-faults were reactivated, and also new dextral strike-slip faults of that orientation were formed. The maximum principal stress axis was E-W. The faults may be related to rapakivi magmatism.

N-trending strike-slip faults formed after the normal faulting. They are sinistral and associated with minor conjugate NNW-SSE-oriented en echelon joints and faults indicating that the maximum principal stress axis was NW-SE. At this time the pre-existing WNW- to NNW-trending normal faults could have been reactivated by more horizontal movements.

Low-angle brittle thrust faults of four dip directions were formed in unknown time and stress field. Possibly some of them were coeval with some other described brittle fault systems.

ACKNOWLEDGEMENTS

The results of this study were mainly produced in the project "Construction potential modelling of bedrock in urban areas" carried out in 1999–2002 in the metropolitan area. We thank the Technological Agencies of Finland (TEKES), Helsinki, Espoo and Vantaa cities and the private companies Viatek Ltd and Rockplan Ltd for their financial support.

Lassi Pakkanen is thanked for microanalysis and Mirja Saarinen for XRD determinations. Jouko Pääkkönen and Andrej Wennström are thanked for preparing the thin sections.

We are thankful for the official reviewers of the paper, Håkan Sjöström and Kerstin Saalman, for their corrections and suggestions on the text.

We thank Roy Siddall for checking the English of the manuscript.

REFERENCES

- Aarnisalo, J. 1978.** Use of satellite pictures for determining major shield fractures relevant for ore prospecting, northern Finland. *Geologinen tutkimuslaitos, Tutkimusraportti* 21. 59 p. + 4 map pls.
- Airo, M.-L., Elminen, T., Mertanen, S., Niemelä, R., Pajunen, M., Wasenius, P. & Wennerström, M. 2008.** Aerogeophysical approach to ductile and brittle structures in the densely populated urban Helsinki area, southern Finland. In: Pajunen, M. (ed.) *Tectonic evolution of the Svecofennian crust in southern Finland – a basis for characterizing bedrock technical properties*. Geological Survey of Finland, Special Paper 47, 283–308.
- Anderson, E. M. 1942.** *The Dynamics of faulting and dyke formation with applications to Britain*. Edinburgh: Oliver & Boyd. 183 p.
- Gardemeister, R., Johansson, S., Korhonen, P., Patrikainen, P., Tuisku, T. & Vähäsarja, P. 1976.** Rakenusgeologisen kallioluokituksen soveltaminen. Tiedonanto / Valtion teknillinen tutkimuskeskus, Geotekniikan laboratorio 25. 39 p.
- Heeremans, M., Stel, P., van der Beek, P. & Lankreijer, A. 1996.** Tectono-magmatic control on vertical dip slip basement faulting: An example from the Fennoscandian Shield. *Terra Nova* 8, 129–140.
- Heeremans, M. & Wijbrans, J. 1999.** Late Proterozoic tectonic events in southern Finland, constrained by (super 40) Ar/ (super 39) Ar incremental heating and single spot fusion experiments on K-feldspars. *Terra Nova* 11, 216–222.
- Härme, M. 1961.** On the Fault Lines of Finland. *Bulletin de la commission géologique de Finlande* 196, 437–444.
- Härme, M. 1969.** Kerava. Geological map of Finland 1:100 000, Pre-Quaternary Rocks, Sheet 2043. Geological Survey of Finland.
- Koistinen, T. (ed.) 1994.** Precambrian basement of Gulf of the Finland and surrounding area 1:1 000 000. Geological Survey of Finland, Special maps 31.
- Korsman, K. (ed.), Koistinen, T. (ed.), Kohonen, J. (ed.), Wennerström, M. (ed.), Ekdahl, E. (ed.), Honkamo, M. (ed.), Idman, H. (ed.) & Pekkala, Y. (ed.) 1997.** Bedrock map of Finland 1:1 000 000. Geological Survey of Finland.
- Korsman, K., Korja, T., Pajunen, M. & Virransalo, P. 1999.** The GGT/SVEKA transect: structure and evolution of the continental crust in the Paleoproterozoic Svecofennian orogen in Finland. *International Geology Review* 41, 287–333.
- Kosunen, P. 1999.** The rapakivi granite plutons of Bodom and Obbnäs, southern Finland: petrography and geochemistry. *Bulletin of the Geological Society of Finland* 71, 275–304.
- Kosunen, P. 2004.** Petrogenesis of mid-Proterozoic A-type granites: Case studies from Fennoscandia (Fin-

- land) and Laurentia (New Mexico). PhD thesis, University of Helsinki, Department of Geology. 21 p.
- Lahtinen, R., Korja, A. & Nironen, M. 2005.** Paleoproterozoic tectonic evolution. In: Lehtinen, M., Nurmi, P. & Rämö, O. T. (eds.) Precambrian Geology of Finland – Key to the Evolution of the Fennoscandian Shield. Amsterdam: Elsevier B.V., 481–532.
- Laitakari, I. & Simonen, A. 1963.** Pre-Quaternary Rocks of the Lapinjärvi Map-Sheet area. Geological Map of Finland 1:100 000, Explanation to the Map of Pre-Quaternary Rocks, Sheet 3022. Geologinen tutkimuslaitos. 48 p.
- Laitakari, I., Rämö, O. T., Suominen, V., Niin, M., Stepanov, K. & Amantov, A. 1996.** Subjotnian: rapakivi granites and related rocks in the surroundings of the Gulf of Finland. In: Koistinen, T. J. (ed.) Explanation to the map of Precambrian basement of the Gulf of Finland and surrounding area 1:1 mill. Geological Survey of Finland, Special Paper 21, 59–97.
- Laitala, M. 1960.** Siuntio. Geological map of Finland 1:100 000, Pre-Quaternary Rocks, Sheet 2032. Geological Survey of Finland.
- Laitala, M. 1967.** Helsinki. Geological map of Finland 1:100 000, Pre-Quaternary Rocks, Sheet 2034. Geological Survey of Finland.
- Laitala, M. 1994.** Lohja. Geological map of Finland 1:100 000, Pre-Quaternary Rocks, Sheet 2041. Geological Survey of Finland.
- Lindberg, B. & Bergman, L. 1993.** Vehmaan karttalueen kallioperä. Summary: Pre-Quaternary Rocks of the Vehmaa Map-Sheet area. Geological Map of Finland 1:100 000, Explanation to the Maps of Pre-Quaternary Rocks, Sheet 1042. Geological Survey of Finland. 56 p. + 4 app
- Mertanen, S., Airo, M.-L., Elminen, T., Niemelä, R., Pajunen, M., Wasenius, P. & Wennerström, M. 2008.** Paleomagnetic evidence for Mesoproterozoic – Paleozoic reactivation of the Paleoproterozoic crust in southern Finland. In: Pajunen, M. (ed.) Tectonic evolution of the Svecofennian crust in southern Finland – a basis for characterizing bedrock technical properties. Geological Survey of Finland, Special Paper 47, 215–252.
- Pajunen, M. 1986.** Deformation analysis of cataclastic structures and faults in the Tervo area, central Finland. In: Korsman, K. (ed.) Development of deformation, metamorphism and metamorphic blocks in eastern and southern Finland. Geological Survey of Finland, Bulletin 339, 16–31.
- Pajunen, M., Airo, M.-L., Wennerström, M., Niemelä, R. & Wasenius, P. 2001.** Preliminary report: the “Shear zone research and rock engineering” project, Pori area, south-western Finland. In: Autio, S. (ed.) Geological Survey of Finland, Current Research 1999–2000. Geological Survey of Finland, Special Paper 31, 7–16.
- Pajunen, M., Airo, M.-L., Elminen, T., Niemelä, R., Salmelainen, J., Vaarma, M., Wasenius, P. & Wennerström, M. 2002a.** Kallioperän rakennettavuusmalli taajamiin. Raportti I. Menetelmäkehitys ja ohjeistus. Geological Survey of Finland, unpublished report K 21.42/2002/5. 95 p., 8 app. pages.
- Pajunen, M., Airo, M.-L., Elminen, T., Niemelä, R., Salmelainen, J., Vaarma, M., Wasenius, P. & Wennerström, M. 2002b.** The Construction Potential of Bedrock 1:50 000 Espoo, Helsinki, Vantaa. Geological Survey of Finland, unpublished map K.21.42/2002/7.
- Pajunen, M., Airo, M.-L., Elminen, T., Mänttari, I., Niemelä, R., Vaarma, M., Wasenius, P. & Wennerström, M. 2008.** Tectonic evolution of the Svecofennian crust in southern Finland. In: Pajunen, M. (ed.) Tectonic evolution of the Svecofennian crust in southern Finland – a basis for characterizing bedrock technical properties. Geological Survey of Finland, Special Paper 47, 15–160.
- Parkkinen, J. 1975.** Deformation analysis of a Precambrian mafic intrusive, Haukivesi area, Finland. Geological Survey of Finland, Bulletin 278. 61 p.
- Passchier, C. & Trow, R. 1996.** Microtectonics. Springer-Verlag Berlin Heidelberg, 289 p.
- Pietikäinen, K. J. 1994.** The geology of the Paleoproterozoic Pori shear zone, southwestern Finland, with special reference to the evolution of veined gneisses from tonalitic protoliths. Dissertation, Michigan Technological University, 1994. U.S.A.
- Ploegsma, M. 1991.** A pilot Rb-Sr dating of the Suomusjärvi ultramylonite: evidence for major Post-Svecofennian deformation in SW Finland. Bulletin of the Geological Society of Finland 63 (1), 3–13.
- Ploegsma, M. & Westra, L. 1990.** The early Proterozoic Orijärvi Triangle (Southwest Finland); a key area on the tectonic evolution of the Svecofennides. Precambrian Research 47:1–2, 51–69.
- Puura, V., Amantov, A., Tikhomirov, S. & Laitakari, I. 1996.** Latest events affecting the Precambrian basement, Gulf of Finland and surrounding areas. In: Koistinen, T. (ed.) Explanation to the Map of Precambrian basement of the Gulf of Finland and surrounding area 1:1 million. Geological Survey of Finland, Special Paper 21, 115–125.
- Reches, Z. 1983.** Faulting of rocks in three-dimensional strain fields; II, Theoretical analysis. Tectonophysics, vol.95, no.1–2, 133–156.
- Rämö, O. T. 1991.** Petrogenesis of the Proterozoic rapakivi granites and related basic rocks of southeastern Fennoscandia: Nd and Pb isotopic and general geochemical constraints. Geological Survey of Finland, Bulletin 355. 161 p. + 1 app. map.
- Sederholm, J. 1910.** Murrosviivat Fennoskandiassa teoksessa Suomen kartasto. Suomen Maantieteellinen seura. Fracture lines in Fennoscandia in Atlas of Finland. Geographical Society of Finland.
- Suominen, V. 1991.** The chronostratigraphy of southwestern Finland with special reference to Postjotnian and Subjotnian diabases. Geological Survey of Finland, Bulletin 356. 100 p. + 5 app.
- Talvitie, J. 1971.** Seismotectonics of the Kuopio region, Finland. Bulletin de la Commission Géologique de Finlande 248. 41 p. + 1 app.
- Vaasjoki, M. & Sakko, M. 1989.** The radiometric age of the Virmaila diabase dyke: evidence for 20 Ma of continental rifting in Padasjoki, southern Finland. In:

- Autio, S. (ed.) Geological Survey of Finland. Current Research 1988. Geological Survey of Finland, Special Paper 10, 43–44.
- Vaasjoki, M., Rämö, O. T. & Sakko, M. 1991.** New U-Pb ages from the Wiborg rapakivi area: constraints on the temporal evolution of the rapakivi granite-anorthosite-diabase dyke association of southeastern Finland. In: Haapala, I. & Condie, K. C. (eds.) Precambrian granitoids: petrogenesis, geochemistry and metallogeny : symposium on Precambrian granitoids, Helsinki, Finland, August 14–17, 1989. Precambrian Research 51 (1–4), 227–243.
- Waldron, J. 2004.** Extensional fault arrays in strike-slip and transtension. *Journal of Structural Geology* 27, 23–34.
- Wennerström, M., Airo, M.-L., Elminen, T., Niemelä, R., Pajunen, M., Vaarma, M. & Wasenius, P. 2008.** Orientation and properties of jointing in Helsinki area, southern Finland. In: Pajunen, M. (ed.) Tectonic evolution of the Svecofennian crust in southern Finland – a basis for characterizing bedrock technical properties. Geological Survey of Finland, Special Paper 47, 253–282.

PALEOMAGNETIC EVIDENCE FOR MESOPROTEROZOIC – PALEOZOIC REACTIVATION OF THE PALEOPROTEROZOIC CRUST IN SOUTHERN FINLAND

by

Satu Mertanen, Meri-Liisa Airo, Tuija Elminen, Reijo Niemelä,
Matti Pajunen, Pekka Wasenius and Marit Wennerström*

Mertanen, S., Airo, M.-L., Elminen, T., Niemelä, R., Pajunen, M., Wasenius, P. & Wennerström, M. 2008. Paleomagnetic evidence for Mesoproterozoic – Paleozoic reactivation of the Paleoproterozoic crust in southern Finland. *Geological Survey of Finland, Special Paper 47*, 215–252, 30 figures and 2 tables.

Paleomagnetic and rock magnetic studies have been carried out on fault and shear zones in the capital area of Finland, southern Fennoscandian Shield. Part of the study locations show markedly consistent remanence directions, and give clear evidences of multiple reactivation of the Paleoproterozoic crust, although most of the studied shear zones are weakly magnetized and give no stable paleomagnetic results. Some of the studied locations have preserved the original remanent magnetization, component A, that was acquired during cooling of the crust in the late stages of the Svecofennian orogeny at ca. 1.9–1.8 Ga. Frequent occurrence of a Subjotnian remanence, component SB₁, implies that the emplacement of the rapakivi granites and associated dykes at ca. 1.64–1.63 Ga has affected the shear zones all over the study area as new magnetic material, hematite, was precipitated from hydrothermal fluids circulating in the fault structures. The most extensive structure, the Porkkala-Mäntsälä shear zone, was remagnetized some 50 Ma later, at ca. 1.58 Ga, when due to partial oxidation of titanomagnetite to titanomaghemite component SB₂ was acquired. Alternatively, based on comparison of pole SB₂ to the Fennoscandian Phanerozoic APW path, component SB₂ was acquired during Early Silurian, at ca. 440 Ma. This interpretation lends support from the most persistent remagnetization of the studied shear zones, component C, carried also by titanomaghemite, the pole of which matches well on the Silurian – Devonian APW path and gives an age of ca. 415 Ma. It is suggested that tectonic reactivation coupled with following sedimentation after the Caledonian orogeny are mainly responsible for the Paleozoic remagnetizations. A weakly defined component B was obtained sporadically in some of the studied sites, and it is interpreted to be ca. 300–230 Ma. These are the first indications of Paleozoic remagnetizations in the Paleoproterozoic crust of the southern Finland. It is implied that the remagnetizations are especially seen in the shear zones which have been most vulnerable to later reactivation due to fluid migration. For reference, paleomagnetic studies were carried out also on Subjotnian diabase dikes in Kopparnäs and Nummela. The Kopparnäs dikes carry remanence component SB that is suggested to represent the primary, ca. 1.63 Ga magnetization of the dikes, whereas it is possible that the Nummela dyke is younger or it was remagnetized at ca. 415 Ma.

Key words (GeoRef Thesaurus, AGI): crust, shear zones, reactivation, dikes, paleomagnetism, remagnetization, thermomagnetic analysis, Paleozoic, Mesoproterozoic, Paleoproterozoic, Uusimaa, Finland

* *Geological Survey of Finland, P.O. Box 96, FI-02151 Espoo, Finland*

* *E-mail: satu.mertanen@gtk.fi*

INTRODUCTION

Paleomagnetic studies have been carried out on shear zones in southern Finland as a part of a larger investigation which aims to resolve the tectono-thermal evolution of the area. The practical geological interpretations of the research are done for the purposes of building and environmental use of rock reservoirs in urban environment (e.g. Pajunen et al. 2001, 2002 and 2008). In order to assess full knowledge of the area, several geological and geophysical methods have been adopted in the study. They are presented as separate papers within this volume. Pajunen et al. (2008) present the overall investigations of the tectono-thermal evolution of the Svecofennian crust in southern Finland, Elminen et al. (2008) have concentrated on the semi-brittle to brittle faulting structures in southern Finland, Wennerström et al. (2008) present the jointing patterns in southern Finland, and Airo et al. (2008) show geophysical investigations, mainly focusing on airborne method. Aeromagnetic maps show that the shear zones are most often weakly magnetized, which is probably due to hydrothermal alteration of magnetic minerals to silicates or other less magnetic Fe-oxides. However, in hydrothermal alteration, new magnetic minerals can also be formed either by alteration from older oxides or silicates or by precipitation and growth of new magnetic minerals accompanied by fluid flow. These phenomena have been used as a basis for paleomagnetic investigations.

In this study we have used palaeomagnetism in order to address timing of the geological processes that have acted within the shear zones. In the preliminary study (Mertanen et al. 2001) from one site

on the extensive Porkkala-Mäntsälä shear zone, it was shown that the shear zone has experienced multiple events of fluid flow and reactivation, seen as three remanent magnetization components of different age. In the present study we have continued the work by collecting samples from shear zones and faults of different styles and rock types. Paleomagnetic studies on shear zones in the Paleozoic Caledonides of Norway (Torsvik et al. 1992, Eide et al. 1997 and Andersen et al. 1999) have shown clearly the usefulness of shear zones to record late remagnetization events. In southern Finland where the basement rocks are of Paleoproterozoic age, several and more complicated processes, even as young as Mesozoic (Larson et al. 1999 and Murrell 2003), may have taken place during the long evolutionary history of the old cratonic Fennoscandian Shield area. One of the purposes of the paleomagnetic study was to estimate the ages of the events from the paleomagnetic poles.

Although the results are not conclusive at this stage, mainly due to statistically limited amount of stable data, they are interpreted in the framework of global geodynamic events. The evolution of Precambrian cratons is delineated by amalgamation of different continents by repeated collisions and the formation of supercontinents, starting from Precambrian up to present. Likewise, extension and crustal thinning due to break up of supercontinents are the phenomena that have also affected to the formation and reactivation of shear and fault zones where remagnetizations have most probably taken place.

GEOLOGICAL SETTING

Geological evolution of the Svecofennian domain in southern Finland has been intensely studied by several authors since the end of 19th century. The Svecofennian bedrock has experienced a complex and multi-stage tectono-thermal evolution. It is delineated by collisional and extensional tectonic events coupled with medium to high-grade metamorphism, intense melting and predominantly felsic intrusive pulses of different ages. Here, a brief summary is given of the evolution in the Southern Finland Granite Zone in the Helsinki area based on the studies of Pajunen et al. (2008, this volume) and on the studies referred to therein.

Svecofennian events

The evolution of the Svecofennian orogeny is related to an oblique collision of a growing Svecofennian island arc system against the Archaean continent and to subsequent continental deformation, metamorphism and crust forming magmatism at ca. 1.9–1.8 Ga. The Svecofennian orogeny was a continuous event that gets younger towards south/south-west.

The oldest rocks of the area are dated at 1.90–1.88 Ga, comprising supracrustal volcanic and sedimentary rocks that indicate varying depositional envi-

ronments. These oldest supracrustal sequences were deformed and metamorphosed during an early major collision and thrusting deformation at ca. 1.90–1.88 Ga when the supracrustal rocks were intruded by syntectonic tonalitic and granodioritic intrusive rocks. The following extensional stage at ca. 1.88–1.87 Ga is related to an island arc collapse, characterized by prograde low-pressure metamorphism and emplacement of large amounts of intermediate igneous rocks. The extension was rapidly followed by a collision due to N-S compression that deformed the supracrustal series and the early magmatic rocks into tight, often northwards overturned folds. In these geotectonic events the Svecofennian arcs were already accreted to the Archaean craton and a new coherent continental crust was formed.

The new continental crust was deformed and metamorphosed at the time of the formation of the Southern Finland Granitoid Zone at ca. 1.87–1.80 Ga, characterized by significant rotations of the stress field and vast magma production. The Porkkala-Mäntsälä shear/fault zone and wide-scale folding are the results of a N-S shortening of the crust at ca. 1.85 Ga. The later evolution of southern Finland from ca. 1.84 to 1.80 Ga, is characterized by SE-NW transpression, formation of N-trending shear zones and emplacement of late Svecofennian diabase dykes. The crust was migmatized as the amount of granitic intrusions increased. High-grade metamorphic conditions were achieved at ca. 1.82–1.81 Ga. Extensional stages were accompanied by compressional events in these stages of the southern Finland granitoid zone evolution. The Svecofennian orogeny ceased at ca. 1.80 Ga, when post-tectonic granite intrusions and pegmatites were emplaced.

Post-Svecofennian events

The post-Svecofennian deformations and magmatic events are strongly controlled by the older Svecofennian structures. After the Svecofennian orogeny about 200 Ma later, anorogenic rapakivi granites and associated dyke swarms were emplaced in southern Finland. The study area is located between the small Bodom and Obbnäs rapakivi granite plu-

tons (age ca. 1640 Ma, Vaasjoki 1977 and Kosunen 2004) and the small Onas body (1630 Ma, Laitala 1984) in the west and the massive Wiborg batholith (1615–1645 Ma, Vaasjoki et al. 1991) in the east. Diabase dykes and quartz porphyry dykes, genetically related to the rapakivi granite intrusions, occur throughout the study area. Diabase dykes and quartz porphyry dykes related to the Onas rapakivi granite pluton in Sipoo area have been studied paleomagnetically by Mertanen and Pesonen (1995).

According to contact metamorphic studies carried out on the Wiborg batholith, the rapakivi granites were emplaced in high crustal levels of about 5 km. The structures formed during the Svecofennian orogeny control the emplacement of the granites. It has been interpreted that the emplacement of the Bodom and Obbnäs rapakivi granites took place within the Porkkala-Mäntsälä shear zone that had its origins during the Svecofennian tectonic regime. Later on, this shear zone was repeatedly reactivated (Elminen et al. 2003).

Subsequently, the western and southwestern Fennoscandian Shield was affected by two orogenic events, the Sveconorwegian orogeny at ca. 1 000 Ma and the Caledonian orogeny at ca. 350–450 Ma ago. Their significance on the geological evolution of Finland is under geological study as will be discussed here in the light of the results, presented in section 'Discussion'.

The bedrock of southern Finland, including the study area, is divided into different tectonic terranes that are separated by shear and fault zones. The zones of weakness represent both old ductile deformation structures as well as brittle fractures. Based on structural studies (e.g. Pajunen et al. 2002 and 2008) it is generally implied that the zones of weakness were originally formed during Svecofennian orogenic events, although they have been reactivated in several younger tectonic events. For instance, the rapakivi granites show evidences of younger cross-cutting shearing. Likewise, the Porkkala-Mäntsälä shear zone is transected by later brittle faults. The orientations of zones of weakness vary at different outcrops, but in general, NE-SW and NW-SE joint sets show more regional than local strain (Wennerström et al. 2008).

SAMPLING

Samples for paleomagnetic studies were taken from 17 shear zones (Fig. 1). The studied sites were chosen according to their mineralogy, location and strike of the shear structure. In addition to shear zones, samples were also taken from seven mafic

dikes and from one acidic dike in order to get reference data for the shear zones. Examples of studied rock types are shown in Figure 2. Three of the mafic dikes, in Kopparnäs and in Nummela, were regarded as Subjotnian (ca. 1.65–1.54 Ga), based on the

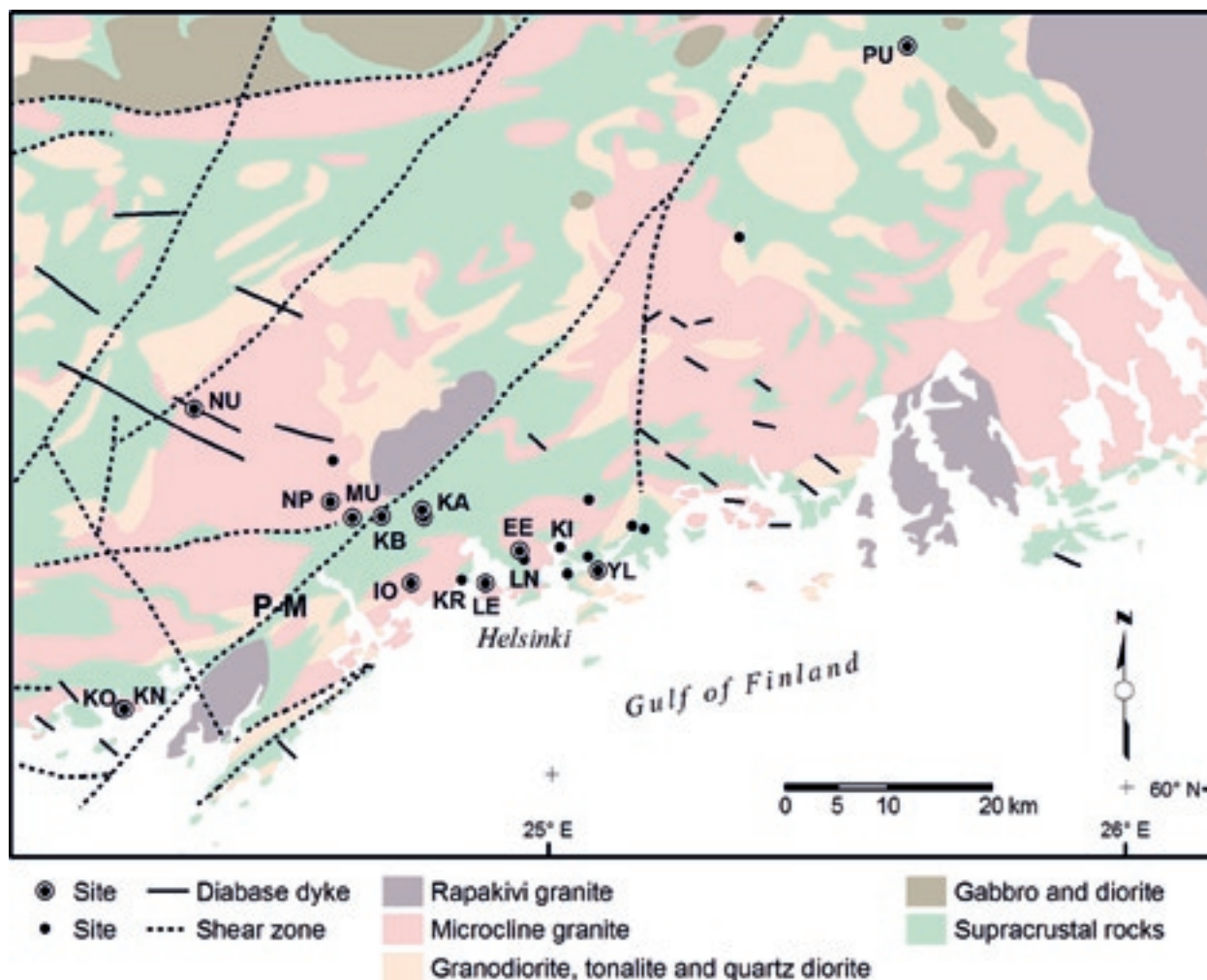


Figure 1. Generalized geological map of the study area where the studied sites are shown as circles. The labelled circles with surrounding rings identify sites that give stable paleomagnetic results. The labelled circles without rings are sites with some indications of stable results.

typical NW-SE strike and fresh mode of occurrence. Previously, Mertanen and Pesonen (1995) studied Subjotnian diabase and quartz porphyry dikes in Siipoo, some ten kilometers east of the present study area. The Subjotnian dikes studied now were taken much further in the west so that most of the shear zones are located between these two dike sets. Four other sampled mafic dikes are clearly altered and deformed and thus are probably of Svecofennian age. The number of samples taken from each site is

limited (approximately 3–5 samples), and therefore, the results presented here are regarded as preliminary.

Samples were either drilled in the field as 2.5 cm diameter cores or taken as oriented blocks and drilled in the laboratory. Orientation in the field was done by using sun compass and/or magnetic compass. Approximately 2–6 specimens of the length of 2.2 cm were cut from each sample or core in the laboratory.

METHODS

Petrophysical properties, ie density and magnetic susceptibility, were measured for each specimen before the palaeomagnetic measurements were made. Intensity of remanence (NRM) was measured from those samples that were also demagnetized and studied paleomagnetically. All remanence measurements were done on a 2G-Enterprises SQUID mag-

netometer. Demagnetization was done mainly by alternating field (AF) up to peak field of 160 mT. Some of the samples that did not show decay of remanence intensity were further thermally demagnetized. Thermal demagnetization up to 680° was also carried out on some of the fresh specimens. Between each demagnetization step, the samples were stored



Figure 2. (a.) Protomylonitic gneiss from site PU. (b.) Reddish gneiss from site PU. (c.) Breccia from site EE. (d.) Mylonitic rock from site LE. (e.) Mylonitized intermediate volcanic rock from site YL. (f.) Mylonitic tonalitic gneiss from site KA. (g.) Pegmatite-granite dike from site KB.



Figure 2. (h.) Calcite-hematite vein from site IO. (i.) Granite with hematite veins from site NP. (j.) Diabase dike from site KO. (k.) Diabase dike from site NU. Photos (a.), (b.), (c.), (d.), (f.), (g.), (h) and (i.) by S. Mertanen, Photo (e.) by T. Elminen and Photos (j.) and (k.) by M. Pajunen.

in a μ -metal shield to avoid acquisition of VRM between heating and subsequent thermal demagnetization. Remanence components were obtained using principal component analysis (Kirschvink 1980) and they were visually inspected in Zijderveld diagrams (Zijderveld 1967 and Leino 1991).

Magnetic carriers were identified by thermomagnetic analysis using an Agico CS2-KLY2 Kappabridge, applying stepwise heating up to 700°C. The acquisition of isothermal remanent magnetization (IRM) was studied in four selected specimens that showed stable remanence directions. The specimens were first stepwise demagnetized in alternating fields up to 160 mT. They were then progressively pulse magnetized in a Molspin pulse magne-

tizer in fifteen steps between 25 and 1500 mT to produce IRM. The IRM intensity was measured on the SQUID magnetometer. Minerals in four selected specimens were determined with electron microprobe by using a Cameca Camebax SX50 instrument at the Geological Survey of Finland. One or two polished thin sections were studied from each site.

AMS measurements were carried out on most specimens that showed stable magnetization directions. Measurements were done both on fresh specimens and on the sister specimens that were previously demagnetized with alternating field. No difference in AMS directions was observed between the two procedures (see Puranen et al. 1992).

PALEOMAGNETIC RESULTS

Paleomagnetic results are shown in Figure 3 and in Tables 1 and 2. Altogether five remanence components were isolated in nine shear zones, and in addition, three of the studied dikes carry a sixth remanence component. In general, the studied shear zones are weakly magnetized, and many of the study locations do not carry a stable remanent magnetization. However, in most cases the intensities were high enough above the noise level (0.03 mA/m) of the SQUID magnetometer. The coercivities are typically high. Those samples, where AF demagnetization up to a peak field of 160 mT did not result to decay of intensity, were then thermally demagne-

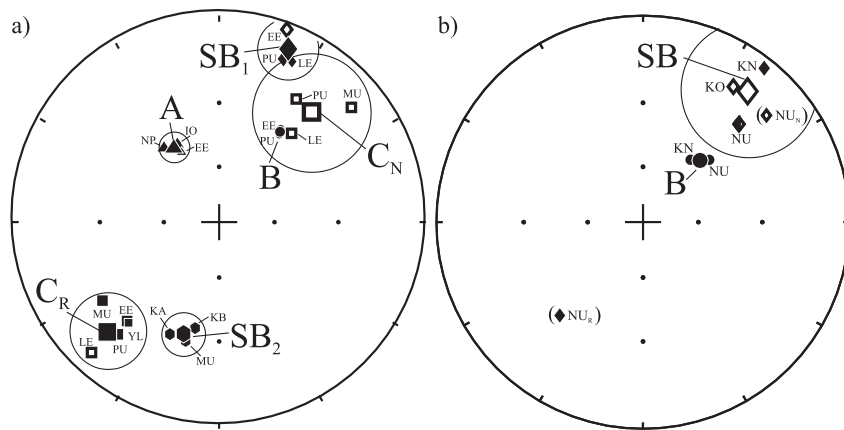
tized resulting to the drop of intensity. During thermal demagnetization the samples in many cases are either unstable or magneto-mineralogical changes take place during heating, indicating the formation of new magnetic phases. Typically, mineralogical alteration was observed at a temperature of ca. 350–500°C by monitoring the susceptibility during thermal demagnetization. Thus, thermal demagnetization was an unuseable method in many cases to distinguish the remanence direction carried by hematite. In the following, paleomagnetic results from different sites are discussed separately.

Table 1. Palaeomagnetic results from the shear zones in Helsinki-Espoo area (Glat = 60.2°N, Glong = 24.9°E).

Component/ Site	B/N/n	Dec (°)	Inc (°)	α_{95} (°)	k	Plat (°N)	Plong (°E)	dp (°)	dm (°)	A95
<i>Component A</i>										
EE	*2/3	331.9	47.8	-	-	53.4	248.7	-	-	-
IO	*2/3	332.1	43.5	-	-	50.3	246.2	-	-	-
NP	*3/5	323.6	41.7	25.6	24.2	46.0	255.8	19.2	31.4	-
<i>Mean</i>	*3/7/11	329.1	44.4	7.2	297.1	50.0	250.4	5.7	9.1	7.6
										K = 268
<i>Component B</i>										
EE	*3/4	33.4	33.2	35.3	13.3	42.3	158.3	22.8	40.1	31.3
PU	*8/19	34.6	35.7	11.9	22.8	43.4	159.0	8.0	13.8	11.4
<i>Mean</i>	*2/11/23	34.0	34.5	-	-	42.8	158.6	-	-	-
						-42.8	338.6			
<i>Component C</i>										
EE	*5/6	222.8	23.6	28.8	8.0	9.8	162.5	16.4	30.7	24.4
YL	*2/4	222.1	23.5	-	-	10.1	163.4	-	-	-
(LE (R))	*3/6	224.4	-7.1	26.2	23.2	24.1	155.0	13.2	26.3	19.9
(LE (N))	*3/4	39.2	-32.3	11.2	108.2	6.1	167.6	7.6	13.4	10.0
LE (C)	*6/10	222.0	12.8	21.1	11.0	15.6	161.3	11.0	21.5	12.7
(PU (R))	*7/15	222.1	17.6	13.7	20.3	12.5	162.8	7.4	14.2	11.0
(PU (N))	*2/3	32.0	-19.9	-	-	14.7	173.0	-	-	-
PU (C)	*8/18	219.5	16.6	12.1	22.0	14.2	165.1	6.4	12.5	8.9
(MU (R))	*2/4	236.2	21.5	-	-	5.9	149.5	-	-	-
(MU (N))	*3/6	49.1	-9.6	29.6	18.5	14.6	153.5	15.1	29.9	-
MU (C)	*4/10	233.3	17.5	27.4	12.0	8.2	151.5	14.7	28.4	18.0
<i>Mean</i>	*5/25/48	224.0	18.9	6.6	137.0	11.6	160.7	3.6	6.8	5.8
						-11.6	340.7			
										K = 174
<i>Component SB₁</i>										
EE	*10/24	19.6	-0.5	6.5	57.0	27.6	182.6	3.2	6.5	5.4
LE	*3/3	24.4	9.1	16.0	60.4	31.4	176.1	8.2	16.1	15.8
PU	*6/6	21.5	9.4	11.3	35.9	31.8	180.1	5.8	11.5	9.4
<i>Mean</i>	*3/19/33	21.8	6.0	9.3	175.3	30.3	179.6	4.7	9.4	5.6
										K = 489
<i>Component SB₂</i>										
KA	*6/18	203.7	28.8	9.3	52.8	12.0	181.6	5.6	10.2	9.1
KB	*6/13	192.8	34.6	8.5	63.7	9.9	192.4	5.6	9.7	7.9
(MU (N))	1/*3	23.0	-27.1	-	-	13.2	181.7	-	-	-
(MU (R))	1/*3	188.4	29.0	-	-	14.0	196.2	-	-	-
MU (C)	1/*3	195.8	28.2	-	-	13.7	188.9	-	-	-
<i>Mean</i>	*3/13/34	197.5	30.6	9.1	182.9	11.9	187.6	5.7	10.2	8.7
						-11.9	7.6			
										K = 201

Note. B/N/n, number of sites/samples/specimens used for mean calculations, (N), (R) and (C) denote normal, reversed and combined polarity, * denotes the statistical level used for mean calculation. D and I are the mean declination and inclination respectively; α_{95} is the radius of the circle of 95% confidence; k is the Fisher's (1953) precision parameter; Plat and Plong are the paleolatitude and paleolongitude for the Virtual Geomagnetic Poles; inverted poles (Plat, Plong) are shown in italic; dp and dm are the semi-axes of the oval of 95% confidence; A95 is the radius of the circle of 95% confidence of the mean pole, K is the Fisher's precision parameter of the mean pole.

Figure 3. Site mean paleomagnetic directions for (a.) the shear zones and (b.) the dikes. Components A, B, C (with normal and reversed polarities), SB₁ and SB₂ were isolated in the shear zones, and components B and SB in the dikes. Small symbols display the site mean directions and large symbols the overall mean direction of a remanence component. Circles indicate cones of $\alpha 95$ confidence about the means.



Sites with stable remanent magnetization

Pukkila (site PU)

At site PU in Pukkila, the intensely folded and migmatitic mica gneiss was deformed in shearing and faulting events that indicate varying deformation conditions. The early deformation was already retrogressive with respect to the higher-grade regional metamorphic assemblages characterizing the terrane. The gneiss is cut by coarse-grained pegmatitic granite dykes. In the latest phase of the Svecofennian compressional event, EW-trending protomylonitic structures were formed. The structures of the area are overprinted by semi-ductile to brittle deformations that have fragmented the bedrock in a very complex pattern. These late faulting structures show intense retrogressive alteration by chloritization, epidotization and hematitization. On the outcrop the late movements exhibit as narrow reddish hematitic and greenish epidotic faults and fractures (Fig. 2a) that parallel the EW-trending protomylonitic foliation.

Samples for paleomagnetic studies were taken from different rock types: fourteen samples came from the protomylonitic gneiss at the base of the Porvoo river, seven samples from a reddish gneiss that contains red hematite veins (Fig. 2b), and two samples from a grey gneiss.

Seven samples from the protomylonitic gneiss show consistent results. The characteristic remanent magnetization has a SW-pointing low-inclination direction that was named as component C_R. It was isolated only in the protomylonitic gneiss, and not in other gneisses. In AF demagnetization, the C_R component was isolated in low coercivities, even below 10 mT (Fig. 4). Thermal demagnetization was in most cases not successful in isolating the C_R component, because of magneto-mineralogical alterations during heating. However, in some samples the susceptibility was not increased and the C_R component was isolated in a temperature range of 320–520°C. Specimen PU2–1B (Fig. 5) is an example of thermal demagnetization which shows a slight increase of intensity at 320°C probably indicating

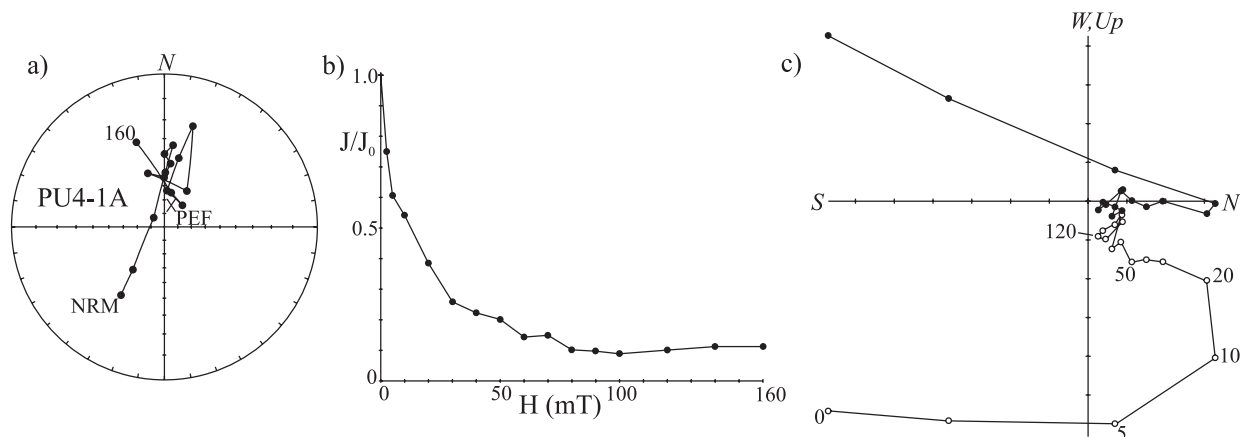


Figure 4. Example of AF demagnetization behaviour of a protomylonitic gneiss sample from site PU that carries a low coercivity component C_R. (a.) stereographic projection where closed (open) symbols indicate downward (upward) pointing remanence directions, (b.) relative NRM intensity decay curve upon AF demagnetization, (c.) orthogonal vector projections where closed (open) circles denote projections onto horizontal (vertical) planes. Numbers at demagnetization steps denote peak alternating field (mT). The Present Earth's magnetic Field (PEF) at the sampling locality is shown as a cross.

that some alteration has taken place. As will be shown later, inversion of titanomaghemite to titanomagnetite or alteration of iron sulphides to magnetite during heating may be explanations to the increase of magnetization.

After isolation of the low coercivity SW directed C_R component, the remanence direction then typically swings to the opposite NE direction, to component C_N . Due to high coercivity that does not decay during AF demagnetization or due to unstable behaviour, in many cases the C_N component is not properly isolated. However, in two thermally demagnetized protomylonitic gneiss samples, a consistent C_N component was isolated in a temperature range of 320–560°C (Specimen PU18-1C, Fig. 5) suggesting that the remanence may reside both in titanomagnetite and/or titanomaghemite. In these samples the susceptibility does not increase upon heating during thermal demagnetization, until at 570° C.

In addition to the dual-polarity C component, a remanence direction with a NE declination and a shallow downward or upward directed inclination was isolated in six samples, ie in five protomylonitic gneiss samples and in one reddish gneiss. This component is called component SB_1 . Separation of components C_N and SB_1 is not always straightforward because despite the much shallower inclination of component SB_1 , the declinations are about the same. Component SB_1 was isolated by AF demagnetization in the coercivity range of 20–70 mT. In the protomylonitic gneiss, thermal demagnetization could not isolate this low inclination direction. Figure 6 is an example of a specimen from the reddish gneiss that was thermally demagnetized after AF cleaning. Unblocking temperatures up to 680°C suggest hematite is the main remanence carrier.

Six samples from the protomylonitic gneiss and two from the reddish gneiss display a third component, called component B. It has a NE declination

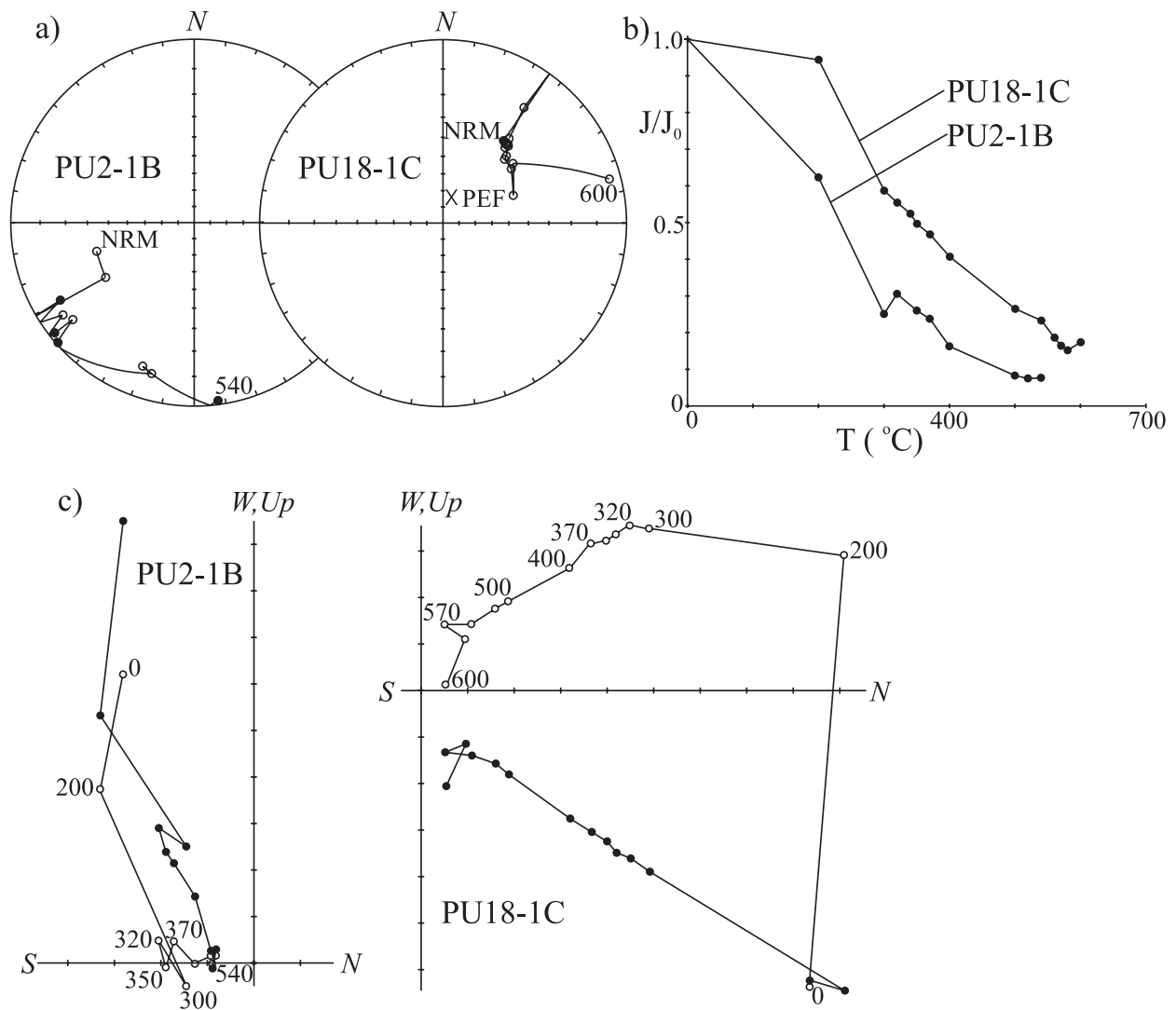


Figure 5. Thermal demagnetization behaviour of two protomylonitic gneiss samples from site PU. Specimen PU2-1B displays a reversed polarity C_R component, and specimen PU18-1C a normal polarity C_N component. In both specimens the C component is isolated in a temperature range of ca. 320–540°C. Numbers at demagnetization steps denote temperatures. For other notes, see Figure 4.

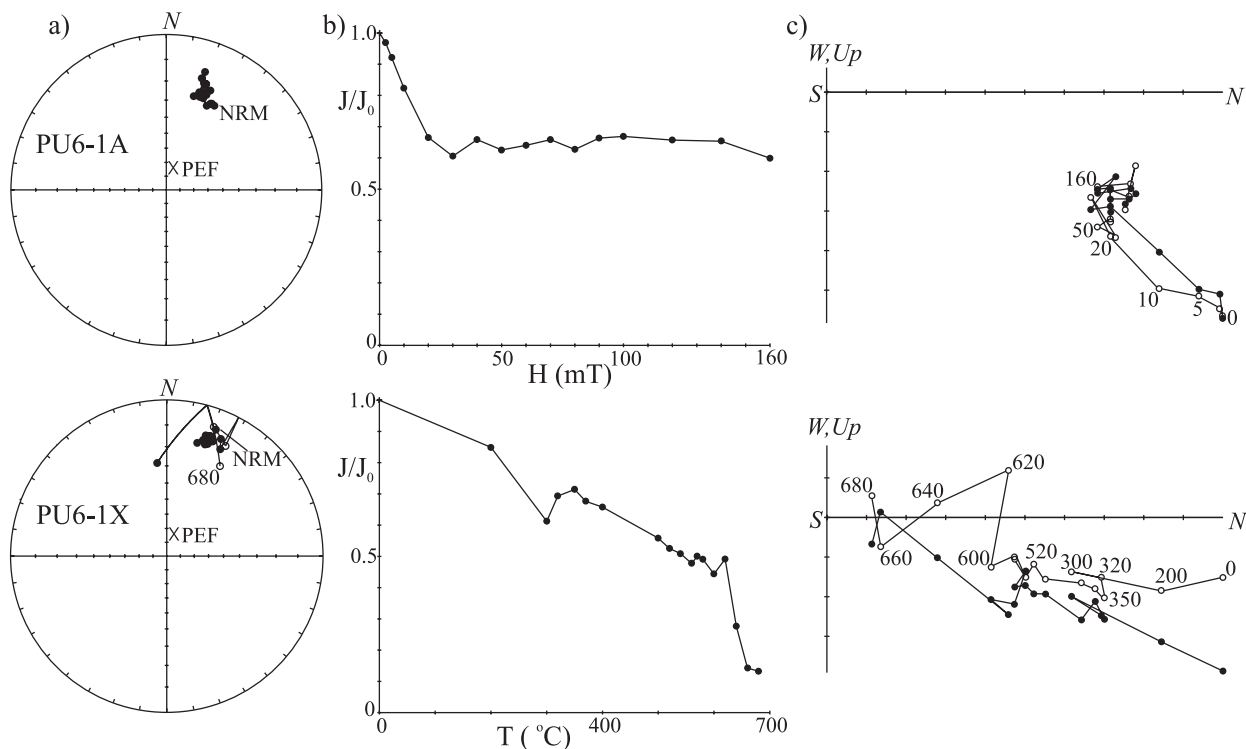


Figure 6. Example of a reddish gneiss sample at site PU that carries component SB₁. After AF treatment to 40 mT, the magnetization did not show decay of intensity. Subsequent thermal demagnetization indicates a maximum unblocking temperature of 680°C; thus the stable magnetization resides in hematite.

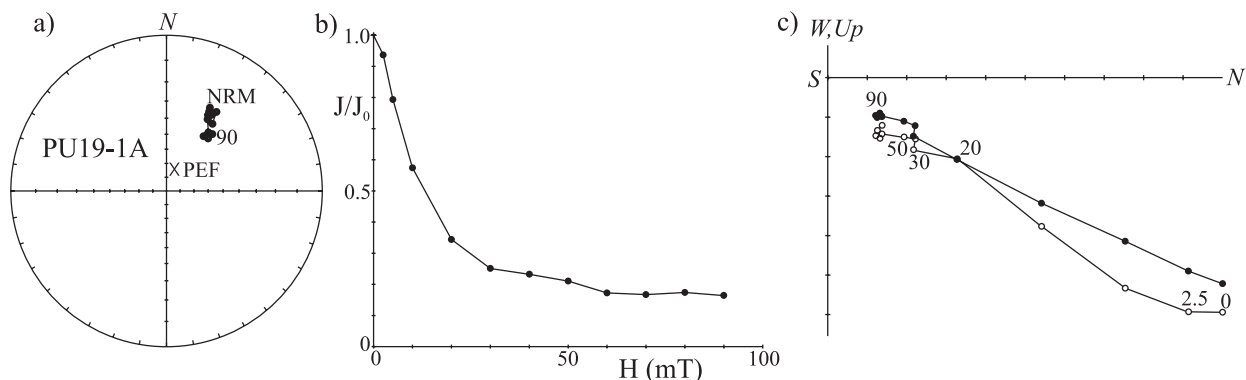


Figure 7. Specimen PU19-1A from the protomylonitic gneiss carries component B that was isolated in a coercivity range of 0–90 mA/m. For explanations, see Figure 4.

and moderately positive inclination. The inclination is higher than that of component SB. Component B was isolated by AF demagnetization in intermediate coercivities (Fig. 7) and by thermal demagnetization below 400°C.

Samples from the grey gneiss did not yield stable results, although their NRM direction is close to the SB/B direction, which is seen as a trend from a steep down PEF direction towards a lower inclination NE direction.

Eläintarha (site EE)

Site EE (Fig. 1) in Helsinki consists of medium-grained granitoid that is composed of two phases:

an intrusive foliated tonalite-granodiorite and a later migmatizing granite phase 'ghosting' the earlier structure of the granitoid. The studied outcrop is situated in a Svecofennian tectonic dome-and-basin structure where supracrustal associations surround the granitoid dome. The early, locally protomylonitic, steep, EW-trending foliation was cut by late-Svecofennian NE-trending shearing, which was later reactivated in a brittle event. The brittle deformation zone is characterized by an intensely altered, rather homogeneous, deeply reddish albite-epidote-hematite breccia with hematite as a main mineral constituent (Fig. 2c). The breccia cuts the host protomylonitic granitoid so that the granitoid is non-identifiable in the intense central part of the fault.

The brittle deformation is well indicated by narrow hematite-rich, still cohesive microbreccia zones. In the vicinity of the outcrop there are brittle structures like ones that cut the 1.65 Ga (Vaasjoki 1977) rapakivi granites.

Twelve samples were taken from the breccia and five samples from the host granitoid. Petrophysical properties of the breccia and granitoid are fairly similar, remanence intensities ranging within 0.7–39 mA/m and susceptibilities within 16–450 $\times 10^{-6}$ SI.

A characteristic remanence direction was established in nine breccia samples and in one granitoid sample. The remanence has a shallow NE pointing inclination corresponding to component SB_1 at site PU. Component SB_1 has high coercivity, which is shown also as decay to the origin in some samples where the remanence could be cleaned by AF method (Fig. 8). In such samples no underlying components seem to exist. However, typically, the remanence of the breccia and the granitoid is incompletely demagnetized by AF method. The magnetization is evidently carried by a hard coercivity hematite. Three samples carry a steeper NE directed declination with positive inclination, corresponding to component B in Pukkila. Typically B was isolated in higher coercivities than component SB_1 .

The SB_1 and B directions and the magnetization behaviour of breccias display a rather similar pattern, as was observed in a previous study on quartz porphyry dikes in Sipoo (Mertanen & Pesonen 1995). Upon AF demagnetization, the NRM is moving from a steeply down PEF direction to a shallow downward or upward NE direction, SB_1 and from there to component B. Component B is not always confidently isolated, although it may exist together with SB_1 , shown as off-origin Zijderveld trajectories which may imply the presence also of a high coercivity component.

In addition to component SB_1 , five breccia samples carry a similar SW pointing intermediate to shallow inclination component C_R that was isolated at site PU. Here also, the C_R component is isolated in very low coercivities (Fig. 9). Only one sample shows exceptionally high coercivity. As at site PU, component C_R was not isolated in the granitoid. At site EE, no opposite polarity component C_N was observed. In addition to component C_R , specimen EE4-1A (Fig. 9) may also carry component A. The high coercivity component goes slightly off the origin, indicating that an underlying component may be present.

Thermal demagnetization typically resulted in the formation of a new magnetic mineral, probably magnetite, in temperatures of ca. 400–500°C, but even as low as 320°C in some specimens, which prevented the observation of hematite. In specimen EE1-1B (Fig. 10) the susceptibility does not show a considerable increase during demagnetization. The intensity of remanence dropped prior to 350°C and to 680°C. The remanence components isolated are a small SB_1 which is obtained in a T_{UB} range of 500–570°C, and component B, isolated close to 680°C. Hence, in this specimen the B component is probably carried by hematite and SB_1 by magnetite. The main magnetic mineral at site EE is hematite although, due to the inability of the AF method to demagnetize and to magneto-mineralogical changes during thermal treatment, it is unlikely that the remanence components residing in hematite were isolated completely. Separation of components according to their magnetic carriers is difficult, because both the SB_1 and B components seem to reside in hematite, although in some specimens (Ti-)magnetite and titanomaghemite are also the remanence carriers. Typically, the breccia contains only small amounts of magnetite which is probably the main carrier of the PEF component.

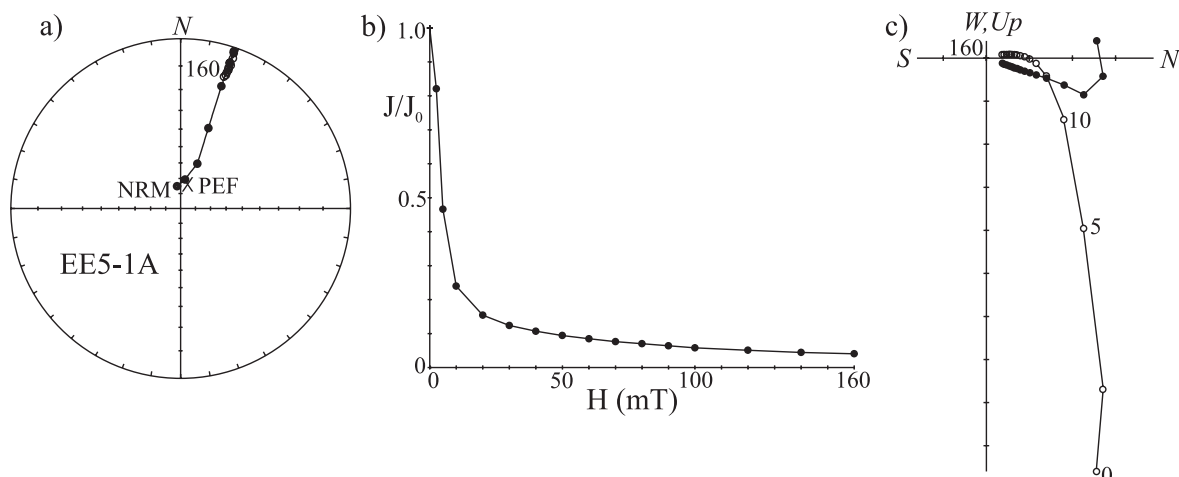


Figure 8. Example of the AF demagnetization of breccia from site EE. After removal of a large PEF component, a hard coercivity component SB_1 is revealed. For explanations, see Figure 4.

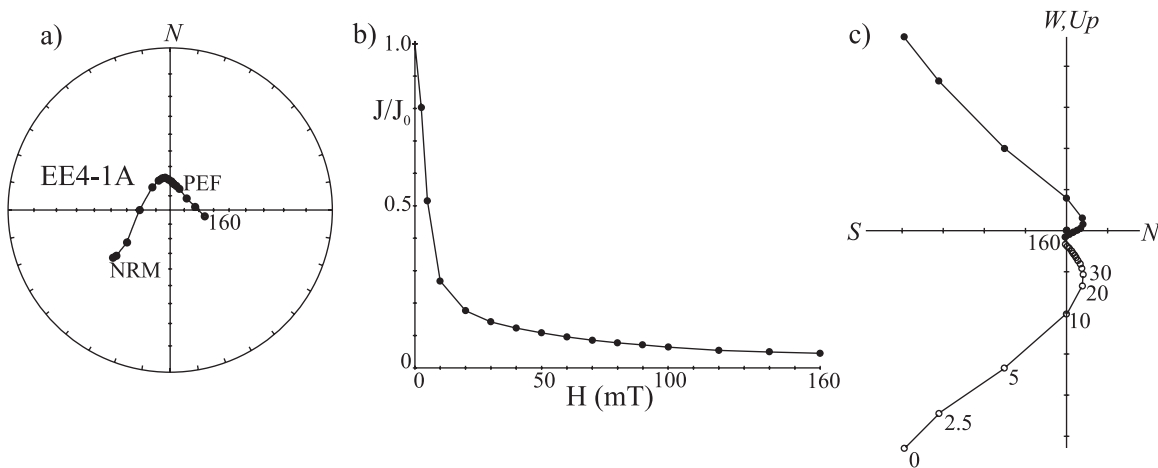


Figure 9. Specimen EE4-1A from the breccia at site EE carries a similar low coercivity C_R component that was characteristic also for the protomylonitic gneiss at site PU. Component A is isolated in higher coercivities of 30–100 mA/m. For explanations, see Figure 4.

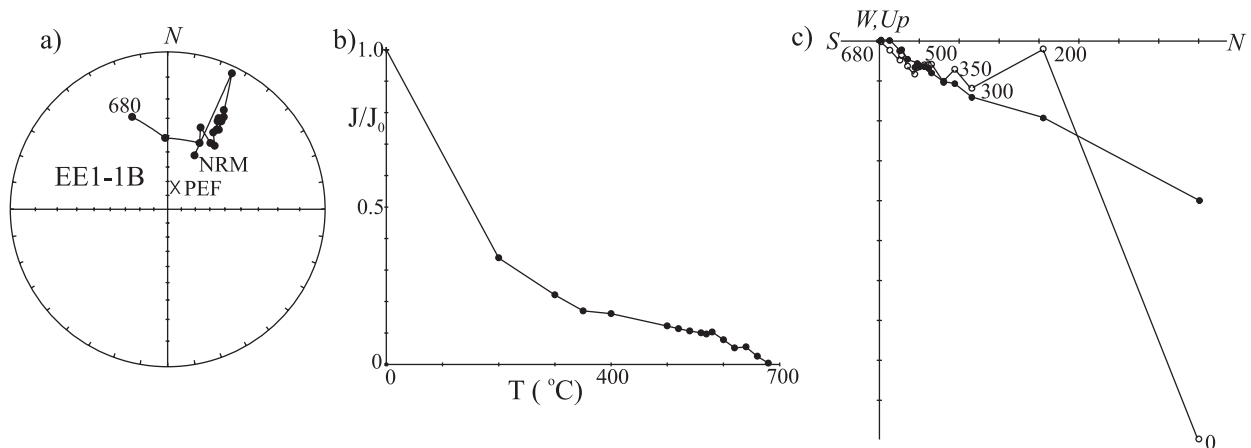


Figure 10. Thermal demagnetization of a breccia sample that carries a small SB_1 component (in 500–570°C) and a larger component B (in 600–680°C). For explanations, see Figure 5.

The breccias and granitoids differ from each other in that the remanence of the granitoid is more unstable than the remanence of the breccia. Five samples were taken from the granitoid. Component SB_1 was isolated properly only in one sample. In other granitoid samples a similar remanence direction is evident, but it cannot be reliably isolated. In addition to SB_1 component, the host granitoid carries also component A. Hence, the granitoid yields indications of three components, PEF, SB_1 and A. Component B was not isolated.

Scatter of remanence directions between specimens for component SB_1 is high, especially the declination that ranges between ca. 10–50° (Table 1). At site EE all the shallow inclination NE pointing remanence directions have been calculated together to give a common mean direction. Because component SB_1 is the characteristic remanence of the breccia, it may be related to its formation. On the other hand, since the same SB_1 component was isolated also in the granitoid (although only in one sample), it is

suggested that the remanence may represent a more pervasive remagnetization, but still, most probably concentrated in zones of crustal weakness. It is probable that the host granitoid was also remagnetized due to fluid activity.

Lemissaari (site LE)

At site LE (Fig. 1) the lithological environment is quite similar as at site EE. The main rock type in the area is a medium-grained granitoid, that generally includes amphibolitic enclaves that are from either a gabbroic intrusive or dyke of local origin. The studied outcrop represents an unaltered, foliated medium-grained gabbro with a weakly retrograde mineral assemblage. The rock is cut by a ductile, sharply-bordered ultramylonitic to protomylonitic fault (Fig. 2d) that exhibits weak retrograde mineral formation of new biotite and pale amphibole, although the older amphibole generation is still preserved as porphyroclasts. Its conspicuous tectonic

flow structure in the NE-SW direction indicates sinistral, east-side up movement. Outside the main fault, only narrow fault seams exist. Nine samples were taken from a mylonitic rock, and five samples from the gabbro.

The magnetization values are lower in the mylonitic rocks and in gabbro samples taken within one meter of the mylonite zone (intensity of remanence 0.3–8.1 mA/m and susceptibility $235\text{--}810 \times 10^{-6}$ SI), than in the gabbro samples taken more than 10 meters away from the mylonite zone (intensity of remanence 6.4–23.5 mA/m and susceptibility $923\text{--}1\,265 \times 10^{-6}$ SI), indicating reactivation and hydrothermal alteration in the mylonitic rock and its vicinity.

Consistent paleomagnetic results were obtained from six samples of the mylonitic rocks, however the rest of the mylonitic samples and the host gabbro did not give stable results. Site LE displays a rather similar behaviour as sites PU and EE. At all sites the mylonitic rocks (breccia at site EE) carry the C component (at sites PU and LE both normal and reversed), and the SB1 component, while the host rocks are magnetically more complex and typically do not yield stable remanence directions.

In a typical case for a mylonitic rock, the direction moves from a steep down PEF component to a shallow inclination C_R component that is isolated in AF fields of 20–40 mT (Fig. 11) in one sample and in 30–160 mT in two samples. At site LE, the coercivity is thus higher than at sites PU and EE. Intensity of remanence does not decay much after 30 mT, seen also as off-origin trajectory, obviously indicating the existence of a remanence carrier with harder coercivity. Component C_R could not be isolated by thermal demagnetization due to mineralogical changes during heating.

An opposite polarity C_N component was isolated by AF demagnetization in two mylonitic samples in the coercivity range of 40–160 mT. In one speci-

men, demagnetized thermally, the C_N component was isolated in the temperature range of 400–520°C (Fig. 12). The direction has an intermediate negative inclination, which, however, being much steeper, deviates from the low inclination C_R component. Therefore, its origin and its correspondence to the C_R component is subject to controversy. However, the similarity of the direction with the sporadically occurring C_N direction in the protomylonitic gneiss of site PU (two samples) is significant.

In two samples, a NE pointing low inclination component was also isolated. The direction corresponds to component SB_1 isolated at sites PU and EE. It was isolated by AF demagnetization in the coercivity range of 30–60 mT, thus, in a lower coercivity range than the C component. In the thermally demagnetized specimen LE14–1B (Fig. 12), where the C_N component was isolated in higher temperatures of 400–520°C (see above), component SB_1 was isolated at lower temperatures of 200–400°C.

In the host gabbro samples, the direction of remanence is typically close to the PEF direction. Otherwise the host samples behave in about the same manner as the mylonitic rocks. They are magnetically soft and the direction is rather unstable. Intensity of remanence does not decay after 50 mT. Sample LE8 (Fig. 13) is taken close to the mylonitic rock from the host gabbro where the rock is visibly fractured. In this sample, a small C_R component may exist in a narrow temperature range of 330–350°C after which the direction moves to the opposite direction. The remanence direction, isolated in the temperature range of 370–560°C is close to the Svecofennian A direction. However, although giving some indications of similar remanence directions as the mylonitic rocks, as well as some indications of a possibly existing primary Svecofennian direction, the result is obtained only in one sample and is not used in mean calculations.

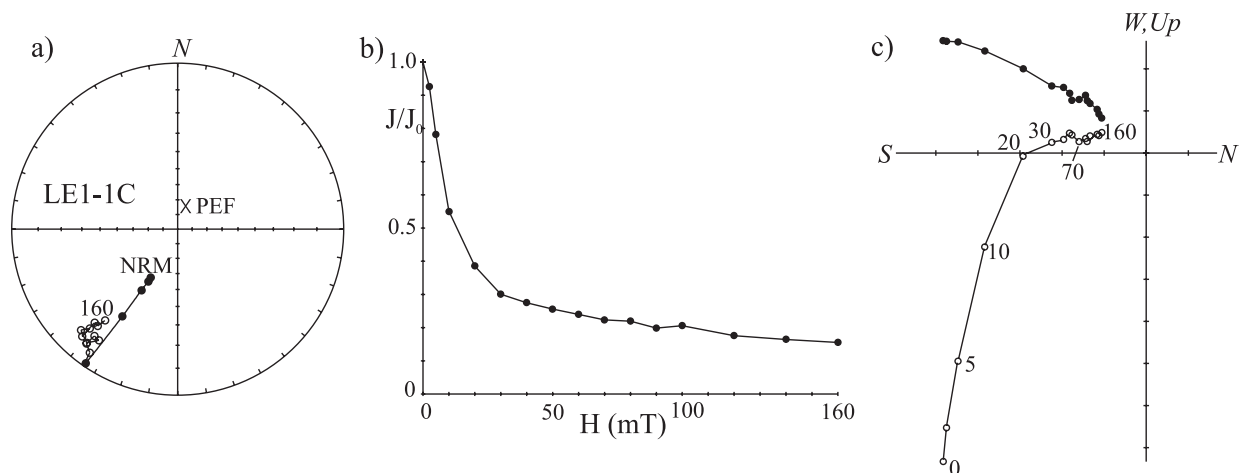


Figure 11. A mylonitic rock sample from site LE displays a corresponding C_R component that was isolated at sites PU and EE. AF demagnetization does not clean the remanent magnetization completely. For explanations, see Figure 4.

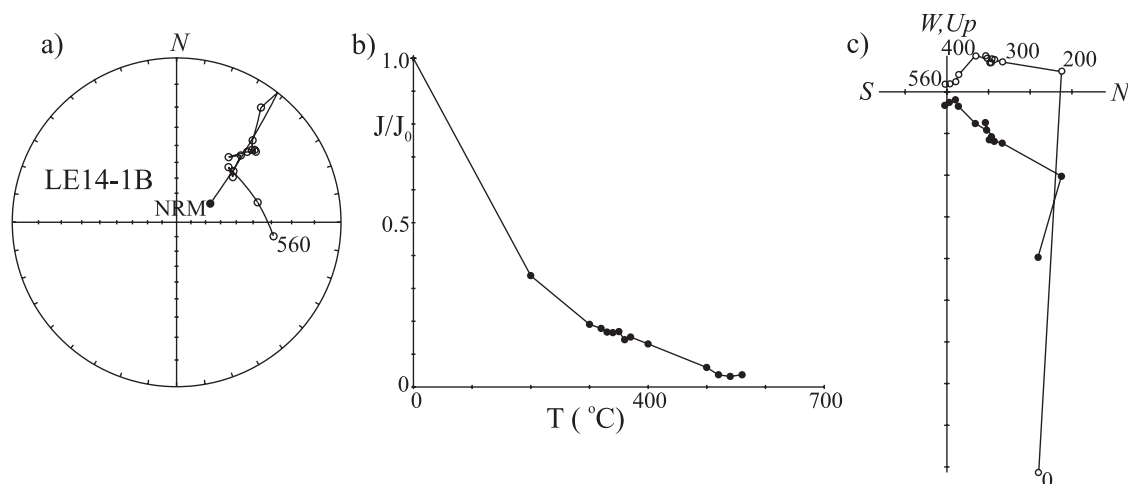


Figure 12. Specimen LE14-1B from the mylonitic rock at site LE carries two remanence components, component SB_1 that was isolated in a temperature range of 200–400°C, and component C_N , obtained in higher temperatures of 400–520°C. For explanations, see Figure 4.

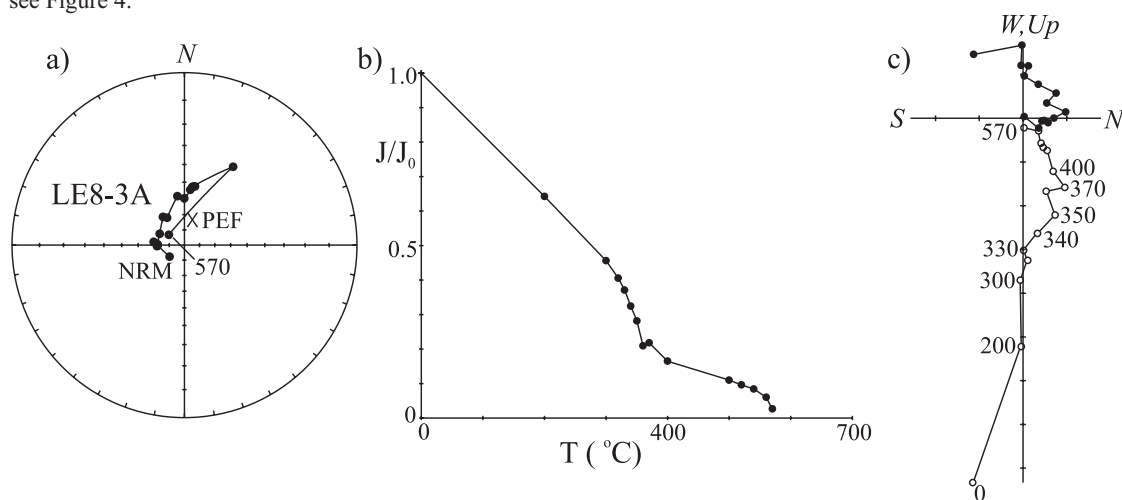


Figure 13. Specimen LE8-3A is taken from the fractured host gabbro at site LE. A possible small C_R component is isolated in a temperature range of 330–350°C and A component in a temperature range of 370–560°C. For explanations, see Figure 5.

Yliskylä (site YL)

Site YL (Fig. 1) represents the so-called 'Vuosaari triangle' that is composed of the best-preserved volcanic associations in the area. Primary features like pillow lava, primary bedding and porphyric structures are often identifiable. Mostly, however, the rocks are isoclinically folded, intensely foliated and stretched. The studied intermediate volcanic rock is near the western border zone of the tectonic 'triangle'. It shows relics of porphyric microstructure, but mostly it has suffered intense dynamic deformation. The deformation is accompanied by a comprehensive epidotic alteration that demonstrates a retrograde stage during faulting (Fig. 2e). The ductile to semi-ductile mylonitic structures indicate dextral reverse faulting in ca. E-W direction. These rather steep faults often branch off into narrow fault seams with varying directions. The youngest component of movement produced narrow prehnite-bearing fracture and breccia zones.

For this paleomagnetic study, five samples were taken from an intermediate volcanic rock, which is mylonitized and partly strongly epidotized. Generally, the remanence directions are scattered. However, in two samples the directions are similar. The remanence direction is close to the C_R component of sites PU, EE and LE. The coercivity of remanence is typically so hard that AF demagnetization cannot isolate the component. In one sample (two specimens), the C_R direction was obtained in 0–70 mT, and in the second sample (one specimen), it was obtained in 90–120 mT although the direction is quite scattered. Specimen YL4-1C (Fig. 14) was thermally demagnetized and in its susceptibility stays constant during the demagnetization procedure, indicating that no mineralogical changes took place during heating. Thermal demagnetization shows a small decay at ca. 350°C and a profound decay at 570°C, suggesting that the remanence possibly resides both in magnetite and Ti-maghemite. The intensity is quite hard and the remanence direction is compara-

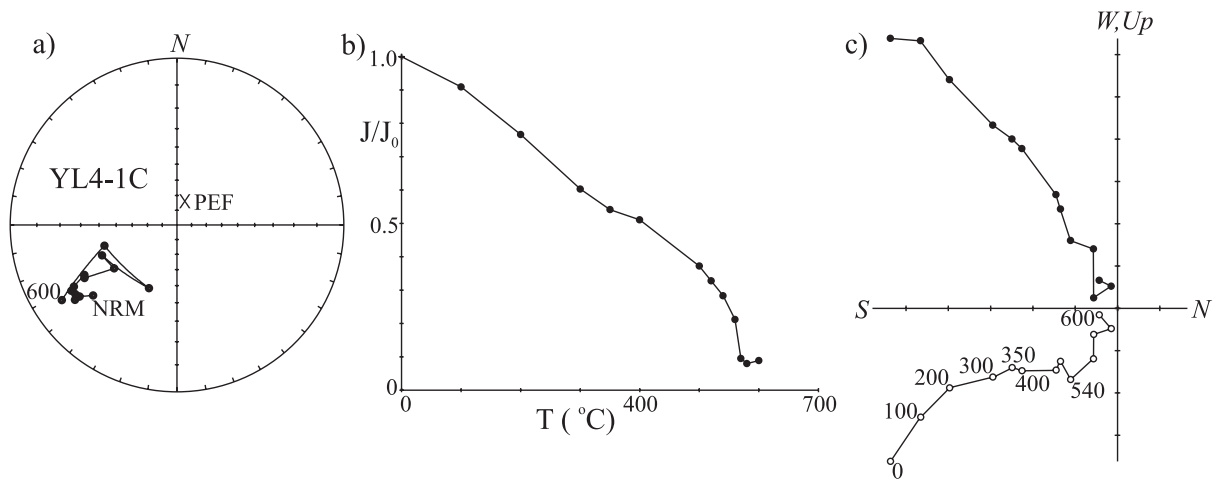


Figure 14. Thermal demagnetization of a mylonitic rock specimen from site YL. The remanence direction corresponds to component C_r of sites PU, EE and LE. For explanations, see Figure 5.

tively stable and similar to the direction obtained by AF demagnetization.

Porkkala-Mäntsälä shear zone

The Porkkala-Mäntsälä shear zone is about 100 km long and about one kilometer wide. It shows hydrothermal alteration and structures from blastomylonites to fault breccias. Three sites located within or close to the Porkkala-Mäntsälä shear zone were studied paleomagnetically. Site MU in Muurala was studied in the preliminary investigation (Mertanen et al. 2001) where the ability of shear zones of southern Finland to carry geologically meaningful remanent magnetizations was first tested. Site KA is represented by both strongly sheared rocks and by less altered rocks, mainly tonalites. The rock types at site KB comprise mylonitic gneissic tonalite and a cross-cutting pegmatite-granite dike.

Karakallio I (site KA)

Site KA is situated in an E-W-trending Svecofennian high-strain zone that was translated to its present location in a ductile transpressional tectonic bend and slide along the Porkkala-Mäntsälä shear zone during the latest phase of the Svecofennian orogeny. The mylonitic gneissic roots of this E-W-trending belt originate from the preceding Svecofennian tectonism (Pajunen et al. 2008). The host rock in the studied outcrop is a foliated medium-grained tonalite that includes boudinaged and folded remnants of earlier supracrustal rocks, predominantly migmatitic intermediate gneisses and amphibolites. The old Svecofennian structure of the host rock is sheared. In the first stage a biotitic spaced cleavage with some retrograde chlorite was formed. Shearing intensified to E-W-trending mylonitic and, more

often, to brittle, sliced, altered and rusty fault rocks. These steep, semi-brittle faults show mostly near-horizontal slickenside lineations that indicate late strike-slip faulting.

Three samples were taken from a visibly fractured mylonite (Fig. 2f), three samples from a less mylonitized tonalite, and three samples from an amphibolite. The Q-values are highest in the tonalite, ranging between 0.3 and 1.5, whereas in the mylonites, the Q-values are in most cases significantly lower in the range of 0.1–0.6. Q-values of the amphibolites range between 0.01–0.7. Stable and mutually consistent paleomagnetic results were obtained from the tonalites and mylonites. The amphibolites gave no stable paleomagnetic results.

The characteristic remanence component of site KA, whether taken from the less altered tonalite or from the mylonitic rock, has a low inclination SSW direction. This is called component SB_2 . In addition, most samples yield a remanence component in the PEF direction. No other remanence components were revealed at this site. Component SB_2 is extremely stable, and displays high coercivities that could not be efficiently demagnetized with alternating field. Although the intensity of remanence does not decay properly, the direction stays stable and goes towards origin (Fig. 15, KA6–1A, mylonitic rock and KA5–1A, tonalite), thus suggesting that no underlying component exist. Thermal demagnetization reveals a similar remanence component. During thermal demagnetization, the intensity drops between 300 and 370°C, indicative for Ti-maghemite or slightly oxidized pyrrhotite as the remanence carrier (Fig. 16, KA1–1B, mylonite and KA5–3B, tonalite). Within $\alpha 95$ error limits, the mean remanence direction of the characteristic component deviates from the C_r direction of sites PU, EE, LE and YL, although some single specimens carry a similar direction as component C_r .

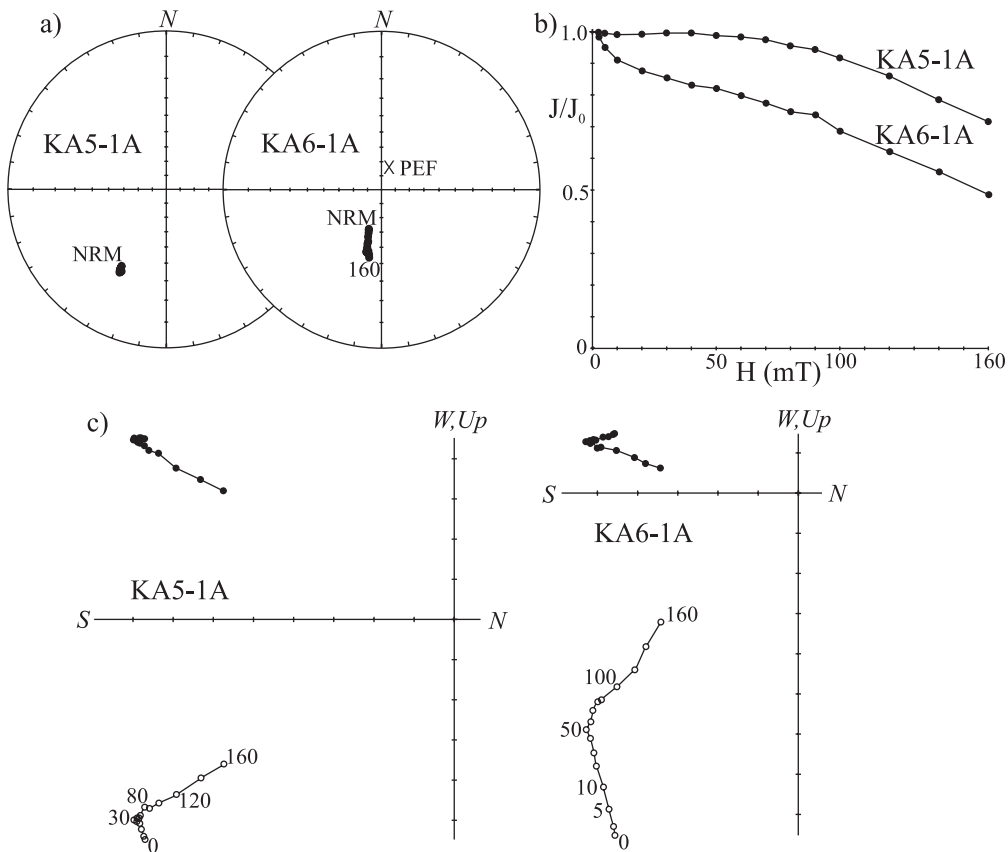


Figure 15. Examples of AF demagnetization of a foliated tonalite (specimen KA5-1A) and a mylonitic gneissic tonalite (specimen KA6-1A) from site KA in the close vicinity of the Porkkala-Mäntsälä shear zone. Both specimens display a similar SB_2 component. Although the intensity of remanence is not decayed properly, the directions go towards the origin, thus implying that no underlying components occur. For explanations, see Figure 4.

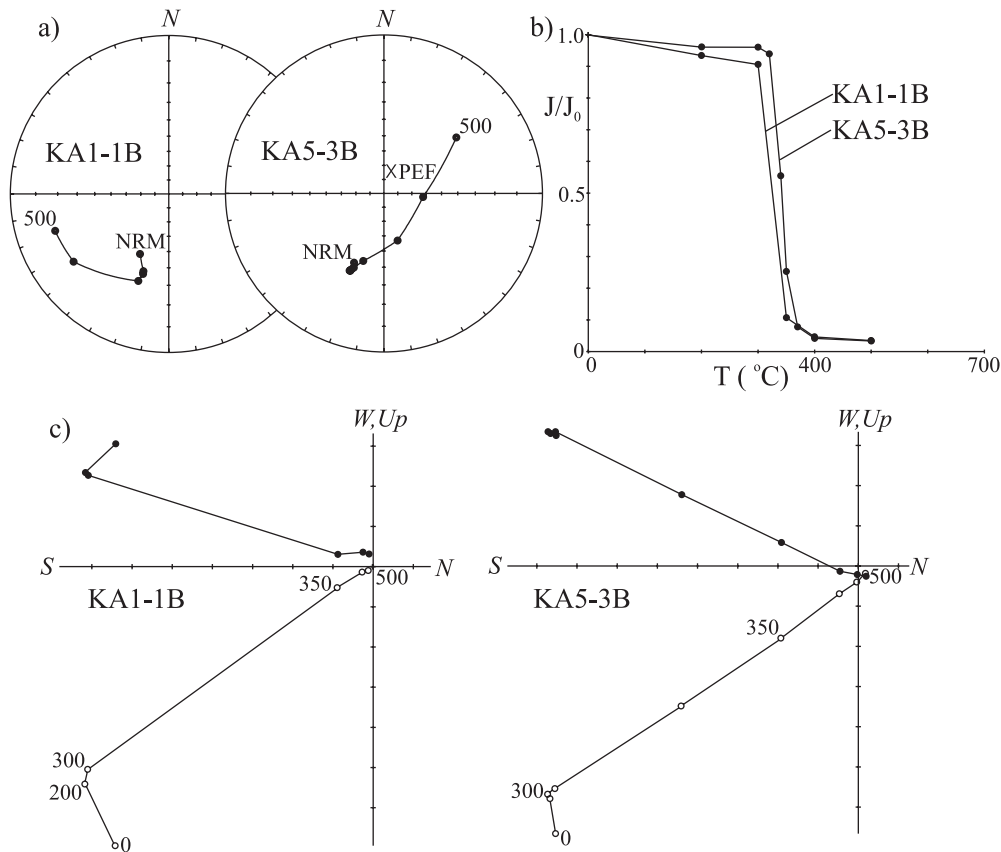


Figure 16. Thermal demagnetization of the foliated tonalite (specimen KA5-3B) and the mylonitic gneissic tonalite (specimen KA1-1B) reveal a similar SB_2 component as was obtained by AF demagnetization. In both specimens the drop of intensity at a temperature range of 300–370 °C may imply that the magnetization resides in Ti-maghemite. For explanations, see Figure 5.

Karakallio II (site KB)

Site KB is situated close to the most intensely faulted Porkkala-Mäntsälä zone, further west from the KA-site within the same E-W-trending high-strain zone, ca. 2 km southwards from the Bodom rapakivi granite intrusion. The host rock on the studied outcrop is protomylonitic or mylonitic gneissic tonalite that is intruded by a narrow boudinaged amphibolitic dyke. The nearly horizontal lineation as at site KA is also seen at site KB. A ca. 15 cm wide, coarse-grained, unaltered porphyritic pegmatite-granite dyke is sharply cutting the sheared structures characterizing the outcrop. It is weakly deformed with undulate quartz and elongated grains. The dyke shows fine-grained chilled margins against the host granitic gneiss (Fig. 2g), a micrographic texture in feldspar, and some sub-idiomorphic quartz against feldspar which probably indicate a rapakivi origin. Two samples were taken from a granitic dyke. One sample was taken in the baked contact zone, ca. 1 cm from the dike margin. Six samples were taken from the unbaked host Svecofennian gneisses at varying distances up to 5 meters from the dike.

The remanence direction of the dike, as well as the baked and the unbaked gneiss, display a similar SB_2 direction as obtained at site KA. AF cleaning did not cause a decay of the intensity (Fig. 17, KB4-1B, dike and KB3-1A, gneiss) in most of the samples. In the samples from the dike and from the gneiss, the characteristic remanence direction is isolated in a temperature range of 320–370°C (Fig. 18, KB1-1X, dike and KB8-1C, gneiss) implying Timagemite or pyrrhotite as the remanence carrier. In the dike, the susceptibility, monitored during thermal demagnetization, decreases dramatically after 370°C. Specimen KB1-1X (Fig. 18) has a slightly off-origin behaviour suggesting that a harder component may exist, however, magneto-mineralogical changes during thermal demagnetization prevented its isolation.

Because both the baked and unbaked gneiss carry a similar remanence direction as the dike, a negative baked contact test is ascertained. Therefore, remanence component SB_2 must be a secondary overprint, representing a later remagnetization event that has affected both the dike and the Svecofennian host gneiss.

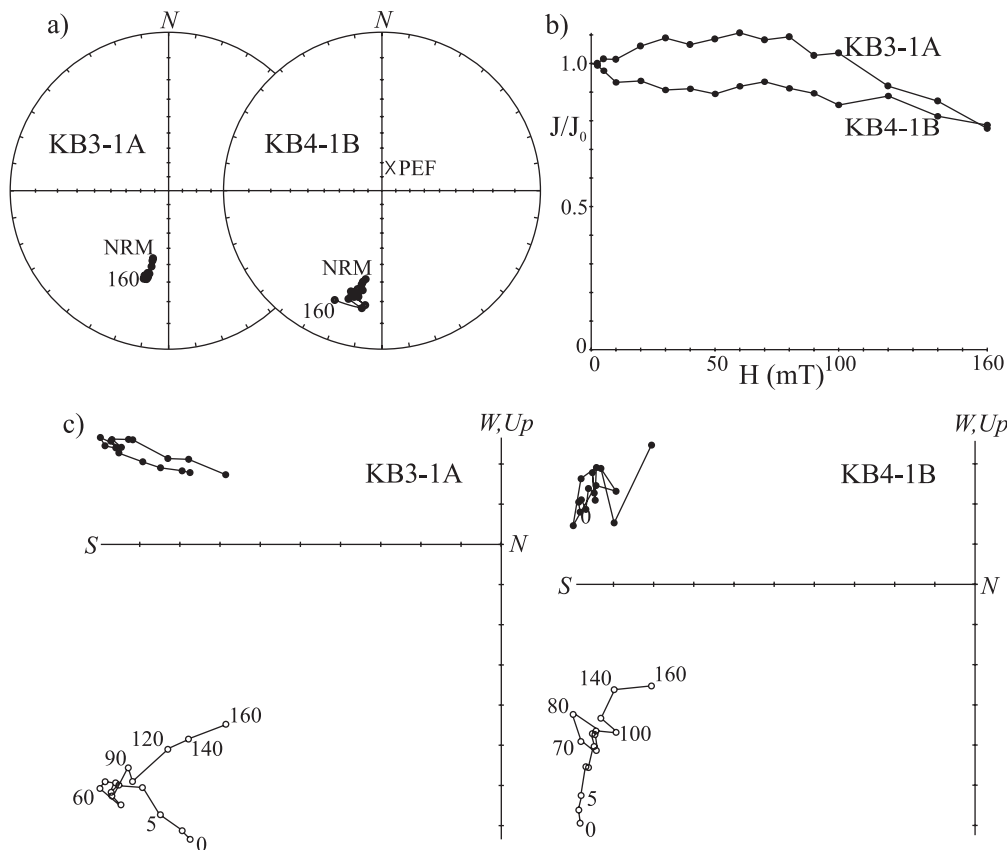


Figure 17. Examples of AF demagnetization of the granitic 15 cm wide dike (specimen KB4-1B) and the unbaked host gneiss (specimen KB3-1A), taken ca. 70 cm from the dike at site KB. Both rock types carry a similar SB_2 remanence component. AF demagnetization was, however, ineffective in removing the remanence completely. For explanations, see Figure 4.

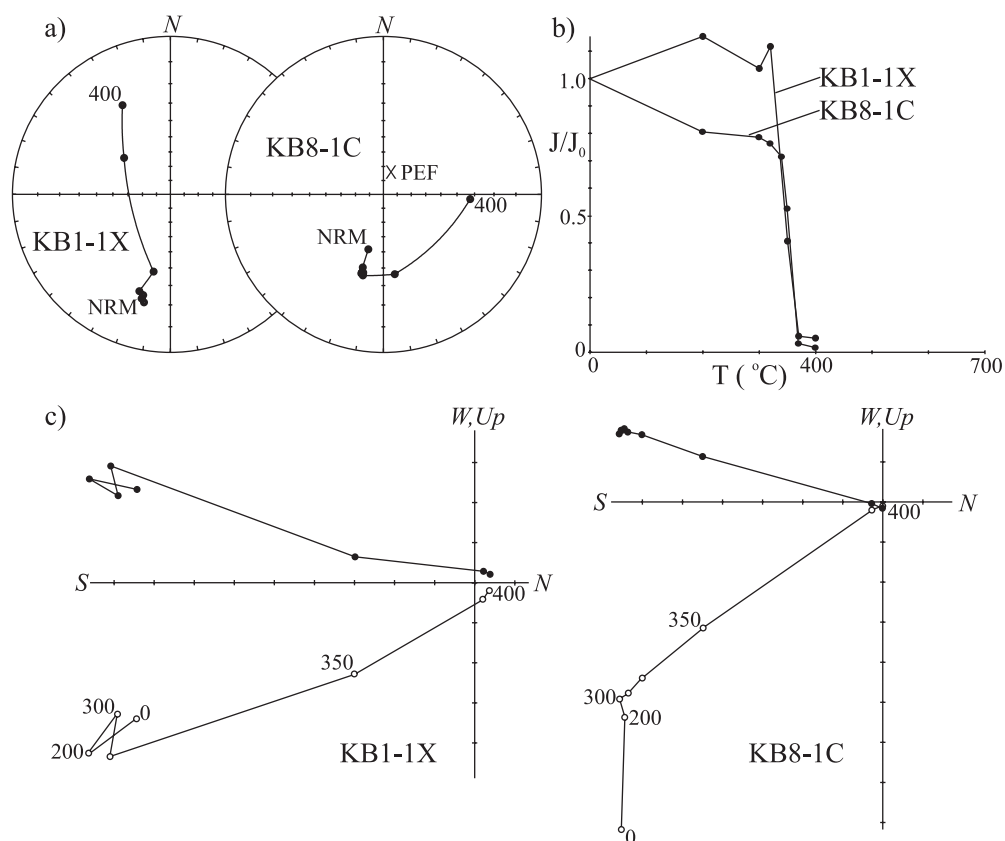


Figure 18. Examples of thermal demagnetization of the granitic dike (specimen KB1-1X) and the unbaked host gneiss (specimen KB8-1C), taken ca. 3 m from the dike at site KB. Both rock types carry a similar SB_2 component isolated in a temperature range of 320–370°C. For explanations, see Figure 5.

Muurala (site MU)

Paleomagnetic results from the site at Muurala, which is located at the center of the Porkkala-Mäntsälä shear zone, are described in Mertanen et al. (2001). At this site, several remanence components were isolated, reflecting the multiphase evolution of the zone. No superimposed components occur but the components were revealed in different samples.

The most typical component isolated both in the host albite-quartz rocks, amphibolite and ultramylonite, is the C component. In two of the samples the C component has a normal SW-pointing direction, and in three of the samples the polarity is reversed. In one sample both polarities occur, but in different specimens. Both the normal and reversed polarity components are isolated in low coercivities below 60 mT. In Table 1 the two opposite polarities are shown separately.

One of the most stable components, although obtained only in one sample taken from an amphibolite, has a similar SSW declination and low inclination as component SB_2 that was obtained at sites KA and KB. Here, component SB_2 was isolated in three specimens at coercivities with peak fields up to 30 mT. The direction then swings to the reversed NNE pointing direction in high coercivities up to 160 mT.

A reversed polarity for component SB_2 was obtained only in this one sample at site MU, although it was not revealed at sites KA and KB.

Iso Omena (site IO)

Site IO is situated in a granitoid area that tectonically resembles the sites EE and LE. The outcrop comprises gabbroic (or amphibolitic) remnants that are foliated in the ENE direction. A brittle NW-SE-trending, altered rusty fracture system was formed later. The fracture system is strongly altered with dark red hematite and opaque pigment masking biotite and feldspar that show mortar and brittle fracturing structures (Fig. 2h). The outcrop is characterized by thin brittle fractures filled with carbonate. These kinds of fractures have a wide distribution as similar carbonate-filled joints have been found, for example, on the western side of the Porkkala-Mäntsälä shear zone. Three samples were taken: one from the hematite zone, one in close contact with the hematite zone, and one from amphibolite that does not show hematitization.

The sample from the hematite zone yields the highest remanence intensity (5.8–7.2 mA/m) and Q-value (0.7). The sample has a very high coercivity that decays only slightly during AF demagnetization

and is thus probably carried by hematite (Fig. 19). Thermal demagnetization was not successful due to breaking up of the sample at 540°C. The susceptibility starts to increase at 500°C suggesting an alteration of hematite to magnetite. The remanence has an intermediate inclination and NW direction, isolated in 0–160 mT. This direction corresponds to the Svecofennian A direction obtained at other sites. Because the intensity does not decay towards the origin, it is possible that a third high coercivity component still exists in this sample. It is implied that the remanence is carried by magnetite and could represent the primary remanence of the rock while the main Fe-oxide, hematite, formed as a chemical precipitation from hydrothermal fluids, could not be isolated. The sample from the amphibolite is magnetically softer and more unstable than the hematite sample. However, in one specimen the remanence direction has a similar A direction as the hematite sample. The sample close to the hematite zone is soft and unstable and does not give reliable results although in this sample there is also a trend for the direction to be in the NW quarter.

its present appearance during the late Svecofennian extensional event at ca. 1.83–1.82 Ga ago. The extension was soon followed by compressional-transpressional events that formed open fold structures characterizing the surrounding granitoids. In general, the structure is simple with nearly horizontal, weak foliation in a medium-grained granitoid that is composed of two phases: the early medium-grained foliated tonalite-granodiorite, and a later non-foliated granitic component that was formed during late high-grade melting phase. Foliated porphyritic granite that preceded the late melt phase also occurs in the outcrop. The area is characterized by intense late fault structures that occur in topographic valleys and lakes. On the studied outcrop these late semi-brittle to brittle fault structures exhibit as narrow hematitized and prehnite-bearing fault and fracture seams.

For paleomagnetic study, five samples were taken from the granite that contains thin hematite veins (Fig. 2i). The samples are magnetically soft. In three samples a direction that is close to the component A was isolated (Fig. 20). In thermally demagnetized specimens the A component is isolated in a temperature range of 370–520°C. However, the susceptibility decreases after 400°C, suggesting that some mineralogical changes have taken place during heating. As with site IO, no remanence directions close to the C or SB components were obtained.

Nupuri (site NP)

Site NP is located on the western side of the Porkkala-Mäntsälä zone in a granitoid area that achieved

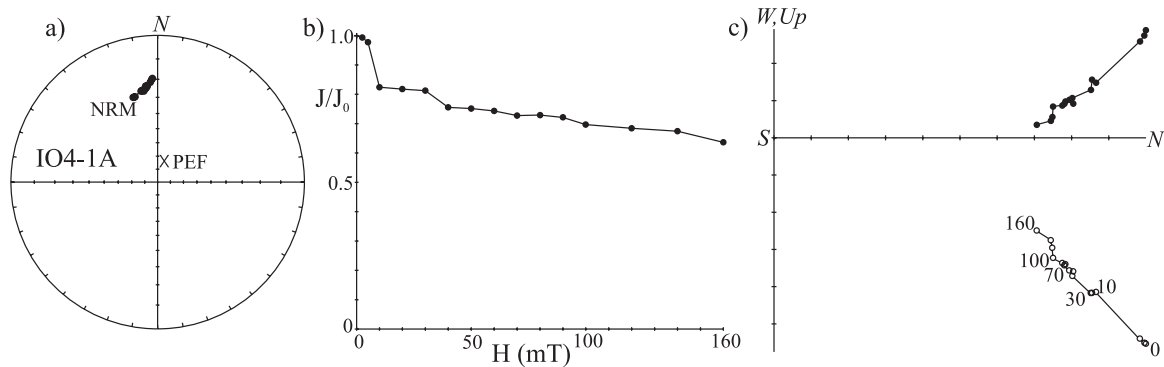


Figure 19. AF demagnetization of a calcite-hematite vein that cross cuts an amphibolite at site IO. AF treatment does not cause decay of intensity of magnetization due to hard coercivity hematite. The remanence direction is close to the A direction obtained at site EE. For explanations, see Figure 4.

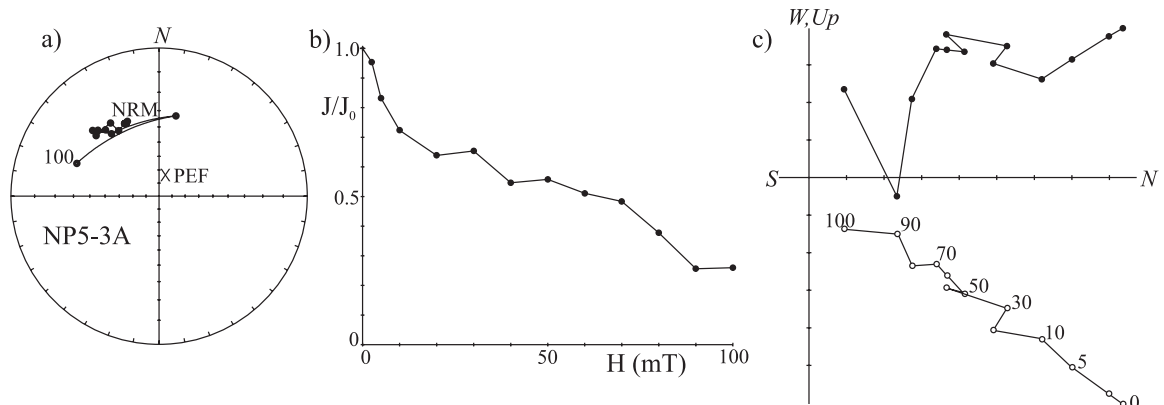


Figure 20. AF demagnetization of a granite that is cross-cut by thin hematite veins at site NP. The remanence component corresponds to A direction obtained at sites IO and EE. For explanations, see Figure 4.

Sites that give not consistent results

Three sites, LN, KI and KR (Fig. 1), where the main sampled rock types display mylonitic structures, show some indications of a similar SW directed remanence component C_R as obtained at sites PU, EE, LE and YL. However, the remanence directions are unstable in all samples, and are not used in mean calculations. Anyway, the mylonite zone of site LN gives some indications of the occurrence of the C component whereas the more solid host granite shows some indications of the Svecofennian A direction. Also at site KI there is a tendency for the directions to be close to the C_R directions. Site KR represents a mega-structure where the host rock is a highly metamorphosed amphibolite that is biotitized on the cross-cutting sheared surfaces. In one specimen the remanence direction behaves similarly as the remanence at site PU, swinging from a stable SW pointing C direction towards NE.

In addition, samples were taken from other sites (Fig. 1) that show mylonitization. However, no stable directions were identified from these sites. These results thus reflect the irregular distribution of the secondary magnetizations. This is probably due to hydrothermal alteration that, depending on the composition of the host rocks and on the circulating fluids, has removed the remanent magnetization without the formation of new magnetic material.

Kopparnäs and Nummela diabase dikes

In order to get reference palaeomagnetic data for the shear zones, diabase dikes were studied in Kopparnäs and Nummela areas (Fig. 1), located west of the studied shear zones. The Kopparnäs area is characterized by a magmatic association which is composed of an earlier gabbro that is cut by a tonalitic granitoid. Both rock types are migmatized and cut by later granitic pulse that is represented by ductile granitic migmatization and rather sharply-cutting pegmatitic granite dykes. This late-Svecofennian extensional event began ca. 1.83 Ga ago (Pajunen et al. 2008). It also produced mafic magmas, such as composite diabase and pegmatite-granite dykes. All the Svecofennian structures are sharply cut by post-Svecofennian rapakivi-related diabase dykes (Fig. 2j). The dykes are thin, about 50 cm wide at maximum, and they form en échelon structures. The samples for paleomagnetic study were taken from two fresh-looking, weakly-deformed post-Svecofennian dikes, KO and KN, and from a Svecofennian amphibolite-facies dyke, KP, with a width of ca. 1.5 m.

Rapakivi-related dike, NU, in Nummela (Fig. 2k) belongs to the Vihti dike swarm, described by

Kosunen (2004). The dike has a width of ca. 10 m, has a coarser grain size than the Kopparnäs dikes, and is visibly tectonized.

The intensity of remanence are highest in dikes KN and NU (664 and 483 mA/m, respectively) and lowest in dike KO (45 mA/m). Likewise, in dikes KN and NU the susceptibilities (19 600 and 16 000) and Q-values (0.8 and 0.7) are higher than those in dike KO (susceptibility 1 900 and Q-value 0.6). On the other hand the density (2920 g/cm³) of dike NU is significantly lower than that of dikes KO and KN (3060 and 3050 g/cm³) suggesting that the silicate minerals of dike NU are more altered compared to those in dikes KO and KN.

At the sample level, the most stable paleomagnetic data were obtained from dike KO. Figure 21 shows an example of AF demagnetization (specimen KO1-1A) where, after removing a steep PEF component, a high coercivity remanence direction with NE direction and shallow inclination is isolated. A similar NE-pointing remanence direction was also obtained in dike KN (Fig. 22). This remanence is called component SB. The direction of component SB is in close agreement with the primary Subjotnian component obtained from the quartz porphyry dikes related to the Onas rapakivi granite in Sipoo area, some 70 km to the east of the Kopparnäs area (Mertanen & Pesonen 1995).

Thermal demagnetization was less effective in isolating the characteristic component, with most samples showing only the steep PEF direction. Specimen KO1-1C (Fig. 21) is an example of thermal demagnetization where the same NE direction with low inclination is obtained as by AF demagnetization. The unblocking temperature of ca. 560°C suggests that the remanence is carried by Ti-magnetite. In some of the thermally demagnetized samples, where the low temperature component (200–520°C) has a similar low NE directed inclination as revealed by AF demagnetization, another steeper inclination component with higher temperature (520–560°C) seems to occur. However, the demagnetization data are scattered, thus preventing isolation of any stable component.

A consistent, characteristic NE direction was obtained in 3 samples of dike KO and in 3 samples of dike KN (Table 2), although the directions between different samples are quite scattered. Dike NU from Nummela differs from the Kopparnäs dikes KO and KN. The remanence of dike NU shows dual polarity with the polarity being reversed in two samples and normal in one sample (Fig. 23). The reversed direction was switched to normal polarity to give a common mean direction, although the reversed direction has a steeper inclination than the normal polarity direction (Table 2). The reversal test (McFadden &

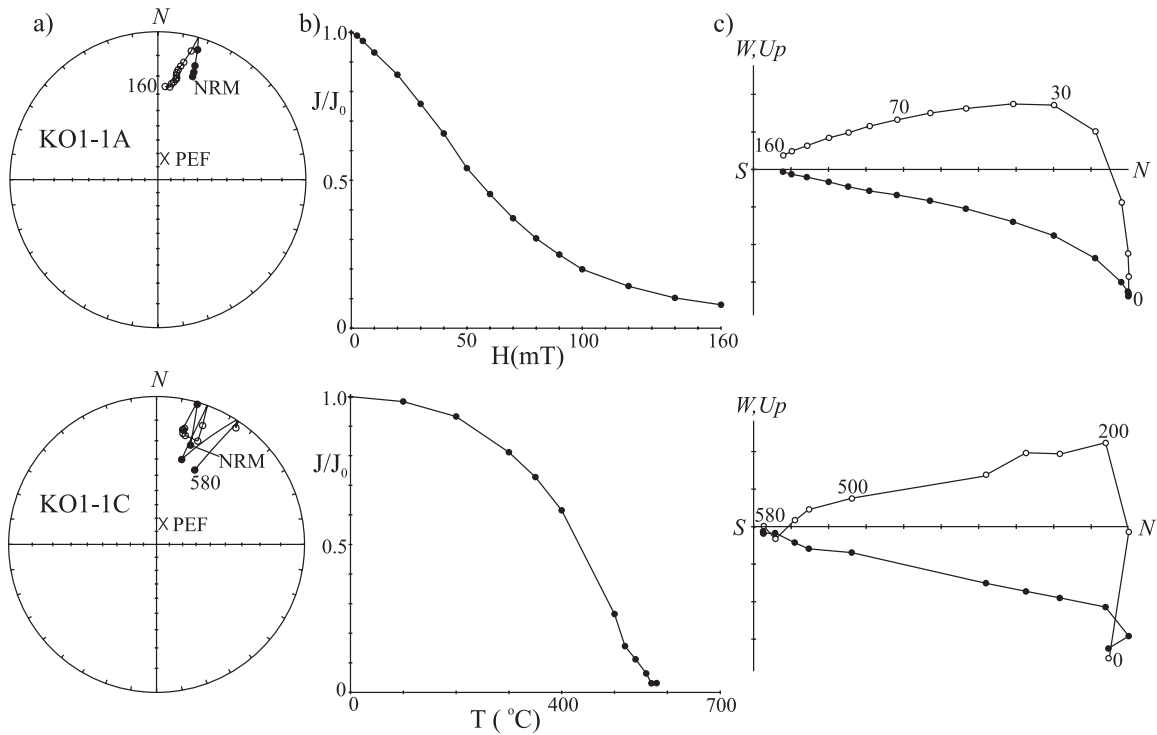


Figure 21. Examples of AF and thermal demagnetizations of a sample from the Kopparnäs dike KO. After removal of the PEF component, both demagnetization methods reveal the same SB component, in a coercivity range of 30–160 mT (KO1-1A) and in temperature of 200–580°C (KO1-1C), indicative of Ti-magnetite as the remanence carrier. For explanations, see Figs. 4 and 5.

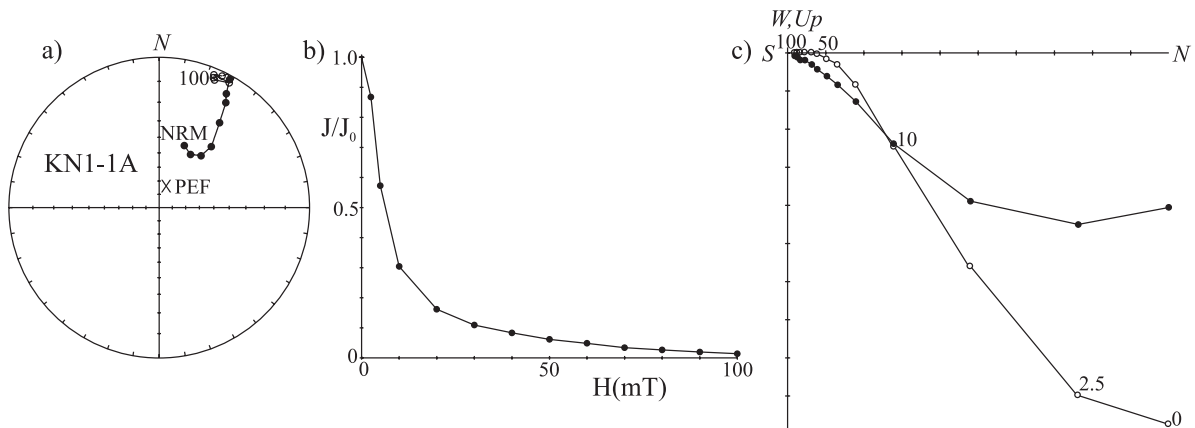


Figure 22. Example of an AF demagnetization of a sample from the Kopparnäs dike KN. The remanence yields a similar SB direction as dike KO. For explanations, see Figure 4.

McElhinny 1990) was not carried out due to small number of samples. The combined mean direction of dike NU has a higher declination and a steeper inclination than that of the Kopparnäs dikes. However, because some individual samples from the Kopparnäs dikes give higher declinations which correspond to the mean NU direction, a mean remanence direction was calculated for all three dikes; KO, KN and NU. As will be discussed later, the possibility that the remanent magnetization of the Kopparnäs dikes represents a different magnetization event than the remanence of the Nummela dikes, is not excluded.

In addition to the NE-pointing low-inclination component, another component, B, with NE declination and moderate inclination was revealed in dikes KN and NU. It was also isolated in one sample of dike KO (not in Table 2). Component B is typically obtained in the coercivity range of 5–50 mT, below the coercivity of the characteristic low-inclination NE component. Thermal demagnetization revealed component B in two specimens in the unblocking range of 100–580°C, thus implying that Ti-magnetite is the carrier of remanence.

The deformed Svecofennian dike KP in Kopparnäs yields significantly lower magnetization

Table 2. Palaeomagnetic results from the Kopparnäs-Nummela dykes (Glat = 60.1°N, Glong = 24.3°E)

Component/ Site	B/N/n	Dec (°)	Inc (°)	α_{95} (°)	k	Plat (°N)	Plong (°E)	dp (°)	dm (°)	A95
Component B										
KN	*3/5	37.3	48.4	16.6	56.1	50.5	149.2	14.3	21.8	16.5
NU	*2/2	46.7	42.5	-	-	42.2	141.2	-	-	-
Mean B	*2/5/7	42.3	45.6	-	-	46.3	145.2	-	-	-
Component SB										
KN	*3/5	38.2	3.0	25.3	24.8	24.5	162.5	12.7	25.3	16.9
KO	*3/7	33.7	-13.6	48.6	7.5	18.0	168.9	25.4	49.7	40.5
(NU (N))	1/*2	49.4	-13.3	-	-	12.6	153.8	-	-	-)
(NU (R))	*2/3	221.7	27.6	-	-	7.9	163.8	-	-	-)
NU (C)	*3/5	44.6	-22.7	31.8	16.1	9.7	160.7	17.9	33.8	31.1
Mean SB	*3/9/17	38.7	-11.2	21.7	33.4	17.5	164.0	11.2	22.0	13.0

K = 91

Note. For explanations, see Table 1.

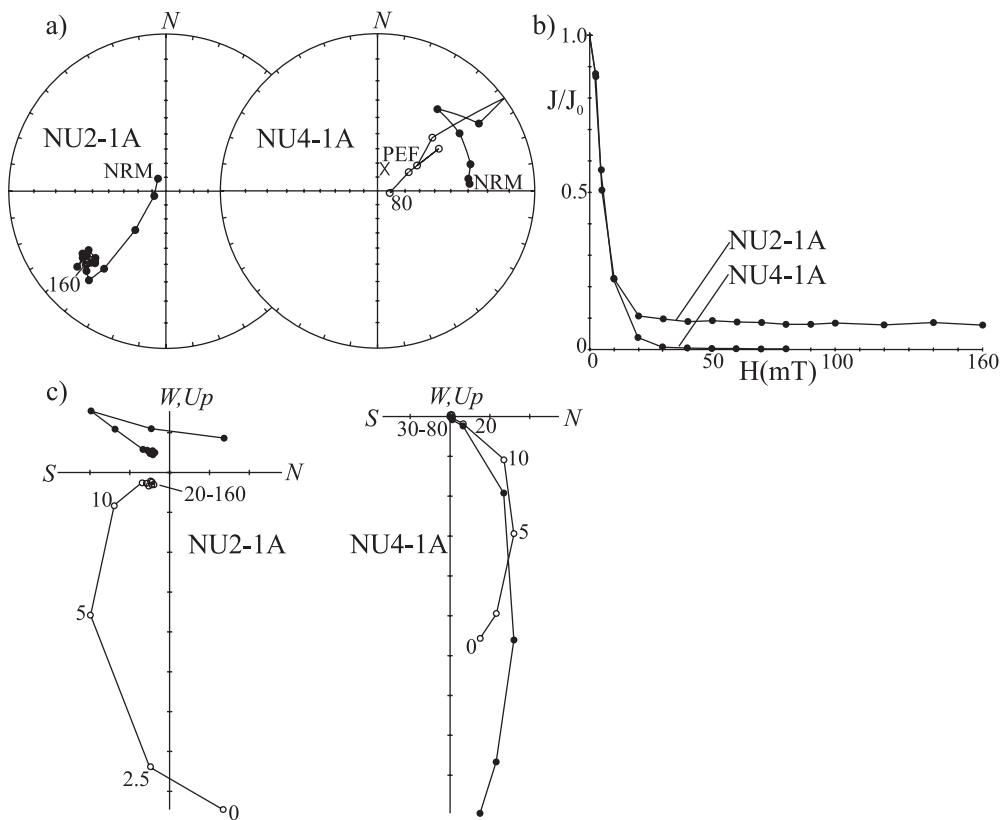


Figure 23. Two examples of AF demagnetization of the dolerite dike NU in Nummela. Specimen NU2-1A displays reversed polarity and specimen NU4-1A normal polarity for component SB. For explanations, see Figure 4.

values than the other dolerite dikes. The low susceptibility (654), intensity of remanence (1.1 mA/m) and Q-value (0.04) all indicate that the dike is metamorphosed and the primary magnetic minerals are altered. Remanence directions of the dike are highly scattered and no common mean direction could be calculated. No indications of any Svecofennian

direction was observed either. Although poorly defined, two samples show similar NE remanence directions as the other Kopparnäs dikes, hinting at the possibility that the dike was overprinted during the emplacement of the other dikes or during a common remagnetization event when the other dikes acquired their remanence.

THERMOMAGNETIC ANALYSES

Shear zones

The principal remanence carriers in magmatic and metamorphosed igneous and supracrustal rocks are minerals belonging to the titanomagnetite ($\text{Fe}_{3-x}\text{Ti}_x\text{O}_4$, $0 < x < 1$) series. In nature, the titanomagnetites often undergo low-temperature (< ca. 250°C) oxidation to form nonstoichiometric, cation-deficient titanomaghemite ($(\text{Fe}, \text{Ti}, \square)_3\text{O}_4$, where the square denotes vacancies in the nonstoichiometric crystal structure which retains the spinel structure of titanomagnetite (e.g. Özdemir 1987, Kelso et al. 1991 and Zhou et al. 2001). This maghemitization takes place typically in mild hydrothermal environments. Rock magnetic studies on the magnetization of oceanic crust have shown that maghemitization is a phenomenon that decreases the magnetization of rocks as a function of time (e.g. Kelso et al. 1991 and Zhou et al. 1999, 2001), although the coercivity of titanomaghemites is higher than that of unoxidized titanomagnetites (Dunlop & Özdemir 1997). In the oceanic crust, the permeability to seawater can play an important role in the oxidation state of titanomagnetite and magnetic properties (Zhou et al. 1999 and Wang & Van der Voo 2004). It has been shown that the oxidation proceeds slowly, typically on a time scale of several million years (Zhou et al. 2001), during which the Earth's magnetic field may reverse several times from one polarity to another.

During the process when titanomagnetite oxidizes to titanomaghemite, the primary thermoremanent magnetization (TRM) evolves into one or more generations of chemical remanent magnetization (CRM) (Dunlop & Özdemir 1997). CRM due to maghemitization of SD-size titanomagnetites is shown to parallel the original TRM (Özdemir & Dunlop 1985). On the other hand, PSD- and MD-size titanomagnetites probably acquire the CRM along the applied field at all stages of oxidation (Kelso et al. 1991).

It is suggested that the studied rocks originally contained titanomagnetite as the primary magnetic mineral of TRM origin. In later geological events the primary titanomagnetite was partly or totally oxidized to titanomaghemite or pyrrhotite. Titanomaghemites are single-phase minerals, but they are metastable (Özdemir 1989). Upon laboratory heating, titanomaghemites invert to multiphase intergrowths, to titanomagnetite, ilmenite, hematite and other minerals. Inversion of titanomaghemite to other magnetic phases takes place above approximately 350°C (O'Reilly 1983) and the inversion can be observed as irreversible thermomagnetic curves.

In most of the studied samples (Figs. 24 and 25) a distinct drop in the thermomagnetic curves is observed at ca. 350°C. It is implied that this behaviour may indicate the inversion of titanomaghemite to intergrowths of other magnetic minerals, probably titanomagnetite or hematite. Formation of new (titanom-)magnetite during heating was observed in the cooling curves of thermomagnetic analyses, and it was also visible in the increase of susceptibility during thermal demagnetization. It is suggested, however, that not all titanomaghemite inverts to magnetite, because the same drop of intensity at 350°C is still preserved in the cooling curves, implying the existence of titanomaghemite. On the other hand, titanomagnetite was also qualitatively inferred by thin section studies before heating experiments, thus confirming that not all magnetite observed by thermomagnetic curves was formed due to inversion of titanomaghemite.

A third mineral identified is goethite. Goethite is typically intergrown with hematite and it is probably also a carrier of remanent magnetization. It was not observed during thermal demagnetization, but in some samples thermomagnetic curves show a drop of intensity at ca. 100–150°C, indicative of goethite. Goethite dehydrates to hematite in the temperature range of 250–400°C (Dunlop & Özdemir 1997). Hence the increase of susceptibility during thermal demagnetization at these temperatures is probably related not only to inversion of titanomaghemite to intergrowth with titanomagnetite, but also to alteration of goethite to hematite. The fact that in many of the samples the remanent magnetization could not be erased by AF demagnetization, can also be evidence of the existence of goethite (Dunlop & Özdemir 1997).

Hematite is probably one of the most common iron oxide minerals in the studied rocks, as evidenced in thin sections and seen visibly as a red colour in most of the ultramylonites and breccias. Precipitation of ultra-fine-grained hematite cement from iron-rich solutions in the pore spaces of clastic sediments is the main mechanism and source for red beds (Butler 1992). The same mechanism may be applied to the hematization of breccias and ultramylonites, although thermomagnetic analyses rarely revealed the Curie point of hematite (ca. 680°C) due to stronger magnetizations in other coexisting minerals.

Figures 24 and 25 show examples of typical thermomagnetic curves of different sites where stable remanence directions were obtained. At site PU, the measurements of the protomylonitic gneiss (Fig. 24a) indicate the occurrence of both magnetite with

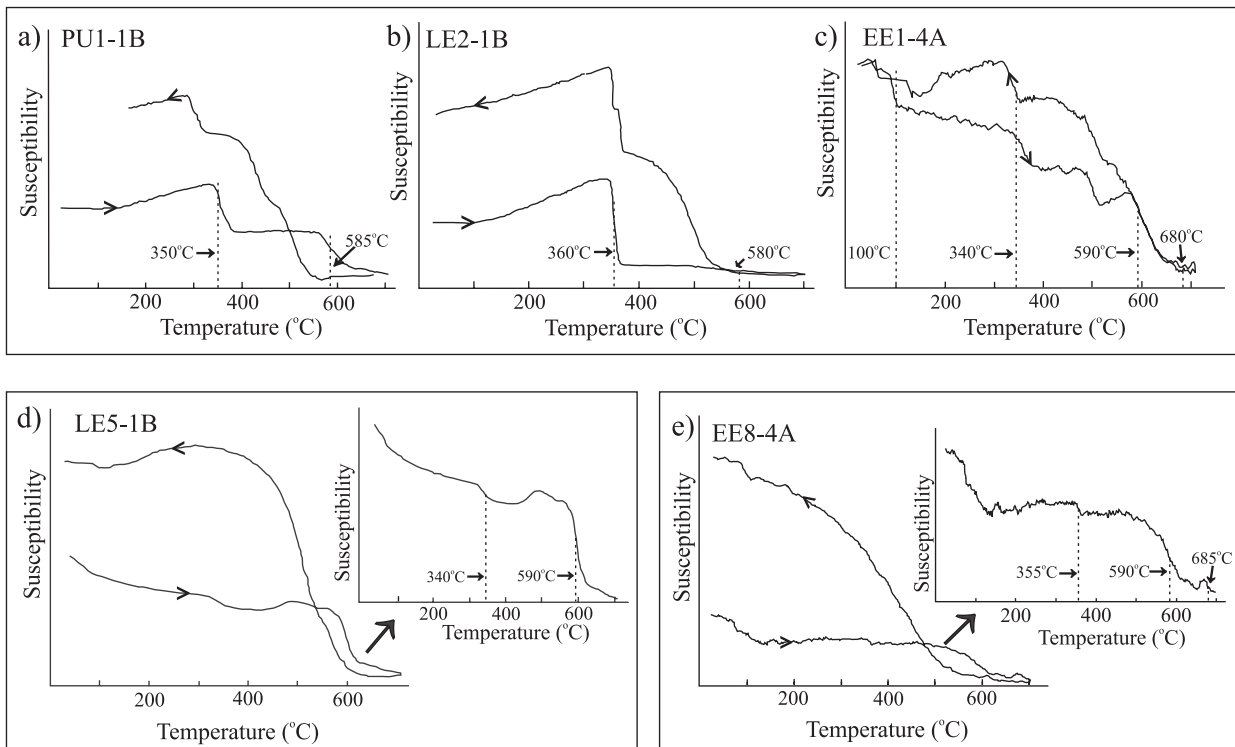


Figure 24. Results of thermomagnetic measurements of mylonitic samples from sites PU (a.) and LE (b.), and from a breccia at site EE (c.). Thermomagnetic analyses for host rocks are shown for a gabbro at site LE (d.) and for a granitoid at site EE (d.). The heating curves are indicated by arrows to the right and the cooling curves by arrows to the left. Insert figures in (d.) and (e.) show the heating curves. All heating curves display a drop of intensity at ca. 340–360°C which is implied to reflect inversion of titanomaghemite to titanomagnetite. Curie temperature of titanomagnetite at ca. 580–590°C is also visible in all samples. Furthermore, the samples from site EE, both from the breccia or host granitoid, give indications of hematite (680°C) and goethite (100°C). Irreversibility of the heating (arrow to the right) and cooling (arrow to the left) curves indicate considerable mineralogical alterations during heating.

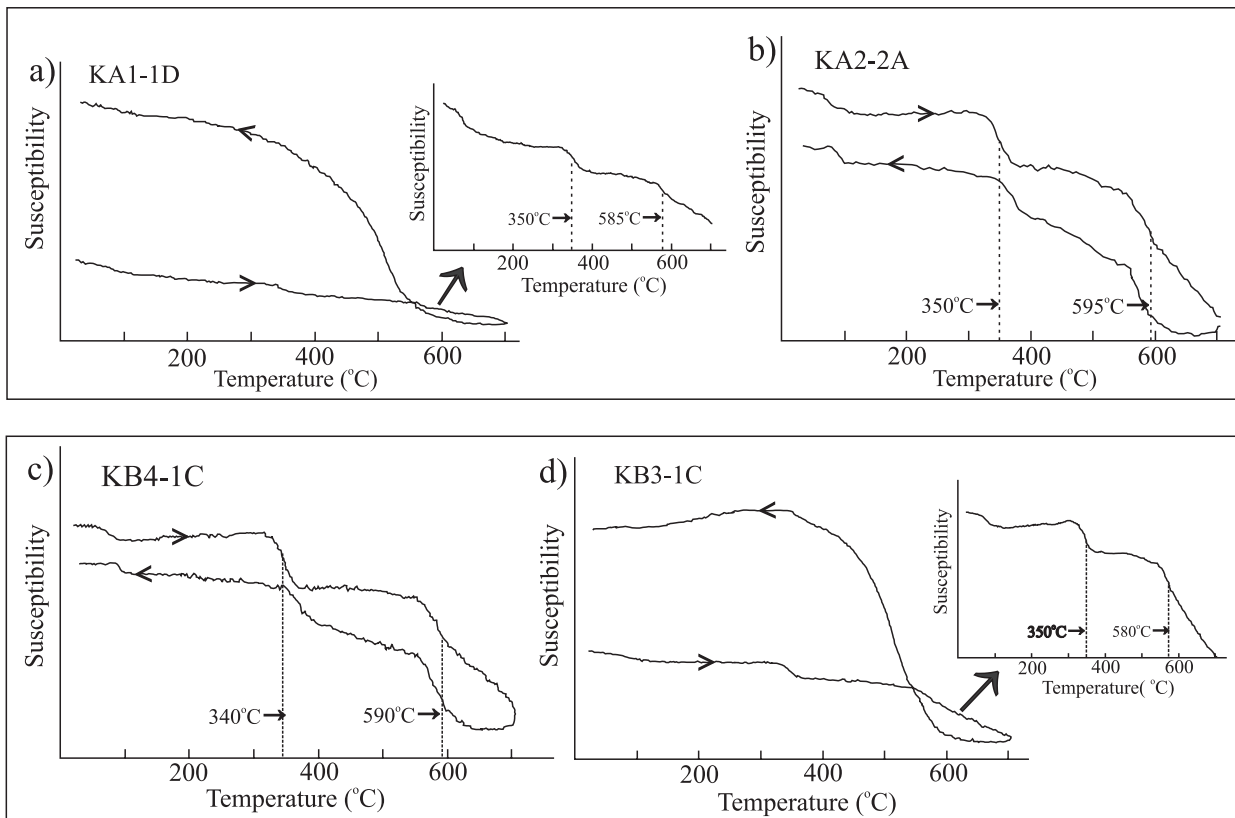


Figure 25. Thermomagnetic curves for samples from the Porkkala-Mäntsälä shear zone. Specimen KA1-1D (a.) is from a mylonitic gneissic tonalite and specimen KA2-2A (b.) from a foliated tonalite at site KA. Specimen KB4-1C (c.) is from the granitic dike and specimen KB3-1C (d.) from the host gneiss at site KB. All specimens display a drop of intensity at ca. 340–350°C, probably indicating the inversion of titanomaghemite to titanomagnetite. The occurrence of magnetite is shown as the drop of intensity at a temperature range of ca. 580–590°C. For other explanations, see Figure 24.

Curie temperature of 585°C and titanomaghemite (or possibly slightly oxidized pyrrhotite) that inverts probably to titanomagnetite in 350°C. Thin section studies indicate the occurrence of original titanomagnetite which is also seen at lower intensity in the cooling curve at temperatures of 680–560°C. Although new magnetite is formed during heating, the titanomaghemite is still shown in the cooling curve, but now with a lower temperature of about 300°C. The thermomagnetic curve of the mylonitic rock at site LE (Fig. 24b) shows similar behaviour as at site PU. Magnetite, with Curie temperature at ca. 580°C, also contributes to the total magnetization and is probably the carrier of the viscous PEF component.

The thermomagnetic curve for the host gabbro at site LE (Fig. 24d) displays an even more conspicuous irreversibility than the mylonitic rock. In the inset figure, only the heating curve is presented. The effect of the furnace was reduced according to the method by Hrouda (1994). The main magnetic carrier is titanomagnetite, but the occurrence of titanomaghemite is seen as a slight decrease of intensity at the temperature of 340°C. The result thus suggests that the occurrence of titanomaghemite at site LE is not restricted just to the proper mylonitic rock, but that it also occurs to a lesser extent in the host rocks.

The main rock type at site EE is a red breccia, that occurs irregularly within the Svecofennian granitoids. The occurrence of red breccia is an indication of the formation of the rock at shallow crustal levels in an oxidizing environment. The thermomagnetic curve for specimen EE1–4A (Fig. 24c) from the breccia shows a complex behaviour with contributions from possibly four magnetic minerals. Curie temperatures of ca. 100, 340, 590 and 680°C are probably indications of goethite, titanomaghemite, titanomagnetite and hematite, respectively. Heating and cooling curves deviate moderately, but compared to the thermomagnetic curves for the host granitoid (Fig. 24e), only minor alteration takes place. The granitoid (inset of Fig. 24e) displays a heating curve with indications of the same minerals as in the breccia. The significant difference between the heating and cooling curves after ca. 550°C of cooling, indicate considerable creation of magnetite during heating, probably due to inversion of titanomaghemite to titanomagnetite. Like in previous sites, however, titanomagnetite was present also before heating, as evidenced by petrographic studies.

Thermomagnetic analysis for samples of sites KA and KB (Fig. 25) at the Porkkala-Mäntsälä shear zone indicate rather similar behaviour as for sites PU, LE and EE, although the oxidation of titanomagnetite to titanomaghemite is less pronounced.

Magnetic mineralogy was further studied by producing isothermal remanent magnetization (IRM) for representative samples from sites PU, LE, EE and KA (Fig. 26). All the IRM curves are dominated by high-coercivity mineral phases because none of the samples were saturated by 1.5 T. Sample EE1 from the breccia shows very slow IRM acquisition suggesting that the main magnetic mineral is hematite. Also site KA is dominated by a high coercivity phase, most obviously hematite. As shown above, thermomagnetic curves from site EE and KA also indicated the existence of titanomagnetite and titanomaghemite which in minor part also contribute to the IRM curve. Thermal demagnetization and thermomagnetic analyses of specimens from sites PU and LE indicated that the remanence resides in titanomaghemite-titanomagnetite. IRM acquisition curves further support the occurrence of these minerals, shown as rapid increase in lower steps below 0.2 T. The existence of hematite is evident in the higher fields.

Diabase dikes

Thermomagnetic analyses were carried out also on samples from the Kopparnäs and Nummela diabase dikes. The notable feature in the Kopparnäs dikes KN and KO is the slight drop in magnetization intensity at the temperature of ca. 350–370°C (Fig. 27a and b), although the principal loss of magnetization takes place in the temperature of 570–590°C.

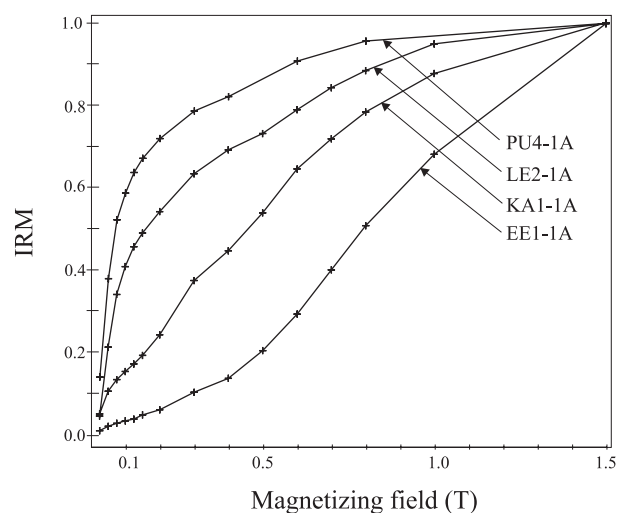


Figure 26. Normalized IRM acquisition curves for mylonite samples from sites PU, LE and KA, and for a breccia sample from site EE. Saturation was not achieved in any of the samples by 1.5 T, indicating the occurrence of a high coercivity hematite. The more rapid IRM acquisition of samples PU4 and LE2 compared to samples KA1 and EE1 indicates the more conspicuous occurrence of magnetite in these samples.

The result indicates that some oxidation of titanomagnetite leading to formation of titanomaghemite (or pyrrhotite) has taken place also in the Kopparnäs dikes. Maghemitization is most pronounced in the altered dike KP (Fig. 27d). The analyses of the Nummela dike shows the existence of a single magnetic phase, a low titanium magnetite (Fig. 27c). As will

be discussed later, the Kopparnäs dikes right at the vicinity of the Porkkala-Mäntsälä shear zone may have been affected by hydrothermal activity within the shear zone. Furthermore, petrophysical properties and the slightly tectonized appearance of the Nummela dike indicate that also the Nummela dike has been affected by later geological events.

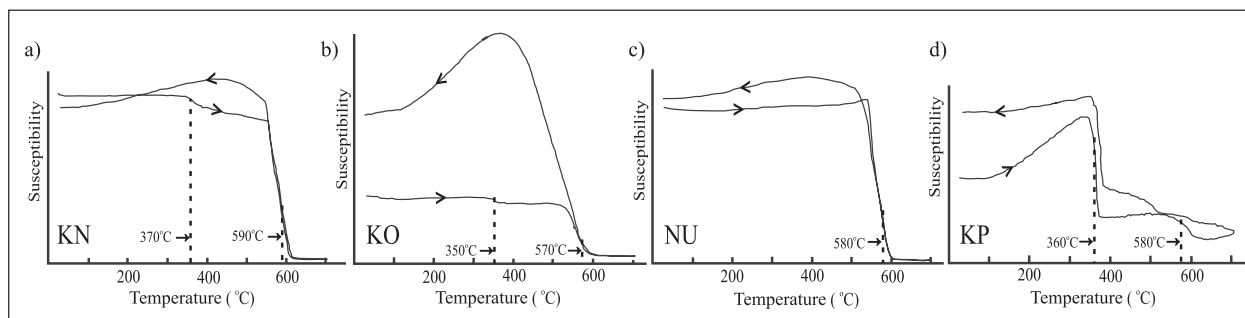


Figure 27. Thermomagnetic curves for samples from the Kopparnäs (a,b and d) and Nummela diabase (c.) dikes. The post-Svecofennian Kopparnäs dikes KN (a.) and KO (b.) show (titano)magnetite (Curie temperatures in 575–590°C) as the main magnetic mineral. A slight decrease in intensity at temperatures of 350–370°C probably indicates that slight oxidation of titanomagnetite to titanomaghemite has taken place. The sample from the Nummela dike NU (c.) shows only the Curie temperature of magnetite. The Svecofennian Kopparnäs dike KP (d.) shows a conspicuous drop of intensity at 360°C probably indicating that the original titanomagnetite has almost totally oxidized to titanomaghemite. For other explanations, see Figure 24.

MICROANALYSES

Microanalyses of four specimens, EE5-1A, PU3-1A, LE2-1B and KA1-1C indicate very small amounts of iron oxides. Small grains of rutile occurs sporadically and goethite was observed in the sample from site EE. However, the analyses reveal only small amounts of hematite and magnetite, but no titanomaghemite or titanomagnetite nor ilmenite were observed. The samples do contain abundant titanite. In samples PU and EE there occurs a highly titanium bearing Ti-Si-mineral that could not be identified owing to the small grain size. The unidentified mineral invariably contains some amounts of aluminium and iron. According to O'Reilly (1983), titanomagnetite-titanomaghemite intergrowths can contain other metallic species like Al, Mn and Mg. Furthermore, studies on oceanic basalts have shown that strongly altered titanomagnetite-titanomaghemite grains show dissolution of titanomaghemite with neocrystallization of a Ti-rich phase (TiO_2), possibly anatase (Zhou et al. 2001). Although not conclusively ascertained, the unknown submicroscopic mineral could be titanomagnetite-titanomaghemite intergrowth that is partly dissolved to a Ti-rich phase.

Xu et al. (1997) propose that submicrometer Fe-Ti oxides may be significant carriers of the magnetic remanence. Zhou et al. (2001) have shown in oceanic basalts that the high degree of oxidation

depends on small grain size or porosity and permeability due to lithological factors (fractures and pore space) or both. Al and Mg act to decrease the lattice parameter (see references in Zhou et al. 2001). Moreover, they conclude that the samples with the highest degree of oxidation, thus maghemitization, contain fine grained remanence carriers, in grain sizes in the superparamagnetic and single-domain range. Threshold between superparamagnetic and SD grain sizes is 0.05 μm for hematite and equant grains of magnetite (Butler 1992). Thus, it is possible that in the studied samples, the remanence carrying minerals may be under the limit of resolution of the electron microprobe. Thermomagnetic analyses and thermal demagnetization experience indicate that the samples do exhibit these minerals. Based on high coercivities and microanalyses that revealed only extremely small amounts of iron oxides, it is possible that the samples carry very small SD grains. These observations could be indications of the high degree of alteration of titanomagnetite leading to formation of titanomaghemite with small grain sizes which carry a stable CRM. As will be discussed later, it is probable that the latest alteration within the studied shear zones took place in higher crustal, possibly high subsurface levels, in the late stages of crustal evolution, and the different rock types were thus vulnerable to oxidation.

ANISOTROPY OF MAGNETIC SUSCEPTIBILITY (AMS)

The anisotropy of magnetic susceptibility (P value) is typically more than 5% and thus comparatively high for most studied locations. Due to shearing, such high values are expected. High anisotropy values indicate a strong deformation (Tarling & Hrouda 1993) which may also have biased the remanence directions. In the studied shear zones the magnetic foliation plane, defined by the direction of the maximum susceptibility axis, is approximately in the ENE-WSW direction (Fig. 28). The most common remanence components trend in the NE-SW direction, and hence, close to the main trend of the shear zones. Therefore, the remanence directions may be related to the overall strain effects of the study area. However, when the AMS data of separate sites are inspected, it is evident that the maximum and minimum susceptibility directions are quite scattered and no clear correlation between the remanence components and AMS are observed. Therefore, it is possible that AMS reflects the orientation of primary (titano)magnetite grains or the shape-alignment of paramagnetic phases. Rock magnetic analyses combined with thermal demagnetization data and

microanalyses indicated that the characteristic remanent magnetizations reside in small-grained, possibly SD sized titanomagnetite and hematite which were obviously formed in secondary geological processes and the remanences thus represent (thermo) chemical remanent magnetizations. The different minerals may have been formed at various times, but the AMS represents a summation of the anisotropic susceptibilities of all the mineral grains within a sample. The existence of magnetite was demonstrated by different methods. It is interpreted, although not unquestionably, that magnetite is probably the original primary mineral in the studied rocks, is the main carrier of the large PEF component in most of the samples, and is also responsible for the AMS.

As will be shown below, the remanence directions and the ages of the poles derived from the remanences are deemed to record correctly the direction of the paleofield at the time they were acquired. However, as stated before, the resemblance of the AMS directions to the main remanence directions cannot be exclusively ignored.

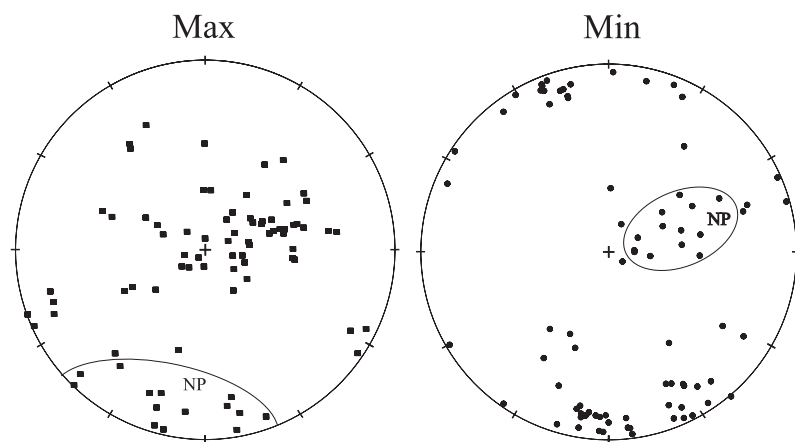


Figure 28. Directions of maximum (squares) and minimum (dots) susceptibility for the specimens from all the studied shear zones. The most exceptional directions from site NP are shown within circles. For explanations, see text.

DISCUSSION

Origin of components

The occurrence of different remanence-carrying minerals and remanence components indicates that the shear and fault zones were reactivated in several geological events. Five remanence components were obtained: A, B, C, SB₁ and SB₂. In addition, the Koppärnäs-Nummela dikes exhibit a sixth remanence component, SB (Fig. 3). Due to weak intensities and unstable magnetizations, only a minor part of the studied shear zones show consistent, stable

remanence results. Nevertheless, the results bear significant geological importance.

Fault and shear zones represent crustal weakness zones in the bedrock, providing path-ways for fluid migration. As shown by aeromagnetic data, hydrothermal alteration typically reduces the magnetization as the Fe of oxide minerals is released to form Fe-silicates (e.g. Airo 2002). However, provided the fluids are capable of forming new remanence carrying minerals, paleomagnetism can be used to date fluid migration. There are different mechanisms that

can cause remagnetization of the rocks, the most typical being the formation of chemical remanent magnetization (CRM) when new magnetic minerals are formed or altered from existing minerals, thermochemical remanent magnetization (TCRM) acquired as the formation of new or altered magnetic mineral is accompanied by the excess of heat, or viscous/ thermoviscous remanent magnetization (VRM/ TVRM, respectively) typically formed during burial.

Magnetic minerals can precipitate by different mechanisms such as fluid migration driven by tectonic stress, sediment compaction or magmatic activity. Considering magmatic events, southern Finland is delineated by the Subjotnian extensional regime, resulting to the emplacement of rapakivi granites and associated dikes at about 1.64 Ga ago. These events have had an obvious impact on the magnetizations. Moreover, southern Finland represents the marginal part of the exposed Precambrian craton, south of which, in Estonia and NW Russia, the Precambrian basement is covered by Cambrian – Silurian sedimentary layers. Therefore, although such sedimentary rocks do not appear in Finland, the past presence of sedimentary cover over the Shield forms one possible source for remagnetization. Furthermore, one of the geodynamic effects which may have affected the occurrence of shear zones in southern Finland, is the Caledonian orogeny in the western part of the Fennoscandian Shield. The Caledonian orogeny took place during Silurian-Devonian (at ca. 440–350 Ma) when the Fennoscandian Shield collided with Laurentia. Compressional stress released from the collisional events may have been partly responsible for the formation of the shear zones in southern Finland.

In the following, the origin of different remanence components is discussed in the light of geological evidence. The age of remanence components is defined by comparing the pole positions with those of the Precambrian ‘key poles’ (Fig. 29) (see Buchan et al. 2000) and the Paleozoic APWP of the Fennoscandian Shield (Fig. 30). The Phanerozoic APWP of the Fennoscandian Shield is well defined from the end of the Early Ordovician up to Jurassic (e.g. Torsvik et al. 1996 and Smethurst et al. 1998), and can thus be used to date the remanence components in that age range.

At present the APW path scenario for the oldest Precambrian poles has not been attempted because of the large age gaps between different poles. Instead, a ‘key pole’ approach, where only the best defined poles with isotopically dated ages, has been adopted. Six of the ‘key poles’ are shown in Figure 28. The 1.88 Ga pole is obtained from 1.88 Ga old Svecofennian synorogenic gabbroic intrusions in

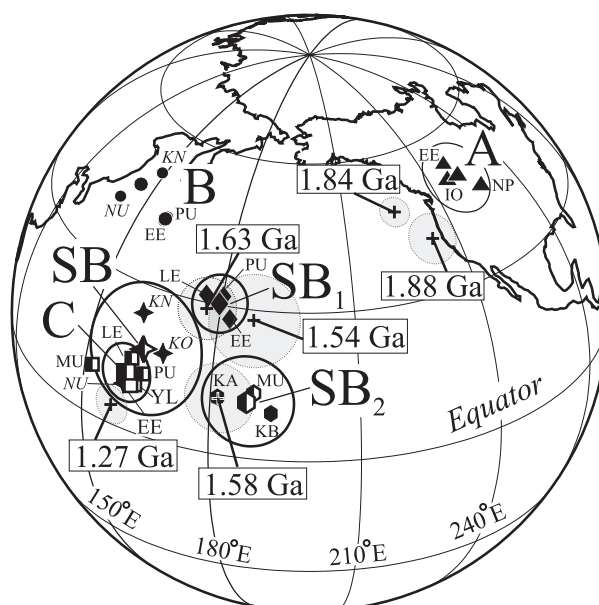


Figure 29. Mean palaeomagnetic poles for components A (triangles), B (circles), C (squares), SB₁ (quadrangles), and SB₂ (pentagons) from the shear zones (B also from the dikes), and SB (stars) from the diabase dikes. The A95 confidence circles are shown around the mean poles (no A95 values were calculated for the B poles because only two sites from both rock types). Closed (open) symbols denote normal (reversed) polarity and half opened symbols mixed polarity. For abbreviations of the sites, see Tables 1 and 2. The crosses with shaded A95 circles denote the ‘key poles’, the ages of which are indicated (see Buchan et al. 2000, Pesonen et al. 2003 and Mertanen & Pesonen 2005). Comparison of the poles from the shear zones with the ‘key poles’ implies that component A was acquired during the Svecofennian orogeny at ca. 1.88–1.84 Ga ago. Component B does not match with any of the known Precambrian ‘key poles’. Component C is close to the 1.27 Ga old ‘key pole’, but like for pole B, Phanerozoic origin is suggested, as shown in Figure 29. Pole SB from the dolerite dikes is, within error limits, similar to pole C from the shear zones. Poles SB₁ and SB₂ are suggested to represent Subjotnian remagnetizations at 1.63 and 1.58, respectively. For an alternative, Phanerozoic origin for pole SB₂, see text, and Figure 30.

Finland (Pesonen & Stigzelius 1972, Neuvonen et al. 1981, Elming 1985, 1994 and Mertanen & Pesonen 1992). The 1.84 Ga pole is obtained from the 1837 Ma Haukivesi lamprophyric dikes (Huhma 1981 and Neuvonen et al. 1981) in central Finland. Three ‘key poles’, the 1.63, 1.58 and 1.54 Ga poles, are related to the Subjotnian magmatic events when rapakivi granites and associated mafic and acid dikes were intruded in the southern Fennoscandian Shield. The 1.63 Ga ‘key pole’ is defined as the average of two ca. 1630 Ma poles, the quartz porphyry dikes related to the Wyborg (Neuvonen 1986) and to the Onas (Törnroos 1984 and Mertanen & Pesonen 1995) rapakivi granites in southern Finland. A mean paleopole with assigned age of 1580 Ma is obtained from the Kumlinge-Brändö diabase and quartz porphyry dikes associated with the Åland rapakivi granite (Pesonen & Neuvonen 1981) and a younger pole with an age of 1540 Ma is obtained from the Föglö-Sottunga dikes (Pesonen & Neuvonen 1981) also related to the Åland rapakivi massif.

Component A

Component A was obtained only sporadically at some of the studied sites (EE, NP and IO, Fig. 29). It is the principal component at two sites, IO and NP which are characterized by hematite bearing veins. As shown before, it is implied that the youngest component related to the hematite veins was not isolated, but the obtained remanence component represents the original magnetization residing in magnetite.

The age of the pole A can be inferred by its pole position with respect to the ‘key poles’ (Fig. 29). Although the pole does not match with the known key poles, it is fairly close to them, and hence it can be inferred that the A component was acquired during the Svecofennian orogenic events at about 1.88–1.84 G ago. The pole is defined by only seven samples from three sites and therefore cannot be regarded as statistically reliable, albeit the poles from all three sites give very consistent results.

Component B

Component B was isolated at two sites (EE and PU) in the shear zones, in the Kopparnäs dike KN, and in the Nummela dike NU. Several other studied shear zones show clear indications of the B component, although it could not be properly isolated.

Figure 28 shows the pole positions for component B. The poles from different formations are close to each other, suggesting a common origin for the acquisition of remanence. A similar B pole has been obtained in several previous studies in the Fennoscandian Shield, for instance in the rocks of the Karelian Province in eastern and northern Finland and in NW Russia. In the Varpaisjärvi area in western Karelian Province, the age of a pole corresponding to the B pole was interpreted as ca. 2.15 Ga (e.g. Neuvonen et al. 1997). In the 2.45 Ga Koillismaa layered intrusions, a similar component was regarded as ca. 1.75 Ga (Mertanen et al. 1989). A comparable pole was also obtained in the Early Palaeoproterozoic rocks of the Kola Province (Mertanen et al. 1998) where this pole occurred also in the one studied Paleozoic dike, which questioned the Proterozoic origin for the remanence. In southern Finland, a similar pole was previously obtained in the Sipoo quartz porphyry dikes (Mertanen & Pesonen 1995) where it was thought to represent a magnetization related to the late Mesoproterozoic rifting event at ca. 1.3 Ga, which later led to the emplacement of the Postjotnian dikes at ca. 1.27 Ga ago. The age of the B pole was determined by its pole position on the APW path (Mertanen & Pesonen

1995 and Elming 1994). As discussed before, the APW path approach is not favoured anymore, and besides, the 1.3 Ga poles used in the APW path determination are not well defined and are not regarded as key poles.

In summary, most of the previous studies indicate that the B pole is of secondary origin. Its occurrence over the whole Fennoscandian Shield thus implies that it could represent a pervasive remagnetization event of the entire shield and may, thus, have regional importance. However, the position of the B pole does not match with any known Precambrian poles of the Fennoscandian Shield. Therefore, the possibility that pole B represents a Paleozoic overprint is considered. Figure 30 shows the present Paleozoic APWP where the B pole has been inverted. This option will be discussed later.

Components SB₁ and SB₂

SB₁

Component SB₁ was obtained in three shear zones, PU, EE and LE. The same remanence component was isolated in part of the host Svecofennian rocks close to the shear zones. Based on comparison of the SB₁ pole with the ‘key poles’ (Fig. 29), remanence component SB₁ was acquired at ca. 1.63 Ga. The pole is in accord with the pole obtained from the quartz porphyry dikes related to the Wyborg (Neuvonen 1986) and the Onas (Törnroos 1984 and Mertanen & Pesonen, 1995) rapakivi granites in southern Finland.

Subjotnian rapakivi granites and associated diabase and quartz porphyry dikes were emplaced in high crustal levels, close to the present erosional levels during the intracontinental rifting and extensional stage of the already cooled Svecofennian basement (Kosunen 2004, Rämö 1991 and Vaasjoki 1977). Simultaneously with the emplacement of rapakivi intrusions and dikes, the basement was affected by a NW-SE directed stress field which caused normal faulting in that direction. The basement between the NW-SE faults is transected by both NE-SW and NW-SE trending brittle structures that also cut the rapakivi granites (Elminen et al. 2008, this volume). It is suggested that these brittle fractures have been most vulnerable to later reactivation and remagnetizations.

It is interpreted that the SB₁ remanence component was acquired at the time of the emplacement of rapakivi intrusions and related dikes. It is implied that fluids migrating along fractures were locally able to remagnetize the Svecofennian basement rocks. The remanence is interpreted as a chemical

remanent magnetization (CRM) residing in hematite. The CRM and associated alteration in the shear zones are direct evidence for later activity, in which the shear zones may have also vented excess heat during the regional crustal extension. Accordingly, the remanence may also represent a thermochemical remanent magnetization (TCRM).

Site EE with breccia shows a variety of remanence components. It is interpreted that the breccia was formed during Subjotnian time when fluids were probably expelled from the rapakivi granites and were moving in the shear zones. New hematite was formed in this process and its remanence was blocked. The host granitoids were influenced by the same fluids, but because of being much more impervious they were not totally remagnetized, but still show the Svecofennian A direction. On the other hand, preservation of an A direction in one of the breccia samples suggest that the fluidization took place at low temperatures.

In the case of the protomylonitic gneiss at site PU, the mechanisms of remagnetization may be several. Site PU is located within a distance of possible contact metamorphic heating effect of the Wiborg rapakivi batholith which may be partly responsible for the occurrence of remanence component SB₁. Although not reliably determined, the host gneiss at site PU also carries the SB₁ component, thus implying a more pervasive remagnetization in the area.

SB₂

Remanence component SB₂ was obtained at three sites, MU, KA and KB in the Porkkala-Mäntsälä shear zone. The similarity of remanence directions between the sites suggest that the rocks in the Porkkala-Mäntsälä shear zone, whether taken from clearly deformed mylonitic rocks or from the less deformed granite dike (site KB), acquired their remanence simultaneously in the same geological event. The pole position of component SB₂ deviates significantly from pole SB₁ (Fig. 29). Based on the similarity of the SB₂ pole to the 'key poles', the age of SB₂ is ca. 1.58 Ga (Fig. 29). It is curious that component SB₂ was isolated in the Porkkala-Mäntsälä shear zone in particular because it is thought to have been active at ca. 1.64 Ga, during the emplacement of the Bodom and Onas rapakivi granites (Kosunen 2004 and Elminen 1999). However, contrary to expectations, no remanence component comparable to SB₁, defined as 1.63 Ga, was obtained. Furthermore, compared to the low intensity and rather unstable behaviour of component SB₁ in the other shear zones, component SB₂ is extremely stable.

It is probable that the main reactivation and remagnetization of the Porkkala-Mäntsälä shear zone

took place at ca. 1.64 Ga. However, it is possible that due to the extensive size of the Porkkala-Mäntsälä shear zone, it was more vulnerable to repeated reactivation and eventually to total overprinting that resulted in the acquisition of component SB₂ at ca. 1.58 Ga. The remagnetization event at late stages of the rapakivi event lent support from ⁴⁰Ar/³⁹Ar studies (Heeremans & Wijbrans 1999 and Murrell 2003) that indicate local reactivation of the Porkkala-Mäntsälä shear zone even as late as at ca. 1.5 Ga.

However, the source of ca. 1.58 Ga remagnetizing fluids in the study area is not clear. Thermal demagnetizations and thermomagnetic analyses indicate that component SB₂ may reside in titanomagnetite that has been partly oxidized from titanomagnetite, whereas component SB₁ is principally carried by hematite. Therefore, it is possible that hydrothermal flow events took place in two different pulses during Subjotnian, at ca. 1.63 Ga and 1.58 Ga.

Furthermore, like for component B, another origin is considered for component SB₂. As was evident from the other shear zones, Ti-magnetite is probably the principal remanence carrier of component C. As will be discussed later, it is implied that magnetization C was acquired during Middle Paleozoic time. Therefore, based on the observation that both component C and component SB₂ are carried by the same magnetic mineral, the alternative explanation for the origin of component SB₂ may be a reactivation during Paleozoic. This alternative will be discussed later.

Component SB of the diabase dikes

Component SB was obtained in the Kopparnäs dikes KO and KN and in the Nummela dike NU. As discussed before, the remanence directions from the Kopparnäs and Nummela dikes were combined to give a common mean direction, although there were some discrepancies that point to a different origin of remanences in the two dike sets. The corresponding poles with the combined mean pole is shown in Figure 29. The poles are shifted westward from the known Subjotnian key poles with the ages of 1.63, 1.58 and 1.54 Ga. The A95 confidence circles cut the A95 circles of the 1.63, 1.58 and 1.27 Ga key poles, suggesting that within error limits the SB pole could be of any of those ages. Consequently, based purely on comparison with the known Precambrian key poles, no certain age for the SB magnetization can be defined.

The poles from the Kopparnäs dikes are close to the 1.63 Ga key pole obtained from the Sipoo quartz porphyry dikes (Plat = 26.4°N, Plong = 180.4°E)

and the Sipoo diabase dikes (Plat = 31.6°N, Plong = 183.6°E, Mertanen & Pesonen 1995). In the Kopparnäs diabase dikes, the remanence has normal polarity (NE pointing remanence direction), whereas the Sipoo diabase dikes display reversed polarity (the remanence pointing SW). In Sipoo area the normal polarity pole was obtained only in the quartz porphyry dikes where it was interpreted to represent a slightly later magnetization than the reversed polarity pole of the diabase dikes. The age difference between different polarity episodes is not significant within the framework of geological time and therefore the paleopoles of the Kopparnäs dykes may record the magnetic field at ca. 1.63 Ga.

Pole SB from the Kopparnäs dikes deviates slightly from the pole of the Nummela dike where it was isolated in three samples, two of the samples showing reversed polarity and one showing normal polarity. The dikes are not isotopically dated, but according to Kosunen et al. (2004), the initial Nd values of the Kopparnäs and Vihti (Nummela) dikes imply a different magma source for the two dike sets, and hence, they could be of different age. The Nummela SB pole is concordant with the 1.27 Ga key pole and also with the C pole of the shear zones, which is inferred to represent a secondary magnetization. The limited number of samples prevents proper considerations of the age of magnetization SB of the Nummela dykes, although it can be speculated that either the Nummela dykes are younger than the Kopparnäs dykes or they are totally remagnetized.

Component C

Pole C (Fig. 29) represents the characteristic remanence of the shear zones. The remanence has dual polarity. The reversed polarity direction is dominating in most of the studied shear zones, whereas normal polarity magnetization was observed rather sporadically. Pole C matches well with the 1.27 Ga key pole of the Fennoscandian Shield and, consequently, it may represent a Postjotnian remagnetization.

Postjotnian time is delineated by rifting and emplacement of mafic dike swarms in western and SW Finland and in Sweden at ca. 1.27 Ga (e.g. Suominen 1991). However, in the present study area there is no evidence of magmatic activity of that age. Coeval mafic dike swarms occur worldwide in other cratons such as the Laurentian and Amazonian cratons. Based on recent continental reconstructions (Elming & Mattson 2001, Pesonen et al. 2003 and Mertanen & Pesonen 2005), rifting both in the Fennoscandian Shield and Laurentia, where the cra-

ton is transected by the extensive Mackenzie and Sudbury dike swarms (e.g. LeCheminant & Heaman 1989), resulted from the separation of the two continents. The rifting was a globally extensive event and, consequently, it may have been partly responsible also for the formation of faults and fractures in southern Finland, and may have resulted to the remagnetization of these structures. In Mertanen et al. (2001) it was suggested that the so-called pole J (pole C of this work) isolated in the Porkkala-Mäntsälä shear zone, could represent reactivation during the Postjotnian. Hence, the pole could be an expression of Postjotnian tectono-magmatic events far from the sites where these formations are exposed. Based on $^{40}\text{Ar}/^{39}\text{Ar}$ datings in southern Finland, Heeremans and Wijbrans (1999) suggested that a fault activation, including the Porkkala-Mäntsälä shear zone, took place during the Postjotnian tectonic events and that the latest brittle fracturing of the Porkkala-Mäntsälä shear zone took place during the Sveconorwegian orogenic events. Thus, based on $^{40}\text{Ar}/^{39}\text{Ar}$ data, the reactivation covers a time span from of ca. 1300–950 Ma.

However, the overall dual polarity, coupled with the dominance of reversed polarity of the C component does not fit with the interpretation of Postjotnian age. The Postjotnian magnetization is shown to be exclusively of normal polarity (Neuvonen 1965, 1966, 1973 and Neuvonen & Grundström 1969). Therefore, although a Postjotnian magnetization age is not conclusively excluded, another source for the origin of component C is considered.

When pole C is switched to opposite polarity (Fig. 30), it matches well with the Early Ordovician to Permian segment of the APWP (e.g. Torsvik et al. 1996, Smethurst, et al. 1998 and Torsvik & Rehnström 2001 and 2003), giving an age of ca. 415 Ma. The origin of magnetization is discussed in the light of this age.

The geological evolution of the central Fennoscandian Shield is mainly restricted to events that took place during the Precambrian, with a few exceptions of younger Paleozoic events. However, in the areas surrounding the craton, in NW Russia, Estonia, and Denmark, the bedrock is largely covered by Neoproterozoic to Late Paleozoic sedimentary deposits. Based mainly on previous fission track dates for the Fennoscandian Shield (Larson et al. 1999), it has been proposed that the entire Fennoscandian Shield has experienced several Paleozoic tectonic phases with considerable uplift and subsidence with characteristic rock records since Neoproterozoic (Kohonen & Rämö 2002 and 2004).

It has been suggested that during Neoproterozoic (> 650 Ma), the crystalline basement of the Fennoscandian Shield was exposed over large areas due to

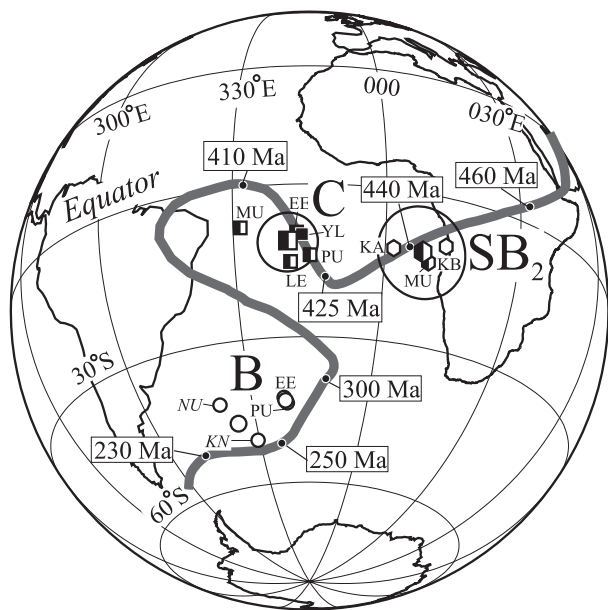


Figure 30. Fennoscandian APW path (Torsvik et al. 1996, 2001, Torsvik & Rehnström 2001, 2003 and Smethurst et al. 1998) with relevant ages indicated. Components B, C and SB₂ are switched to opposite polarity from their positions in Figure 29. For explanations, see Figure 29.

uplift and exhumation of the Shield (Kohonen & Rämö 2004 and Konsa & Puura 1999). No sedimentary rocks of Late Neoproterozoic age occur, comparable to the deposition of Cryogenian (850–600 Ma) sediments directly on top of the crystalline basement in Estonia and Russia. According to Kohonen & Rämö (2004), a sedimentary cover was present during a subsequent platform stage at ca. 600–415 Ma, as a response of break-up of the Rodinia supercontinent and opening of the Iapetus Ocean in the west, when shallow marine continental margin sediments were deposited. These, and younger deposits are still preserved in Estonia and NW Russia, in the Bay of Bothnia and sporadically on some inland outcrops in Finland. It has been suggested, however, that the entire Fennoscandian Shield may have been covered by thick platform sediments during Early Paleozoic (Kohonen & Rämö 2004). During Silurian-Devonian, the Fennoscandian Shield collided with Laurentia resulting to the closure of the Iapetus Ocean and formation of the Caledonian orogenic belt. During the collisional event at about 425 Ma, the Fennoscandian Shield and Laurentia were located at the equator, and the Fennoscandian Shield was still drifting slightly northward, whereas Laurentia was stationary (Torsvik et al. 1996).

Based on fission-track thermochronometry analyses (Larson et al. 1999 and Tullborg et al. 1996) that indicate a slight increase of temperature due to burial under sedimentary cover, it has been suggested that sediments eroded from the Caledo-

nian orogen were deposited as far as eastward of the Fennoscandian Shield. On the basis of recent apatite fission-track thermochronometry analyses, Murrell (2003) argues, however, that the Caledonian foreland basin did not extend to Finland, but the area is delineated by passive margin and platform deposition during Cambro-Silurian. Furthermore, it is suggested (Larson et al. 1999 and Kohonen & Rämö 2004) that at 250 Ma ago, the thickness of the platform sediments in Finland was 0.5–1.5 kilometers and that the final exhumation of the Fennoscandian Shield took place no earlier than during Late Paleozoic.

Based on the location of the C pole on the APWP (Fig. 30), the age of pole C of ca. 415 Ma matches well with the timing of the Caledonian orogeny. So far, there are no other paleomagnetic evidence from the Precambrian basement that points to a Paleozoic remagnetization in Finland. However, considering the position of Finland between the margins of the Caledonian orogens (the Caledonian Front in the North, Caledonian margin in the West, and Tornquist margin in the SW), the most probable origin for the C component is related to tectono-sedimentary events of the Caledonian orogeny. According to Airo et al. (2008, this volume), the magnetic lineament related to the NE-SW striking Porkkala-Mäntsälä shear zone may extend for more than 200 km SW from southern Finland over to Latvia. The lineament, which thus represents a megastructure of the crust, parallels the Caledonian front, although the original zone of weakness may derive from Svecofennian tectonic events. It can be implied anyway that the tectonic structures in the study area are of more regional than of local scale.

Several mechanisms may be responsible for the remagnetization. Based on magneto-mineralogical evidence that verifies a low-temperature oxidation, it is suggested that the main origin of C remagnetization may be basinal fluids that have moved along the fault zones and resulted to the formation of a chemical remanent magnetization (CRM). The source of fluids may be simply tectonic (see Oliver 1986), originating from the Caledonian front proper, as a result of collision between the Fennoscandian Shield and Laurentia. The mylonitic rocks and shear zones have evidently played a vital role as the channels for fluids, although the effect of fluid flow may have been more pervasive, and not just locally restricted to the shear zones proper.

On the basis of the occurrence of component C both in the mylonitic rocks as well as in some of the Precambrian basement rocks, it is implied that the causal mechanism involved in the remagnetization, may have been burial diagenesis. Remagnetization involving burial, coupled with movement of fluids

in the underlying basement, may record the previous existence of a platform cover (see Elmore et al. 1998 and McCabe & Elmore 1989). The remagnetizations were likely to involve chemical and low-temperature thermal processes acting during burial. It is possible that the overlying sediments have imparted excess heat to the fluids and thus the remanence could be TCRM. Studies on the Athabasca basin (Kotzer et al. 1992) have shown that uranium deposits and coeval remagnetization were formed due to mixing of basement and basinal fluids that moved upwards near and across the unconformity between the basement rocks and sediments. Similarly, Geissman and Harlan (2002) have shown the acquisition of a secondary magnetization due to fluids migrating within the nonconformity between the Archaean-Proterozoic basement rocks and late Paleozoic sedimentary rocks in Rocky Mountains. An analogous process seems to have prevailed also in the shear and fault zones in southern Finland where a pervasive mild reheating event related to burial after Caledonian orogeny, coupled with tectonic uplift, resulted in the movement of fluids in the fractures that were responsible for the remagnetizations.

The C component was not isolated at the two sites, KA and KB, close to the Porkkala-Mäntsälä shear zone. The characteristic component of sites KA, KB and MU is component SB₂. Site KA is defined by brittle structures, but the same well-defined and well-grouped magnetization also occurs at site KB within the porphyritic granitic dike and the Svecofennian host gneisses. Because of the closeness of the rapakivi granites and Porkkala-Mäntsälä zone, the most probable origin for this magnetization is Subjotnian fluid related reactivation, as discussed before. On the other hand, because of the diversity of rock types where the SB₂ magnetization occurs, it is also possible that it represents a secondary magnetization related to Paleozoic regional reactivation event. The pole fits well with the Phanerozoic APW path (Torsvik et al. 1996) and gives an Early Ordovician age of ca. 440 Ma. Furthermore, pole SB from the Kopparnäs-Nummela dikes, especially the Nummela dike, compares well with the C pole. Therefore, as pointed out before, there is a possibility that the Nummela dike may have been remagnetized also in the same Paleozoic event as the shear zones, at about 415 Ga ago.

Isotopic evidences supporting Paleozoic remagnetization

The protomylonitic gneiss of site PU in Pukkila was investigated already in late 1970's, when Vaasjoki (1977) studied galena mineralization associated

with rapakivi granites. According to the results, and based on recent results on U-Pb analyses of uraninites and allanites from sheared deposits (Vaasjoki et al. 2002 and 2004), oxidizing supergene fluids (< 100°C) in the fracture zones caused enrichment of uranium at ca. 450–400 Ma. Vaasjoki et al. (2002 and 2004) suggest that the remobilisation of fluids is probably related to the Precambrian – Paleozoic unconformity after Paleozoic sedimentation and burial of the stable platform. The age represents a mean age from several uraninite formations in southern Finland. Furthermore, recent Sm-Nd isotopic (Alm et al. 2004 and Sundblad et al. 2004) and Pb-Pb (Sundblad et al. 2002) studies on fluorite-calcite-galena bearing veins in the southern Fennoscandian Shield also point to a reactivation at ca. 400 Ma. According to these studies, fluorite-calcite-galena bearing veins cut both the Precambrian basement and Cambrian sedimentary rocks in Sweden and southern Finland. For instance, the Sm-Nd age of the fluorites in Lovisa, augmented by representative data from the host Wyborg rapakivi granite, is 402±32 Ma (Sundblad et al. 2004). Sundblad et al. (2004) suggest that these mineralized zones were formed from low-temperature (60–190°C) fluids that leached the elements from Precambrian crystalline rocks, and that the vein formation is possibly related to the stress field induced by the Caledonian orogeny.

As presented before, the fission-track ages in southern Finland (Murrell 2003) point to the Paleozoic reactivation of the crust between 250–500 Ma. According to Murrell (2003) the Paleozoic re-heating culminated at ca. 430 Ma in the order of 75 °C. The apatite fission-track thermochronometry age of the sample from the Porkkala-Mäntsälä shear zone is 419±15 Ma, which is in agreement with paleomagnetic data presented in this study.

Paleozoic origin of component B

As pointed out previously, pole B, which was obtained both in the shear zones and in the dikes, does not match with any known Precambrian key poles of the Fennoscandian Shield. However, it compares well with the known Permian poles when inverted to opposite polarity, and plotted on the Phanerozoic APWP (Torsvik et al. 1996 and Torsvik & Rehnström 2003). Furthermore, the obtained poles are remarkably similar to the secondary pole obtained in the Cambro-Ordovician sediments in Estonia (Plado et al. 2001 and 2002). In Estonia, the well-dated Cambro-Ordovician sediments have experienced pervasive dolomitization. However, the exact age and mechanisms of dolomitization are still

poorly known. Puura et al. (1996) suggested that the dolomitization reflects a thermal effect of the Oslo rifting during Carboniferous-Permian time. As dolomitization is accompanied by recrystallization of magnetic minerals, the dolomites have acquired a chemical remanent magnetization, which has been dated by using the APWP. Preliminary paleomagnetic results from the Estonian sediments suggest

that, in addition to occurrence of other older secondary remanence components, the latest dolomitization event took place during Permian (Plado et al. 2001 and 2002). Therefore, although based on limited data, it is implied that the same late 'secondary' processes seen in the Estonian sediments, are possibly seen in the shear and fault zones as remagnetizations in Finland.

CONCLUSIONS

The complexity of remagnetizations in the fault and shear zones of the Paleoproterozoic crust of southern Finland is reflected both in the variety of magnetic minerals and in the existence of several remanence components. This indicates the multiphase evolution of the crustal weakness zones that have been repeatedly reactivated in successive regional and global scale geological events during Mesoproterozoic and Paleozoic time.

- 1) Based on the closeness of the virtual geomagnetic pole to the known 1.88 and 1.84 Ga key poles, the oldest remanence component A was acquired during the Svecofennian orogenic events. Although not fully matching with the known key poles, the remanence probably represents the original Svecofennian magnetization that has preserved in some of the studied locations.
- 2) The first major reactivation of the shear zones after the Svecofennian events took place during Subjotnian time, evidently in different stages at ca. 1.63 and 1.58 Ga when components SB₁ and SB₂, respectively, were acquired.

It is suggested that component SB₁ was acquired at ca. 1.63 Ga during the extensional phase at the time of the rapakivi intrusions and related dikes, when chemical or thermochemical remanent magnetizations (CRM/TCRM) were formed due to fluid migration along the faults. In that process, new hematite, which is the main carrier of magnetization SB₁, was precipitated.

Remanence component SB₂ was obtained at three studied sites, all located in the Porkkala-Mäntsälä shear zone. Based on comparison to the Precambrian key poles, the age of component SB₂ is ca. 1.58 Ga. The difference of ages of poles SB₁ and SB₂ may thus imply fluid activity and remagnetization that lasted about 50 Ma. Component SB₂ possibly resides in titanomaghemite that has been partly oxidized from titanomagnetite.

Consequently, magnetic minerals, precipitated in the two hydrothermal fluid flow events during Subjotnian at 1.63 Ga and 1.58 Ga, signify different compositions of fluids. On the other hand, pole SB₂ fits well to the Phanerozoic APW path, giving an age of 440 Ma. It is therefore suggested that remanence component SB₂ may also have been formed in the tectonic events related to the Caledonian orogeny.

- 3) The most common remanence component obtained in the shear zones, is component C. It probably resides in titanomaghemite, and it shows dual polarity. Based on its pole position on the Phanerozoic APW path, component C was acquired during Late Silurian – Early Devonian, at ca. 415 Ma. It is proposed that component C was formed due to tectonic stress caused by the Caledonian orogeny, which resulted in the movement of fluids in the shear zones and fractures. In addition, it is implied that pervasive mild reheating event related to burial after the Caledonian orogeny is partly responsible for the remagnetization.
- 4) Pole B represents a magnetization that has been sporadically obtained over the whole Fennoscandian Shield. In this study it was obtained both in the shear zones and in the diabase dikes. Pole B does not match with any known Precambrian key poles, but it compares well with the Phanerozoic paleopoles, attesting to a Carboniferous-Permian age of ca. 300–230 Ma. It is implied that it may be related to the late sedimentary processes after the Caledonian orogeny.
- 5) In addition to shear zones, three Subjotnian diabase dikes were studied; two in Kopparnäs and one in Nummela. The dikes carry remanence component SB that is suggested to represent the

primary, ca. 1.63 Ga remanence of the dikes. However, the pole from the Nummela dike differs to some extent from the Kopparnäs dikes, being in more agreement with pole C. Therefore, there is a possibility that the Nummela dike was more affected by the fluid events related to the Caledonian orogeny, and acquired its remanence at ca. 415 Ma. Alternatively, the remanence of the Nummela dike may be of primary origin, in which case the Nummela dike is slightly younger than the Kopparnäs dikes.

In this study we have investigated the usefulness of paleomagnetic method to date multiple events in the shear zones. The results have shown that a variety of magnetic minerals were formed in the later geological processes and as well as the complexity of tectonic stress effects onto the magnetization. The results shown here were obtained sporadically in the faults and shear zones throughout the capital area of Finland. In order to verify these results, more thorough investigations on single structures need to be carried out in the future.

ACKNOWLEDGEMENTS

Matti Leino is acknowledged for all his assistance in the field and in the paleomagnetic laboratory of GTK, and for constantly improving the analysing programs. Markku Kääriä and Tuula Laine made the paleomagnetic and rock magnetic measurements. Markku Kääriä also helped out in drawing the figures. Peik Aura, Gustav Westerlund and Viveca

Lindqvist assisted in sampling in the field. Lassi Pakkanen made the microprobe analysis. The work of all these people are sincerely appreciated. The manuscript was reviewed by David T.A. Symons who is greatly acknowledged for his constructive remarks.

REFERENCES

- Airo, M.-L. 2002.** Aeromagnetic and aeroradiometric response to hydrothermal alteration. *Surveys in Geophysics* 23, 273–302.
- Airo, M.-L., Elminen, T., Mertanen, S., Niemelä, R., Pajunen, M., Wasenius, P. & Wennerström, M. 2008.** Aerogeophysical approach to ductile and brittle structures in the densely populated urban Helsinki area, southern Finland. In: Pajunen, M. (ed.) *Tectonic evolution of the Svecofennian crust in southern Finland – a basis for characterizing bedrock technical properties*. Geological Survey of Finland, Special Paper 47, 283–308.
- Alm, E., Huhma, H. & Sundblad, K. 2004.** Preliminary Palaeozoic Sm-Nd ages of fluorite-calcite-galena mineralization in the margins of the Fennoscandian Shield. In: Kaakinen, A. (ed.) *Geologian 3. tutkijapäivät 10.–11.3.2004*, Helsinki, 47.
- Andersen, T. B., Torsvik, T. H., Eide, E. A., Osmundsen, P. T. & Faleide, J. I. 1999.** Permian and Mesozoic extensional faulting within the Caledonides of central south Norway. *Journal of the Geological Society of London* 156, 1073–1080.
- Buchan, K., Mertanen, S., Elming, S.-Å., Park, R. G., Pesonen, L. J., Bylund, G. & Abrahamsen, N. 2000.** The drift of Laurentia and Baltica in the Proterozoic: a comparison based on key paleomagnetic poles. *Tectonophysics* 319, 167–198.
- Butler, R. F. 1992.** *Paleomagnetism: magnetic domains to geologic terranes*. Blackwell Scientific Publications, USA. 319 p.
- Dunlop, D. J. & Özdemir, Ö. 1997.** *Rock Magnetism: Fundamentals and Frontiers*, Cambridge Studies in Magnetism. Cambridge: Cambridge University Press. 573 p.
- Eide, E. A., Torsvik, T. H. & Andersen, T. B. 1997.** Absolute dating of brittle fault movements; Late Permian and Late Jurassic extensional fault breccias in western Norway. *Terra Nova* 9, 135–139.
- Elminen, T. 1999.** Porkkala-Mäntsälä -siirrosvyöhykkeen kuvaus ja tulkinta. Unpublished M.Sc thesis, University of Helsinki. 87 p. (in Finnish)
- Elminen, T., Airo, M.-L., Mertanen, S. & Pajunen, M. 2003.** Multiple reactivations of the Porkkala-Mäntsälä shear zone, southern Finland. In: *Deformation mechanisms, rheology and tectonics*, St. Malo, France, 14–16 April 2003. Abstract volume, 53.
- Elminen, T., Airo, M.-L., Niemelä, R., Pajunen, M., Vaarma, M., Wasenius, P. & Wennerström, M. 2008.** Fault structures in the Helsinki Area, southern Finland. In: Pajunen, M. (ed.) *Tectonic evolution of the Svecofennian crust in southern Finland – a basis for characterizing bedrock technical properties*. Geological Survey of Finland, Special Paper 47, 185–213.
- Elming, S.-Å. 1985.** A palaeomagnetic study of Svecofennian basic rocks from northern Sweden. *GFF* 107, 17–35.
- Elming, S.-Å. 1994.** Palaeomagnetism of Precambrian rocks in northern Sweden and its correlation to radiometric data. *Precambrian Research* 69, 61–79.
- Elming, S.-Å. & Mattson, H. 2001.** Post Jotnian basic intrusions in the Fennoscandian Shield, and the break

- up of Baltica from Laurentia; a palaeomagnetic and AMS study. *Precambrian Research* 108, 215–236.
- Elmore, R. D., Campbell, T., Banerjee, S. & Bixler, W. G. 1998.** Palaeomagnetic dating of ancient fluid-flow events in the Arbuckle Mountains, southern Oklahoma. In: Parnell, J. (ed.) *Dating and duration of fluid flow and fluid-rock interaction*. Geological Society Special Publications 144, 9–25.
- Fisher, R. 1953.** Dispersion on a sphere. *Proceedings of the Royal Society of London, Serie A* 217, 293–305.
- Geissman, J. W. & Harlan, S. S. 2002.** Late Paleozoic remagnetization of Precambrian crystalline rocks along the Precambrian/Carboniferous nonconformity, Rocky Mountains; a relationship among deformation, remagnetization, and fluid migration. *Earth and Planetary Science Letter* 203, 905–924.
- Heeremans, M. & Wijbrans, J. 1999.** Late Proterozoic tectonic events in southern Finland, constrained by $^{40}\text{Ar}/^{39}\text{Ar}$ incremental heating and single spot fusion experiments on K-feldspars. *Terra Nova* 11, 216–222.
- Hrouda, F. 1994.** A technique for the measurement of thermal changes of magnetic susceptibility of weakly magnetic rocks by the CS-2 apparatus and KL-2 Kappabridge. *Geophysical Journal International* 118, 604–612.
- Huhma, A. 1981.** Youngest Precambrian dyke rocks in North Karelia, East Finland. *Bulletin of The Geological Society of Finland* 53 (2), 67–82.
- Kelso, P. R., Banerjee, S. & Worm, H.-U. 1991.** The effect of low-temperature hydrothermal alteration on the remanent magnetization of synthetic titanomagnetites: A case for acquisition of chemical remanent magnetization. *Journal of Geophysical Research* 96, 19,545–19,553.
- Kirschvink, J. L. 1980.** The least-squares line and plane and the analysis of palaeomagnetic data. *Geophysical Journal of the Royal Astronomical Society* 62, 699–718.
- Kohonen, J. & Rämö, T. 2002.** Sedimentary record and magmatic episodes reflecting Mesoproterozoic-Phanerozoic Evolution of the Fennoscandian Shield. In: Lahtinen, R., Korja, A., Arhe, K., Eklund, O., Hjelt, S.-E. & Pesonen, L. J. (eds.) *Lithosphere 2002 – Second symposium on the structure, composition and evolution of the lithosphere in Finland*. Programme and extended abstracts. Institute of Seismology, University of Helsinki, Report S–42, 23.
- Kohonen, J. & Rämö, T. 2005.** Sedimentary rocks, diabases, and late cratonic evolution. In: *Precambrian geology of Finland: key to the evolution of the Fennoscandian Shield*. Developments in Precambrian geology 14. Amsterdam: Elsevier, 563–603.
- Konsa, V. & Puura, V. 1999.** Provenance of zircon of the lowermost sedimentary cover, Estonia, East European Craton. *Bulletin of the Geological Society of Finland* 71, 253–273.
- Kosunen, P. 2004.** Petrogenesis of mid-Proterozoic A-type granites: case studies from Fennoscandia (Finland) and Laurentia (New Mexico). PhD thesis, University of Helsinki, Department of Geology. 170 p.
- Kotzer, T. G., Kyser, T. K. & Irving, E. 1992.** Paleomagnetism and the evolution of fluids in the Proterozoic Athabasca Basin, northern Saskatchewan, Canada. *Canadian Journal of Earth Sciences* 29, 1474–1491.
- Larson, S. Å., Tullborg, E.-L., Cederbom, C. & Stiberg, J.-P. 1999.** Sveconorwegian and Caledonian foreland basins in the Baltic Shield revealed by fission-track thermochronology. *Terra Nova* 11, 210–215.
- LeCheminant, A. N. & Heaman, L. M. 1989.** Mackenzie igneous events, Canada: middle Proterozoic hotspot magmatism associated with ocean opening. *Earth Planet. Sci. Lett.* 96, 38–48.
- Leino, M. A. H. 1991.** Paleomagneettisten tulosten monikomponenttianalyysi pienimmän neliösumman menetelmällä. (Multicomponent analysis of palaeomagnetic results by least square method). Laboratory for Palaeomagnetism, Department of Geophysics, Geological Survey of Finland, unpublished report Q 29.1/91/2. 15 p. (in Finnish)
- McCabe, C. & Elmore, R. D. 1989.** The occurrence and origin of late Paleozoic remagnetization in the sedimentary rocks of North America. *Reviews of Geophysics* 27, 471–494.
- McFadden, P. L. & McElhinny, M. W. 1990.** Classification of the reversal test in palaeomagnetism. *Geophysical Journal International*, 103, 725–729.
- Mertanen, S., Pesonen, L. J., Huhma, H. & Leino, M. A. H. 1989.** Palaeomagnetism of the Early Proterozoic layered intrusions, northern Finland. *Geological Survey of Finland, Bulletin* 347. 40 p.
- Mertanen, S. & Pesonen, L. J. 1992.** Palaeomagnetism of the Early to Middle Proterozoic mafic intrusions in northern Finland. In: *International Symposium, IGCP Project 275 – Deep Geology of the Baltic (Fennoscandian) Shield and IGCP Project 257 – Precambrian Dike Swarms, Petrozavodsk 1992*. Abstracts, 57–59.
- Mertanen, S. & Pesonen, L. J. 1995.** Palaeomagnetic and rock magnetic investigations of the Sipoo Subjotnian quartz porphyry and diabase dykes, southern Fennoscandia. *Physics of the Earth and Planetary Interiors* 88, 145–175.
- Mertanen, S., Pesonen, L. J. & Vuollo, J. 1998.** Preliminary study of the palaeomagnetism of mafic dykes in the Kola Peninsula. *Geological Survey of Finland, unpublished report Q 29.1/98/2*. 19 p.
- Mertanen, S., Pajunen, M. & Elminen, T. 2001.** Applying palaeomagnetic method for dating young geological events. In: Autio, S. (ed.) *Geological Survey of Finland, Current Research 1999–2000*. Geological Survey of Finland, Special Paper 31, 123–129.
- Mertanen, S. & Pesonen, L. J. 2005.** Drift history of the shield. In: *Precambrian geology of Finland: key to the evolution of the Fennoscandian Shield*. Developments in Precambrian geology 14. Amsterdam: Elsevier, 645–668.
- Murrell, G. R. 2003.** The long-term thermal evolution of central Fennoscandia, revealed by low-temperature thermochronometry. PhD thesis, Vrije Universiteit Amsterdam. 219 p.
- Neuvonen, K. J. 1965.** Palaeomagnetism of the dike systems in Finland, i. Remanent magnetization of Jotnian

- olivine dolerites in southwestern Finland. *Comptes Rendus, Geol. Soc. Finl.*, 37, 153–168.
- Neuvonen, K. J. 1966.** Palaeomagnetism of the dike systems in Finland, ii. Remanent magnetization of dolerites in the Vaasa archipelago. *Comptes Rendus Geol. Soc. Finl.*, 38, 275–281.
- Neuvonen, K. J. 1973.** Remanent magnetization of the Jotnian sandstone in Satakunta, SW-Finland. *Geol. Surv. Finl. Bull.* 45, 23–27.
- Neuvonen, K. J. 1986.** On the direction of remanent magnetization of the quartz porphyry dikes in SE Finland. *Bull. Geol. Soc. Finland* 58 (1), 195–201.
- Neuvonen, K. J. & Grundström, L. 1969.** Paleomagnetism of the dike systems in Finland, iv. Remanent magnetization of the dolerite and related dikes in the land archipelago. *Geol. Surv. Finl. Bull.* 41, 57–63.
- Neuvonen, K. J., Korsman, K., Kouvo, O. & Paavola, J. 1981.** Paleomagnetism and age relations of the rocks in the Main Sulphide Ore Belt in central Finland. *Bull. Geol. Soc. Finland* 53, 109–133.
- Neuvonen, K. J., Pesonen, L. J. & Pietarinen, H. 1997.** Remanent Magnetization in the Archaean Basement and Cutting Diabase Dykes in Finland, Fennoscandian Shield. *Geophysica* 33(1), 111–146.
- Oliver, J. 1986.** Fluids expelled tectonically from orogenic belts: their role in hydrocarbon migration and other geologic phenomena. *Geology* 14, 99–102.
- O'Reilly, W. 1983.** The identification of titanomagnhemites: model mechanisms for the magnetization and inversion processes and their magnetic consequences. *Physics of the Earth and Planetary Interiors* 31, 65–76.
- Özdemir, Ö. 1987.** Inversion of titanomagnhemites. *Physics of the Earth and Planetary Interiors* 46, 184–196.
- Pajunen, M., Elminen, T. & Wennerström, M. (ed.) 2001.** Kallioperän heikkousvyöhyke- ja rakennettavuusmallin kehittäminen taajamaympäristöön. Geological Survey of Finland, unpublished report K 21.42/2000/1. 61 p. (in Finnish)
- Pajunen, M., Airo, M.-L., Elminen, T., Niemelä, R., Salmelainen, J., Vaarma, M., Wasenius, P. & Wennerström, M. 2002.** Kallioperän rakennettavuusmalli taajamiin. Menetelmäkehitys ja ohjeistus. Geological Survey of Finland, unpublished report K 21.42/2002/5. 95 p. (in Finnish).
- Pajunen, M., Airo, M.-L., Elminen, T., Mänttari, I., Niemelä, R., Vaarma, M., Wasenius, P. & Wennerström, M. 2008.** Tectonic evolution of the Svecofennian crust in southern Finland. In: Pajunen, M. (ed.) Tectonic evolution of the Svecofennian crust in southern Finland – a basis for characterizing bedrock technical properties. Geological Survey of Finland, Special Paper 47, 15–160.
- Pesonen, L. J. & Stigzelius, E. 1972.** On petrophysical and paleomagnetic investigations of the gabbros of the Pohjanmaa region, Middle-West Finland. *Geol. Surv. Finland, Bull.* 260, 1–27.
- Pesonen, L. J. & Neuvonen, K. J. 1981.** Paleomagnetism of the Baltic Shield – Implications for Precambrian Tectonics. In: Kröner, A. (ed.) Precambrian Plate Tectonics. Amsterdam: Elsevier, 623–648.
- Pesonen, L. J., Elming, S.-Å., Mertanen, S., Pisarevski, S., D'Agrella-Filho, M. S., Meert, J., Schmidt, P. W., Abrahamsen, N. & Bylund, G. 2003.** Palaeomagnetic configuration of continents during the Proterozoic. *Tectonophysics* 375, 289–324.
- Plado, J., Kirsimäe, K. & Pesonen, L. J. 2001.** Palaeomagnetic Data of Early Cambrian clays from northern Estonia. In: Airo, M.-L. & Mertanen, S. (eds.) XX Geofysiikan päivät. Helsinki: Geological Society of Finland, 173–178.
- Plado, J., Pesonen, L. J., Kirsimäe, K., Puura, V., Pani, T. & Elbra, T. 2002.** Magnetic overprints in the Silurian Dolomites, central Estonia. In: Lahtinen, R., Korja, A., Arhe, K., Eklund, O., Hjelt, S.-E. & Pesonen, L. J. (eds.) Lithosphere 2002 – Second symposium on the structure, composition and evolution of the lithosphere in Finland. Programme and extended abstracts. Institute of Seismology, University of Helsinki, Report S-42, 111.
- Puranen, R., Pekkarinen, L. J. & Pesonen, L. J. 1992.** Interpretation of magnetic fabrics in the early Proterozoic diabase dykes of Keuruu, central Finland. *Physics of the Earth and Planetary Interiors* 72, 68–82.
- Rämö, O. T. 1991.** Petrogenesis of the Proterozoic rapakivi granites and related basic rocks of southeastern Fennoscandia: Nd and Pb isotopic and general geochemical constraints. Geological Survey of Finland, Bulletin 355. 161 p.
- Smethurst, M. A., Khramov, A. N. & Pisarevsky, S. A. 1998.** Paleomagnetism of the Lower Ordovician Orthoceras Limestone, St. Petersburg, a revised drift history for Baltica in the early Paleozoic. *Geophysical Journal International* 133, 44–56.
- Sundblad, K., Vaasjoki, M. & Alm, E. 2002.** Radiogenic leads from fissures and sandstones within the Fennoscandian shield: Indications of Paleozoic weathering-related enrichment of base metals. In: Lahtinen, R., Korja, A., Arhe, K., Eklund, O., Hjelt, S.-E. & Pesonen, L. J. (eds.) Lithosphere 2002 – Second symposium on the structure, composition and evolution of the lithosphere in Finland. Programme and extended abstracts. Institute of Seismology, University of Helsinki, Report S-42, 129–132.
- Sundblad, K., Alm, E., Huhma, H., Vaasjoki, M. & Sollien, D. B. 2004.** Early Devonian tectonic and hydrothermal activity in the Fennoscandian Shield; evidence from calcite-fluorite-galena mineralization. In: Mertanen, S. (ed.) Supercontinents, remagnetization and geomagnetic modelling. 5th Nordic Paleomagnetic Workshop, Suitia-Helsinki, Finland, September 25–30, 2004. Geological Survey of Finland, unpublished report Q 29.1/2004/1, 67–71.
- Suominen, V. 1991.** The chronostratigraphy of southwestern Finland with special reference to Postjotnian and Subjotnian diabases. Geological Survey of Finland, Bulletin 356, 1–100.
- Tarling, D. H. & Hrouda, F. 1993.** The magnetic anisotropy of rocks. London: Chapman & Hall, 217 p.
- Törnroos, R. 1984.** Petrography, mineral chemistry and petro-chemistry of granite porphyry dykes from Sibbo, southern Finland. *Geol. Surv. Finland, Bull.* 326. 43 p.

- Torsvik, T. H., Stuart, B. A., Swensson, E., Andersen, T. B. & Dewey, J. F. 1992.** Palaeomagnetic dating of fault rocks; evidence for Permian and Mesozoic movements and brittle deformation along the extensional Dalsfjord Fault, western Norway. *Geophysical Journal International* 109, 565–580.
- Torsvik, T. H., Smethurst, M. A., Meert, J. G., Van der Voo, R., McKerrow, W. S., Brasier, M. D., Sturt, B. A. & Walderhaug, H. J. 1996.** Continental break-up and collision in the Neoproterozoic and Palaeozoic – A tale of Baltica and Laurentia. *Earth Science Reviews* 40, 229–258.
- Torsvik, T. H. & Rehnström, E. F. 2001.** Cambrian paleomagnetic data from Baltica: Implications for true polar wander and Cambrian paleogeography. *Journal of the Geological Society of London* 158, 321–329.
- Torsvik, T. H. & Rehnström, E. F. 2003.** The Tornquist Sea and Baltica-Avalonia docking. *Tectonophysics* 362, 67–82.
- Tullborg, E.-L., Larson, S. Å. & Stiberg, J.-P. 1996.** Subsidence and uplift of the present land surface in the southeastern part of the Fennoscandian Shield. *GFF* 118, 126–128.
- Vaasjoki, M. 1977.** Rapakivi granites and other postorogenic rocks in Finland: their age and the lead isotopic composition of certain associated galena mineralizations. *Geological Survey of Finland, Bulletin* 294. 64 p.
- Vaasjoki, M., Rämö, O. T. & Sakko, M. 1991.** New U-Pb ages from the Wiborg rapakivi area: constraints on the temporal evolution of the rapakivi granite-anorthosite-dyke association of southeastern Finland. In: Hapaala, I. & Condie, K. C. (eds.) *Precambrian granitoids – petrogenesis, geochemistry and metallogeny*. *Precambrian Research* 51, 227–243.
- Vaasjoki, M., Appelqvist, H. & Kinnunen, K. A. 2002.** Paleozoic remobilisation and enrichment of Proterozoic uranium mineralisation in the East-Uusimaa area, Finland. In: Lahtinen, R., Korja, A., Arhe, K., Eklund, O., Hjelt, S.-E. & Pesonen, L. J. (eds.) *Lithosphere 2002 – Second symposium on the structure, composition and evolution of the lithosphere in Finland*. Programme and extended abstracts. Institute of Seismology, University of Helsinki, Report S–42, 139.
- Vaasjoki, M., Sundblad, K., Alm, E. & Huhma, H. 2004.** Paleozoic supergene processes in the Precambrian Fennoscandian Shield: radiogenic isotopic evidence. In: Mertanen, M. (ed.) *Supercontinents, remagnetization and geomagnetic modelling*. 5th Nordic Paleomagnetic Workshop, Suitia-Helsinki, Finland, September 25–30, 2004. *Geological Survey of Finland, unpublished report Q 29.1/2004/1*, 67–71.
- Wang, D. & Van der Voo, R. 2004.** The hysteresis properties of multidomain magnetite and titanomagnetite/titanomaghemite in mid-ocean ridge basalts. *Earth and Planetary Science Letters* 220, 175–184.
- Wennerström, M., Airo, M.-L., Elminen, T., Niemelä, R., Pajunen, M., Vaarma, M. & Wasenius, P. 2008.** Orientation and properties of jointing in Helsinki area, southern Finland. In: Pajunen, M. (ed.) *Tectonic evolution of the Svecofennian crust in southern Finland – a basis for characterizing bedrock technical properties*. *Geological Survey of Finland, Special Paper* 47, 253–282.
- Zijderveld, J. D. 1967.** A.C. demagnetization in rocks: analysis of results. In: Collinson, D.W., Creer, K. M. & Runcorn S. K. (eds.) *Methods in paleomagnetism*. New York: Elsevier, 254–286.
- Zhou, W., Van der Voo, R. & Peacor, D. R. 1999.** Preservation of pristine titanomagnetite in older ocean-floor basalts and its significance for paleo-intensity studies. *Geology* 27, 1043–1046.
- Zhou, W., Van der Voo, R., Peacor, D. R., Wang, D. & Zhang, Y. 2001.** Low-temperature oxidation in MORB of titanomagnetite to titanomaghemite; a gradual process with implications for marine magnetic anomaly amplitudes. *Journal of Geophysical Research* 106, B4, 6409–6421.
- Xu, W., Van der Voo, R., Peacor, D. R. & Beaubouef, R. T. 1997.** Alteration and dissolution of fine-grained magnetite and its effects on magnetization of the ocean floor. *Earth and Planetary Science Letters* 151, 279–288.

ORIENTATION AND PROPERTIES OF JOINTING IN HELSINKI AREA, SOUTHERN FINLAND

by

*Marit Wennerström**, *Meri-Liisa Airo*, *Tuija Elminen*, *Reijo Niemelä*,
Matti Pajunen, *Markus Vaarma* and *Pekka Wasenius*

Wennerström, M., Airo, M.-L., Elminen, T., Niemelä, R., Pajunen, M., Vaarma, M. & Wasenius, P. 2008. Orientation and properties of jointing in Helsinki area, southern Finland. *Geological Survey of Finland, Special Paper 47*, 253–282, 29 figures and 2 tables.

Joint properties in the Paleoproterozoic Svecofennian bedrock in the Helsinki area were studied using joint set observations from 687 ice-polished outcrops, road cuts and quarries. Orientations, dimensional and joint wall properties were used for describing the regional pattern of jointing. The study area was divided using lithology and tectonic structures into 6 main sub-areas, the jointing properties of which are described separately.

The joint data show six main orientation groups, which occur in variable frequency across the area. The mapping method of joint set orientations, used in the present study, finds the main joint orientations when compared to tightly measured joint data. The jointing geometry in the Helsinki area involves that early deformation structures control the development of joints and their orientation. One joint set at the outcrops often parallels the main foliation, especially the steep NE-trending foliation in gneisses. Joint zones and shear joints with smooth and slickensided surfaces follow locally the orientation of semi-ductile to semi-brittle fault structures. Long sub-horizontal joints are regular in microcline granites. The frequent occurrence of steeply dipping NE- and NW-trending joint sets in the area implies the connection to regional strain. Sub-vertical NNE-trending cutting joint sets close to the NNE-trending faults probably suggest a new joint phase due to change in the local stress fields as a result of movements in the faults. Well-defined magnetic lineaments show correspondence to parallel joint sets in the field. Jointing which parallels diabase dykes in the western part of the study area refers to brittle fracturing already during the rapakivi magmatism (ca. 1650 Ma).

Key words (GeoRef Thesaurus, AGI): structural analysis, bedrock, joints, orientation, properties, urban environment, Paleoproterozoic, Helsinki, Espoo, Vantaa, Finland

* *Geological Survey of Finland, P.O. Box 96, FI-02151 Espoo, Finland*

* *E-mail: marit.wennerstrom@gtk.fi*

INTRODUCTION

Since the end of the 19th century the Geological Survey of Finland (GTK) has been carrying out a bedrock mapping program. The regional bedrock mapping on the scale of 1 to 100,000 covers almost the whole Finland. Mapping and regional studies of bedrock have predominantly been focused on the characteristics of ductile deformation in the crust. During the last decades more attention has been paid to compilation and appliance of geological data for rock mechanical and environmental applications. The importance of brittle structures in rocks has increased simultaneously with the increase in requirements of underground space for civil activities or the needs of fresh water supply in bedrock. Studies in bedrock fractures, zones of weakness and jointing, will get a great importance in the future in urban areas, where more construction will be directed underground, more traffic lanes will be constructed and the risk of discharges to the ground water increases.

The fractures in bedrock are represented by mechanical breaks involving discontinuities in displacement across surfaces or narrow zones. Joints are opening mode fractures that propagate normal to the least principal stress (σ_3) and in the plane containing σ_1 and σ_2 (e.g. Pollard & Segall 1987). In dilating displacements, in joints, the surfaces have moved away from each other in a direction perpendicular to the surfaces (mode I). In shearing displacements, movement is parallel to the fracture surface, and either perpendicular (mode II) or parallel (mode III) to the propagation front. Joints may contain mixtures of shearing modes as well (e.g. Pollard & Aydin 1988). According to Segall and Pollard (1983) there is good evidence in many areas for the fact that the fractures formed predominantly by opening and were sheared at a later date. Faults or zones of weakness may have developed through the coalescence of the microcracks, joints (Hancock 1972).

Several authors have studied joint properties in regional scale and the relations of jointing to regional folding or faulting. Zhao and Johnson (1992), Cruikshank and Aydin (1995) and Ohlmacher and Aydin (1995) have described the progressive deformation and relative age of joints. In their studies of granitic rocks Granier (1985), Martel (1990) and Bürgmann and Pollard (1994) show how fault or shear zones grow from pre-existing joint sets. Wilkins et al. (2001) have analysed faulted joints in sandstones and shales, where early joints were reactivated in shearing. Reches (1976) investigated the time relationships of five joint sets in sedimentary rocks and concluded that four of them developed prior to regional folding and were later rotated by this folding. On the contrary Kattenhorn et al. (2000)

illustrated that the disturbance of a fault slip in the local stress field may result in an unexpected orientation of induced secondary fractures. Using a large amount of earlier works Peacock (2001) studied the temporal relationship between joints and faults. He deduced the existence of three types of relationships: joints that pre-date, are synchronous with faults or post-date the faults.

Using sedimentary rocks, for instance Babcock (1974) studied the orthogonal cross joints in order to imply the mode of fracturing in rocks. Caputo (1991 and 1995) and Bai et al. (2002) estimated the behavior of the regional stress field in sedimentary rocks applying orthogonal joint sets. According to Pollard et al. (1982), Olson and Pollard (1989) and Arlegui and Simón (2001) the geometry and distribution of regional joint sets may be used in inferring spatial or temporal changes in the orientation of principal stresses in the crust.

The brittle properties of bedrock in the local scale have been intensively studied in Finland only during the last few decades. Niini (1968) studied rock fracturing in the valleys on the course of the conveyance of fresh water from Lake Päijänne to the Helsinki area. The study was based on 100 drill holes mainly from the soil-covered valleys. Structural geological mapping was done at Olkiluoto in Eurajoki in order to describe the tectonic history of the bedrock and its various deformation phases and to assess their effect on fracturing (Paulamäki & Koistinen 1991). Olkiluoto is one of the sites in which Teollisuuden Voima Oy (Anttila (ed.) 1992) and Posiva Oy (Anttila et al. 1999) investigated the bedrock for the final disposal of spent nuclear fuel. Fracture measurements were made from outcrops and in two 400 m long and 1–3 m wide investigation trenches during the geological surface mapping (Paulamäki 1995 and 1996). These studies were carried out in order to detect possible constraints on the disposal (Anttila et al. 1999).

In Finland only a few regional studies of jointing properties in the Precambrian bedrock have been carried out. In the Pori region ductile to brittle deformation and jointing were regarded in examining the basis of tectonic evolution to rock mechanical properties (Pajunen et al. 2001a). The control of ductile tectonic structures to even joint set orientations became evident in Pori region (Pajunen et al. 2001a). Studies of fracturing in the regional scale continued in Espoo, Helsinki and Vantaa (Helsinki Area) during 1999–2002 (e.g. Pajunen et al. 2001b and 2008), where jointing was one of the main issues in the project “Construction potential modelling of bedrock in urban areas”. The bedrock mapping methods of urban areas were developed and the mapped geological

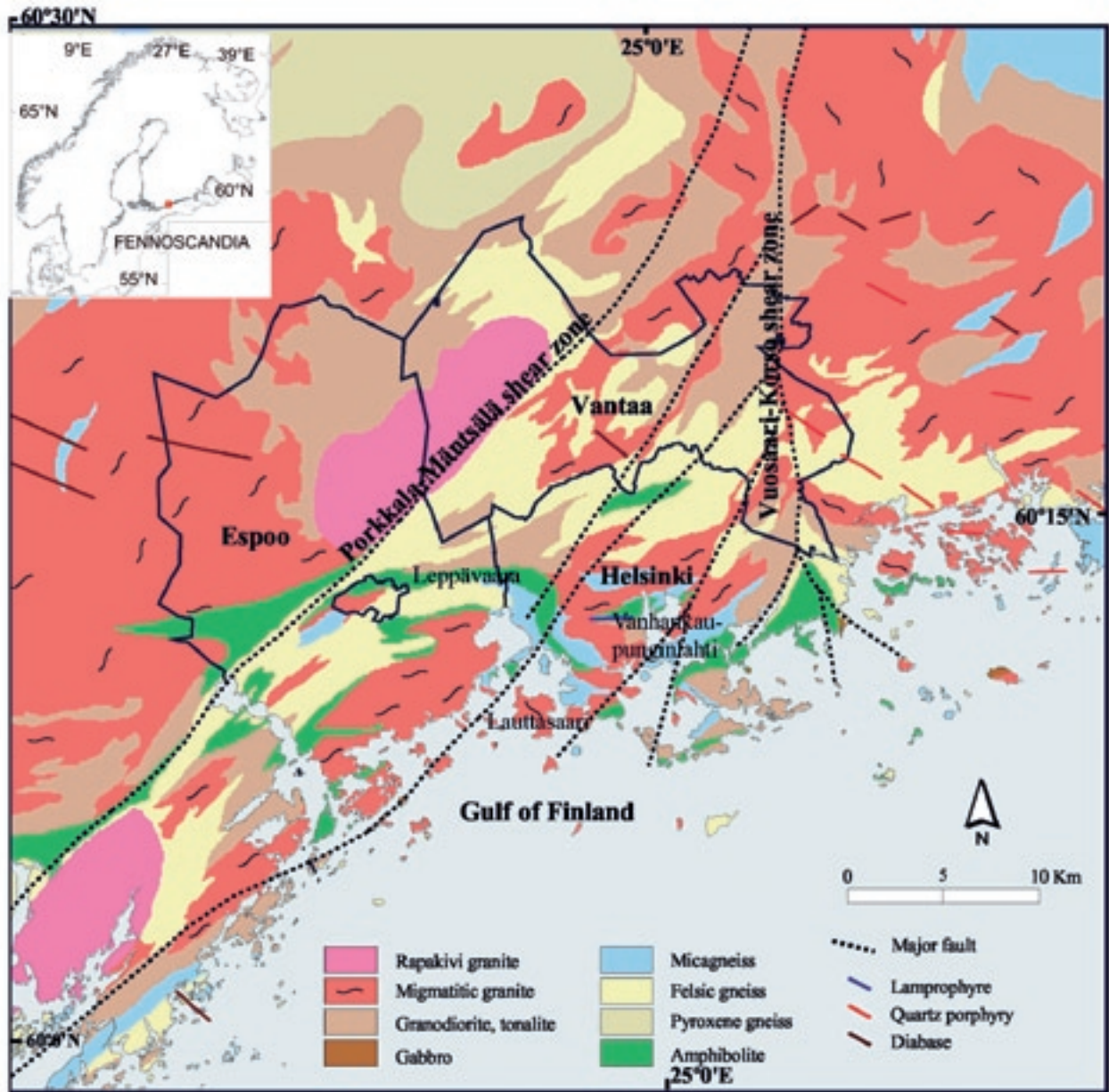


Figure 1. The lithological map of the study area, modified from the Geological Maps of Finland 1:100 000, Sheets 2032 (Laitala 1960), 2034 (Laitala 1967), 2041 (Laitala 1994) and 2043 (Härme 1969). In the upper left corner the location of the study area in Fennoscandia is shown with a red square. Base map © National Land Survey of Finland, permit No. 13/MML/08.

data were processed to suit rock mechanical applications (Pajunen et al. 2008). One of the results of the project was the map “The Construction Potential of Bedrock 1:50 000 – Espoo, Helsinki, Vantaa” (Pajunen et al. 2008, Appendix 1, this vol., back cover).

The purpose of this paper is to describe the regional pattern of jointing, the orientations and properties of joints in the Helsinki Area (Figure 1). The regional relationships between jointing features and tectonic structures like foliation and faulting are discussed. The study area was divided into 26 structurally and lithologically uniform sub-areas, jointing patterns of which are described. The adequacy of the used mapping method for observing the orientations of the main joint sets was tested using mapping data from two tunnels and older bedrock mapping data. The results are presented in this paper. The rocks in the study area are structurally

anisotropic and have a complex strain history. The preliminary results concerning the regional pattern of jointing in terms of regional and local deformation and stress field are presented. More detailed fieldwork is required for verifying these outcomes. The main goal of our studies is to construct a functional model of methods to predict the outlines of the brittle structure of bedrock in new areas of interest using bedrock mapping and geophysical data of GTK.

M.-L. Airo is responsible for the presentation and interpretations of the geophysical data in the study. M. Pajunen is responsible for the ductile deformation analyses. T. Elminen has carried out the fault studies. During the project M. Vaarma, R. Niemelä and P. Wasenius participated in several stages, the field work and data analyses. M. Wennerström is responsible for all the interpretation concerning jointing characteristics in the paper.

GEOLOGICAL AND TECTONIC SETTING

The Helsinki study area (Figure 1) is situated in the southern Svecofennian domain, primarily representing an island arc terrane characterized by ca. 1.9–1.88 Ga felsic to mafic metavolcanic sequences (e.g. Korsman et al. 1999). Locally, they show well-preserved primary structures. Metasedimentary sequences are low-water metasediments, like iron formations and calcareous rocks, and pelitic to psammitic turbiditic sediments. The supracrustal sequences are more or less migmatized by several thermal pulses. The terrane developed in a complex tectonic, metamorphic and magmatic evolution between 1.9–1.8 Ga ago (e.g. Korsman et al. 1999 and Pajunen et al. 2008). The post-Svecofennian events are represented by the 1.65-Ga-old Obbnäs and Bodom rapakivi batholiths and related mafic to felsic dykes (e.g. Haapala et al. 2005), and by the strong reactivation of the late-Svecofennian faults (Elminen et al. 2008) during the rapakivi stage and still during the Caledonian orogeny (e.g. Vaasjoki 1977).

When analyzing the jointing patterns of the study area the structures formed during the post-Svecofennian are of great importance. However, the Svecofennian structural evolution affected remarkably the anisotropy of the rock masses and, thus, determines effectively the joint sets formed in different tectono-magmatic terranes (Pajunen et al. 2001b). The oldest tectonic evolution is seen in the supracrustal sequences as isoclinal-folding events related to crustal thickening (E_1 of Pajunen et al. 2008). Development of the early regional penetrative horizontal foliation and the earliest stage of migmatization, caused by a strong extensional event, were related to island arc collapse (E_2 of Pajunen et al. 2008). Also mafic to intermediate magmatic rocks evolved during the early history were deformed and fragmented during these tectonic-magmatic processes. The associations were deformed into isoclinal dome-and-basin structures (E_{3-4} of Pajunen et al. 2008) showing metamorphism of amphibolite to granulite facies. During this early Svecofennian history a new continental crust formed. Deformation continued as complex transpressional events under varying stress fields that produced a tectonic pattern characterized by oblique extensional and constructional structures, and locally development of granulite facies metamorphism (E_4 of Pajunen et al. 2008). The continuous belt of the Southern Finland Granite Zone (SFGZ) was generated during the transpressional events at c. 1.86–1.80 Ga ago (Pajunen et al. 2008). The zone is character-

ized by intense pulses of intermediate to felsic magmas that cut the previous structures sharply in a brittle or ductile manner depending on the depth of the terrane in question at that time. A minority of mafic magmas also intruded, and the late sedimentary-volcanic sequences related to pull-apart basin tectonics formed (Pajunen et al. 2008). In the study area the Espoo Granite Complex (EGC) situates between the Southern volcanic-sedimentary belt (SVB) in the south and the West Uusimaa Granulite Complex (WUC) in the north.

The Southern Finland Granitoid Zone tectonic history with syntectonic wide-scale crustal folding structures typifies the Helsinki area (Figure 1). The Porkkala-Mäntsälä and Vuosaari-Korso shear/fault zones break the continuous ENE structural trend of the southern Svecofennian. The outcropping of different terranes like the Nuuksio granite area is strongly determined by the open folds: the earlier folding with E-trending axial planes form with the later folds with NE-trending axial planes wide-scale dome-and-basin structures (Pajunen et al. 2008). The folding with NE-trending axial planes broke in its latest phase to partitioned faulting in NNE to N directions that were reactivated still during the post-Svecofennian time (Elminen et al. 2008). A late folding with N-trending axial planes with a wavelength up to 300 km still strengthened the crustal bend in the Helsinki area (E_5 of Pajunen et al. 2008).

During the latest stage of the Svecofennian history ductile to semi-ductile shear and fault zones formed in NNE and N-directions (Pajunen et al. 2008 and Elminen et al. 2008). During the rapakivi event the crust was cooled and deformation occurred along the older crustal zones of weakness and a new set of semi-brittle, steep normal faults was formed into NW-direction. This normal fault pattern was later cut by N-S-trending strike-slip faults and low-angle thrust faults (Elminen et al. 2008). The latest dated reactivation in the pre-existing faults was Caledonian in age (Vaasjoki 1977). The reactivation of the old Svecofennian faults is a typical feature as demonstrated by polyphase character of the faults, e.g. the Porkkala-Mäntsälä shear/fault zone in the study area. Outcomes of the structural and metamorphic history of the area, intrusion stages of the igneous rocks and the late faulting episodes appear in the present bedrock as separate geotectonic units. The division of the area to 26 sub-areas for description of jointing properties has been done on this structural basis.

FIELD DATA AND PARAMETERS OF THE JOINT PROPERTIES

An important goal of the study 'Construction potential modelling of bedrock in urban areas' (Pajunen et al. 2008) was to develop bedrock mapping methods for different infrastructural and environmental applications in urban areas. The focus was on the brittle structure, but the ductile deformation history was seen as the basis, which controls the geometry of fracturing. For mapping purposes an observation form was developed during the studies in Pori and Helsinki (Pajunen et al. 2002). Lithological, tectonic and joint properties were mapped very accurately, and the local relationships between them were detected already in the field.

In the present study joint sets and joint zones were measured at 557 ice-polished outcrops, 126 road cuts and 5 quarries (Figure 2). These kinds of sites represent unbroken bedrock compared to shear zones and zones of weakness, subject to the other study of the project (Elminen et al. 2008). The geometry and regional pattern of jointing are observable in the rock blocks between these fracture zones.

A uniform net of observation points was created. Due to some poorly exposed or tightly populated areas the net is less uniform in places. The average distance between observation points is approximately one kilometre. The observation area was chosen to represent a typical jointing pattern in the point, and its mean extent was 400 m². Well-defined joints, which form parallel joint sets, were taken into account (2455 joint sets) (Figure 3). Properties of joints were investigated as joint sets. The parallel repetitive joints were tried to locate, because the connection of these recurring joints as joint sets to other tectonic structures is possible. In addition special attention was paid to exclude the fresh joints caused by excavation processes. At outcrops the slopes and gentle to sub-horizontal planes were studied carefully and included in the data when the orientations of these surfaces were recurring. Joint zones, narrow tabular bands where spacing of joints was exceptionally dense compared to the whole joint set (Figure 4), were regarded as one joint. The allowed deviation of

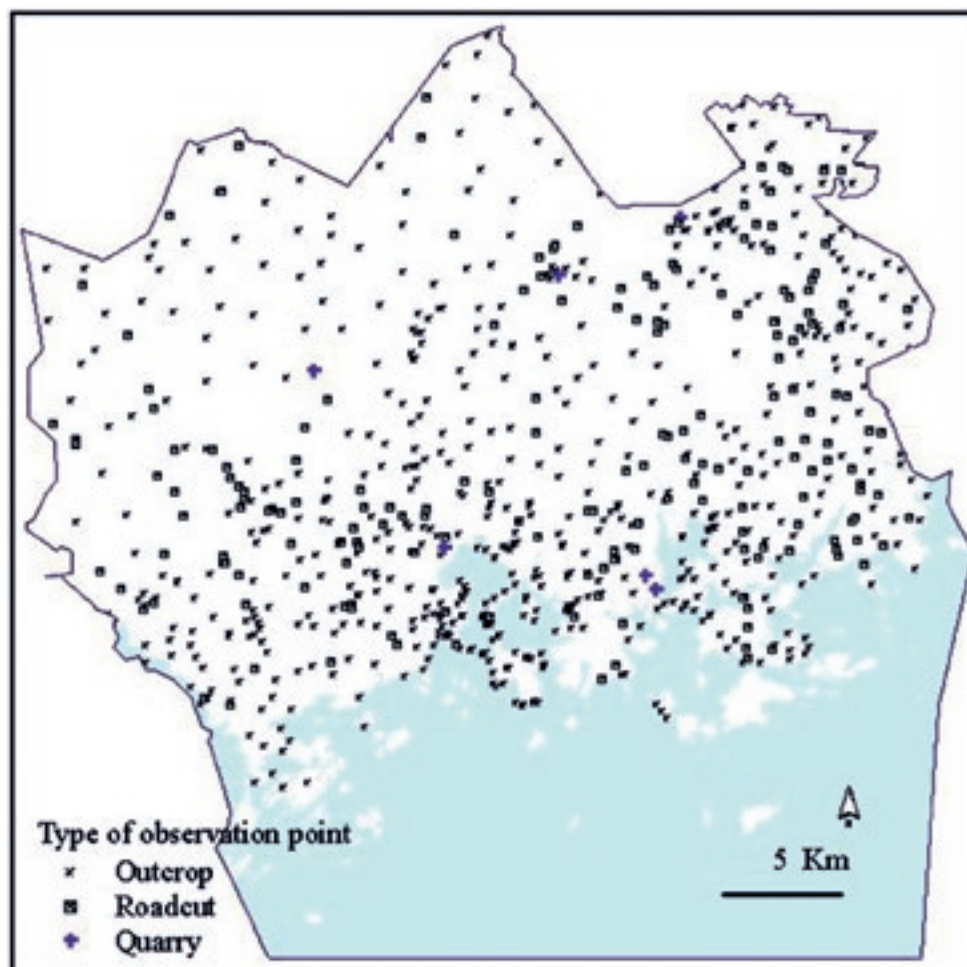


Figure 2. Observation points in the study area (N=922). Properties of joint sets and joint zones at 557 ice-polished outcrops, 126 road cuts and 5 quarries were measured. Base map © National Land Survey of Finland, permit No. 13/MML/08.



Figure 3. Well-defined joints forming parallel joint sets were taken into account. Trends of four different joint sets are shown with yellow stippled lines. The rock type is microcline granite, x=6680328 y=2556236.



Figure 4. Joint zone with exceptionally dense spacing of joints. The rock type is biotite-plagioclase gneiss, x=6716384 y=2543622.

the directions in observed joint sets was at the most $\pm 15^\circ$ in strike and $\pm 20^\circ$ in dip, respectively.

Particular joint characteristics were selected for describing the regional pattern of jointing. These properties were classified in the project ‘Construction potential modelling of bedrock in urban areas’ for presenting the construction potential of the bedrock (Pajunen et al. 2002). The joint properties at issue are based on the features in the engineering classification of rock masses, the Q-system (Barton et al. 1974). The number values of Q-system (Jr etc.) were not directly usable in the project. Because every mapped feature could be separately linked to deformation, properties of the Q-system were demerged suitable for geological inspection (Table 1).

Table 1. Joint properties measured in the field during the project and related parameters of the Q-method (Barton et al. 1974). Comparable features are marked with dotted lines in between.

Features in the study	Q-value parameters
Joint trace length	
Joint Spacing	
Joint zone	
Joint set number	: Joint set number (Jn)
Joint Wall outline	: Joint roughness number
Joint wall roughness	(Jr)
Joint type	: Joint alteration number (Ja)

For instance parallel oriented planar joint sets in neighbouring outcrops may be linked to a same deformation phase. Joint sets with fillings of the same mineralogy, respectively, from separate observation points may be connected to same processes and may show a relationship with faulting.

In the Q-system joint trace length is not taken into account. In the study it was measured as the maximum and mean length of every joint set. Joint trace length was divided into three classes: short (mean length < 5 m), moderately long (mean length 5–10 m) and long (mean length > 10 m). Spacing of jointing is a number of crossing joints along a line perpendicular to the average orientation of the joint set. Densely spaced joint sets have joints at distances of about 0.4 m. The frequency of joints in a joint zone was measured as a number of joints cutting the perpendicular line, which define the width of the zone. Joint types, joint wall geometry and alteration

were mapped, too. Slickensided joints were studied separately in the manner to detect directions of semi-ductile or semi-brittle faulting. As the data measured in natural bedrock are not always unambiguous, some generalizations were required for describing the jointing properties in the Helsinki Area.

Elminen et al. (2008) have studied the zones of weakness. The zones were deduced from topographic data and they represent straight valleys with a minimum length of 0.5 km. The zones of weakness cut Svecofennian and rapakivi related structures.

Using the field observations the joint set number (J_n), the average total number of joints per m^3 (J_v) and the RQD value (%) were calculated for each outcrop and a crude measure of the average block size (RQD/J_n) was computed based on Barton et al. (1974). A VisualBasic application, which automatically completed the field measurement Excel-files of outcrop data with these derived parameters, was built up.

REGIONAL JOINTING PATTERN

In order to construct a regional view of the jointing characteristics in the area, the jointing orientations were analysed and compared to aeromagnetic features and tectonic structures. Orientations of the joint sets ($N=2211$) are presented with a stereoplot in Figure 5. Sub-horizontal (dips $0-10^\circ$) joint sets are excluded, because the orientations of moderately dipping (dips $45-74^\circ$, $N=608$) and steep (dips $75-90^\circ$, $N=1338$) joint sets are then more easily detectable in the diagram. Gentle joint sets (dips $11-44^\circ$) are few in number ($N=263$) in the measured data in the Helsinki area. The data show six main orientation groups trending E, NE, NNE, N, NW and WNW, into all cardinal points (Figure 5).

The NE-trending joints are most abundant. When comparing joint set orientations at mapped outcrops and road cuts, respectively, differences occur

(Figure 6 a, b) (See also Niini et al. 2001). In both data steep NE-trending joints and moderate joints trending NW are abundant. In road cuts deviation into NE- and NNE-trending groups is well defined. Steep joints trending N are present in both data being more abundant at outcrops. Gently or moderately dipping joints have been measured more often in road cuts. Subhorizontal joints cover 6 per cent at outcrops and 12 per cent in road cuts of the data, respectively. The road cuts in the study area trend variously in direction. The joints, which parallel this trend in places, may have been underestimated in number. The road cuts have been mapped in 3 dimensions and at least the joint sets the spacing of which is below 1 meter have been detected. The purpose was to construct a regional view of the jointing characteristics in the area. In more detailed work more

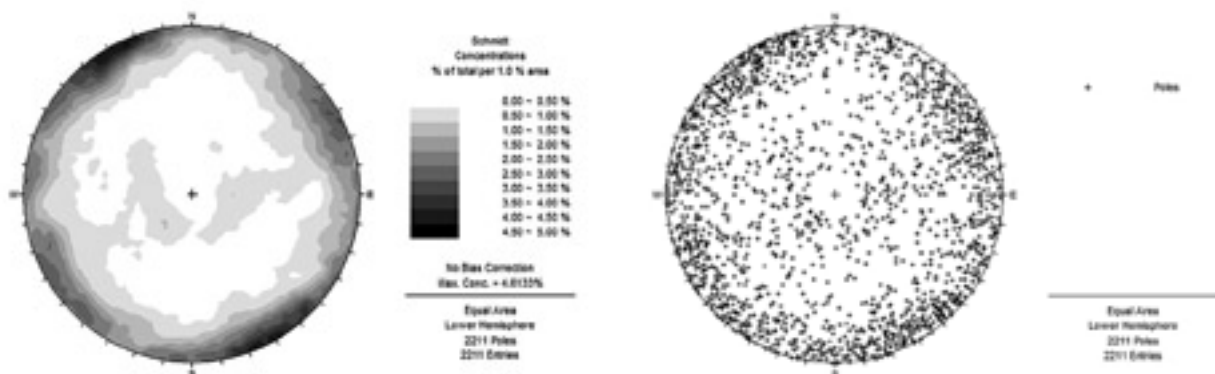


Figure 5. Poles to joint set planes shown as (a.) contours and (b.) poles on equal area lower hemisphere plots. 2211 measurements were carried out. Sub-horizontal joint sets (dips $0^\circ-10^\circ$) are not presented ($N=228$). The data show 6 main orientations: E, NE, NNE, N, NW and WNW.

attention should have been paid on equal consideration of jointing orientations in road cuts.

Steep NE-trending foliation has effectively controlled the jointing propagation (Figure 7). According to Pollard and Aydin (1988) in highly anisotropic rocks planes of weakness may be favoured for jointing even though they are not perpendicular to the least compressive stress. The natural heterogeneity of rock can produce shear stresses at front of a propagating joint, resulting in tilted and twisted paths (Pollard & Aydin 1988). In the Helsinki area one joint set often parallels locally the main foliation.

In aeromagnetic data the structural form lines of strongly foliated migmatitic rocks appear as banded anomalies, which can be followed on a regional

scale (Figure 8). These bands often show the trend of one of the main joint sets observed at outcrops. Sub-perpendicular cuttings in anomaly trends may lead to another joint set at high angle to the set parallel to the foliation. On the outcrop scale the aeromagnetic data may not give a straight reference of fracturing, but where jointing builds up regionally continuous structures or joint zones and zones of weakness, the joint sets can often be identified.

Two steep main joint orientations trending NE and NW show systematic occurrence in the study area (Figure 9). They are quite uniformly present among the whole area, and thus imply a regional strain. The steep joint sets trending NNE concentrate close to the Vuosaari-Korso shear zone (V-K

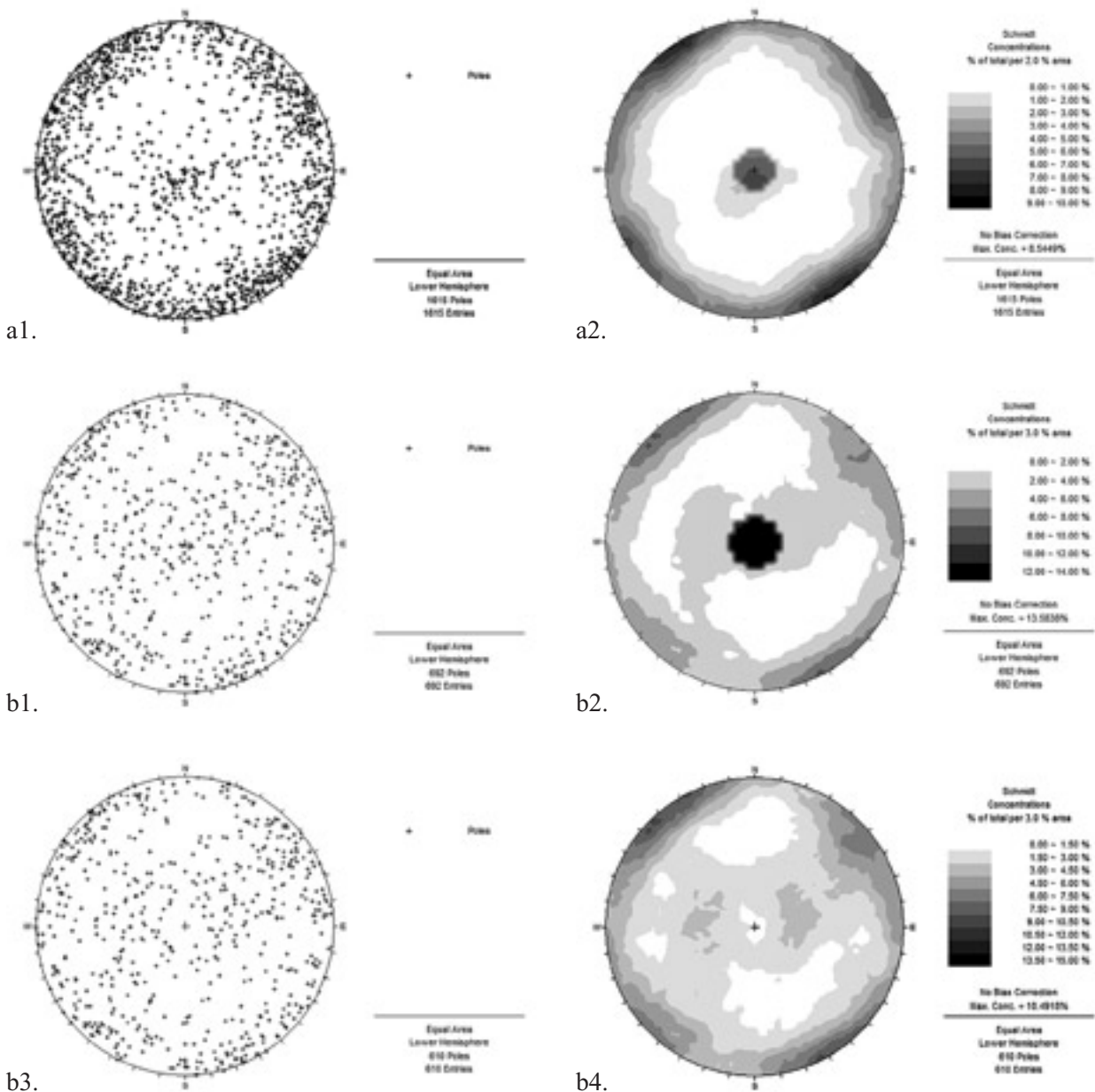


Figure 6. Orientations of joint sets of the whole study area (a1) at outcrops (N=1615) and (b1) in road cuts (N=692) (poles to planes shown as contours on equal area lower hemisphere). If the sub-horizontal joint sets are ignored, the details of the other directions in the road cuts are more detectable (b3 and b4).

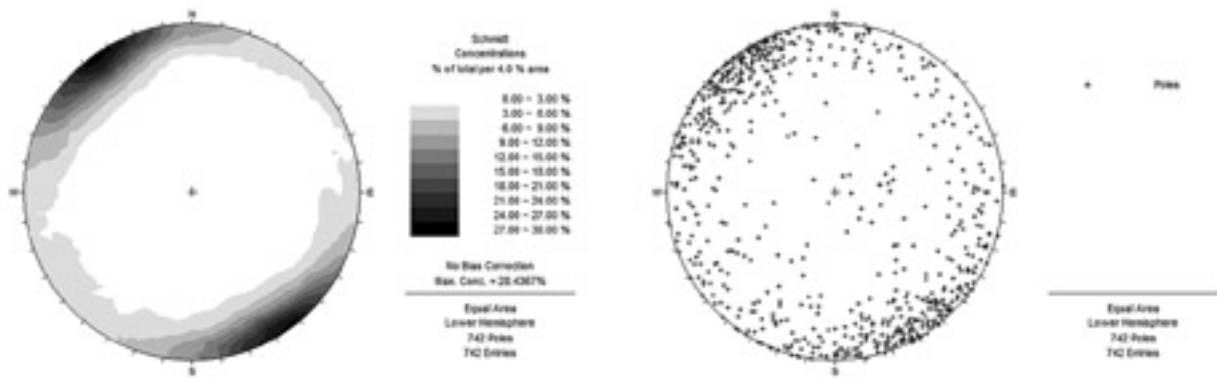


Figure 7. All measured foliation orientations of rocks in the study area (N=742) are shown on the stereoplots (poles to planes shown as poles and contours on equal area lower hemisphere) (a.) contours and (b.) poles. Sub-horizontal planes are ignored. An overwhelming majority of the foliation orientations trend NE.

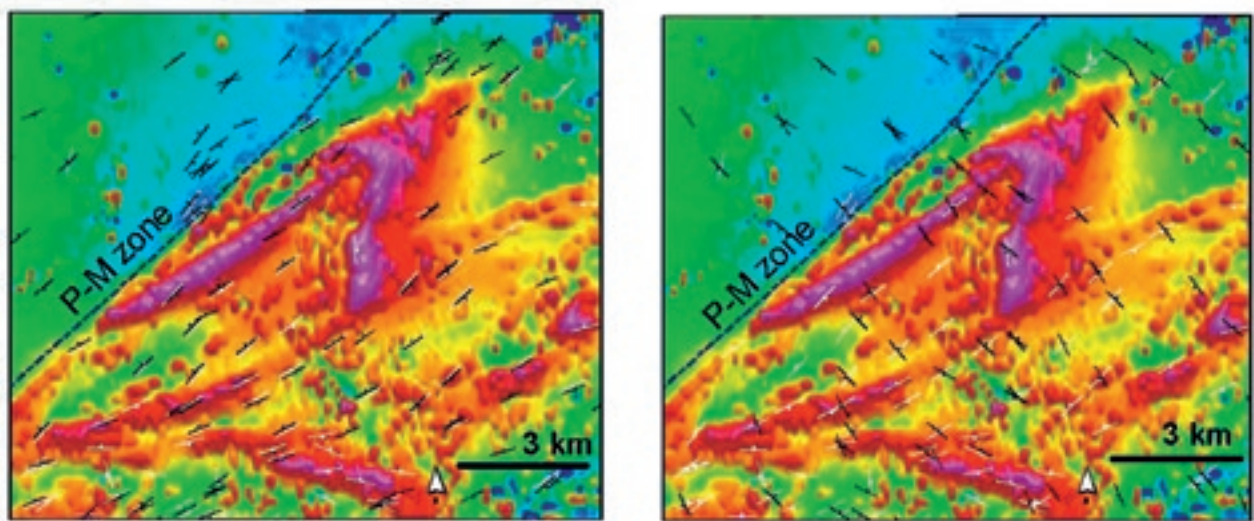


Figure 8. Sub-vertical foliation planes of strongly orientated migmatites (white symbols) and sub-vertical joint sets (black symbols) a) trending NE and b) trending NW on an aeromagnetic shaded relief map (50 m grid cell size). The Porkkala-Mäntsälä (P-M zone) is marked with a black dashed line. Coordinates of the lower left corner $x=6678003$ $y=2539978$ and of the upper right corner $x=6690025$ $y=2554002$, respectively.

zone) and to the other NNE-trending faults (Elminen et al. 2008) (Figure 10). The NE- and NNE-trending joint sets occur mostly at separate outcrops, respectively. The NNE trending joints show crosscutting nature towards the local main foliation (Figure 11 a, b). Joints have smooth or weakly rough, stepped surfaces and contain shear in between tightly spaced joints (Figure 11 a). After the joints have originated, some shearing has taken place. The NNE-trending joints probably indicate a new jointing phase originated due to rotation in the local stress fields followed by movements in the NNE-trending faults.

A directional analysis of aeromagnetic data was carried out on the basis of the original survey data by using trend-analyses algorithm of the Oasis Montaj software. The programme finds continuity trends in pre-defined directions of preferred angles (see Airo et al. 2008). The window to seek trends was 500 m. The results of this directional analysis were

compared with field observations. The compatibility is outstanding in the directions of systematically occurring joint sets trending NE and NW (Figure 12). The joint set directions often even locally follow the analyzed minor lineaments. The reliable use of this method in predicting jointing orientations in bedrock is promising but needs further careful studies to compare the lineaments to field observations.

On the aeromagnetic horizontal gradient map (interpolated grid, 50 m grid cell size) the banded, rectilinear anomalies trending NW and WNW represent diabase dyke swarms (Figure 13). Two main steep joint sets parallel the two trends of brittle fractures, into which the diabase magma intruded indicating relationship to rapakivi intrusion (ca. 1650 Ma) (Haapala et al. 2005). Field observations evidence parallel jointing with these diabase dykes even at outcrop scale. It is obvious that the first appearance of jointing in bedrock in the Helsinki Area dates back at least to the intrusion of these dykes.

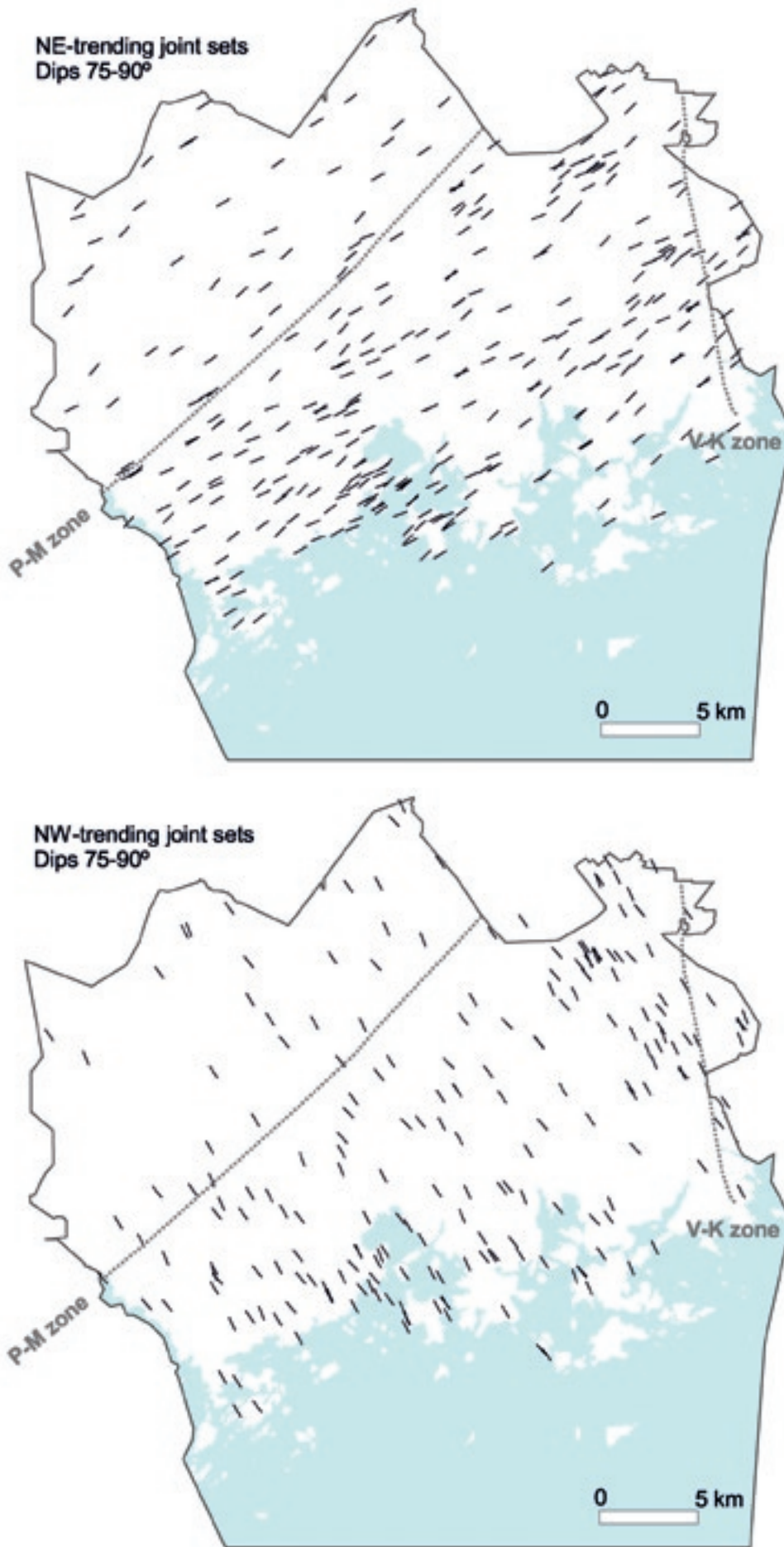


Figure 9. NW-trending and NE-trending sub-vertical joint sets show a systematic occurrence over the study area.

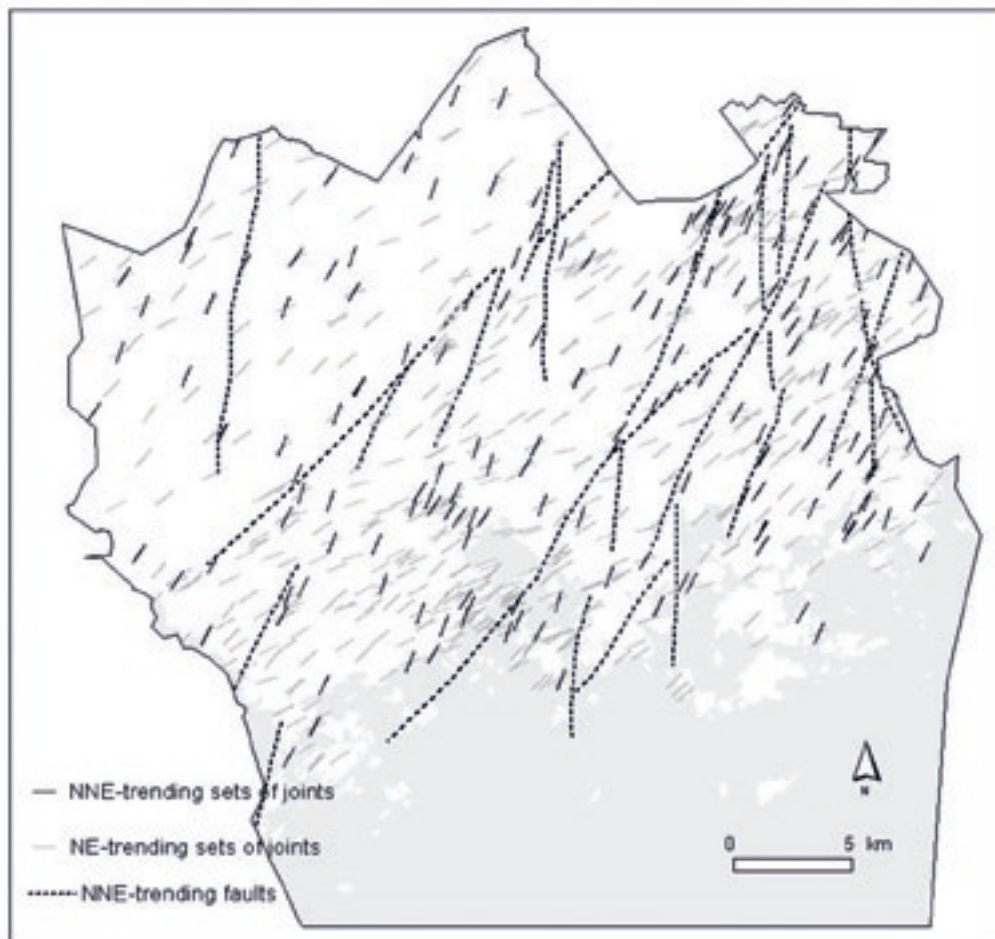


Figure 10. Orientations of sub-vertical NE-trending and NNE-trending joint sets. NNE-trending joints show parallel orientation to a NNE-trending semi-ductile fault or shear zones and are abundant close to the zones.

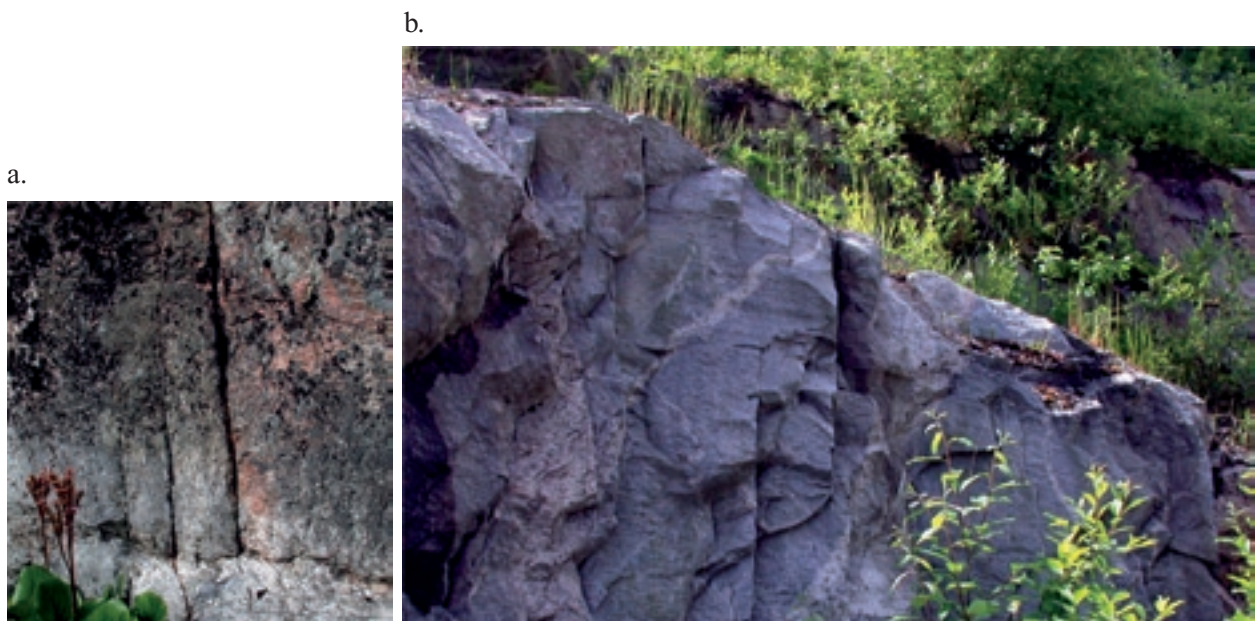


Figure 11. The NNE-trending joints show cross cutting nature towards the ductile structures. In (a.) pegmatitic, partly migmatitic granite, $x=6685087$ $y=2563148$ and (b.) migmatitic biotite-plagioclasegneiss, $x=6693156$ $y=2560100$.

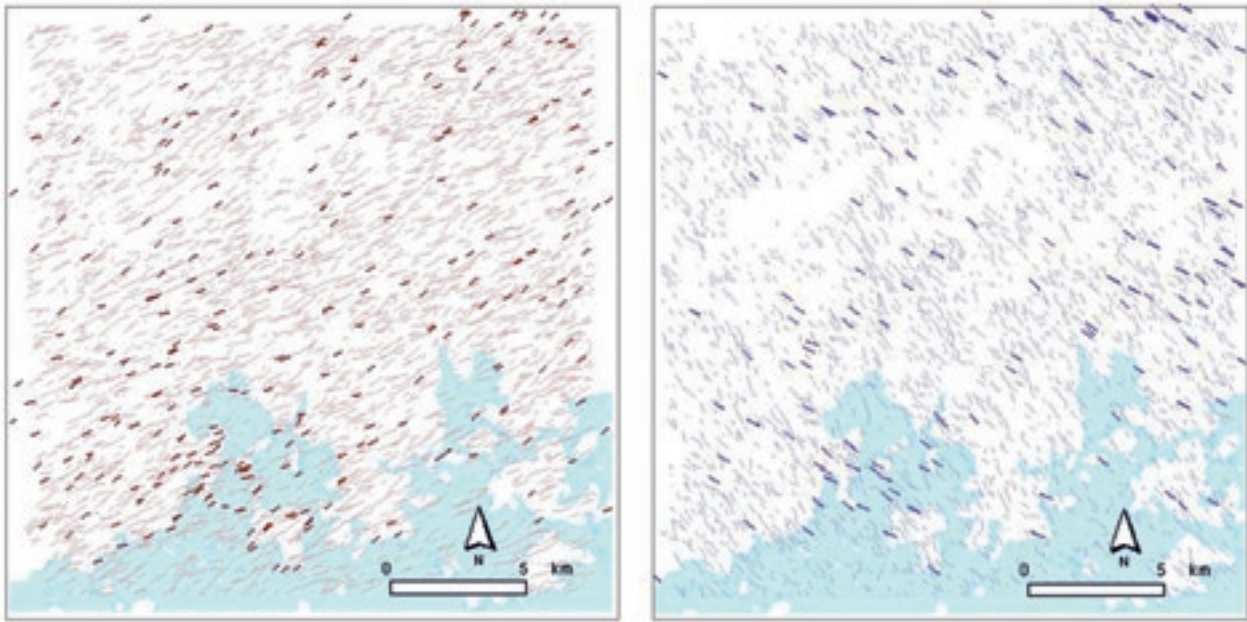


Figure 12. Two regional joint set orientations trending NE (left) and NW (right) compared with interpreted magnetic lineament orientations. The directional analyses of minor magnetic lineaments were done in six preferred orientations, based on the original survey data, using the trend-analysis algorithm of Geosoft Oasis Montaj. The sampling interval of the aeromagnetic survey is ca. 6 m with 200 m line spacing and two wing-tip magnetometers. The compatibility between the observed and interpreted directions is remarkable.

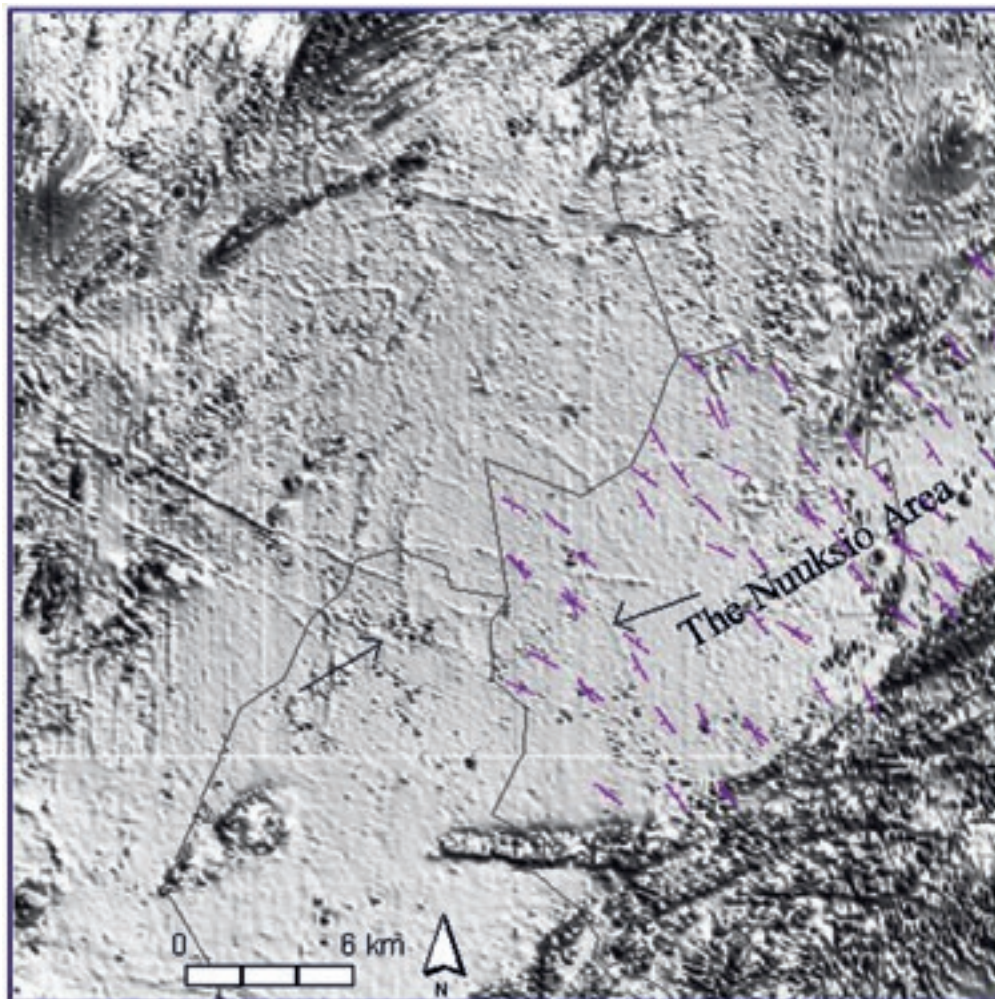


Figure 13. Some observed trends of diabase dyke swarms in the northwestern part of the study area. Two main subvertical joint sets parallel the lineament orientations (shown with arrows) revealed on the aeromagnetic horizontal gradient map (50 m grid cell size). Horizontal gradients in preferred orientations enhance the weak lineament patterns where the magnetic contrast to the background is poor. Coordinates of the lower left corner $x=6671386$ $y=2511839$ and of the upper right corner $x=6706393$ $y=2546582$, respectively.

ORIENTATIONS OF THE JOINT SETS

The Helsinki area was divided into 26 sub-areas based on tectonic and metamorphic history of the area. The lithological associations, main tectonic shear zones and brittle faults were exploited in the definition of these internally uniform 'blocks'. Orientations of the joint sets in the sub-areas are presented with stereoplots in figures 15, 17, 18, 20, 21 and 22. In order to describe the jointing orientations, 26 sub-areas have been grouped into six main areas; The Nuuksio area, The Espoonlahti area, The Central Vantaa area, The Central Helsinki area, The Malmi area and The Vuosaari-Korso area (Figure 14).

The Nuuksio area

In the sub-areas 1–5 to the west of the Porkkala-Mäntsälä shear zone (P-M zone), granitoid rocks predominate, coarse- to medium-grained, mainly homogeneous and locally porphyritic granites in the west, granodioritic-granitic rocks in the north-west and the Bodom rapakivi batholith (Figure 1) next to the P-M zone. In the northernmost part quartz-feldspar gneisses exist with granite migmatizing it. Close to the P-M zone in the southwest mafic, banded rocks with gabbroic fragments occur with feldspathic gneisses and granodiorites.

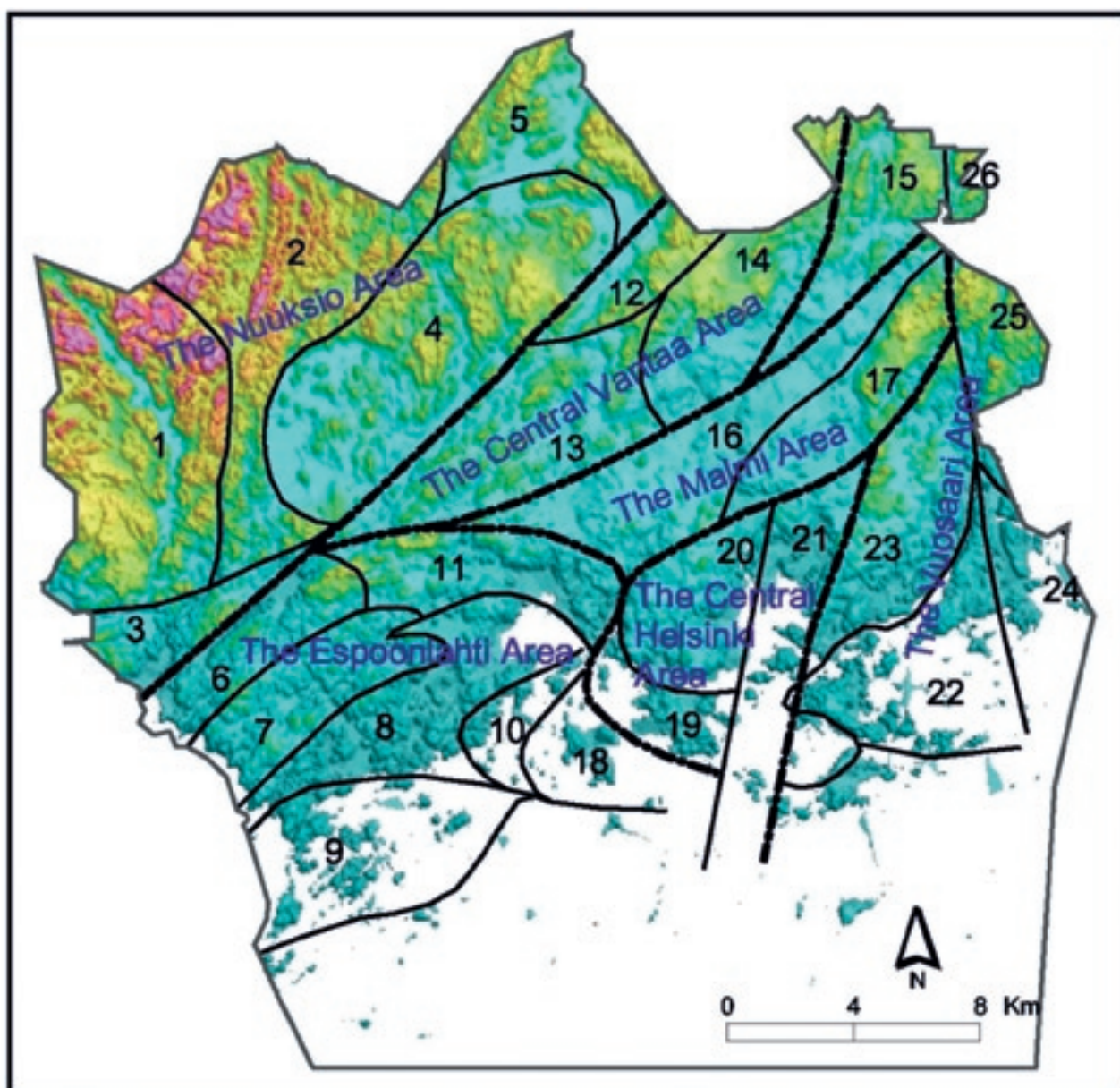
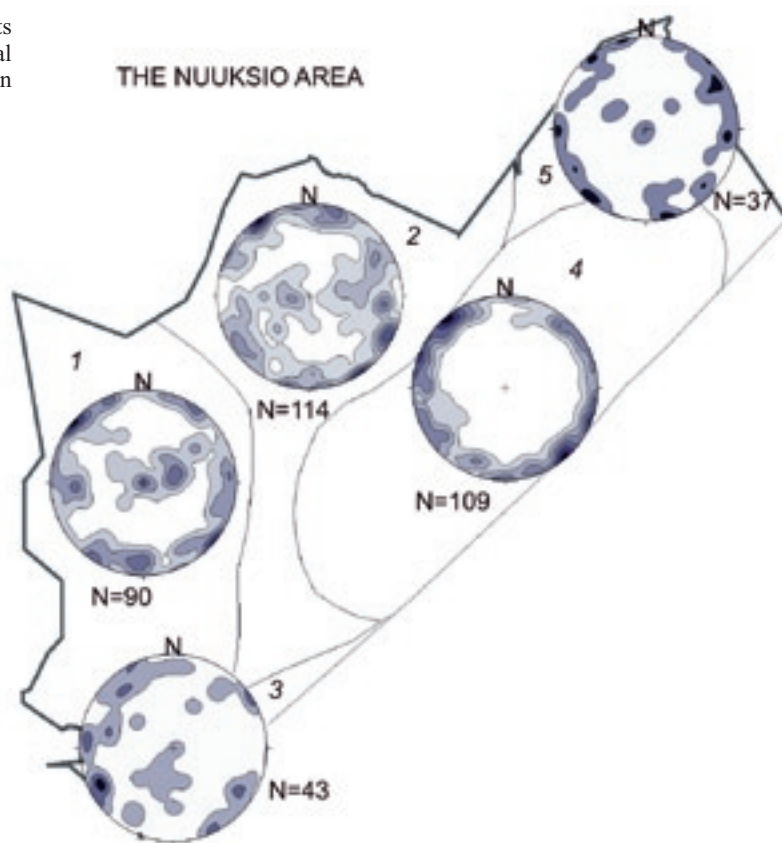


Figure 14. The main areas and sub-areas of the study on shaded topographic data of National Land Survey of Finland, permit No. 13/MML/08.

Figure 15. Orientations of the joint sets (poles to planes shown as contours on equal area lower hemisphere) in the sub-areas in the Nuukksio Area (393 observations in all).



To the west of the P-M zone an upland area predominates the landscape. Two major valleys divide the highlands in N-S and NW-SE directions. In these valleys longitudinal lakes follow the main zones of weakness in the area. In the northeastern part of the area the relative difference in altitude is not as big as in the west. The topographic data show systematic depressions in the NW-SE direction over the whole area indicating weathering of rock in this direction. Because no construction strains are directed to this region, only a sparse net of observation points with an average distance of 2 kilometres was arranged here.

Gentle foliation dominates in the granites of the sub-area 1. Closer to the Bodom rapakivi batholith foliation gets steeper trending NE or N. The main foliation in granodioritic-granitic rocks in the sub-area 2 dips to 70° to the west. Near the P-M zone orientation of foliation bents trending systematically NE and implicating the control of shearing in the fault zone. In the southwestern part (sub-area 3) in amphibolites, in hornblende gneisses and in granodiorites the main foliation follows the steep orientation of the P-M zone.

In the Nuukksio granites one joint set follows the gentle foliation (Figure 15). Steep jointing trending NE occurs over the whole area and is frequent near the P-M Zone. Directing to NW steep joint sets include long traces of joints in the sub-area 1 and short and locally dense traces in the sub-areas 2,3 and 5

(Figure 16). In the sub-area 2 moderately long and long traces of joints exist trending N with dips $60\text{--}70^\circ$ either to the west or to the east. Gentle jointing dipping to the west or to the east is typical in the sub-area 2. In the Nuukksio Area faulted joints trending N, NW and WNW have been detected.

The Bodom rapakivi batholith (sub-area 4) is elongated parallel to the P-M zone which probably controlled its emplacement (Härme 1961, Kosunen 1999, Elminen et al. 2008 and Pajunen et al. 2008). Steep joint sets in the orientation of the P-M zone occur in the whole area of the batholith. The most common NW-SE jointing orientation forms a high angle with the P-M zone. In this direction there are a few moderately long joint sets (Figure 16) and brittle fault structures have been found (Elminen et al. 2008). Steep joints trending N are moderately long in places (Figure 16). Sub-horizontal jointing appears occasionally in the Bodom rapakivi.

The Espoonlahti Area

The major part of the Espoonlahti area (sub-areas 6–11, 18) is located in the lowland and outlines a densely populated region. It is bordered by the Espoonlahti Bay in the southwest, the P-M Zone in the west and the Leppävaara Zone in the north (Figure 1). All these zones are detectable in topography and

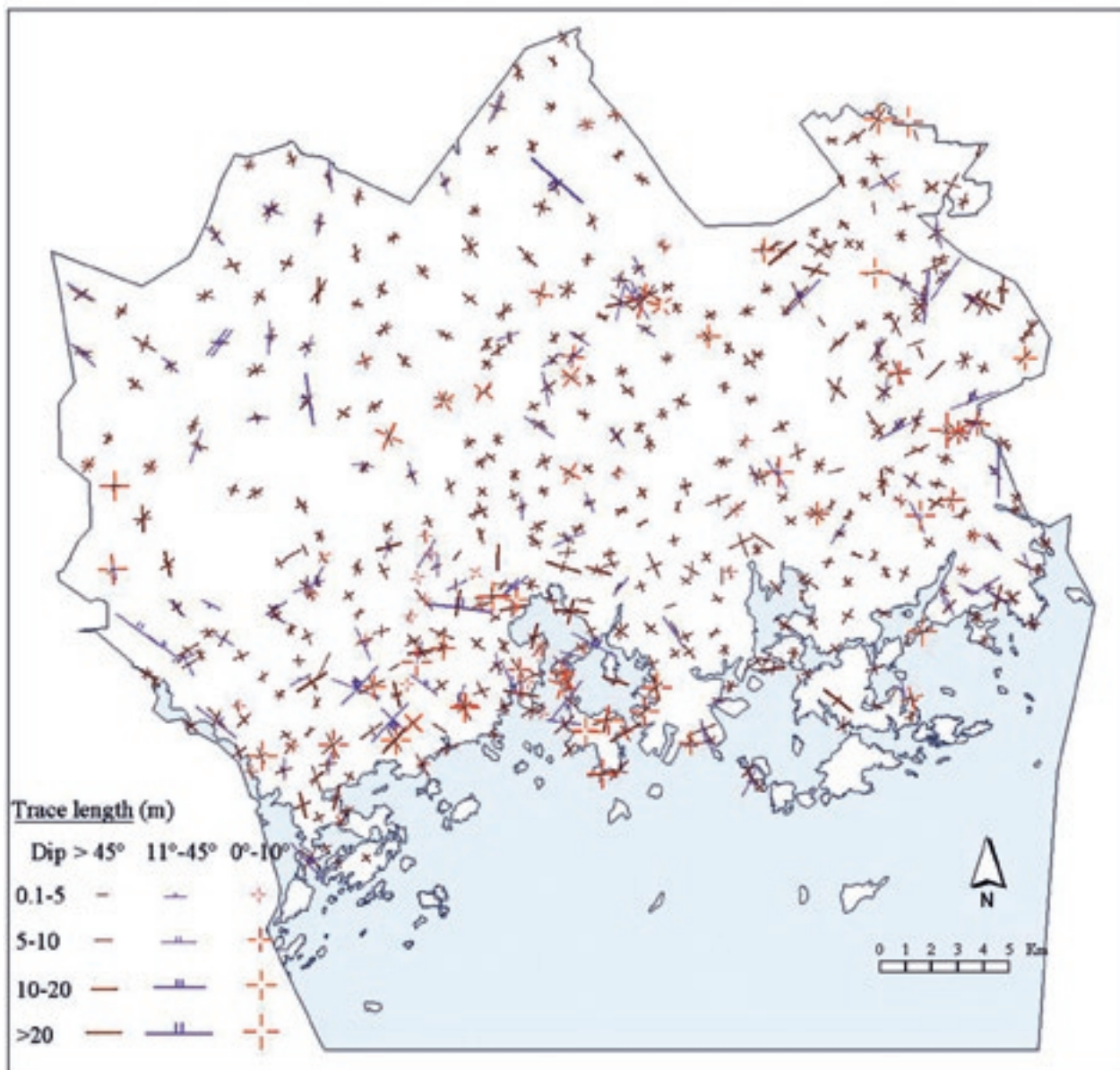


Figure 16. Mean trace lengths of three main joint set orientations at every observation point. The trace lengths have been classified into four categories: 0.1–5 m, 5–10 m, 10–20 m and over 20 m. The dips of the joint set planes have been classified into three categories: over 45°, 11°–45° and 0°–10°.

are followed by parallel depressions within the area (Figure 14).

This Area establishes quite a uniform tectonic basin-and-dome structure in SW-NE direction in the west and almost in E-W direction in the northeast, correspondingly. The division of rock types in the area follows almost precisely the basin-and-dome structure even on the outcrop scale creating small elliptical structures. Supracrustal rocks consist of felsic to intermediate gneisses and amphibolites. Widely distributed medium- to coarse-grained microcline granite is homogeneous in the northern part, but contains various gneisses and mafic inclusions in the south.

East of the P-M zone the foliation trending NE is predominant until the main structure bends to the east near Leppävaara (Figure 1) (Pajunen et al. 2008). In the E-trending zone foliation forms two main orientations striking parallel to the zone or trends to NE (sub-area 11). To the south of Laajalahti (Figure 1) a late-Svecofennian shearing deformation has reoriented the regional structure (Pajunen et al. 2008) (sub-area 10).

Near the P-M zone one course of jointing frequently follows the parallel steep foliation trending NE (Figure 17). Besides this orientation, joint sets controlled by the steep foliation in almost E-W direction are regular in the Espoonlahti area. Schistos-

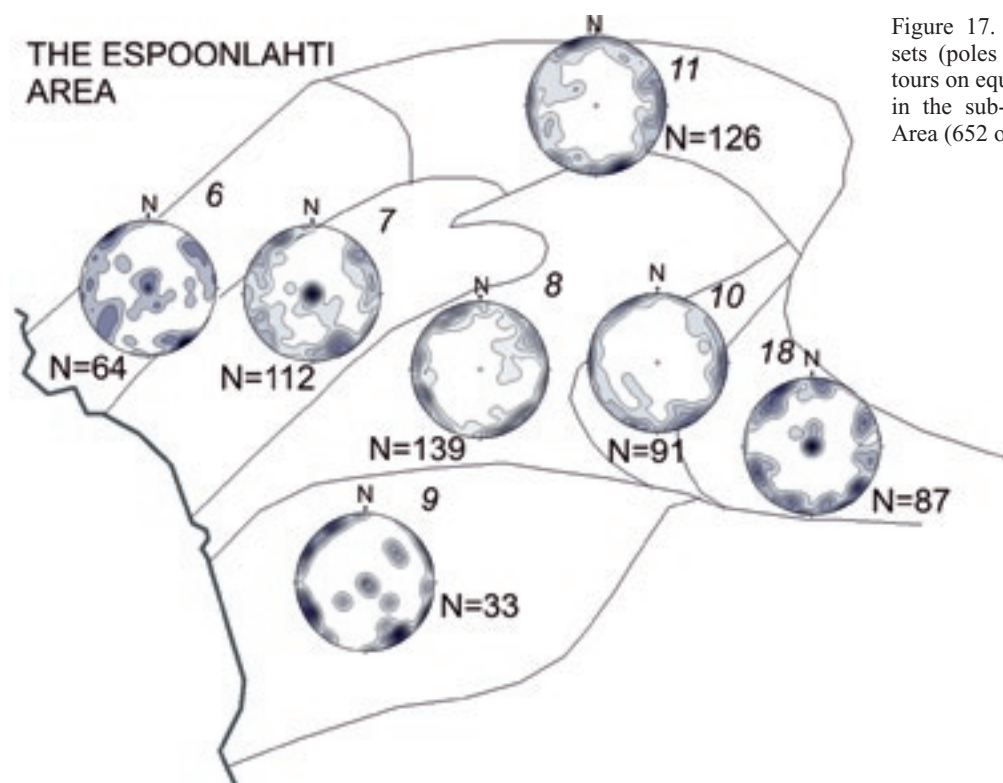


Figure 17. Orientations of the joint sets (poles to planes shown as contours on equal area lower hemisphere) in the sub-areas in the Espoonlahti Area (652 observations in all).

ity in the microcline granite is weaker compared to the surrounding supracrustal rocks, but NE-trending joint sets show the most common jointing orientation also there (sub-area 8).

Joint sets trending NW and occasionally N include moderate joints with dips between 40–80° (Figure 17). They contain mainly short, fairly tightly spaced joints and joint zones. In microcline granite joints are locally long or moderately long and near the Espoonlahti Bay long joint sets parallel the course of the shoreline (sub-area 7). Sub-horizontal jointing occurs frequently in the sub-areas 6, 7, 9 and 18, and show long traces of joints in microcline granite in the sub-areas 8 and 18 (Figure 17).

Near Laajalahti moderately long traces of joints parallel the foliation in the zone that has bent towards southwest (Figure 16). Another occasionally long jointing cuts the main foliation at a high angle. In this sub-area (sub-area 10) quite abundant steep N-trending joint sets include faulted joints. Slip markers have been measured in joint sets trending E.

In Lauttasaari (Figure 1) (sub-area 18) red microcline granite predominates including steep and moderately dipping joint sets trending mostly NW or NE. Sub-horizontal long jointing characterizes this granite (Figure 16).

The Central Vantaa area

The Central Vantaa Area to the east of the P-M zone (sub-areas 12–14, Figure 14) is divided lithologically into two parts: felsic gneisses and amphibolites cut by tonalites and granodiorites in the southwest and coarse granites and migmatitic micagneisses in the northeast. Folded dome-basin structures trending NE appear as relatively high chains of outcrops. In the south they follow the P-M zone direction and turn to the east in the middle of the area.

The southern and southeastern parts of the area consist of lowland areas including the valleys of River Vantaa and River Kerava. The soil is clayey and locally thickness of overburden is more than 17 metres (Pajunen et al. 2002).

The main, steep foliation trends NE. Close to the eastern border of the sub-area 14 foliation turns to the north. One joint set follows regularly the main foliation (Figure 18). In the east jointing parallels only the steepest foliation planes. These main jointing orientations contain long joint sets (Figure 16). In sub-areas 13 and 14 gentle joint sets dip to the northeast. Faulted joints trending NE, N and E have been observed.

In sub-areas 13 and 14 the orthogonal joint system is well developed and dominates the jointing

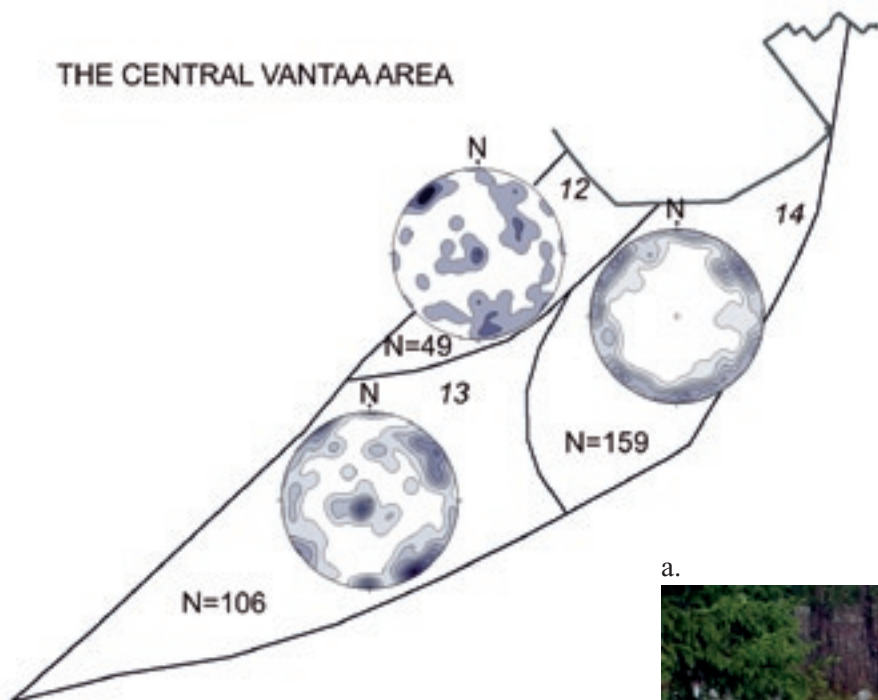


Figure 18. Orientations of the joint sets (poles to planes shown as contours on equal area lower hemisphere) in the sub-areas in the Central Vantaa Area (314 observations in all).

pattern at the outcrops concerned (Figure 19 a, b). One joint set parallels the main, steep foliation trending NE and the other one is perpendicular to it. Timing of crosscutting joint sets in orthogonal systems has raised discussion in the literature (e.g. Bai et al. 2002 and Caputo 1995). Joints are basically fractures that propagate normal to the least principal stress (σ_3) and in the plane containing σ_1 and σ_2 . In the orthogonal system the existence of two joint sets indicate a rotation of regional principal stresses by 90° after the formation of the first joint set (Bai et al. 2002). But some switch in the local stress may happen due to decrease in spacing of fractures because of the infilling (Bai et al. 2002) and a cross joint set may form. The stress field may also be distorted locally by the drop, which follows the stress release after the formation of the first joint set, and a second fracture may form perpendicular to the first one (Caputo 1995).

a.



b.



Figure 19. The orthogonal joint system in the sub-areas 13 and 14 is well developed and dominates the jointing pattern in all lithologies at outcrops concerned. (a.) quartzfeldspargneiss $x=6685467$, $y=2546882$ and (b.) pegmatitic granite $x=6684717$, $y=2546312$.

The Central Helsinki Area

The Central Helsinki area is comprised of granodioritic and tonalitic rocks with a younger granitic phase (sub-areas 19–21, Figure 14). Migmatitic gneisses and amphibolites form minor enclaves in them. These granitoids form rounded topographic highs in the area. In the east the Vanhan Kaupunginlahti bay (Figure 1) and its surroundings forms a plain area with wetlands.

The most frequent, steep foliation trends to NE. Around the rounded granitoid formations steep foliations follow their contacts to the schists. In the eastern border of the area foliation bends northwards.

Jointing parallels regularly the main foliation (Figure 20). Steep joints trending N are abundant. Traces of joints are usually short, but joint sets trending E and NW occasionally include long joints (Figure 16). Sub-horizontal jointing exists frequently.

In the Central Helsinki area faulted joints are present in joint sets trending N and E. Further brittle fault structures have been described by Elminen et al. (2008).

The Malmi area

Bedrock in the Malmi lowland area is poorly exposed until the eastern part, where upland predominates the landscape (sub-areas 16 and 17, Figure 14). Main rock types are tightly folded and migmatitic, metavolcanic felsic gneisses and amphibolites intruded by pegmatitic granites. A steep foliation trends NE and close to the V-K zone it bends more to N direction. Near the southern border of the sub-area 16 joint zones parallel the NE-trending foliation.

At the outcrops one joint set is regularly controlled by a NE-trending foliation (Figure 21). In the western part joints are mainly short (Figure 16). Long joint sets appear in fractures striking SW-NE, SE-NW and S-N close to the V-K zone. Slip markers like slickenside striations are typical on these long joint planes. The vicinity of the V-K Zone is characterized by several gently-dipping joint sets that often show strong alteration and a shear component. These gentle joint sets appear at five main trends: NW, NE, N, WNW and E.

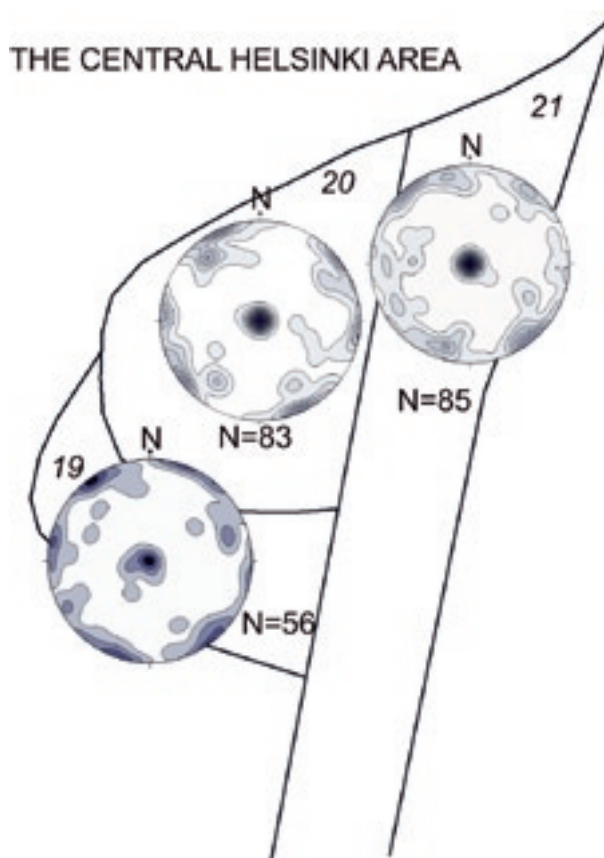


Figure 20. Orientations of the joint sets (poles to planes shown as contours on equal area lower hemisphere) in the sub-areas of the Central Helsinki Area (224 observations in all).

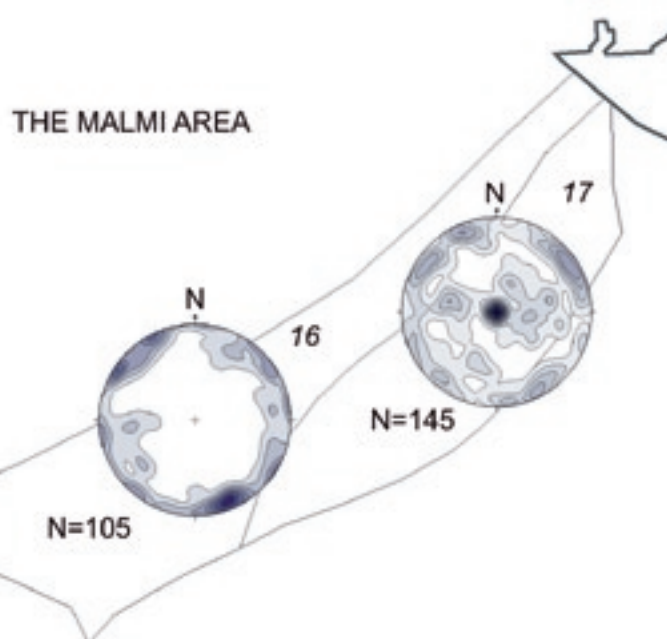


Figure 21. Orientations of the joint sets (poles to planes shown as contours on equal area lower hemisphere) in the sub-areas of the Malmi Area (250 observations in all).

The Vuosaari area

In the eastern part of the study area the Vuosaari-Korso (V-K fault zone) fault zone dominates the bedrock structures (sub-areas 22–26 and 15, Figure 14). In the Vuosaari area there are big differences in altitude. The main fault zone runs in the valley and cuts sharply the other structures. In the western part outcrops dip steeply to the west and in the east an extensive area of highlands predominates.

Granodioritic-tonalitic rocks prevail in the southern part of the Vuosaari Area (sub-areas 22 and 24). Two kilometres to the north volcanic rocks with primary structures are well preserved although rocks have been deformed both in ductile and brittle conditions. In the middle (sub-area 23) zones of supracrustal and more abundant granitoid rocks alternate. The proportion of granites increases northwards (sub-areas 15, 25 and 26).

The main trend of foliation bends northwards near the V-K fault zone and signs of shearing are common. The main strikes align to NE in the west and to NW in the eastern side of the V-K fault zone. The southernmost rocks strike mainly E-W.

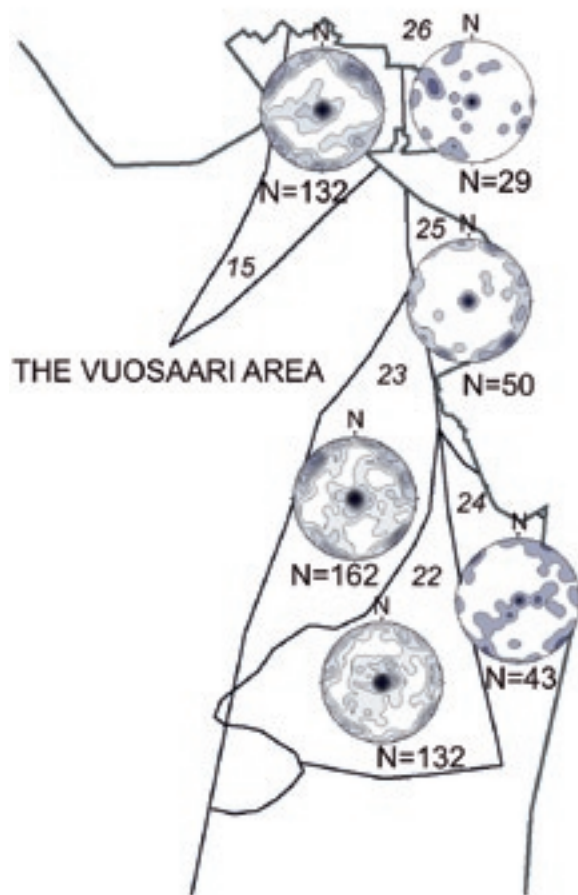


Figure 22. Orientations of the joint sets (poles to planes shown as contours on equal area lower hemisphere) in the sub-areas of the Vuosaari Area (548 observations in all).

Jointing following the main foliation is common in areas with steep foliation orientation (Figure 22). West of the V-K fault zone traces of joints are mainly short even when they follow the main foliation (Figure 16). In the eastern side some long traces of joint sets parallel the foliation in felsic gneisses and metavolcanic rocks. Long joint sets occur also trending WNW and N. In the most intensely deformed part of the V-K fault zone foliation is strong and steep. Long joints and joint zones follow the foliation or cut it at a high angle. Faulted joints and joint zones appear trending NE and NW.

Conclusion of the jointing orientations in the sub-areas

The Porkkala-Mäntsälä Zone (P-M Zone) controls the tectonic structure in its vicinity. Foliation parallels the zone and one joint set at outcrops usually follows this steep orientation near the P-M Zone. In the Nuuksio area, the westernmost part of the study area, jointing parallels the gentle foliation in granites. Besides NE-trending joints, joints at a high angle with the P-M Zone and sub-horizontal joints appear occasionally in the Bodom rapakivi batholith.

In the Espoonlahti area near Leppävaara the main structure bends to the east and a steep foliation in an almost E-W direction controls one jointing orientation. Joint sets trending NW and occasionally N include moderate joints with dips between 40°–80°. Sub-horizontal jointing occurs frequently and shows long traces of joints in microcline granite.

In sub-areas 13 and 14 in the Central Vantaa area the orthogonal joint system is well developed and one jointing orientation parallels the steep foliation trending NE. The Central Helsinki area is characterized by steep N-trending joint sets.

In the eastern part of the study area the Vuosaari-Korso fault zone (V-K Zone) defines the structural main orientation near by. The new NNE-trending strong steep foliation appears close to the V-K Zone and one jointing orientation follows it. In the vicinity of the V-K Zone steep or gentle joint sets trending NE or NW occasionally include strong alteration and shear component.

TESTING THE ADEQUACY OF DENSITY OF THE REGIONAL JOINT DATA

In the study area the average distance between the observation points was one kilometre. The adequacy of density of the mapped joint sets was tested with two joint data; from two tunnels and the densely measured data gathered in the bedrock mapping programme of GTK on the scale of 1 to 100,000. The purpose of the tests was to detect if the used mapping method finds the main jointing orientations in the area. The position of the bedrock mapping data is presented in Figure 23. The traces of the tunnels are not shown for security reasons.

The 1.2 kilometer long Salmisaari-Lauttasaari tunnel was studied during the project. Special attention was paid to jointing and zones of weakness. All the observed joints in the tunnel are included in the data. The data was divided into two parts cut by the border between sub-areas 18 and 19 (Figure 14). Sub-horizontal joint sets (dip 0°–10°) are frequent in the tunnel. They are not shown in the stereoplots (Figures 24 a, b), because compared to other orientations they dominate too much in the diagrams.

In Lauttasaari 5 observation points at outcrops are located close to the tunnel (at a distance less than 1 km and without any detected zone of weakness between them and the tunnel section). The field observations of jointing orientation fit well with the joint sets in the tunnel (Figure 24 a). A horizontal

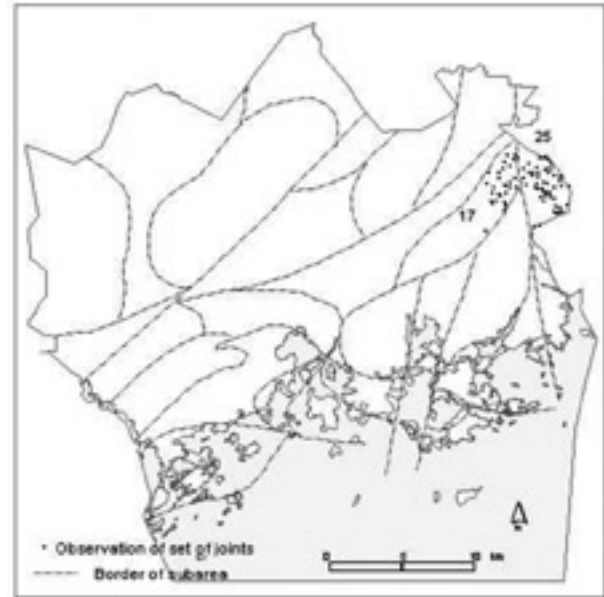


Figure 23. Location of the old joint data gathered during the bedrock mapping in 1958 and 1959.

joint set has been measured, but gently sloping joint sets were not exposed at the analyzed outcrops on the surface. The rock type in Lauttasaari is homogeneous microcline granite and steep joint sets trend similarly in the tunnel and at the outcrops.

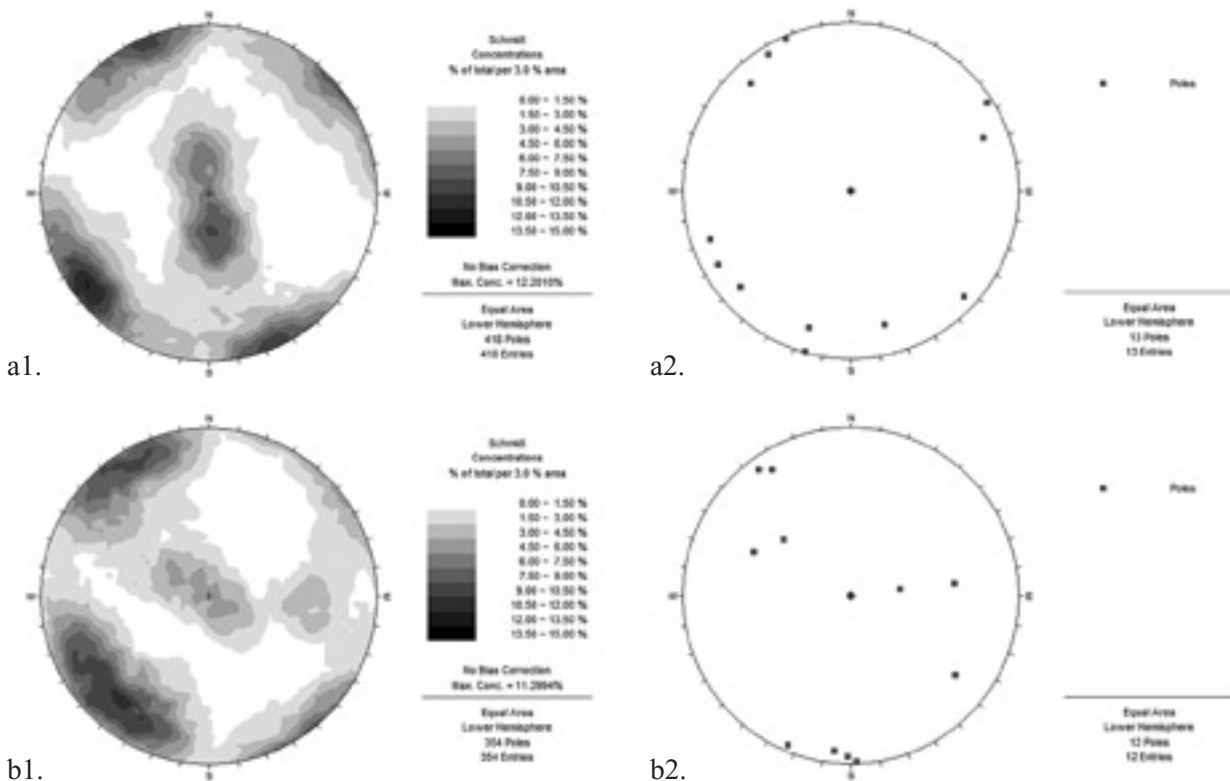


Figure 24. (a.) Joints measured in the tunnel as contours (N=418) and at 5 outcrops with square symbols (N=13) from Lauttasaari, (b.) joints measured in the tunnel as contours (N=354) and at three outcrops and one road cut with square symbols (N=12) from Salmisaari (poles to planes on equal area lower hemisphere).

In Salmisaari (Figure 1) three outcrops were mapped near the tunnel (at a distance less than 1 km from the tunnel trace) and one road cut at the tunnel mouth. Some of the joint sets on the surface parallel the main jointing orientations in the tunnel. The direction of the tunnel is NE-SW and the diagram shows shortage of data in this orientation compared to the direction at a high angle with it (Figure 24 b). The moderately dipping NW-trending (*sensu lato*) joints, which abound in the tunnel data, have not been present at the outcrops.

The Geotechnical expert services of Helsinki City Real Estate Department mapped the soil water tunnel from Kerava to the shore of the Gulf of Finland in the 1970's. Using this construction-engineering mapping data, orientations of tightly spaced joints in the tunnel between Vanhakaupunki and Kaivopuisto were digitized and utilized in this study. The data are plotted on the stereographic projections in two sets (Figure 25 a, b) divided by the border between sub-areas 19 and 20 (Figure 14). Sub-horizontal joint sets are not shown because of their dominant appearance in the tunnel. Both diagrams show considerable consistency between the tunnel and outcrop data. In Figure 25 b the NE-trending joints are underestimated in the tunnel data because the direction of the tunnel is the same. As shown,

tightly spaced joint sets in the tunnel are often present at outcrops, respectively. In a study, concerning a civil shelter in Helsinki Saari and Ylinen (1979) conclude that the joint orientations in the tunnel are very similar to those at the outcrops above.

During the national bedrock mapping on the scale of 1 to 100,000 several local measurements of joints were carried out in the eastern part of the study area. The data in Malmi and Sotunki have been digitized in the present study. In two sub-areas (17 and 25, Figure 14) these joint orientations are presented with joints measured at outcrops in the current project (Figure 26 a, b). According to the data, directional distributions correspond well to each other. Steep joints prevail in the bedrock mapping data. The gentle joint sets, shown in Figure 26 a, are from road cuts excavated after the bedrock mapping in the area.

The diagrams show that the mapping method of joint set orientations in the present study finds quite well the main joint orientations (seen in Figures 24, 25, 26). Sub-horizontal joints are relatively regular at the outcrops, but in the project data gentle joints remain underestimated. The observation density used in the study seems to be adequate for detecting frequent and essential jointing orientations in the study area.

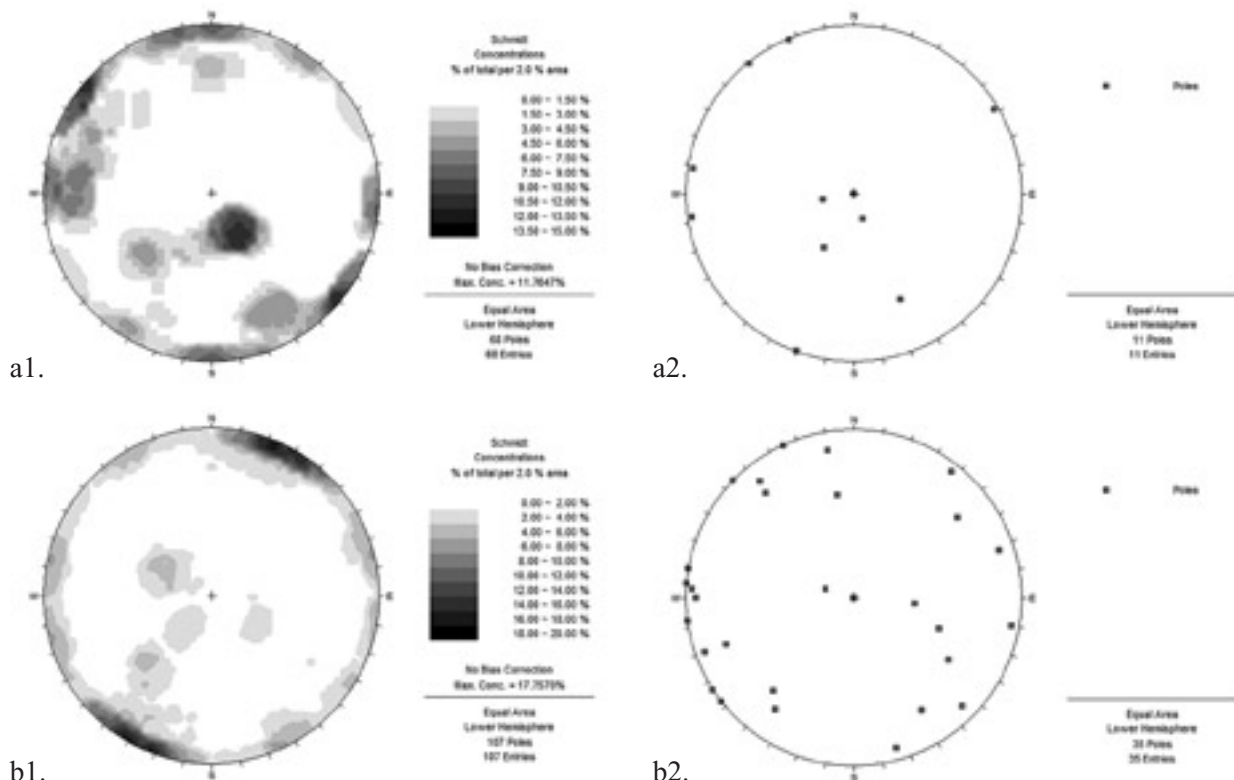


Figure 25. (a.) Tightly spaced joints measured in the soil water tunnel (southern part) as contours (N=68) and at 3 observation points with square symbols (N=11), (b.) tightly spaced joints measured in the soil water tunnel (northern part) as contours (N=107) and at 13 observation points with square symbols (N=35) (poles to planes on equal area lower hemisphere).

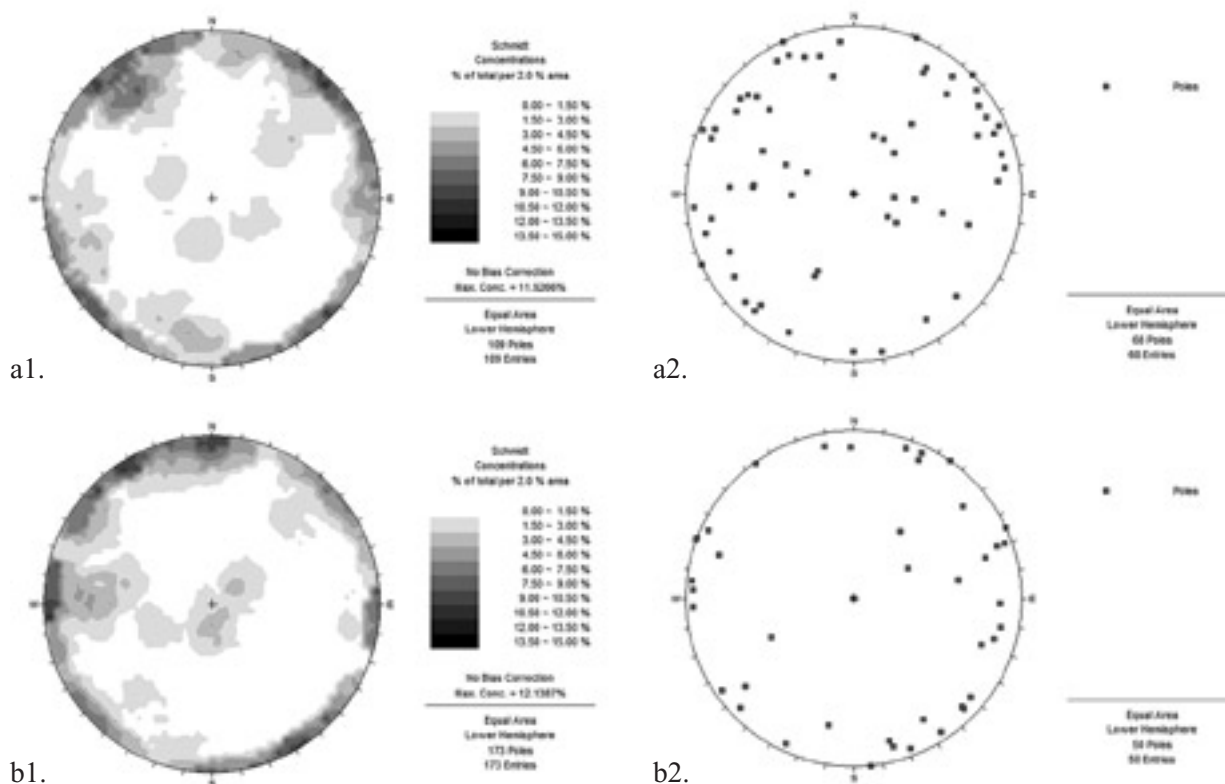


Figure 26. (a.) The old joint mapping data (contours, N=109) and joint sets measured in the present study (points, N=68) in the sub-area 17, (b.) the old joint mapping data (contours, N=173) and joint sets measured in the present study (points, N=50) in the sub-area 25.

PROPERTIES OF JOINTS

The joint properties, mapped in this study, include trace length, spacing, aperture, fillings and properties of joint walls (Table 1). The first three properties, and partly joint wall properties, are used in describing the nature of fracturing of rocks in the Helsinki area. Joint fillings and joint wall alteration types will need a separate study. The possibilities to pick up joint properties from outcrops and road cuts vary. For instance at outcrops weathering has often removed evidences of joint fillings. In road cuts such properties often have remained. Fresh, obscure joints caused by quarrying were not taken into account.

Trace length

Two trace length values were measured – the maximum length and the mean length. In the study the mean values were used. These values were corrected using the relative number of joints traversing the entire area of observation calculated as follows:

- when the relative number of joints in the joint set traversing the observation area was $\leq 33\%$,

1 was added to the mean value, e.g. $1+0,12$ ($=12\%$) = 1.12

- when the relative number was more than 33 %, the mean value was multiplied by 4; e.g. $(4 \times 0,35$ ($=35\%$)) = 1.40).

With this method the mean trace length increased in 28% of measurements and the mode of the correction in them was 1 meter (Table 2). The corrected joint length data, presented in Figure 16, are used in the description of joint set orientations in the sub-areas above.

Long trace lengths occur in joint sets parallel to and cutting the local main foliations (Figure 16). Compared to other lithologies long joint sets are more abundant in granitoids. Joint sets with mean trace lengths 10 meters or more often follow the trend of the near zone of weakness (See the zones of weakness in Elminen et al. 2008). Long sub-horizontal joint sets occur mainly in microcline granites. Variously orientated, long sub-vertical joint sets including slickensides are present close to the Vuosaari-Korso zone (V-K zone).

Table 2. The joint length values, presented in the study, have been corrected considering the relative number of joints traversing the entire area of observations. Corrections were made in 521 joint sets the mean correction being nearly +2 metres. The mode +1 metre was applied to the measured mean trace length.

Summary statistics	
Mean	1,814415
Standard Error	0,168443
Median	0,71
Mode	1
Range	35,97
Minimum	0,03
Maximum	36
Count	521

Spacing of jointing

The major part of the investigated outcrops is sparsely or slightly fractured. The most densely spaced 10 percent of the joint sets (211 exceptionally dense joint sets) have spacing values equal to or less than 0.4 m. Joint sets, in which spacing of jointing corresponds to this proportion, are concentrated in zones of gneissic rocks. In the P-M zone densely spaced joint sets parallel the zone, especially in the Bodom rapakivi batholith. The dense joint sets have two main orientations. One follows the steep foliation trending NE, and the other strikes at a high angle with this foliation (Figure 27 a). In general, in the southern part of the V-K zone gently sloping dense joint sets cut the main foliation. Approximately 70 % of densely spaced joint sets have dips $> 60^\circ$.

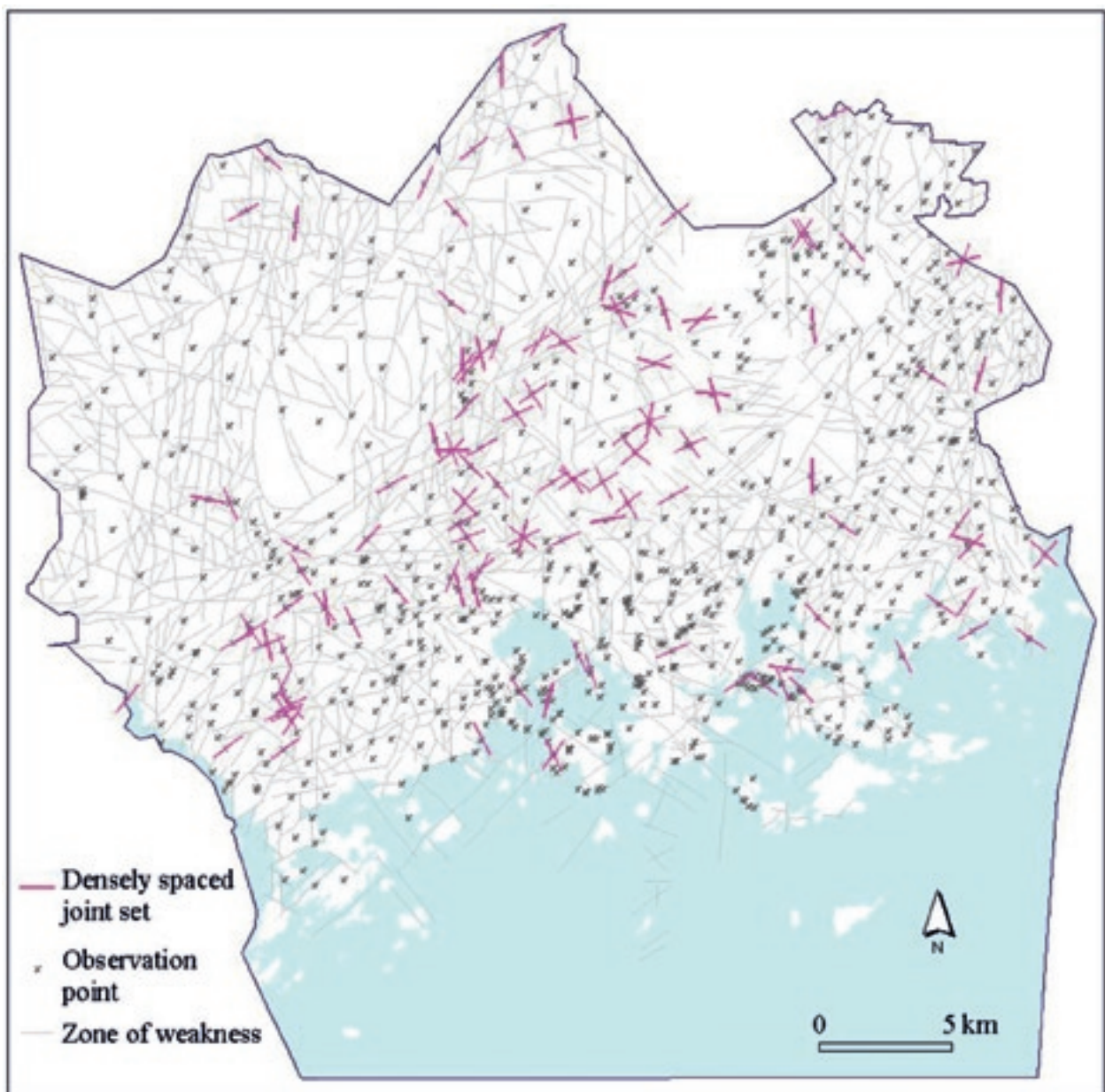


Figure 27. (a.) Densely spaced joint sets with spacing equal to 0.4 m or less (N=145). Joint sets with dips $> 60^\circ$ are presented.

Tight joints are common in densely spaced joint sets. Some open or filled joints were also observed. Most dense joints have planar surfaces regardless of the joint set orientation.

Joint zones are narrow tabular bands, where spacing of joints is exceptionally dense compared to the whole joint set in question. At outcrops 445 joint zones in 279 joint sets were observed (Figure 27 b). The widths of joint zones varied from 0.1 m to 1.5 m with median density of 12.5 joints/m (space 0.08 m) and with maximum density of 100 joints/m. In the study area joint zones occur in all kind of rocks. In the southern Espoonlahti steep joint zones parallel the foliation in granites and the strong foliation in southern V-K zone (mainly trending NE). Another main joint zone direction trends NW. Close to the V-K zone and the southern P-M zone some joint zones include slickensides.

Tightly spaced joints and joint zones occur mainly at separate locations (Figure 27 a, b). The main orientations are quite well comparable, but joint zone directions are more scattered. The joint zones are, as a whole, steeper than dense joint sets. Sub-horizontal sets are present in both data.

Tightly spaced joint sets and joint zones are often located close to zones of weakness and parallel them (Figure 27 a, b). The increase in joint frequency toward the fault zone indicates the relationship of these joints to the faulting (Peacock 2001). Niini (1968) showed in his studies of the Pääjärve bedrock tunnel in southern Finland that exceptionally fractured bedrock (fracture frequency $\geq 5/m$, Figure 11, Niini 1968.) was discovered at a distance of 100 metres from the centre of the fracture zone. However, the frequency of observations in the Helsinki Area is too sparse to ascertain this kind of connection.

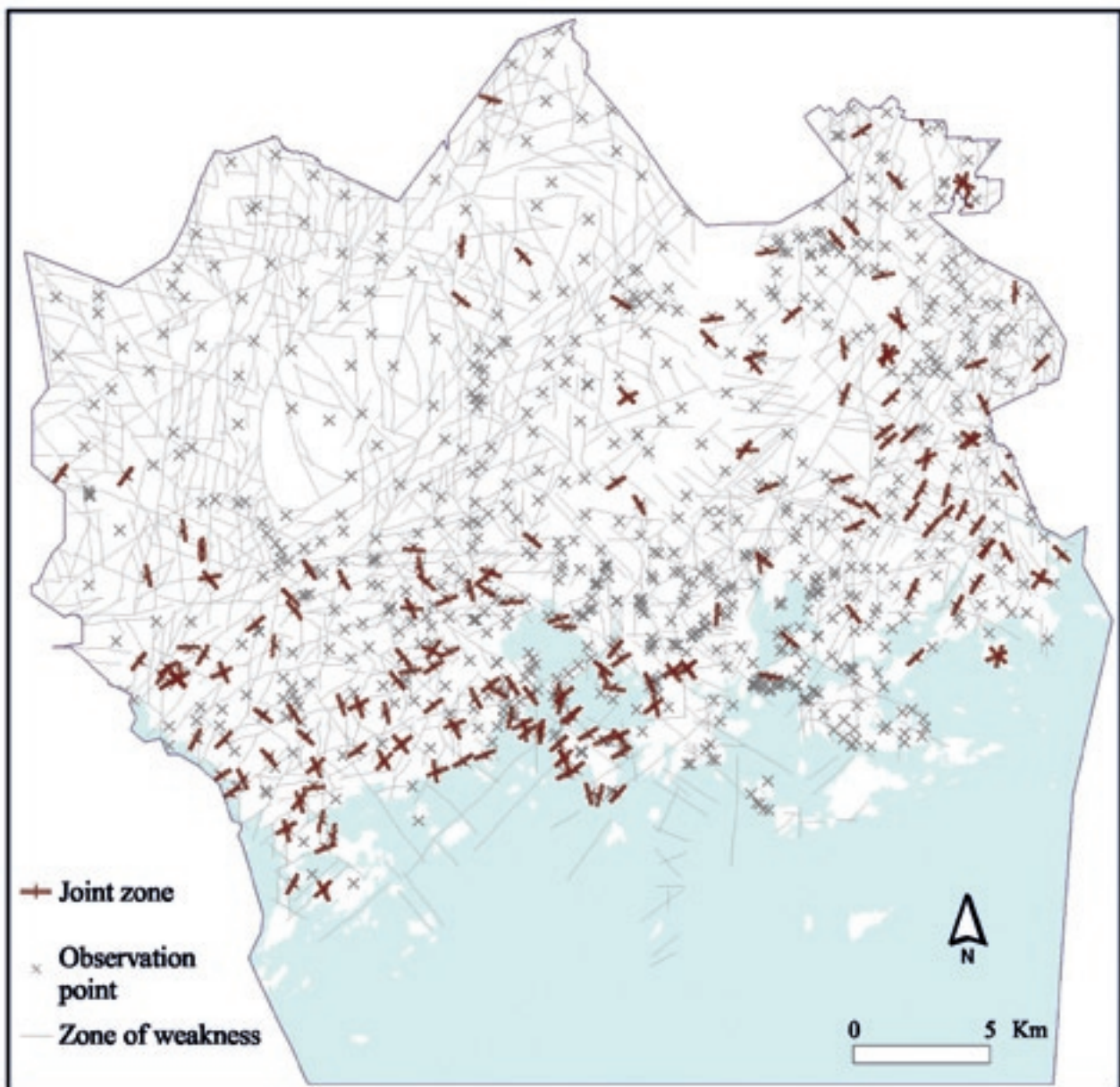


Figure 27. (b.) Joint zones in 212 joint sets. Joint sets with dips $>60^\circ$ are presented.

Relative Block size

The joint set number (J_n), total number of joints per m^3 (J_v) and the RQD value (%) were calculated for each observation point. Based on these calculations a crude measure of the average block size (RQD/J_n) (see Barton et al. 1974) was computed and presented on map (Figure 28). A small dark block size symbol indicates dense jointing at the outcrop concerned. In the Helsinki Area small block sizes characterize moderately or strongly foliated supracrustal rocks in places.

Other joint properties

In open joint sets joints with an aperture of 1 mm or more (between 1–55 mm according to the data)

were included. Open joint sets occur in the six main joint orientations defined in the beginning of this paper (Figure 29 a). NE-trending open joint sets (35 %) as well as NW-trending open joint sets (26 %) are well represented in the data. In order to bring out sub-vertical orientation groups in the diagram, sub-horizontal joints (dip 0° – 10°) were excluded.

Joint sets with slickensides are concentrated in the southwestern and eastern parts of the study area (Figure 29 b). In strongly foliated supracrustal rocks joint sets containing slickensides in southern P-M zone, in Leppävaara and in the Vuosaari-Korso fault zone parallel the strong foliation.

Joint sets with planar walls occur all over the study area, but show a scattered deviation in orientation (Figure 29 c). Joint sets, which include joints with smooth surfaces, show no particular trend either

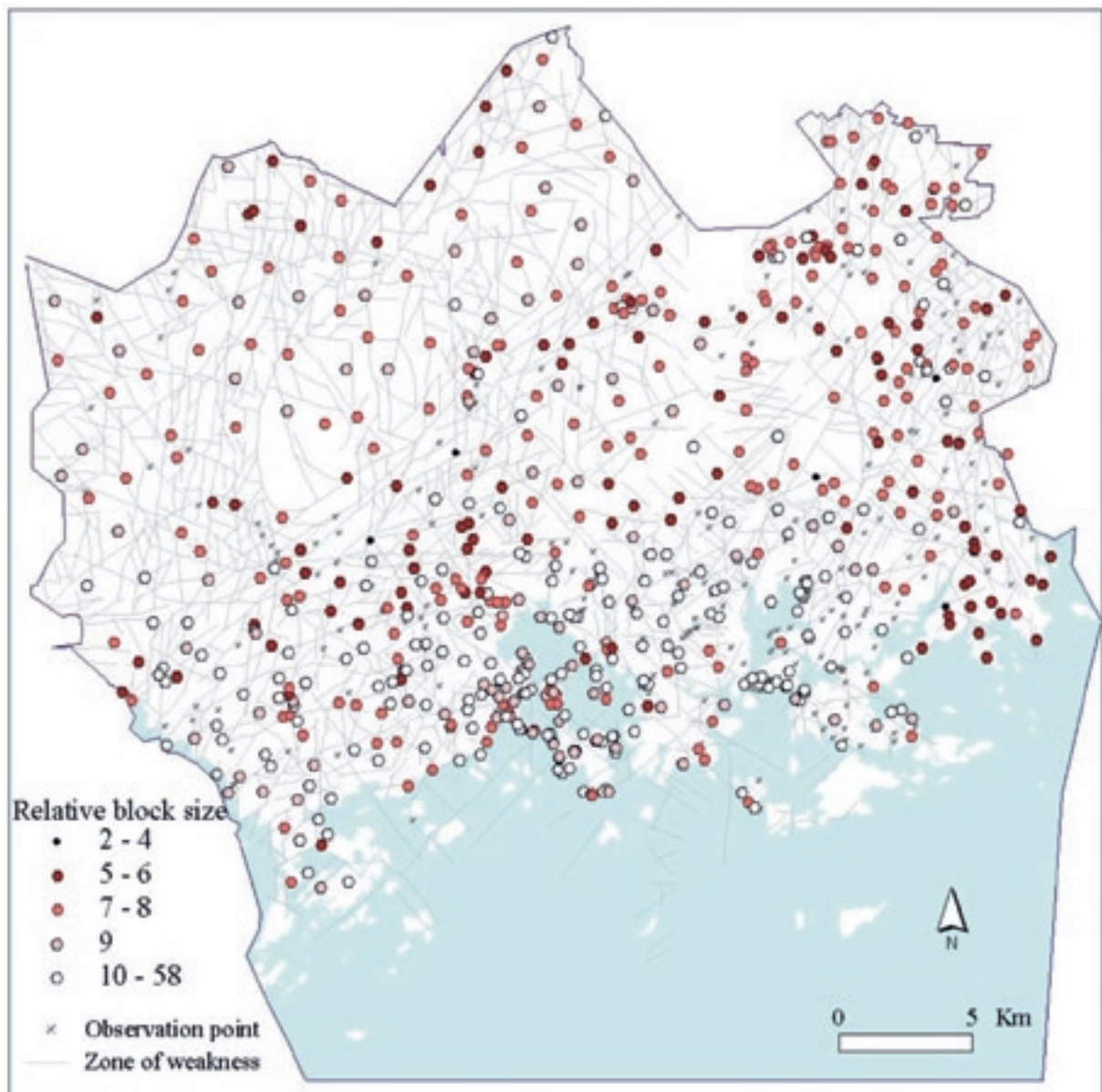


Figure 28. The relative block size (RQD/J_n) according to Barton et al. 1974. Small, dark symbols indicate dense jointing in the observation point.

(Figure 29 d). The smooth joints are concentrated in strongly foliated supracrustal rocks in the south-western and southeastern parts of the study area.

The very interesting study on the connection of these jointing properties to tectonic evolution in the area waits for completion.

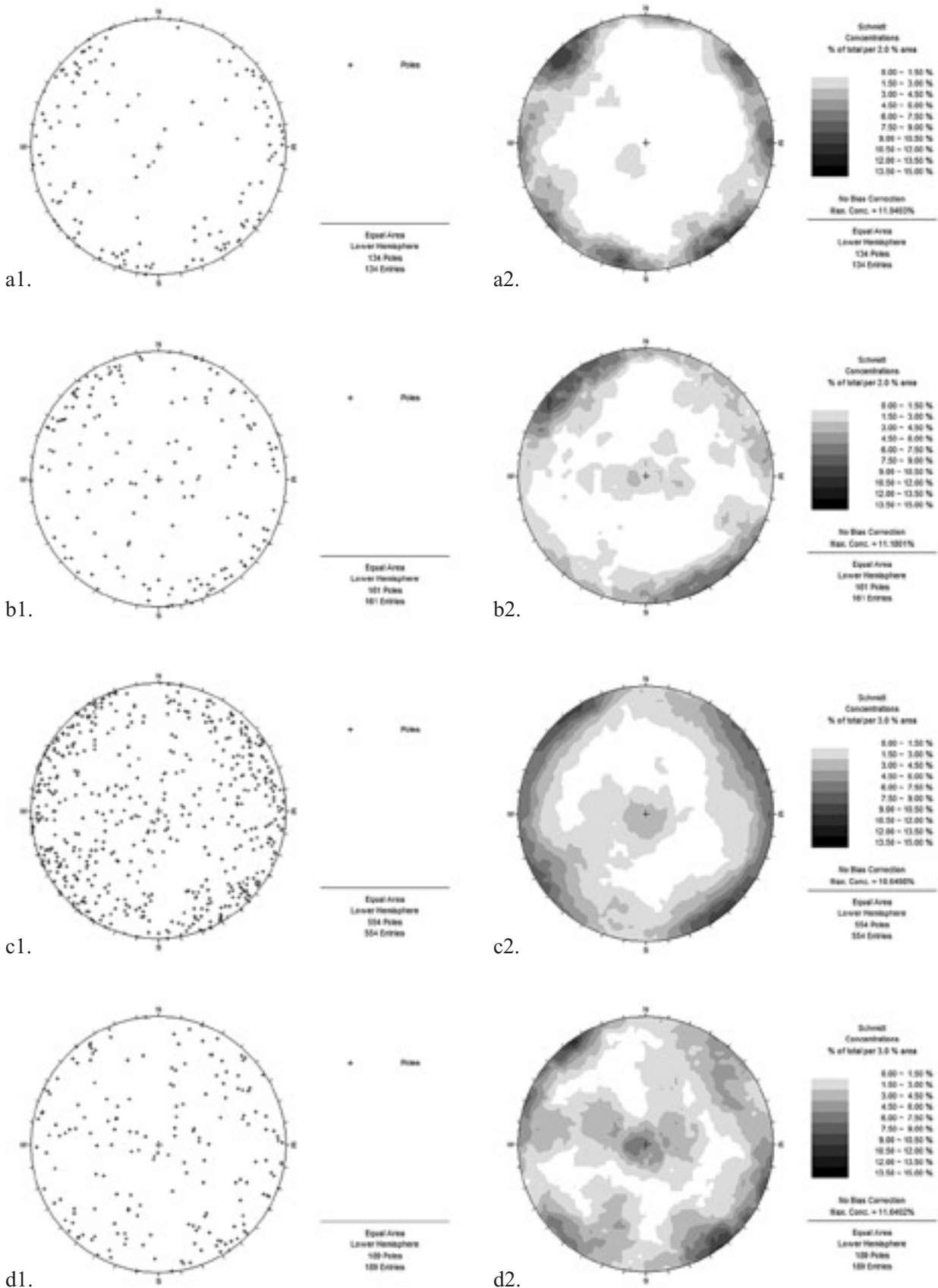


Figure 29. (a.) Orientations of open joint sets (N=134), (b.) orientations of joint sets, which include slickensided planes (N=161), (c.) orientations of joint sets with planar surfaces (N=554) and (d.) orientations of joint sets with smooth surfaces (N=189).

DISCUSSION

Regional studies of joint properties are few in Finland, especially, when compared to studies of ductile deformation succession. Some attempts on assessing the deformation history to fracturing of bedrock have been carried out (e.g. Paulamäki & Koistinen 1991 and Pajunen et al. 2001a and b). In the present study in the Helsinki area jointing was one of the main themes, and dimensional and quality features of fracturing were studied. Orientations of joint sets were combined with ductile and semi-brittle deformation features like foliation, folds and faulting structures. Properties of joints were classified and displayed on the 'Construction Potential of Bedrock' map in sub-areas defined using lithology and tectonic structure.

On a regional scale orientations of joint sets show regular patterns and match locally quite well with the tightly measured reference data used in the study. In our data in joint properties some lithological and tectonic relationships occur. For instance long joint sets, especially sub-horizontal long joints, are common in granitoid rocks. Smooth joints are concentrated in strongly foliated supracrustal rocks. Densely spaced joints and joint zones often parallel the zones of weakness in their vicinity. Close to the main fault zones in the area, the P-M zone and the V-K zone, joints with smooth slickensided walls regularly parallel the zones. In the study area migmatitic gneisses and granites dominate and they have a complex strain history. Usually the rocks do not form any exact lithological units; on the contrary they contain mixed parts of different rock types. In the study area the connection between the jointing patterns and the rock type is more complicated than expected and should be studied more carefully in the future.

The regular joint orientation trending NE and its parallelism with the main foliation are strong evidence of the control of an older deformation stage to jointing emplacement (Figures 5, 7). The P-M fault zone and V-K fault zone clearly control the jointing development nearby. One joint set parallels the foliation in the zone and the other cuts across it at a high angle (Figure 9). The diabase dyke swarm in the western part of the study area represents fracturing of the bedrock that dates back to the Rapakivi magmatism (Figure 13).

The uniform occurrence of NW- and NE-trending joint sets in the study area implies a regional, more than local strain (Figure 9). The concentration of steep NNE-trending joint sets close to the Vuosaari-Korso shear zone (V-K zone) and to the other NNE-trending faults (Figure 10) (See NNE-trending faults in Elminen et al. 2008), shows a tectonic

connection between these two structures. The NNE trending joints show crosscutting nature towards the local main foliation (Figure 11 a, b). The smooth surfaces indicate shearing after the initiation of the joints. The NNE-trending joints probably indicate a new jointing phase originated due to rotation in the local stress fields followed by movements in the NNE-trending faults.

The NW trending joint sets show moderately dipping planes both to NE and to SW. The same trends are present in the fault structure data (Elminen et al. 2008), but the relationship between these two structures has not yet been analysed. Granites in the southern part of the study area would be the best targets for this examination because the terrain has experienced only the latest phases of deformation events (Pajunen et al. 2008).

Orthogonal jointing pattern characterizes the central part of the study area (Figure 19). The appearance of the orthogonal jointing system indicates a rotation of regional principal stresses by 90° (Bai et al. 2002), or some switch in the local stress may lead to initiation of a new crosscutting joint set (Caputo 1995).

In the study area migmatitic gneisses and granites dominate and the rocks are mostly highly anisotropic in structures indicating complex strain history (Pajunen et al. 2008). In order to use jointing orientations as strain indicators more research concerning the relationships of joint to joint and joints to fault structures is required.

In aeromagnetic data the structural form lines of strongly foliated migmatitic rocks often show the trend of one of the main joint sets observed at outcrops (Figure 8). At the outcrop scale the aeromagnetic data may not give a straight reference of fracturing, but in places where jointing builds up regionally continuous structures or joint zones, the joint sets often can be detected.

In a directional analysis of aeromagnetic data continuity trends in pre-defined directions of preferred angles were found (Airo et al. 2008). The compatibility with field observations is outstanding in the directions of systematically occurring joint sets trending NE and NW (Figure 12). The joint set directions often even locally follow the analyzed minor lineaments. The reliability of this method for predicting jointing orientations will be studied forward.

The banded rectilinear anomalies, shown on the aeromagnetic map, parallel two steep joint sets trending NW and WNW follow the directions of diabase dyke swarms (Figure 13). It is obvious that the first appearance of jointing in the Helsinki Area bedrock dates back at least to the intrusion of these dykes.

The control of earlier deformation structures to joint set emplacement proved to be strong. The relationship is multiform and not always easily found. A new framework of the brittle deformation in the Helsinki area could be constructed in the future studies by using these observations in connection

with fault structures (Elminen et al. 2008). The increased knowledge about the relationships between separate deformation structures makes it possible to prefigure jointing patterns in new study and mapping areas.

CONCLUSION

In the present study joint set orientations, dimensions and quality properties were examined in 687 observation points in the Helsinki Area. The distance between the points was approximately one kilometre, which proved to be adequate for regional inspection and the local orientations match quite well the reference data. The purpose was to study jointing geometry and the control of earlier deformation structures to jointing orientations on a regional scale. This information will be used in predicting fracturing in future study areas.

This paper describes jointing characteristics in the study area. Bedrock in the area is sparsely or slightly fractured. Long traces of joints, densely spaced joint sets and joint zones locally decrease the construction potential of rock. Long trace lengths occur in joint sets parallel to local main foliations and long sub-horizontal joints are frequent in microcline granite. Tightly spaced joint sets and joint zones are often located close to zones of weakness, which may indicate the relationship of these joints to the faulting.

The whole joint data include six main orientation groups with varying frequencies across the area. In six sub-areas the jointing orientations deviate to some extent, but NE- and NW-trending joint sets display uniform occurrence in the area. They imply a regional strain.

The steep NNE-trending joint sets close to the NNE-trending faults probably indicate a new jointing phase originated due to rotation in the local

stress fields followed by movements in the faults.

In aeromagnetic data the structural form lines of strongly foliated migmatitic rocks appear as banded anomalies. They show the trend of frequent joint set, which parallels the main foliation orientation. Also the results of the directional analysis of aeromagnetic data are outstanding in compatibility with the directions of systematically occurring joint sets trending NE and NW. The reliability of this method for predicting jointing orientations in bedrock is promising, but it still requires further studies. On the aeromagnetic horizontal gradient map the banded, rectilinear anomalies indicate a parallel jointing with diabase dykes in the western part of the study area referring to brittle fracturing already during the rapakivi magmatism (ca. 1650 Ma).

Underground activities in civil engineering targets are mostly directed to the upper most 100 metres of the bedrock. The importance of knowledge in jointing properties of bedrock in urban areas increases with the intensification of subjecting new bedrock areas to construction activities. Especially the information about orientation and properties of zones of weakness and systematic joint zones would direct construction activities of communities to suitable localities. Studies on a regional scale highlight regular fracturing patterns in bedrock. At the same time the relation of jointing to other tectonic features, fault structures and foliation is detectable at a regional scale.

ACKNOWLEDGEMENTS

The project "Construction potential modelling of bedrock in urban areas" was a co-operation project financed by Geological Survey of Finland (GTK), National Technology Agency of Finland, Cities of Espoo, Helsinki and Vantaa and two companies, Rockplan Ltd. and Viatek Ltd. We would like to express our gratitude to these establishments for providing possibilities to realize our studies. Eevaliisa Laine from Technical university of Helsinki has acted as an advisor in geostatistics. We express our

gratitude to her for useful ideas and comments. Nils Gustavsson from GTK has constructed the applications for counting joint length and density parameters in the study. We would also like to thank all other persons involved in this work – Juha Salmelainen from Rockplan Ltd and Christer Ahlsved, Anneli Lindh, Satu Mertanen, Tuomo Turunen and Markku Väisänen from GTK. Reviews by H. Niini, L. Persson and L. Albrecht are gratefully acknowledged.

REFERENCES

- Airo, M.-L., Elminen, T., Mertanen, S., Niemelä, R., Pajunen, M., Wasenius, P. & Wennerström, M. 2008.** Aerogeophysical approach to ductile and brittle structures in the densely populated urban Helsinki area, southern Finland. In: Pajunen, M. (ed.) Tectonic evolution of the Svecofennian crust in southern Finland – a basis for characterizing bedrock technical properties. Geological Survey of Finland, Special Paper 47, 283–308.
- Anttila, P. (ed.), Paulamäki, S., Lindberg, A., Paananen, M., Koistinen, T., Front, K. & Pitkänen, P. 1992.** The geology of the Olkiluoto area, summary report. Helsinki, Finland: Nuclear Waste Commission of Finnish Power Companies, Report YJT–92–28. 83 p.
- Anttila, P., Ahokas, H., Front, K., Hinkkanen, H., Johansson, E., Paulamäki, S., Riekkola, R., Saari, J., Saksa, P., Snellman, M., Wikström, L. & Öhberg, A. 1999.** Final disposal of spent nuclear fuel in Finnish bedrock – Olkiluoto site report. Helsinki, Finland: Posiva Oy, POSIVA 99–10. 206 p.
- Arlegui, L. & Simon, J. L. 2001.** Geometry and distribution of regional joint sets in a non-homogeneous stress field; case study in the Ebro Basin (Spain). *Journal of Structural Geology* 23:2–3, 297–313.
- Babcock, E. A. 1974.** Jointing in Central Alberta. *Can. J. Earth Sci.*, v. 11, 1181–1186.
- Bai, T., Maerten, L., Gross, M. R. & Aydin, A. 2002.** Orthogonal cross-joints; do they imply a regional stress rotation? *Journal of Structural Geology* 24:1, 77–88.
- Barton, N., Lien, R. & Lunde, J. 1974.** Engineering classification of rock masses for the design of tunnel support. *Rock Mechanics* 6, 189–236.
- Bürgmann, R. & Pollard, D. D. 1994.** *Journal of Structural geology* 16:12, 1655–1674.
- Caputo, R. 1991.** A comparison between joints and faults as brittle structures used for evaluating the stress field. *Annales Tectonicae*, Vol.V, n. 1, 74–84.
- Caputo, R. 1995.** Evolution of orthogonal sets of coeval extension joints. *Terra Nova*, 7, 479–490.
- Cruikshank, K. M. & Aydin, A. 1995.** Unweaving the joints in Entrada Sandstone, Arches National Park, Utah, U.S.A. *Journal of Structural Geology* 17:3, 409–421.
- Elminen, T., Airo, M.-L., Niemelä, R., Pajunen, M., Vaarma, M., Wasenius, P. & Wennerström, M. 2008.** Fault structures in the Helsinki Area, southern Finland. In: Pajunen, M. (ed.) Tectonic evolution of the Svecofennian crust in southern Finland – a basis for characterizing bedrock technical properties. Geological Survey of Finland, Special Paper 47, 185–213.
- Granier, T. 1985.** Origin, damping, and pattern of development of faults in granite. *Tectonics*, vol. 4, no. 7, 721–737.
- Haapala, I., Rämö, O. T. & Frindt, S. 2005.** Comparison of Proterozoic and Phanerozoic rift-related basaltic-granitic magmatism. *Lithos* 80, 1–32.
- Hancock, P. L. 1972.** The analysis of en-echelon veins. *Geological Magazine* 109:3, 269–275.
- Härme, M. 1961.** On the Fault Lines of Finland. *Bulletin de la commission géologique de Finlande* 196, 437–444.
- Härme, M. 1969.** Kerava. Geological map of Finland 1:100 000, Pre-Quaternary Rocks, Sheet 2043. Geologinen tutkimuslaitos.
- Kattenhorn, S. A., Aydin, A. & Pollard, D. D. 2000.** Joints at high angles to normal fault strike; an explanation using 3-D numerical models of fault-perturbed stress fields. *Journal of Structural Geology* 22:1, 1–23.
- Korsman, K., Korja, T., Pajunen, M. & Virransalo, P. 1999.** The GGT/SVEKA transect: structure and evolution of the continental crust in the Paleoproterozoic Svecofennian orogen in Finland. *International Geology Review* 41, 287–333.
- Kosunen, P. 1999.** The rapakivi granite plutons of Bodom and Obbnäs, southern Finland: petrography and geochemistry. *Bulletin of the Geological Society of Finland* 71, 275–304.
- Laitala, M. 1960.** Siuntio. Geological map of Finland 1:100 000, Pre-Quaternary Rocks, Sheet 2032. Geologinen tutkimuslaitos.
- Laitala, M. 1967.** Helsinki. Geological map of Finland 1:100 000, Pre-Quaternary Rocks, Sheet 2034. Geologinen tutkimuslaitos.
- Laitala, M. 1994.** Lohja. Geological map of Finland 1:100 000, Pre-Quaternary Rocks, Sheet 2041. Geological Survey of Finland.
- Martel, S. J. 1990.** Formation of compound strike-slip fault zones, Mount Abbot Quadrangle, California. *Journal of Structural Geology* 12:7, 869–882.
- Niini, H. 1968.** A study of rock fracturing in valleys of Precambrian bedrock. *Fennia*, 97: 6, 1–60.
- Niini, H., Uusinoka, R. & Emekeokhale, S. 2001.** Bedrock parameters of natural surfaces differing from those of excavated road cuts. *Bull. Eng. Geol. Env.* 60, 103–108.
- Olmacher, G. C. & Aydin, A. 1995.** Progressive deformation and fracture patterns during foreland thrusting in the Southern Appalachians. *American Journal of Science* 295:8, 943–987.
- Olson, J. & Pollard, D. D. 1989.** Inferring paleostresses from natural fracture patterns; a new method. *Geology* 17:4, 345–348.
- Pajunen, M., Airo, M.-L., Wennerström, M., Niemelä, R. & Wasenius, P. 2001a.** Preliminary report: The “shear zone research and rock engineering” project, Pori area, south-western Finland. Geological Survey of Finland, Special Paper 31, 7–16.
- Pajunen, M., Elminen, T., Airo, M.-L. & Wennerström, M. 2001b.** Structural evolution of bedrock as a key to rock mechanical properties. In *Rock Mechanics. A Challenge for Society. Proceeding of Regional Symposium EUROCK 2001*. Rotterdam: A. A. Balkema, 143–148.
- Pajunen, M., Airo, M.-L., Elminen, T., Niemelä, R., Vaarma M., Wasenius P. & Wennerström M. 2002.** Kallioperän rakennettavuusmalli taajamiin. The Con-

- struction Potential of Bedrock. Menetelmänkehitys ja ohjeistus. Geological Survey of Finland, unpublished report K.21.42/2002/5. 95 p. (in Finnish)
- Pajunen, M., Airo, M.-L., Elminen, T., Mänttari, I., Niemelä, R., Wasenius, P., Vaarma, M. & Wennerström, M. 2008.** Tectonic evolution of the Svecofennian crust in southern Finland. In: Pajunen, M. (ed.) Tectonic evolution of the Svecofennian crust in southern Finland – a basis for characterizing bedrock technical properties. Geological Survey of Finland, Special Paper 47, 15–160.
- Paulamäki, S. 1995.** Geological bedrock and fracture mapping of the investigation trench TK1 at the Olkiluoto study site, Eurajoki, western Finland (in Finnish with an English abstract). Helsinki, Finland: Teollisuuden Voima Oy, Work Report PATU–95–81. 40 p.
- Paulamäki, S. 1996.** Geological bedrock and fracture mapping of the investigation trench TK2 at the Olkiluoto study site, Eurajoki, western Finland (in Finnish with an English abstract). Helsinki, Finland: Posiva Oy, Work Report PATU–96–61. 47 p.
- Paulamäki, S. & Koistinen, T. J. 1991.** Interpretation of the geological structures of the Olkiluoto area, Eurajoki, Western Finland. Espoo, Geological Survey of Finland, Nuclear Waste Disposal Research. TVO/Site Investigations, Work Report 91–93. 26 p. (in Finnish)
- Peacock, D. C. P. 2001.** The temporal relationship between joints and faults. *Journal of Structural Geology* 23: 2–3, 329–341.
- Pollard, D. D., Segall, P. & Delaney, P. T. 1982.** Formation and interpretation of dilatant echelon cracks. *Geological Society of America Bulletin* 93:12, 1291–1303.
- Pollard, D. D. & Segall, P. 1987.** Theoretical displacements and stresses near fractures in rock: with applications to faults, joints, veins, dikes, and solution surfaces. In: Atkinson, B. K. (ed.) *Fracture mechanics of rock*. London, England: Academic Press, p. 277–349.
- Pollard, D. D. & Aydin, A. 1988.** Progress in understanding jointing over the past century. *Geological Society of America Bulletin* 100:8, 1181–1204.
- Reches, Z. 1976.** Analysis of joints in two monoclines in Israel. *Geological Society of America Bulletin* 87:11, 1654–1662.
- Saari, K. & Ylinen, A. 1979.** Mapping of joints in Precambrian granitic rock masses. *Bulletin of the International Association of Engineering Geology* 19, 190–195.
- Segall, P. & Pollard, D. D. 1983.** Joint formation in granitic rock of the Sierra Nevada. *Geological Society of America Bulletin* 94:5, 563–575.
- Vaasjoki, M. 1977.** Phanerozoic resetting of U- Pb ages in some South-Finnish uraninites. In: ECOG V. Fifth European Colloquium of Geochronology, Cosmochronology and Isotope Geology, Pisa, September 5–10, 1977. 2 p.
- Väisänen, M. & Mänttari, I. 2002.** 1.90 – 1.88 Ga arc backarc basin in the Orijärvi area, SW Finland. *Bulletin of the Geological Society of Finland* 74, 185–214.
- Wilkins, S., Gross, M. R., Wacker, M., Eyal, Y. & Engelder, T. 2001.** Faulted joints; kinematics, displacement-length scaling relations and criteria for their identification. *Journal of Structural Geology* 23:2–3, 315–327.
- Zhao, G. & Johnson, A. M. 1992.** Sequence of deformations recorded in joints and faults, Arches National Park, Utah. *Journal of Structural Geology* 14:2, 225–236.

AEROGEOPHYSICAL APPROACH TO DUCTILE AND BRITTLE STRUCTURES IN THE DENSELY POPULATED URBAN HELSINKI AREA, SOUTHERN FINLAND

by

Meri-Liisa Airo, Tuija Elminen, Satu Mertanen, Reijo Niemelä,
Matti Pajunen, Pekka Wasenius and Marit Wennerström*

Airo, M.-L., Elminen, T., Mertanen, S., Niemelä, R., Pajunen, M., Wasenius, P. & Wennerström, M. 2008. Aerogeophysical approach to ductile and brittle structures in the densely populated urban Helsinki area, southern Finland. *Geological Survey of Finland, Special Paper 47*, 283–308, 13 figures and 2 tables.

The whole Helsinki area is covered by high-resolution aerogeophysical surveys, including magnetic, electromagnetic and gamma-ray spectrometric measurements. Interpretation of these data aimed at outlining the regional structural framework with respect to the present structural pattern of bedrock, and at discovering systematic trends for shallow, near-surface geological features. Standard interpretation methods were expanded by using directional analysis of horizontal derivatives (HDR) of aeromagnetic data. The main results include:

1. Aeromagnetic lineaments are related to fracture zones, faults and joints and their regional distribution and orientations can be mapped by using directional analysis of aeromagnetic HDR data.
2. Aeromagnetic data mirror extremely well the structural domains of bedrock and the character of their overall fragmentation and fracturing. Regular patterns of faults and joints are found along geophysical domain boundaries and demonstrated in aeromagnetic data by local lineaments paralleling the boundaries.
3. Bedrock fabric plays an important role in localizing the development of faults and fractures. Aeromagnetic anomaly trends are consistent with the strike of fold axes and foliation of bedrock – similarly, the intersecting magnetic lineaments correspond to schistosity.
4. The geometry of magnetic lineaments is consistent with topographic morphology, supporting the idea that the late stage, brittle deformational pattern of bedrock surface is well described by high-resolution aeromagnetic data.

Key words (GeoRef Thesaurus, AGI): geophysical surveys, airborne methods, magnetic methods, gravity methods, petrophysics, structural geology, lineaments, urban environment, Paleoproterozoic, Helsinki, Espoo, Vantaa, Finland

* *Geological Survey of Finland, P.O. Box 96, FI-02151 Espoo, Finland*

* *E-mail: meri-liisa.airo@gtk.fi*

INTRODUCTION

The so-called Helsinki area in southern Finland comprises the neighbouring cities of Helsinki, Espoo and Vantaa, with a population of more than 1 million people altogether. Structural mapping of this densely populated and built-up area was carried out between 1999 and 2002 as a pilot project: “Construction potential modeling of bedrock in urban areas” (e.g. Pajunen et al. 2001a). The project focused on detecting, characterizing and categorizing crustal weakness zones in the Helsinki area for the needs of infrastructural planning and underground construction. The results were presented on a thematic structural bedrock map on a scale of 1:50 000 (Pajunen et al. 2008a, this volume). The map outlines bedrock provinces showing different structure and construction potential, with classification of crustal weakness zones and fractured parts of bedrock. The mapping context was based on new fieldwork focusing on structural observations, on previous geological studies and on high-resolution airborne geophysical data covering the whole area. Since the completion of the pilot project, the same method of structural re-mapping in urban areas has been adopted to cover a wider area – the Helsinki area – including the municipalities surrounding the cities of Helsinki, Espoo and Vantaa.

Soil cover and cultivated fields in southern Finland hinder the straight geological observation of bedrock structure and lithology. In densely built-up urban areas, where road and street network and building complexes obstruct the geological observation coverage, regional geophysical data are crucially important in crustal investigations. Particularly in geologically complex areas of limited outcrop, geophysical methods improve mapping the outline of geological units, their continuity and the distribution and organization of fault and fracture zones.

Geophysical data, in particular magnetic and gravity data are valuable in crustal studies, because they can give the vertical dimension to the lateral variation of geological features and their continuity under cover. However, the geophysical crustal investigations must be bound by an understanding of the basement structure and the geological history of the study area. Airborne geophysical surveys provide cost-effective, coherent, multifaceted information on the variation of the physical properties of bedrock and soil cover. The whole Helsinki area is covered by high-resolution aerogeophysical surveys, including magnetic, electromagnetic and gamma-

ray spectrometric measurements. Interpretation of these data is aimed at 1) outlining the regional structural framework controlling the present structural pattern of bedrock, and 2) expanding the standard interpretation methods to discover such shallow, near-surface geological features, which were produced by brittle deformation at the late stage of tectonic history, and whose geophysical signature may be very weak and local. Furthermore, the cultural component of magnetic field in densely developed areas may have significant amplitude and strongly disturb or mask the sometimes very low-amplitude geological signature. Different methods of removing the artificial anomaly component were compared.

Of geophysical methods, the magnetic method gives a good description and is often solely sufficient for investigation of crustal structure, provided that the geological history and the main features of the basement structure are known to some extent. Other geophysical data sets, including airborne electromagnetic and radiometric data, petrophysical properties and regional Bouguer-anomaly data, played a supportive role in explaining and classifying the results of magnetic interpretation. Structural interpretation of aeromagnetic data in areas of limited outcrop requires the use of relevant data enhancement techniques for accurate positioning of magnetic sources – body outlines and structural relationships of the lithological provinces. In defining indications of brittle deformation, we applied directional horizontal derivatives (HDR), which emphasize small variations in magnetic susceptibility thus highlighting perpendicular structural trends. For enhancing the brittle structure especially in areas of weak magnetic contrast, we used the so-called total horizontal derivative THDR (the sum vector of two perpendicular derivative directions). In addition to detailed scale investigations, we used horizontal derivatives in analyzing regional scale folding.

Geoscientific mapping, based on integration of geophysical, geological and geographic information, enables the production of geoscience databases and thematic maps in urban and highly developed areas. These databases will be important for the planning of future land-use, underground construction and for environmental follow-up. Future importance may rest in the prediction of environmental – ecological hazards, which may depend on geological factors.

AIRBORNE GEOPHYSICAL SURVEYS IN THE HELSINKI AREA AND DATA DESCRIPTION

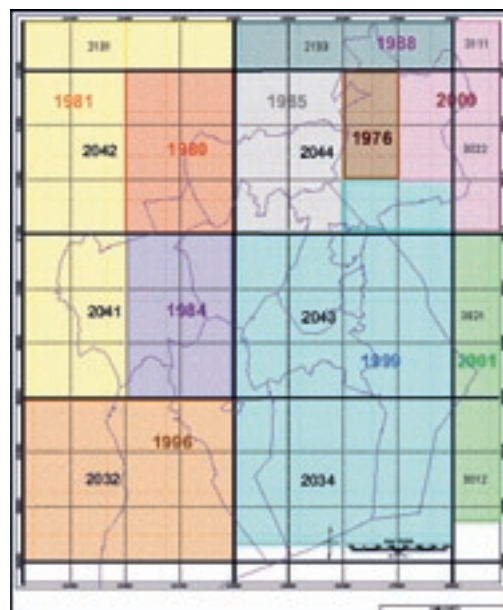
The Helsinki area is covered by high-resolution aerogeophysical surveys. They were separate flights covering separate survey areas over a period of several years as part of the nationwide aerogeophysical mapping project in Finland. The Geological Survey of Finland (GTK) has conducted nationwide surveys by applying a nominal terrain clearance of 35 m and a line spacing of 200 m. The flying direction was either NS or EW, depending on the main geological trend of the survey area. Throughout the surveys, the GTK “Three-in-One” concept applied comprises simultaneous measurement of the Earth’s magnetic field, the electromagnetic field (after 1996 dual-frequency) and gamma-ray spectrometric data in one survey flight (Hautaniemi et al. 2005). High-sensitivity magnetometers register even the slightest lateral variation in the magnetic properties of bedrock. Electromagnetic measurements detect electrical conductivity of the ground, including the conductivity variation of both the bedrock and soil. The gamma-ray spectrometric method measures the natural gamma-radiation of the ground (K, Th and U). Gamma-rays emitted from the ground surface relate to the primary mineralogy and geochemistry of the bedrock, and the secondary weathered materials

composing the soil cover. The aeroradiometric data are complementary to aeromagnetic data in terms of the lithological characterization of bedrock.

Survey characteristics in the Helsinki area and map sheets covered are illustrated in Table 1. To promote regional crustal mapping in urban areas, GTK and Malmilento Oy conducted a new airborne survey covering the cities of Helsinki, Espoo and Vantaa in 1999. The flights were carried out using a Twin-Otter aircraft (wing span 21.36 m) and the GTK Three-in-One concept: two Cesium magnetometers mounted on the wing tips; a dual-frequency AEM system consisting frequencies of ~3 kHz and ~14 kHz, and a radiometric crystal volume 41 l. The size of the surveyed area was about 45 km x 60 km. By using differential GPS, the accuracy of positioning is less than one meter. The line spacing of EW- trending flight lines was 200 m and occasionally 100 m. The nominal terrain clearance was mainly 35 m – in areas of denser population it was 70 m, and above Helsinki city the altitude was raised to 160 m. The wide range in flight altitude variation meant that extra care had to be taken when processing and interpreting the aerogeophysical data.

Table 1. System specifications for airborne geophysical surveys in the Helsinki area. Map sheet index for the countrywide 1:100 000 aerogeophysical mapping program. Helsinki 1999 survey area in light blue.

Year	Map sheet	Line spacing	Flight direction
1999	2034 and 2043 (1:100 000)	200 m	EW
	2034 03	100 m	EW
	2032 12C-D	100 m	EW
	2043 05 and 06C-D	100 m	EW
	2043 08A-B, 09A-B	100 m	EW
1976	2044 08–09	200 m	NS
1981	2041 01–06	200 m	NS
	2042 01–06	200 m	NS
	2131 01, 04, 07, 10	200 m	NS
1984	2041 07–12	200 m	NS
1985	2044 01–06	200 m	NS
1988	2133 01, 04, 07, 10	200 m	NS
1996	2032 01–12	200 m	NS
2000	2044 11–12	200 m	NS
	3022 10–12	200 m	NS
	3111 01	200 m	NS
2001	3012 02–03	200 m	NS
	3021 01–03	200 m	NS



GEOLOGICAL AND GEOPHYSICAL OUTLINE

The bedrock of the Helsinki area, on the northern coast of the Gulf of Finland, belongs to the Proterozoic Svecofennian Domain in the central part of the Precambrian Fennoscandian Shield (Korsman et al. 1999). The supracrustal rocks were folded, metamorphosed and migmatized during the Svecofennian Orogeny (1.95 to 1.8 Ga). Large massifs of plutonic rocks, especially granitoids, were intruded during the Lower Proterozoic. After this, there were only minor rock-building processes, such as the intrusion of rapakivi granites in the Middle Proterozoic (Vaasjoki & Sakko 1988). Thick sediments, which covered the region during the Phanerozoic, are now eroded and have vanished due to the continental glacier. The geological outline of the Helsinki area is described in more detail in Pajunen et al. 2008b (this volume).

The geophysical of the Helsinki area is best determined by aeromagnetic data. The regional gamma-radiation data reveal regional variation in the overall K-, U- and Th-radiation, largely related with variation in bedrock composition and deformation. The regional electromagnetic data sets show very few bedrock conductors.

Comparison of lithological and aeromagnetic maps (Figure 1) verifies that in general, the whole region is characterized by regional magnetic lows (blue areas), which correspond to wide areas of granite (red areas on the lithological map). Svecofennian gneisses and migmatites appear on the aeromagnetic map as concentrated, elongated narrow magnetic anomalies with alternating amplitudes. In a broad scale, the anomaly strikes follow the structural aniso-

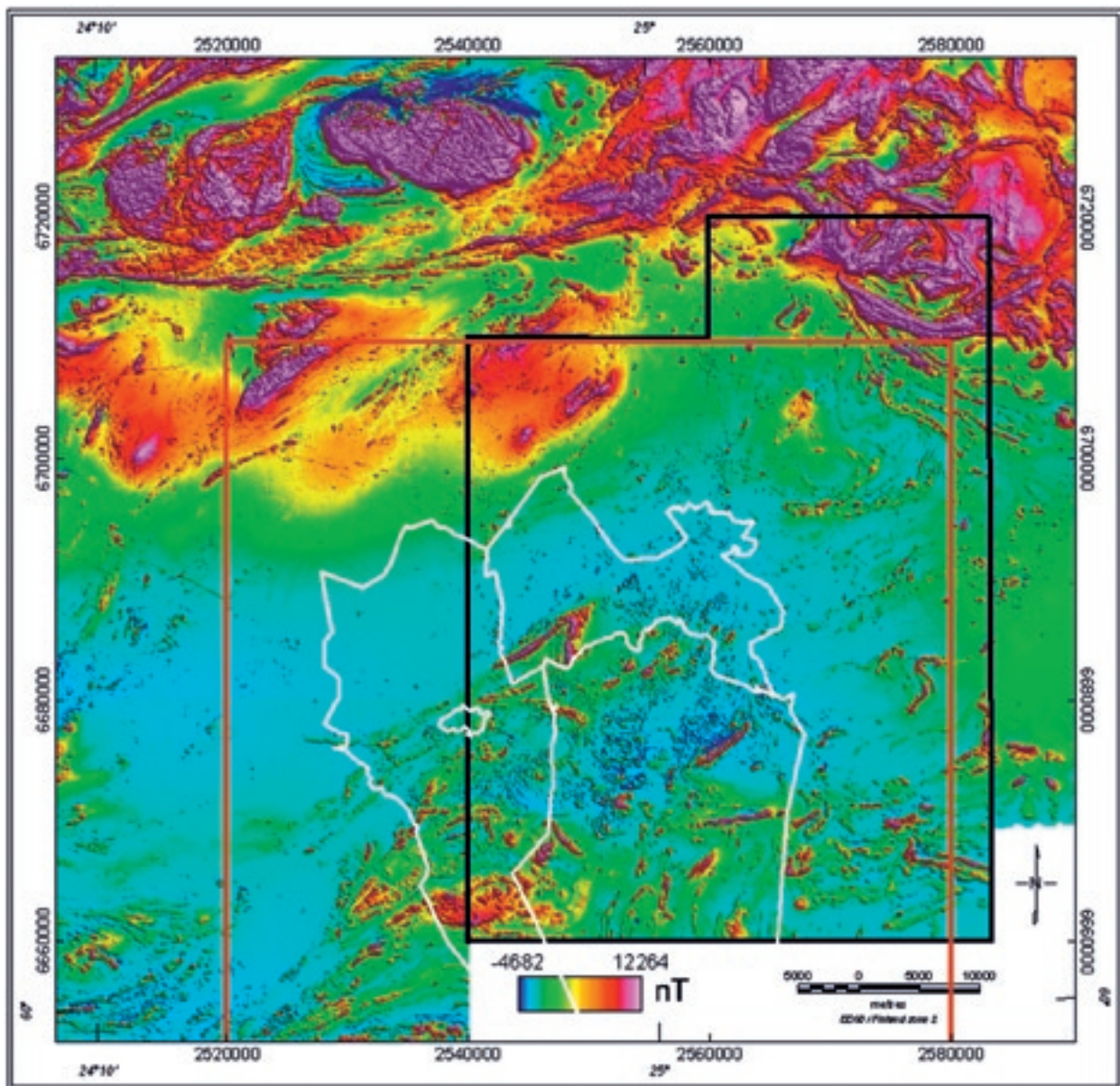


Figure 1 (a). Compiled aeromagnetic map covering the Helsinki area. Black outline: Helsinki aerogeophysical survey 1999; white outlines: the cities of Helsinki, Espoo and Vantaa; red outline: the lithological map area in Figure 1b.

tropy of the gneisses, and their folded structure is also recognized on the aeromagnetic map. Similar banded anomalies are related to the E-trending metavolcanic belt in the southern part of the area. Directly to the north of the outlined Helsinki aerogeophysical survey area, highly magnetic granitic rocks dominate the aeromagnetic image. Boundaries between granite and gneiss are commonly poorly defined, but are displayed as a gradual change in the magnetic signature. Where the boundary is of tectonic nature, it is indicated by weakly magnetic lineaments representing faults. Some magnetic lineaments traverse through the whole map area suggesting their great depth. Some of the lineaments are slightly curved – indicating crustal scale shear zones – occasionally with remnants of magnetic anomalies. The rapakivi granite intrusions are weakly magnetic, oval shaped magnetic structures with their positions closely con-

nected to the crustal scale shear zones (Elminen et al. 2008, this volume). The latest ductile (Svecofennian) deformation events dominate the nature of ductile magnetic anomalies and the variation in magnetic field intensity in southern Finland. After the ductile period, the response to tectonic stress of the more cooled crust has a more brittle character (Sibson 1977). In magnetic data, the brittle deformational signatures are represented by discontinuities in the ductile and coherent magnetic patterns. However, the geometrical systematics of the magnetic indications of the late brittle deformational features are strongly dependent on bedrock structures formed already during earlier tectonic stages, as evidenced in our earlier study in the Pori Area (Pajunen et al. 2001a and b). It is obvious that older structures control the shape and outline of structural bedrock provinces also in the Helsinki area.

RESTRICTIONS IN AEROGEOLOGICAL SURVEYING OF DENSELY POPULATED AREAS

In crustal investigations of urban areas, all cultural anomalies due to human activity can be regarded as noise. The Helsinki area is a highly developed, densely populated and constructed urban area, and the non-geological noise caused by buildings, road and railway networks, power-lines etc. disturbs the

recognition of a proper geological signal. The level of cultural noise encountered in the Helsinki area, as revealed by airborne gamma-ray and electrical conductivity maps, is high. Regional magnetic data are less sensitive to man-made effects than the two other methods.

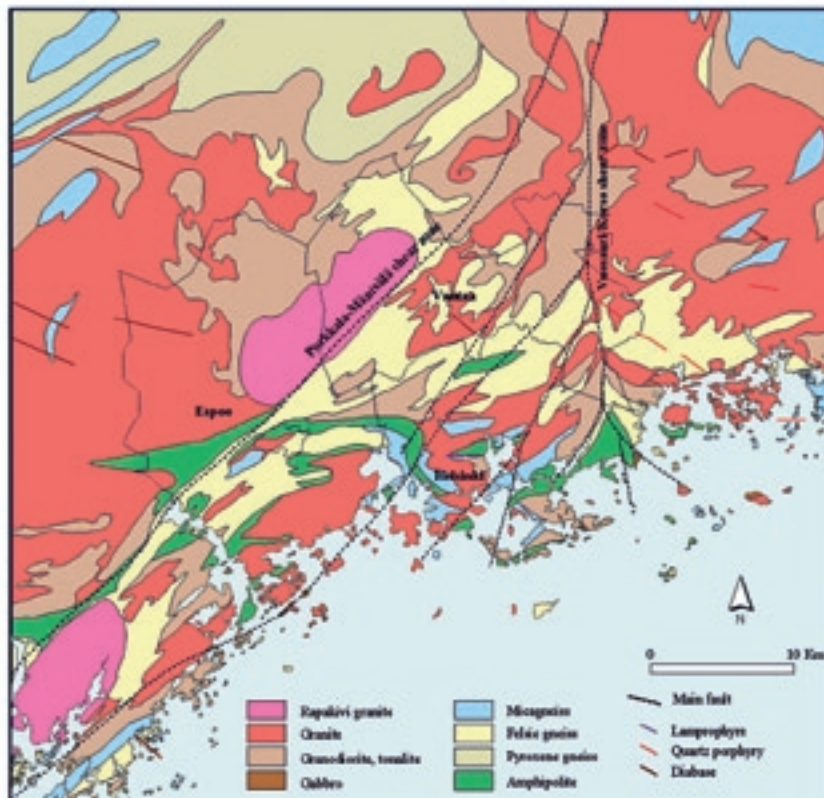


Figure 1 (b). Lithological map of the Helsinki area. Simplified from the Bedrock Map of Finland (Korsman et al. 1997).

Regional non-geological signal

Of the three geophysical data sets, the magnetic method describes best the lithology and structure of bedrock, and most of the regional magnetic anomalies in the magnetic field map are due to geological sources (Figure 2a). Although the amplitude of magnetic response of man-made objects is high, they commonly cause only local anomaly peaks. The response of geological sources are continuous and more extended, and may be followed for several data points in airborne data, commonly they can be observed at least in a few adjacent flight lines. The local signal caused by building complexes or domestic waste disposal sites does not disturb the regional, long wavelength crustal component of magnetic data.

An airborne radiometric image is a kind of geochemical map showing the distribution of potassium, uranium and thorium in rocks and soils. Water content or precipitation in soil attenuates the radiation coming through, so that a 0.5–1 m thick layer of water may totally suppress the radiation. That is why the lakes, rivers, swamps and the Gulf of Finland are shown in black on the regional radiometric image (Figure 2b). The image displays mainly four different provinces in different colours – in addition to the non-geological noise of the highly constructed areas (the yellow region). The overall compositional variation in bedrock and soil cover controls the radiometric signal of the other provinces. The bluish regions have proportionally enhanced Th relative to K or U radiation. In the reddish province, the U radiation values are enhanced but K radiation is relatively

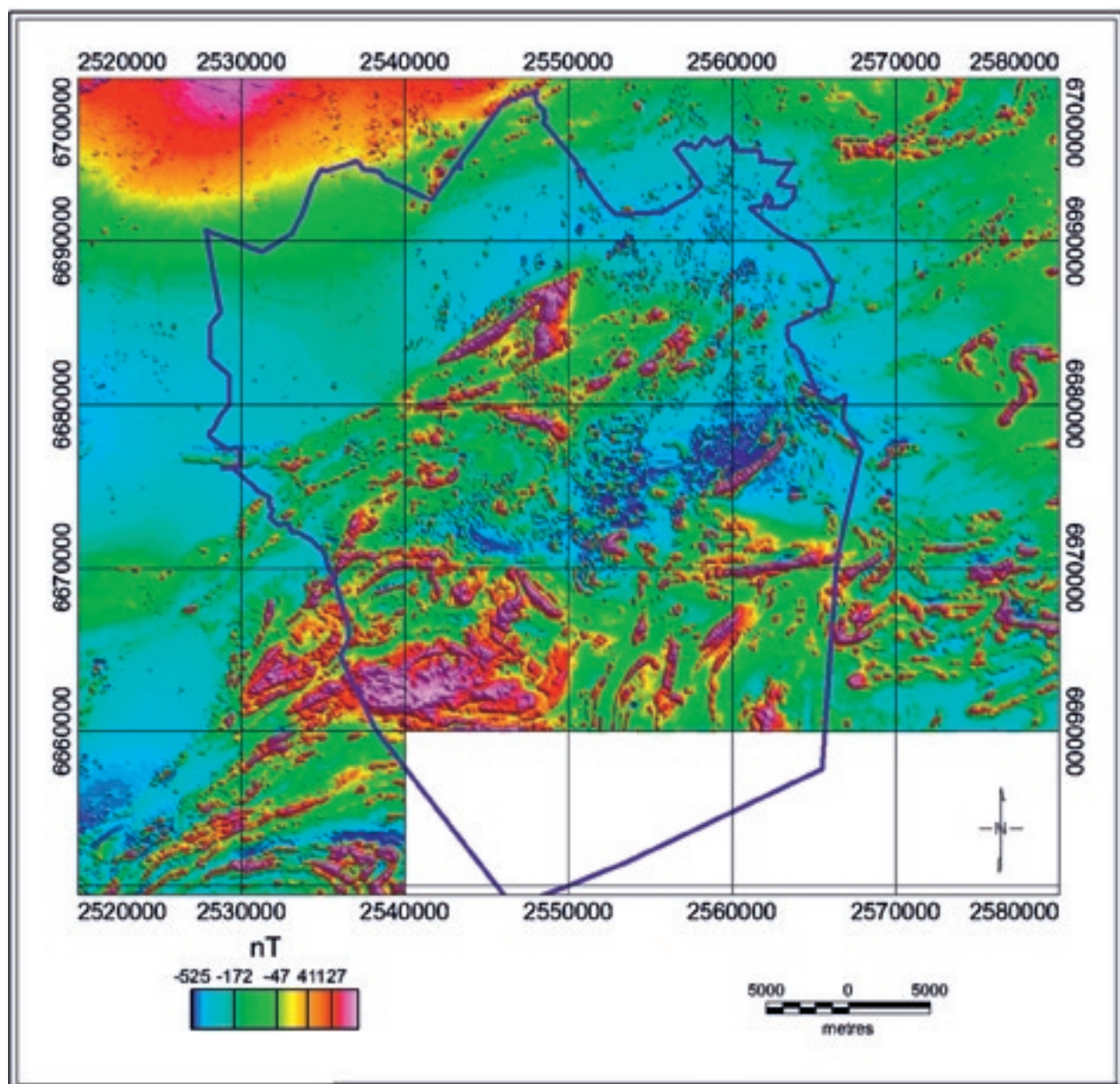


Figure 2 (a). Aerogeophysical image with the blue border showing the area of Helsinki, Espoo and Vantaa. Aeromagnetic image.

low. The green province in the south is due to the predomination of K in the area of rapakivi granite. Cultivated fields have specific K radiation values due to fertilizers, while low K but enhanced U and Th radiation values reflect a more clayish composition in soil.

Non-geological noise in urban areas disturbs the electrical conductivity data strongly (Figure 2c). In general, practically no bedrock conductors were detected in the study area. The electrical conductivity anomalies (in purple: low apparent resistivity) are connected to power-lines, roads, railways and buildings, and they mask the geological information coming from bedrock. However, in detailed inspection of individual electromagnetic components, overburden characteristics (conductivity and information on the thickness of overburden) could

be interpreted from the dual-frequency EM data. This kind of interpretation was outside the scope of this project, but can be worthwhile in future projects.

Local anomalies due to non-geological noise

Aerogeophysical responses due to non-geological noise are represented in Figure 3 for comparison of the same anomaly sources in different data sets and for correlation with topography and the base map. Typical sources of cultural noise are building complexes or waste disposal sites, railroads, pipelines or power lines. Their locations in the small example area are shown in Figure 3a. In magnetic data, building complexes or waste disposal sites are typically

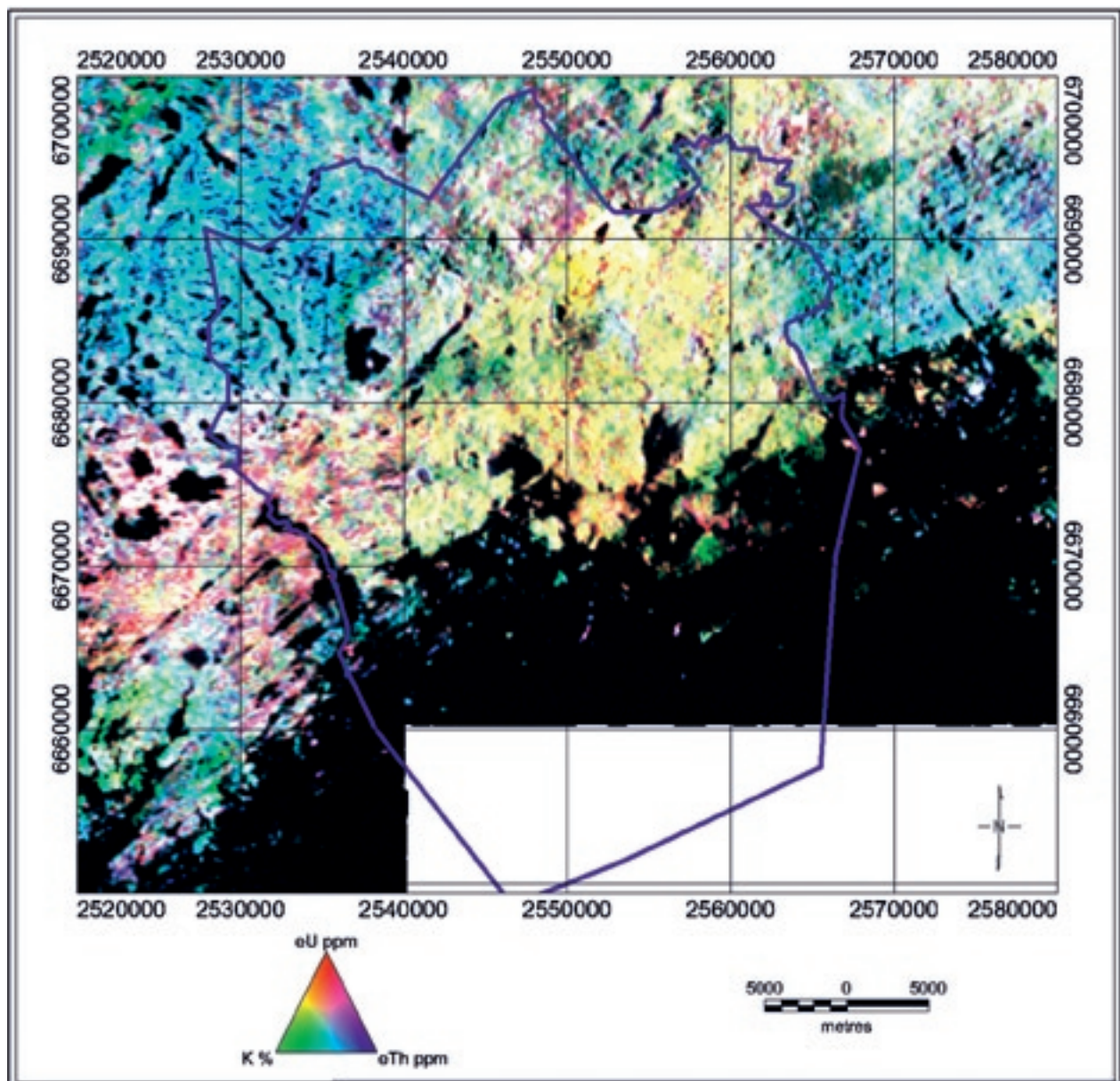


Figure 2 (b). Aerogeophysical image with the blue border showing the area of Helsinki, Espoo and Vantaa. Radiometric ternary image. Non-geological noise (shown as yellow) masks the most densely populated Helsinki City area.

represented by singular, isolated magnetic anomalies of high amplitude and they often show bimodality (Figure 3c). Other types of cultural noise may be long linear magnetic features following railroads, pipelines or power lines. In electromagnetic data, power lines and streets or roads and the swamp at Koukkusuo are recognized as enhanced conductivity while the outcropping bedrock is related to regions of low conductivity (Figures 3d–h). In radiometric data, roads, asphalt surfaces around buildings, landfills, gravel heaps and pits are typical sources of a cultural signal affecting the U and Th radiation (Figures 3i–l). Outcropping bedrock in the example area is mostly granitic and is associated with enhanced K-, Th- and U-radiation. The Fågelbacken gravel heap and the waste disposal site are seen as regions of high K-radiation, and the in-

habited areas, buildings and constructed areas are associated with moderate radiation values as well.

In the course of the project, attempts were made to remove cultural component by manual correction of magnetic data, but application of existing automated de-culturing routines produced an unacceptable result. The high content of cultural noise masks much of the subtle geological/structural signal. When removing the cultural anomaly peaks, part of the geological signal may also be removed at the same time. Since the 1:20 000 scale topography maps in Finland provide adequate and recent detail for the identification of most cultural noise sources, it was agreed that the best way of recognizing man-made objects is the correlation of geophysical data with topographic base maps. This can easily be organized using modern GIS-tools and image processing

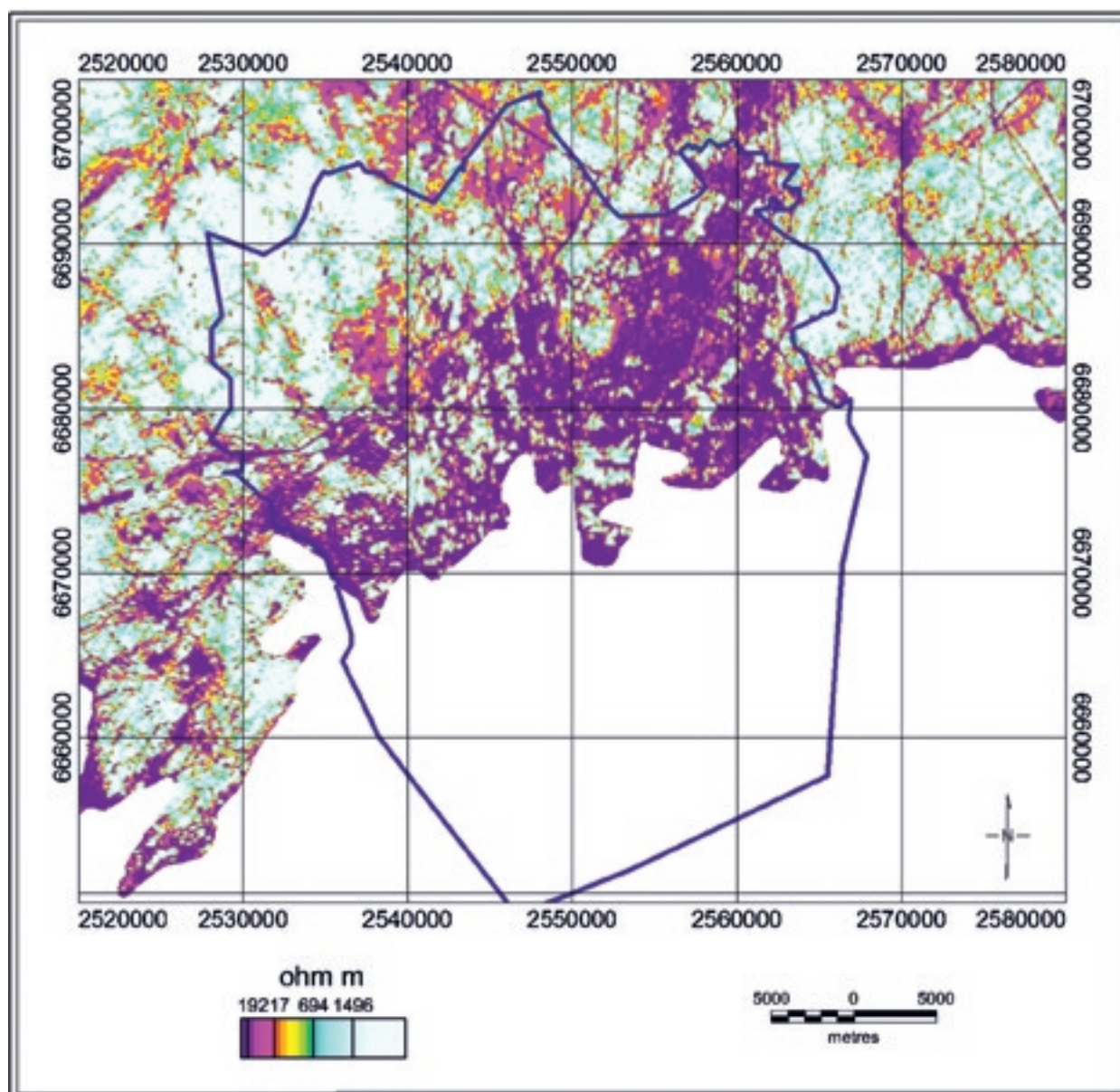


Figure 2 (c). Aerogeophysical image with the blue border showing the area of Helsinki, Espoo and Vantaa. Apparent resistivity map enhancing electrically conductive areas in purple. Non-geological noise strongly masks the geological signal.

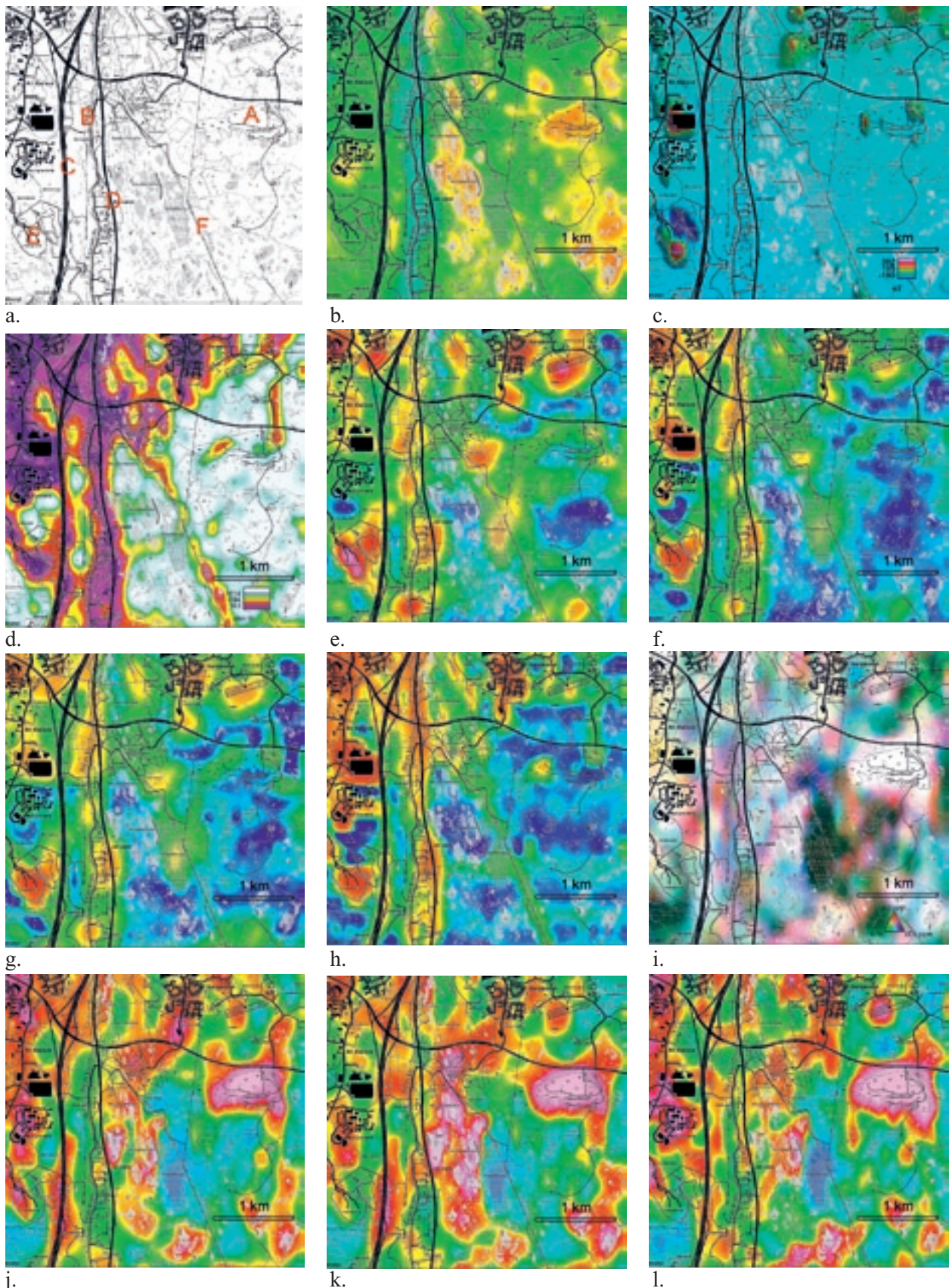


Figure 3. Aerogeophysical responses due to non-geological noise. Comparison of 1:20 000 scale topography maps and aerogeophysical data sets helps to identify different non-geological anomaly sources. (a.) Topographic base map showing locations discussed in text. A = Fägelbacken gravel heap, B = river valley, C = main road, D = road, E = domestic waste disposal site, F = power line. (b.) Topographic digital elevation model. Bedrock hills are exposed on both sides of the N-trending river valley. (c.) Magnetic field (red= high, blue = low). Bedrock is mainly weakly magnetic with very few geological anomalies. (d.) Apparent resistivity (half-space model) calculated on the basis of EM components (white = high resistivity, purple = low). (e.) EM high-frequency (14 kHz) quadrature component (red= good conductivity, blue = poor). (f.) EM high-frequency (14 kHz) in-phase component (red= good conductivity, blue = poor). (g.) EM low-frequency (3 kHz) quadrature component (red= good conductivity, blue = poor). (h.) EM low-frequency (3 kHz) in-phase component (red= good conductivity, blue = poor). (i.) Radiometric ternary image indicating ratios between K, U and Th radiation. Wet soils attenuate radiation (dark regions). (j.) K radiation (red = high, blue = low). (k.) Th radiation (red = high, blue = low). (l.) U radiation (red = high, blue = low). Base map © National Land Survey of Finland, permit No. 13/MML/08.

methods. Manual de-culturing using topographic maps has been found effective elsewhere too: Cuss (2003) compares different methods for removing

non-geological noise from airborne data in surveys flown over the English Midlands and uses the data for comparison with topographic 1:25 000 scale maps.

REGIONAL POTENTIAL FIELD CHARACTERISTICS FEATURING GEOLOGY

Gravity and magnetic fields

The bedrock in the Helsinki area can be divided into 9 geophysical domains on the basis of variation in field intensity and discontinuity of structures in magnetic and gravity data (Figure 4 and Table 2). These domains differ in their regional radiometric signal too, referring to their geochemical variation. Discontinuities in the internal magnetic patterns of these domains suggest later fragmentation, which occurred after the main ductile deformation stage. The 9 main domains can further be divided into smaller sub-domains on the basis of dislocations and interruptions in the morphology of the magnetic units. These smaller magnetic sub-domains are discussed in more detail later in this article.

Two major tectonic zones control the regional potential field structure of the Helsinki area: the Porkkala-Mäntsälä (P-M) crustal scale shear zone and the Korso-Vuosaari (K-V) zone. Their importance to the tectonic image and history of the area are described in Elminen et al. 2008 (this volume) and Mertanen et al. 2008 (this volume). On the Magnetic Anomaly Map of the Fennoscandian Shield (Korhonen et al. 2002), the SW-NE trending magnetic lineament related to the Porkkala-Mäntsälä shear zone extends over 200 km SW from

southern Finland towards Latvia. The lineament cuts sharply the regional, almost E-trending magnetic anomaly assemblages, whose general strike is parallel to the Tornqvist margin (see Mertanen et al. 2008, this volume). The P-M zone separates between domains 4 and 7, and between 5 and 8, respectively. The N-trending K-V zone is the domain boundary between domains 2 and 3, and 5+8 and 6. Along the P-M shear zone, there occur two known rapakivi intrusions (see also Figure 2a), i.e. Bodom and Obbnäs rapakivi granites (Elminen et al. 2008, this volume). In the magnetic data, the rapakivi intrusions are illustrated as oval shaped magnetic lows with quite smooth internal magnetic fabric. In the gravity data they are associated with oval shaped gravity minima due to the light specific density of rapakivis' – commonly below 2630 kg/m³ (Elo 1997). Two other magnetic and gravity lows are located along the domain boundaries and K-V zone, at similar structural culmination points of regional weakness zones (the red ovals in Figure 4). The same kind of geophysical appearance of the known rapakivi intrusions raises the question about the existence of more numerous intrusions than previously known, but lacking outcrops. Because of the similarity between densities and susceptibilities of a rapakivi body and the strongly fractured bedrock,

Table 2. Regional geophysical properties for the 9 domains illustrated in Figure 4.

Geophysical domains	Magnetic field intensity	Magnetic pattern	Gravity field	Radiometric classification
Domain 1	Moderate	Banded, curved, organized, E-W to SW-NE trend	Medium	Th + U
Domain 2	Extremely low	Irregular, disturbed, SW-NE trend	Local min	Th + U; urban area: non-geological noise
Domain 3	Low	Deformed, banded, bedded, nearly E-W trend	Province boundary, low	Th + K; low U
Domain 4	Low	Banded, sheared, organized	Province boundary	Th + U
Domain 5	Moderate (locally high)	Banded, partly irregular	Low, province boundary	Urban area: non-geological noise
Domain 6	Low	Banded, curved, organized	Low, local max	K + U
Domain 7	Extremely low	Smooth, faint organized fabric	Slope of regional max	Th + K; low U
Domain 8	Partly high	Banded, sheared	Slope of regional max	K + U
Domain 9	Partly high	Deformed, sheared	Low, crossection of province boundaries	High K

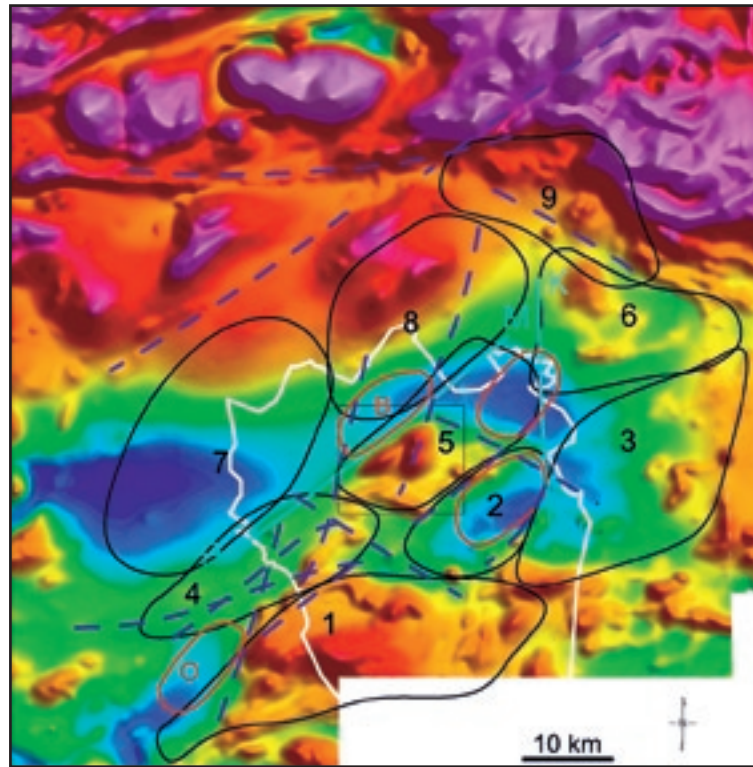


Figure 4 (a). The 9 regional geophysical domains in the Helsinki area, based on aeromagnetic and gravity data. The outline of Helsinki, Espoo and Vantaa is shown. P-M is the Porkkala-Mäntsälä shear zone discussed in text, and K-V is the Korso-Vuosaari zone. Red ovals denote the known rapakivi intrusions of Bodom (B) and Obbnäs (O) and two other geophysically and structurally similar units. Blue dotted lines = major structural zones. Aeromagnetic data, continued upwards to 800 m to reduce local signal.

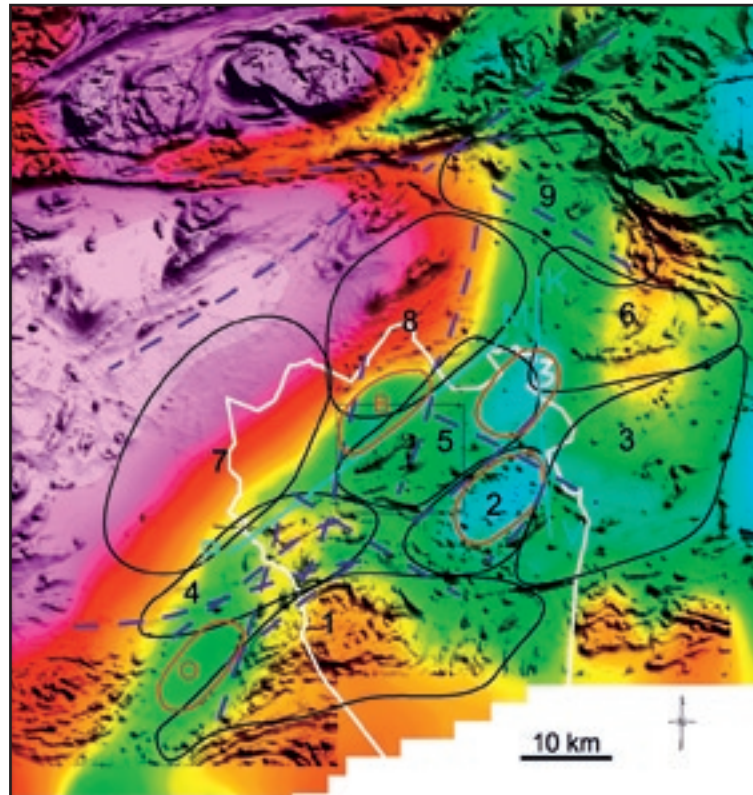


Figure 4 (b). The 9 regional geophysical domains in the Helsinki area, based on aeromagnetic and gravity data. The outline of Helsinki, Espoo and Vantaa is shown. P-M is the Porkkala-Mäntsälä shear zone discussed in text, and K-V is the Korso-Vuosaari zone. Red ovals denote the known rapakivi intrusions of Bodom (B) and Obbnäs (O) and two other geophysically and structurally similar units. Blue dotted lines = major structural zones. Gravity (in colour) with aeromagnetic shaded relief in grey (200 m continued upwards to reduce local signal). Gravity data is based on the interpolated 2 km grid (5 km station spacing), by the Finnish Geodetic Institute and GTK.

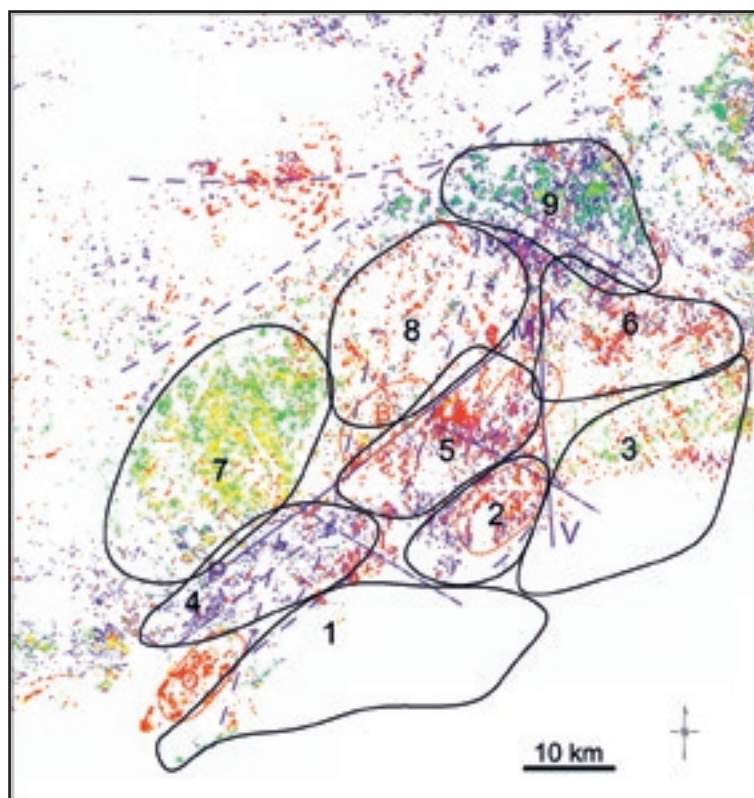


Figure 4 (c). The 9 regional geophysical domains in the Helsinki area, based on aeromagnetic and gravity data. The outline of Helsinki, Espoo and Vantaa is shown. P-M is the Porkkala-Mäntsälä shear zone discussed in text, and K-V is the Korso-Vuosaari zone. Red ovals denote the known rapakivi intrusions of Bodom (B) and Obbnäs (O) and two other geophysically and structurally similar units. Blue dotted lines = major structural zones. Classification of the airborne radiometric data (red = K; green = Th; blue = U).

the modeled magnetic and gravity profiles across the suspected bodies could not clearly verify their source. The petrophysical properties of rapakivis and other rock types in the Helsinki area will be discussed further in the following section.

Petrophysical analysis (density and magnetic properties)

In the course of various bedrock mapping and specific projects in the study area, rock samples were collected for laboratory measurement of their petrophysical properties (density, magnetic susceptibility and the intensity of remanent magnetization). The results are stored in the national petrophysical database, maintained by GTK, including more than 2900 samples from the Helsinki area. The statistical characteristics of densities and magnetic properties for different rock types was analyzed to explain the variation in geophysical potential field anomalies (Figure 5). Most of the samples have, disregarding their lithology, susceptibilities of about or below 1000×10^{-6} (SI- units). These values correspond approximately to the paramagnetic susceptibility of mafic silicates, meaning that the rocks in the study area mainly lack ferromagnetic minerals (e.g., mag-

netite or monoclinic pyrrhotite). The intensities of remanent magnetization are low for the same reason. The densities for most of the samples are below 2800 kg/m^3 . Higher densities common to mafic and ultramafic compositions are rare and the sample densities are generally low, typical for felsic or intermediate varieties (migmatite gneisses, granodiorites, granites etc.). Commonly, for any rock type or any study area in the Finnish Precambrian, any sample set can be divided into at least two magnetic populations: weakly and strongly magnetic populations (Puranen et al. 1968, 1978, Puranen 1989, Korhonen 1992 and Airo 1999). The poor representation of magnetite-bearing varieties can thus be regarded as characteristic for the Helsinki area. This results in mainly low-amplitude magnetic anomalies, except for some varieties of metamorphosed gneisses and local ultramafic or mafic (gabbroic) intrusions. One reason for the weak overall magnetization could be the extensive migmatization, which resulted in magnetite deficient rock compositions.

Scatter diagrams between density and magnetic susceptibility for selected rock types are presented in Figure 6. The division into two magnetic populations – a weakly and a more highly magnetic population – is seen for samples with broad lithological names such as “granites” or “gneisses”. However,

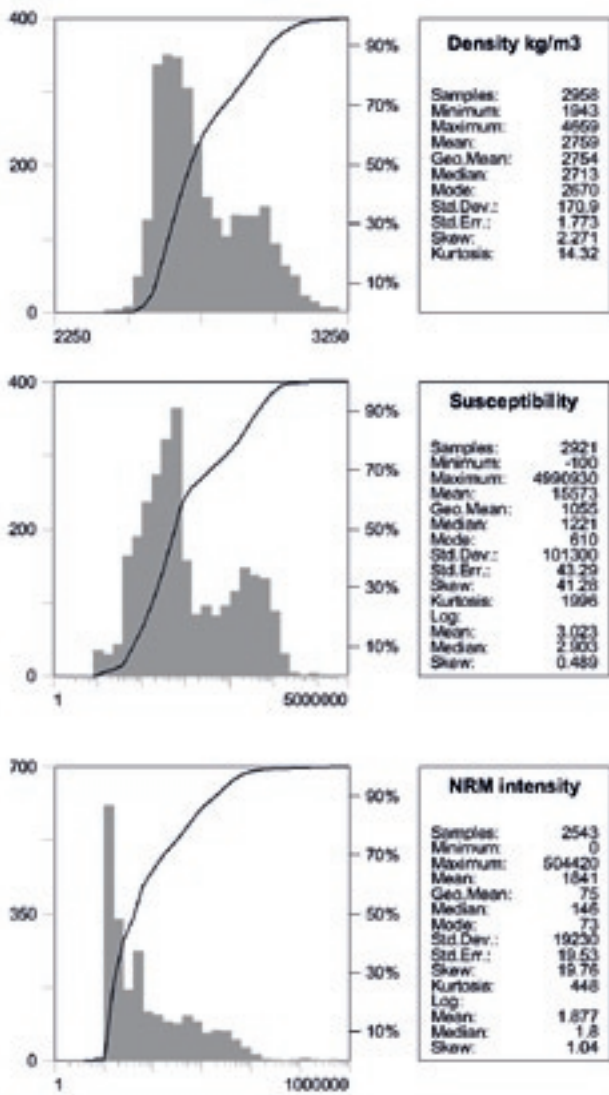


Figure 5. Frequency histograms for petrophysical properties: density (kg/m³), magnetic susceptibility (x 10⁻⁶) and intensity of remanent magnetization (mA/m) for the >2900 samples from the Helsinki area.

there are few samples with susceptibilities > 1000 x 10⁻⁶ (SI-units). The number of gabbro samples somewhat overestimates the susceptibilities for gabbros in the whole Helsinki study area, because the gabbro sample set contains numerous samples representing one highly magnetic gabbroic intrusion, which has been studied in more detail. The magnetic susceptibilities for rapakivis in the petrophysical database are commonly below 0.01 (SI units), although highly magnetic varieties also exist. They cluster into three main magnetic populations (averaging at 200, 1000 and 10000 x 10⁻⁶ (SI-units), depending on differences in their main mineral composition.

The distribution of sampling sites is shown in Figure 7, with proportional values for densities. Inspection of measured densities and magnetic properties for outcropping provinces can be used to explain variations in potential field intensities. Unfortunately, domains 7 and 8 (Table 2), which have moderate to high gravity, are generally poorly exposed and therefore lack petrophysical samples. The gravity field data for these domains, corresponding to gneisses and migmatites, refer to a higher proportion of heavy minerals in the exposed rocks or a more dense body underneath. The high density may be due to a greater mafic silicate component or to a higher metamorphic grade. Because there is also a magnetic response, it can be expected that these are mainly mafic silicates with accompanying magnetic minerals. The increase in metamorphic grade tends to increase the amount (the proportion) of heavy, mafic silicates in the composition, and results in a gravity and magnetic maximum.

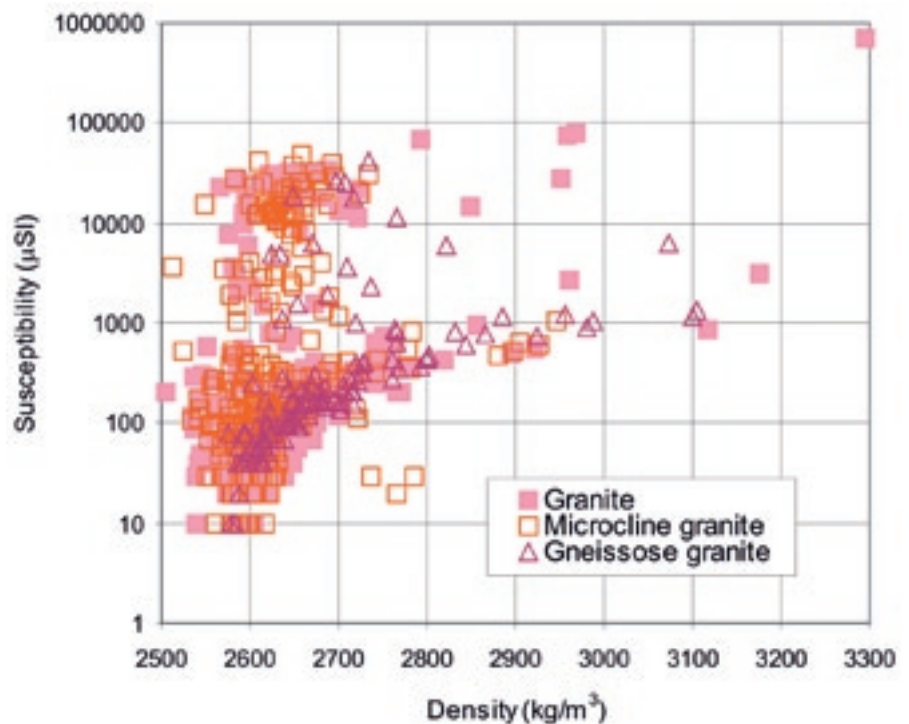
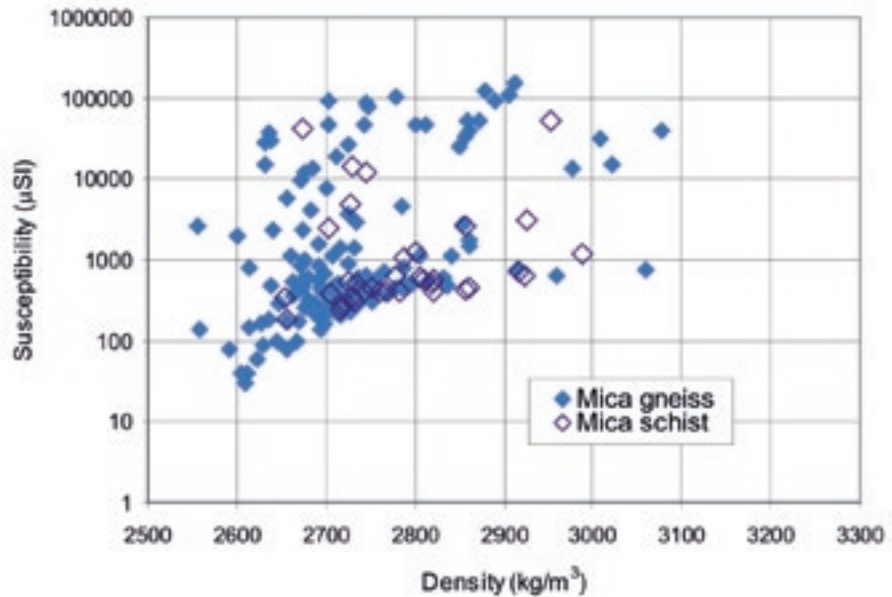
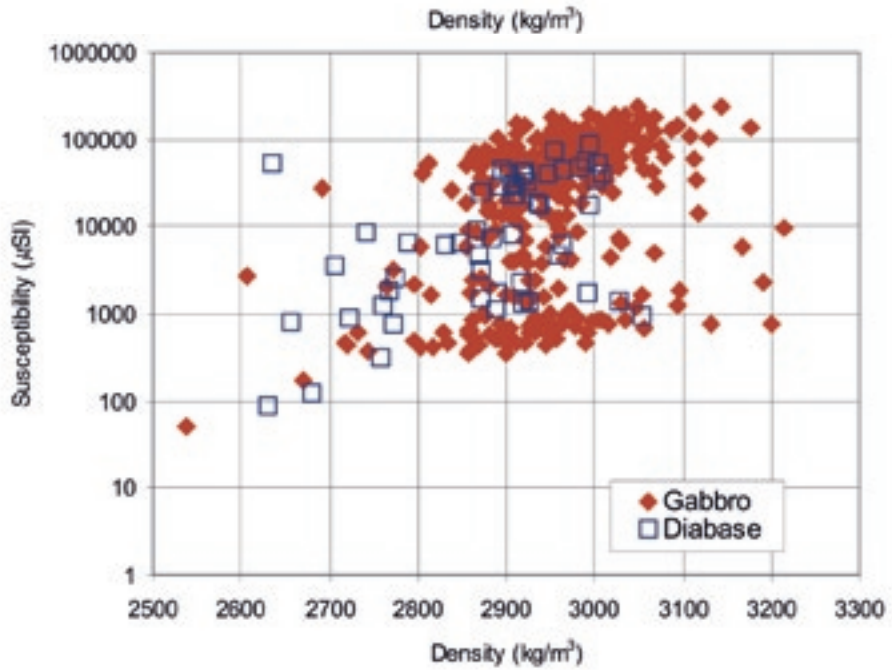
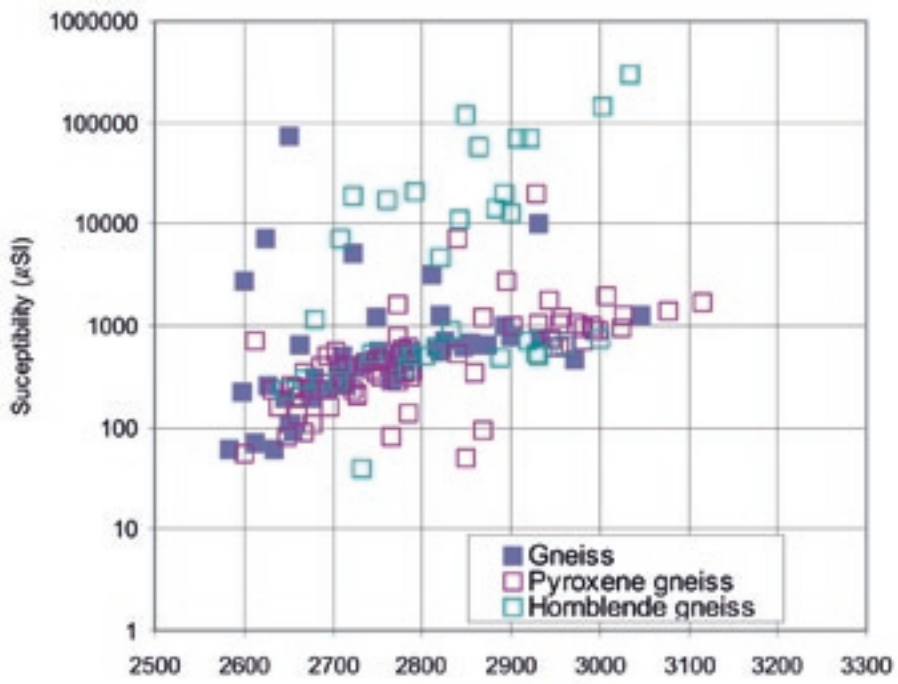


Figure 6. Scatter diagrams showing the relationship between densities and susceptibilities for selected rock types (by L. Kivekäs, GTK).



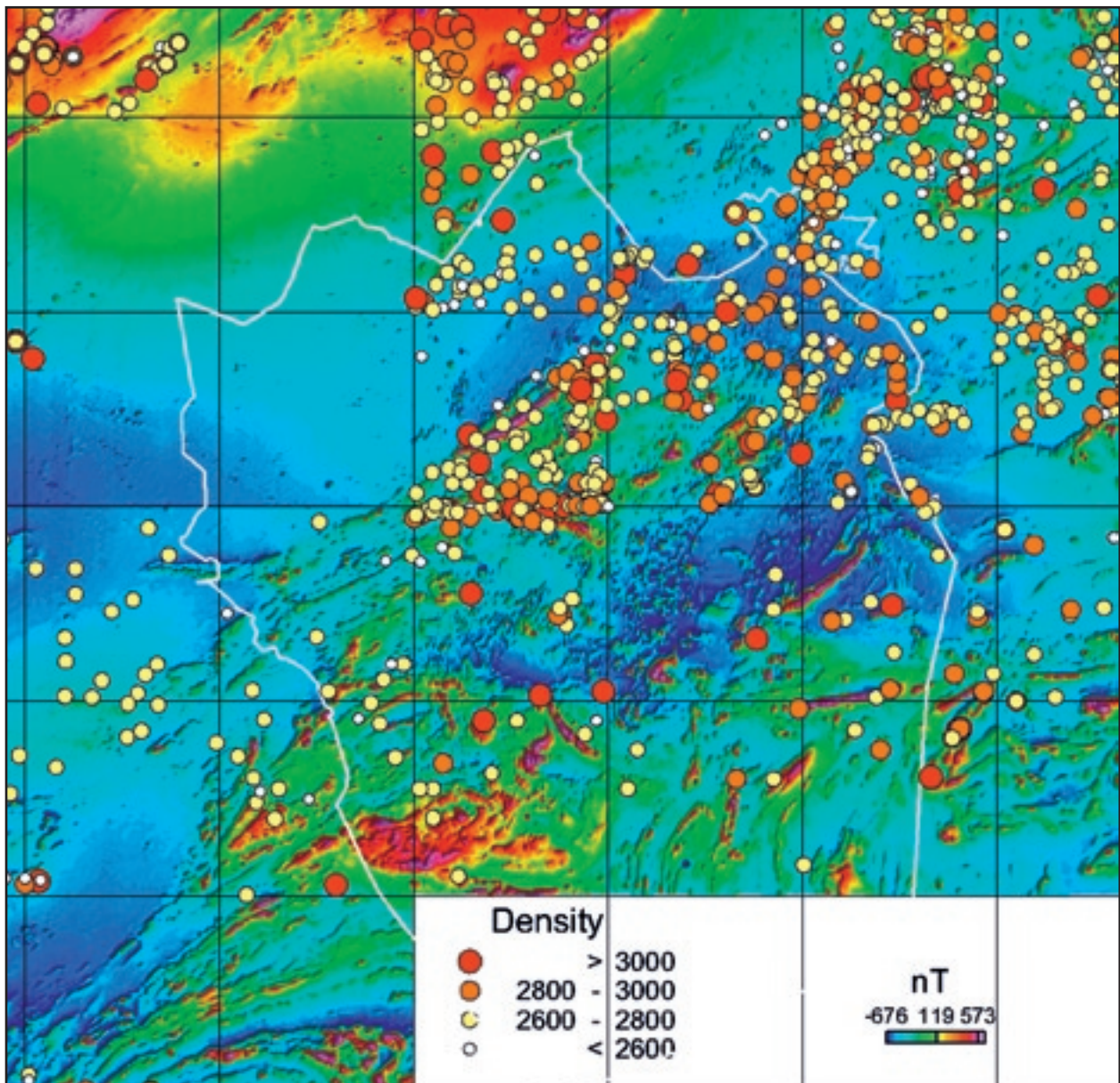


Figure 7. Distribution of petrophysical sampling sites in the Helsinki area, with proportional values for sample densities.

INTERPRETATION METHODOLOGY AND RESULTS

From data analysis to structural synthesis

The standard approach for airborne data analysis in crustal mapping includes classification of geophysical signatures by amplitude, identification of regions of coherent field intensity or texture, and recognition of structural trends within the units and the weakness zones between them. Continuous, banded magnetic anomalies are commonly related to bedrock units, which were produced or deformed under a ductile evolutionary stage. Crustal investigations in the Helsinki area focused on mapping the shallow basement structure and detecting weakness zones in bedrock. Particular

interest was laid on brittle structures and the factors controlling their distribution and directional trends. The magnetic signal due to brittle bedrock features may be very weak, local and obscured, and superimposed by other anomaly sources of intense magnetization situated close by or below. In the magnetic field data, the responses for near-surface, brittle structures are in the short-wavelength component and one aim of this project was to develop and test methods of enhancing this signal. Generous geological field observations were correlated with the enhanced magnetic data, thus giving a good reference for estimating the validity of the processed results.

Regional geological/structural interpretation of airborne geophysical data is a multistage process. It begins with analyses of the different data sets, classification of data properties and estimation of the limitations (of the suitability of data resolution to the proposed geological aspects in the study area). In densely populated areas, estimation of the influence of the cultural component on the geophysical signal is also required at an early stage, in order to establish the need for any de-culturing methods to be applied.

The geophysical data analyses stage included:

- 1) estimation of non-geological signal and the need for de-culturing
- 2) outlining of magnetic provinces and their characterization
 - assemblages of magnetic and non-magnetic units
 - textural analysis
 - narrow anomalies represented by a line
- 3) boundaries of magnetic units (shear zones, regional lineaments, gradual)
- 4) estimation of depth, attitude (dip) or any superposition of magnetic units
 - analysis of short-wavelength signal (shallow sources and structures, explained by susceptibility) or long-wavelength signal (doming, regional folding, deep sources, regional highs and lows)
- 5) lineament analysis (narrow anomalies; their nature and spatial distribution)

The data analysis stage was succeeded by integration of different geophysical data sets – gravity and regional radiometric and electromagnetic data, and comparison with the geological information:

- 1) geological reasons for geophysical signatures
 - lithology and/or chemical changes
 - regions displaying concentrations of organized or random magnetic anomalies
 - trends within magnetic units: folding or faulting
- 2) specific geological aspects
 - mapping of crustal weakness zones
 - signatures due to ductile or brittle deformation
- 3) computer modeling studies using rock property data.

In the final stage of the interpretation process, a structural synthesis can be drawn. It should justify all the observed geophysical and geological signal. The details of the structural synthesis for the Helsinki area are represented in Pajunen et al. 2008b (this volume).

Magnetic provinces and their boundaries

Magnetic provinces are regions of organized magnetic anomalies regarding patterns, intensities and trends. In most situations magnetic units correspond to geological units, such as a particular lithology or lithological assemblage. The potential field domains were first outlined on the basis of regional, long-wavelength magnetic and gravity field characteristics (Figure 8). The boundaries of superimposed magnetic provinces were confirmed by using different data enhancement and filtering methods. As a general rule, boundaries are close to anomaly inflection points for sources with almost vertical sides. When plotted on the short-wavelength magnetic data that describe the shallow, near-surface anomaly sources, the division into magnetic domains differs slightly in some details. For outlining different domains and describing the structural trends we preferred using directional horizontal derivatives (HDR) of both the magnetic and gravity fields. HDRs were effective structural indicators both when calculated from regional, long-wavelength data, and from the 50 m gridded magnetic data (Figure 8a). The analytical signal of the magnetic field is often used in drawing the edges of magnetically uniform areas. However, we found the total horizontal derivatives (THDR) calculated on the basis of two perpendicular derivative directions very informative and suitable for the high-resolution data surveyed at a very low altitude (Figure 8b). In particular, the subtle indications of fracture zones were remarkably enhanced in areas of poor susceptibility contrast. Vertical derivatives (VDR) of 50 m-grid magnetic data proved not as useful as the HDRs, but in defining very faint indications of brittle deformation, the zero-contours of VDR were applied coupled with HDR data. The VDR of regional gravity data (Figure 8c) enhances the zones of gravity gradient and was used for the first estimate of crustal weakness zones representing domain boundaries. In fact the main domain boundaries could be drawn on the basis of gravity gradient.

As was discussed earlier, the Helsinki area is an area of very low magnetic field intensity with few distinct isolated discrete magnetic anomalies. The internal patterns of the regional magnetic (e.g., domain 7 in Figure 8) lows are not uniform, but on enhanced data they show organized internal fabric. Also the Helsinki city area (domain 2) is recognized as a regional magnetic low, with an E-trending southern boundary against domain 1. Swarms of organized or random anomalies cover domains 1, 3, 4, 5, 6 and 8, typically with a NE or EW internal trend. Some individual high amplitude anomalies occur sporadically within these areas. The boundaries between the

magnetic units are commonly gradual and superimposed, except the Porkkala-Mäntsälä (P-M) shear zone. This crustal scale shear zone is a wider zone composed of several, almost parallel fault planes. It can be drawn partly as a single line, which separates the regional magnetic lows in the western part of the

study area from the more highly magnetic unit comprising regions in northern Espoo and Vantaa.

The magnetic signature of the P-M zone suggests nearly vertical or SE dipping geometry. The zone was reactivated several times during its tectonic history (Mertanen et al. 2008 and Elminen et al. 2008, this

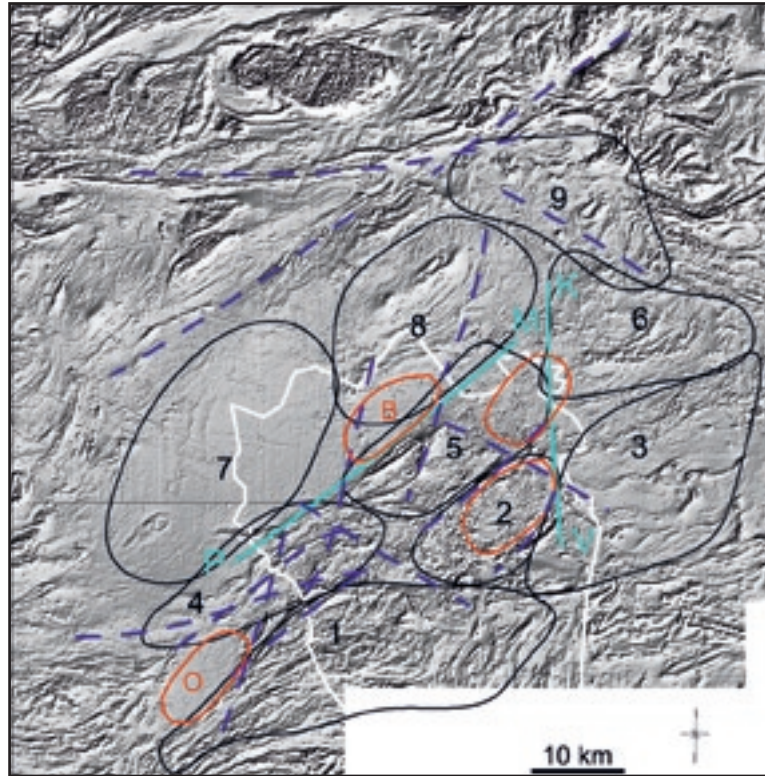


Figure 8 (a). Interpreted major lineaments and tectonic features in the Helsinki area. Horizontal derivative of magnetic field.

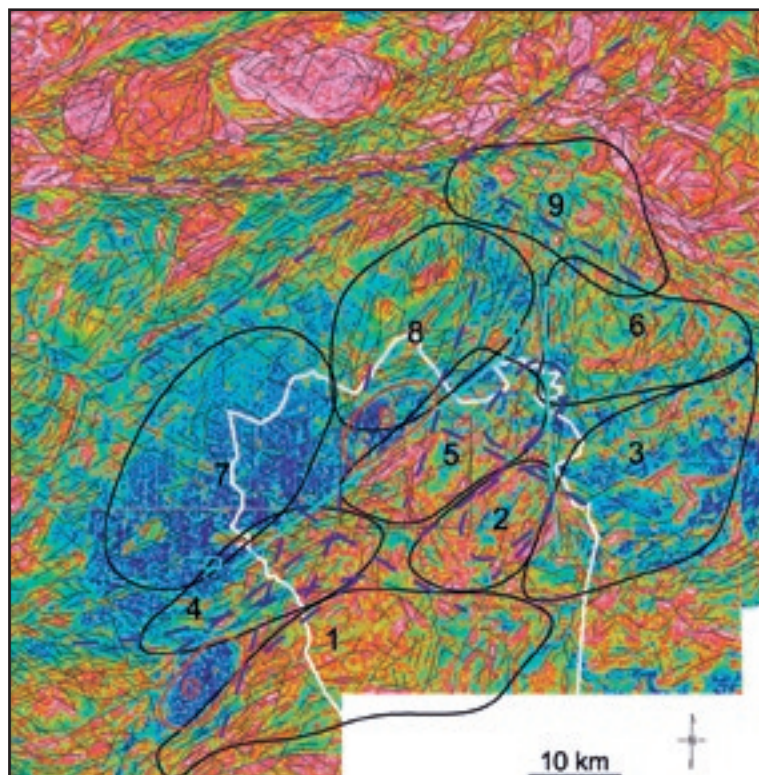


Figure 8 (b). Interpreted major lineaments and tectonic features in the Helsinki area. Total horizontal derivative of magnetic field.

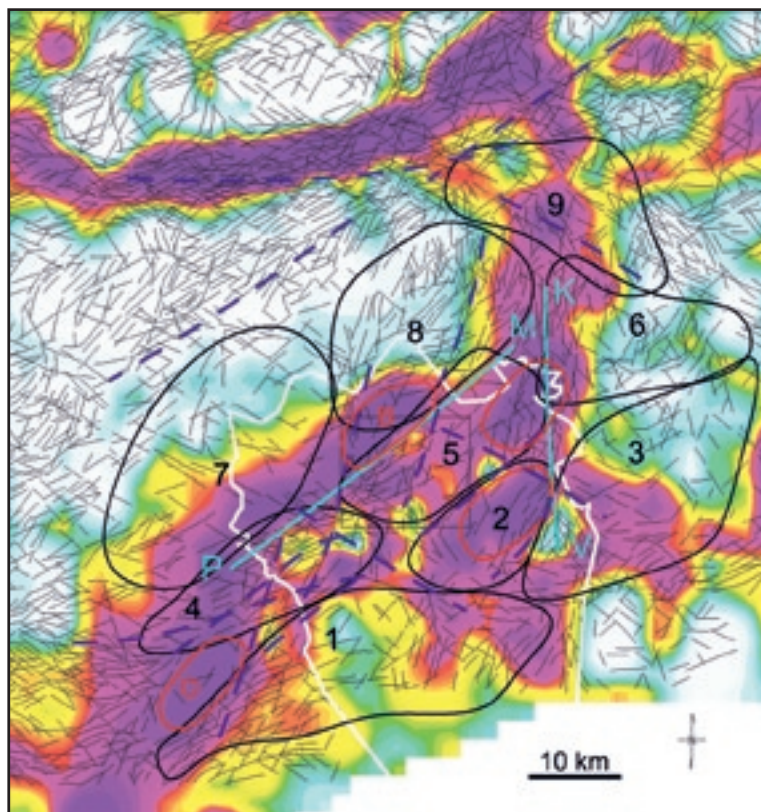


Figure 8 (c). Interpreted major lineaments and tectonic features in the Helsinki area. Vertical derivative of gravity.

volume), resulting in a more or less ductile zone, with an internal trend caused by anomaly remnants trending according to the main strike. The other major zone, the Korsso-Vuosaari (K-V) zone, has no direct response in the aeromagnetic data, but it forms a clear N-trending boundary between magnetic crustal units. The boundary separates regions displaying two different internal trends – domains 2, 5, and 8 versus domains 3 and 6 – and is related to the major Bouguer-anomaly discontinuity (Figure 8c).

Directional analysis for regional lineaments: faults and folding

Faults: lineaments that intersect other magnetic units. Regional faults and shear zones are commonly associated with major topographic valleys, filled with an overburden of glacial material and as such are poorly exposed for field observations. Faulting is recognized from sudden discontinuities of magnetic units, offsets in apparently continuous magnetic patterns or coherent texture, or an abrupt change in depth to magnetic sources. In the case of a linear magnetic low, weathering along a fault plane has oxidized magnetic minerals into non-magnetic minerals. Hematite, chlorite or biotite was observed in many of the weakly magnetic zones. In a shear zone, alteration due to fluid injection commonly produces the same result,

but often leaves remnants of magnetic anomalies paralleling the general strike of the shear zone. If magnetic minerals (magnetite or monoclinic pyrrhotite) are precipitated in the fault plane, the lineament may be a positive magnetic anomaly.

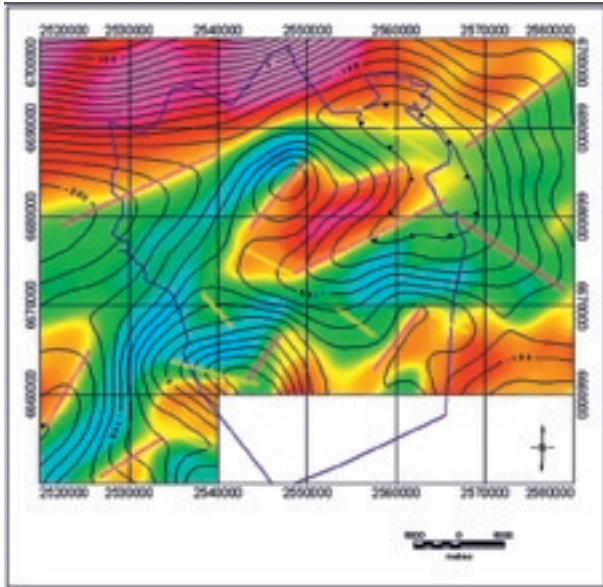
Folding: weakness zones parallel to the long axis of regional magnetic highs and lows. Folded magnetic units contain curved and bending magnetic anomalies, commonly with alternating anomaly intensities. They are recognized by patterns of linear magnetic anomalies in much the same way that folds can be recognized in outcropping geology. It was noticed that in the Helsinki area the last ductile stage – the latest folding event – predominates the magnetic signature. After that, the gradually cooling crust responded to deformation in an increasingly brittle manner. Regional, long-wavelength folding (or gentle doming) is evidenced by smooth, generally elongated, alternating magnetic highs and lows. However, signs of several folding stages may superimpose each other and result in a mixed pattern.

The overall magnetic NE trend in the Helsinki area was demonstrated by directional analysis of the long axis of regional highs and lows in magnetic and gravity data (Figures 9 and 10). Regional highs and lows in magnetic field and Bouguer-anomaly data were visualized by contouring – the magnetic data continued upwards to reduce the local and to

enhance the regional signal. The gravimetric station spacing is 5 km, so that the data as such reflect regional features. The strike of the long axis of highs and lows was defined on the basis of the inflection line of the HDRs calculated from the upward-continued magnetic data (Figures 9a and b) and in the same way from the Bouguer-anomaly data. Directions 70° and 40° dominate the regional axial orientations in both of the data sets. On a geological basis, these directions are known to be common weakness zone trends in the area. In order to enhance the $40\text{--}70^\circ$ axis trends, the HDRs were calculated in a perpendicular direction of 320° . Two other magnetic axis zone trends, perpendicular to the former, were

found: 330° and 310° , respectively. The directions revealed by directional analysis are in harmony with geological evidence on the regional folding axis in the area (Pajunen et al. 2008b, this volume). The same orientations also comply with the location and orientation of major magnetic lineaments in the study area, suggesting crustal weakness zones depending on the fold axial planes. Many of the fault systems form organized, parallel fault groups, and are commonly associated with a family of concentrated small, faint indications of brittle fractures. The NW fault strike is occupied by the Subjotnian diabase dykes, possibly abusing the previous crustal weakness zones by their intrusion.

a.



b.

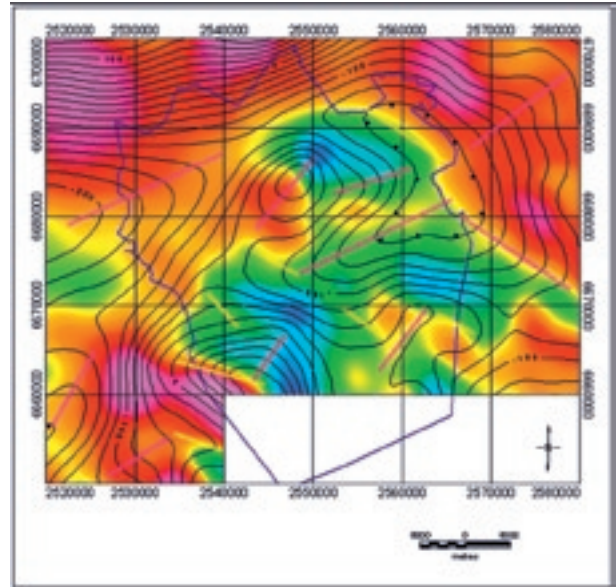
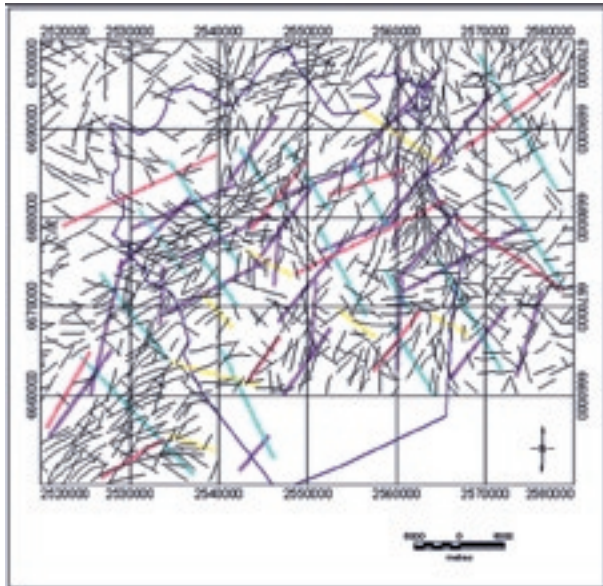


Figure 9. Directional analysis of axis plane orientations for the long axis of regional magnetic highs and lows. The location and orientation of the long axis were described according to the inflection line of horizontal derivatives of upwards continued (to 3 km) magnetic data. (a.) magnetic data: enhancement of $40\text{--}70^\circ$ (dx130), (b.) enhancement of $310\text{--}330^\circ$ (dx40).

a.



b.

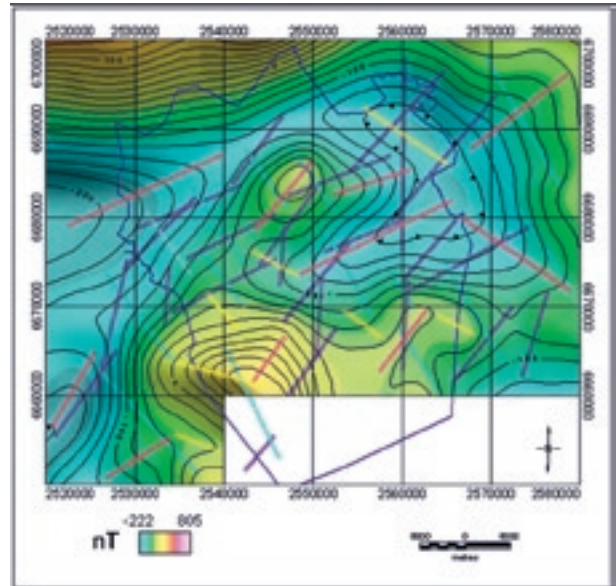


Figure 10. Distribution of regional and local scale magnetic lineaments in the Helsinki area. (a.) Minor lineaments (black) and axial plane orientations (red and yellow for magnetic data, purple and light blue for gravimetric data). (b.) Regional lineaments on upwards continued (to 3 km) magnetic data.

Minor lineaments

Lineaments in magnetic data are often related to fault and fracture zones and show their location, regional continuity and systematic trends. Mapping of magnetic lineaments in the Helsinki area was based on different data enhancements depending on the desired scale. The generalized distribution of magnetic minor lineaments and their relationship to regional potential field lineaments is shown in Figure 10. Elongated lines of magnetic minima, representing crustal scale faults and fractures, were mainly detected from shaded relief maps. These maps are very informative because both the intensity variation and the structural geometry are well defined. They also allow for estimates of the attitude of the zones. The directional distribution of minor lineaments follows the directional pattern of regional lineaments. Horizontal derivatives (HDR) of magnetic field data were found most useful for observing local scale lineaments, often associated with very subtle indications. HDRs calculated in different directions enhance the faintest susceptibility variations. In the presence of high-amplitude cultural anomalies, as in the Helsinki area, the subtle geological signal is often attenuated. In the most densely populated parts of the study area, upward-continued magnetic field data were needed for reducing the cultural noise component. For example, the HDR high-resolution data were combined with the shaded relief of upward-continued data and this revealed the connection of local anomalies to the more regional overall geological trend. Minor lineaments focus on the geophysical province boundaries and their orientations follow their main trend, or interrupt them steeply. This was expected since the fracturing, as a response to the present day stress field, is most easily released along previous weakness zones. The correlation between the focal mechanism of recent earthquakes elsewhere in Finland and the related surface faults evidences their close relationship to the brittle aeromagnetic signatures (Uski et al. 2003).

Characterization of different groups of weakness zones was one of the main aims of the structural mapping of the Helsinki area. Comparison of magnetic lineaments, topographic depressions interpreted from 1:20 000 scale base maps and ground geological observations on weakness and fracture zones verified that the same lineament orientations are evident in magnetic, topographic and field observation data. Aeromagnetic data were thus useful in detecting and predicting systematic trends, regularity and similarities of weakness zone distribution. Characteristics and discussion of the weakness zones are represented elsewhere in this volume (Elminen et al.

2008, this volume). The distribution of selected groups of the ground observations on semi-brittle to brittle weakness zones is illustrated in Figure 11, where four different sets of topographic lineaments are represented on the aeromagnetic processed image. Compared with the interpreted aeromagnetic lineaments in Figure 10a, there is a good correspondence between the directional trends of the interpreted and observed data.

We also tested methods to map very small / local magnetic lineaments for predicting signal of foliation or jointing. Figure 12 illustrates an example of observed foliation and joint sets (Wennerström et al. 2008, this volume) represented on the aeromagnetic map. The strike of magnetic lineament was found to be related to joint patterns, either parallel to the strong cleavage orientation or the fracture orientation intersecting the main cleavage, and to follow the deformational / structural trend inside a structural domain. The large number of field observations on shear and fracture zones in the Helsinki area strongly suggest that the fracture trends inside the structural domains reflect and multiply the large-scale tectonic trends in the area.

Special application: directional analysis of minor lineaments. During field checking, it was clear that an improved method for enhancing the faintest susceptibility variations would be needed to aid mapping of the regional distribution and organization of small-scale brittle features. Directional analysis was carried out on the basis of individual flight line data utilizing the trend gridding algorithm of Oasis Montaj software (by Geosoft), which finds continuity trends in pre-defined directions of preferred angles. In this case the preferred angles were 60°, 30°, 0°, 330° and 300°, the permitted deviation was $\pm 25^\circ$ and the window to seek trends was 500 m. The resulting trends for the test area in Otaniemi are illustrated in Figure 13. They are in harmony with the trends of brittle structural features interpreted from geological observations and topographic data and represented by Elminen et al. (2008) and Wennerström et al. (2008). Orientations 70° and 45° correspond to the main strike of magnetic anomalies and the main foliation strike direction. Orientations 30–40° are related to the brittle to semi-brittle zones. The NS trend is obvious from magnetic and topographic interpretations, although ground evidence is poor. Directions 310–330° and 300° are recognized both in observed brittle fault orientations and fracture trends. The comparisons between observed and calculated trends support the usefulness of this kind of directional analysis for estimating and mapping regional organization of shallow basement structures.

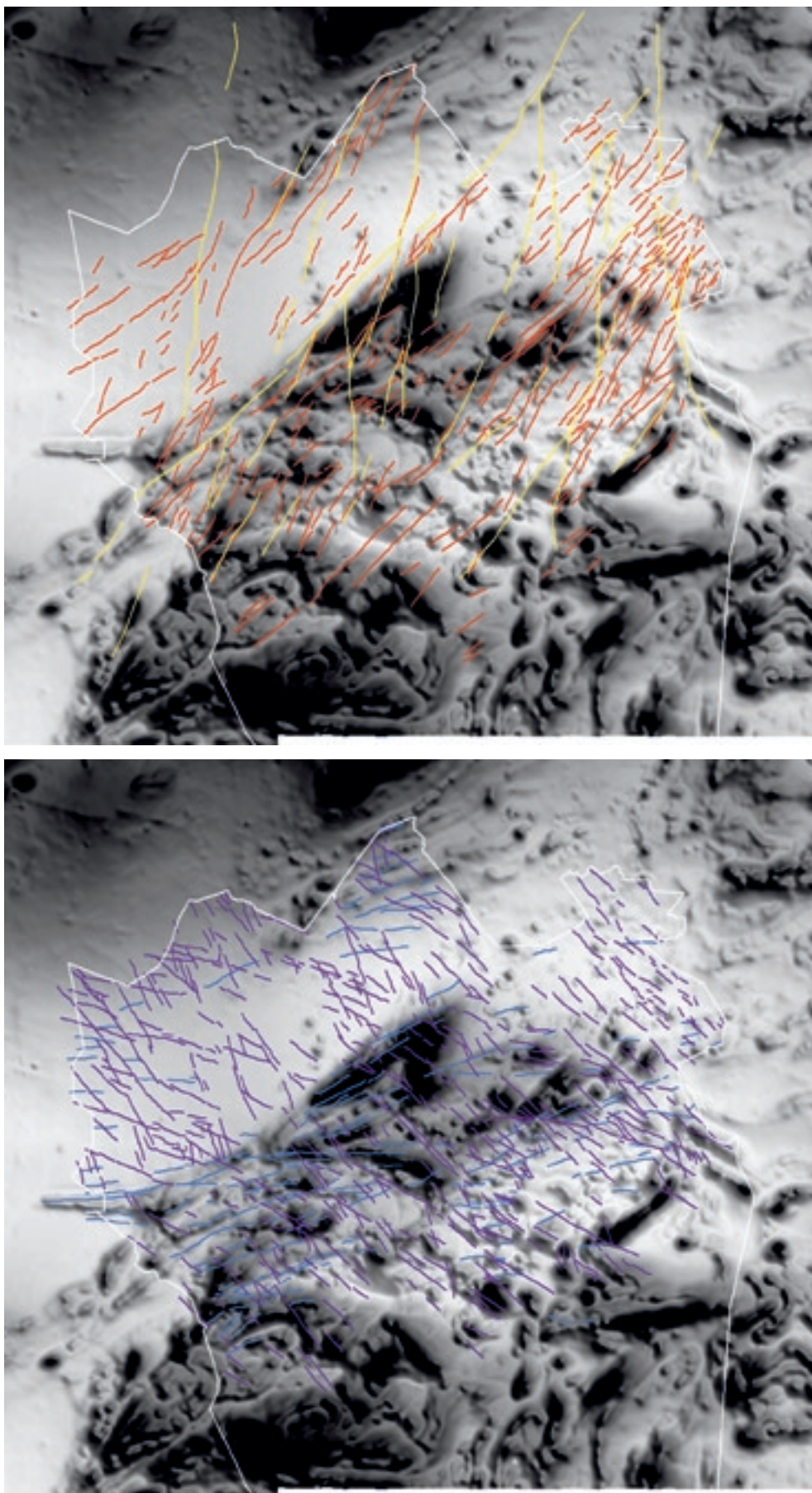


Figure 11. Comparison between magnetic lineaments, topographic depressions interpreted from 1:20 000 base maps and ground geological observations on weakness and fracture zones. Size of view is 50 km x 45 km. Characterization of different groups of weakness zones was integrated with topographic lineament analysis (Elminen et al. 2008). (a.) Interpreted topographic NE lineaments (red and yellow lines) on magnetic shaded relief image. (b.) Interpreted topographic EW to NE-EW lineaments (blue lines) and WNW-ESE brittle faults (purple lines) on magnetic shaded relief image.

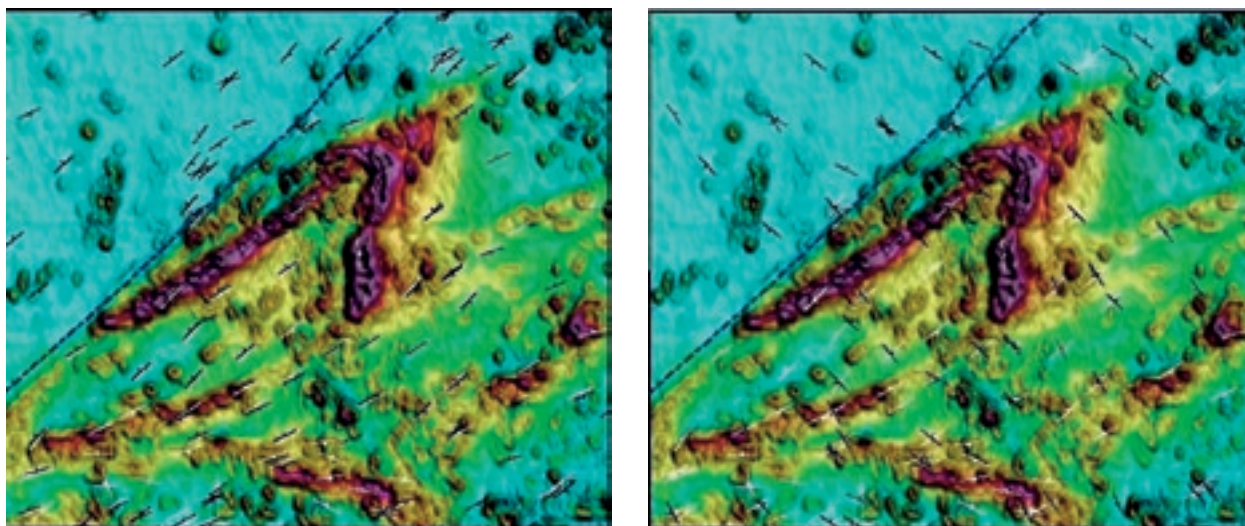


Figure 12. Observations on subvertical foliations and joint sets in migmatites (analysis by Wennerström et al. 2008) on aeromagnetic horizontal derivative data. SW-NE trend (left) along strike of magnetic anomalies and SE-NW trend (right), intersecting the anomaly strike. Size of view is 15 km x 10 km.

SUMMARY

The pilot project for crustal mapping of the Helsinki area offered the possibility of comparing the results of airborne geophysical interpretation with generous geological ground observations. It was found that the available airborne data are detailed enough and the positioning accurate enough for mapping even the shallow, brittle basement structure. Different data enhancement techniques were adopted to map continuity or organization and to highlight magnetic texture. We preferred using directional horizontal derivatives of magnetic field data, in particular for detecting subtle, local, weak magnetic features that indicate shallow, brittle to semi-brittle joint or fracture patterns.

Svecofennian ductile formations are described in aeromagnetic data by assemblages of magnetic and non-magnetic, continuous units, which follow the structural pattern of geological units. The cleavage-oriented or intersecting jointing and fracturing seem to inherit the strike orientation from the Svecofennian units. The late, regional folding of these units produced regional magnetic highs and lows. The axial plane orientations of these highs and lows were determined by utilizing horizontal derivatives of upward-continued magnetic data, and they show systematic NW trends that correlate well with the geological axial trends (Pajunen et al. 2008b, this volume). Later rupturing and fracturing of these structures are represented by the shallow fault and shear patterns interpreted from horizontal derivatives (HDR), calculated in different directions, and from total horizontal derivative (THDR) data (based on two perpendicular derivatives). Directional

analysis of HDR data reveals and enhances the distribution of even the faintest structures. The results of HDR analysis were correlated with the analysis of semi-brittle to brittle fault and shear zones (Elminen et al. 2008, this volume), and with the analysis of the joint set data (Wennerström et al. 2008, this volume). Mapping of organized trends in near-surface fracturing is based on the development of fractures and jointing along the main strike of the structural anisotropy, which actually reflects the anisotropy of silicate minerals. This again is well defined by the shaded relief magnetic data, which illustrate the susceptibility variation of mafic silicates along the anisotropy strike. In general it can be verified that the directional main trends in jointing are reflected by the main magnetic lineament trends. However, the comparison evidenced that, although the regional directional trends are well described, the nature of the weakness zone – a shear zone, a fracture zone, jointing – could not definitely be differentiated solely on the basis of magnetic data characteristics.

From these integrated studies it is evident, that specific aeromagnetic fingerprints are related to the brittle deformational stage. They can be recognized and mapped by using the following routines: 1) related to late folding: regional axial plane orientation from gradients of the regional magnetic field data; 2) faulting, coupled with this late folding and utilized later by diabase magmatism; 3) low angle thrust faults due to compression from NW and glacial rebound: THDR or HDR in different directions, especially in areas of very low magnetic field intensity.

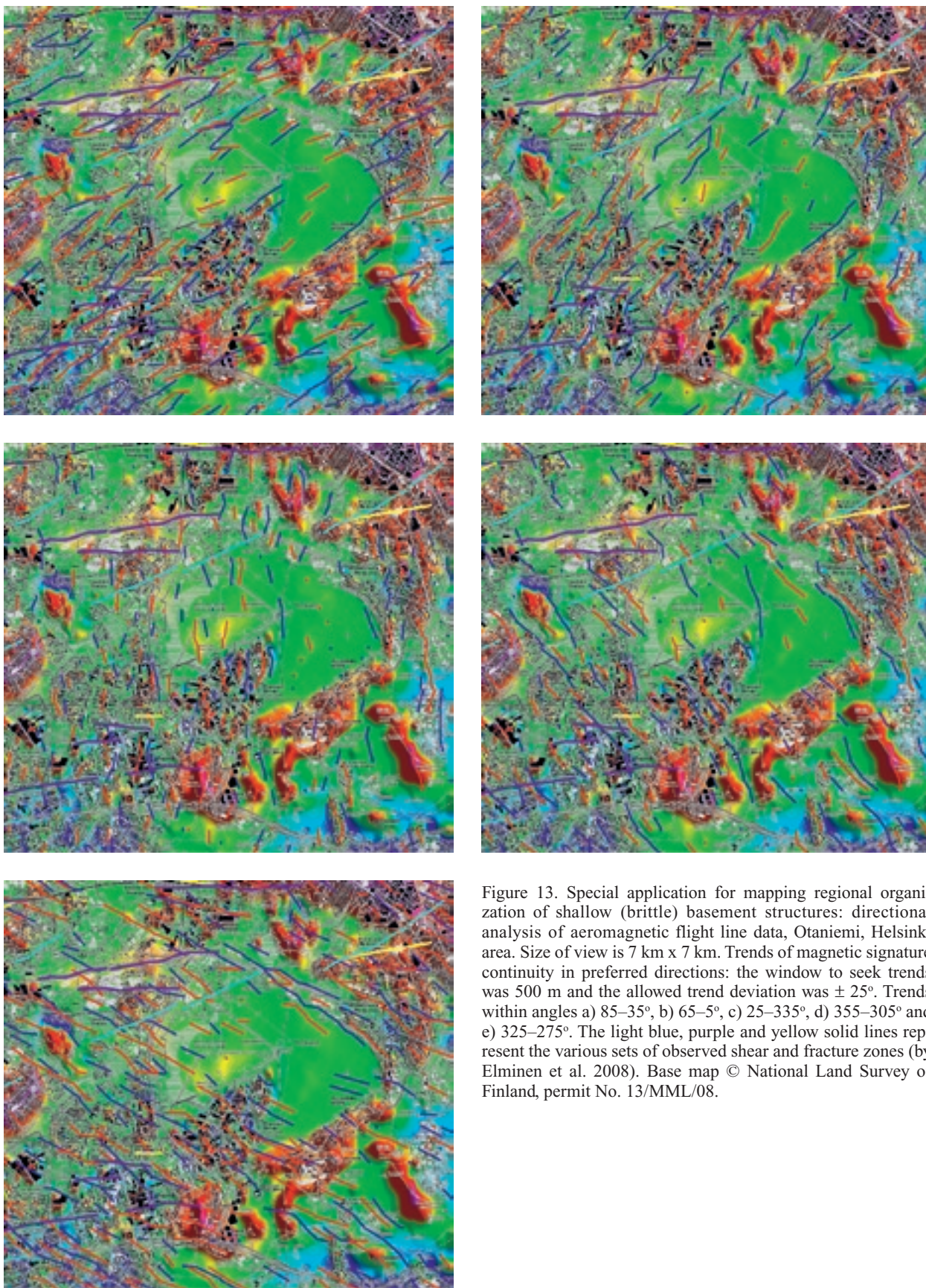


Figure 13. Special application for mapping regional organization of shallow (brittle) basement structures: directional analysis of aeromagnetic flight line data, Otaniemi, Helsinki area. Size of view is 7 km x 7 km. Trends of magnetic signature continuity in preferred directions: the window to seek trends was 500 m and the allowed trend deviation was $\pm 25^\circ$. Trends within angles a) 85–35°, b) 65–5°, c) 25–335°, d) 355–305° and e) 325–275°. The light blue, purple and yellow solid lines represent the various sets of observed shear and fracture zones (by Elminen et al. 2008). Base map © National Land Survey of Finland, permit No. 13/MML/08.

Some main results may be pinpointed:

- Aeromagnetic data mirror the structural domains of bedrock and the character of their overall fragmentation and rupture extremely well
- The geophysical structure is somewhat different from the geological one, but is reasoned by the additional third dimension given by potential field methods
- The organized geometry of fault and fracture zone distribution and their concentration along geophysical domain boundaries are highlighted
- Lineaments in magnetic data are related to fault and fracture zones and their location is well expressed, but the geological nature of the source structure (minor or regional fault, shear zone or jointing) cannot be differentiated
- The regional distribution of the strike direction of joint sets and fracture zones can be mapped by aeromagnetic data
- The strike of foliation of migmatites and the strike orientation of magnetic anomalies correspond to each other – similarly, the intersecting magnetic lineaments correspond to the schistosity cutting the foliation
- The geometry of minor magnetic lineaments strongly controls the topographic morphology, e.g. the outlines of lakes such as the elongated Nuuksion Pitkäjärvi or Tuusulanjärvi – supporting the idea that the brittle, late stage deformational pattern of the surface of the Svecofennian crust is well described by high-resolution aeromagnetic data.

In the geophysical interpretation of the Helsinki area, aeromagnetic data played a leading role because one of the main aims of the project was mapping the crustal structure. Further investigations, applying electromagnetic and gamma-ray spectrometric data, should also be considered in the future, e.g. for environmental or ecological applications. Geoscience database collected from the Helsinki area, or any densely populated area, offers a basis for more effective integrated use of other geophysical, geographic, ecological, biological etc. data in the future, for infrastructural and land-use planning, groundwater studies or monitoring and predicting environmental hazards.

CONCLUSION

The following geophysical procedures and data are recommended for the geological mapping of urban areas:

Perfect coverage of geophysical data sets

- airborne geophysical surveys using a dense line spacing (75–100 m) and a low flying altitude (i.e., 30–45 m)
 - 1) magnetic: bedrock structure and lithology, crustal weakness zones and lineaments
 - 2) EM 2-or 4-frequency: electrical conductivity of ground, bedrock and soil conductors, thickness and conductivity of soils
 - 3) gamma-ray spectrometry: geochemistry of bedrock and soil; environmental monitoring (coupled with EM)
- regional gravimetric measurements (airborne or ground)
 - bedrock structure and lithology, crustal weakness zones and lineaments, thickness of soils
- follow-up airborne surveys (for environmental monitoring)

- specific ground geophysics
 - super-sensitive gravimetric measurements, seismic sounding, development of near-surface geophysical methods specified for mapping shallow basement structure
- petrophysical sampling for potential field modelling
- palaeomagnetic studies (relative timing of geological events; investigations of shear and fracture zones)

Interpretation coupled with geological and topographic information

- inspection of non-geological noise and need for elimination
 - (topographic base maps scale 1:20 000)
- outlining and geophysical characterization of structural domains
- lineament and texture analysis
- geological field observations: continuity, organization and zoning of structures
- correlation and integration using GIS-tools

ACKNOWLEDGEMENTS

The Project "Construction potential modelling of bedrock in urban areas" was carried out in co-operation of GTK, TEKES, Rockplan Ltd, Viatek Ltd

and the cities of Helsinki, Espoo and Vantaa. The authors thank all those involved with the project.

REFERENCES

- Airo, M.-L. 1999.** Aeromagnetic and petrophysical investigations applied to tectonic analysis in the northern Fennoscandian shield. Geological Survey of Finland, Report of Investigation 145. 51p.
- Cuss, R. J. 2003.** Manual approaches to the removal of cultural noise from high-resolution aeromagnetic data acquired over highly developed areas. First Break Volume 21, October 2003.
- Elminen, T., Airo, M.-L., Niemelä, R., Pajunen, M., Vaarma, M., Wasenius, P. & Wennerström, M. 2008.** Fault structures in Helsinki area, southern Finland. In: Pajunen, M. (ed.) Tectonic evolution of the Svecofennian crust in southern Finland – a basis for characterizing bedrock technical properties. Geological Survey of Finland, Special Paper 47, 185–213.
- Elo, S. 1997.** Interpretations of the Gravity Anomaly Map of Finland. *Geophysica* (1997), 33(1), 51–80.
- Hautaniemi, H., Kurimo, M., Multala, J., Leväniemi, H. & Vironmäki, J. 2005.** The "Three In One" aerogeophysical concept of GTK in 2004. In: Airo, M.-L. (ed.) Aerogeophysics in Finland 1972–2004: Methods, System Characteristics and Applications. Geological Survey of Finland, Special Paper 39, 21–74.
- Korhonen, J. 1992.** Kallioperän magneettiset ominaisuudet / Berggrundens magnetiska Egenskaper / Magnetic properties of the bedrock. In: Alalammi, P. (ed.) Suomen kartasto / Atlas över Finland / Atlas of Finland 123–126, *Geologia / Geologi / Geology*, 26–29 / Bilaga, 14–16 / Appendix, 15. National Board of Survey and Geographical Society of Finland 1992.
- Korhonen, J. V., Aaro, S., All, T., Nevanlinna, H., Skilbrei, J. R., Säävuori, H., Vaher, R., Zhdanova, L. & Koistinen, T. 2002.** Magnetic Anomaly Map of the Fennoscandian Shield 1:2 000 000. The Geological Surveys of Finland, Norway and Sweden and Ministry of Natural Resources of the Russian Federation.
- Korsman, K., Koistinen, T., Kohonen, J., Wennerström, M., Ekdahl, E., Honkamo, M., Idman, H. & Pekkala, Y. (eds.) 1997.** Bedrock map of Finland 1:1 000 000. Geological Survey of Finland.
- Korsman, K., Korja, T., Pajunen, M. & Virransalo, P. 1999.** The GGT/SVEKA transect: structure and evolution of the continental crust in the Paleoproterozoic Svecofennian orogen in Finland. *International Geology Review* 41, 287–333.
- Mertanen, S., Airo, M.-L., Elminen, T., Niemelä, R., Pajunen, M., Wasenius, P. & Wennerström, M. 2008.** Paleomagnetic evidence for Mesoproterozoic – Paleozoic reactivation of the Paleoproterozoic crust in southern Finland. In: Pajunen, M. (ed.) Tectonic evolution of the Svecofennian crust in southern Finland – a basis for characterizing bedrock technical properties. Geological Survey of Finland, Special Paper 47, 215–252.
- Pajunen, M., Elminen, T., Airo, M.-L. & Wennerström, M. 2001a.** Structural evolution of bedrock as a key to rock mechanical properties. In: *Rock Mechanics. A challenge for Society. Proceeding of Regional Symposium EUROCK 2001.* Rotterdam: A.A. Balkema, 143–148.
- Pajunen, M., Airo, M.-L., Elminen, T. & Wennerström, M. 2001b.** Preliminary report: The "Shear Zone Research and Rock Engineering" project, Pori area, south-western Finland. In: Autio, S. (ed.) Geological Survey of Finland, Special Paper 31, 7–16.
- Pajunen, M., Airo, M.-L., Elminen, T., Niemelä, R., Salmelainen, J., Vaarma, M., Wasenius, P. & Wennerström, M. 2008a.** Construction suitability of bedrock in the Helsinki area based on the tectonic structure of the Svecofennian crust of southern Finland. In: Pajunen, M. (ed.) Tectonic evolution of the Svecofennian crust in southern Finland – a basis for characterizing bedrock technical properties. Geological Survey of Finland, Special Paper 47, 309–326.
- Pajunen, M., Airo, M.-L., Elminen, T., Mänttari, I., Niemelä, R., Vaarma, M., Wasenius, P. & Wennerström, M. 2008b.** Tectonic evolution of the Svecofennian crust in southern Finland. In: Pajunen, M. (ed.) Tectonic evolution of the Svecofennian crust in southern Finland – a basis for characterizing bedrock technical properties. Geological Survey of Finland, Special Paper 47, 15–160.
- Puranen, M., Marmo, V. & Hämäläinen, U. 1968.** On the geology, aeromagnetic anomalies and susceptibilities of Precambrian rocks in the Virrat region (Central Finland). *Geoexploration* 6, 163–184.
- Puranen, R. 1989.** Susceptibilities, iron and magnetite content of Precambrian rocks in Finland. Geological Survey of Finland, Report of Investigation 90. 45p.
- Puranen, R., Elo, S. & Airo, M.-L. 1978.** Areal and geological variation of rock densities, and their relation to some gravity anomalies in Finland. *Geoskrifter* (Aarhus University) 10, 123–164.
- Sibson, R. 1977.** Fault rocks and fault mechanisms. *Journal of the Geological Society of London* 133, 191–213.
- Uski, M., Hyvönen, T., Korja, A. & Airo, M.-L. 2003.** Focal mechanisms of three earthquakes in Finland and their relation to surface faults. *Tectonophysics* Volume 363, Issues 1–2, 141–157.
- Vaasjoki, M. & Sakko, M. 1988.** The evolution of the Raahe-Ladoga zone in Finland: isotopic constraints.

In: Korsman, K. (ed.) Tectono-metamorphic evolution of the Raahe-Ladoga zone. Geological Survey of Finland, Bulletin 343, 7–32.

Wennerström, M., Airo, M.-L., Elminen, T., Niemelä, R., Pajunen, M., Vaarma, M. & Wasenius, P. 2008. Orientation and properties of jointing in Helsinki

area, southern Finland. In: Pajunen, M. (ed.) Tectonic evolution of the Svecofennian crust in southern Finland – a basis for characterizing bedrock technical properties. Geological Survey of Finland, Special Paper 47, 253–282.

CONSTRUCTION SUITABILITY OF BEDROCK IN THE HELSINKI AREA BASED ON THE TECTONIC STRUCTURE OF THE SVECOFENNIAN CRUST OF SOUTHERN FINLAND

by

Matti Pajunen¹, Meri-Liisa Airo¹, Tuija Elminen¹, Reijo Niemelä¹, Juha Salmelainen², Markus Vaarma¹, Pekka Wasenius¹ and Marit Wennerström¹

Pajunen, M., Airo, M.-L., Elminen, T., Niemelä, R., Salmelainen, J., Vaarma, M., Wasenius, P. & Wennerström, M. 2008. Construction suitability of bedrock in the Helsinki area based on the tectonic structure of the Svecofennian crust of southern Finland. *Geological Survey of Finland, Special Paper 47*, 309–326, 7 figures, 6 tables and 1 appendix.

The formulation of geological data for various societal demands requires extensive co-operation between geoscientists and the users of the data. The results presented in this paper were derived from projects of the Geological Survey of Finland running from 1999–2004 in the Helsinki capital area, which represents the major growth zone in Finland. Earlier development was carried out in the Pori area from 1998–2000. The aim is to provide an example of the analysis of geological research and mapping of data for various purposes, including land use planning, underground building and the analysis of water or waste movements in the bedrock in urban areas. The formulation of data highlights the significance of reliable geological and geophysical data on crustal evolution in achieving definite solutions for commercial applications.

Comprehensive data on the Finnish Precambrian bedrock have been compiled in geological and geophysical mapping programmes and research carried out during more than one hundred years. This study is based on analyses of c. 1000 observations of outcrops from the Helsinki study area. The main emphasis was on lithology and on structures that are measurable using routine geological mapping and laboratory methods. Characterization of the properties of jointing and semi-ductile to brittle faults takes priority, because they determine the major properties of rock masses for most applications. The relationships between semi-brittle and brittle structures and the lithology and ductile structure of the crust form the basis for dividing the bedrock into coherent terranes or blocks. Our first target was the purely geological classification of tectonic structures. The geological classes were transformed into a usable, technical form by means of pre-existing classifications (Q system and Finnish RG classification) applied in engineering geology.

The technical classification of geological structures presented in this paper is the first attempt to regionally formulate the bedrock properties, particularly the construction suitability of zones of weakness and of coherent crustal blocks, by fixing the classes according to recent knowledge of crustal evolution in the area. In the Helsinki area this means combining the structures with the polyphase development of the Svecofennian, c. 1.9–1.8-Ga-old lithologies and structures. These were later modified by tectonic-magmatic events of the rapakivi stage at 1.65 Ga ago and by minor movements during the Caledonian and even post-glacial times. The results are represented in the form of a “construction suitability map” of the Espoo, Helsinki and Vantaa areas.

Keywords (GeoRef Thesaurus, AGI): engineering geology, bedrock, structural geology, shear zones, fault zones, joints, classification, construction, Espoo, Helsinki, Vantaa, Finland

¹ *Geological Survey of Finland, P.O. Box 96, FI-02151 Espoo, Finland*

² *Rockplan Ltd, Asemamiehenkatu 2, FI-00520 Helsinki, Finland*

¹ *E-mail: matti.pajunen@gtk.fi*

INTRODUCTION

The need for geological information in different urban tasks, such as in building (Roinisto 1986, Saari 1988 and Rönkä & Ritola 1997) and community planning (Tarkkala 2004), has considerably increased along with the increased responsibilities for the safety of our natural environments and for making definite decisions in exploiting bedrock resources. In Finland the basis for all kinds of geological work is formed by the multifaceted knowledge gathered during more than one hundred years of research, mapping and exploration, and by developments in geophysical mapping methods at the Geological Survey of Finland (GTK). This Geological Survey of Finland, Special Paper 47 is a compilation of articles presenting recent results on the structural characteristics and evolution of the Svecofennian crust in the southernmost part of Finland. Depending on the application, the way of approaching bedrock properties varies. Different information is needed if prospecting processes are allocated to the bedrock material itself, or if the bedrock acts as a target of construction. Special formulations of geological data are also demanded when prospecting water circulation in the fracture framework or when analyzing the movements of harmful components in the bedrock. However, the prediction of most bedrock properties, e.g. the strength and isotropy of rock types, characters of the zones of weakness channeling water or creating problems for underground construction, or jointing patterns affecting local stress field patterns and the stability of rock masses, are predominantly determined by the tectonic, metamorphic and magmatic evolution of the crust. In-depth study of these processes and kinematic relations and the factors controlling ductile to brittle structures helps us to interpret the extensions of structures and rock types into soft-sediment-encrusted areas; here, geophysical data plays an important role. The accompanying papers of this Geological Survey of Finland, Special Paper 47 place their main emphasis on the geological characteristics that can be reformulated for various applications. The main interest was in semi-brittle to brittle structures, faulting and jointing, and on their connections to the ductile events and lithology of the Svecofennian crust.

Recent developments in information technology have improved the possibilities to distribute various kinds of information in defined ways to users and applicators. In Finland, such approaches are generally company- or municipality-centered. The projects

described in this volume of the Special Paper, in Pajunen et al. (2001a and b) and in the preliminary reports of Pajunen et al. (2002a, b, c and d) along with the extensive studies during nuclear waste site investigations (e.g. Paulamäki & Koistinen 1991, Paulamäki et al. 2006 and Mattila et al. 2008), have smoothed the path for an information technological development project, GeoTIETO (Geo Information System), at GTK (Kuivamäki et al. 2005 and Kuivamäki 2006). It aims at distributing applied geodata for several purposes in society. When dealing with geological information, difficulties particularly arise in the mutual understanding of geodata in the geoscientist-applier interface. What kind of geodata is important and in which forms should it be provided to benefit various applications?

The results presented in this paper were derived from projects in the surroundings of the urban Helsinki area from 1999–2002 (Pajunen et al. 2002a, b, c and d), with some revision and field mapping from 2003–2004 (Wennerström et al. 2006 and 2008). The early development of the research methods was achieved in a project in the Pori area of southwestern Finland from 1998–2000 (Pajunen et al. 2001a). The aim of this study was primarily to test the possibilities to characterize the carefully collected observations on bedrock properties in a technically usable form. Field data from outcrops on lithology, ductile deformation, shearing/faulting and jointing properties were collected for geological interpretation and classification. The purpose was to characterize the structures as a part of the polyphase tectonic evolution of the crust, and use this information as a basis for classifications and regional analyses of the structures. The geologically-classified data were combined with the pre-existing technical classifications (Barton et al. 1974 and Gardemeister et al. 1976) and properties of the bedrock to form a construction suitability map. The study area, comprising Espoo, Helsinki and Vantaa, is shown in Figure 1. This paper is a brief presentation of the formulation of the geological and geophysical data that is predominantly reported in the accompanying articles (Pajunen et al. 2008, Elminen et al. 2008, Wennerström et al. 2008 and Airo et al. 2008); the workflow followed is presented in Figure 2. All attempts to construct information for application purposes also needs co-operation with applicators of the data; in this approach the collaboration was carried out with the municipalities and private planning companies acting in the study area.

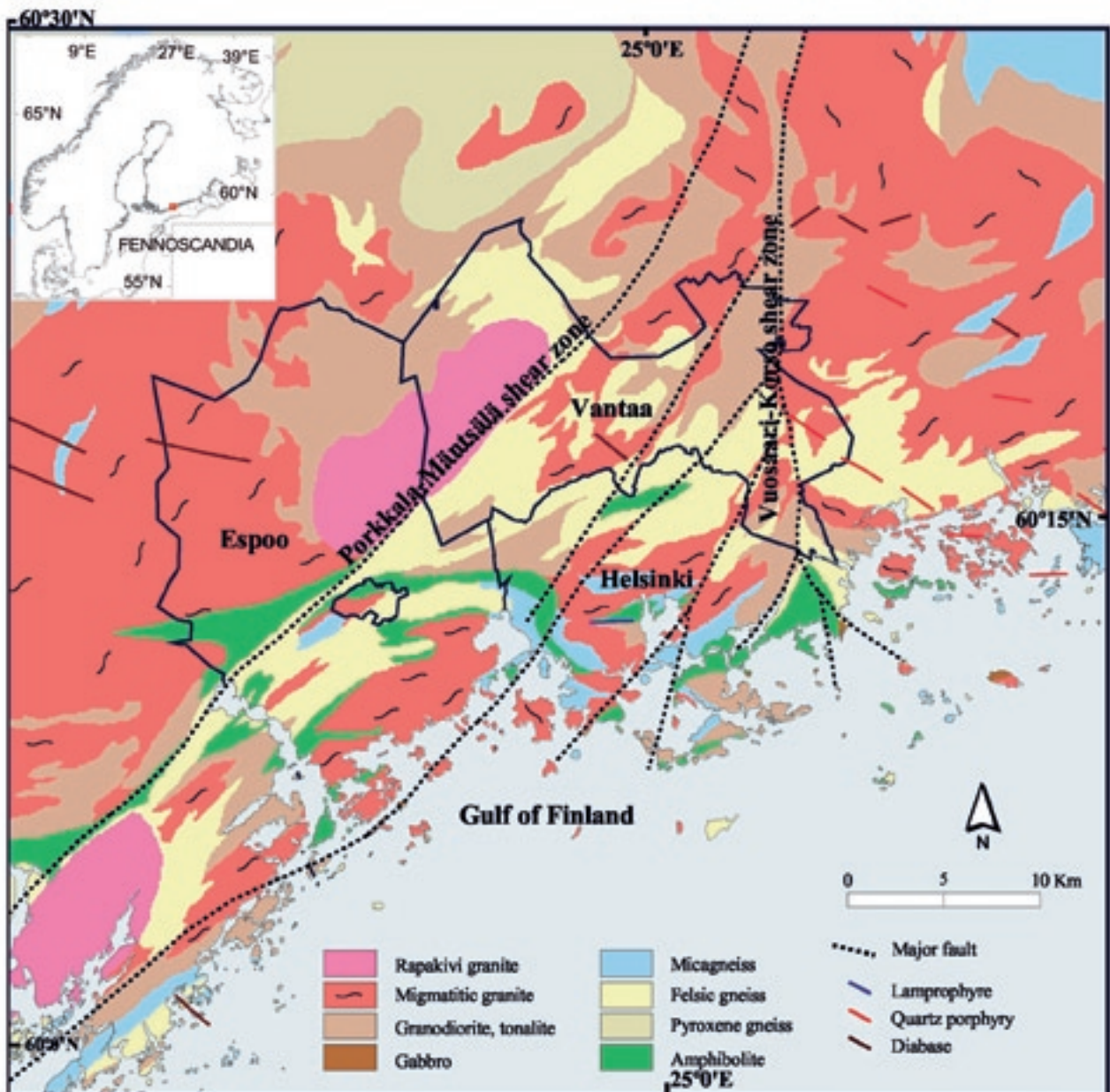


Figure 1. Study area in Espoo, Helsinki and Vantaa on the lithological map of the Helsinki Metropolitan Area. Base map © National Land Survey of Finland, permit No. 13/MML/08.

DATA AND METHODS

During the project in the Helsinki Metropolitan Area, comprehensive data were collected from c. 1000 outcrops. The data including, both geological and rock mechanical properties, are discussed in detail in the accompanying papers: Pajunen et al. (2008) for ductile deformation and lithology, Elminen et al. (2008) for shearing and faulting structures, Wennerström et al. (2006 and 2008) for jointing characteristics and Airo et al. (2008) for geophysical data and methods. The purpose was to standardize the mapping methods and field measurements as well as possible, and to classify the rock properties in the field. In addition to the standard geological mapping data on lithology, attention was

focused on the characterization of ductile structures, magmatic phases and metamorphic events, ductile to brittle shearing/faulting structures and jointing (Table 1).

The technically classified data (RG classification of Gardemeister et al. 1976) for the mapped faults were compiled from the corresponding zones of weakness in tunnels; the tunnel mapping had been carried out by the Geotechnical Division of the City of Helsinki. The mapped joint data include properties that are inconsistent with the engineering classification (Q system) of Barton et al. (1974). However, most of the observations are from ice-polished outcrops that show only minute possibilities

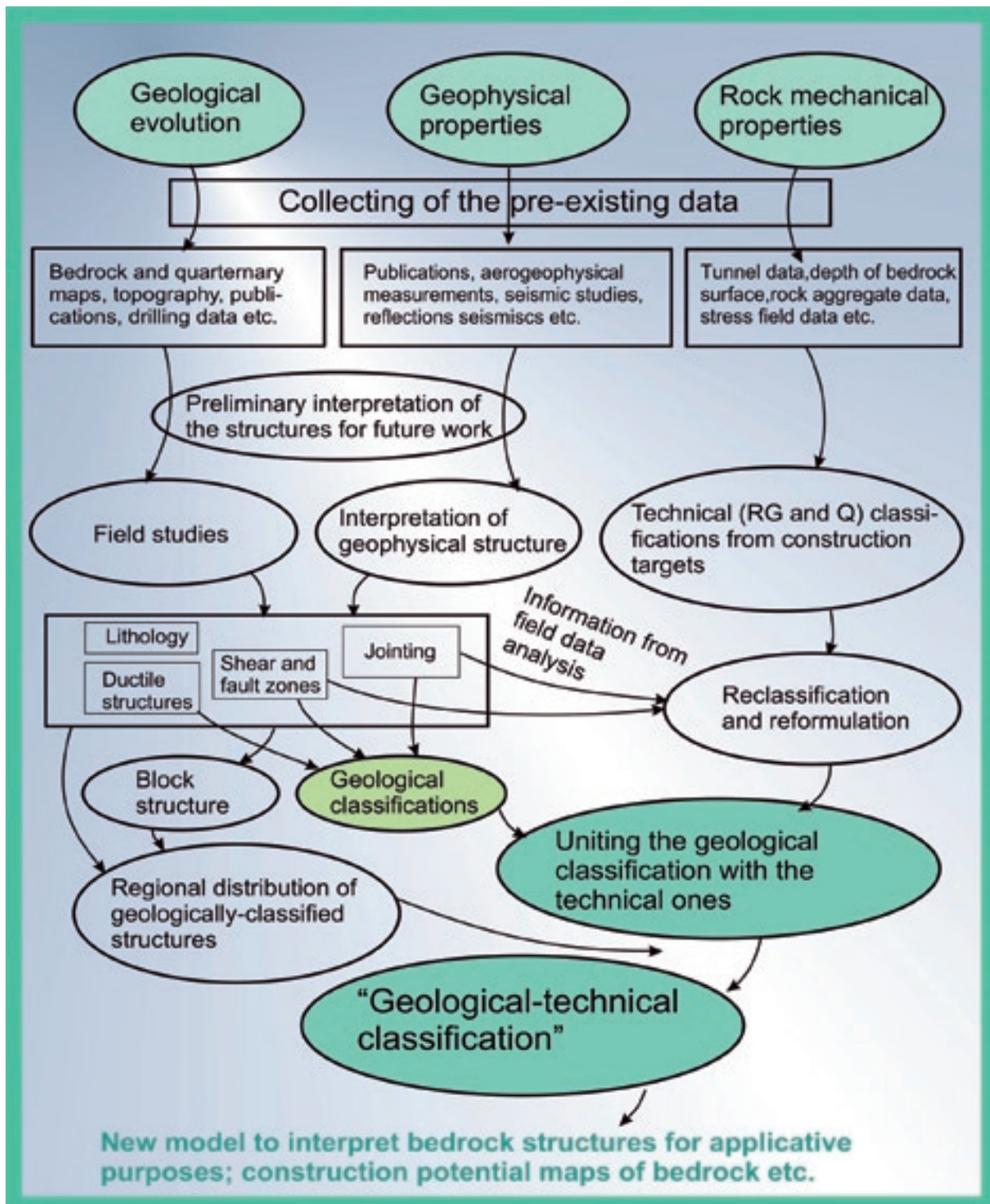


Figure 2. Workflow diagram for the project.

for three-dimensional analyses. Observations from road cuts and quarries gave a good 3D reference. For this reason, some properties, such as joint surface properties, collected during the normal technical mapping in tunnels were impossible to gather comprehensively during the field mapping. Normally, geological mapping data encompass several requirements of investigation, prospecting or planning, but are not as detailed as those collected in this

development project. Hence, more research is needed in the future to formulate more suitable field mapping methods in order to cover the separate requirements of technical and other applications. The blanket data collected during the projects nevertheless form a good starting point for further more thorough analyses; here, the data are used to construct a map that exhibits the consistency/brokenness of bedrock in the study area.

Table 1. Characterization of the collected field data.

DATA COLLECTED DURING THE FIELD WORK	
1	<u>Location information:</u> situation, coordinates, extent of the observation area
2	<u>Type of outcrop:</u> outcrop, road cut, quarry, tunnel
3	<u>Observation dimensions:</u> 2-D or 3-D; 3-D observation if the joint spacing can be measured from three dimensions
4	<u>General description of outcrop:</u> relations of rock types and structures
5	<u>Rock quality:</u> alteration, characters of contacts, slickensides
6	<u>Rock type:</u> lithology, fabric, grain size, structures, rock aggregate quality, building rock estimate, etc.
7	<u>Metamorphism and migmatization:</u> metamorphic assemblages, migmatization type and relations to structures and magmatic rocks
8	<u>Ductile deformation:</u> directions and types of foliation, fold and lineation and polydeformation analysis
9	<u>Faults:</u> fault plane strike and dip, dimensions, slickenline trend and plunge, sense of shear, fault type (Anderson's classification 1942), estimates of net slip, character of fault (brittle to ductile), fault rock texture, structural relationships
10	<u>Joints:</u> general description, extent of the measurement area, number of joint sets, orientation of each joint set <u>properties of each joint set:</u> type, opening, slickensides, joint fillings, joint length, spacing of joints, jointing zones, joint surface, extent of alteration of joint surfaces, en echelon joints, relations with other structures, water conductivity

DUCTILE EVOLUTION DETERMINING THE LATER EVOLUTION AND PROPERTIES OF BEDROCK

The study area is situated in the 1.9–1.8 Ga Svecofennian domain, in the c. 100 km wide WSW-trending granitoid-dominant zone of southern Finland (e.g. Korsman et al. 1997). It shows a polyphased ductile deformation concomitantly with magmatic and high-T/low-p metamorphic processes produced by highly complex crust-building processes of collisional and transpressional events (Pajunen et al. 2008). In the study area the most obvious post-Svecofennian events are related to the rapakivi stage at c. 1.65 Ga ago that already manifest the semi-ductile to brittle behaviour of the crust (Elminen et al. 2008, Mertanen 2001, Mertanen et al. 2001, 2004 and 2008). Some of the latest identified fault movements accompanied with fluid activity continued to produce coherent fault rocks during the Caledonian events c. 450 Ma ago (Vaasjoki 1977). Post-glacial movements have become evident as faults in glacial sediments (Kuivamäki et al. 1998) and as recent seismic tremors or earthquakes.

The ductile tectonic framework can be described by formlining the tectonic elements, such as foliation trends or shear zones, on the map plane or by modelling the structures into three-dimensional space. Three-dimensional modelling requires data fixed into 3-D; such modelling is suitable for and widely used in mines and local construction programmes (Paulamäki et al. 2006). The geological data gathered from outcrops is mostly two-dimensional point data. Three-dimensional extensions of lithology and structures incorporating depth can be modelled by analyzing the tectonic structures concomitant with the geophysical, tunnel or drilling data. Structural field data and several forms of integrated geophysical maps (Airo et al. 2008) are used to form the two-dimensional formline interpretation of the study area in Figure 3. The Svecofennian crustal evolution was polyphase and this is also reflected in a complex manner in its lithology and distribution (cf. Pajunen et al. 2008).

The sedimentary or volcanogenic belts representing the earliest Svecofennian geotectonic history still display relics of their primary, depositional features. These rocks underwent a series of successive geotectonic events that produced a very complex structural pattern (Pajunen et al. 2008). Several folding, foliation, migmatitic veining generations and pulses of intrusive rocks can be detected. Following the interpretation of Pajunen et al. (op. cit.), the earliest deformation events (D_{A-B}) tore the earliest primary sequences apart and made it difficult to predict the present-day occurrence of these rocks in a wider context. The D_B was related to crustal extension that caused strong migmatization and vertical shortening predominantly producing horizontal structures. The regional folding generations during the early contractional (D_C) and transpressional events (D_D) pushed the flat-lying structures (mainly D_B) and lithological associations into the steep D_{C-D} dome-and-basin structures. These dome-and-basin structures still characterize the areas that were not strongly impacted by the later transpressional events.

Wide-scale crustal transpression may cause oblique contractional deformation to act in one part of the terrane, whereas simultaneous oblique extension and magmatism act in another. During continuous deformation, extension may turn quickly to contraction. In such cases, highly differentiated local structural successions may form that are sometimes impossible to fix into the regional structural scheme without a wide structural context.

In the Svecofennian domain of southern Finland, extensional processes occurred with characteristic vertical shortening, extensional shearing, strike-slip faulting and strong felsic magmatism; in the early stage, at c. 1.87–1.84 Ga ago, the oblique extension occurred in the SE-NW direction (D_E , Pajunen et al. 2008). The crust cooled in several places below the ductile-brittle transition conditions before the D_E extension initiated; thus a new tectono-metamorphic pulse with new migmatite phases was generated. However, the timing of this tectono-metamorphic discordance varies between locations. In granulite areas, such as in the West Uusimaa complex (WUC), the discordance is difficult to distinguish due to more continuous heat flow in these areas (Pajunen et al. 2008). A following contractional regime produced wide-scale folding with E-W-trending axial planes (D_G). The extent of the extensional magmatism, represented by the widespread granites and granodiorites in the Southern Finland Granitoid Zone (SFGZ) continued during the SE-NW transpression at c. 1.84–1.80 Ga ago (D_H). The maximum principal stress rotated to more E-W-trending at the end of the Svecofennian orogeny and large open folds with N-S-trending axial planes (D_I) generated.

These late wide-scale folding phases caused large-scale tectonic dome-and-basin structures (F_{G-I} , Pajunen et al. 2008). Due to high thermal gradient, the concomitant structures varied significantly both horizontally and with depth during the Svecofennian orogeny. Because of the high thermal gradient also metamorphic conditions and amount of melting of the rocks varied significantly with depth. Consequently, the late large-scale folding structures with amplitudes of up to three kilometers determine the present-day exposition of rock types and structures that evolved at different crustal depths. The ductile tectonic-lithological framework that was generated during the complex Svecofennian evolution formed the foundation for the later post-Svecofennian geotectonic events.

As discussed (Pajunen et al. 2008), Svecofennian evolution already exhibited more or less brittle events (e.g. at the beginning of D_H), but the later progressive metamorphism and magmatism healed these old fractures to form cohesive structures. However, often these, and especially the zonal structures that formed during the latest stages of Svecofennian evolution, acted as zones of weakness during the post-Svecofennian zonal shearing/faulting deformations. Therefore, understanding of Svecofennian tectonic history opens possibilities to predict the regions prone to generating later brittle structures that, depending on the application target, present the biggest threats or bring the greatest benefits.

The fracturing and rock strength properties of the rock types, testable in laboratory experiments, are dependent, among others, on foliation characteristics, mineral composition and grain boundary characteristics. On a regional scale, fracturing properties of bedrock show more dependence on wider-scale structures, such as foliation trends, folding patterns and shear/fault zones, and lithology (e.g. Pajunen et al. 2001a, 2001b, Wennerström et al. 2006 and 2008). In the Precambrian Shield areas these properties result from the complex evolution of the rocks; the important properties can be recorded during geological mapping in the field. The bedrock often shows areas of systematic internal tectono-metamorphic and lithological characteristics that can be regarded as a basis for dividing the bedrock into varying terranes/blocks. In this example we divided the bedrock of the study area according to its ductile structural characteristics into 94 sub-areas (Figure 3) that were separately examined for their jointing properties. Shear zones and faults and lithological boundaries form the natural borders for such terranes. Some borders, covered by a thick layer of quaternary sediments, are based on geophysical interpretation (Airo et al. 2008).

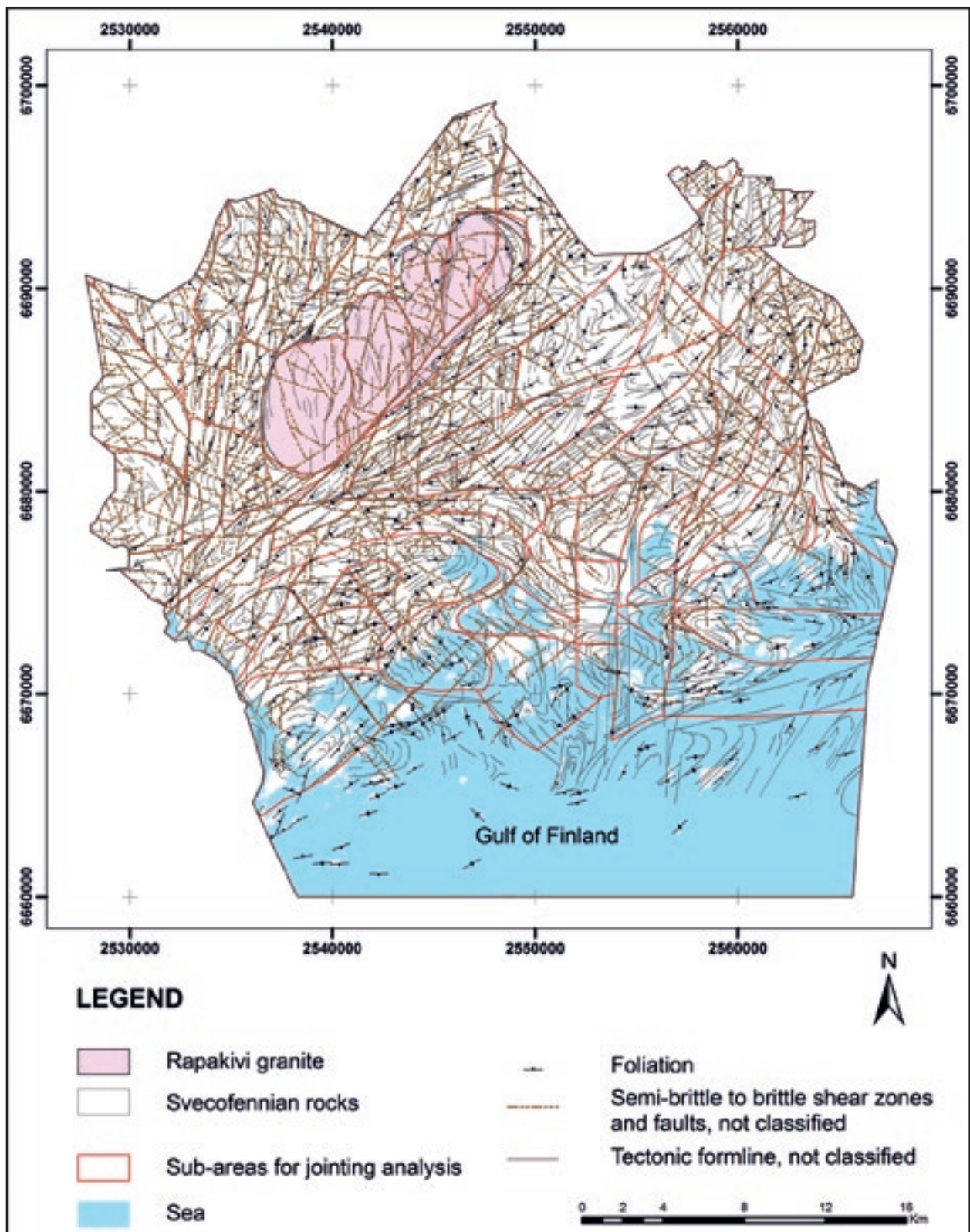


Figure 3. Division of the study area into terranes/blocks showing coherent internal lithological and structural characteristics. The terranes/blocks were characterized by their jointing properties and classified according to their brokenness (cf. Figure 6) to determine the construction suitability of the bedrock in the study area (Appendix 1). Base map © National Land Survey of Finland, permit No. 13/MML/08.

CLASSIFICATION OF SHEAR AND FAULT ZONES FOR CONSTRUCTION SUITABILITY

Ductile to semi-brittle shearing/faulting to brittle faulting already occurred during the Svecofennian, especially during its latest evolution, and are exhibited as long, topographic valleys or linear anomalies on aeromagnetic maps (Sederholm 1932, Tuominen 1957, Härme 1961, Talvitie 1971, Pajunen 1986, Elminen et al. 2008 and Airo et al. 2008). The post-Svecofennian tectonic movements often concentrated in these pre-existing zones or planar structures; polyphase zones were generated. In the Helsinki area these zones of weakness were located by using several modifications of topographic (Elminen et al. 2008) and geophysical data (Airo et al. 2008). The fault rock properties were examined in the field and by analyzing the structures under a microscope (Elminen et al. 2008); c. 470 detailed fault observations were made. The relative ages of the fault zones were determined by field observations and by using the fault rock properties for relative characterization (Table 2 and Figure 4); younger faults and those formed closer the erosion surface show more brittle characteristics than the older and deeper-generated ones. Paleomagnetic studies (Mertanen et al. 2008) fixed hydrothermal activity in some faults into the rapakivi age and some of them show signatures of Caledonian remagnetization. Kinematic analysis of

the faults helps to combine differently-oriented fault zones and to give an idea of how the regional framework of the faults was produced; the same stress field simultaneously formed both contractional and extensional fault/shear zones in different directions (Elminen et al. 2008).

The shear and fault structures are classified by their geological characteristics into several groups, indicating a change from ductile shear zones to transitional, mylonitic shear zones and finally to brittle zones with breccias and fault breccias. In the present-day erosion level the brittle faults and, because of brittle reactivation, also the ductile zones are often expressed as valleys covered by Quaternary sediments. When exposed in tunnels the brittle zones often are composed of non-cohesive fault rocks and various weathering products. The Porkkala-Mäntsälä shear/fault zone represents the major crustal deformation zone of the NE trend in southern Finland, and the Vuosaari-Korso shear/fault is a N-trending shear/fault zone in the eastern part of the study area. According to Elminen et al. (2008, Table 2 and Figure 4 in Elminen et al. 2008, this volume), the geological characteristics of the shear and fault zones in the study area are as follows:

Table 2. Classification of fault rocks (modified from Wise et al. 1984 and Higgins 1971).

Non-oriented	Fault gouge	<ul style="list-style-type: none"> • Fragments: < 30% in fine-grained matrix. Also oriented types with lense-shaped fragments • Angular fragments > 30% 	Incohesive
	Fault breccia		
	Cataclasite Microbreccia Breccia	<ul style="list-style-type: none"> • Fragments: < 30% in fine-grained matrix • Fragments > 30% 	
	Pseudotachylite	<ul style="list-style-type: none"> • Glass, possibly recrystallized 	
Oriented	Ultramylonite	<ul style="list-style-type: none"> • Porphyroclasts < 10%, matrix grain-size < 0.5 mm • Porphyroclasts > 10% 	Cohesive
	Proto- ja ortomylonite		
	Augen gneiss Blastomylonite*	<ul style="list-style-type: none"> • Matrix grain-size > 0.5 mm, porphyroclasts or porphyroblasts 	
	Gneiss Mylonite gneiss*	<ul style="list-style-type: none"> • Matrix recrystallized to grain-size of protolith or coarser 	

*according to Higgins (1971)

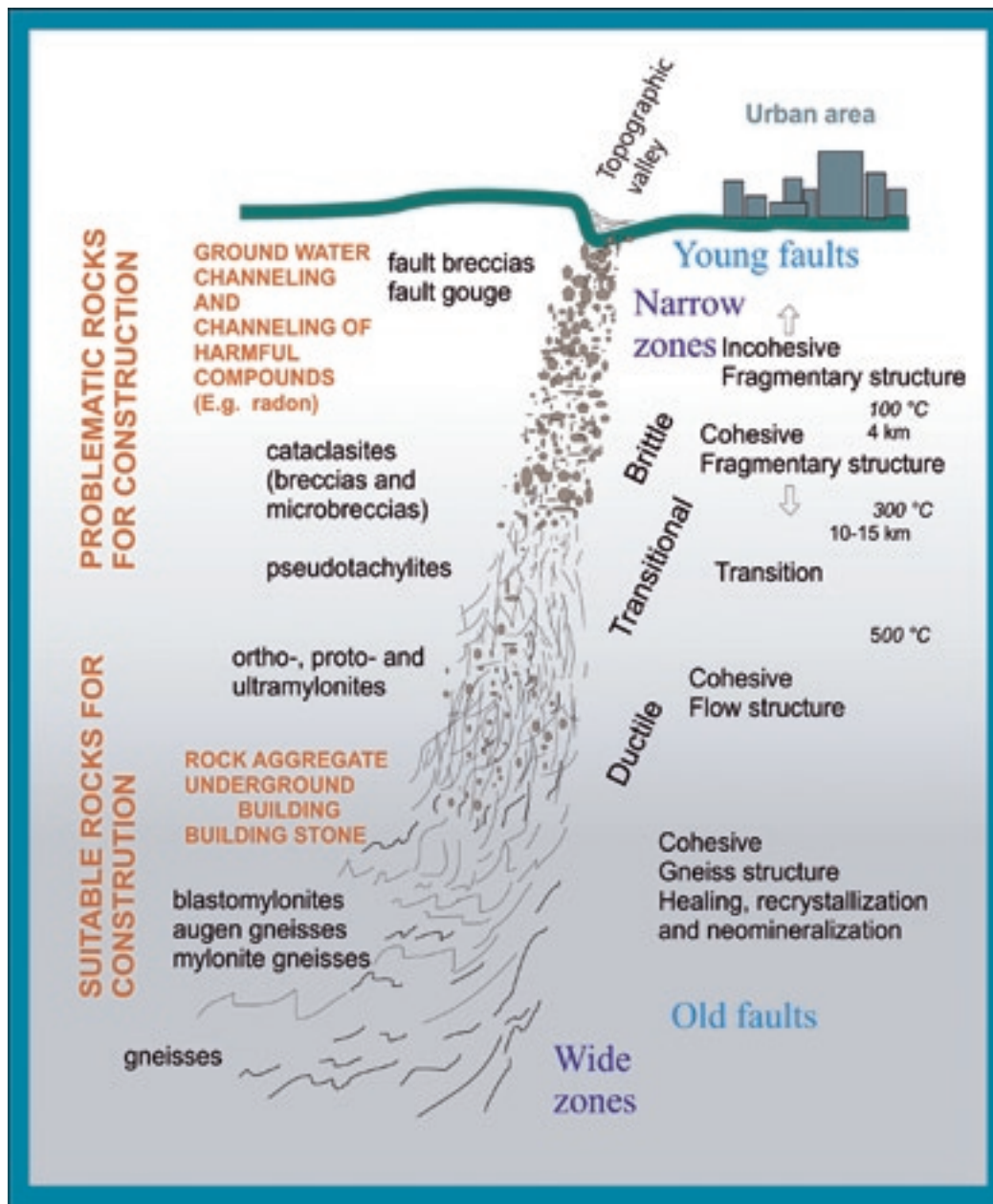


Figure 4. Characterization of fault rock properties in a schematic shear/fault zone; see also Table 2. Applicational properties of fault rocks are dependent on several factors affecting the fault rock generation, for example on the deformational depth, metamorphic p/T conditions, strain rate, amount and composition of accompanying fluids, composition and pre-existing structures of the rock.

SZ_A: Ductile E-W and ENE-trending steep mylonites and mylonite gneisses. Svecofennian. Brittle overprinting by SZ_F.

SZ_B: Ductile to semi-brittle NE steep mylonites, mostly ultramylonites. Late-Svecofennian. Compressional event. Brittle overprinting in SZ_C. Main structures of the Porkkala-Mäntsälä shear/fault and Vuosaari-Korso shear/fault.

SZ_C: Brittle steep NE faults and reactivation of ductile NE major faults (SZ_B). Narrow micro breccias, slickensides. Strike-slip regime. Rapakivi-related, similarly to SZ_D.

SZ_D: Brittle steep to moderate WNW and NNW breccia faults, also fault breccias and jointing.

Normal faulting in transcurrent regime. Rapakivi-related, similarly to SZ_C.

SZ_E: Brittle steep and long N faults with breccias, quartz and carbonate filled joints. Strike-slip movements. Later than the rapakivi. Possibly reactivates SZ_D.

SZ_F: Brittle E-W chloritic (altered) steep slickensides, fault gouge. Strike-slip movements. Later than the rapakivi. Concentrates in pre-existing SZ_A E-W zones.

SZ_G: Brittle low angle thrust faults, dips to N, E, S and W. Fault breccias, strongly weathered. Later than the rapakivi; not related to a single event.

The geologically-classified shear and fault zones have been combined with the corresponding zones in tunnels; these zones were technically classified at the time of tunnel excavation. These technically-classified zones have been used as a basis in determining the construction suitability of shear zones (SZ_A), transitional fault zones (SZ_B) and brittle zones of weakness (SZ_{C-G}) (Table 3). The technical rock classification (RG classification, Gardemeister et al. 1976) includes information on the weathering properties (Rp1–4, Table 4) and brokenness (RiI-V, Table 4) of the rock mass; the amount of water flow is an approximation made in the studied tunnels. The shear and fault zones were classified into three categories according to their geological and technical characteristics and dimensions (Table 3). The

three-fold classification of the zones of weakness was transformed into a practical form for the users (Table 5) by co-operation at the geology-engineering interface and by using experience of the technical demands in corresponding zones of weakness in tunnels. The classification provides estimates of the technical properties for the geologically-determined shear and fault zones by taking into account the excavation as well as the stabilization properties of the rock mass. The classification of the zones of weakness is illustrated in Figure 5. The zones are classified as “observed” when there are observations of the zone properties on outcrops or in tunnels or as “interpreted” when geological, kinematic and geophysical interpretation is used to classify the zone.

Table 3. Properties of the shear/fault zones in the study area. Brokenness and weathering classification are shown in Table 4.

SZ class	PM zone	SZ _A (ENE)	SZ _{A+F} (E-W)		SZ _B	SZ _C and SZ _E	SZ _D	SZ _G	
RG classification	strongly weathered and fractured	no tunnel observation	Rp1-3 RiIII-IV		Rp1-2 (3) RiII / IV	Rp0-2 RiIV-V	Rp1-2 RiIII-IV	Rp0-2 RiI-V	
Water			minute	moderate	minute	rather abundant	rather abundant		
Size→ Technical class↓		Length (km)	Width (m)	Length (km)	Length (km)	Length (km)	Width (m)	Length (km)	Width (m)
1		2-5	< 2	< 2	2-5	2-5	< 2	< 2	< 1
2		> 5	2-5	2-5	> 5	> 5	2-5	2-5	1-2
3	always class 3	> 5 + factors reducing class	> 5	> 5	> 5 + factors reducing class	> 5 + factors reducing class	> 5	> 5	> 2
Other	(properties from the drilling data)		If fault breccia, strong alteration or weathering exist the primary class is reducing						

Table 4. Jointing (brokenness RiI-V) and weathering (RpI-IV) classification of Gardemeister et al. (1976). The classification has been used to describe the weak zones in tunnels for engineering purposes.

Jointing		
RiI	plane-like joints divide the rock into two or more parts	
RiII	abundant jointing	no joint filling
RiIII	dense jointing	some joint filling
RiIV	abundant or dense jointing	clay or couge as joint filling
RiV		abundant clay or couge
Weathering		
Rp1	no weathering	
Rp2	some weathering	
Rp3	abundant weathering	
Rp4	totally weathered	

Table 5. Technical classification of shear/fault zones of the study area.

Class	Rock structures effecting on		
	blasting/quarrying	stabilization	stopping
1	Rock quality non-weathered or slightly weathered (Rp1) Joints open or filled with clay Joints with slickensides Small joint openings (<2 mm) Rock quality RiIII-RiIV	Moderate block size (>30 dm ³) Clearly visible jointing system Small dimensions of zone (<2m)	Small water conductivity of jointing Small underground water pressure
2	Rock quality slightly or strongly weathered (Rp1-2) Joints open or filled with clay Joints with slicken sides Moderate joint openings (2-5 mm) Rock quality RiIV	Moderate–small block size (30-10 dm ³) Weakly visible jointing system Moderate dimensions of zone (2-5 m)	Moderate water conductivity of jointing Moderate underground water pressure
3	Rock quality strongly or penetratively weathered (Rp2-4) Joints open or filled by clay Joints with slickensides Small joint openings (<2 mm) Joints filled with rock grains or clay Wide joint openings (>5 mm) Rock quality RiIV-RiV	Small block size (<10 dm ³) Jointing system not visible Large dimensions of zone (>5m)	High water conductivity of jointing High underground water pressure

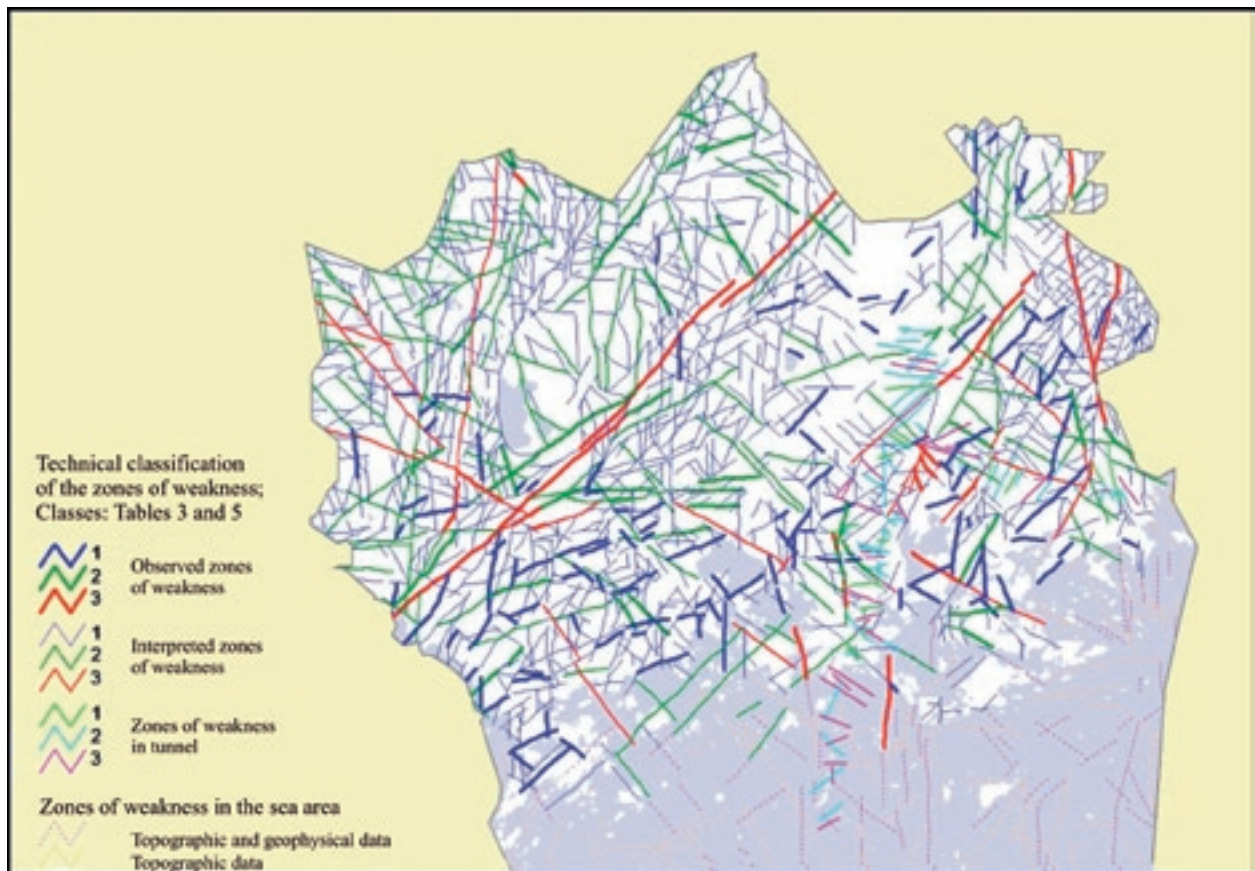


Figure 5. Technical classification of the zones of weakness in the study area; see also Tables 4, 5 and 6. Base map © National Land Survey of Finland, permit No. 13/MML/08.

TECHNICAL CLASSIFICATION OF JOINTING

In Finland, studies on jointing properties have generally been related to local construction programmes (Paulamäki 1989, Saksa et al. 1992, Anttila et al. 1992, Anttila et al. 1999, Posiva 2005 Mattila et al. 2008), but regional characterizations have seldom been done. The systematic NE and NW orientation of the major lineaments in the Finnish Precambrian bedrock was pointed out by Härme (1961). According to Grad and Luosto (1992), fracturing continues in the bedrock to a depth of c. 1–2 km. One of the main purposes in the projects carried out in the Pori and Helsinki areas (Pajunen et al. 2001a, 2001b and Pajunen et al. 2002a) was to consider the variations in jointing patterns with respect to the penetrative, ductile structures of the crust as well as the zoned deformations, shearing and faulting. Pajunen et al. (2001a) described coherent jointing patterns in tectonically uniform blocks in the Pori area. Wennerström et al. (2008) combined the orientations of joint sets with regional deformation features such as foliation, folding and faulting structures. The directions characterizing the regional lineament pattern in Finland (Härme 1961) also characterize the jointing pattern in the study area; the pattern behaves independently on the lithological boundaries. The systematic array of joints suggests generation by a homogeneous stress field that affected a large area, but the tectonic event causing the pattern is not known (Wennerström et al. 2008). There have been only a few attempts to assess the fracturing of bedrock in relation to the deformation history of the bedrock (e.g. Paulamäki & Koistinen 1991 and Pajunen et al. 2001a). Preliminary observations have been made on the kinematic control of joints by the faults of rapakivi stage (SZ_{C-D}). At least the joints, sometimes slightly altered, sitting parallel and outcropping in the same terrane with the constantly WNW-oriented rapakivi-related diabase dykes provide evidence that at least at 1.65 Ga ago the bedrock behaved in such a brittle way that jointing was able to form (Wennerström et al. 2008).

In the Helsinki area, dimensional and quality features of jointing were recorded from c. 700 outcrops to analyse regional variations in jointing properties. The mapped joint properties are presented in Table 1. Properties of c. 2420 joint sets forming a coherent observation net in the study area were investigated. A comprehensive discussion of the methods for collecting jointing data is included in Wennerström et al. (2006 and 2008). The aim was to collect joint properties that are comparable with the existing classification of rock masses, such as Q

system of Barton et al. (1974). We were forced to concentrate on data that can be collected from ice-polished outcrops, often showing only poor three-dimensional sections. Thus, not all the properties included in engineering classifications could be collected during normal geological field mapping; the trace length, spacing of joints and number of joint sets are the main characterizing properties in our studies. The use of joint wall properties is more restricted. For example, weathering at outcrops has often removed the evidence of joint fillings, whereas in road cuts such properties have often remained. Joint fillings and joint wall alteration types will require a separate study. Fresh, artificial joints caused by quarrying were not taken into account. Classification of the brokenness of the bedrock in the Helsinki Metropolitan Area was formed as follows.

Properties of joints were classified and displayed on a construction suitability of bedrock map in sub-areas defined using lithology and the tectonic structure. The study area was divided into blocks by using the ductile deformation structures, shear and fault zones and lithology (Figure 3); the distribution of rock types on the present-day erosion surface are strongly determined by the late, ductile, open folding structures (Pajunen et al. 2008). Each block was separately dissected according to its jointing characteristics. The main properties, namely the trace length, spacing of joints and number of joint sets, determine the basic construction suitability of each block; the classification factors are presented in Table 6. Each observation point was separately classified into four classes; A (the most solid) to B, C and D (the most broken), and the class obtained for each block represented the average value of the observation points for the block. If the block included some dominant additional properties that reduced the solidity of the rock mass, the class was lowered by one or more depending on the extent of these weakening characters. The additional properties were tightly-spaced joints (r), slickensides (h), open jointing (a), planar jointing (s), smooth jointing (i), intensely altered or strongly weathered joint surfaces (m) and clay- or soil-filled or weathered joints (t) (Table 6). The construction suitability, A-D, of the blocks were determined by their main properties, but if the class was lowered due to the existing additional properties, the lowered class is symbolized on the left-hand side of the slash; the original value and the factors reducing the construction suitability follow the slash (Figure 6).

Table 6. Technical classification based on the main components of jointing.

Class	A	B	C	D
Spacing (m)	> 1	0.5...1	0.5...0.3	< 0.3
Length (m)	< 10	< 10	< 20	> 20
Number of sets (s=random)	1-2 (Jn: 2-4)	2+s or 3 (Jn:6-9)	3+s (Jn: 12)	4-> (Jn: 15)
Slickenside (appear)	no	single	moderate	numerous
Tightly spaced	no	if predominates class decreases	if predominates class decreases	
Other properties	no	if predominates class decreases	if predominates class decreases	

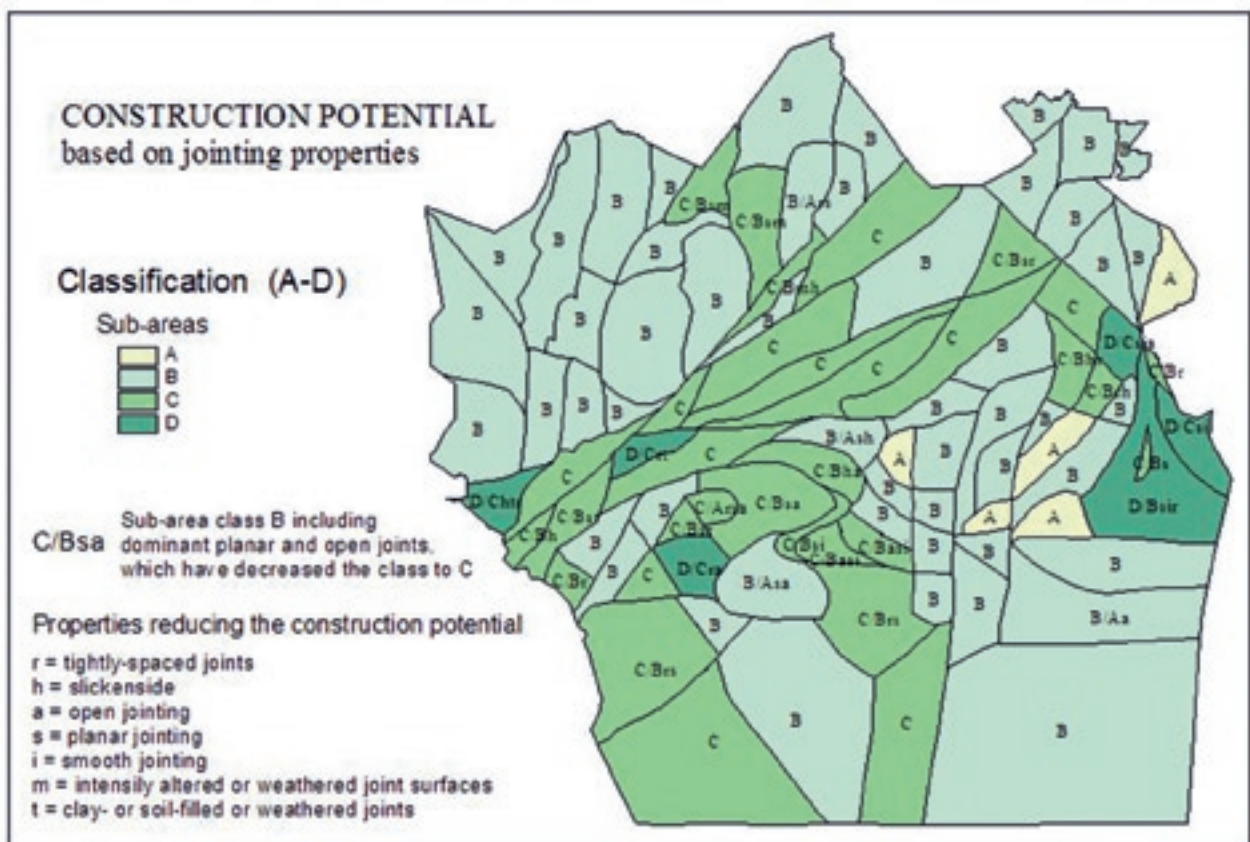


Figure 6. Tectonically determined terranes/blocks of the study area (see Figure 3) are classified according to their jointing properties (Table 6). The base classification, classes A-D, was formed using the three main properties: the trace length, spacing of joints and number of joint sets. The base classifications were lowered when additional harmful components, such as tightly-spaced joints (r), slickensides (h), open jointing (a), planar jointing (s), smooth jointing (i), intensely altered or strongly weathered joint surfaces (m) and clay- or soil-filled or weathered joints (t) were prominent in the studied terrane/block. Base map © National Land Survey of Finland, permit No. 13/MML/08.

EXAMPLE APPLICATION – CONSTRUCTION SUITABILITY OF BEDROCK

The geological data on zones of weakness and on crustal terranes/blocks determined by lithological characteristics and structural analyses and by benefiting geophysical interpretations is presented in the form of a “construction suitability of bedrock” map covering the Espoo, Helsinki and Vantaa areas (1:50 000) in Appendix 1 (back cover). The inset maps include the characterization of the data: 1. Ductile structures determining the major tectonic structures on the aeromagnetic map and the observation points in the study area; 2. Characterization of shear/fault rock observations on outcrops and tunnels on the topographic slope map; 3. Jointing observations classified according to relative block size on the spacing of jointing map, and 4. Length of jointing on the construction suitability map showing the number of observations on which the classification is based within each block. The construction suitability of bedrock map is an integrated presentation of these different data classified by the means discussed in the previous chapters. Lithological data are included only as point data on the map indicating the main rock type on the outcrops. The data were collected during the study and the geological mapping of GTK (Härme 1969, Laitala 1960, 1967 and 1994). The foliations are from the same sources. The thicknesses of overburden from the drillings of GTK are also included.

For readers unfamiliar with geological bedrock maps, it is not always self-evident how the data needed can be obtained from the maps. One problem in using the preliminary map (Pajunen et al. 2002d) arose from the different ways of reading maps. Common road and topographic maps show the data on the map area as they are, because the data are measured and presented using similar methods. The same partly applies dealing with the characters of aerogeophysical data such as magnetic maps, but in this case different variables affect the results in different ways (such as the characteristics of overburden and non-geological noise; see Airo et al. 2008). In contrast, geological field observations are point data and the information must be interpolated by different methods (e.g. using tectonic interpretation and geophysics) to the unexposed areas shown on the map. This means that geological bedrock maps, like the construction suitability map presented here, should be read in a slightly different way! This problem will be illustrated with an example.

Example

The map (Appendix 1), showing interpolated classification of point data, gives a good overall estimate of the construction suitability in the area, but a more detailed estimation of the target must be performed by carefully investigating the information in the vicinity of the study site. The more data is recorded in the vicinity, the more precisely the data can be interpolated. In this respect, however, the accuracy of the data differs between geological terranes/blocks. In homogeneous and simply deformed areas, as in many granitoid areas of the Svecofenian bedrock, interpolation is more reliable than in areas showing complexly folded variable lithology (see Pajunen et al. 2008). In such a way different areas are indicated in inset 1 (see above).

The example area in Vantaa, Koivuhaka (Figure 7), is situating in the vicinity of Helsinki-Vantaa airport in the NNE part of the construction suitability map area. The example area is located in area C in Inset 1, which is characterized by NE flexures of lithological associations and NE and N-trending faults. In the northern part of the area there are some outcrops, but the area is mostly covered by Quaternary soils. In the SE corner of the area there is labelling according to which the thickness of the soil exceeds 17 m in that location.

Aided by the records of the area and surroundings concerning the lithologies, orientations and structural forms, an assessment of the nature of the prevailing bedrocks can be made. The area is intersected by a zone of weakness (status interpreted) in the direction of NE-SW, and in addition, just near the northern border of the area there is an intersection zone of this and two other zones of weakness in directions of N-S and NW-SE, respectively. The construction suitability class of these zones of weakness is moderate. The construction suitability class of bedrock in the western and middle parts of the area is B, solid. In the eastern parts it is C/Bsr, broken. The annotation means that the bedrock of this part is also solid (construction suitability class B), but more abundant occurrences of planar joints (s) and tightly spaced joints (r), respectively, makes the bedrock more broken (construction suitability class C). The interpretation of factors determining the construction suitability presented in the map may include following features:

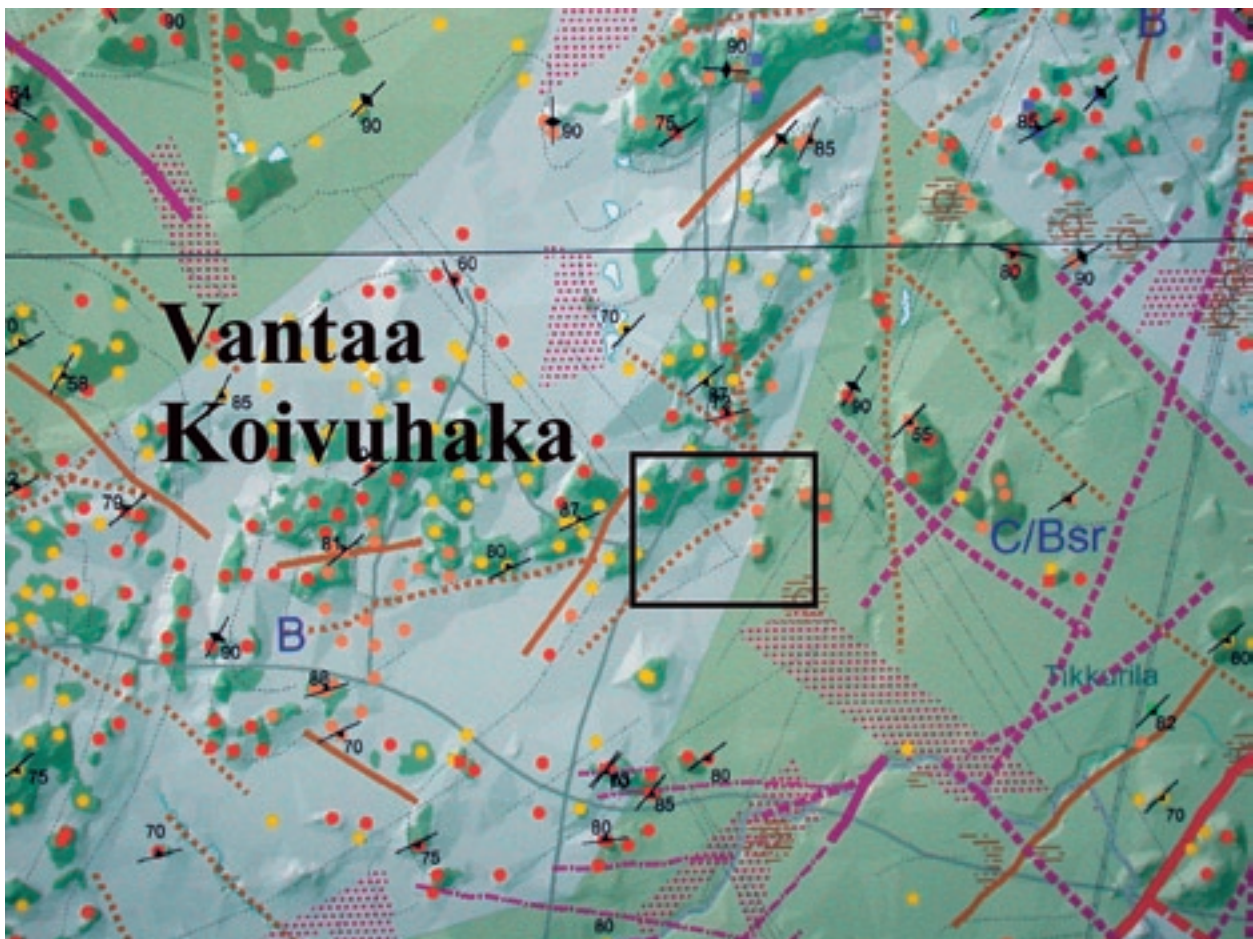


Figure 7. An example area (1 km²) in Koivuhaka, Vantaa (Finnish grid coordinates KKJ2 of the SW corner: x = 6688750 and y = 2554900) on the construction suitability map of Espoo, Helsinki and Vantaa areas (appendix 1). See discussion in the text. Base map © National Land Survey of Finland, permit No. 13/MML/08.

1. There is significant variation in the topography of the bedrock surface. The soil is rather thin in northern parts and thickens towards the south and southwest.
2. The northern parts of the area mostly consist of granite and granodiorite, whereas in the middle and southern parts quartz-feldspar gneisses and migmatitic rocks prevail.
3. The lithology is oriented and the prevailing strike is SW-NE, but some NW-SE orientation and strike also occur.
4. The number of main jointing directions is two or three and in addition some occasional joints may occur. The spacing between joints varies, being 0.3–1 m. The length of joints is mostly less than 10 m, but lengths of over 20 m may occur in places.
5. The strikes of the two main jointing directions are c. SW-NE and NW-SE, and the dips are steep. The NW jointing nearly parallels the regional strike of the lithology. The strike of the third main jointing direction is c. E-W and the dip is quite gently sloping to the north.
6. Occasional slickensides and tightly-spaced joints may occur, mostly due to the steeply dipping main jointing directions. They may be more abundant when connected to zones of weakness and when accompanied by quartz-feldspar gneisses and migmatitic rocks.
7. The change in the strike of lithological associations may be related to the NE zone of weakness. If so, it may indicate ductile shear zone with rather solid and trouble-free rock masses within the zone. The brittle joint faults and breccias may still exist. Some problems may also occur in the intersection of zones of weakness in the north and in the southern and south-eastern parts with a thick overburden.
8. The relative block size (RQD/J_n) varies between 8–5 within the area.

This map is by no means the final possible compilation of the geological-geophysical data, even for those it was addressed to. The main purpose was to point out, that it is possible to construct usable applications by leaning on geological information based on the extensive work carried out during the regional mapping programmes and intensive research in the target areas. The more the applications are based on the thorough investigation results, the safer and more

reliable the results offered will also be. The consensus between the geoscientists and application users is far from solved and much work and co-operation will be necessary to narrow this gap. This study has been a small step closer and demonstrates that this kind of development work is important and such data are needed and sought after. However, further and longer leaps must be taken before the current and future needs of the society are met.

ACKNOWLEDGEMENTS

The co-operation project of the Geological Survey of Finland (GTK) was financed by the National Technology Agency of Finland (TEKES), the cities of Espoo, Helsinki and Vantaa, and the planning companies Rockplan Ltd and Viatek Ltd, who we for providing the possibilities to realize our studies. Kalevi Korsman and Tapio Koistinen showed great interest during the long evolution of the structural investigations in the study areas and provided their valuable advice on the formulation of the results presented in this study. Seppo Paulamäki and Aimo

Kuivamäki read the early version of the manuscript and suggested several improvements. Roy Siddall checked the English of the manuscript, and Pekka Särkkä and Ossi Ikävalko acted as official reviewers. Co-operation during the projects has been extensive and we want to express our gratitude to all those mentioned, as well as to many people not mentioned here who have helped to compile these papers and provide this possibility to formulate geological information for general use.

REFERENCES

- Airo, M.-L., Elminen, T., Mertanen, S., Niemelä, R., Pajunen, M., Wasenius, P. & Wennerström, M. 2008.** Aero-geophysical approach to ductile and brittle structures in the densely populated urban Helsinki area, southern Finland. In: Pajunen, M. (ed.) Tectonic evolution of the Svecofennian crust in southern Finland – a basis for characterizing bedrock technical properties. Geological Survey of Finland, Special Paper 47, 283–308.
- Anderson, E. M. 1942.** The Dynamics of faulting and dyke formation with applications to Britain. Edinburgh: Oliver & Boyd. 183 p.
- Anttila, P., Paulamäki, S., Lindberg, A., Paananen, M., Koistinen, T., Front, K. & Pitkänen, P. 1992.** The geology of the Olkiluoto area, summary report. Tiivistelmä: Olkiluodon alueen geologiset olosuhteet: yhteenvetoraportti. Helsinki: Voimayhtiöiden ydinjätetoimikunta, Report YJT-92-28. 37 p.
- Anttila, P., Ahokas, H., Front, K., Hinkkanen, H., Johansson, E., Paulamäki, S., Riekkola, R., Saari, J., Saksa, P., Snellman, M., Wikström, L. & Öhberg, A. 1999.** Final disposal of spent nuclear fuel in Finnish bedrock – Olkiluoto site report. Tiivistelmä: Käytetyn polttoaineen loppusijoitus Suomen kallio-perään – Olkiluodon paikkaraportti. Helsinki: Posiva Oy, Posiva-raportti 99-10. 206 p.
- Barton, N., Lien, R. & Lunde, J. 1974.** Engineering classification of rock masses for the design of tunnel support. Rock Mechanics 6, 189–236.
- Elminen, T., Airo, M.-L., Niemelä, R., Pajunen, M., Vaarma, M., Wasenius, P. & Wennerström, M. 2008.** Fault structures in the Helsinki Area, southern Finland. In: Pajunen, M. (ed.) Tectonic evolution of the Svecofennian crust in southern Finland – a basis for characterizing bedrock technical properties. Geological Survey of Finland, Special Paper 47, 185–213.
- Gardemeister, R., Johansson, S., Korhonen, P., Patrikainen, P., Tuisku, T. & Vähäsarja, P. 1976.** Rakennusgeologisen kallioluokituksen soveltaminen. Tiedonanto / Valtion teknillinen tutkimuskeskus. Geotekniikan laboratorio 25. 39 p. (in Finnish)
- Grad, M. & Luosto, U. 1992.** Fracturing of the crystalline uppermost crust beneath the SVEKA profile in central Finland. Geophysica 28 (1–2), 53–66.
- Härme, M. 1961.** On the fault lines in Finland. C.R. Soc. Géol. Finlande, Vol. 33, 437–444, illus.; also Bull. Comm. Géol. Finlande, n:o 196.
- Härme, M. 1969.** Kerava. Geological Map of Finland 1:100 000, Pre-Quaternary Rocks, Sheet 2043. Geological Survey of Finland.
- Higgins, M. H. 1971.** Cataclastic Rocks. U.S. Geological Survey Professional Paper 687. 97 p.
- Korsman, K., Koistinen, T., Kohonen, J., Wennerström, M., Ekdahl, E., Honkamo, M., Idman, H. & Pekkala, Y. (eds.) 1997.** Bedrock map of Finland 1:1 000 000. Geological Survey of Finland.
- Kuivamäki, A. (ed.) 2006.** GeoTIETO.informaatiojärjestelmän kehittäminen yhdyskunta- ja ympäristö-

- suunnittelua varten (in Finnish with English summary). Vaihe II: Geotieto-käyttöliittymän ja 1:20 000 rakennettavuusmallien viimeistely sekä 1:50 000 rakennettavuusmallien kehittäminen. Geological Survey of Finland, unpublished report K 21.42/2006/2. 166 p.
- Kuivamäki, A., Vuorela, P. & Paananen, M. 1998.** Indications of postglacial and recent bedrock movements in Finland and Russian Karelia. Nuclear Waste Disposal Research, Geological Survey of Finland, Report YST-99. 92 p.
- Kuivamäki, A., Lampio, E., Jarva, J., Wennerström, M., Airo, M.-L., Valjus, T., Ojala, A., Tarvainen, T., Säätuvuori, H., Pajunen, M., Elminen, T. & Grönholm, S. 2005.** A new internet based information system GeoTIIETO for land use planning in the Helsinki capital region, Finland, Abstract to the 27th Nordic Geological Winter Meeting.
- Laitala, M. 1960.** Siuntio. Geological Map of Finland 1:100 000, Pre-Quaternary Rocks, Sheet 2032. Geological Survey of Finland.
- Laitala, M. 1967.** Helsinki. Geological Map of Finland 1:100 000, Pre-Quaternary Rocks, Sheet 2034. Geological Survey of Finland.
- Laitala, M. 1994.** Lohja. Geological Map of Finland 1:100 000, Pre-Quaternary Rocks, Sheet 2041. Geological Survey of Finland.
- Mattila, J., Aaltonen, I., Kemppainen, K., Wikström, L., Paananen, M., Paulamäki, S., Front, K., Gehör, S., Kärki, A. & Ahokas, T. 2008.** Geological model of the Olkiluoto site, Version 1.0. Posiva Oy, Working Report 2007-92. 509 p.
- Mertanen, S. 2001.** Sekundääriset remanenssit kallioperän geologisten prosessien ilmentäjänä. In: Airo, M.-L. & Mertanen, S. (eds.) XX Geofysiikan päivät Helsingissä 15.-16.5.2001, Geofysiikan Seura, Geophysical Society of Finland, 129-134. (in Finnish)
- Mertanen, S., Pajunen, M. & Elminen, T. 2001.** Applying palaeomagnetic method for dating young geological events. In: Autio, S. (ed.) Geological Survey of Finland, Current Research 1999-2000. Geological Survey of Finland, Special Paper 31, 123-129.
- Mertanen, S., Pajunen, M. & Elminen, T. 2004.** Multiple remagnetization events of shear zones in southern Finland. In: Mertanen, S. (ed.) Supercontinents, remagnetizations and geomagnetic modelling. 5th Nordic Paleomagnetic Workshop, Suitia-Helsinki, Finland, September 25-30, 2004, 39-44.
- Mertanen, S., Airo, M.-L., Elminen, T., Niemelä, R., Pajunen, M., Wasenius, P. & Wennerström, M. 2008.** Paleomagnetic evidence for Mesoproterozoic - Paleozoic reactivation of the Paleoproterozoic crust in southern Finland. In: Pajunen, M. (ed.) Tectonic evolution of the Svecofennian crust in southern Finland - a basis for characterizing bedrock technical properties. Geological Survey of Finland, Special Paper 47, 215-252.
- Pajunen, M. 1986.** Deformation analysis of cataclastic structures and faults in the Tervo area, central Finland. Geological Survey of Finland, Bulletin 339, 16-31.
- Pajunen, M., Airo, M.-L., Wennerström, M., Niemelä, R. & Wasenius, P. 2001a.** Preliminary report: The "Shear zone research and rock engineering" project, Pori area, south-western Finland. Geological Survey of Finland, Special Paper 31, 7-16.
- Pajunen, M., Elminen, T., Airo, M.-L. & Wennerström, M. 2001b.** Structural evolution of bedrock as a key to rock mechanical properties. In Rock Mechanics. A Challenge for Society. Proceeding of Regional Symposium EUROCK 2001. Rotterdam: A. A. Balkema, 143-148.
- Pajunen, M., Airo, M.-L., Elminen, T., Niemelä, R. J., Vaarma, M., Wasenius, P. & Wennerström, M. 2002a.** Kallioperän rakennettavuusmalli taajamiin. Menetelmänkehitys ja ohjeistus. Raportti I. Geological Survey of Finland, unpublished report K 21.42/2002/5. 95 p. (in Finnish)
- Pajunen, M., Airo, M.-L., Elminen, T., Niemelä, R., Salmelainen, J., Vaarma, M., Wasenius, P. & Wennerström, M. 2002b.** Rakennettavuuskartan selitys. "Kallioperän rakennettavuusmalli taajamiin" -projekti. Raportti II. Geological Survey of Finland, unpublished report K 21.42/2002/4. 42 p. (in Finnish)
- Pajunen, M., Airo, M.-L., Elminen, T., Niemelä, R., Salmelainen, J., Vaarma, M., Wasenius, P. & Wennerström, M. 2002c.** Projekti pätkinänkuoressa. "Kallioperän rakennettavuusmalli taajamiin" -projekti. Raportti III. Geological Survey of Finland, unpublished report K 21.42/2002/4. 28 p. (in Finnish)
- Pajunen, M., Airo, M.-L., Elminen, T., Niemelä, R., Salmelainen, J., Vaarma, M., Wasenius, P. & Wennerström, M. 2002d.** Kallioperän rakennettavuuskartta 1:50 000 - Espoo, Helsinki, Vantaa. "Kallioperän rakennettavuusmalli taajamiin" -projekti. Geological Survey of Finland, unpublished report K 21.42/2002/7. (in Finnish)
- Pajunen, M., Airo, M.-L., Elminen, T., Mänttari, I., Niemelä, R., Wasenius, P., Vaarma, M. & Wennerström, M. 2008.** Tectonic evolution of the Svecofennian crust in southern Finland. In: Pajunen, M. (ed.) Tectonic evolution of the Svecofennian crust in southern Finland - a basis for characterizing bedrock technical properties. Geological Survey of Finland, Special Paper 47, 15-160.
- Paulamäki, S. 1989.** Geological bedrock mapping of the Olkiluoto study site, Eurajoki, western Finland (in Finnish with English abstract) TVO/Site investigations. Helsinki: Teollisuuden Voima Oy, Work Report 89-25. 63 p.
- Paulamäki, S. & Koistinen, T. 1991.** Interpretation of the geological structures of the Olkiluoto area, Eurajoki, western Finland (in Finnish with English summary). TVO/Site investigations. Helsinki: Teollisuuden Voima Oy, Work Report 91-62. 34 p.
- Paulamäki, S., Paananen, M., Gehör, S., Kärki, A., Front, K., Aaltonen, I., Ahokas, T., Kemppainen, K., Mattila, J. & Wikström, L. 2006.** Geological model of the Olkiluoto Site, Version O. Posiva Oy, Working Report 2007-37. 355 p.
- Posiva Oy 2005.** Olkiluoto site description. Report May 2005. Posiva Oy, POSIVA 2005-03. 444 p.

- Roinisto, J. (ed.) 1986.** Kalliorakentaminen Suomessa. Rakentajain kustannus, Maanalaisten tilojen rakentamisyhdistys r.y. Jyväskylä: Gummerus Oy. 190 p. (in Finnish)
- Rönkä, K. & Ritola, J. (ed.) 1997.** Kalliorakentamisen neljäs aalto: ympäristövastuullinen maanalainen rakentaminen, suunnittelu ja toteutus. MTR (Maanalaisten tilojen rakentamisyhdistys r.y.), VTT (Valtion teknillinen tutkimuskeskus, yhdyskuntateknikka). Porvoo: WSOY. 137 p.
- Saari, K. (ed.) 1988.** Kalliorakentamisen mahdollisuudet. Maanalaisten tilojen rakentamisyhdistys r.y. Jyväskylä: Gummerus Oy. 207 p. (in Finnish)
- Saksa, P., Paananen, M., Paulamäki, S., Anttila, P., Ahokas, H., Pitkänen, P., Front, K. & Vaittinen, T. 1992.** Bedrock model of the Romuvaara area, summary report. Tiivistelmä: Kuhmon Romuvaaran kallioperämalli, yhteenvetoraportti. Helsinki: Voimayhtiöiden ydinjätetoimikunta, Report YJT-92-06. 97 p.
- Sederholm, J. J. 1932.** Über die Bodenkonfigurationen des Päijänne-Sees. Bulletin de la Commission Géologique de Finlande 100. 23 p.
- Talvitie, J. 1971.** Seismotectonics of the Kuopio region, Finland. Bulletin de la Commission Géologique de Finlande 248. 41 p.
- Tarkkala, J. 2004.** Helsingin maanalaisten toimintojen osayleiskaava, suunnitteluohjelma. Helsingin kaupunkisuunnitteluviraston yleissuunnitteluosaston selvityksiä 2004:8. Helsingin kaupunki. (in Finnish).
- Tuominen, H. V. 1957.** The structure of an Archean area: Orijärvi, Finland. Bulletin de la Commission Géologique de Finlande 177, 1–31.
- Vaasjoki, M. 1977.** Phanerozoic resetting of U- Pb ages in some South-Finnish uraninites. In: ECOG V. Fifth European Colloquium of Geochronology, Cosmochronology and Isotope Geology, Pisa, September 5.10, 1977. 2 p.
- Wennerström, M., Airo, M.-L., Elminen, T., Pajunen, M. & Salmelainen, J. 2006.** Structural evolution of the crust as a means of determining the technical properties of bedrock. In: Proceedings of the IAEG2006 Congress of 'Engineering geology for tomorrow's cities'. Nottingham, United kingdom. 6–10 September 2006. Extended abstract. 9 p.
- Wennerström, M., Airo, M.-L., Elminen, T., Niemelä, R., Pajunen, M., Vaarma, M. & Wasenius, P. 2008.** Orientation and properties of jointing in Helsinki area, southern Finland. In: Pajunen, M. (ed.) Tectonic evolution of the Svecofennian crust in southern Finland – a basis for characterizing bedrock technical properties. Geological Survey of Finland, Special Paper 47, 253–282.
- Wise, D., Dunn, D., Engelder, J., Geiser, P., Hatcher, R., Kish, S., Odom, A. & Schamel, S. 1984.** Fault-related rocks: Suggestions for terminology. Geology 12, 392–394.

The tectonic structures formed during the Svecofennian orogeny determined the tectonic framework for orienting the post-Svecofennian deformations. The deformation events were studied by using extensive field data and careful analyses of key structures on outcrops on ductile events, shear and fault zones and jointing. Structural interpretations were supported by new isotopic age data, paleomagnetic investigations and geophysical interpretations, especially developed for analyses in urban areas. The main goal of the seven papers in the volume was to produce geological baseline information for different applications to meet the various demands of society. In these applications the brittle structures, faulting and jointing, play an important role; they may provide benefits or disadvantages depending on the target application. A test application of the obtained geological data is presented here as a construction suitability map of bedrock in the study area, the Helsinki region of southern Finland.

ISBN 978-952-217-044-6 (paperback)
ISBN 978-952-217-045-3 (PDF)
ISSN 0782-8535



9 789522 170446